International VLBI Service for Geodesy and Astrometry

2004 GENERAL MEETING PROCEEDINGS

Ottawa, Canada
February 9-11

IVS 3rd GENERAL MEETING 2004 Ottawa, Canada • February 9-11

NASA/CP-2004-212255

International VLBI Service for Geodesy and Astrometry
2004 GENERAL MEETING PROCEEDINGS
NASA/CP-2004-212255

International VLBI Service for Geodesy and Astrometry

IVS Coordinating Center
NASA Goddard Space Flight Center
Code 926
Greenbelt, MD 20771

http://ivscc.gsfc.nasa.gov
ivscc@ivscc.gsfc.nasa.gov

phone: 301-614-5939
fax: 301-614-6099

Geodetic Survey Division
Natural Resources Canada

IVS International VLBI Service
for Geodesy and Astrometry

National Aeronautics and
Space Administration

The NASA STI Program Office … in Profile

Since its founding, NASA has been dedicated to the advancement of aeronautics and space science. The NASA Scientific and Technical Information (STI) Program Office plays a key part in helping NASA maintain this important role.

The NASA STI Program Office is operated by Langley Research Center, the lead center for NASA's scientific and technical information. The NASA STI Program Office provides access to the NASA STI Database, the largest collection of aeronautical and space science STI in the world. The Program Office is also NASA's institutional mechanism for disseminating the results of its research and development activities. These results are published by NASA in the NASA STI Report Series, which includes the following report types:

- TECHNICAL PUBLICATION. Reports of completed research or a major significant phase of research that present the results of NASA programs and include extensive data or theoretical analysis. Includes compilations of significant scientific and technical data and information deemed to be of continuing reference value. NASA's counterpart of peer-reviewed formal professional papers but has less stringent limitations on manuscript length and extent of graphic presentations.
- TECHNICAL MEMORANDUM. Scientific and technical findings that are preliminary or of specialized interest, e.g., quick release reports, working papers, and bibliographies that contain minimal annotation. Does not contain extensive analysis.
- CONTRACTOR REPORT. Scientific and technical findings by NASA-sponsored contractors and grantees.
- CONFERENCE PUBLICATION. Collected papers from scientific and technical conferences, symposia, seminars, or other meetings sponsored or cosponsored by NASA.
- SPECIAL PUBLICATION. Scientific, technical, or historical information from NASA programs, projects, and mission, often concerned with subjects having substantial public interest.
- TECHNICAL TRANSLATION. English-language translations of foreign scientific and technical material pertinent to NASA's mission.

Specialized services that complement the STI Program Office's diverse offerings include creating custom thesauri, building customized databases, organizing and publishing research results . . . even providing videos.

For more information about the NASA STI Program Office, see the following:

- Access the NASA STI Program Home Page at http://www.sti.nasa.gov/STI-homepage.html
- E-mail your question via the Internet to help@sti.nasa.gov
- Fax your question to the NASA Access Help Desk at (301) 621-0134
- Telephone the NASA Access Help Desk at (301) 621-0390
- Write to:
  NASA Access Help Desk
  NASA Center for AeroSpace Information
  7121 Standard Drive
  Hanover, MD 21076–1320

International VLBI Service for Geodesy and Astrometry

2004 GENERAL MEETING PROCEEDINGS

Ottawa, Canada

February 9-11

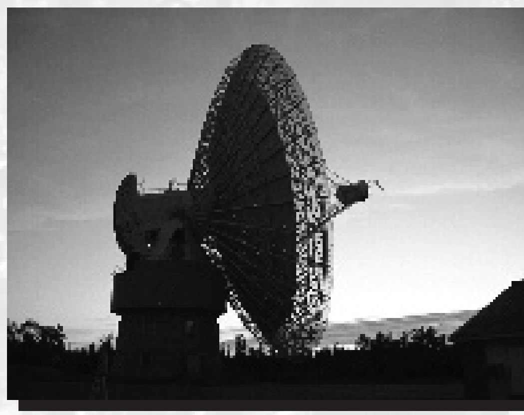

IVS 3rd GENERAL MEETING 2004 Ottawa, Canada • February 9-11

NASA/CP-2004-212255

Available from:

NASA Center for AeroSpace Information
7121 Standard Drive
Hanover, MD 21076-1320
Price Code: A17

National Technical Information Service
5285 Port Royal Road
Springfield, VA 22161
Price Code: A10

Preface

This volume is the proceedings of the third General Meeting of the International VLBI Service for Geodesy and Astrometry (IVS), held in Ottawa, Canada, February 9–11, 2004. The contents of this volume also appear on the IVS web site at

`http://ivscc.gsfc.nasa.gov/publications/gm2004`

The third General Meeting was held at the Lord Elgin Hotel in Ottawa, Canada. The meeting was hosted by the Geodetic Survey Division of Natural Resources Canada, an IVS member organization.

The keynote of the third General Meeting was visions for the next decade following the main theme of "Today's Results and Tomorrow's Vision", with a recognition that the outstanding VLBI results available today are the foundation and motivation for the next generation VLBI system requirements. The goal of the meeting was to provide an interesting and informative program for a wide cross section of IVS members, including station operators, program managers, and analysts.

Photographs taken during the meeting are available on the web at

`http://ivscc.gsfc.nasa.gov/meetings/gm2004/#Pictures`

This URL will display a section of the 2004 General Meeting web page with links to pages of photographs taken by several of the meeting's participants.

The April 2004 issue of the IVS Newsletter has a feature article about the meeting. The Newsletter is available at

`http://ivscc.gsfc.nasa.gov/newsletter/issue8.pdf`

This volume contains the following:

- **Welcome address.** This section contains the welcome address from Natural Resources Canada.
- **The papers presented at the meeting.** There are six major sections of this volume, each corresponding to a meeting session. Poster and oral papers are mixed. This volume includes 99 papers, as well as the abstracts of two papers that were not provided for publication. Poster papers about IVS component status are not included in this volume; they have been published in the 2003 Annual Report, available on the web.
- **A splinter meeting report.** Included is a report about the fifth Analysis Workshop.
- **A list of registered participants.**
- **The meeting program.**
- **An author index.**

Page intentionally left blank

Table of Contents

Preface ..... **iii**

Welcome Address **1**

Welcome Address of Natural Resources Canada **3**

Session 1. VLBI: Today's Results and Tomorrow's Vision **5**

Wolfgang Schlüter: Chair's Report at the Third IVS General Meeting **7**

Patrick Charlot: The ICRF: 2010 and Beyond **12**

Martine Feissel-Vernier, Jim Ray, Zuheir Altamimi, Véronique Dehant, Olivier de Viron: VLBI and Earth Rotation: Geophysical and Geodetic Challenges **22**

Hermann Drewes, Christoph Reigber: The IAG Project "Integrated Global Geodetic Observing System (IGGOS)" – Setup of the Initial Phase **32**

Benjamin F. Chao: Earth Rotational Variations Excited by Geophysical Fluids **38**

Zinovy Malkin: 5,000,000 Delays—Some Statistics **47**

Session 2. VLBI2010 ..... **53**

John LaBrecque: The International Global Network of Geodetic Fiducial Stations **55**

Ari Mujunen, Jouko Ritakari: VLBI2010: Commercial-off-the-Shelf Techonology Perspectives in 1996, 2003, and 2010 ..... **56**

Bill Petrachenko, Brian Corey, Ed Himwich, Chopo Ma, Zinovy Malkin, Arthur Niell, David Shaffer, Nancy Vandenberg: VLBI2010: Networks and Observing Strategies **60**

Hayo Hase, Brian Corey, Yasuhiro Koyama, David Shaffer, Bill Petrachenko, Wolfgang Schlüter: Preliminary Results of the VLBI2010 Subgroup "RF/IF, Frequency and Time" **65**

C.S. Jacobs, G.E. Lanyi, C.J. Naudet: Standard Observing Bands: Is Now the Time to Replace S/X with X/Ka? **70**

Christopher S. Jacobs, Patrick Charlot, Ed B. Fomalont, David Gordon, Gabor E. Lanyi, Chopo Ma, Charles J. Naudet, Ojars J. Sovers, Liwei D. Zhang, KQ VLBI Survey Collaboration: Extending the ICRF to Higher Radio Frequencies: 24 and 43 GHz Astrometry **75**

Gino Tuccari, Alan Whitney, Hans Hinteregger, Yasuhiro Koyama, Tetsuro Kondo: Backend Systems – Perspectives in 2010 ..... **80**

Alan R. Whitney, Hans F. Hinteregger, Tetsuro Kondo, Yashuhiro Koyama: Data Acquisition and Transport - Looking 2010 and Beyond **85**

Yasuhiro Koyama, Tetsuro Kondo, William T. Petrachenko, Hans Hinteregger, Alan R. Whitney: Correlators in 2010 and Beyond **90**

Harald Schuh: Report of the Subgroup "Data Analysis" of Working Group 3 VLBI2010 (Outline) **95**

Chopo Ma: Data Longevity Beyond 2010 ..... **97**

R. Craig Walker: Future Directions on the VLBA **100**

Wolfgang Winkler, Boris Bogensberger, Wilfried Karel, Michael Kistenich, Gerold Pacher, Andrea Pany, Andreas Roncat, Gerhard Summer, Johannes Boehm, Thomas Hobiger, Robert Weber, Harald Schuh: VIEPROJ1 - A Students' VLBI Project **105**

David L. Jauncey, James E. J. Lovell, Roopesh Ojha, Alan L. Fey, Yasuhiro Koyama, Hayley E. Bignall, Lucyna Kedziora-Chudczer, Jean-Pierre Macquart, Barney J. Rickett, Oleg Titov, Anastasios K. Tzioumis: The Impact of Interstellar Scintillation on Astrometric VLBI **109**

Session 3. Network Stations, Operation Centers, Correlators **113**

Arno Müskens, Walter Alef, David Graham, Kerry Kingham: Operational Experience with the Mark 5 Recording System at the Bonn and USNO Correlator **115**

Alessandra Bertarini, Arno Müskens, Alexandra Höfer: Overview of Geodetic Experiments at the Bonn Correlator **120**

Robert M. Campbell: Recent Results from the EVN Mark IV Data Processor at JIVE **123**

Andrey Finkelstein, Valery Gratchev, Alexander Ipatov, Zinovy Malkin, Ismail Rahimov, Elena Skurikhina, Sergey Smolentsev: Some Results of the First Year of Participation of the Svetloe Observatory in IVS Observing Programs **128**

Zhihan Qian, Shuhua Ye, Xiaoyu Hong, Xiuzhong Zhang, Jin Zhang, Xizheng Zhang, Hongbo Zhang: Present Status and Future Plan on the Chinese VLBI Network **133**

Shigeru Matsuzaka, Yoshimitsu Masaki, Hiromichi Tsuji, Kazuhiro Takashima, Takashi Tsutsumi, Yoshimasa Ishimoto, Morito Machida, Hirohito Wada, Shinobu Kurihara: VLBI-GPS Co-location Results in Japan **138**

Hayo Hase, Sergio Sobarzo, Cristobal Jara, Roberto Aedo, Gonzalo Remedi, Marcos Moreno, Gonzalo Hermosilla, Oscar Cifuentes: Projects at TIGO **143**

Maria Hennes, Cornelia Eschelbach: New Technologies for the Real 3D Reference Point Determination **146**

Seiji Manabe, Yoshiaki Tamura, Takkaki Jike, Koji Horiai, VERA Team: Status and Plan of Geodetic and Astrometric Observations with VERA **151**

Young Chol Minh, Hyun-Goo Kim, Seog-Tae Han, Duk-Gyoo Roh: Present Status of the KVN Construction Project **156**

Andrey Finkelstein, Alexander Ipatov, Sergey Smolentsev: Radio Astronomy Observatories Svetloe, Zelenchukskaya and Badary of VLBI Network QUASAR **161**

Igor Molotov, Yuri Gorshenkov, Alexander Stepanov, Alexander Dementiev, Gino Tuccari, Valerii Saurin, Alexis Zinoviev: VLBI Status of the Bear Lakes Radio Astronomy Station **166**

Alexandr Volvach, Larisa Volvach, Yuri Y. Kovalev: Single Dish Flux Density Monitoring of Geodetic VLBI Sources **170**

Session 4. New Technology Developments in VLBI **175**

Alan R. Whitney: The Mark 5B VLBI Data System **177**

Jouko Ritakari, Ari Mujunen: Gbit/s VLBI and eVLBI with Off-The-Shelf Components **182**

Tetsuro Kondo, Moritaka Kimura, Yasuhiro Koyama, Hiro Osaki: Current Status of Software Correlators Developed at Kashima Space Research Center **186**

Stephen T. Lowe: Softc: an Operational Software Correlator **191**

Valery Gratchev: New Correlator PARSEC **195**

Hiroshi Takeuchi, Tetsuro Kondo, Yasuhiro Koyama, Junichi Nakajima: VLBI@home – VLBI Correlator by GRID Computing System **200**

Stephen Parsley: eVLBI Research in the European VLBI Network **205**

Zheng Weimin, Zhang Xiuzhong, Shu Fengchun: e-VLBI Progress of the Chinese VLBI Network **210**

David Lapsley: A Practical Approach to e-VLBI over Long Fast Networks **215**

Yasuhiro Koyama, Tetsuro Kondo, Hiro Osaki, Masaki Hirabaru, Kazuhiro Takashima, Kazuo Sorai, Hiroshi Takaba, Kenta Fujisawa, David Lapsley, Kevin Dudevoir, Alan Whitney: Geodetic VLBI Experiments with the K5 System **220**

Gino Tuccari, Igor Molotov, Salvatore Buttaccio, Gaetano Nicotra, Alexander Dementiev, Alexander Konovalenko, Alexis Zinoviev, Yuri Gorshenkov, Xiang Liu, Xiaou Hong, Alexander Volvach: A Near Real Time e-Radar/VLBI Network **225**

Seog-Tae Han, Do-Heung Je, Duk-Gyoo Roh, Sek-O Wi, Se-Jin Oh, Min-Gyu Song, Chang-Hoon Lee, Kwang-Dong Kim: The Multi-Channel Millimeter Wave Receiver for VLBI **229**

Gino Tuccari: DBBC - a Wide Band Digital Base Band Converter **234**

Hans Hinteregger: Low-Cost Wideband Digital Back-Ends for LOFAR⇒e-VLBI⇒SKA **238**

Alexander Ipatov, Nikolay Koltsov, Leonid Fedotov: The Data Acquisition System Developed for Quasar Network **243**

Duk-Gyoo Roh, Kwang-Dong Kim, Se-Jin Oh, Hyun-Soo Chung, Han-Kyu Choi: A Design of Data Acquisition System for Korean VLBI Network **248**

Ryuichi Ichikawa, Mamoru Sekido, Hiroo Ohsaki, Yasuhiro Koyama, Tetsuro Kondo, Takafumi Ohnishi, Makoto Yoshikawa, Wayne Cannon, Alexander Novikov, Mario Bérubé, NOZOMI DVLBI Group: An Evaluation of VLBI Observations for the Deep Space Tracking of the Interplanetary Spacecrafts **253**

Mamoru Sekido, Ryuichi Ichikawa, Hiro Osaki, Tetsuro Kondo, Yasuhiro Koyama, Makoto Yoshikawa, Takafumi Ohnishi, Wayne Cannon, Alexander Novikov, Mario Bérubé, NOZOMI VLBI Group: VLBI Observation for Spacecraft Navigation (NOZOMI) - Data Processing and Analysis Status Report **258**

Session 5. Analysis Strategies and Software 263

David Gordon: CALC: The Next Upgrade **265**

Oleg Titov, Volker Tesmer, Johannes Boehm: OCCAM v.6.0 Software for VLBI Data Analysis **267**

Ojars J. Sovers, Christopher S. Jacobs, Gabor E. Lanyi: MODEST: a Tool for Geodesy and Astrometry **272**

Johannes Boehm, Harald Schuh: Vienna Mapping Functions in VLBI Analyses **277**

Volkmar Thorandt, Gerald Engelhardt: Residual Plotting and Ambiguity Resolution (REPA) **282**

Wolfgang Schwegmann: An Embedded Expert System for the Automation of VLBI Data Analysis: Concept, Implementation and Results **287**

Wolfgang Schwegmann, Gerald Engelhardt, Volkmar Thorandt: Towards an Operational Automatic VLBI Data Analysis Tool for INTENSIVE Sessions **292**

Volker Tesmer, Hansjörg Kutterer: An Advanced Stochastic Model for VLBI Observations and its Application to VLBI Data Analysis **296**

Hansjörg Kutterer: Reliability Measures for Geodetic VLBI Products **301**

Thomas Hobiger, Harald Schuh: Modelling Vertical Total Electron Content from VLBI Observations **306**

Volker Tesmer, Hansjörg Kutterer, Hermann Drewes: Simultaneous Estimation of a TRF, the EOP and a CRF **311**

V.S. Gubanov, Yu.L. Rusinov, I.F. Surkis, S.L. Kurdubov, C.Y. Shabun: Project: Global Analysis of 1979-2004 VLBI Data **315**

Zinovy Malkin: Towards IVS Analysis Conventions **320**

Gerald Engelhardt, Volkmar Thorandt, Dieter Ullrich: Activities of the IVS Analysis Center at BKG in 2003 ..... **324**

David M. Hall, David A. Boboltz, Alan L. Fey, Kerry A. Kingham: VLBI Analysis at the U.S. Naval Observatory **329**

Session 6. Results and Geodetic/Geophysical/Astrometic Interpretation 335

Chopo Ma: Refinement of the ICRF 337

Alan L. Fey: Status of the International Celestial Reference Frame 341

Martine Feissel-Vernier: Stability of the VLBI-Derived Celestial Reference Frame 346

David Gordon: VLBA Impact on Geodesy and Astrometry 351

Alan L. Fey, Roopesh Ojha, David L. Jauncey, Kenneth J. Johnston, John E. Reynolds, James E. J. Lovell, Anastasios K. Tzioumis, Jonathan F. H. Quick, George D. Nicolson, Simon P. Ellingsen, Peter M. McCulloch, Yasuhiro Koyama: VLBI Astrometry of 22 Southern Hemisphere Radio Sources 356

David A. Boboltz, Alan L. Fey, Patrick Charlot, Edward B. Fomalont, Gabor E. Lanyi, Liwei D. Zhang, KQ VLBI Survey Collaboration: Extending the ICRF to Higher Radio Frequencies – Imaging and Source Structure 361

Nicole Capitaine, Patrick Wallace: The VLBI Contribution to Precession (Present and Future) 366

D. E. Smylie, Andrew Palmer: Ring Downs of Free Core Nutations in the GSFC and USNO VLBI Nutation Series 371

Véronique Dehant, Olivier de Viron, Martine Feissel-Vernier: Investigation of Nutation beyond the IAU2000 Model 381

George A. Krasinsky: Viscosity of the Earth's Fluid Core from VLBI Data 383

Zinovy Malkin: A New Free Core Nutation Model with Variable Amplitude and Period 388

Daniel Gambis, Christian Bizouard: Contribution of VLBI to Earth Orientation Monitoring: State-of-the-Art and Future Prospects 393

Karen Baver, Daniel MacMillan, Leonid Petrov, David Gordon: Analysis of the VLBI Intensive Sessions 394

Dorothee Fischer, Axel Nothnagel, Richard Kilger, Shinobu Kurihara, Wolfgang Schlüter, Kazuhiro Takashima: UT1 Intensive Series Using K4 Technology 399

Rüdiger Haas, Raymundo Del Cojo López, Juan Mata Lozano: Investigations of High-Frequency Earth Rotation Variations from VLBI CONT Observations 403

Jolanta Nastula, Barbara Kolaczek, Robert Weber, Johannes Boehm, Harald Schuh: High Resolution Earth Rotation Parameters Determined During the CONT02 Campaign 408

Christoph Steinforth, Axel Nothnagel: Considering a Priori Correlations in the IVS Combined EOP Series 413

Manuela Krügel, Volker Tesmer, Detlef Angermann, Daniela Thaller, Markus Rothacher, Ralf Schmid: CONT02 Campaign - Combination of VLBI and GPS 418

Markus Vennebusch: First Results of SINEX Combinations **423**

Mamoru Sekido, Tetsuro Kondo, Eiji Kawai, Michito Imae: Evaluation of Global Ionosphere TEC by Comparison with VLBI Data **427**

Thomas Hobiger, Harald Schuh: How VLBI Contributes to Ionospheric Research **437**

Thomas Hobiger, Sonya Todorova, Harald Schuh: Ionospheric Parameters Obtained by Different Space Geodetic Techniques during CONT02 .... **442**

Sten Bergstrand, Rüdiger Haas: Comparison of Ionospheric Activity Derived from GPS and Different VLBI Networks **447**

Gabor Lanyi, David Gordon, Ojars J. Sovers: Limitations to Dual Frequency Ionosphere Corrections for Frequency Switched K-Q-Band Observations with the VLBA **452**

Monia Negusini, Paolo Tomasi: Tropospheric Parameters Estimated by Geodetic VLBI Data IVS .. **456**

Harald Schuh, Kristyna Snajdrova, Johannes Boehm, Pascal Willis, Gerald Engelhardt, Roberto Lanotte, Paolo Tomasi, Monia Negusini, Daniel MacMillan, Iraida Vereshchagina, Vadim Gubanov, Rüdiger Haas: IVS Tropospheric Parameters - Comparison with DORIS and GPS for CONT02 .... **461**

Elena Skurikhina: Long Time Wet Tropospheric Delay Series for Some Stations **466**

Bisser Stoyanov, Rüdiger Haas, Lubomir Gradinarsky: Calculating Mapping Functions from the HIRLAM Numerical Weather Prediction Model **471**

Daniel MacMillan, Jean-Paul Boy: Mass Loading Effects on Crustal Displacements Measured by VLBI **476**

Zhigen Yang, Mario Bérubé, Anthony Searle: Relative Deformations between Co-located VLBI Stations and Comparisons with VTRF2003 .... **481**

Axel Nothnagel: First Results of the IVS Pilot Project "Time Series of Baseline Lengths" **486**

Daniel MacMillan, Steven Cohen: Postseismic Transient after the 2002 Denali Fault Earthquake from VLBI Measurements at Fairbanks **491**

Oleg Titov, Paul Tregoning: Post-Seismic Motion of Gilcreek Geodetic Sites Following the November, 2002 Denali Earthquake **496**

Leonid Petrov: Preliminary Results of the IVS Gravity Experiment Grav01 .... **501**

Splinter Meeting Report **507**

Axel Nothnagel: Summary of the Fifth IVS Analysis Workshop **509**

Registered Participants **515**
Program **521**
Index of Authors **535**

Welcome Address

Page intentionally left blank

Welcome Address of Natural Resources Canada, IVS 2004 General Meeting Proceedings, p.3–4
http://ivscc.gsfc.nasa.gov/publications/gm2004/welcome-nrcan

Welcome Address of Natural Resources Canada

Dr. Susan M. Till

It is an honour for Natural Resources Canada to host the third IVS General Meeting in Canada's national capital. Holding this meeting in Canada reflects NRCan's commitment to the IVS program and the IVS international community, more than 76 components representing 30 national agencies, universities and research institutions, from 15 nations. I commend each of you and your organisations for your dedication to the IVS and welcome you to the third IVS General Meeting.

Canada is the world's second-largest country, larger than the continent of Europe (excluding Russia), and covers six time zones. Given this, it is not surprising that the Natural Resources sector is a very important part of the Canadian economy, amounting to over 12 percent of Canada's GDP. Nearly a million Canadians are directly involved in forestry, mining and energy.

Natural Resources Canada (NRCan) is a Canadian federal government department specializing in the sustainable development and use of natural resources, energy, minerals and metals, forests and earth sciences. Natural Resources Canada (NRCan) conducts leading-edge science and technology to provide Canadians with ideas, knowledge and technology. This helps Canadians use their country's resources wisely, reduce costs, protect the environment and create new products and services. We build and maintain a national knowledge infrastructure on Canada's land and resources, so all Canadians can easily access the latest information about our landmass and our resources. In partnerships such as the IVS, we promote shared international interests. This helps NRCan meet its commitments related to natural resources, and keeps access open to Canadian and global markets for products, services and technology.

Canada has a long successful history in VLBI. In the 1960s Canadians were in the forefront of the development of this technique, obtaining the first set of VLBI fringes in a race with our U.S. counterparts. And that is not all: our measurement of the distance between Algonquin Radio Observatory and an antenna in Saskatchewan was the first successful geodetic VLBI experiment. Since the IVS began about 5 years ago, NRCan has been a strong supporter and contributor. At present, this support includes operation of three VLBI antennas, including the Algonquin Radio Observatory. In the past year or so we have been coordinating an international experiment on a monthly basis using VLBI equipment developed in Canada (at CRESTech/York University and NRCan).

The stable reference frame produced by these systems strengthens positioning on earth. We could say that the positioning of an engineering project or climate change study in Canada's Arctic is tied through GPS and then VLBI to the most stable reference frame in the world, made up of quasars billions of light years away. NRCan views its contribution to the IVS as a two-way relationship, in that it benefits from the IVS as much as it contributes.

We recognize that our participation in the IVS, the International GPS Service (IGS) and the International Earth Rotation Service (IERS) generates outputs that are essential to the maintenance of Canada's national reference frame. This national reference frame, based on the results of international collaboration, provides Canadians with access to geospatial coordinates that are precise and consistent over time for many important applications linked to key issues in Canada, such as Sustainable Development, Natural Hazards and Safety and Security of Canadians.

Canada supports IVS evolution and its efforts to enhance its capabilities. The keynote of the third General Meeting will be visions for the next decade following the main theme of "Today's Results and Tomorrow's Vision". NRCan, through the Geodetic Survey Division, continues to contribute its expertise through national and international collaboration in support of positioning requirements. In doing so, NRCan provides for more effective and efficient use of geospatial data and supports integrated geomatics initiatives with its Canadian partners and abroad.

I hope you have time to visit the some of the sites around our beautiful capital city, take in some of the Winterlude events, and go skating on the Rideau Canal. I hope the meeting in Ottawa is productive and pleasant. We certainly extend a welcoming hand and look forward to seeing you in Canada in the future. The local organizing committee is available to address any specific questions you may have about the city or your visit. Don't hesitate to ask for their help. Once again thank you and I hope you have a very productive meeting.

Susan M. Till
Associate Assistant Deputy Minister
Earth Sciences Sector
Natural Resources Canada

Session 1

VLBI: Today's Results and Tomorrow's Vision

Page intentionally left blank

Wolfgang Schlüter: Chair's Report at the Third IVS General Meeting, IVS 2004 General Meeting Proceedings, p.7–11
http://ivscc.gsfc.nasa.gov/publications/gm2004/schlueter

Chair's Report at the Third IVS General Meeting

Wolfgang Schlüter

Bundesamt für Kartographie und Geodäsie, Fundamentalstation Wettzell
e-mail: `Wolfgang.Schlueter@bkg.bund.de`

Abstract

This report presents the status of the IVS and gives some prospects for the future.

1. General

The International VLBI Service for Geodesy and Astrometry holds its General Meetings (GM) every two years. The first IVS GM in Kötzting, Germany, held February 21-24, 2000, was guided by the keynote "Highlights and Challenges of VLBI". The goal was to provide an interesting and informative program for a wide cross section of IVS members on the high goals of VLBI technology and its potential for the future. The keynote for the second IVS GM in Tsukuba, Japan, held February 4-7, 2002, was "Prospectives for the Future" in keeping with the reorganization of IAG around the motivation of geodesy as "an old science with a dynamic future" and noting the challenging role of IVS in maintaining global reference frames on the highest accuracy level. Products and observing programs were reviewed in the Working Group 2 report, and proposals were made and discussed with the goal of having a common plan for improvements in the coming years, in order to meet the service requirements. The keynote of the third IVS GM in Ottawa, Canada, held February 9-11, 2004, is visions for the next decade following the main theme of "Today's Results and Tomorrow's Vision". The outstanding VLBI results available today are the foundation and motivation for the next generation VLBI system requirements. All speakers were encouraged to address the results of today and to consider possible future directions.

So far the GMs have been held in Europe, Asia and North America, which reflects the global task and the global international collaboration of IVS. It is obvious that the next GM should be in the southern hemisphere. I thank the University of Concepción, Chile, where the German Transportable Integrated Geodetic Observatory (TIGO) is located, for their willingness to host the IVS GM in 2006.

Much work was done for GM 2004 by the Local Organizing Committee and also by the IVS Coordinating Center. I express my thanks to the Geodetic Survey Division, Natural Resources Canada for hosting the third IVS GM and for organizing the meeting in Ottawa, in particular to the members of the Local Organizing Committee:

- Calvin Klatt
- Anthony Searle
- Mario Bérubé.

I also thank the IVS Coordination Center, in particular Nancy Vandenberg, for strong support.

For the preparation of the GM 2004 program I thank the Program Committee and the session conveners. They were:

- Wayne Cannon (SGL/Crestech, Canada)
- Rüdiger Haas (Onsala Space Observatory, Sweden)
- Hayo Hase (BKG-TIGO, Germany)
- Ed Himwich (NVI, Inc./GSFC, USA)
- Kerry Kingham (USNO, USA))
- Yasuhiro Koyama (CRL, Japan)
- David Lapsley (MIT Haystack, USA)
- Zinovy Malkin (IAA, St. Petersburg, Russia)
- Arthur Niell (MIT Haystack, USA)
- Axel Nothnagel (Univ. Bonn, Germany)
- Bill Petrachenko (NRCan, Canada)
- Wolfgang Schlüter (BKG, Germany)
- Harald Schuh (TU-Vienna, Austria)
- Volker Tesmer (DGFI, Germany)
- Oleg Titov (Geoscience Australia, Australia)
- Nancy Vandenberg (NVI, Inc./GSFC, USA)
- Alan Whitney (MIT Haystack, USA).

I thank all the participants for making the meeting successful by attending and by preparing and presenting papers, chairing sessions and more. We have six very interesting sessions:

- VLBI: Today's Results and Tomorrow's Vision (4 oral presentations, 1 poster)
- VLBI2010 (13 oral presentations, 2 posters)
- Network Stations, Operation Centers, Correlators (9 oral presentations, 7 posters)
- New Technology Developments in VLBI (12 oral presentations, 7 posters)
- Analysis Strategies and Software (8 oral presentations, 10 posters)
- Results and Geodetic/Geophysical/Astrometric Interpretation (18 oral presentations, 16 posters.)

with 64 oral presentations and 43 posters, which is remarkable as we have 111 registered participants.

2. "Today's Results, Tomorrow's Vision"

In general VLBI provides products for the Celestial Reference Frame (CRF) uniquely, for the Terrestrial Reference Frame (TRF), and delivers the combining elements between both frames as the Earth Orientation Parameters (EOP), uniquely the complete set in particular the velocity of the rotation as DUT1. As no other technique is capable of providing the fundamental products for CRF and for the EOP, and in particular the DUT1, in the future IVS will continue to place emphasis on its strengths. We will have to carry on the fundamental role of VLBI for contributing to research programs related to global and climate change, natural hazards and Earth observations and for many applications in navigation, in positioning and for space missions as well.

Considering the keynote "Today's Results and Tomorrow's Vision" I will focus on two events which recently have demonstrated the excellence of VLBI/IVS products. "Today's Results ...." are basic products for research and for many applications.

The MARS Mission, which was reported in the newspapers recently, is a good example of the application of VLBI products. Precise VLBI results were needed to point antennas to the space vehicles for communication. As a spectacular event, the mission was recognized by German newspapers and "by accident" the contribution of VLBI, supporting the mission with EOPs, was mentioned in various articles to the public.

As a significant application of the excellence of VLBI products in research, the work done by the IAU Working Group "Non-Rigid Earth Nutation Theory" chaired by Dr. Veronique Dehant, Royal Observatory Belgium, has to be mentioned. The working group won the Decartes Prizes 2003, which is the highest award for science in Europe. VLBI contributed the precise EOP time series needed to confirm the theory. I would like to express my respect and congratulations to the Working Group.

Geodetic VLBI has been successful over the past three decades; however, a number of factors are converging to make progress more difficult. Most antennas and equipment were developed in the 70's and 80's and are close to being worn out today. Increasing interference (in particular at S-Band) decreases the data quality. The network distribution and locations of antennas are not ideal and are unbalanced. The operational costs vs. efficiency (due to old equipment) have to be improved. Overall new technology and improved strategies will be required.

To develop plans for the future or even to think about a new VLBI generation, visions are needed. The IVS Working Group 3: "VLBI2010" was established by the IVS Directing Board at its 10th Meeting, in order to come up with recommendations to be presented in a vision paper as VISION 2010. Such a document is strongly needed for:

- planning the long term developments
- planning budgets of contributing agencies
- initiating new developments
- motivating contributors
- optimizing future resources.

With the adoption of the keynote "Today's Results and Tomorrow's Vision" for this General Meeting, it is expected we will initiate additional input from the attendees. The Program Committee invited well known keynote speakers, who were asked to focus to future requirements they would like to see realized in VLBI in their field. It is with pleasure that I thank the keynote speakers for their willingness to present a paper:

- Patrick Charlot: "The ICRF: 2010 and Beyond"
- Martine Feissel-Vernier et al.: "VLBI and the Earth Rotation: Geophysical and Geodetic Challenges"
- Hermann Drewes and Chris Reigber: "IGGOS–Its Mission, Scientific Rationale, and First Steps and Ideas for its Design and Development."
- Benjamin Chao: "Earth Rotation Dynamics: Review and Prospects"
- John LaBrecque: "The International Global Network of Geodetic Fiducial Stations".

3. Important Steps Since GM 2002

Since the General Meeting 2002 significant improvements have been made to meet the service requirements. In January 2002 the new IVS observing program was introduced. The quality and quantity of observations were increased and additional resources were included, following the resolution released at the GM 2002. All together this resulted in strong improvements in the IVS products. For research investigations CONT02 was carried out, providing an important data set to investigate VLBI capabilities and to support research in the combination with other techniques. The transition from Mark IV (tape recording systems) to Mark 5A (disk recording systems) was organized and realized successfully and in a remarkably short period of time. This transition opened up new capabilities and increased the efficiency by decreasing the operation costs. Using the VLBI Standard Interface (VSI) the newly developed disk-based recorders such as Mark 5 (USA) and K5 (Japan) can be combined in observing sessions, which gives more flexibility in the use of network stations. Employing disk-based recorders pushed forward the development of e-VLBI. Several e-VLBI experiments have been performed successfully in national, international and global experiments. The developments for e-VLBI are close to being employed in routine operation, e.g. for the Intensives. It also has to be mentioned that troposphere time series are provided now regularly as an official IVS product.

4. Concern to Guarantee Product Availability with High Quality and Timeliness

Recognizing the urgent need for the products that the IAG services such as the IVS, the ILRS and the IGS are providing today, and considering the resulting responsibility of the services, I take, as Chair of IVS, the opportunity to express some concern.

Due to lack of money, agencies might be forced to consider reduction of support for IVS. Consequently this might result in a decrease of quality of the generated products. Finally it could result in a collapse, if major contributors might be forced to withdraw their support. In any case, it should be considered that IVS is dependent on contributions of agencies, as they proposed in their response to the call for participation. The product generation through collaboration – as the IAG services are doing – is most effective: all agencies contribute according to their ability and in return all partners benefit from products which could never be achieved from a national institution by itself. I emphasize that IVS optimizes the use of VLBI resources to obtain the best products. It is obvious that this kind of service organization is sensitive to any reductions of support, but this approach keeps the costs low and results in high quality products. I remind you that IVS needs the long term continuous support which ultimately remains the responsibility of all members and member institutions. I urge everybody to do their best to continue the excellent work, which will be the best argument for being respected in, and for maintaining the support of, society.

5. From the Directing Board

With the beginning of the year 2003 the second four-year Directing Board terms commenced and some changes have to be mentioned. James Campbell, University of Bonn, Germany, withdrew from the board as IAG representative. He was replaced by Harald Schuh from the University of Vienna, Austria. Harald was appointed by the IAG. Nicole Capitaine, Paris Observatory, France as IAU representative was replaced by Patrick Wallace, Rutherford Appleton Labatory, U.K. By a decision of the board, the new representative for the Analysis and Data Centers became Zinovy Malkin, Institute of Applied Astronomy, St. Petersburg, Russia. The term expired for the at large members Wayne Cannon, Space Geodetic Laboratory, Ottawa, Canada and Paolo Tomasi, Istituto di Radioastronomia CNR, Bologna, Italy. The new members elected by the board were William Petrachenko, Natural Resources Canada, and Franco Mantovani, Istituto di Radioastronomia CNR, Bologna, Italy.

I like to take this opportunity to express my sincere thanks to James Campbell, to Nicole Capitaine, to Wayne Cannon and to Paolo Tomasi for their important support and their significant contributions in the IVS Directing Board. It was a pleasure to collaborate with all during the first four years. I congratulate Harald Schuh, who is also one of the representatives of the services in the new IAG Executive Committee, William Petrachenko and Franco Mantovani on being elected to the IVS Directing Board.

Patrick Charlot: The ICRF: 2010 and Beyond, IVS 2004 General Meeting Proceedings, p.12–21
http://ivscc.gsfc.nasa.gov/publications/gm2004/charlot

The ICRF: 2010 and Beyond

Patrick Charlot

Observatoire de Bordeaux – CNRS/UMR 5804
e-mail: charlot@obs.u-bordeaux1.fr

Abstract

This paper considers future directions for improving the International Celestial Reference Frame (ICRF) over the next 10 years. The current ICRF includes a total of 717 extragalactic objects, most of which have position accuracies of 250–1000 microarcseconds (μas). Beyond 2010, the radio realization of the ICRF may be disputed by new instruments like the GAIA optical astrometric satellite which will observe 500 000 extragalactic objects with astrometric precision of 10–100 μas. The IVS should prepare for this challenge by improving as far as possible the present ICRF accuracy and source density. Position accuracies better than 100 μas may soon be achievable considering possible modeling refinements (troposphere, source structure) and improved instrumentation. Recent initiatives to densify the ICRF as well as future possibilities to massively increase the number of sources are discussed. Over 10+ years, the realization of an ultra-accurate extragalactic reference frame at both optical and radio wavelengths is an exciting perspective not only for astrometry but also for studying physics of active galactic nuclei.

1. Introduction

The International Celestial Reference Frame (ICRF) is a unique VLBI product because no other astrometric technique has been able to derive a similar highly-accurate extragalactic frame. The ICRF became effective as the fundamental celestial reference frame on 1 January 1998, following a resolution adopted at the XVIII General Assembly of the International Astronomical Union held on 1997 August 20 in Kyoto, Japan [1].

The ICRF differs from the previous realization of the celestial frame, the FK5 stellar catalog, in two important ways: (i) it relies on extragalactic objects (quasars and active galactic nuclei), and (ii) its axes are no longer related to the equator and ecliptic planes. Instead, the ICRF axes are specified through quasi-inertial coordinates of 212 *defining* extragalactic sources observed by VLBI between August 1979 and July 1995 [1]. The accuracy of the individual source positions is as small as 250 microarcseconds (μas) while the orientation of the ICRF axes is good to the 20 μas level. Positions for 294 less-observed *candidate* sources and 102 *other* sources with less-stable coordinates were also reported, primarily to densify the frame. Continued VLBI observations through May 2002 have provided positions for an additional 109 *new* sources along with refined coordinates for candidate and "other" sources [2]. The sky distribution and position accuracy of the current 717 ICRF sources are shown in Fig 1.

While there is presently no competition for the realization of the fundamental extragalactic frame, the situation may evolve within the next decade because new instruments will come on line, which may dispute the realization of the frame to VLBI. In the radio band, the e-MERLIN instrument (a development of the present MERLIN array using fiber-optics cables to transmit wide-band signals from telescopes)[1] will conduct geodetic-mode observations to measure absolute

[1]See the e-MERLIN science case and technical specification at http://www.jb.man.ac.uk/e-merlin.

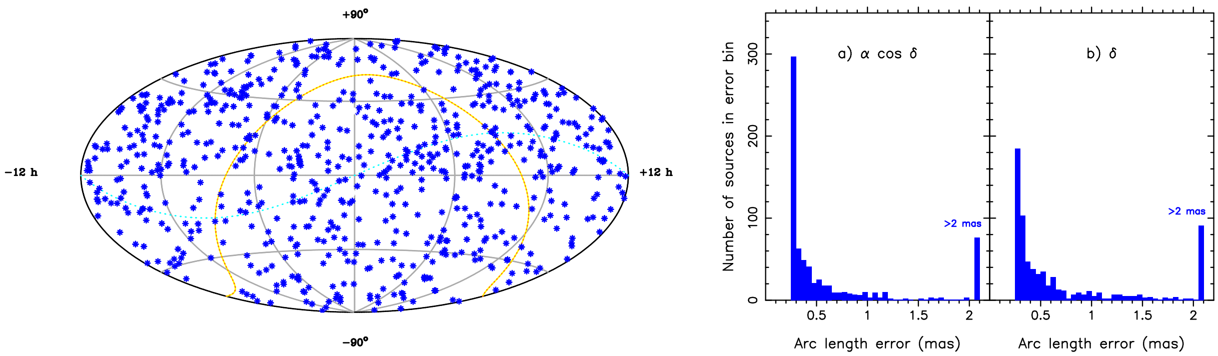

Figure 1. *Left panel:* Distribution of the current 717 ICRF sources on an Aitoff equal-area projection of the celestial sphere. *Right panel:* Histogram of source position errors in *(a)* right ascension and *(b)* declination.

positions to within a few milliarcsecond (mas) for milliJansky (mJy) sources. Plans are prepared for a survey of up to 100 000 such sources with observing starting by 2008 [3]. Though not up to the ICRF accuracy, this survey will be 100 times denser than the ICRF and will constitute a natural extension of the frame towards weaker objects north of approximately $-20°$ declination.

At optical wavelengths, the GAIA space mission, a second-generation astrometric satellite to be launched by 2010–2012, will survey all stars and quasars down to an apparent magnitude of 20 [4]. Position accuracies will range from 10–40 μas at magnitude 15–18 to 100–200 μas at magnitude 20. Based on current estimates from local surveys, it is expected that 500 000 such quasars should be detected. Hence, there will be plenty of material to construct the extragalactic frame from *direct* observations of defining sources in the visible wavebands. Simulations show that with a sample of 10 000 defining sources the residual spin of the GAIA reference frame could be determined to 0.5 μas/yr [5]. In practice, the ultimate accuracy of the frame may be limited by random instability of the sources which may show extended and variable structure on these spatial scales, similar to that observed at radio wavelengths [6, 7]. Despite this limitation, the GAIA reference frame will clearly surpass the current ICRF, both in accuracy and in source density. Hence, the realization of the fundamental celestial frame is likely to be brought back to visible wavebands in about 10 years.

This perspective should be regarded as a strong motivation to further improve the current ICRF, design ambitious VLBI programs, and possibly invent new VLBI instruments that will challenge the future optical realization of the extragalactic frame by GAIA. Sections 2 and 3 below consider possible future directions for improving the accuracy and source density of the ICRF with the GAIA perspective in mind. In Sect. 4, I will give my own view on how such improvements may be accomplished and propose a time frame for the work to be done from now to beyond 2010.

2. Improving the Accuracy of the ICRF

Improving the accuracy of VLBI astrometric results require improving the entire VLBI observing, calibration and analysis system. This includes modeling capabilities, data acquisition technology, and astrometric target selection. Overall, the largest contributor to ICRF inaccuracy is the propagation in the troposphere (150–250 μas error), followed by the data acquisition technology (50–100 μas error), and source structure (widely-variable error) [8]. Recent or foreseeable improvements for each of these three major error components are discussed below.

2.1. Troposphere Modeling

While the charged particle propagation media effects (ionosphere) have been effectively calibrated using two observing frequencies, the modeling of the troposphere has improved in discrete steps associated with consideration of asymmetry and variability [9] and development of new troposphere mapping algorithms [10]. Current research is directed toward the use of global weather data in computing the mapping function through ray tracing or a proxy. However, computational limits as well as temporal and spatial resolution of the weather models preclude direct ray tracing for every observation in place of estimating troposphere variations.

Another approach would be to install advanced water vapor radiometers at each VLBI site to calibrate the atmospheric path delay along the line of sight for every observation [11]. This technology, developed for the Cassini gravitational wave experiment, has been very successful. However, it is very expensive and there are no plans to replicate such instruments at the moment. Further engineering studies should be carried out to determine whether the cost for these instruments could be lowered so that a wider use may be considered.

Reducing the impact of tropospheric mismodeling also implies devising optimum observing strategies for improving the estimation of troposphere variations. Such strategies may be facilitated by future increased baseline sensitivities (see below) which will permit integration over shorter scans and hence observation of more sources over a given period of time for improving the local sky coverage around each VLBI station.

2.2. Data Acquisition Technology

This category covers a wide range of instrumental errors, among which atomic clock instabilities, phase-calibration errors, and recording-media deficiencies. When taken altogether, these errors may be the second largest contributor to inaccuracy in astrometric VLBI results.

While fiber optics have greatly reduced the errors in distributing the frequency standard to the antennas, atomic clocks (hydrogen masers) still wander at a level VLBI is sensitive to. There is ongoing research with mercury-ion clocks that shows promise especially on the long time scales (many hours to days) but this technology is not yet operational for VLBI [12]. The pulse generation and process of injecting phase-calibration tones into the signal chain are imperfect and do not calibrate the antenna optics (primary dish, subreflector, feed). Additionally, there is usually no polarization calibration while it is known that polarization leakage may be a potentially significant error. Overall, imperfect calibration produces phase instabilities in both time and frequency which affect the measurements at some level. While certainly a long process, scrutinization of all such errors appears to be a necessary step to further improve data quality.

Tape-based recording has constantly suffered from varying amounts of data lost due to tape dropouts and tape synchronization up time, thus contributing to measurement errors. Fortunately, these problems are about to go away with the introduction of disk-based recording. This new system greatly improves data reliability and is a huge step forward in collecting uniformly-sampled data in time and frequency. Another practical effect of disk-based recording is that recording data rates are increasing (up to 1 Gb/s with the Mark 5 system), hence improving signal-to-noise-ratios. In the longer term, the introduction of modern digital video converters, replacing the present Mark IV analog video converters, will make it possible even higher data rates. According to [13], there is reasonable hope that a recording rate of 4 Gb/s be available by 2010. The astrometric consequence of such improved sensitivities will be examined in Sect. 3 below.

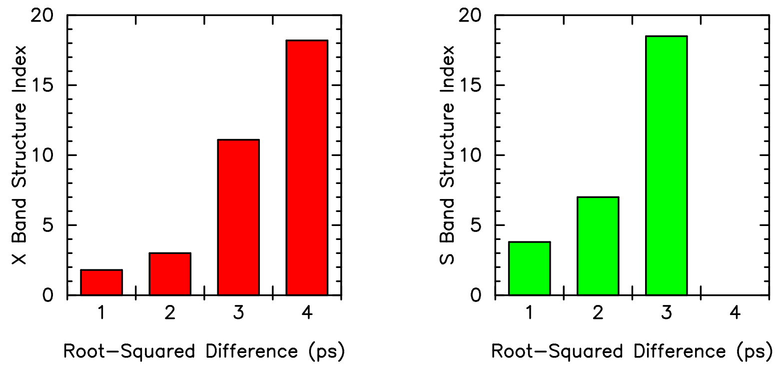

Figure 2. Delay residual improvements upon introducing source maps to model the structure delays. The improvement is given as a function of the structure index at 8 GHz (left panel) and 2 GHz (right panel). See [15] for further details on this analysis.

2.3. Source Structure

Various imaging programs have shown that extragalactic radio sources are generally not point-like on VLBI scales [6, 7]. While having a very compact core, they also often display extended jet emission and thus do not make perfect fiducial targets for building a reference frame. Source structure and changes in source structure put a floor on the stability of estimated source positions using VLBI astrometric data. A useful indicator of source quality is the "Structure Index" introduced in [6]. Values of the structure index range from 1 to 4 with increasing values indicating increasing average structural VLBI group-delay corrections on an approximately logarithmic scale. The current structure index distribution, available for 450 ICRF sources, shows that 57% of the sources for which a structure index is available, have a value of either 1 or 2 at the standard 8 GHz geodetic observing frequency, indicating compact or very compact structures for these sources, while the rest of the sources, with a value of either 3 or 4, show more extended structures [7, 14].

The impact of source structure effects on astrometric VLBI results has been tested on massive scales with a data set including 155 sources and a total of 800 maps to correct for such effects in multi-epoch observations [15]. Figure 2 shows the delay residual improvement as a function of structure index, indicating larger improvements for increased values of the structure index. These range from a few picoseconds (ps) for structure index 1 values to about 20 ps for structure index 4 values. Overall, the weighted rms delay residuals were found to decrease by 8 ps in quadrature upon introducing source maps to model the structure delays. The angular equivalent of this improvement is approximately 100 μas for typical VLBI baselines and amounts to a significant fraction of the 250 μas systematic error of the ICRF, thus confirming that source structure does affect VLBI analysis even though it is not currently the dominant error.

Such modeling, however, is very labor-intensive because of the many sources to be mapped at many epochs due to unpredictable evolution of source structure. An alternate approach, which would limit structural VLBI delay effects, would be to select only the most compact sources for the realization of the celestial frame. Structure index studies show that the more extended sources do have larger position uncertainties and are less positionally stable than the more compact sources [7]. The selection of targets could also be based on analyses of source position stability, as proposed in [16]. Interestingly, the vast majority (92%) of the 199 ICRF sources identified as stable in [16] have a value of the structure index of either 1 or 2, indicating compact or very compact structures.

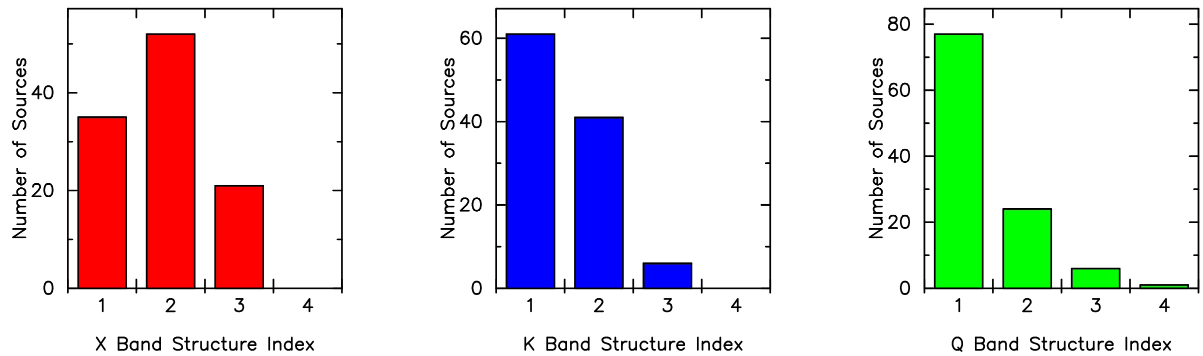

Figure 3. The structure index distribution at 8 GHz (X band), 24 GHz (K band) and 43 GHz (Q band) for 108 ICRF sources.

Such studies also revealed that the ICRF-defining sources are not as good as could be hoped for defining the celestial frame with the highest accuracy [7, 16]. This suggests that revision of source categories would be mandatory upon realization of a new ICRF.

Another approach to reduce structural VLBI effects would be to observe at higher radio frequencies. On average, active galactic nuclei are expected to be more compact at higher frequencies since extended jet emission has a steep spectrum and thus usually weakens (as regard to the core brightness) as observing frequency increases. Regular VLBI astrometric and imaging observations at 24 GHz and 43 GHz have been conducted since May 2002 to investigate this possibility [17, 18]. As shown in Fig. 3, the comparison of the structure index distribution at 8 GHz, 24 GHz, and 43 GHz for the first 108 sources observed in this survey is striking, indicating a larger proportion of structure index values of 1 as observing frequency increases (32% at 8 GHz, 56% at 24 GHz, and 71% at 43 GHz). Hence, these initial results already suggest that the sources make significantly better fiducial targets at 24 GHz and 43 GHz than at the standard 8 GHz observing frequency.

3. Increasing the ICRF Source Density

The current ICRF with a total of 717 sources has an average of one source per $8^\circ \times 8^\circ$ on the sky (Fig. 1). While this density is sufficient for geodetic purposes, it is clearly too sparse for differential-VLBI astrometric applications (phase-referencing of weak targets, spacecraft navigation), which require reference calibrators within a-few-degree angular separation. Additionally, the frame suffers from inhomogeneous distribution of the sources. For example, the angular separation to the nearest ICRF source for any randomly-selected location is up to 13° in the northern sky and 15° in the southern sky [19]. Another deficiency of the frame is the deficit of defining sources in the south and their less-accurate astrometric positions, as a result of the lack of well-established VLBI networks in the southern hemisphere.

The next subsection (3.1) reviews the current ICRF densification programs aimed at correcting these deficiencies. As the celestial frame fills up, increasing further the source density will require observing weaker and weaker targets. The number of sources that could be effectively observed in the future is thus closely connected to the evolution of the sensitivity of VLBI arrays. Future ICRF densification programs should also be devised with a long-term view, keeping in mind the GAIA perspective of an optical frame with 500 000 extragalactic objects in 10–15 years. This perspective raises the question (to be addressed in subsection 3.2 below) of the feasibility of massively increasing the ICRF source density (e.g. by one or two orders of magnitude) on this time scale.

3.1. Current Densification Programs

A specific observational effort is being devoted to the southern sky in order to attempt to correct the existing ICRF deficiency in the south. This effort is accomplished through dedicated astrometric and imaging observations using telescopes of the Australia Telescope National Facility plus other geodetic stations in the southern hemisphere [20]. The goals of this program are to image all southern ICRF sources at least twice for structure monitoring and to search for new astrometric sources for densification of the ICRF in the south. Astrometric positions for 22 new sources and first-epoch images for 69 ICRF sources have just been reported [21, 22]. Ultimately, the astrometric sessions should provide a strong tie between the northern and southern sky through the overlapping common sources at moderate southern declinations whose positions have already been measured with the northern VLBI networks.

In the northern sky, an observing program is currently underway to densify the ICRF using the European VLBI Network and other geodetic antennas [19]. The approach used in this program has been designed to improve the overall source distribution in the ICRF. More specifically, the goal is to add 150 new sources at specific sky locations in order to fill the holes in the current frame. As shown in [19], this extension would reduce the angular separation to the nearest ICRF object from a maximum of 13° to a maximum of 6° for any location in the northern sky, and thus would largely contribute to homogenizing the source distribution. A secondary goal of this project is to identify new sources of high astrometric value which could potentially serve as defining sources in a future realization of the ICRF. This was accomplished by filtering out the potential targets using images from the VLBA Calibrator Survey (see below) in order to select only sources with no or limited extended structure for these observations.

The basis for current ICRF densification programs is the Very Long Baseline Array (VLBA) Calibrator Survey (VCS1). This survey reports previously-unmeasured VLBI astrometric positions for 1332 sources between −30° and +90° declination along with survey VLBI images at 2 GHz and 8 GHz for most of these sources [23]. This is the largest high-resolution radio survey ever undertaken and it triples the number of sources available for VLBI applications. The VCS2 extension reports positions for an additional 276 sources, most of which are in the declination range −20° to −45° and near the galactic plane [24]. Although not acquired in standard geodetic VLBI mode, these data may be useful for future ICRF extensions. Evaluation of the astrometric suitability of the VCS1 and VCS2 sources based on the available survey images would also be worthwhile to identify the most promising candidates for future inclusion in the ICRF.

3.2. How Many Sources in the ICRF by 2010?

As stated above, increasing further the ICRF source density will closely depend on how fast the sensitivity of VLBI arrays improves in the future. Disk-based recording with the Mark 5 system now permits data rates up to 1 Gb/s, a gain by a factor of 4 as compared to the standard 256 Mb/s data rate used so far on geodetic networks. A gain by an additional factor of two will be possible when Mark 5B units are available (two of these used in parallel will support up to 2 Gb/s), while the introduction of modern digital video converters opens up hope for recording data rates up to 4–8 Gb/s on the longer term. New large antennas that are being built, e.g. in Spain (40 m

Table 1. Present and future sensitivity of the baselines Algonquin–Medicina and Algonquin–Effelsberg. The sensitivity (in mJy) is given as a function of data rate and integration time for a signal-to-noise ratio of 20.

Epoch	Data rate	Algonquin–Medicina			Algonquin–Effelsberg		
	(Gb/s)	10 sec	60 sec	240 sec	10 sec	60 sec	240 sec
2004	1	140	60	30	36	14	7
2006	2	100	40	20	25	10	5
2010	4	70	30	15	18	7	3.5

telescope in Yebes to be inaugurated later this year), Italy (64 m telescope in Sardinia planned for 2006), or China (50 m telescope in Miyun and 40 m in Kunming planned for 2006) will also directly contribute to improving the sensitivity of VLBI arrays in the near future.

Table 1 compares the baseline sensitivity for recording data rates of 1 Gb/s (possible now), 2 Gb/s (likely available by 2006), and 4 Gb/s (foreseen by 2010). The sensitivity is given as a function of integration time (10 sec, 60 sec, and 240 sec) for the "standard" baseline Algonquin–Medicina and the highly-sensitive baseline Algonquin–Effelsberg. The results in Table 1 indicates that most ICRF sources should be detectable with 10-second long observations on standard baselines since the vast majority of these sources are stronger than 100 mJy. Use of such short scans will considerably increase the number of observations per day, hence permitting the monitoring of a larger portion of the frame within each session. Longer integration times will permit detection of sources as weak as 15 mJy on standard baselines, while inclusion of big antennas (e.g. Effelsberg) in the array will bring the detection threshold down to a few mJy.

This expected enhancement in sensitivity raises the question of how many of such weak sources do exist over the entire sky and whether they are compact enough for detection by VLBI arrays. Some insights into this questioning have recently been obtained from VLBI test experiments using the ultra-sensitive baseline Arecibo-Effelsberg [25]. The aim of these experiments was to explore the source compactness on a statistical basis by observing a sample of 1000 weak sources (> 1 mJy) randomly-selected from the FIRST survey[2]. Each source was observed for 1 minute at a recording data rate of 512 Mb/s, which provides a 7σ detection threshold of about 1 mJy at 21 cm wavelength. Preliminary results based on a subset of the data show that roughly 20% of the targets have been detected [25], hence indicating the portion of the sources that are potentially useful for building a dense and precise reference frame at this sensitivity level.

The total number of radio sources for a given flux threshold may be derived from the NRAO VLA Sky Survey [26]. This catalog contains 2 million radio sources, of which 50 000 are stronger than 50 mJy at 1.4 GHz, approximately equivalent to 15 mJy at 8 GHz, the expected threshold to be reached by 2010 (Table 1). As noted above, if 20% of these have at least one compact component on VLBI scales, this implies that 10 000 sources should be detectable with standard VLBI arrays by that time. Assuming 250–500 sources may be observed per 24 hours, a reasonable assumption if using large VLBI arrays, the observing load represents a total of 20–40 experiments, equivalent to observing once per month during 2–4 years. This observing load is only twice that of the current bi-monthly Research & Development VLBA program (RDV) and thus is not unrealistic.

[2]The FIRST Survey is available at http://sundog.stsci.edu/

4. Proposed Plan and Timeframe

4.1. Build ICRF–2 (2004–2006)

The ICRF has accomplished its primary goal of providing an accurate and stable celestial reference frame conceptually independent of the motion of the Earth in space. However, it was recognized from the beginning that there were several intrinsic deficiencies in its realization, in particular the uneven distribution of defining sources and the weakness of the criteria for selecting these sources. Since the inception of the ICRF in 1995, a wealth of VLBI data (including those from the highly-accurate RDV experiments) has been acquired, modeling has been refined (e.g. for troposphere propagation effects), and improved criteria based on source structure and position stability have been devised to categorize the sources. With such additional data and analysis improvements, the source position error floor is now most probably at the 100 μas level or below [27], a significant gain as compared to the 250 μas systematic error of the ICRF. For this reason, I feel that it is now time to initiate a new realization of the celestial frame. Targeting the completion of this second realization, ICRF–2, by 2006 sounds like a reasonable objective.

4.2. Initiate a Massive Survey (2006–2010)

The next step I see once ICRF–2 is done is a massive increase in source density. As noted above, observing 10 000 sources will be feasible on a time scale of a few years when data rates of a few Gb/s are available. For higher efficiency, large networks of 15–20 telescopes should be used so that both imaging and astrometry could be carried out simultaneously (as currently done with the RDV experiments). Inclusion of sensitive telescopes (40–50 m class antennas) would also be desirable to pick up the weakest sources. Such a survey may be handled jointly with the astrophysical community which is considering similar surveys for studies of radio source population and cosmology. More generally, obtaining a large set of accurate radio positions would be invaluable for comparison with the future GAIA optical positions, not only for astrometric purposes but also for astrophysical goals. Pinpointing the relative positions of the optical and radio counterparts in active galactic nuclei is indeed especially useful for investigating emission processes in these objects. This massive survey is a long-term work with sustained observations over several years, therefore it should start as soon as the required sensitivity is available so that results could be obtained by the end of this decade or soon after, prior to the realization of the GAIA frame.

4.3. Get Involved in SKA (Beyond 2010)

On the longer term, the astrometric VLBI community should keep a close eye on the development of future radio instruments such as the Square Kilometer Array (SKA)[3]. This instrument, envisioned by 2015–2020, would have one square-kilometer collecting area (equivalent to 100 times that of the Effelsberg telescope), making the nanoJy sky accessible to radio observations. While the general SKA concept is agreed, there are many different designs still competing at this point. Will the collecting area consist of big antennas (e.g. 100 "Effelsberg" telescopes) or smaller antennas (e.g. 10 000 telescopes with a diameter of 10 m)? Will this instrument observe only at low frequencies or will the frequency coverage go up to 22 GHz? Will the baselines be limited to a few hundred kilometers or be intercontinental? High frequencies and long baselines would be of most

[3] See http://www.skatelescope.org/

interest for building a future accurate and ultra-dense celestial frame down to the nanoJy level. Multi-beaming, a specific SKA feature considered for observing up to 100 sources simultaneously, is also highly interesting as it would permit the construction of a celestial frame free of terrestrial frame and Earth orientation errors by using measurements of the arc length between sources [28].

Overall, I feel the geodetic, astrometric but also astrophysical VLBI communities should express their views as regard to the design of the SKA instrument and should especially push towards higher-frequency and longer-baseline capabilities. A SKA-VLBI workshop[4] held in Bonn in 2001 could serve as a basis for future detailed studies and proposals regarding these issues. On the astrometric side, SKA is the only radio instrument that may be able to compete with GAIA for the realization of the celestial reference frame. Therefore, it is important that the astrometric VLBI community get involved in SKA if the decision to build this instrument is taken.

5. Acknowledgements

I am indebted to Chris Jacobs for many useful discussions regarding VLBI modeling and instrumentation, to Richard Porcas for providing VLBI results prior to publication, and to Simon Garrington for providing e-MERLIN information.

References

[1] Ma, C., E. F. Arias, T. M. Eubanks, A. L. Fey, A.-M. Gontier, C. S. Jacobs, O. J. Sovers, B. A. Archinal, P. Charlot, The International Celestial Reference Frame as Realized by Very Long Baseline Interferometry, AJ, 116, 516–546, 1998.

[2] Fey, A. L., C. Ma, E. F. Arias, P. Charlot, M. Feissel-Vernier, A.-M. Gontier, C. S. Jacobs, J. Li, D. S. MacMillan, The Second Extension of the International Celestial Reference Frame. ICRF-Ext.2, AJ (in press), 2004.

[3] Garrington, S. T., private communication, 2004.

[4] Perryman, M. A. C., GAIA: An Introduction to the Project, In: GAIA: A European Space Project, O. Bienaymé and C. Turon (eds.), EAS Publication Series, Vol. 2, 3–26, 2002.

[5] Mignard, F., Observations of QSOs and Reference Frame with GAIA, In: GAIA: A European Space Project, O. Bienaymé and C. Turon (eds.), EAS Publication Series, Vol. 2, 327–339, 2002.

[6] Fey, A. L., P. Charlot, VLBA Observations of Radio Reference Frame Sources. II. Astrometric Suitability Based on Observed Structure, ApJS, 111, 95–142, 1997.

[7] Fey, A. L., P. Charlot, VLBA Observations of Radio Reference Frame Sources. III. Astrometric Suitability of an Additional 225 Sources, ApJS, 128, 17–83, 2000.

[8] Jacobs, C. S., O. J. Sovers, C. J. Naudet, R. F. Coker, R. P. Branson, The JPL Extragalactic Radio Reference Frame: Astrometric Results of 1978–96 Deep Space Network VLBI, TMO Progress Report 42-133, 1–55, 1998.

[9] MacMillan, D. S., C. Ma, Atmospheric Gradients and the VLBI Terrestrial and Celestial Reference Frames, Geophys. Res. Lett., 24, 453–456, 1997.

[10] Niell, A. E., J. Tang, Gradient Mapping Functions for VLBI and GPS, In: IVS 2002 General Meeting Proceedings, N. R. Vandenberg and K. D. Baver (eds.), NASA/CP-2002-210002, 215–218, 2002.

[4]See http://www.euska.org/workshops/hr_ws_MPIfR_Bonn.html.

[11] Naudet, C. J., S. Keihm, G. Lanyi, R. Linfield, G. Resch, L. Riley, H. Rosenberger, A. Tanner, Media Calibration in the Deep Space Network - A Status Report, In: IVS 2002 General Meeting Proceedings, N. R. Vandenberg and K. D. Baver (eds.), NASA/CP-2002-210002, 194–198, 2002.

[12] Prestage, J. D., R. L. Tjoelker, L. Maleki, Mercury-Ion Clock Based on a Linear Multi-Pole Ion Trap, TMO Progress Report 42-143, 1–8, 2000.

[13] Whitney, A. R., private communication, 2004.

[14] Charlot, P., Extended Emission Structure in Extragalactic Sources, In: IAU XXV General Assembly, Joint Discussion 16: The International Celestial Reference System, Maintenance and Future Realizations, R. Gaume, D. D. McCarthy and J. Souchay (eds.) (in press), 2004.

[15] Sovers, O. J., P. Charlot, A. L. Fey, D. Gordon, Source Structure in Astrometric VLBI: A Large-Scale Test, In: The Interplanetary Network Progress Report (in preparation), 2004.

[16] Feissel-Vernier, M., Selecting stable extragalactic compact radio sources from the permanent astrogeodetic VLBI program, A&A, 403, 105–110, 2003.

[17] Jacobs, C. S., P. Charlot, E. B. Fomalont, D. Gordon, G. E. Lanyi, C. Ma, C. J. Naudet, O. J. Sovers, L. D. Zhang, and the K–Q VLBI Survey Collaboration, Extending the ICRF to Higher Radio Frequencies: 24 and 43 GHz Astrometry, these Proceedings, 2004.

[18] Boboltz, D. A., A. L. Fey, P. Charlot, E. B. Fomalont, G. E. Lanyi, L. D. Zhang, and the K–Q VLBI Survey Collaboration, Extending the ICRF to Higher Radio Frequencies – Imaging and Source Structure, these Proceedings, 2004.

[19] Charlot, P., B. Viateau, A. Baudry, C. Ma, A. L. Fey, T. M. Eubanks, C. S. Jacobs, O. J. Sovers, A Proposed Astrometric Observing Program for Densifying the ICRF in the Northern Hemisphere, In: IVS 2000 General Meeting Proceedings, N. R. Vandenberg and K. D. Baver (eds.), NASA/CP-2000-209893, 168–172, 2000.

[20] Fey, A. L., K. J. Johnston, D. L. Jauncey, J. E. Reynolds, A. K. Tzioumis, J. E. J. Lovell, P. M. McCulloch, M. E. Costa, S. P. Ellingsen, G. D. Nicolson, A Southern Hemisphere Observing Program to Strenghen the ICRF, In: IVS 2000 General Meeting Proceedings, N. R. Vandenberg and K. D. Baver (eds.), NASA/CP-2000-209893, 164–167, 2000.

[21] Fey, A. L., R. Ojha, D. L. Jauncey, K. J. Johnston, J. E. Reynolds, J. E. J. Lovell, A. K. Tzioumis, J. F. H. Quick, G. D. Nicolson, S. P. Ellingsen, P. M. McCulloch, Y. Koyama, Accurate Astrometry of 22 Southern Hemisphere Radio Sources, AJ, 127, 1791–1795, 2004.

[22] Ojha, R., A. L. Fey, K. J. Johnston, D. L. Jauncey, J. E. Reynolds, A. K. Tzioumis, J. F. H. Quick, G. D. Nicolson, S. P. Ellingsen, R. G. Dodson, P. M. McCulloch, VLBI Observations of Southern Hemisphere ICRF Sources – I, AJ (in press), 2004.

[23] Beasley, A. J., D. Gordon, A. B. Peck, L. Petrov, D. S. MacMillan, E. B. Fomalont, C. Ma, The VLBA Calibrator Survey – VCS1, ApJS, 141, 13–21, 2002.

[24] Fomalont, E. B., L. Petrov, D. S. MacMillan, D. Gordon, C. Ma, The Second VLBA Calibrator Survey: VCS2, AJ, 126, 2562–2566, 2003.

[25] Porcas, R., private communication, 2004.

[26] Condon, J. J., W. D. Cotton, E. W. Greisen, Q. F. Yin, R. A. Perley, G. B. Taylor, J. J. Broderick, The NRAO VLA Sky Survey, AJ, 115, 1693–1716, 1998.

[27] Jacobs, C. S. private communication, 2003.

[28] Arias, E. F., M. S. De Biasi, A New Method of Analysis and Reduction of VLBI Observations, In: Radio Interferometry: Theory, Techniques and Applications, IAU Colloquium 131, T. J. Cornwell and R. A. Perley (eds.), ASP Conference Series, Vol. 19, 317–320, 1991.

Martine Feissel-Vernier et al.: VLBI and Earth Rotation: Geophysical and Geodetic Challenges, IVS 2004 General Meeting Proceedings, p.22–31
http://ivscc.gsfc.nasa.gov/publications/gm2004/feissel

VLBI and Earth Rotation: Geophysical and Geodetic Challenges

Martine Feissel-Vernier [1], Jim Ray [2], Zuheir Altamimi [3], Véronique Dehant [4], Olivier de Viron [4]

[1] *Institut Géographique National/LAREG and Observatoire de Paris/SYRTE*
[2] *National Geodetic Survey and Bureau International des Poids et Mesures*
[3] *Institut Géographique National/LAREG*
[4] *Royal Observatory of Belgium*

Contact author: Martine Feissel-Vernier, e-mail: `feissel@ensg.ign.fr`

Abstract

We examine some current limitations in the interpretation of VLBI Earth rotation measurements due to factors inherent in existing observing programs and we propose directions for possible future improvements to enhance the contributions to geophysics.

1. The Roles of Earth Rotation Observations

We distinguish two roles for observations of the Earth's rotation (referred to in terms of Earth orientation parameters or EOPs): 1) to relate the terrestrial (rotating) and the celestial (inertial) reference frames; 2) for the study of signatures of the Earth's structure and dynamics. There are many applications (e.g., satellite tracking) that depend on accurate knowledge of the relationship between the terrestrial and celestial frames. VLBI contributes uniquely in this regard by providing direct measurements of Universal time (UT1) and precession-nutation; satellite-based techniques cannot provide comparably unbiased information.

The topics of interest here are both roles; i.e., providing geophysical insights as well as high-accuracy unification of reference frames. Space geodetic techniques contribute information both unique and complementary to that obtained from independent geophysical methods. The global scope, sub-ppb (parts-per-billion) sensitivity, accuracy, and stability are especially important, and, again, the VLBI ability to observe unbiased UT1 and nutation is critical.

1.1. Signal Spectrum

We consider the Earth rotation signal spectrum in three broad regimes. Tidal signals are strictly periodic, driven by the gravitational forcings of the sun, moon, and planets. Because the forcing properties are very well known, the unknown characteristics of the Earth can be inferred from the observed tidal responses limited only by the geophysical inversion itself and in some cases by overlying non-tidal signals. A weakness of tidal studies is that the Earth response can only be examined at discrete frequencies, corresponding primarily to periods near 12 h, 24 h, fortnightly, monthly, semiannual, annual, and some longer.

Non-tidal, quasi-periodic signals arise either from some feeback process operating on a recurring cycle (e.g., el Niño) or as an amplification of broadband geophysical "noise" near some natural resonant frequency (e.g., Chandler wobble). These phenomena provide an opportunity to explore the Earth's response over wider bandwidths but their interpretation is usually complicated by uncertainties in the underlying excitations as well as in the geophysical inversion.

The third spectral category is the background continuum. Geophysical processes normally generate "red" power-law variations (apart from the tidal and quasi-periodic signals already mentioned), with the largest power being in the longest temporal and spatial scales. These signals are usually the most challenging to understand because so many different factors can be entangled. The observed power level at any given frequency, which should be useful, is often difficult to evaluate accurately because the measurement and analysis processes can be sensitive to subtle or unintended filtering.

For a detailed discussion of Earth orientation excitation, please refer also to the review by B. Chao (this volume).

2. VLBI EOP Measurements Today – The Radio Sources

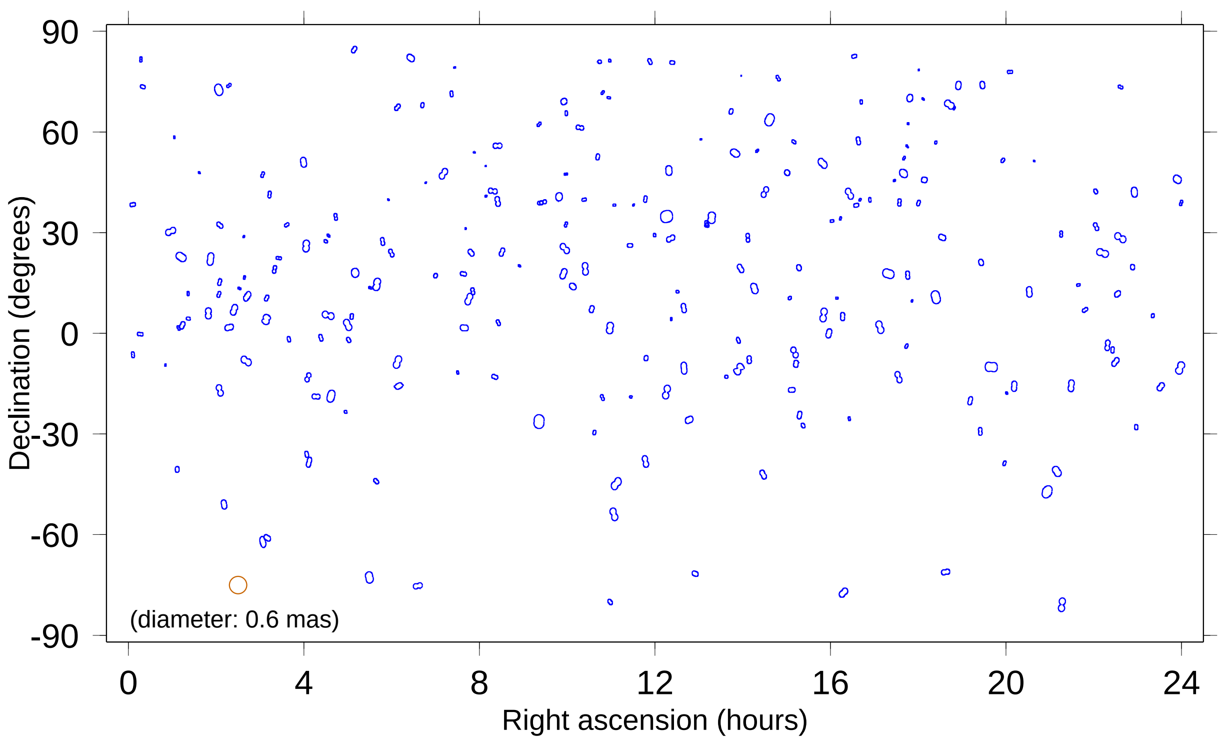

Figure 1. Map of 245 well-observed radio sources (1989.5-2002.4) with one-year standard deviations smaller than 0.35 mas. Envelopes show the standard deviation of the yearly average coordinates in local equatorial frames ($\alpha \cos \delta$, δ).

The celestial reference frame is materialized by a set of quasars and galactic nuclei that are compact when observed at X-band (4 cm) and S-band (13 cm) with terrestrial baselines. However, at the current level of sub-milliarcsecond (mas) precision, no object is really pointlike. Most of the known quasar activity takes the form of jets; i.e., aligned emissive structures that cause an apparent motion of the observed brightness center. While the background source structure is assumed to stay fixed, oscillations may exist in the observed direction as well as apparent drift rate which are unlikely to continue indefinitely; the temporal characteristics are not well known. In principle, it is possible to accurately correct this effect if repeated maps are available (P. Charlot, this volume). However, such source structure corrections are not implemented in existing astrogeodetic analysis software. As a result, most objects exhibit time variations of their position in some preferred direction. This is illustrated in Figure 1, which shows the envelopes of the standard deviation of yearly weighted average source positions in local equatorial frames for the most stable sources. The deficiency of sources south of declination -30^o is an effect of their relatively sparse observation history due the biased network distribution (§3).

2.1. Effects of Source Instability

Studying the influence on nutation of the variable torque exerted by the atmosphere and the ocean, Dehant et al. [3] showed that apparent variability in the celestial frame can lead to changes in estimates of precession or long-period nutation coefficients at a level comparable to that of the variable nutation excited by the Earth's fluid layers (a few tens of μas). Figure 2 shows an example of the sensitivity of the estimates of the precession constant, the obliquity rate, and the 18.6-year nutation term to source selection. While the common practice to estimate these terms is to use observations of all sources, the figure shows that, depending on the set of radio sources considered in the analysis, the precession and obliquity rates may change by 20 μas/year and the 18.6-year prograde component by 30 μas.

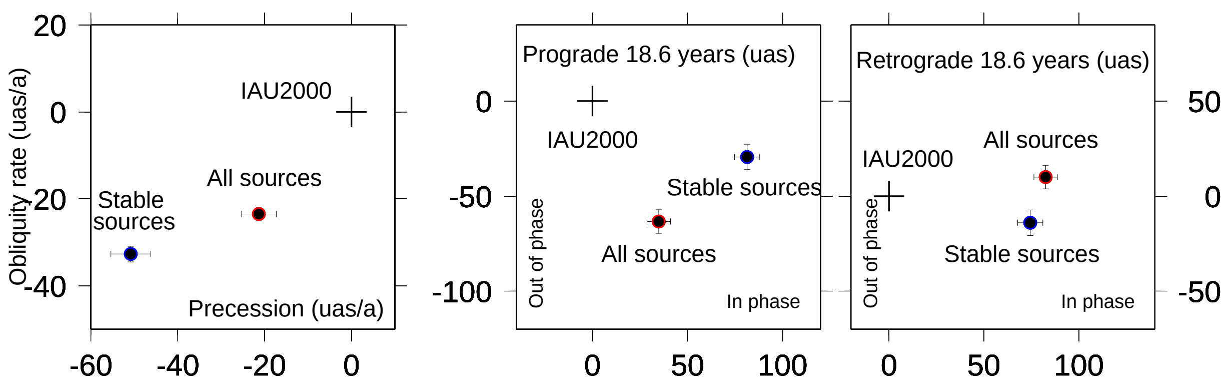

Figure 2. Corrections to IAU2000 precession-nutation components using all sources or selected stable sources.

The stable sources mentioned in Figure 2 result from a selection scheme proposed by Feissel-Vernier [5]. As shown by M. Feissel-Vernier (this volume), this source selection agrees only partially with the quality criteria for the original ICRF (Ma et al. [6]) that made use of qualitative and quantitative factors such as apparent drift, formal uncertainty of the global coordinates over 1980-1995, and source structure index. It is expected that replacing the ICRF defining sources by the stable ones for constraining the axes of a future ICRS realization would improve its long-term stability by nearly a factor of five (6 μas vs 29 μas).

The Free Inner Core Nutation (FICN) is a prograde free oscillation with an expected period between 930 and 1140 days according to the IAU2000 model (Mathews et al. [8]). The search for the FICN provides an opportunity to test the detectability of weak variable oscillations by VLBI in the interannual frequency band. V. Dehant et al. (this volume) studied the residuals between the observed nutation and the adopted IAU2000 nutation model. By considering the proposed stable sources selection, they found residuals more physically meaningful. They observed in the period 1990-1995 a large peak around 870 days, which is close to the FICN frequency as expected from the forced nutation [8]. Unfortunately, the theoretical estimation of a random noise excitation of the FICN by the ocean and the atmosphere is expected to be much smaller, below 1 mas. It is always possible, but not likely, that an harmonic excitation of the ocean and/or atmosphere would excite the FICN exactly at that time. But contamination by source instability must be considered. While VLBI estimates suggest a potential candidate for the detection of the FICN with an amplitude 37 ± 10 μas, when considering the stable sources the spurious celestial pole motion resulting from random apparent motions of the sources amounts to 20 ± 13 μas (M. Feissel-Vernier et al., in preparation). They therefore concluded that the prograde oscillation that appears in various VLBI spectra is probably an artifact due to radio source instabilities, although effects related to VLBI network variations could also play some role (see next section).

3. VLBI EOP Measurements Today – The Antenna Network

3.1. The Antenna Network

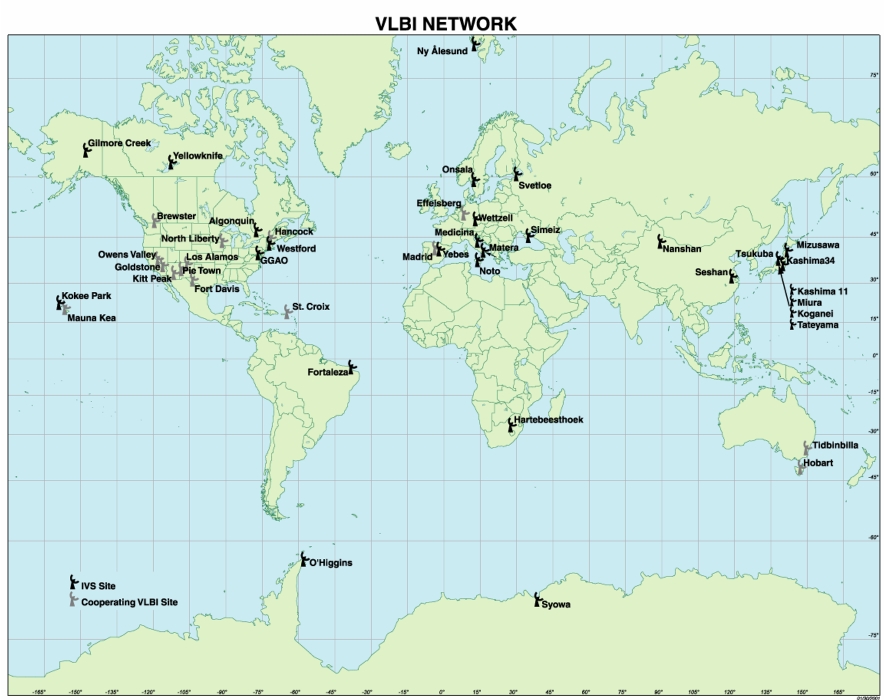

Figure 3. Geodetic VLBI network.

As seen in Figure 3, the most striking feature of the VLBI antenna network is its non-uniformity. Only a handful of stations are located in the southern hemisphere. The network is essentially two continental subnetworks (N. America and Europe) with a few stations scattered elsewhere. For measurements of global quantities, such as EOPs and the terrestrial frame, this can seriously limit performance. On account of the weak geometrical coverage of the Earth's surface, correlations among EOP estimates and among Helmert network parameters can often exceed 0.5. For instance, the weekly IVS R4 network normally has a correlation coefficient between polar motion X and UT1 of about -0.6.

3.2. Network Effects on EOP Measurements

We show three examples of the impact of network distribution on the consistency of the EOP results. The first concerns the weekly operation of the IVS R1 and R4 24-hour EOP sessions, each using different networks. They have run since 2002 on Mondays and Thursdays, respectively, and each includes five to seven stations. Three stations are common: Gilcreek, Wettzell and Conception. Table 1 gives estimates of the differences between the two EOP series, taking into account the Earth rotation changes during the three to four days between them. The magnitude of the differences is equivalent to 3 to 5 mm on the Earth's surface, probably reflecting station coordinate inconsistencies at a similar level.

Table 1. EOP differences between R1 & R4 sessions (2002.0-2003.8)

Parameter	Bias	Wrms residual
Nutation		
$d\psi \sin(\epsilon)$	-1 μas	114 μas
$d\epsilon$	2 μas	105 μas
Polar motion		
X	57 μas	132 μas
Y	-20 μas	110 μas
Orientation		
UT1	1.9 μs	9.6 μs

The next example is based on two different combinations of unconstrained session solutions for station coordinates and EOPs together with the full covariance matrices (SINEX files). The global combination of these parameters in a unique terrestrial reference frame is done using the CATREF (Combination and Analysis of Terrestrial REference Frames) software (Altamimi et al. [1]). The datum definition attaches the results to ITRF2000 using a subset of stations that are judged reliable over the data span. Two combination strategies were compared: 1) a global analysis over 1990-2003, using an appropriate set of long-term reliable stations for the datum definition; 2) yearly analyses, with different suitable sets of datum stations for each year. The EOP differences derived from the two approaches are plotted in Figure 4 in the form of yearly weighted averages. The annual averages of the rotation angle A3 of yearly celestial reference frames from a similar computation [5] are also included in the figure, as errors in UT1 may result from either terrestrial or celestial frame axial instabilities. The year-to-year EOP changes, which increase after 1996, are significant with respect to their internal consistencies, reaching the few-mm level for rotation on the Earth's surface. The effects presumably reflect mostly inconsistencies with the VLBI terrestrial frame and weaknesses in the longer-term interconnection of the network.

The third example is also based on a rigorous combination of terrestrial frames and EOPs except that it includes both VLBI and GPS results over 1999-2003. The VLBI data are a subset of above while the GPS data are unconstrained SINEX files from the IGS containing weekly station coordinates and daily pole coordinates. The combination using CATREF included a weighting of the inputs according to their respective scatters. The datum definition uses a set of 23 sites with co-located VLBI and GPS stations and reliable local ties. The post-fit polar motion residuals are plotted in Figure 5 and the weighted RMS residuals are, for the X and Y components respectively:

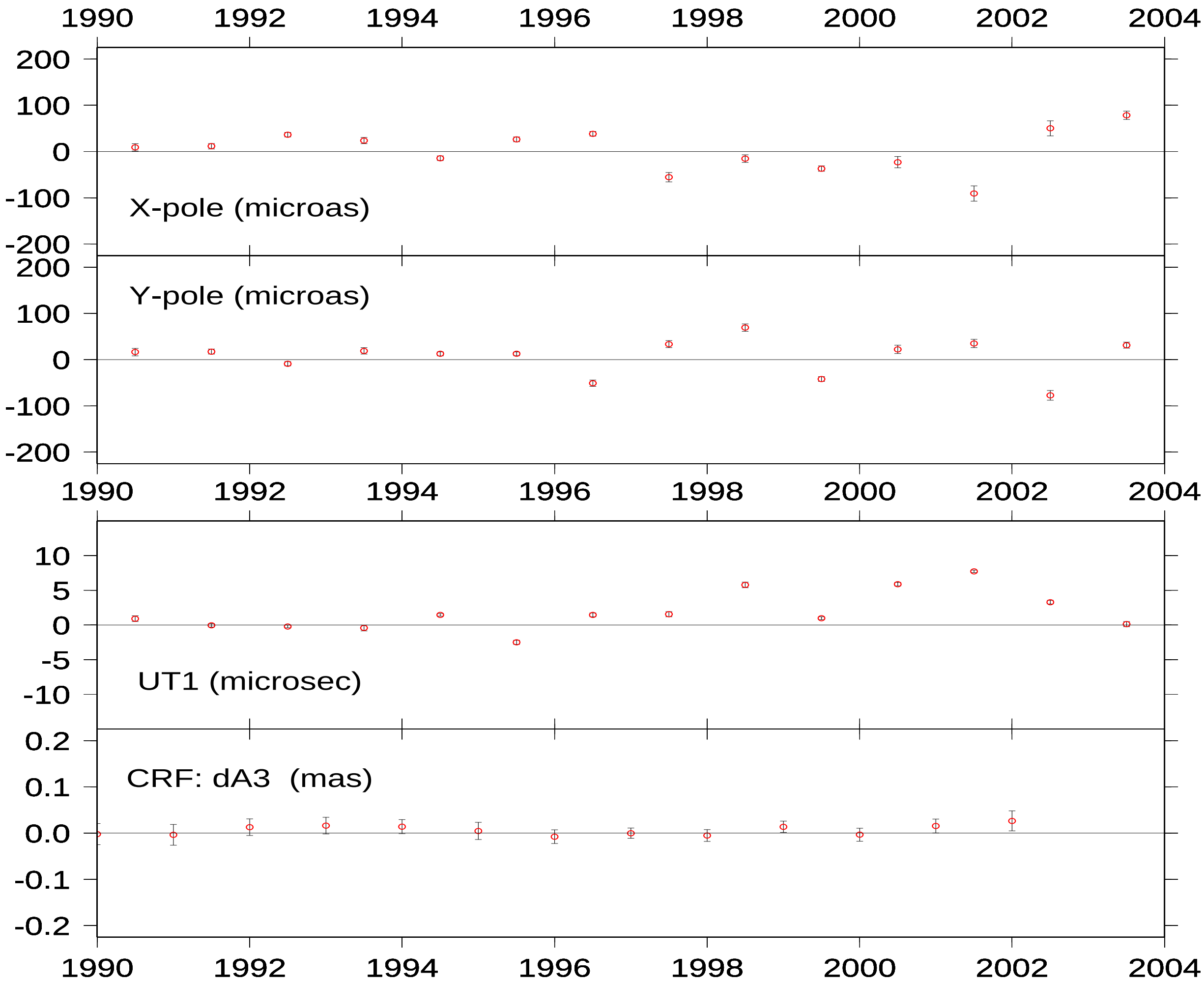

Figure 4. Yearly average EOP differences between solutions with the ITRF2000 tie performed separately each year and globally over 1990-2003. Similar variations of the axial rotation of yearly celestial reference frames are shown in the bottom panel. Note that all four plots have the same scale.

124 and 101 μas per VLBI session; 40 and 55 μas per day for GPS. The VLBI session scatters are equivalent to 3 to 4 mm on the Earth's surface, two to three times larger than for GPS. A difference in drift is also evident for the Y component, most likely due to discrepancies in the respective reference frames. One may question the precise source of the VLBI random noise and the extent to which terrestrial frame inconsistencies may be responsible versus other causes.

We conclude from the above tests that the effects of terrestrial frame inconsistencies on VLBI EOP measurements are equivalent to a few mm of surface rotation for individual sessions, and around 1 to 2 mm in the longer term. Further efforts in the direction of inter-technique combination and co-location, as well as in network stability studies generally, are necessary to improve the precision and accuracy of current EOP determinations.

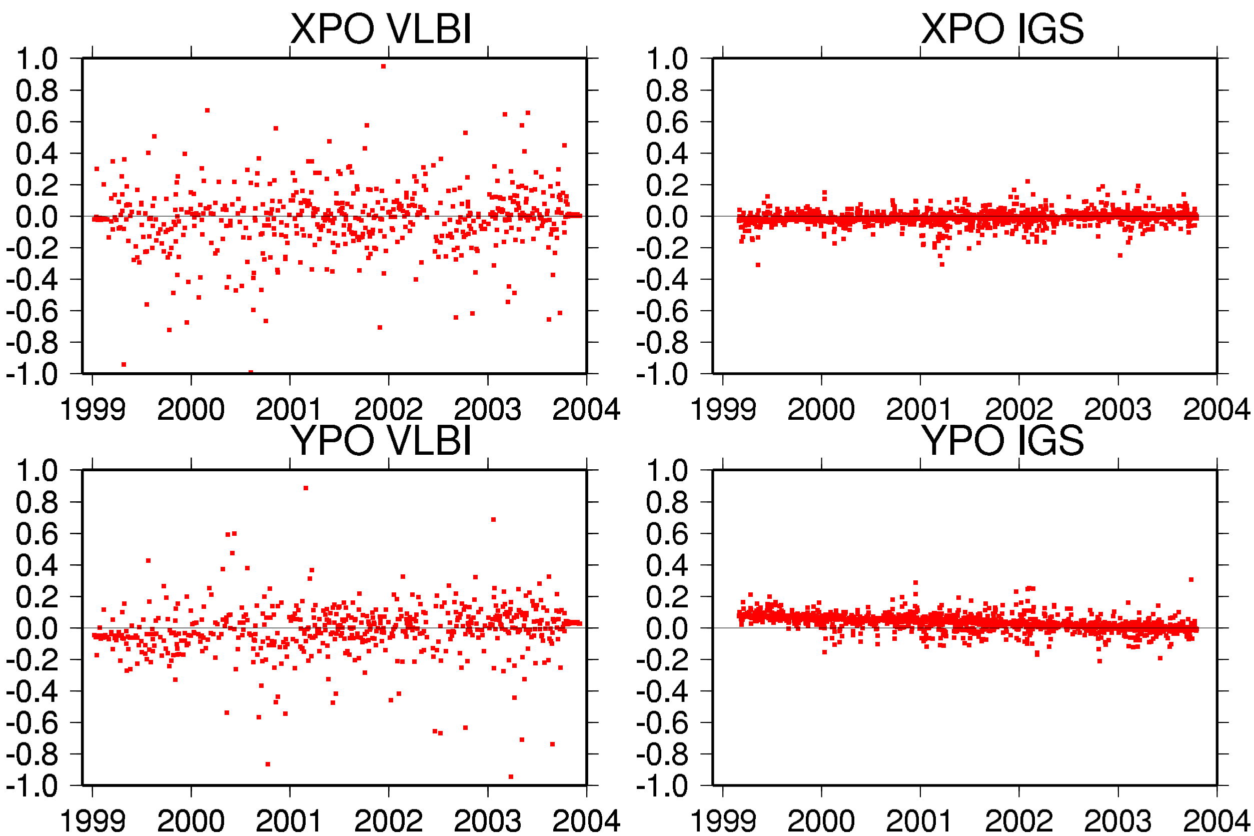

Figure 5. Post-fit polar motion residuals from a joint combination of VLBI and GPS solutions.

4. Geophysical Challenges in the Next Decade

4.1. Long-Term Changes in LOD and UT1

At long time scales, LOD variations are attributed to the interaction between the Earth's core and the mantle. Consequently they are supposed to be correlated with the core angular momentum (CAM). The dynamics inside the fluid core are presently not very well known, though, and LOD is the best proxy available for the long-term core angular momentum. Independent CAM series are also computed from magneto-hydrodynamics considerations, under strong hypotheses, and their success can be tested against the LOD variations (Van Hoolst et al. [9]). In that sense, monitoring LOD variations is very important for the future development of models for core dynamics.

In the last two years, the analysis of J_2 variations from Satellite Laser Ranging (SLR) data (Cox et al. [2]) has generated large interest from both the geodetic and geophysics communities. The study of this time series is very important as it reflects the global scale mass variations in the Earth system and is a big challenge for our understanding of the geophysical fluids (Dickey et al. [4]). Computing J_2 variations from SLR data necessitates an a priori knowledge of UT1 variations that is not currently possible without VLBI.

4.2. Inner Core Signature in Polar Motion

Theoretical studies (Mathews et al. [7]) predict the existence of a rotational normal mode in polar motion related to the presence of a solid inner core within the outer liquid core: the Inner Core Wobble (ICW). This mode has not been detected yet though its observation would increase strongly our knowledge of the properties of the inner core, in particular the density jump at the inner core boundary and the flattening of the inner core. Its period is predicted to be around 2400 days. Consequently, its observation would require high precision and long-term stability of the VLBI network.

4.3. Nutations

Nutations are mainly excited by the gravitational action of the moon, sun, and planets on the equatorial bulge of the Earth. The Earth responds to that forcing as a complex system and, in particular, the Earth internal structure deeply impacts the amplitudes of the nutations. In addition, the external geophysical fluids (atmosphere and ocean) create additional nutational motion of the Earth, but of smaller amplitudes. In order to interpret the nutation observations in terms of Earth interior parameters, it is important to be able to separate external fluids and interior effects. Depending on the frequency, the relative amplitudes of these effects will be different. For periods close to the Free Core Nutation (FCN) resonance, the Earth interior effect strongly dominates, whereas the atmosphere impact is strong on the prograde annual nutation as it corresponds to one solar day in the terrestrial reference frame. For some other nutation periods, perturbations from both the interior and exterior of the Earth must be considered. From the first category, we can learn about the physics of the Earth interior, and the second category can be used to: (a) constraint the diurnal cycle of the fluid models and (b) determine which atmospheric model is the most relevant for nutation studies. This will allow us to separate atmospheric and interior effects in the case of the third category (both impacting). A consistent set of high-precision VLBI nutation data would immediately increase our knowledge of the Earth interior.

5. Geodetic Challenges in the Next Decade

5.1. Near-term Assumptions

Any attempt to assess future challenges should first try to specify the expected conditions likely to be influential:

- GPS, Galileo, and related satellite navigation systems will continue to provide the widest user access to the ITRF indirectly via precise orbits and directly through dense ground networks.
- While satellite methods already dominate determinations of polar motion, they will probably not improve much in measuring LOD or nutation rates, where only the high-frequency components provide useful geophysical information due to time-varying technique biases.
- Uncertainties in the absolute scale of satellite-based terrestrial reference frames will not be reduced to better than about 1 ppb due to lack of accurate knowledge of the satellite transmit antenna characteristics.
- The global VLBI geodetic network will continue to evolve but is unlikely to grow much. The VLBI observing program will continue to be constrained by costs.

- Optimal user benefits will increasingly require a balanced combination of VLBI and satellite geodetic results.

5.2. Priority Contributions from VLBI

If our assumptions of future trends prevail, the areas of global geodesy that will continue to require substantial VLBI contributions (preferably with improvements) are: 1) maintaining the celestial reference frame; 2) providing the definitive link between the ICRF and ITRF through UT1 and nutation observations; 3) establishing the absolute scale of the ITRF (together with SLR). In all these respects, it is vital to maintain the highest level of long-term stability, especially considering the older observing history of VLBI.

5.3. Goals for the Next Decade

To maximize the utility of VLBI during the coming years, we emphasize these objectives:

- Schedule more fully global VLBI networks as often as feasible. Doing so will strengthen the celestial and terrestrial frames by reducing the presently high internal correlations. Network-dependent biases in other parameters will also be reduced.
- Improve the UT1 accuracy and sampling by expanding and upgrading the current Intensive series. Better use of GPS results should be studied as a way to reduce the effects of polar motion errors.
- Improve the quality of the celestial frame by dynamic monitoring of radio source stability.
- Improve co-location ties with the other techniques, especially GPS and DORIS. This will allow a more robust combination of VLBI results with the satellite techniques and permit inter-technique biases to be identifiable. Doing so requires that the intra-VLBI components of the local ties be accurately modeled (i.e., antenna effects).

6. Summary

VLBI will remain the unique source of our knowledge of the Earth's sidereal rotation (UT1, precession-nutation) for at least one more generation. Some exciting new geophysical challenges facing the technique may remain unmet if further enhancements cannot be implemented, but the present data quality will continue to be needed to interpret aspects of the dynamical Earth system, including information useful for climatology, global change research, and for deep interior studies. To infer new levels of insight and to address the currently unsatisfied challenges will require heightened attention to instabilities in the celestial and terrestrial reference frames, among other concerns.

Until VLBI is operated worldwide and continuously (if ever), developers and analysts are urged to maximize the quality of the CRF and TRF that can be derived from VLBI observations, enhance the use of geodetic information from the satellite techniques (GPS, DORIS, SLR, and in the future Galileo), and actively participate in the IERS multi-technique combination effort. In the current context, VLBI will only attain its fullest potential significance by exploiting the complementary strengths of its competitors, the satellite techniques.

References

[1] Altamimi, Z., P. Sillard and C. Boucher, 2002, JGR 107B, 1, 2002.

[2] Cox, C., B.F. Chao, Detection of large-scale mass redistribution in the terrestrial system since 1998, Science, 297, 831-832, 2002.

[3] Dehant, V., M. Feissel-Vernier, O. de Viron, C. Ma, M. Yseboot, C. Bizouard, J. Geophys. Res., 108B, 2275, 2002.

[4] Dickey, J.O., S.L. Marcus, O. de Viron, I. Fukumori, Recent changes in Earth oblateness: separating the geodetic signatures of climate variability and post-glacial rebound, Science, 298, 1975-1977, 2002.

[5] Feissel-Vernier, M., A&A, 403, 105, 2003.

[6] Ma, C., E.F. Arias, T.M. Eubanks, A.L. Fey, A.-M. Gontier, C.S. Jacobs, O.J. Sovers, B.A. Archinal, P. Charlot, Astron. J., 116, 516, 1998.

[7] Mathews, P.M., B.A. Buffett, T.A. Herring, I.I. Shapiro, Forced nutations of the Earth: Influence of inner core dynamics. 1. Theory, J. Geophys. Res., 96(B5), 8219-8242, 1991.

[8] Mathews, P.M., T.A. Herring, B. Buffett, J. Geophys. Res., 107B, 10.1029, 2002.

[9] Van Hoolst, T., V. Dehant, W. Kuang, Special Bureau for the Core, in: Proc. IERS Workshop, Munich, Germany, November 2002, IERS Technical Note, 30, eds. B. Richter, W. Schwegmann, W. Dick, 168-179, 2003.

Hermann Drewes et al.: The IAG Project "Integrated Global Geodetic Observing System (IGGOS)" – Setup of the Initial Phase, IVS 2004 General Meeting Proceedings, p.32–37
http://ivscc.gsfc.nasa.gov/publications/gm2004/drewes

The IAG Project "Integrated Global Geodetic Observing System (IGGOS)" – Setup of the Initial Phase

Hermann Drewes [1], *Christoph Reigber* [2]

[1] *Deutsches Geodätisches Forschungsinstitut*
[2] *GeoForschungsZentrum*
Contact author: Hermann Drewes, e-mail: drewes@dgfi.badw.de

Abstract

The Integrated Global Geodetic Observing System (IGGOS) was established in 2003 as the first and only Project of the International Association of Geodesy (IAG). The project structure shall be installed during an initial phase in the years 2003 to 2005. The vision, mission, objectives and the first ideas of the overall structure are described in the paper.

1. Introduction

The Project "Integrated Global Geodetic Observing System" (IGGOS) of the International Association of Geodesy (IAG) was installed within the new structure of IAG during the XXIII General Assembly of the International Union of Geodesy and Geophysics (IUGG) in Sapporo, Japan, July 2003. According to its bylaws, projects of the IAG are of a broad scope and of highest interest and importance for the entire field of geodesy. They serve as the "flagship" of the Association for a long time period. At the same event in Sapporo, IGGOS was endorsed by the IUGG through the Resolution No. 3.

2. Vision

IGGOS integrates different techniques, different models and different approaches in order to achieve a better consistency, long-term reliability and understanding of geodetic, geodynamic and global change processes. It is geodesy's contribution to Earth sciences and the bridge to the other disciplines; it asserts the position of geodesy in geosciences, integrates the work of IAG and emphasizes the broad spectrum of geodetic research and application fields. IGGOS provides the scientific and infrastructure basis for all global change research in Earth sciences. In the frame of IGGOS, the Earth system is viewed as a whole including the solid Earth as well as the fluid components, the static as well as time-varying parameters.

3. Mission

IGGOS is to collect, archive and ensure the accessibility of geodetic observations, results and models covering the three fundamental fields of geodesy:

- geometry and kinematics of the Earth's surface,
- Earth orientation and rotation, and

- the Earth's gravity field and its variability.

IGGOS shall identify a complete set of geodetic products in these fields and establish the requirements concerning the products' accuracy, time resolution, and consistency. It will identify eventual gaps in the products provided by the IAG services and develop strategies to close them. Intensive cooperation between existing and new IAG services shall be stimulated and the visibility of scientific research in geodesy shall be promoted and improved. By these means a maximum benefit for science shall be achieved. IGGOS is geodesy's central interface to the scientific community and to society in general.

4. Objectives

In the first phase IGGOS aims at maintaining the stability of and providing the ready access to the existing time series of geometric and gravimetric reference frames. It focuses on all aspects relevant to ensure the consistency of geometric and gravimetric products. This includes space-borne and terrestrial techniques. The targeted overall accuracy and consistency of the products is of the order of 10^{-9} or better. IGGOS ensures the consistency between the different geodetic standards used in the geosciences community in agreement with the international unions and aims at improving the geodetic models at the level required by the observations.

IGGOS shall actively participate in the IGOS, the United Nation's Integrated Global Observing Strategy. IGOS brings together the major satellite and surface-based systems for global environmental observations in a strategic planning process. It shall support the environmental information needs of scientists, operational environmental programmes, as well as national and international decision makers.

5. Scientific Rationale

IGGOS shall have a central theme and a master product. The central theme "Global deformation and mass exchange processes in the System Earth" must include all the activities IGGOS might envisage in future. It comprises the Earth's geometry, rotation and gravity field. In addition, it may easily be translated and broken down into tangible individual sub-themes and sub-products. From the general theme one general product may be derived, encompassing the following scientific questions/areas:

- Deformation (loading as well as expansion) of the Earth due to the mass transfer between atmosphere, hydrosphere (including ice) and solid Earth, separating the effects of mass changes from motion and from thermal expansion;
- The global pattern of tectonic processes including inter-plate and intra-plate deformation;
- The global pattern of height changes in one datum and on all time scales, of geodynamic as well as of anthropogenic origin, on land, of ice covers, and of sea level, separating the effects from solid Earth and from the oceans ("absolute" sea level);
- Quantification of the mass exchange between all the components of the System Earth.

The above list is not meant to be final and will be further developed.

The central theme and the main results (master products) derived from it will address the relevant science issues related to geodesy and geodynamics in the 21st century, but also issues relevant to society in general (global risk management, natural resources, climate change, ocean forecasting and others). It is an ambitious project of a dimension that cannot be achieved by the geodetic community alone, and which requires a strong cooperation inside and outside this community.

In order to shape IGGOS through its master-theme and its master-products, a sound and comprehensive "IGGOS Science Plan" is required. The IGGOS Science Plan shall provide a logic framework for the work of IGGOS. The central theme and the corresponding master product(s) must be put into a broader science and application context. It should also include an analysis of the state-of-art in the science field under discussion, strength and deficiencies, recommendations of what should be done.

The IGGOS Science Plan should serve as the basis for the implementation of IGGOS in 2005. A work plan should be derivable from it. Furthermore it should become an attractive document for presentation to potential future partners and clients.

6. Initial Structure

The IAG Project Planning Group proposed and the IAG Executive Committee accepted to establish the following key elements of IGGOS:

1. The "IGGOS Project Board" as the central oversight entity.
2. "Working Groups" the tasks of which are to a high degree independent of the tasks of the IAG services.
3. A "Science Council" representing the geodetic and geophysical community.

The initial IGGOS structure (for the definition phase 2003-2005) is illustrated by Figure 6.3.

6.1. Project Board and Steering Committee

The IAG Bylaws ask for the establishment of a Steering Committee consisting of representatives appointed by the commissions, two members at large, and the chairs of the IAG project sub-groups. The Steering Committee is a subset of the IGGOS Project Board. In the initial phase of IGGOS it is composed of the following members which is to a large extent the same as the composition of the IGGOS Planning Group 2001-2003 (Steering Committee members are marked by an asterisk):

- Chair: *Chris Reigber**
- Members related to reference frames: *Claude Boucher, Hermann Drewes* (Representative of Commission 1), Markus Rothacher*
- Members related to gravity field and sea level: *Rene Forsberg* (Representative of Commission 2), Reiner Rummel, C.K. Shum*
- Members related to Earth rotation and geodynamics: *Veronique Dehant, Kosuke Heki, Susanna Zerbini* (Representative of Commission 3)*
- Members related to services for geometry: *Norman Beck, Chopo Ma, Mike Pearlman*
- Members related to services for gravity and sea level: *Fernando Sanso, Phil Woodworth, Mike Watkins*
- Members related to networks: *Wolfgang Schlüter, John Manning, Ruth Neilan*

6.2. Working Groups

Setting up the IGGOS working groups the following general principles are observed:

- IGGOS will be based on the existing IAG Services. It is in particular *not* taking over tasks of existing, and well working IAG services. IGGOS will provide a framework for existing or future services and ensure their long-term stability.
- New entities will be established only if there is a stringent requirement.
- IGGOS must be recognized by partners outside IAG, e.g., by UNESCO, ICSU, IGOS, GOOS, GTOS, governments, inter-government organizations, WCRP, IGBP, etc., as geodesy's most important contribution to Earth sciences. For this purpose contacts have to be established to these organizations.
- IGGOS must promote its master product and the related sub-products.
- IGGOS must promote interdisciplinary research in geodesy.
- IGGOS will provide standards and enforce quality management (validation, calibration, ensure the 1 ppb level) either by a new IGGOS entity or by delegating this task to one or several of the existing services.

6.3. Science Council

The primary task of the science council is to develop the IGGOS science plan based on the science rationale. The Inter-Commission Committee on Theory shall be represented in the Science Council.

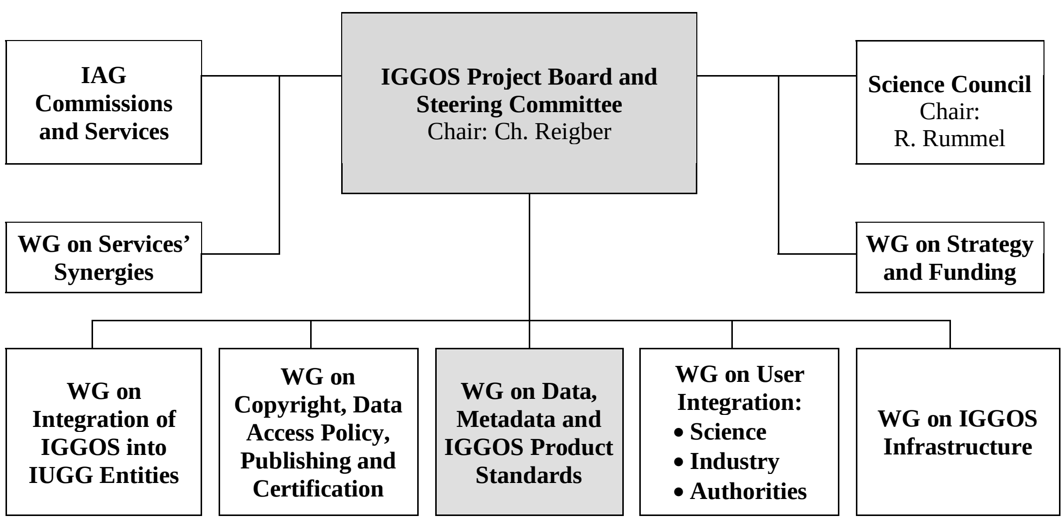

Figure 1. Initial IGGOS Structure.

7. Initial Program of Activities

WG on IAG Services' Synergies: The key issue within this WG is a thorough analysis of the existing IAG structure. Does it make sense to combine certain services into one? What new services should be set up? Is it correct to distinguish within IAG between *level 1 services* (e.g., IGS, ILRS, IVS), dealing with raw observations and generating products which are more or less based on these observations only, and *level 2 services* (e.g., IERS) using the products of several level 1 services and generating new products, which are consistent with all the information from level 1? Shall additional level 2 services be established?

WG on Strategy and Funding: In the long run, funding has to be addressed by all permanent IAG entities requiring a complex infrastructure. As IGGOS per se (at least initially) will be based —exactly like all IAG services— on voluntary contributions of the relevant research organizations in the field, an IGGOS funding strategy must be developed in close coordination with these organizations. It seems therefore appropriate to establish a working group related to this topic. This aspect is clearly not dealt with at a sufficient rate within the existing IAG services structure.

WG on Integration of IGGOS in IUGG entities: This WG has the task to set up (so-to-speak) the foreign ministry of IGGOS. It must be the goal to have IGGOS acknowledged as a member in the important international programs dealing with global change, etc. The IGOS is but one important example.

WG on Copyright, Data Access Policy, Publishing and Certification: This WG should deal with the consistent assignment of the *Digital Object Identifier* (DOT Û) framework for IGGOS products and the usage of *Data Set Citation* rules in metadata documents for the definition and realization of copyright, data access, publishing and certification objectives.

WG on Data, Metadata, and IGGOS Product Standards: This WG has to deal with IGGOS products and standardization issues. The definition of IGGOS *Products* consisting of data and metadata, driven by user, application and service requirements using international *Standardization* specifications, constitutes the precondition for the creation of state-of-the-art value-added public and science IGGOS services.

WG on User Integration: This task is in part dealt with by the IAG services. A common policy on the IAG level is, however, missing. This WG must be set up in close cooperation with the services.

WG on IGGOS Infrastructure: The infrastructure of IGGOS has to be setup in accordance with the objectives. In the initial phase the following sub-groups shall be installed to study and to configure the corresponding tasks:

- SG on Fundamental Station Network
- SG on Data Centres
- SG on Mission Operations
- SG on Global Communication
- SG on TR/TTC Networks

8. Schedule for the Realization of IGGOS

The following plan to develop IGGOS is based on the decisions taken at the last IGGOS planning group meeting in Sapporo.

1. The IGGOS definition phase lasts from 2003-2005. The main tasks are:
    - Definition of the final IGGOS structure

- Development of the IGGOS Science Plan

2. The "final" IGGOS structure and the science plan will have to be approved by the IAG Executive Committee at the IAG Scientific Assembly in Cairns, Australia.
3. The IGGOS, as IAG's first project, should become operational in 2005.
4. IGGOS, in particular the science plan developed between 2003 and 2005, will be a central issue of the IAG Scientific Assembly 2005.

Benjamin F. Chao: Earth Rotational Variations Excited by Geophysical Fluids, IVS 2004 General Meeting Proceedings, p.38–46
http://ivscc.gsfc.nasa.gov/publications/gm2004/chao

Earth Rotational Variations Excited by Geophysical Fluids

Benjamin F. Chao

NASA Goddard Space Flight Center

e-mail: benjamin.f.chao@nasa.gov

Abstract

Modern space geodetic measurement of Earth rotation variations, particularly by means of the VLBI technique, has over the years allowed studies of Earth rotation dynamics to advance in ever-increasing precision, accuracy, and temporal resolution. A review will be presented on our understanding of the geophysical and climatic causes, or "excitations", for length-of-day change, polar motion, and nutations. These excitations sources come from mass transports that constantly take place in the Earth system comprised of the atmosphere, hydrosphere, cryosphere, lithosphere, mantle, and the cores. In this sense, together with other space geodetic measurements of time-variable gravity and geocenter motion, Earth rotation variations become a remote-sensing tool for the integral of all mass transports, providing valuable information about the latter on a wide range of spatial and temporal scales. Future prospects with respect to geophysical studies with even higher accuracy and resolution will be discussed.

1. Introduction

For over two decades, the very-long-baseline interferometry (VLBI) has been a most powerful geodetic technique for measuring the Earth's rotation. Compared to other "workhorse" techniques of satellite-laser-ranging (SLR) or Global Positioning System (GPS) based on satellites, VLBI has the unique strength of being able to observe the geometrical orientation of the rotating Earth relative to the inertial space. (The celestial reference frame is best defined by distant celestial bodies, which is the subject of other invited papers in this Proceedings.) As such, geodetic VLBI data contain the information of:

1. The rotational speed, free from uncertainties suffered by satellite techniques due to their orbit drifts. These data yield the length-of-day (LOD) variation (used conveniently when the temporal sampling is longer than 1 day) or the universal-time (UT) variation (for sub-daily sampling where LOD loses its meaning.)

2. The rotational axis orientation, in both nutations and polar motion. In conventional terminology, nutations (including precession) are variations of the axis orientation relative to the inertial space, while polar motion is that relative to the terrestrial frame. Satellite techniques are unable to see nutations as can VLBI (because VLBI refers to the celestial frame), whereas VLBI can see polar motion as can satellite techniques (as the VLBI antennas are fixed on the terrestrial frame.)

Based on these Earth rotation data, this paper means to give a brief overview of the geophysical causes, or "excitations", of Earth rotation variations.

2. Angular Momentum Variations in Geophysical Fluids

Mass transports occurring in the atmosphere-hydrosphere-cryosphere-solid Earth-core system (the "global geophysical fluids") occur on all temporal and spatial scales. Large-scale mass transports in the Earth system produce variations in Earth's rotation, gravity field, and geocenter. See Chao et al. (2000), and the website of IERS' Global Geophysical Fluids Center http://ggfc.gsfc.nasa.gov/.

To illustrate the effect on Earth rotation, consider a simple "solid Earth + atmosphere" system where an air mass moves across the surface of an otherwise uniformly rotating solid Earth. Regardless of its driving mechanism, via surface torques the relative motion of the air mass imparts changes in the solid Earth's rotation, just as a circus seal does by balancing itself on a rolling ball. Furthermore, the associated redistribution of mass changes the Earth's inertia tensor and hence its rotation. A familiar analogy is a spinning ice skater changing his rotation by moving his arms — he'd spin faster when drawing his arms closer to his body and vice versa, and he'd "wobble" if he does so in an asymmetric way. The above two effects (whose sum is what's observed) are consequences of the conservation of angular momentum, which here dictates that the total angular momentum of the Earth + atmosphere system stays constant.

Our real Earth is of course a lot more complex, and exciting, than the above Earth + atmosphere system. Any geophysical process involving fluid mass transport will excite its own Earth rotation variations depending on its spatial and temporal characteristics. The signal observed by space geodetic techniques is the sum of all the individual contributions, which enter in the form of angular momentum (AM) variations. The latter consists of a "motion term" (due to relative motion of the geophysical fluids mass, e.g. winds and ocean currents) and a "motion term" (due to mass redistribution, e.g. air pressure changes and land water impoundment). As far as Earth rotation variation is concerned, these AM variations act as "excitation" sources, where the Earth responds in accordance with its physical properties: A schematic "Earth filter" for LOD and polar motion is given in Figure 1; for details see, e.g. Munk and MacDonald (1960).

<u>The atmospheric AM (AAM):</u> The most prominent contributions are perhaps weather effects, driven originally by solar radiation input, and related over much of the globe to the Earth's rotational Coriolis force and modified by atmosphere-ocean and atmosphere-land interactions. The meteorological pressure systems appearing on weather maps indicate that different masses of air move around the planet as part of the general circulation. The wind thus produced shows a variation on short timescales of these synoptic motions, but they are strong as well on longer scales related to intraseasonal, seasonal, and interannual oscillations. Interannual anomalies associated with El Niño/La Niña are of particular interest.

<u>The oceanic AM (OAM):</u> Mass transport also occurs in the oceans where it is mainly caused by tidal forcing, surface wind forcing, atmospheric pressure forcing, and thermohaline fluxes. Satellite altimetry can measure changes in the sea surface height caused by these forcing mechanisms, and the GRACE mission is currently measuring the time-variable gravity signals coming from the ocean-bottom pressure changes. Numerical models of the oceanic general circulation allow the response of the oceans to these forcing mechanisms to be investigated in detail.

<u>The tidal AM (TAM):</u> Large mass transports/redistributions occur as tides at all tidal periods. The tides involve mass transports and angular momentum exchanges within the Earth system at periods ranging from subdaily to 18.6 years. The Earth's body tide is responsible for large length-of-day variations at monthly and fortnightly periods; the ocean tides are the dominant cause of

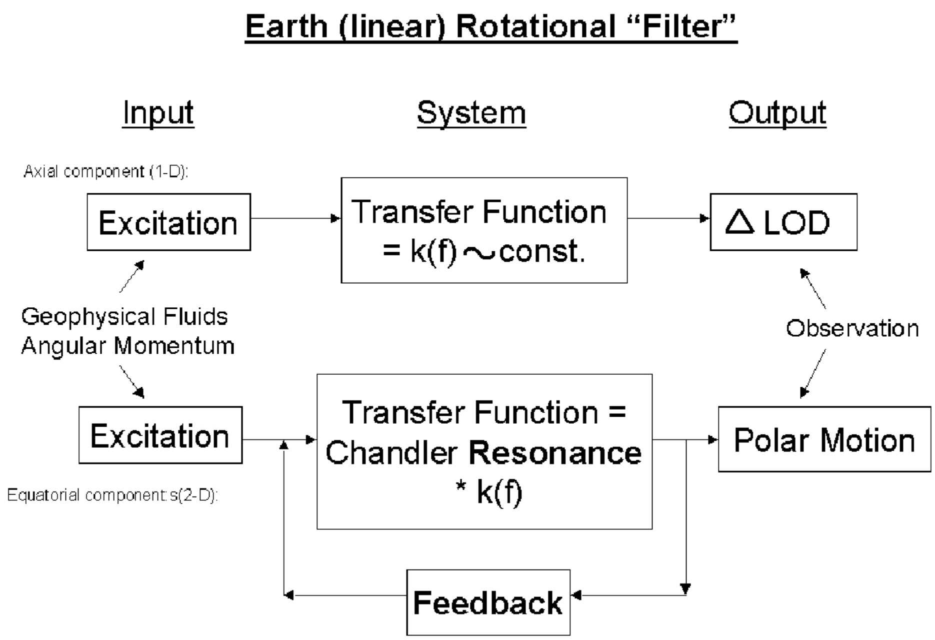

Figure 1. Schematic "Earth filter" for LOD and polar motion, linking the input excitations to the output observations.

diurnal and semidiurnal variations in both rotational rate and polar motion.

The hydrological AM (HAM): Redistribution of water mass stored on the continents occurs on a variety of timescales. Seasonal and shorter time scales involve precipitation, evaporation, and runoff, with storage of water in lakes, streams, artificial reservoirs, soil, and biomass. Over longer timescales, storage variations in ice sheets and glaciers signal climate change, while ground water storage changes take place in deeper aquifers. Some of these hydrological processes are fundamentally regulated by vegetation; but all are ultimately exchanged with and hence reflected in atmospheric water content and sea level in an intricate budget. Water mass redistribution involving these various reservoirs and mechanisms has been shown to have observable effects on Earth rotation, geocenter and gravity field changes. However, the variety of transport mechanisms and storage reservoirs makes the task of globally monitoring water storage on land an extremely challenging task. Indeed, this is considered to be a first order problem for the climate community, and is being pursued at every major climate research center.

The mantle AM (MAM): The solid, but non-rigid, Earth is perpetually in motion as well. There are motions caused by external forces, including tidal deformation, atmospheric and oceanic loading, and occasional meteorite impacts. For internal processes, volcanic eruptions and pre-seismic, co-seismic and post-seismic dislocations associated with an earthquake act on short timescales. On longer timescales, present-day post-glacial rebound, surface processes of soil erosion and deposition, and tectonic activity such as plate motion, orogeny, and internal mantle convection, all transport large masses over long distances. Finally, the entire solid Earth undergoes an equilibrium adjustment in response to the secular slowing down of the Earth's spin due to tidal friction.

The core AM (CAM): Deeper in the solid Earth, the fluid outer core is constantly turning and churning in association with the geodynamo's generation of the magnetic field. The variation of the core angular momentum can evidently be inferred from surface observations of the geomagnetic field or modeled by physical hypotheses and the equations of motion that drive and govern the geodynamo and hence the core flow. This core angular momentum has been compared to the observed variations of the length-of-day at decadal timescales, while torques at the core-mantle and inner core boundaries have been evaluated. The recent seismological finding of a differential rotation of the solid inner core is also under evaluation in this context.

3. LOD/UT1 Variations and Polar Motion

Figure 2 shows a sample of modern LOD and polar motion data, obtained by weighted combination of VLBI, SLR, and GPS observations (Gross, 2000). Figure 3 gives a schematic spectrum of the LOD/UT1 variations expected (and observed) in terms of geophysical fluids contributions. Many periodic and quasi-periodic signals peak above a generally red spectrum, much of which is known to be due to AAM and, to a lesser extent, OAM and HAM. The long-period tidal signals are much stronger than the diurnal and semidiurnal ones because the long-period tidal potential's (and hence the corresponding TAM in the solid Earth) zonal nature strongly influences LOD/UT, while the diurnal + semidiurnal tidal signals (as well as a small portion of the long-period tidal signals) in LOD/UT1 only come from the oceanic TAM (e.g., Chao and Ray, 1998). The annual and semiannual peaks are excited by the combination of AAM + OAM + HAM, which all have strong seasonality (for a review, see, e.g., Dickey, 1993; Eubanks, 1993).

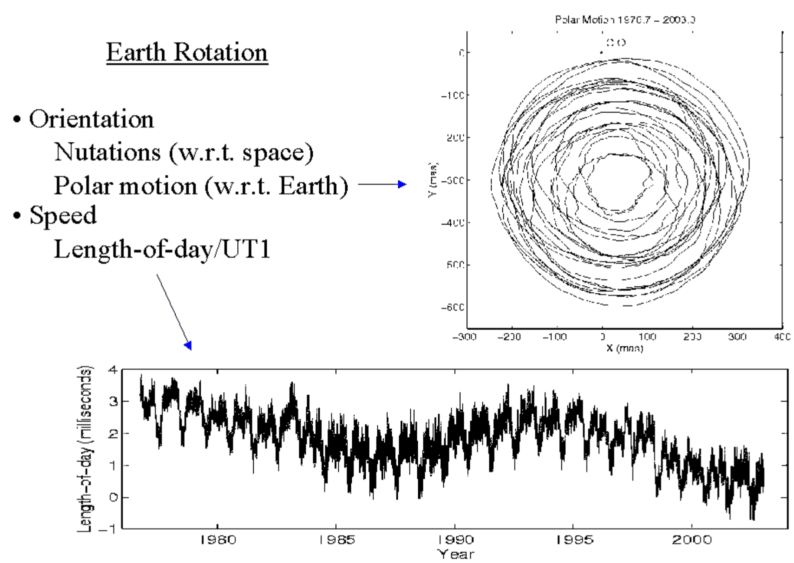

Figure 2. A sample of modern LOD and polar motion data, obtained by weighted combination of space geodetic observations including VLBI.

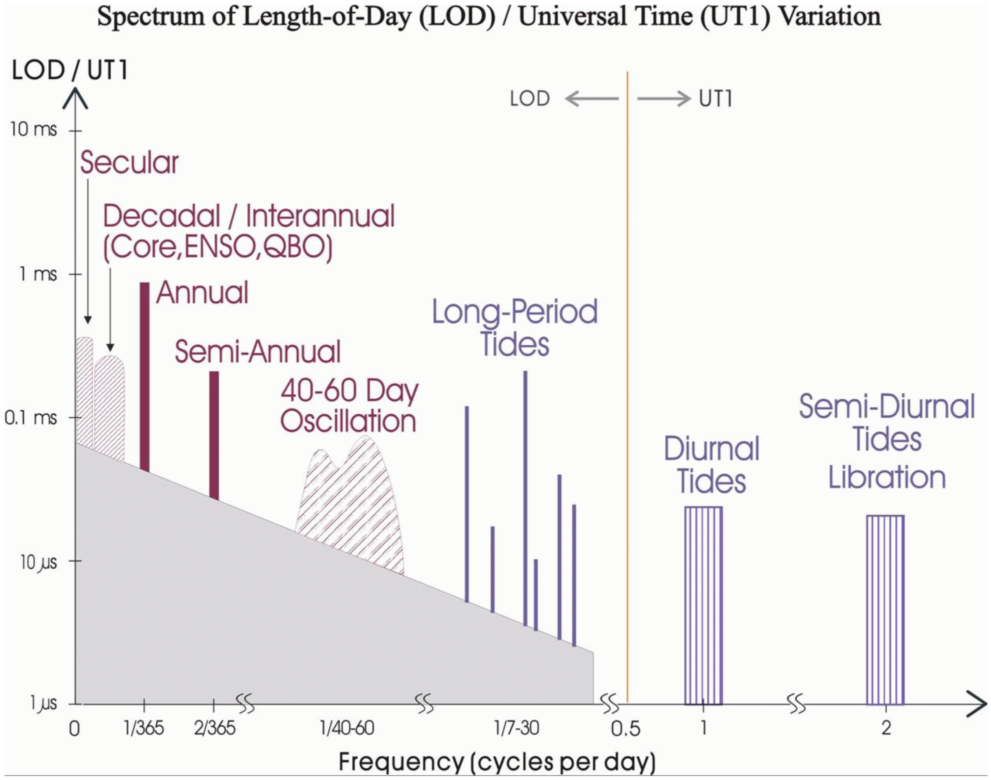

Figure 3. A schematic spectrum of the LOD/UT1 variations expected (and observed) in terms of geophysical fluids contributions.

Figure 4 illustrates some of the most important findings in the geophysical excitation of LOD/UT variations over the years (Chao, 2003). A series of zoom-in views allows finer details to be studied with respect to various geophysical excitation sources ranging from core flow, to El Niños, to ocean tides. In the top panel, the good correspondence between the curves implies that the mass transport in the fluid core is the dominant cause of the decadal LOD change over the last 1-2 centuries. The middle panel zooms in on the last 20 years. One sees that the interannul LOD variation is mainly caused by the anomalous mass transport (mostly in the east-west wind field) of the Southern Oscillation in the tropical Pacific-Indian Ocean. The bottom panel further zooms in on a 2-week period during the VLBI Cont94 campaign, showing that the ocean tides are responsible for most of the diurnal/semidiurnal LOD changes. Clearly, very distinct geophysical processes are at work in exciting Earth rotation variations on very distinct timescales, with a wide range of magnitude.

Figure 5 gives the counterpart schematic spectrum of the polar motion, showing a much more complex physical nature than Figure 3. The positive frequency means prograde motion/excitation while the negative frequency the retrograde motion/excitation. Also given is the "nutation" frequency scale, which is shifted with respect to the polar motion frequency by 1 cycle per day, which is the conversion between the terrestrial reference frame and the inertial reference frame as realized by the celestial frame observed by VLBI.

The Earth presents two rotational resonances across the spectrum. One is the Chandler wobble resonance (as mentioned in Figure 1), representing the elastic Earth's version of the Eulerian

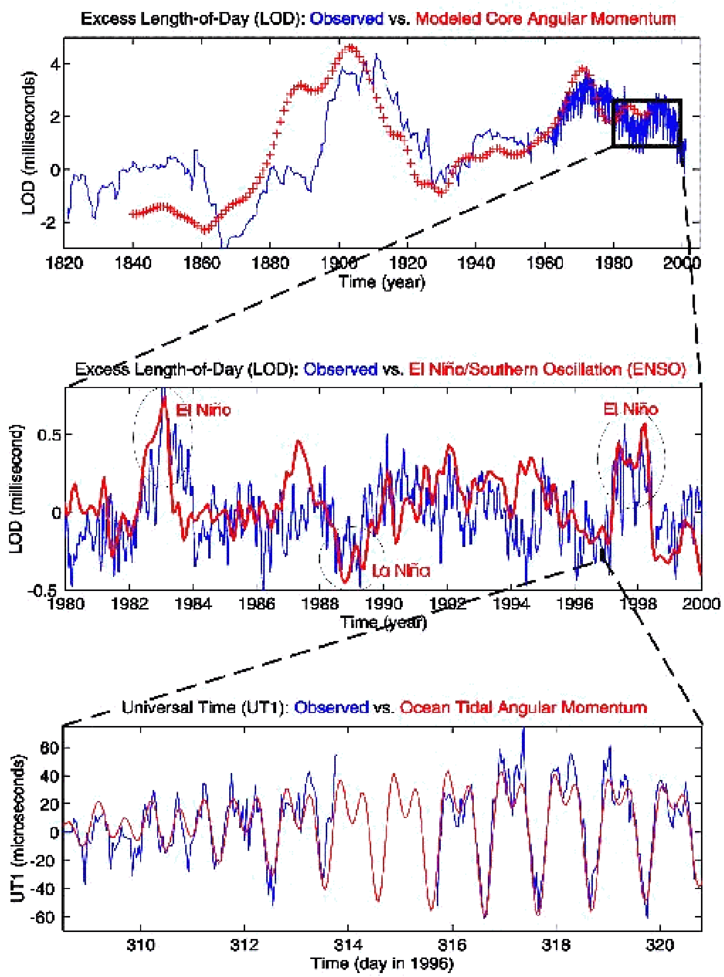

Figure 4. Zoom-in views examining the LOD/UT1 variations with respect to various geophysical excitation sources ranging from core flow, to El Niños, to ocean tides.

wobble. The other is the so-called free-core-nutation (FCN) resonance due to the dynamical motion of the fluid outer core. FCN resides in the nutation band although its origin has nothing to do with tides, some of which are close enough so that their responses are magnified by this resonance. There is a third resonance, but at the zero nutation frequency (hence not "oscillatory"), giving rise to the astronomical precession. It should be emphasized that VLBI is currently the only technique that is sensitive to, and precise enough to measure the signals in the nutation band, although gyrometers are beginning to show exciting potentials, such as large ring-laser interferometers (Schreiber and Klugel, 2003).

As a result of the resonances in the Earth's polar motion "filter" as depicted in Figure 1, the observed polar motion is not the excitation function; rather it is the convolution of the excitation function with the resonance functions (e.g., Munk and MacDonald, 1960). Therefore, a numerical procedure of de-convolution has to be conducted to convert the observed polar motion into its

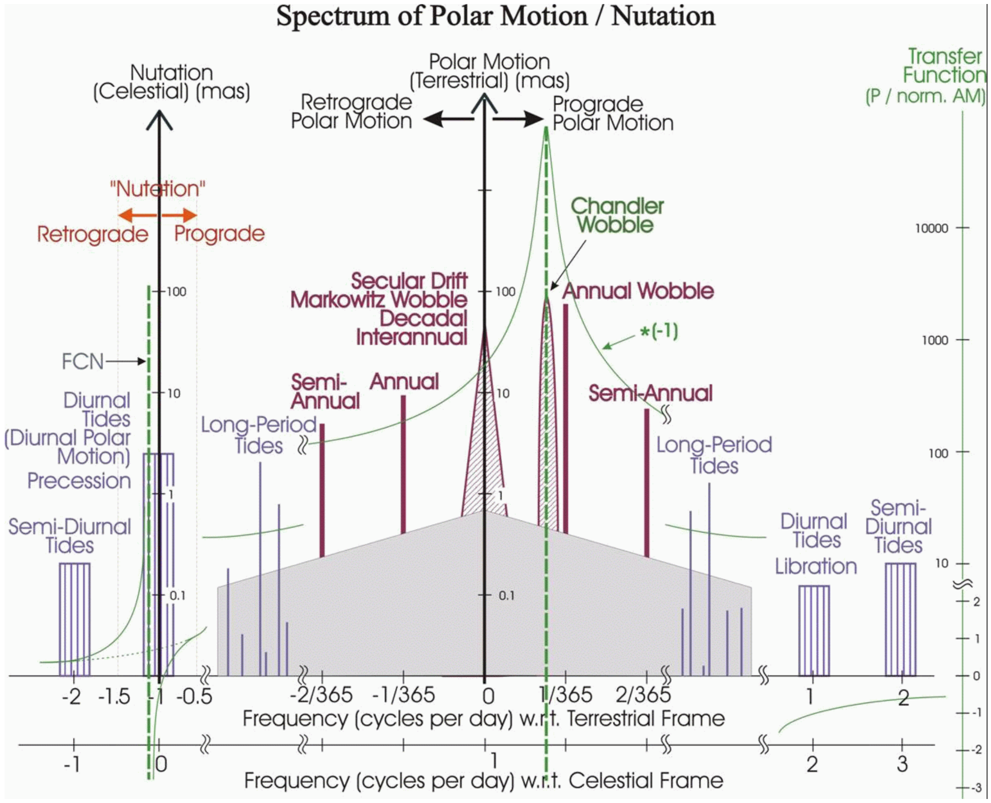

Figure 5. A schematic spectrum of the polar motion/nutation expected (and observed) in terms of geophysical fluids contributions.

excitation function, before it can be compared with the geophysical fluids' AM variations. Among other things, the frequencies and Q-values of the resonances need to be well-determined for the de-convolution. Considerable research has been devoted to this subject (see Figure 6 below.)

For the most part, geophysical and meteorological excitations for the polar motion are similar to those for the LOD/UT1 variation (for a review, see, e.g., Dickey, 1993; Eubanks, 1993). For example, the AAM and to a lesser extent the OAM have been found to be the major contributors in exciting the polar motion (e.g., Gross, 2003). For the TAM, the main difference from the case of LOD/UT1 excitation is that the largest contribution comes from the tesseral terms in the tidal potential corresponding to the retrograde diurnal tides generated in the solid Earth (while, as in the case of LOD/UT1, other smaller tidal signals come from oceanic TAM) (e.g., Chao and Ray, 1998). Empirically, the frequency band around the retrograde diurnal is characterized as the "nutation band", where the signals are absorbed into the nominal nutation solutions of VLBI. Hence such signals are absent from VLBI's polar motion solution given, e.g., in Figure 2.

4. Epilogue

VLBI observes the Earth rotation variations in LOD/UT1 and nutation/polar motion. Under the so-called space-geodetic "Moore's law", that space geodesy is seeing a ten-fold advancement in precision and temporal resolution every decade in the last 2-3 decades, these Earth rotation variations have been studied in increasingly more detail, as illustrated in Figure 4. Together with time-variable gravity observations, traditionally coming from SLR but in recent years from the CHAMP and GRACE satellite missions, space geodesy has become a powerful remote sensing tool for monitoring our changing environment on this restless planet (NASA, 2003). The scientific utilities of these data are two-fold: In the forward direction, the data provide information for better understanding of geophysical fluids' mass transports and dynamics, independent of and complementary to other observations for geophysical, meteorological, and climatic changes. In the inverse direction, in investigating the relationship between the excitation sources and the Earth's rotational responses, many important, but often subtle, properties and dynamical behavior of the Earth can be deduced or constrained. Figure 6 gives a list of such parameters, whose better understanding and modeling can benefit by the Earth rotation observations, to different extents depending on the precision and resolutions of the available data.

Inverse Inference

(from Earth rotation data to Earth properties and dynamics)

- Core-mantle coupling (*f*, mechanism, direction)
- Inverted-Barometer (*f*, **r**)
- Love numbers (*f*)
- Ocean tidal response
- Chandler period, Chandler *Q*
- FCN period, FCN *Q* (FCN = Free Core Nutation)
- Core ellipticity/topography
- Libration
- Core equatorial ellipticity
- Inner core parameters
- Mantle conductivity
- Mantle viscosity
- Mantle heterogeneity
- …

Figure 6. A list of many important properties and dynamical behavior of the Earth that can be deduced or constrained by studying the relationship between the excitation sources and the Earth's rotational responses.

References

[1] Chao, B. F., The Geoid and Earth Rotation, in *Geophysical Interpretations of Geoid*, ed. P. Vanicek and N. Christou, CRC Press, Boca Raton, 1994.

[2] Chao, B. F., and R. D. Ray, Oceanic tidal angular momentum and Earth's rotation variations, *Prog. in Oceanog.*, *40*, 399-421, 1998.

[3] Chao, B. F., V. Dehant, R. S. Gross, R. D. Ray, D. A. Salstein, M. M. Watkins, and C. R. Wilson,

Space geodesy monitors mass transports in global geophysical fluids, *EOS, Trans. Amer. Geophys. Union, 81*, 247-250, 2000.

[4] Chao, B. F., Geodesy is not just for static measurements any more, *EOS, Trans. Amer. Geophys. Union, 84*, 145-156, 2003.

[5] Dickey J. O., Atmospheric excitation of the Earth's rotation: Progress and prospects via space geodesy, in Contributions of Space Geodesy to Geodynamics: Earth Dynamics, 55-70, ed. D. E. Smith and D. L. Turcott, AGU, Washington, D. C., 1993.

[6] Eubanks, T. M., Variations in the orientation of the Earth, in Contributions of Space Geodesy to Geodynamics: Earth Dynamics, 1-54, ed. D. E. Smith and D. L. Turcott, AGU, Washington, D. C., 1993.

[7] Feissel-Vernier, Martine, Stability of the VLBI-Derived Celestial Reference Frame, in IVS 2004 General Meeting Proceedings, NASA/CP–2004-212255, ed. N. R. Vandenberg and K. D. Baver, IVS 2004 General Meeting, Ottawa, Canada, 2004 (this volume).

[8] Gross, R.S., Combination of Earth orientation measurements: SPACE97, COMB97, and POLE97, *J. Geodesy, 73*, 627-637, 2000.

[9] Gross, R. S., Atmospheric and oceanic excitation of the Earth's wobbles during 1980-2000, *J. Geophys. Res., 108*, B8, 2370, doi:10.1029/2002JB002143, 2003.

[10] Munk W. H., and G. J. F. MacDonald, *The Rotation of the Earth*, Cambridge Univ. Press, New York, 1960.

[11] NASA Solid Earth Science Working Group Report, *Living on a Restless Planet*, 2002, <http://solidearth.jpl.nasa.gov/>).

[12] Schreiber, K. U., and T. Klugel, Earth tide and tilt detection by a ring laser gyroscope, *J. Geophys. Res., 108*, doi:10.1029/2001JB000569, 2003.

Zinovy Malkin: 5,000,000 Delays—Some Statistics, IVS 2004 General Meeting Proceedings, p.47–51
http://ivscc.gsfc.nasa.gov/publications/gm2004/malk1

5,000,000 Delays—Some Statistics

Zinovy Malkin

Institute of Applied Astronomy of Russian Academy of Sciences (IAA)
e-mail: malkin@quasar.ipa.nw.ru

Abstract

5,000,000 VLBI delays are stored now in the IVS data base and available for scientific analysis. This is a remarkable result of more than 20 years of geodetic VLBI history. This paper presents some statistics related to the VLBI observations during almost 25 years of geodetic VLBI.

At the end of 2004, the number of VLBI delays obtained in the framework of the geodetic and astrometric VLBI programs reached 5,000,000! This is one of the major milestones in the VLBI history resulting from almost 25 years of heroic efforts by astronomers and physicists, engineers and programmers, network stations and correlator teams.

Most of the statistics presented here (when not indicated explicitly) are related to all the observing sessions, independent of their duration. As can be seen from Table 1, only number of sessions substantially depends on the session set taken into account, other statistics are practically the same for all sessions and 24h ones (we consider the session as 24h one if its duration is 18 hours or greater). One can see that most of observations were obtained during the 24h and intensives ($< 2h$) sessions. The sessions with duration 2–18h were, evidently, rather sporadic.

Table 1. Statistics depending on the session duration. Number of observations is given in thousands. Number of stations includes also the experimental ones (KASL, MOJAVLBA, NOTOX, LEFT85_1, VLBA85_3, WIDE85_3).

Session duration	All	≥ 18h	< 18h	< 12h	< 6h	< 2h
Number of observations	5005	4913	92	80	68	64
Number of sessions	8528	3757	4771	4737	4633	4528
Number of stations	159	156	53	40	29	17
Number of baselines	1356	1335	167	94	51	33
Number of sources	2254	2248	406	355	201	119

These observations were collected in 8528 sessions (3757 of them with duration 18h or greater) at 159 stations including experimental ones, on 1356 baselines (there was a misprint in the IVS Newsletter of August 2002, number of baselines 1722 given there should be 1272). Totally, 2254 sources were observed, more the half of them during the VLBA Calibrator Survey program.

Figure 1 shows how the overall result was reached. It is interesting to see how much time was needed to get each million observations (Table 2). Apparently, a limit of the capacity of existing IVS network is reached in the late 1990s.

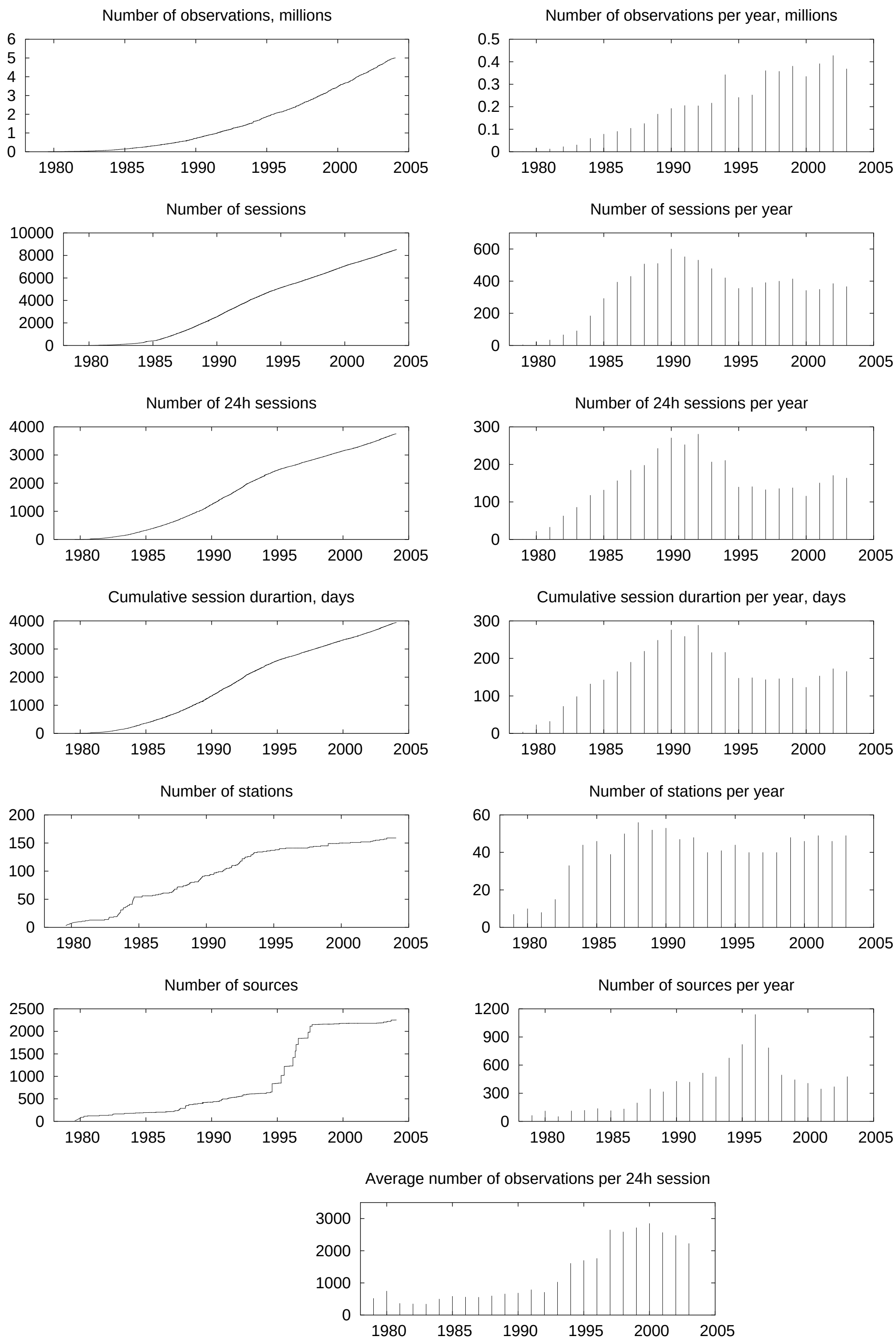

Figure 1. Overall statistics.

Table 2. Time taken to collect each million observations (ΔT), the corresponding period of observations (T_{beg}–T_{end}), and number of sessions. Some inconsistencies between ΔT and T_{beg}–T_{end} are due to rounding.

Million	1st	2nd	3rd	4th	5th
ΔT, years	11.9	3.9	3.3	2.6	2.6
$T_{beg}-T_{end}$	1979.6–1991.5	1991.5–1995.5	1995.5–1998.7	1998.7–2001.4	2001.4–2004.0
# of sessions	3425	1873	1234	1002	976
# of 24h sessions	1628	901	444	348	432

Here are some extreme statistics with examples:

Maximum number of stations:	20	(991220XA)
Maximum number of baselines:	188	(991220XA)
Maximum number of sources:	263	(950715XV)
Maximum number of observations:	34221	(991220XA)
Maximum number of good observations:	30372	(991220XA)
Maximum number of bad observations:	4092	(940812XV)
Maximum percentage of good observations:	100.0	(860223X)
Maximum percentage of bad observations:	90.8	(911205MV)
The longest sessions, h:	99.2	(830520D)

Table 3 shows most active stations during the whole period of observations, and Tables 4–5 present statistics for sources and baselines. The longest attempted baselines is SESHAN25–TIGOCONC (12660 km), but no successful observations (zero quality code in NGS files) was obtained. The longest baseline with successful observations is DSS65–HOBART26 (12520 km). The shortest baselines was KAUAI–KOKEE (39 m)

Table 3. Most active stations, Nobs – number of observations, Nsess – number of sessions.

Ordered by number of observations				Ordered by number of sessions			
All sessions		24h sessions		All sessions		24h sessions	
Station	Nobs	Station	Nobs	Station	Nsess	Station	Nsess
GILCREEK	1016731	GILCREEK	1007188	WETTZELL	6291	WETTZELL	1893
WETTZELL	979313	WETTZELL	916828	WESTFORD	3849	GILCREEK	1731
WESTFORD	876858	WESTFORD	853711	GILCREEK	1937	WESTFORD	1640
KOKEE	541291	KOKEE	529154	KOKEE	1639	KOKEE	953
NYALES20	410231	NYALES20	409257	NRAO20	1389	RICHMOND	734
MATERA	314207	MATERA	311260	NRAO85 3	1145	HRAS 085	732
ONSALA60	292715	ONSALA60	291044	RICHMOND	794	MOJAVE12	726
MOJAVE12	288671	MOJAVE12	286644	HRAS 085	742	FORTLEZA	704
LA-VLBA	268754	LA-VLBA	268754	MOJAVE12	737	HARTRAO	593
ALGOPARK	260134	ALGOPARK	260134	FORTLEZA	706	ALGOPARK	527

Figures 2 and 3 show the evolution of some observational data and EOP uncertainty (IAA EOP series) with time.

Table 4. Most observed sources, Nobs – number of observations, Nsess – number of sessions.

Ordered by number of observations				Ordered by number of sessions			
All sessions		24h sessions		All sessions		24h sessions	
Source	Nobs	Source	Nobs	Source	Nsess	Source	Nsess
0552+398	271721	0552+398	266837	0552+398	5996	0552+398	3517
4C39.25	201307	4C39.25	198602	4C39.25	5137	4C39.25	3231
0059+581	166093	0059+581	163363	0059+581	4299	OJ287	3099
1803+784	146816	1803+784	138602	1803+784	4201	0528+134	2904
OJ287	135129	OJ287	131791	OJ287	3765	1741-038	2640
1739+522	131596	1739+522	131196	1739+522	3333	0727-115	2566
1357+769	125816	1357+769	122314	1357+769	3130	0229+131	2219
0528+134	113163	0528+134	112026	0528+134	2894	1803+784	2162
1308+326	101217	1741-038	99174	1741-038	2814	1334-127	2139
1741-038	99965	1308+326	99173	1308+326	2717	2145+067	2046

Table 5. Most observed baselines, Nobs – number of observations, Nsess – number of sessions.

Ordered by number of observations			
All sessions		24h sessions	
Baseline	Nobs	Baseline	Nobs
WESTFORD WETTZELL	171093	WESTFORD WETTZELL	149602
GILCREEK WESTFORD	134234	GILCREEK WESTFORD	133942
GILCREEK KOKEE	116313	GILCREEK KOKEE	116290
GILCREEK WETTZELL	111450	GILCREEK WETTZELL	111145
NYALES20 WETTZELL	90820	NYALES20 WETTZELL	90703
HRAS 085 WESTFORD	70704	HRAS 085 WESTFORD	70233
KOKEE WETTZELL	65154	MOJAVE12 WESTFORD	63085
MOJAVE12 WESTFORD	63252	FORTLEZA WETTZELL	62451
FORTLEZA WETTZELL	62456	MATERA WETTZELL	59681
MATERA WETTZELL	59945	GILCREEK KAUAI	56883

Ordered by number of sessions			
All sessions		24h sessions	
Baseline	Nsess	Baseline	Nsess
WESTFORD WETTZELL	3312	WESTFORD WETTZELL	1112
KOKEE WETTZELL	1415	GILCREEK WETTZELL	799
NRAO20 WETTZELL	1297	KOKEE WETTZELL	732
GILCREEK WETTZELL	818	GILCREEK WESTFORD	680
GILCREEK WESTFORD	683	HRAS 085 WESTFORD	595
NRAO85 3 WETTZELL	647	GILCREEK KOKEE	591
HRAS 085 WESTFORD	602	FORTLEZA WETTZELL	571
GILCREEK KOKEE	593	RICHMOND WESTFORD	566
FORTLEZA WETTZELL	572	FORTLEZA KOKEE	548
RICHMOND WESTFORD	567	RICHMOND WETTZELL	538

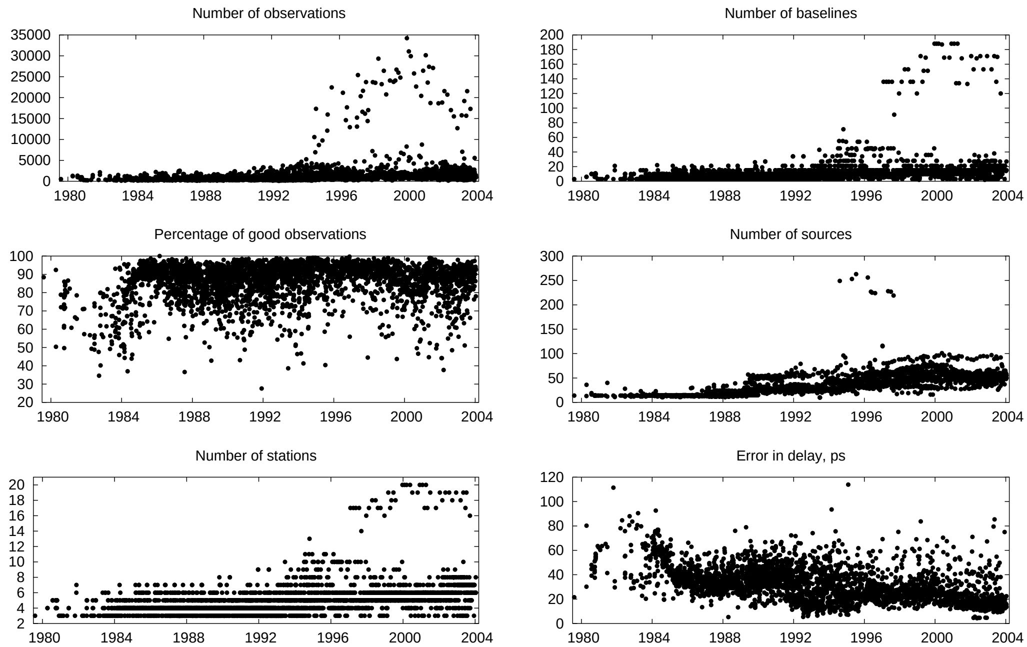

Figure 2. Statistics of the observational data. Each point corresponds to one 24h session. Sessions with the largest numbers of stations/baselines were observed along with VLBA network. Sessions with the largest number of sources were observed in the framework of the VLBA Calibration Survey program.

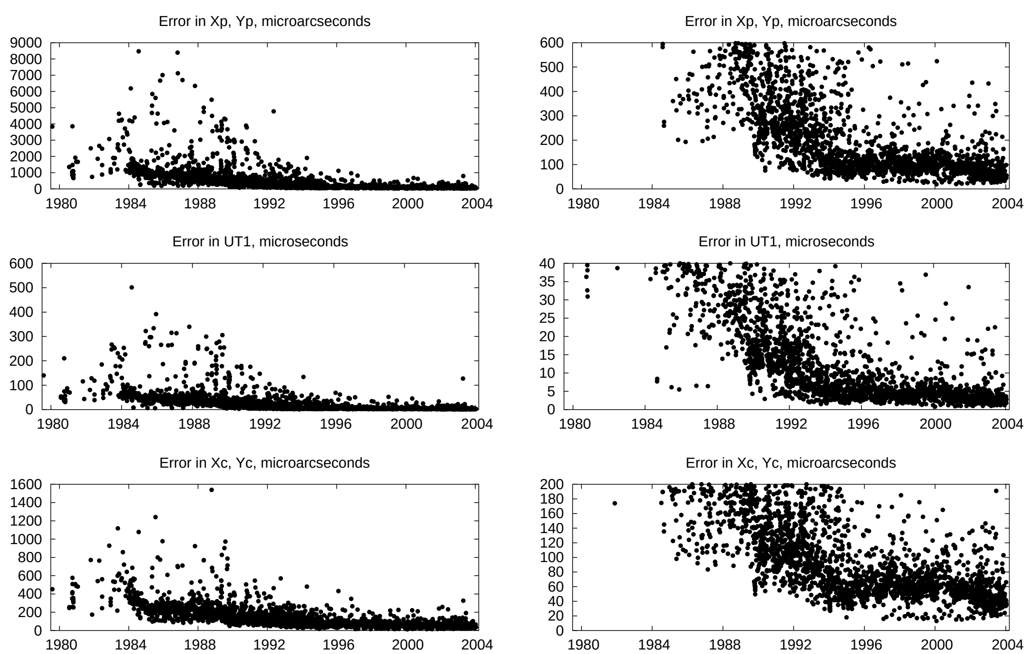

Figure 3. Errors in EOP (on the left are zoomed data). Each point corresponds to one 24h session. Note clear correlation with improvement in delay precision, and also with number of stations/baselines (Figure 2).

Page intentionally left blank

Session 2

VLBI 2010

Page intentionally left blank

John LaBrecque: The International Global Network of Geodetic Fiducial Stations, IVS 2004 General Meeting Proceedings, p.55–55
http://ivscc.gsfc.nasa.gov/publications/gm2004/labrecque

The International Global Network of Geodetic Fiducial Stations

John LaBrecque

Office of Earth Science/NASA

e-mail: John.LaBrecque@nasa.gov

Abstract

Scientific need and technological opportunity require that we move toward implementing a global network of geodetic fiducial stations which feature co-located SLR, VLBI, GNSS, and DORIS instrumentation. Earth science of the next decade will require more accurate global change measurements of sea level topography, sea level change, polar ice mass balance, hydrological and atmospheric mass flux, and topographic deformation, real time mm scale navigation and precision time transfer on a global scale. These scientific requirements have been translated into a goal of mm scale annual stability for the terrestrial reference frame, earth orientation parameters, as well as the orbit and clock determinations for the GNSS systems. To meet these challenges, the four geodetic observing systems must be more tightly integrated in technology, location, and analysis. NASA strongly supports the objectives of the IGGOS initiative vis NASA's National Geodetic Observatory and INDIGO programs. The global networks of GNSS, SLR, and VLBI observatories are for the most part poorly suited for these new demands. These important geodetic networks have evolved with little planning yet these systems are providing essential measurements to a wide swath of society. New signal structures in the GPS and the developing Galileo GNSS will soon require replacement of the GNSS receivers. The SLR network is poorly distributed globally, requires labor intensive observations and analysis, and for the most part relies upon antiquated technology. The VLBI observatories utilize large radio telescopes in remote regions that are poorly distributed globally. Co-location of these networks is sparse and co-location errors contribute significantly to the observing error spectrum. Increasing use of the S and X band by commercial and other government services will also contribute to increased observational errors. The time is upon us for an international effort to develop an optimized global geodetic fiducial network of twelve or more integrated automated geodetic observatories that will provide in near real time high density measurements of Earth orientation, geodetic positioning, and GNSS system monitoring. The strategic goal for the optimized global fiducial network should be efficient autonomous operation, real time data streaming to analysis centers with an integrated near real time analysis capability for all four observing systems. These goals are achievable in the next decade given the dramatic technological improvements in all geodetic systems. For VLBI, the BKG TIGO might be viewed as a preliminary prototype of technology for fundamental stations. Mark 5, PC-VSI, e-VLBI broadband development efforts are laying the groundwork to reduce the aperture of the VLBI antennas and to allow for precision mm level co-location of observing systems. Operating costs and enhanced accuracy would accrue from the elimination of hydrogen maser clocks using double differencing, GNSS time transfer technology, GHz broadband recording, real time analysis, and mm wavelength VLBI observations. A global geodetic fiducial network will not be realizable without international efforts and the support of the four services.

Ari Mujunen et al.: VLBI2010: Commercial-off-the-Shelf Techonology Perspectives in 1996, 2003, and 2010, IVS 2004 General Meeting Proceedings, p.56–59
http://ivscc.gsfc.nasa.gov/publications/gm2004/mujunen

VLBI2010: Commercial-off-the-Shelf Techonology Perspectives in 1996, 2003, and 2010

Ari Mujunen, Jouko Ritakari

Metsähovi Radio Observatory, Helsinki University of Technology
Contact author: Ari Mujunen, e-mail: Ari.Mujunen@hut.fi

Abstract

In the VLBI2010 session we are trying to predict the world a mere seven years in the future. In these seven years the infrastructure in computing and data communications will change more than anybody realizes now. We can get some insight about the rate of change by looking back seven years into year 1996. At that time microcomputers had 133MHz processors, 16MB of main memory and the largest hard disk was 2GB. Mainstream networking technology was 10Mbit/s Ethernet, the first 100Mbit/s equipment was starting to arrive. Global Internet connections were typically 155Mbit/s at their best. Now we have 3GHz processors (22 times improvement), 1GB main memory (62 times more), 200GB hard disks (100 times larger) and 1Gbit/s Ethernet networking (100 times faster). Internet backbone networks routinely use 10Gbit/s connections (66 times faster). If the trend continues, in 2010 we will have 66GHz processors with 60GB main memory and 20TB hard disks. Networks will work at 100Gbit/s speeds. Global connectivity will be available at 660Gbit/s. Of course these numbers are wrong in details, but it is better to use them than to think in terms of today's technology. It is imperative that we do our development work as fast as the computer industry and we must accept that at least one generation (possibly two) of VLBI equipment will become totally obsolete before we reach 2010.

1. Introduction

Historically, custom-designed VLBI data acquisition and data processing (correlation) equipment have enjoyed the status of bleeding-edge technology that no other data processing application area has matched in capacity nor in speed. The continuous advances in general-purpose data processing technology have, however, started to match and/or surpass the capabilities of specialized VLBI equipment.

It is not easy to recognize and comprehend the speed of mainstream technology development, mainly because it is far too easy to overestimate advances in the near future and far too easy to underestimate the development in a longer timescale. In this paper, an attempt is made to predict the level of impact of mainstream technology developments in the scale of seven years from today. The perspective is sought by seeing back into the past seven years from today. The scale of plus/minus seven years is apparently long enough to prevent "short-sightedness" of the true impact of continuing, exponential speed and capacity growth which can easily be seen in every major area of mainstream data processing technology development. Several key areas are being illustrated in Figure 1.

2. Disk Development

The backbone of VLBI data acquisition and processing, acquiring and storing RF data arriving from a sky source at real time, relies exclusively on high-rate, vast-capacity data media. Traditionally, this has been magnetic tape. However, the protected nature of encased magnetic disks has made it easier to enhance the data densities of magnetic disks much further than the data density of magnetic tape. At the same time, the market demand for high-capacity fast disks in the general PC market has increased the volume of hard disk shipments, making it economically viable to invest in developing faster and larger hard disks. As a result of this trend, the hard disks surpassed the general-purpose magnetic tapes (geared at data backup applications) years ago, and at this very moment they are quickly surpassing the capabilities of specialized VLBI magnetic tapes.

The largest standard hard disks of desktop PCs were 2GB in size in 1996. In 2003 we could easily buy 200GB hard disks for regular desktop use. Projecting this to 2010, we can expect standard form-factor hard disks to reach 20TB sizes, with the imminent increase in data transfer speed accompanying the capacity increase. The predictions of hard disk industry in [1] are actually even more optimistic, stating areal bit densities of 1Tb/in^2 by 2010.

What this means to VLBI is that by 2010, every general-purpose desktop PC is capable of recording and storing hours of multi-Gbps VLBI data onto its standard hard disk drive. (20TB is approximately 44 hours of 1Gbps data.) Intermediate buffering of acquired VLBI data will be a non-issue and it can be performed at will as required, not limited by hardware or economical boundary conditions.

3. Networking Development

Transporting VLBI data acquired at participating observing stations to be correlated has been—this far—the second major bottleneck in VLBI operations. Physical shipment of media has been the only viable option but this is being changed by global high-speed networks.

In 1996 the mainstream local area networking technology was 10Mbit/s Ethernet; correspondingly, global Internet connectivity was available at the 155Mbit/s ATM level. In 2003, LANs are quickly migrating to 1Gbit/s Ethernet and the global Internet commonly has 10Gbit/s backbone connections available. This 100x development predicts 100Gbit/s LANs and 660Gbit/s backbone connections in 2010 which greatly surpasses the VLBI transport demands and effectively eradicates the need for physical media shipments. (Transferring one 20TB hard disk (44 hours of 1Gbps data) over a 100Gbit/s connection takes less than half an hour.)

4. Processor Development

Perhaps the most astonishing advances have been made in semiconductor technology and especially in the area of computer CPUs. The desktop processors of 1996 performed at the level of 53 million instructions per second and with 133MHz clock rate. [2] Today in 2003, 3GHz processors routinely crunch 6 billion instructions per second, effectively 113 times faster. Combined with main memory and bandwidth developments this has made it feasible to perform VLBI correlation entirely in software of general-purpose computers. The processors of 2010 will have the processing power of "66 GHz" CPUs with 678 billion instructions per second.

Currently, software correlators can process in the range of 64–128 megasamples per second of a few baseline data in real time. (The exact estimation formulas are shown in [3].) A network of 10 observing stations could correlate the 45 baselines at 1Gbps in real-time using approximately 8 PCs per station. This takes maximum advantage of time-sliced FX architecture where delay tracking, fringe rotation, cross-correlation, and integration consume less Gflops than the initial FFTs—which only need to be calculated per-station and can be "re-used" for all baselines, thus avoiding "baseline explosion".

The architecture where an experiment is divided in time equally to all participating stations to be correlated results in well-balanced full-duplex network traffic. The large main memories make it easy to keep data of a given time slot from all stations in main memory. As a whole, the stations only need $(n-1)/n$ times the disk buffering capacity that they need for their own data to be able to correlate all stations of $1/n$ time of the experiment.

5. VLBI-Specific Hardware Development

Historically, the VLBI data acquisition systems have been constrained by the recording system, thus less emphasis has been put into sampling bandwidth or receiver RF bandwidth. VLBI receivers have had less than 500MHz of RF bandwidth in each frequency channel and this has been largely unchanged since 1978. The last time DAR sampling bandwidth has increased was in 1996 when the Mark IV formatter was introduced with 2048Mbps sampling capability. The previous doubling occurred in 1989 when the VLBA DAR featured 1024Mbps samplers.

Advances in semiconductor technology, especially in high-speed A/D converters, cellular base station RF components, and digital FPGAs all contribute to the fact that it will be increasingly easy to increase the sampling bandwidth using direct IF sampling and digital signal processing and filtering techniques. Thus we will quickly collide into the RF bandwidth limitations of VLBI receivers—2Gbps takes care of the whole 500MHz at two bits per sample.

6. Conclusions

Using short timescales (1–2 years) to estimate technology capabilities can lead to the false impression that "technology at first advances just a little bit and then all development stops." When designing VLBI2010 equipment, falling into this trap would lead to designs which cannot keep pace with the advances in mainstream technology.

In the areas of data storage, networking, and processing speed it is likely that mainstream technology will easily satisfy and surpass VLBI requirements before 2010. It is unclear if VLBI-specific technology (samplers, receivers) can be developed quickly enough to match this capacity increase of COTS devices.

References

[1] Maxtor Corporation, Areal Density Chart, `http://www.maxtor.com/en/images/technologies/add.gif`

[2] van Dorst, Wim, WvD@clifton.nl, `http://www.linux.org/docs/ldp/howto/BogoMips.html`, v34, 2003-08-07, jubilee edition, 2003.

[3] Moritaka Kimura, Junichi Nakajima, Hiroshi Takeuchi, and Tetsuro Kondo, 2-Gbps PC Architecture and Gbps data processing in K5/PC-VSI, In: Technology Development Center News, Communications Research Laboratory (CRL), Serial No. 23, Kashima Space Research Center, Tetsuro Kondo and Yasuhiro Koyama (eds.), 12–13, November 2003.

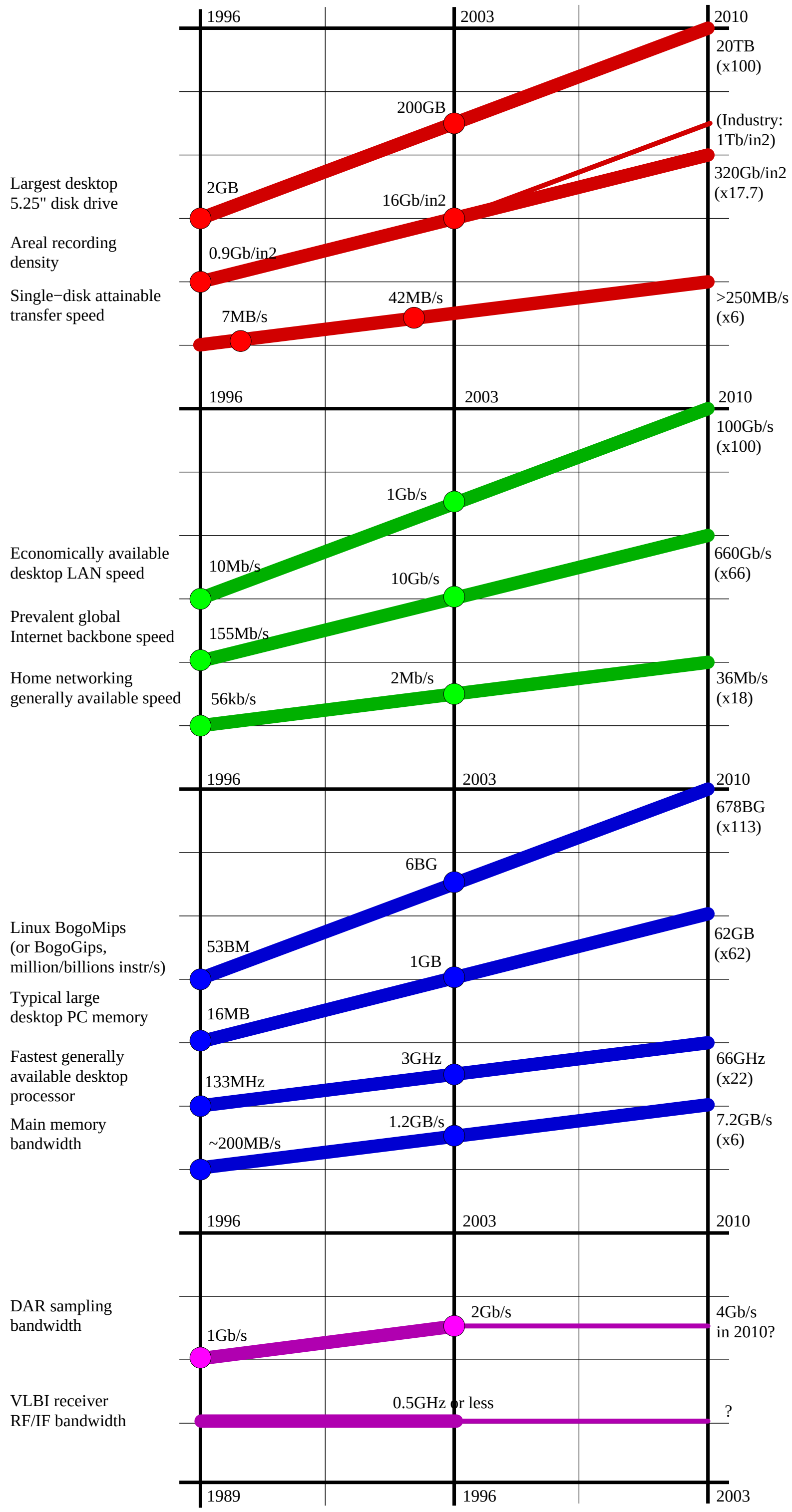

Figure 1. Several key COTS trends in 1996..2010.

Bill Petrachenko et al.: VLBI2010: Networks and Observing Strategies, IVS 2004 General Meeting Proceedings, p.60–64
http://ivscc.gsfc.nasa.gov/publications/gm2004/petrachenko

VLBI2010: Networks and Observing Strategies

Bill Petrachenko [1], Brian Corey [2], Ed Himwich [3], Chopo Ma [4], Zinovy Malkin [5], Arthur Niell [2], David Shaffer [6], Nancy Vandenberg [3]

1) *Natural Resources Canada*
2) *MIT Haystack Observatory*
3) *NVI, Inc./Goddard Space Flight Center*
4) *NASA/Goddard Space Flight Center*
5) *Institute of Applied Astronomy*
6) *Radiometrics, Inc.*

Contact author: Bill Petrachenko, e-mail: `Bill.Petrachenko@nrc-cnrc.gc.ca`

Abstract

The Observing Strategies Sub-group of IVS's Working Group 3 has been tasked with producing a vision for the following aspects of geodetic VLBI: antenna-network structure and observing strategies; source strength/structure/distribution; frequency bands, RFI; and field system and scheduling. These are high level considerations that have far reaching impact since they significantly influence performance potential and also constrain requirements for a number of other WG3 sub-groups. The paper will present the status of the sub-group's work on these topics.

1. Introduction

The formation of Working Group 3: VLBI2010 was motivated by: 1) deficiencies of the current system, e.g. aging electronics and antennas, growing S-band interference, sub-optimal networks, etc; 2) advancing requirements in terms of accuracy, duty cycle and timeliness; and 3) recognition that the cost of currently planned operational modes is not sustainable indefinitely. Early indications are that WG3 is considering a bold vision for the future. For the first time in history, the geodetic VLBI community is contemplating the specification of an internationally funded global "instrument" for the establishment and maintenance of geodetic reference frames.

In order to constrain the scope of this discussion, it will be helpful to begin by looking at future accuracy requirements of geodetic VLBI. The most strict requirements typically come from scientific applications where it is generally agreed that long term accuracy of geodetic reference frames will be needed at the level of 1mm or below. Since WG3 is looking a decade or more into the future, it would be prudent to aim for accuracies significantly below the 1mm level so that its recommendations don't become prematurely obsolete. In addition, it is generally agreed that observations of EOP are required continuously.

What does 1mm accuracy mean in terms of the primary geodetic VLBI observable, the delay? In terms of systematic error, the answer is clear. If you want to guarantee unbiased long term accuracy below the 1mm level, then the sum total of all systematic contributions to delay must be below 3ps (1mm equivalent light travel). It goes without saying that this is a daunting task. With respect to random measurement error, the answer is less clear-cut since the connection between delay precision and baseline precision involves complex interactions that include elements such as network size and geometry, the observing schedule, etc. However, a rough idea of the requirement was obtained by scaling the post-fit residuals of a typical R1 experiment by the ratio of the achieved R1 baseline precision relative to a target precision of 1mm. After applying some reasonable assumptions regarding added contributions due to maser and atmospheric instability, precision for delay of about 4 ps per observation was estimated.

WG3 has been divided into 7 sub-groups. This is the progress report of the Observing Strategies Sub-group. The topics assigned to this sub-group for consideration are:

- antenna-network structure and observing strategies
- source strength/distribution/structure
- frequency bands, RFI
- field system and scheduling

2. Antenna-Network Structure

Currently, there are 27 IVS network stations. Of these, 9 are in Europe, 6 in Japan and 5 in North America, leaving 7 for the rest of the globe. Many of the antennas currently in use were acquired on an "as-is where-is" basis and hence their location and performance were not optimized for geodesy.

2.1. Network Geometry

How can network geometry be improved?

First, since scale and orientation of geodetic reference frames are aggregate parameters, i.e. they are determined by making measurements at a number of stations, having more stations will in general improve the result.

Second, a more uniform distribution of stations will help, e.g.: 1) It will add to the geometric strength of adjustments. 2) If at least three stations are located on each major plate, an independent VLBI TRF can be defined. Since VLBI baseline solutions begin to deteriorate for lengths greater than about 6000km (due to lack of common sky visibility), a final constraint should be added that neighboring stations never be separated by more than 6000km.

Finally, it is worth remembering that an important asset of geodetic VLBI is the twenty years of uninterrupted data. In order to maintain and enhance this asset, these data sets should be carefully continued into the future. Consequently, as many of the new stations as is practical should be co-located at existing sites.

Reducing station capital and operating costs will make it easier to significantly increase the number of geodetic VLBI sites. In this regard, recent advances have been made in reducing the cost of small to moderate size antenna systems, e.g. the Allen Telescope Array. When this is coupled with new low cost disk recording systems and digital data acquisition systems (DAS), the potential exists for a breakthrough in the cost of geodetic VLBI stations.

2.2. Site Selection and Station Design Criteria

Achieving millimeter and submillimeter accuracy will require attention to detail. An exhaustive list of site selection and station design criteria will help minimize site related systematic errors.

With respect to **site selection** criteria, important examples might include: benign tropospheric conditions, good horizon mask; geological stability; accessibility of bedrock; lack of local interference; proximity to other fundamental geodetic measurements; etc.

With respect to **station design** criteria, important examples might include: ease and accuracy of site ties; fast slew rates; low elevation capability; well understood thermal and gravity deformations; interference tolerance; adequate sensitivity; stable and accurately calibrated electronics; etc.

It is likely that significant performance and operating benefits will result from using an identical station design at each site.

2.3. Multi-Beam VLBI

The ability to observe more than one source at a time may have advantages, e.g.: 1) The clock contribution to the delay observable will disappear in the differenced data. 2) It may allow more scans per day. 3) It may allow more than one type of observation to be made at a time, e.g. CRF simultaneous with EOP. In the past, although the benefits of multi-beam VLBI have been appreciated, it has never been implemented due to the high cost of antennas. The recent reduction in cost of high performance small to moderate size antennas, e.g. those of the Allen Telescope Array, may make this option worth reconsidering.

2.4. Site Ties

The integration of all space geodetic techniques is becoming increasingly important. Efficient determination and maintenance of accurate site ties is necessary for effective inter-technique integration. It also allows local movements of the antenna structure and pier to be separated from large scale geologic movements.

Recently, a novel approach has been proposed to improve local ties [Y. Koyama, unpublished]. The position of a small nearby antenna relative to the larger VLBI antenna can be accurately established using connected element interferometry. Since the antenna is small, if designed properly, very accurate ties could be established between it and the local monumentation. Perhaps the process can even be automated. The small antenna could also be used to verify thermal and gravitational deflection models of the large antenna.

2.5. Sensitivity

Increased sensitivity has a number of benefits: 1) The precision of the delay observable increases proportionately. 2) Shorter scans can be used (which is an important element in acquiring more scans per day). 3) System performance can be evaluated more readily. 4) Weaker sources can be observed.

In general, sensitivity is defined based on the weakest source that needs to be observed and the minimum SNR required per observation. Unfortunately, it also comes at a price. Sensitivity is a function of antenna diameter, antenna efficiency, system temperature, bandwidth and integration time. The impact on antenna diameter is of particular interest since antenna cost increases approximately as the cube of the diameter. Making an informed trade-off between sensitivity and antenna diameter will have significant impact both on system cost and future performance potential.

3. Observing Strategies

The IVS delivers global geodetic scale and orientation by contributing to the ITRF, ICRF and EOP through a series of observation types, each optimized for its own specific purposes. This somewhat complex strategy does a good job of making the best use of available resources. However, it requires compromises which limit performance.

For example, the VLBI contribution to the ITRF is established primarily through a series of 8-station observations in which certain core stations are observed repeatedly while the rest are added cyclically. Clearly, observing all stations simultaneously would provide a more robust result. This is currently not possible because of the limited number of inputs to existing correlators. Although the goal of using all available stations simultaneously will not happen immediately, the situation may improve in the not too distant future. All Mark IV correlators were built as 16-station correlators, but they have been equipped with only seven to nine station inputs. With the introduction of the much lower cost Mark 5B to replace both the Mark IV playback system and station unit, the input from all sixteen stations should be affordable.

There are also compromises with respect to the measurement of EOP. For example, the full set of EOP is only quaranteed to be determined twice per week. Although UT1-UTC is determined an additional 5 times per week using short 2-station observations referred to as the Intensives, it would be better to determine the full set of EOP daily and continuously. This is currently not possible due to a lack of station availability. In addition, larger and better distributed networks would make EOP more robust and improve the connection to the ITRF. Unfortunately, increasing network size puts further stress on station availability. This situation is not likely to improve without adding a number of VLBI stations dedicated to geodesy and designed specifically to be operationally efficient, e.g. robust and capable of unattended operation.

Because ITRF and EOP on the one hand, and ICRF on the other, have quite different observational requirements, the challenge for the future will be to find a way to optimally determine all three. A number of interesting scenarios have been considered, but more work will be required before the full range of possibilities can be explored and final contenders proposed.

4. Source Strength/Distribution

As source strength decreases, the number of visible sources increases rapidly. Having more sources available makes it possible to be more selective with respect to the source's positional stability and lack of structure. It also allows better optimization of schedules since it is more likely that a source can be found in a specified target region.

5. Source Structure

As the precision of geodetic VLBI moves into the submillimeter range, it will be necessary to review the contribution that source structure makes to the error budget. Two approaches can be taken with regard to minimizing the effect of source structure. First, an attempt can be made to select only sources with minimal structure. This is the approach taken today. In this regard, it is worth noting that weaker sources tend to have less structure and that sources tend to have less structure at higher frequencies. If required, a second, more labour intensive approach involves actively monitoring source structure and correcting for it.

6. Frequency Bands

Troublesome S-band interference and the move by the NASA Deep Space Network (DSN) from S/X band to X/Ka band are motivating a review of the frequency allocations used for geodetic VLBI. Regardless of which bands are selected, it is clear that a large separation (greater than a factor of 2) is required between the highest and lowest frequencies to effectively calibrate the ionosphere. Reasons have been proposed for frequency coverage all the way from L-band to Ka-band.

There is interest in L-band because it will allow observation of GNSS satellites (GPS, Glonass, Galileo). Direct comparisons can then be made with the GNSS, and observational access to the geocenter by VLBI may be possible.

Observations at S/X band will allow the continuation of the 30-year history of CRF in those bands.

Observations at X/Ka band is attractive because sources tend to have less structure at higher frequency, there is less interference at those frequencies, and the wider bandwidths will allow more precise group delay determinations. Ka-band observations will also support the CRF requirements for planetary navigation of spacecraft by NASA. On the negative side, sources tend to be weaker at Ka-band and everything technological is more difficult, e.g. antenna surface accuracy, support structure and pointing, coherence, etc.

Frequencies near the 22 GHz water vapour line are interesting because they may enable line-of-sight calibration of water vapour content.

More dense frequency coverage may be desirable to allow phase delay determination at moderate SNR. Phase delay is typically about an order of magnitude more precise than group delay.

7. RFI

In this communications intensive world, it is almost certain that problems with RFI will intensify. As a result, it is important for geodetic VLBI to develop a strategy to minimize the impact of RFI.

To begin, it makes sense to avoid spectral regions which are a problem everywhere on Earth, e.g. commercial satellite downlink and broadcast allocations. Fortunately, with these removed, there are still significant spectral regions available, e.g. 2.69 to 3.4 GHz, 4.8 to 6.7 GHz, 7.75 to 10.7 GHz, 12.75 to 17.3 GHz, and 22.0 to 37.5 GHz.

Next, when VLBI sites are being selected, low local interference can be set as a criterion. Sites should typically be located away from large urban areas, airports, military installations, communications repeaters, satellite ground stations, etc. Once a good site has been found, working with local regulatory agencies can ensure that within reasonable limits the low RFI situation will continue into the future.

Finally, the frequency structure used and the DAS design should be robust against RFI. For example, 1) Frequency structures that depend on critically spaced narrow channels should be avoided since RFI can cause serious degradation if even one of the channels is compromised. 2) The DAS should be designed such that only the frequencies affected by RFI will be degraded and not entire broad-band channels.

Hayo Hase et al.: Preliminary Results of the VLBI2010 Subgroup "RF/IF, Frequency and Time", IVS 2004 General Meeting Proceedings, p.65–69
http://ivscc.gsfc.nasa.gov/publications/gm2004/hase1

Preliminary Results of the VLBI2010 Subgroup "RF/IF, Frequency and Time"

Hayo Hase [1], *Brian Corey* [2], *Yasuhiro Koyama* [3], *David Shaffer* [4], *Bill Petrachenko* [5], *Wolfgang Schlüter* [6]

1) *BKG - TIGO*
2) *MIT Haystack Observatory*
3) *CRL - Kashima*
4) *NVI Inc.*
5) *Natural Resources Canada*
6) *BKG - Wettzell*

Contact author: Hayo Hase, *e-mail:* hayo.hase@bkg.bund.de

Abstract

This subgroup discusses how a future VLBI systems should be designed with respect to the problems of existing RFI, the existence of new antenna concepts, the developments of high speed samplers, and the demands for high frequency stability of the reference oscillator. The current status of the discussion is presented in a shortened form.

1. Goals and Limits

Based on the Charter for the IVS Working Group 3 "VLBI2010" [1] this subgroup was examining the future requirements for VLBI geodetic systems focussing on the observed spectra (RF), the signal conversion (IF), the observing instruments (antennas) and its scaling versus time (T&F).

The Charter requests *"highest-precision geodetic and astrometric results"* as a goal. Also the IAG Project of the Integrated Global Geodetic Observing System (IGGOS) in which VLBI will be an important contributor demands the transition from global geodetic measurements to approach in the coming years millimeter precision.

A precision of 1 millimeter in the space domain corresponds to only 3 picoseconds in the time domain. These values should be achieved as design goals for the VLBI2010 vision.

The technical realization of a VLBI observing system introduces another characterizing quantity: the signal-to-noise-ratio (SNR), which finally determines whether or not an observation comes out successfully from the correlation process.

Limiting factors in geodetic and astrometric VLBI are: a. *atmosphere*, b. *radio frequency interference*, c. *instrumentation.*

2. Atmosphere

The propagation of electromagnetic radiation from the radio source to the antenna is affected by a. interstellar and interplanetary plasmas, b. the ionosphere, c. the neutral atmosphere, including tropospheric water vapor.

The largest impact on geodetic measurements is caused by the variability of water vapor in the troposphere and of the electron content in the ionosphere; both vary up to several nanoseconds (S-/X-band).

The idea of eliminating the atmospheric delay requires path length correction based on additional information from other sensors, like humidity sensors and water vapour radiometers. While the humidity sensors are ground based and not very representative of the signal path, the water vapour radiometers even used coaligned to the radio telescope targeting axis did not fulfill their expectations yet, because of the relatively wide beam compared to the narrow beam of the radio telescope. Promising investigations at 183GHz show that it is possible to determine at a high and dry site like Mauna Kea using the primary optics the atmospheric path lengths with an error of 0.2ps [2].

VLBI2010 conclusion: Water vapor radiometry should be further developed and become an integral part of the VLBI2010 system.

The ionospheric delay scales as the inverse of the observed frequency squared. E.g., at observed frequency of 2GHz the ionospheric excess equals the tropospheric excess; thus at 20GHz the ionospheric excess is only about 1% of the tropospheric one. Hence the effect of ionospheric delays is below a few picoseconds at frequencies above 100 GHz ([3], p. 555).

VLBI2010 conclusion: RF below 100GHz must be at least dual-band for ionospheric correction.

3. Radio Frequency Interference

Today RFI is already a problem in the on-going VLBI operations, especially in S-band. RFI can be treated in two ways: avoidance of polluted spectral bands, using unpolluted spectral bands only, or treatment of RFI with mitigation technology.

Given the current situation the S-band needs a replacement with a higher frequency band, because at lower frequencies the situation is worse. S-band was basically needed to do the ionospheric calibration of the X-band observations, on which nowadays the ICRF with its 20 years of recorded data is based.

VLBI2010 conclusion: S-band needs to be replaced by another spectral band, ideally higher than X-band.

Candidate spectral bands are listed in table 1.

Table 1. Existing S/X-band parameters and those of the candidate spectral bands to replace S-band.

Name	ν-range	λ-range
S	2 - 3 GHz	15 - 10 cm
X	8 - 10 GHz	4 - 3 cm
Ku	15 - 17 GHz	2 - 1.75 cm
K	22 - 24 GHz	1.4 - 1.25 cm
Ka	30 - 32 GHz	1.0 - 0.9cm

4. Instrumentation

The instrumention of a VLBI system is defining the geodetic reference point in space and time. The instrumentation is characterized by the achievable signal-noise-ratio.

$$SNR = f \cdot V \cdot \sqrt{\frac{T_{a_1} \cdot T_{a_2}}{T_{s_1} \cdot T_{s_2}} \cdot 2\Delta\nu \cdot \tau} \tag{1}$$

The higher the SNR the lower the errors of the correlation output signal, thus the higher the precision. From (1) it can be seen, that a high SNR can be achieved by a. efficient antennas (T_a), with b. small system temperatures at each site (T_s), c. high sample rates ($2\Delta\nu$) and d. high number of bitquantization (f), long integration time intervals (τ).

VLBI2010 conclusion: New technology promising higher SNR has to be considered in future instrumentation.

4.1. Antenna

Desirable improvements in geodetic VLBI can be achieved by multibeaming in a GPS-like fashion. More data per time unit of different sources will enable a subhourly resolution of Earth-orientation variation - one of the IVS goals. The status quo of geodetic VLBI is based on the concept of monolithic radio telescopes observing sequentially source by source. Observing two or more sources simultaneously can be done in a differential or non-differential mode.

The non-differential mode allows observing more than one source per time unit with larger angular separation simultaneously. This type of observation will be made under almost the same atmospheric conditions and if connected to same frequency standard depending on the same clock modelling. If differenced the dependency on the reference oscillator cancels out.

VLBI2010 conclusion: Multibeam observations in non-differential mode are desired.

Multibeam observations can be made by one antenna with many receivers or many antennas with one receiver each. The ongoing radioastronomical projects like *Square Kilometer Array (SKA)* and *Atacama Large Millimeter Array (ALMA)* are examples for future antenna installations.

The phased array concept looks attractive compared to the monolithic concept: a. sensitivity depends on the number of elements per site and can be easily increased in upgrades; b. splitting the array allows differential measurements by multibeam observations, which allows the cancelation of some equipment errors and reduction of the atmospheric delay, if antenna observation direction are close enough to sample the same part of the atmosphere; c. elements can be smaller and products of mass production. Disadvantages of the array concept are: a. the replacement of one geodetic reference point at the intersecting axes of a monolithic radio telescope by n reference points at each dipol of the elements; b. the requirements for the calibration of path lengths multiple by the number of n-elements.

VLBI2010 conclusion: Multibeam observations should be realized by multiple antennas capable at 8-40 GHz with sufficient directivity.

VLBI2010 conclusion: Antenna construction must allow installation of complementing sensors like WVR and GNSS receivers.

4.2. HF-Components

The characteristics of the feed are defined by the selected RF (table 1). Log periodic pyramidal feeds and wide band amplifiers allow continous RF bandwidth over ranges up to 10GHz. Those feed's focal point varies with frequency, but as VLBI is a differential technique the difference between two antennas at one specific frequency will be constant and should disappear in the clock offset. Another difference to existing S-/X-band feeds is their linear polarization, which requires observing both circular components or rotating the feed during observing.

VLBI2010 conclusion: New feeds and wide band amplifiers enable observing the entire spectral bandwidth, which have previously been spanned by bandwidth synthesis.

The need of a phasecal system is questionable if the entire spanned bandwidth is sampled. Bandwidth synthesis requires a phasecal system in order to compensate for different instrumental delays and to align the phase in the correlation process. As a diagnostic tool at least the phasecal system is indispensible.

VLBI2010 conclusion: Phase calibration systems are needed in coming systems, not to exclude the possibility of bandwidth synthesis.

Delay calibration systems measure the delay due to temperature variations during the 24h cycle between front and back end. Even if data may be processed at the front end, there remains a need to measure cable delays between the frequency standard and the involved phase calibrators.

VLBI2010 conclusion: Delay calibration systems continue to be necessary.

If new generations of uncooled low-noise-amplifiers have lower system temperatures than the cooled one, the maintenance of cryogenic cooling systems becomes superfluous. However precise hot and cold loads for radiometric purposes may be realized by a temperature controlled environment.

VLBI2010 conclusion: Any design should concentrate on minimizing the noise temperature of the front end, especially the LNA.

4.3. Samplers

Classical VLBI has used mostly one-bit sampling. In most cases of recording VLBI, the limit is given by the rate at which data can be stored (or transmitted) at a maximum sustainable bit rate. One-bit (two level), two-bit (4 level), and three-level data sampling (with 5 samples stored in 8 bits) can be used for VLBA observing. All three sampling schemes produce almost the same sensitivity for bit-rate limited observing - which continuum (and geodetic) VLBI will be for the foreseeable future ([3], p. 272).

If we consider as an example a continous RF band from 8-24 GHz, the whole 16 GHz bandwidth were 2-bit Nyquist sampled, then the output data rate per site would be 64 Gb/s. Right now, the maximum practical record rate is 1 Gb/s. We are faced with trying to synthesize a 16 GHz bandwidth using a record rate of a few Gb/s. This cannot be done without using some form of bandwidth synthesis.

VLBI2010 conclusion: Bandwidth synthesis has a future, also in the light of broadband sampling.

There are three ways of doing bandwidth synthesis: a. *Sparse in Frequency.* This is what is done in the Mark III/IV/5. It requires a large number of comparatively narrow bandwidth channels each with its own baseband converter and sampler; b. *Sparse in Time.* In this approach, the fully sampled 16 GHz bandwidth is acquired in bursts using a duty cycle that allows the rapidly sampled data to be sent to the recorders at a much lower rate commensurate with the capability of the record device; c. *Frequency Switching.* In this approach, there is only a single channel, but it can be used to select any portion of the entire 8-24 GHz input RF bandwidth. By cycling through all possible frequencies in sequence, the entire RF band could be acquired (S2). This approach is economical in hardware and is just as robust against RFI as the *sparse-in-time* method.

VLBI2010 conclusion: Frequency switching capabilities are not contradictary to the sparse-in-frequency approach. Several channels with frequency switching allow flexibility.

VLBI2010 conclusion: One- or two-bit sampling IF should enter the correlator. RFI mitigation might require a higher bit quantization at the front end.

4.4. Frequency Standards

1 mm spatial precision depends on the clock offset to be known better than 3 ps. Between remote stations no time transfer allows this accuracy so far.

VLBI2010 conclusion: Better apriori station synchronization should be realized.

VLBI2010 conclusion: The primary reference oscillator should have an Allen variance better than 10^{-15}.

References

[1] Whitney, A., Niell, A.: Proposal to the IVS Directing Board for IVS Working Group 3: VLBI2010, 29.09.2003, http://ivscc.gsfc.nasa.gov/WG/wg3/vlbi2010_charter.doc

[2] Wiedner et al: Ap. J. 553, pp. 1036-1041, 2002

[3] Thompson, A.R., Moran, J.M., Swenson, G.W.: Interferometry and Synthesis in Radio Astronomy, John Wiley & Sons, Inc., 2nd ed., 2001

C.S. Jacobs et al.: Standard Observing Bands: Is Now the Time to Replace S/X with X/Ka?, IVS 2004 General Meeting Proceedings, p.70–74
http://ivscc.gsfc.nasa.gov/publications/gm2004/jacobs2

Standard Observing Bands: Is Now the Time to Replace S/X with X/Ka?

C.S. Jacobs, G.E. Lanyi, C.J. Naudet

Jet Propulsion Laboratory, NASA/Caltech

Contact author: C.S. Jacobs, e-mail: `Chris.Jacobs@jpl.nasa.gov`

Abstract

In this paper we will argue that the VLBI community should be developing a road map to transition from S/X to simultaneous X and Ka-band (32 GHz) observations. There are both negative and positive reasons for planning such a transition. On the negative side, we will outline concerns that S-band observations may be headed toward obsolescence. On the positive side, we will refer to evidence that X/Ka has potential for providing a more stable reference frame than S/X. We will propose timetables for a transition to X/Ka observing starting from the current status of X/Ka and plans that are now taking shape. First X/Ka fringes were obtained in 2001 with the Deep Space Network. Future plans will be discussed including a proposed X/Ka-band upgrade to the VLBA. Lastly, we will consider the need for a period of overlap between S/X and X/Ka so that the long and rich history of astrometric and geodetic VLBI is not compromised.

1. Introduction: the Motivation for Moving to X/Ka-Band

Has the time now come for the VLBI community to consider a new set of standard observing frequencies? We believe that it has. In the early 1970s astrometric and geodetic VLBI work was done at S-band (2.3 GHz). Starting in about 1978 astrometric and geodetic observations were done with simultaneous S (2.3 GHz) and X-band (8.4 GHz) observations thereby allowing one to directly calibrate plasma effects from the Earth's ionosphere and the solar plasma. This simultaneous dual band configuration has been the standard for over two decades during which time it has produced an ongoing stream of scientifically important results (*e.g.* Ma *et al.* 1998, Sovers, Fanselow, and Jacobs, 1998). Why then would one consider moving to a different set of observing bands?

There are a number of developments that are now converging to make the present time an opportune moment to consider moving astrometric and geodetic work to higher frequency bands. First, on the negative side, continued use of S-band is threatened by a radio environment which is increasingly cluttered by radio frequency interference. Second, there seems to be little chance that NASA will launch any more deep space missions that use S-band for telemetry. This is already starting to create pressure to remove S-band equipment from NASA's Deep Space Network (DSN). Both of these factors make it difficult to plan long range continuation of S/X observations for our VLBI program at JPL.

Prior to moving on to the positive motivations for moving to higher frequency bands, we would note that in recent years high frequency radio amplifiers at frequencies such as K (24 GHz), Ka (32 GHz), and Q-band (43 GHz) have become available for use by the VLBI technique. Thus it is no longer just a theoretical issue. It is now practical to make observations at these bands. These higher bands have potential for improved geodesy and astrometry to the extent that the sources become more pointlike and therefore less affected by both static source structure and the apparent proper motions induced by changing source structure. What might observers expect from moving from S/X to X/Ka-band observations? Initial evidence from K- and Q-band systems has confirmed our expectation that sources do indeed tend to become more compact at higher frequencies. The work of Boboltz *et al.* (2004, this volume) shows that sources are more compact—and therefore more astrometrically stable—at these frequencies than at X-band typically by a factor of a few. Thus there is potential for constructing references frames that are superior to the current S/X-based reference frames. These improved frames would provide improved calibrators for narrow field phase referencing work at higher frequencies.

Apart from any advantages for geodetic and astrometric work, the move to higher frequencies is being driven by the desire to achieve higher telemetry rates to interplanetary spacecraft (*e.g* Shambayati, 1999 & 2001). In particular, NASA has already started moving radio systems to Ka-band (32 GHz). The Cassini mission to Saturn is using Ka-band for radio science experiments (*e.g.* Perrot and Giordani, 1998) and the Mars Reconnaissance Orbiter, scheduled for launch in August 2005, is also being equipped with Ka-band. In addition to improving telemetry rates, the move to Ka-band will reduce the contribution of plasmas (*e.g.* Earth ionosphere and solar plasma) to the phase and group delay measurement error for single band spacecraft signals. Noting that plasma effects scale in inverse proportion to frequency squared, moving from X-band to Ka-band will reduce plasma related errors by a factor of ≈ 15.

Of course, most of the above reasoning applies to a greater or lesser extent to any frequency above X-band. So why choose Ka-band over other bands such as K-band or Q-band? Ka-band (32 GHz) is preferred over K-band (24 GHz) because it is further from the 22 GHz H_2O line; Ka-band is preferred over Q-band (43 GHz) because it is farther from the 60 GHz O_2 line. Thus the choice of the 32 GHz frequency band is an attempt to optimize atmospheric transparency. Extreme high frequencies such as W-band (86 GHz) were not chosen because of the difficulty of pointing large antennas at such high frequencies, the very short coherence time due to atmospheric turbulence (*e.g.* Linfield, 2001), and the uncertainty as to whether there are strong enough sources to be detectable within the shorter coherence times.

2. Game Plan

Having settled on Ka-band as the higher frequency band of choice, what is the plan for moving high accuracy astrometric and geodetic work to this band? While the VLBI community has taken 20 years to get S/X to its current accuracy, we expect that X/Ka-band must get to comparable accuracies in a much shorter time. Future spacecraft missions are expected to require sub-mas tracking accuracy within a few years. This is driving the need to start the process of building sub-mas reference frames at Ka-band. Yet, a full set of Ka-band antennas are not yet available. In fact, the first X/Ka-band VLBI fringe test is not scheduled until March 2004.

Because these constraints were anticipated, a plan was developed starting in 2001 (Jacobs *et al.*, 2002) to make use of then existing high frequency VLBI resources to learn as much as possible about source behavior at frequencies above X-band. The approach decided upon was to observe using the VLBA at K-band (24 GHz) and Q-band (43 GHz) in a mode that would allow both high accuracy astrometry and snapshot-based imaging. We assumed that the source properties at Ka-band (32 GHz) could then be obtained by interpolating between the 24 and 43 GHz results.

The interpolated results would then be used to determine the astrometric suitability of sources at Ka-band in advance of actual Ka-band observations. The goal in this initial stage of our plan was to learn whether there were a sufficient number of sources of sufficient strength to enable high accuracy reference frames to be built at Ka-band. Quantitatively, for spacecraft navigation applications, these goals imply a source with about 0.4 Jy or higher flux within $\approx 10^\circ$ of any point along the ecliptic plane in order to have easily detectable sources near any point along most deep space mission trajectories. The next section will briefly discuss the initial results which provide evidence that these goals are obtainable.

Our long term goal remains to move from simultaneous dual frequency S/X-band to simultaneous X/Ka-band observations. Toward that end, over the last several years, construction of X/Ka-band systems has been undertaken. Two antennas at Goldstone, California were equipped with X/Ka in 2001: DSS 13 and DSS 25. A third antenna, DSS 26, was made X/Ka ready in April 2003. The next antenna to be X/Ka equipped was DSS 55 outside of Madrid, Spain in late 2003. X/Ka capability is planned for Canberra, Australia's DSS 34 in the Spring of 2005, for Goldstone's DSS 24 in October 2006, and for Madrid's DSS 54 in August 2007. Thus there are seven antennas with X/Ka now in place or with firm plans to be so equipped within a few years.

3. Initial Observations and Results

While we envision gradually moving our focus away from single band K- or Q-band work to simultaneous X/Ka-band work, at present we must rely on the K- and Q-band results which are in hand in order to characterize the sources at high frequencies. Boboltz *et al.* (2004, this volume) and Jacobs *et al.* (2004, this volume) present the K- and Q-band results from the first two years of effort. The highlights of this work are that 230 K-band sources and 132 Q-band sources have been detected. Typically, the sources are a few times more compact at K-band than at X-band. These results indicate that there are enough strong sources to make pursuing X/Ka-band observations worthwhile.

In order to learn as much as possible as quickly as possible, short baseline tests at Ka-band have been done while the remaining parts of the long baseline system are being built. The first X/Ka-band fringes were obtained on 30 September 2001 on the 10 km DSS 13 to DSS 25 baseline within the Goldstone California tracking complex using connected element interferometry (CEI) [1]. We obtained usable group delays for 54 of 120 scheduled observations. The strongest Ka-band detection was for the source DA 55 for which the measured SNR was 166. This test confirmed that the receiving systems worked at Ka-band but that it was desirable to improve the antenna pointing—work which is currently underway.

We would also note that the group in Kashima, Japan has had a Ka-band system (31.7 GHz to 33.7 GHz) on its 34m antenna since about 2002 (Nakajima *et al.*, 2003). This system is advertised as having a 150 K system temperature. We have been exploring the potential for collaboration between the Kashima Ka-band system and the NASA Ka-band systems.

4. Future Plans

What is the next step toward broad use of X/Ka for astrometry and geodesy? Encouraged by the sucess of the so-called "RDV" sessions (*e.g.* Gordon, 2002; Sovers *et al.*, 2002) which use the VLBA at S/X, a dialogue has been initiated between NASA and the VLBA regarding the possibility of equipping VLBA antennas with simultaneous X/Ka-band systems. While it would be technically desirable to have all ten VLBA antennas equipped with X/Ka before the Mars Reconnaissance Orbiter scheduled launch in August 2005, there are no such plans yet in place.

There is, however, solid technical interest from NASA and VLBA representatives who have started initial estimates of cost and schedule. While for highest accuracy it is highly desirable to have simultaneous X and Ka-bands, detailed cost vs. benefit analysis for a single band Ka system vs. a simultaneous dual band X/Ka system remains to be completed. Issues such as feed design, the assignment of a space on the feed ring of the VLBA antenna, and Ka-band phase calibration generators are amongst the items needing further study.

5. Proposed Roadmap for S/X to X/Ka Transition

As discussed at the start of this paper, we see many potential benefits of moving high accuracy astrometric and geodetic work to X/Ka-band. However, we must at the same time retain the great value of over 20 years of proven S/X results (*e.g.* Ma *et al.*, 1998; Sovers, Fanselow and Jacobs, 1998). Thus it is highly desirable to have a period of overlap during which the accuracy of new X/Ka systems could be verified against existing S/X systems. This should include sufficient overlap of geodetic measurements to insure continuity of the VLBI based terrestrial frames. We suggest that 5-10 years of overlap would be a reasonable goal. We anticipate that by 2007 NASA's X/Ka systems will be mature enough to produce high accuracy astrometry and geodesy. Thus we suggest that the period of overlap would start around 2007 and last to at least 2012 and preferably to 2017.

6. Conclusions

We have presented the motivation for moving astrometric and geodetic observations from S/X to X/Ka-band. We have outlined a plan for establishing high frequency astrometry and geodesy starting with work at K- and Q-bands. This preliminary work has already extended the celestial frame to K-band (230 sources) and Q-band (132 sources) at the sub-mas level. Furthermore, interpolation of the these results suggests that similar results should be obtainable at the intermediate Ka-band. There are currently four antennas in NASA's Deep Space Network equipped with X/Ka-band with seven antennas expected by 2007. Kashima currently has a Ka-band system and the VLBA has begun study of proposals to install either Ka or X/Ka-bands systems in its antennas. Thus there is a potential for having as many as 18 Ka-band equipped antennas within a few years. First fringes have been obtained at X/Ka-band on a short baseline connected element interferometer and long baseline VLBI tests are planned for March 2004. All of these developments suggest that X/Ka-band VLBI is feasible.

We are optimistic about the future of X/Ka-band VLBI for astrometry, geodesy, and spacecraft tracking. We believe that there is great potential for a major step forward in these fields. Therefore, we encourage other VLBI groups to consider joining the move from S/X to X/Ka-band.

7. Acknowledgements

This research was done at the Jet Propulsion Laboratory of the California Institute of Technology under contract with NASA.

References

[1] Boboltz, D. A., Fey, A. L., P. Charlot, E .B. Fomalont, G. E. Lanyi, L. D. Zhang, & KQ VLBI Survey Collaboration, 'Extending the ICRF to Higher Radio Frequencies—Imaging Results', this volume.

[2] Gordon, David, 'RDV Analysis and Mark IV/VLBA Comparison Results', International VLBI Service (IVS) for Geodesy and Astrometry, 2002 General Meeting Proceedings, Tsukuba, Japan, February 4-7, 2002, Eds. Nancy R. Vandenberg and Karen D. Baver, June, 2002.
http://ivscc.gsfc.nasa.gov/publications/gm2002/gordon/

[3] Jacobs, C.S., D.L. Jones, G.E. Lanyi, S.T. Lowe, C.J. Naudet, J.A. Steppe, L.D. Zhang, J.S. Ulvestad, G.B. Taylor, O.J. Sovers, C. Ma, D. Gordon, A.L. Fey, D.A. Boboltz, P.Charlot, 'Extending the ICRF to Higher Frequencies', International VLBI Service (IVS) for Geodesy and Astrometry, 2002 General Meeting Proceedings, Tsukuba, Japan, February 4-7, 2002, Eds. Nancy R. Vandenberg and Karen D. Baver, June, 2002.
http://ivscc.gsfc.nasa.gov/publications/gm2002/jacobs/

[4] Jacobs, C.S., P. Charlot, E.B. Fomalont, D. Gordon, G.E. Lanyi, C. Ma, C.J. Naudet, O.J. Sovers, L.D. Zhang, and the KQ VLBI Survey Collaboration, 'Extending the ICRF to Higher Radio Frequencies: 24 and 43 GHz,' this volume.

[5] R.P. Linfield, 'Mounting a Water Vapor Radiometer on a DSN Antenna Subreflector: Benefits for Radio Science and Millimeter-Wavelength VLBI,' Telecommunications and Mission Operations Progress Report 42-145, Joseph H. Yuen, editor, Jet Propulsion Laboratory, Pasadena CA, 15 May 2001.
http://tmo.jpl.nasa.gov/tmo/progress_report/42-145/145M.pdf

[6] Ma, C., E.F. Arias, T.M. Eubanks, A.L. Fey, A.-M. Gontier, C.S. Jacobs, O.J. Sovers, B.A. Archinal, and P. Charlot, 'The ICRF as Realized by VLBI', AJ, 116, 1, pp. 516-546, July 1998.
http://www.journals.uchicago.edu/AJ/journal/issues/v116n1/970504/970504.html

[7] Nakajima, Junichi, Eiji Kawai, Hiroshi Okubo, Hiroo Osaki, 'Kashima 34m Radio Telescope,' in IVS 2002 Annual Report, N.R. Vandenberg and K.D. Baver, eds., p. 105, NASA/TP-2003-211619, Goddard Space Flight Center, Greenbelt, MD, Feb. 2003.
http://ivscc.gsfc.nasa.gov/publications/ar2002/nskashim34

[8] Perrot,B., and R. Giordani, 'Cassini Huygens Mission: the Exploration of the Saturn System. Radio Science Experiments: Radio Frequency Instrument Subsystem,' Planetary and Space Science, vol. 46, Issue 9-10, p. 1333-1338, Oct. 1998.

[9] Shambayati, S., 'Optimization of a Deep-Space Ka-Band Link Using Atmospheric-Noise-Temperature Statistics,' Telecommunications and Mission Operations Progress Report 42-139, Joseph H. Yuen, editor, Jet Propulsion Laboratory, Pasadena CA, 15 Nov 1999.
http://tmo.jpl.nasa.gov/tmo/progress_report/42-139/139C.pdf

[10] Shambayati, S., 'Maximization of Data Return at X-Band and Ka-Band on the DSN's 34-Meter Beam-Waveguide Antennas,' IPN PR 42-148, October-December 2001, pp. 1-20, February 15, 2002.
http://ipnpr.jpl.nasa.gov/tmo/progress_report/42-148/148E.pdf

[11] Sovers, O.J., J.L. Fanselow, & C.S. Jacobs, 'Astrometry & Geodesy with Radio Interferometry: Experiments, Models, Results', Rev. Mod. Phys., 70, 4, pp. 1393-1454, Oct. 1998.
http://xxx.lanl.gov/abs/astro-ph/9712238

[12] Sovers, Ojars J., Patrick Charlot, Alan L. Fey, David Gordon, 'Structure Corrections in Modeling VLBI Delays for RDV Data,' International VLBI Service (IVS) for Geodesy and Astrometry, 2002 General Meeting Proceedings, Tsukuba, Japan, February 4-7, 2002, Eds. Nancy R. Vandenberg and Karen D. Baver, June, 2002.
http://ivscc.gsfc.nasa.gov/publications/gm2002/sovers/

Christopher S. Jacobs et al.: Extending the ICRF to Higher Radio Frequencies: 24 and 43 GHz Astrometry, IVS 2004 General Meeting Proceedings, p.75–79
http://ivscc.gsfc.nasa.gov/publications/gm2004/jacobs1

Extending the ICRF to Higher Radio Frequencies: 24 and 43 GHz Astrometry

Christopher S. Jacobs [1], *Patrick Charlot* [2], *Ed B. Fomalont* [3], *David Gordon* [4], *Gabor E. Lanyi* [1], *Chopo Ma* [4], *Charles J. Naudet* [1], *Ojars J. Sovers* [1], *Liwei D. Zhang* [1], *KQ VLBI Survey Collaboration* [1]

1) *Jet Propulsion Laboratory, NASA/Caltech*
2) *Observatoire de Bordeaux – CNRS/UMR 5804*
3) *National Radio Astronomy Observatory*
4) *NASA Goddard Space Flight Center*

Contact author: Christopher S. Jacobs, e-mail: `Chris.Jacobs@jpl.nasa.gov`

Abstract

Celestial reference frames have been constructed at K-band (24 GHz) and Q-band (43 GHz) based on VLBI astrometric survey observations of active galactic nuclei. Five VLBA observing sessions covered the full 24 hours of right ascension and declinations down to $-44°$. K-band's 230 sources have median formal position uncertainties of 150 and 290 μas in $\alpha\cos\delta$ and δ, respectively; the corresponding uncertainties for 132 Q-band sources are 215 and 360 μas, respectively. K-band weighted RMS (WRMS) residuals were 33 ps and 48 fs/s in delay and rate, respectively. Comparison of the K-band frame to the S/X-band ICRF shows WRMS agreement of 330 and 590 μas in $\alpha\cos\delta$ and δ, respectively. The motivations for extending the ICRF to higher frequencies are to use more compact sources to construct a more stable frame, to provide phase calibrators, and to support spacecraft navigation at Ka-band.

1. Introduction

Early in the development of the Very Long Baseline Interferometry (VLBI) technique, it was recognized that observations of distant active galactic nuclei had the potential to form the basis of a quasi-inertial celestial reference frame with milli-arcsecond (mas) or better accuracy. In the 1990s, the IAU working group on reference frames created a consensus celestial reference frame known as the International Celestial Reference Frame (ICRF, *cf.* Ma *et al* (1998)) that realized this potential at S/X-band (2.3/8.4 GHz). It was appreciated then that extension of the ICRF to additional frequencies would further enhance the value of the work already done.

A number of developments have now converged to make the present an opportune time to pursue the extension of the ICRF to radio frequencies in the 24–43 GHz range. First, staying at S/X is increasingly threatened by S-band radio frequency interference. Second, low noise amplifiers at K (24 GHz), Ka (32 GHz), and Q-band (43 GHz) are now available for use by the VLBI technique. Third, Boboltz *et al.* (2004) present evidence that sources are more compact—and therefore more astrometrically stable—at these frequencies than at X-band. Thus there is potential for a frame that is superior to the current S/X-based ICRF. Fourth, radio systems for planetary probes are moving to Ka-band and are expected to require sub-mas tracking accuracy. Interpolating the K and Q-band results will provide initial constraints on astrometric suitability of sources at Ka-band thereby allowing one to build a roadmap for high accuracy spacecraft navigation at 32 GHz.

Our long term goal is to move from simultaneous dual frequency S/X-band to X/Ka-band. Ka-band allows for higher telemetry rates to spacecraft and reduces plasma errors by a factor of

≈ 16 compared to X-band. Eventually we will move our focus away from single band K or Q-band work to simultaneous X/Ka-band work. In the meantime, we must rely on K and Q-band results.

2. Observations

The results presented here are based upon five VLBA sessions: 15 May 2002, 25 August 2002, 26 December 2002, 22 May 2003, and 13 September 2003. The first two sessions observed the same set of 65 sources which was selected based on predicted compactness and strength of flux (typically > 0.7 Jy). The third session extended observations to weaker sources; the fourth session was a K-band only survey which nearly doubled the number of sources observed in that band; the 5th session returned to observing both K and Q-bands. Each source was observed with 3–5 snapshots, each of which used the entire array for 2 minutes at K-band and then 2 minutes at Q-band (except for session 4). This strategy was chosen to allow adequate uv coverage for simultaneous imaging while still permitting sub-mas global astrometry based on group delays over a 400 MHz spanned bandwidth. Recorded bandwidth was 128 Mbps. There were 36204 usable pairs of delays and rates which were fit with 1388 degrees of freedom. The VLBA is limited to U.S. territory by design. The longer baselines contribute proportionately more to the astrometric solution. The array has a greater East-West extent compared to its North-South extent. As a result, the VLBA produces better precision in right ascensions than declinations by a factor of ≈ 1.5.

3. Results

Data from our five sessions yielded a global reference frame of right ascensions and declinations for 230 K-band and 132 Q-band sources. The distribution of K-band sources is illustrated in Fig. 1. Note that: 1) Observations covered down to $\delta \approx -30°$ for sessions 1, 2, 3, and 5. Session 4 went down to $\approx -44°$. 2) Declination uncertainty systematically increases as one moves south. Q-band results are similar but with $\sigma_\delta \approx 1.5$ times larger than at K-band due to lower SNR.

When the minimal 3 coordinates are held fixed in order to set the frame orientation, the solution for the right ascensions and declinations yields median formal K-band position uncertainties of 149 and 290 μas in $\alpha \cos\delta$ and δ, respectively. The solution used 3 hour troposphere breaks and one overall tropospheric gradient per site. The WRMS residuals were 33 ps in delay and 48 fs/s in rate. For Q-band the corresponding position uncertainties were 225 and 392 μas in $\alpha \cos\delta$ and δ, respectively. We have assumed that proper motions and parallaxes are negligible. The MODEST software (Sovers, Fanselow & Jacobs (1998)) was used both for the physical modelling and parameter estimation used to build all the references frames compared in this paper.

4. Internal and External Catalog Comparisons

Experience with S/X data analysis suggests that formal uncertainties may underestimate true errors (*e.g.* Jacobs *et al* (1998), Ma *et al* (1998)). In order estimate the true accuracy of our reference frame, we made two comparisons: K vs. S/X frame and K vs. Q-band.

A recent JPL S/X solution labelled DDOR_2002 (3 million delay measurements, 1978–2002) provides an external standard of comparison. This frame is an unpublished extension of the ICRF extension-1 frame verified to be consistent with that frame at the 100 μas (WRMS) level. For the 156 sources in common which have $\leq$ 2 mas formal uncertainties, the mean in $\Delta\alpha \cos\delta$ was 149 μas and the WRMS about the mean was 333 μas. Both these values are too large to be explained by the modelled formal uncertainties and thus indicate the presence of unmodelled systematic errors. The mean of $\Delta\delta$ was 109 μas and the WRMS about the mean was 586 μas, again, indicating the presence of systematic errors in the declinations. While these comparisons do not determine to what extent the systematic errors are in the K vs. the S/X frame, the latter's vastly larger data set and more carefully scrutinized analyses lends more weight to the S/X results. Thus, our working hypothesis is that K-band systematic errors dominate the comparison.

Turning from external to internal consistency, let's compare the two high frequency frames: K and Q-band. Using data from sessions 1, 2, 3, and 5, there were 118 sources in common which had $\sigma_\delta \leq 2$ mas. The coordinate differences were consistent with the formal uncertainties as evidenced by median normalized differences in $\Delta\alpha$ and $\Delta\delta$ of 1.1 and 1.0, respectively. The mean K−Q differences were, respectively, $< \Delta\alpha\cos\delta > = 5 \pm 25$ μas and in $< \Delta\delta >= 13 \pm 36$ μas. The WRMS differences about the mean were 267 μas in $\alpha\cos\delta$ and 389 μas in δ.

We take the K-Q normalized differences to be an indication that plasma effects are not yet dominating our error budget. Thermal noise is still an issue especially at Q-band (*cf.* Lanyi et al, 2004). As further data are added, formal uncertainties will decrease thereby making smaller K vs. Q-band systematic effects visible. Thus we are considering various strategies for dealing with and quantifying plasma systematic effects as they arise in future analyses.

5. Geometric Weakness

Because there is evidence for unmodelled systematic errors, we will now take a closer look at possible underlying causes for the differences. Given the small number of sessions, we suspected that the reference frames might suffer from geometric weakness due to the lack of long southern baselines and the lack of variation in the schedules. To explore this we created two K-band solutions. The first had the minimal 3 coordinate parameters fixed. The second had 8 coordinates (from 4 well spread sources) constrained to the S/X solution values in order to control large scale zonal errors and thereby appropriate some of the geometric strength of the S/X solution.

With 3 coordinates constrained, the mean and WRMS agreement in $\alpha\cos\delta$ were 149 and 333 μas, respectively. With 8 coordinates constrained, the mean and WRMS agreement were reduced to 21 and 229 μas, respectively. The declinations also showed improvement when the extra constraints were added. For 3 constraints, the mean and WRMS agreement in δ were 109 and 586 μas, respectively. Imposing 5 additional constraints improved the mean and WRMS agreement in δ to 83 and 433 μas, respectively.

5.1. Right Ascension Inter-Source Correlations

In further searching for the underlying cause of the systematic errors, we discovered that the position parameters themselves were not yet well separated by the data in hand. Figs. 2a. and b. show the right ascension inter-source correlations vs. the arclength between a given pair of sources. On the left, Fig. 2a. reflects the solution with 3 coordinates fixed whereas Fig. 2b., on the right, reflects 8 coordinates held fixed. The most obvious and important change between the two figures is that the additional 5 constraints on the solution leads to large reductions in inter-source correlations.

From these plots we observe that, with our current data set, the right ascensions are significantly positively correlated especially for separations less than about 35°. This leaves the solution vulnerable to systematic changes of the positions of the sources over the sky—i.e. zonal errors. The deficiency appears to worsen as one moves further south in declination, presumably because the northern-based VLBA's observing geometry is systematically weakened for southern observations. We conclude that *a minimally constrained solution is not yet able to separate adequately the position parameters.*

6. Conclusions

We have presented the motivation for and initial results from our program to develop global celestial reference frames at K and Q-bands. At K-band 230 sources have been observed with median formal position uncertainties of $\sigma(\alpha\cos\delta) \approx 150$ μas and $\sigma(\delta) \approx 300$ μas; the corresponding uncertainties for 132 Q-band sources were $\sigma(\alpha\cos\delta) \approx 215$ μas and $\sigma(\delta) \approx 360$ μas. The true accuracy of our results has been estimated from both internal and external comparisons. K and Q-band solutions showed internal agreement at ≈ 270 and ≈ 390 μas in $\alpha\cos\delta$ and δ, respectively. Comparison with the independent and more strongly established S/X frame gave WRMS agreement in the corresponding parameters to 330 and 590 μas, respectively.

Examination of inter-source correlations shows that after 5 sessions we have not yet well separated the estimated position parameters. Perhaps this should not be a surprise given that the S/X work took two decades to get to its present level. We will need a stronger North-South geometry in order to create a more rigid frame that can stand independently of the S/X frame. Thus our work must be continued and refined before any high frequency frame can surpass the S/X frame.

Before we undertook the work described in this paper, there was very little global astrometric data available at frequencies above X-band (8.4 GHz). There were uncertainties as to whether reference frames at K, Q, and Ka-bands were even feasible. The results presented in this paper have answered our questions well enough that we are now optimistic about the future of high frequency radio frames both for general astrometry and spacecraft tracking. We have a reasonably large catalog of reasonably strong sources detected at both K-band (24 GHz) and Q-band (43 GHz) to begin supporting demonstrations of spacecraft measurements in late 2005. In conclusion, this work is a major step forward for both the astrometry and spacecraft navigation communities.

7. Acknowledgements

This research was done by KQ VLBI survey collaboration members from the Jet Propulsion Laboratory of the California Institute of Technology, Goddard Space Flight Center, U.S. Naval Observatory, (all under under a contract with NASA), the National Radio Astronomy Observatory, and Bordeaux Observatory. NSF support and AUI operation of NRAO's VLBA is acknowledged.

References

[1] Ma, C., E.F. Arias, T.M. Eubanks, A.L. Fey, A.-M. Gontier, C.S. Jacobs, O.J. Sovers, B.A. Archinal, and P. Charlot, "The ICRF as Realized by VLBI", AJ, 116, 1, pp. 516-546, July 1998.

[2] Boboltz, D. A., Fey, A. L., P. Charlot, E .B. Fomalont, G. E. Lanyi, L. D. Zhang, & KQ VLBI Survey Collaboration, "Extending ICRF to Higher Radio Frequencies: Imaging & Source Structure," this vol.

[3] Jacobs, C.S., O.J. Sovers, C.J. Naudet, R.F. Coker, and R.P. Branson, "The JPL Extragalactic Ra-

dio Reference Frame: Astrometric Results of 1978-96 Deep Space Network VLBI", NASA JPL TDA Progress Reports, vol. 133, pp. 1-55, 15 May 1998.

[4] Lanyi, G.E., D. Gordon, O.J. Sovers, "Limitations to Dual Frequency Ionospheric Corrections for Frequency Switched K/Q Observations with the VLBA", this volume.

[5] Sovers, O.J., J.L. Fanselow, & C.S. Jacobs, "Astrometry & Geodesy with Radio Interferometry: Experiments, Models, Results", Rev Mod Phys, 70, 4, Oct. 1998.

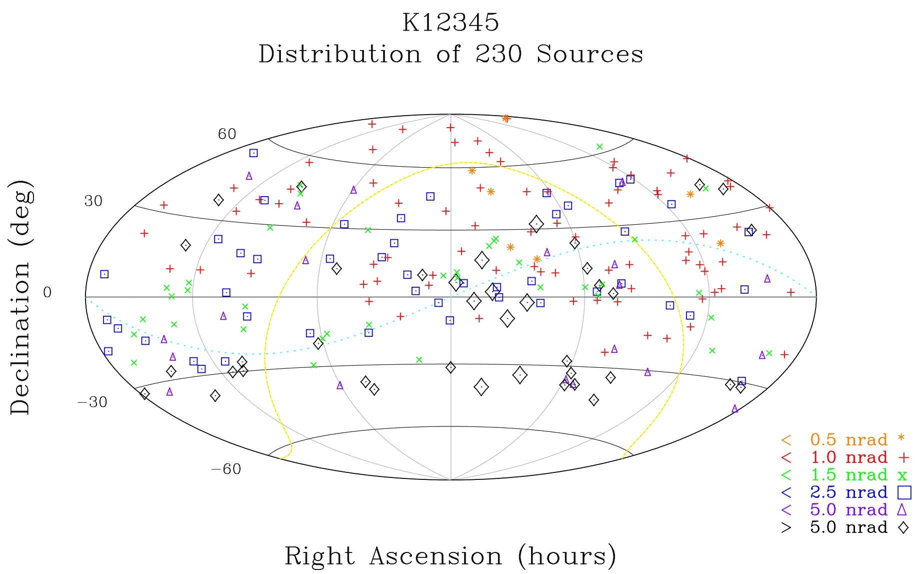

Figure 1. Distribution of the 230 K-band sources. Symbols indicate size of σ_δ.

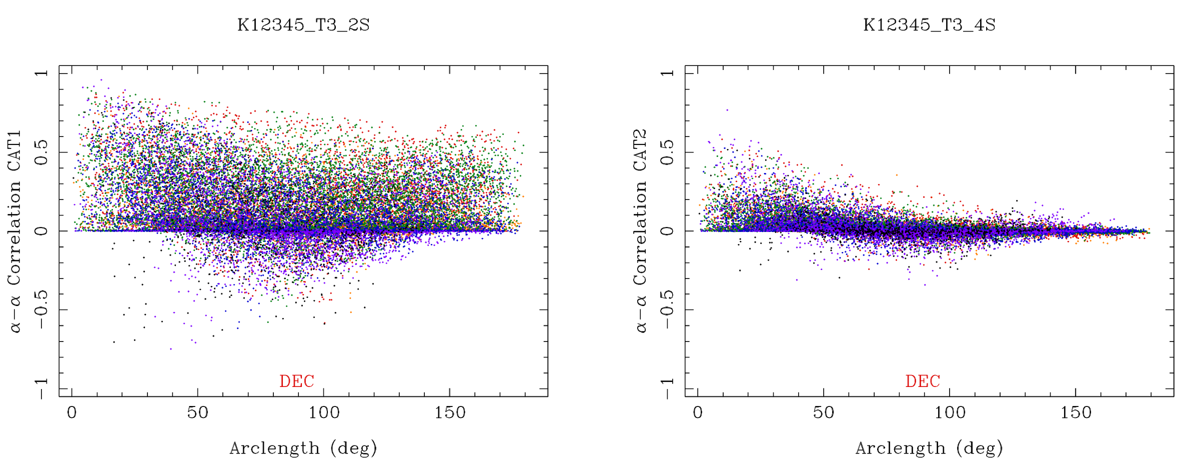

a. Minimal 3 coordinates constrained.

b. Increase to 8 coordinates constrained.

Figure 2. K-band right ascension inter-source correlations. Note in Fig. b. on the left, how constraining an additional 5 K-band coordinates to their S/X values greatly reduces the correlations.

Gino Tuccari et al.: Backend Systems – Perspectives in 2010, IVS 2004 General Meeting Proceedings, p.80–84
http://ivscc.gsfc.nasa.gov/publications/gm2004/tuccari2

Backend Systems – Perspectives in 2010

Gino Tuccari [1], Alan Whitney [2], Hans Hinteregger [2], Yasuhiro Koyama [3], Tetsuro Kondo [3]

[1] *INAF-IRA, Italian National Astrophysical Institute-RadioAstronomy Institute*
[2] *MIT Haystack Observatory*
[3] *CRL, Communications Research Laboratories*

Contact author: Gino Tuccari, e-mail: `g.tuccari@ira.cnr.it`

Abstract

A new technological vision on the future of the VLBI backend area lets us envision a fully digital implementation of what was until now performed in the analog domain. Several advantages can indeed be expected moving the domain's transition point to an earlier stage, at IF frequency instead of at the final base-band. Such a quantum leap can be afforded because of the rapid changes in digital technology that radio observatories continue to look for maintaining their competitive edge. New processing technologies here discussed will make it possible to reconfigure the whole data handling process using digital conversion to base-band and then to fully benefit from the high data rates in new acquisition and data transport systems, while simultaneously improving the reliability and flexibility of the signal path. In addition, a digital representation of the IF and base-band signals will provide the opportunity to correct for various RFI and calibration effects using embedded DSP algorithms. In order to implement these new techniques a number of major modifications are needed at all telescopes for both single-dish and for VLBI operations. Such modifications could greatly enhance the overall sensitivity of the observatories and improve the reliability of operations. The new hardware should comply with the internationally adopted standards for VLBI in order to allow global applications. A further final step we could anticipate is a brief look at a "next" future, after this near future: a trend to move the transition point yet closer to the sky frequency, overlapping with the receiver area.

1. Introduction

Since the VLBI introduction in the radioastronomy community there was evident a deep fusion of the interferometric methodology with the technological solution to implement it. Whether this was pertaining to the receiver area with the introduction of the great deal in the phase stability of the constituting components and particularly with the frequency conversions performed with the best achievable phase lock conditions, the actual complication in the equipment area was related to the back-end instrumentation. Indeed, still maintaining a fundamental need to keep the received signals with a great phase stability all over the process, this section presented the place where the interfacing between receivers and recording media was placed, with all the limitations and compromises this could show.

The evolution up to the present times is then providing us with an aspect from the historical adaptation dictated by the best possible solutions at the time. In particular the limited width in the recorded band with respect to the entire available, and potentially usable, so as the technological limitation in the maximum working frequency in the correlation components, imposed the important architecture development of our present backend systems.

Any new technology now available that could improve the performance and simplify the data process has to be taken into account, and a new perspective should be envisioned to be operative in the near future we are taking into consideration, to the end of the present decade.

Such process is of great importance not only for the opportunity now introduced by the network connections and new recording systems, but even because a further step could be considered: not only improvement and adaptation of new technology with the traditional method, a necessary step to guarantee the continuity, but even a more radical approach from which the VLBI data processing could benefit. Such consideration on the other hand could contribute to addressing other areas, correlators, receivers, data transfer, to converge on solutions of excellence. This description is only a preliminary and limited collection of considerations we think useful in such direction, and for sure more discussions are necessary for achieving a well delineated vision. It could hopefully represent a starting point for discussion.

2. Performance of a VLBI Backend in 2010

A system able to replace a present VLBI terminal would as minimum perform the same functionality and doing the same in a fully digital fashion would immediately represent several advantages. Reproducibility and phase stability are the main elements involved in such scenario: any terminal would be exactly the same with respect to any other, clock stability would be guarantee for the quality in terms of phase stability. A digital version then would represent an obvious goal.

Let's consider a list of elements included in the traditional acquisition terminal and for each element consider the equivalent functionality in a digital system. For each 400 MHz width IF an analog backend has:

- IF distributor, including total power measurement system;
- A number of 8-16 baseband converters, each including functionality for tuning and single side band converting with 10 kHz step in a range from 100 to 500 MHz, or 500 - 900 MHz. Side bands wide in frequency from 0.625, 0.125, 0.25, 0.5, 1, 2 , 4, 8, 16 MHz. Automatic gain control. Total power measurements in both lower and upper side band.
- Samplers at 1 or 2 bits.
- Formatter or VSI-H interface.

In the same circumstances a digital backend needs to have:

- No IF distributor because the first operation to perform, by definition, is the analog to digital conversion. Data distribution of the sampled signal is realized through a dedicated serial gigabit transmission system or through a parallel high speed bus. Total power measurement is needed.
- Frequency conversion can be conceived in more ways, with different architectures, whose choice is deeply affecting the final features and degrees of freedom. In particular we could divide in methods where the single converted channel is independent of the others in terms of bandwidth and zero converted frequency, and methods where channels are equally spaced and wide. Channel bandwidth can be greatly improved because of the lack of limitation typical of tape writing. Total power measurement is needed in each channel.
- Signals for operating in digital need to have a wider representation with respect to the 1 or 2 bits, and this appears more evident whether a control in the RFI area needs to be included.

VSI-H is a standard interface between instrumentation, path or any other item needing a rigorous control on the timing of the data transfer. The traditional formatter is limited in the maximum data rate for future needs, because it was developed for feeding a tape recorder.

Numerous improvements are then possible, taking advantage of very different methods in implementing the needed functionalities.

A first question we could ask is what could be the proper number of IFs to treat in a new back-end system. A minimum number is pretty obvious, just to reflect what is today in use, a maximum is instead not so evident. Multi-frequency observations are indeed an interesting option and interleaving more than putting in parallel more frequency bands could represent an interesting solution for several purposes in radioastronomy.

A perspective analysis regarding geodetic VLBI has anyway to take into consideration the needs for astronomy, because technological developments ran, in our times, together. A possible solution for giving an answer about the number of IFs a backend should support is just to present a modular approach, where more channels could be added, considering the scientific problem to treat and a common output set of channels where data coming from more sources (frequency bands and/or polarizations) could be placed to go on the further recording media, or data transfer.

Let's consider now the bandwidth for a single IF. Numerous developments are in progress in the radioastronomy community (ALMA; SKA, e-VLBI, etc.) and several analyses have been performed to choose the most proper A/D converter, considering of course the total bandwidth to process. This is because different commercial options are in the field to convert with a proper number of representation bits, the received signals. Excellent low cost solutions are possible even if the major bottleneck is represented by the further processing hardware elements. So it is not difficult to find solutions ranging between 500 MS/s up to 1500 MS/s or even more for 500/1000 MHz slices of band.

A trade-off between bandwidth in use with the traditional VLBI receivers and hardware processing method and components capability is necessary to properly set the analog to digital conversion data rate and it appears promising to set such value not too far from 1000 MS/s, for a limitation in the cost.

Let's now evaluate what is needed as channel bandwidth coming out by our new hypothetical backend. It looks useful to have available the common channel width we are using, 1-2-4-8-16 MHz, while we could ask whether the narrower bandwidth are needed. The possibility to increase the channel to 32, 64, 128, 256, or the entire 512 MHz is worth to be taken into consideration, due to the greatly improved recording data rate. So if a trend to increase channel size in frequency looks promising, the necessity to include narrow band channelization should be carefully taken into consideration for limiting development complexity.

The process to produce a single frequency channel, wide or narrow band, can be realized with different methods.

Some authors reported about methods making use of FFT modules, dividing the frequency spectrum in more bands, equally spaced, with channel size depending on the FFT dimension. Such modules are fed by poly-phase digital filters in order to reduce data rate and perform a filtering process.

A different method treats a channel as a single unity giving the possibility to independently tune different channels choosing their bandwidth. This is a more complex implementation, but more flexible.

A crucial element that should be considered for a future backend architecture to adopt is just leaving the possibility to explore different solutions for different observing schemes, adding to the already cited modular aspect, a programmability aspect. Then it would be worth to consider in the future backend a defined architecture with functionally defined modules, implementing inside different methods or technologies, well adapted to the general or particular need to satisfy. A flexible approach can be reflected in the possibility to have tunable or fixed multi-channel modules, to have high data rate transfer modules (ex. 10G technology) or direct bus connections, and so on. A precise relation between different parts should anyway be considered to guarantee an electrical and maximum data rate compatibility. Total power measurements should be included in the digital domain such as a selectable automatic gain control.

A new approach is still possible considering to add in the backend section the functionality to treat delay and fringe rotation control under a station based approach. This, while presenting restrictions for astronomical usage due to the limitation in the field of view, in the geodetic data process could bring great simplification in the correlation process opening yet the possibility to easily share the process in a software approach. On the other hand a more heavy process would be left for the backend side, where a-priori calculation would be needed, with no possibility to recover for calculation errors. A deeper evaluation seems worthwhile considering.

3. On the Opportunity to Move Some Functionalities to Different Sites

Taking in consideration a new vision, as we are trying to do, for a VLBI backend functionality, it appears possible in principle to move some processes to different places, instead of maintaining all together as we are at present used to. It looks interesting to discuss this possibility.

The conversion of the analog IF coming from the receiver is the first stage of the backend process, while being any other further activity performed in the digital domain. So it would be worth to ask whether it could be convenient to physically place the converter in the receiver area and then to transfer sampled data, using high data rate serial technology, as it could be represented by the 10G one. Indeed if data representation is 7-8 bit wide with a rate of about 1 GS/s, such standard technology could be adopted to transfer data inside an observatory or more in general inside the digital backend "area". Some indications could suggest such a useful opportunity, because it could contribute to avoiding frequency dependent performance in the traditional analog cable signal transfer, and it could represent a valid method to minimize cross-talk or interference introduction in the signal path. Still more important, signal injection for phase calibration could be much simplified, due to the single analog to digital conversion point. A great deal would still be given to the reference clock distribution. As drawback a digital front-end in the receivers area could represent a potential source of noise, so that particular care should be taken in the shielding realization.

To talk about backend "area" is in our view pretty valuable, because introducing a standard method to distribute high data rate signals implies the possibility to further process the observed data even in different places. It means that a radio interference mitigation algorithm could be taken into consideration, as was suggested by groups working in such area, adopting a real time cancellation or a more simple digital band filtering. And such process could be realized in a different place, where interference are detected and selected, as a RFI station could represent.

The data transfer technology is quickly growing so that a possibility could also be considered to fully record a received band to process later at the correlator side for tuning or bandwidth selecting. What is traditionally performed in a station could be transferred in some valuable occasions to the correlator, reducing failure risks in the station. With an almost ideal no limitation in data transfer, it would not make any sense to select portion of bands in the stations, while leaving the correlator site free to handle the data in a unique common process for all the stations. Unexpected

RFI could be removed simply tuning all the station at a different band portion. This approach could appear the opposite of creating a delay and fringe rotation station based in the backend, but it is not, because simply this solution could be adopted with the backend terminal placed at the correlator side, and the delay-phase control performed in such terminal. All these solutions should be evaluated including the problems related to the sampling jitter and the consequences on placing sampling process close to the data conversion, considering the reference clock distribution.

4. Moving Towards a Sky Frequency Processing

Already now very fast A/D converters are commercially available, in excess of 20GS/s, so that it could be taken into account the possibility to sample data at sky frequency for the bands at present adopted or even for those higher if the trend will be to increase the frequency of the observed band. As soon as faster digital processing components come to the market, able to "fill" a VLBI network with sampled data, still a much simpler, and faster, process could be adopted, greatly simplifying the backend role, up to its minimization and integration with the correlator.

Alan R. Whitney et al.: Data Acquisition and Transport - Looking 2010 and Beyond, IVS 2004 General Meeting Proceedings, p.85–89
http://ivscc.gsfc.nasa.gov/publications/gm2004/whitney2

Data Acquisition and Transport - Looking 2010 and Beyond

Alan R. Whitney [1], *Hans F. Hinteregger* [1], *Tetsuro Kondo* [2], *Yashuhiro Koyama* [2]

1) *MIT Haystack Observatory*

2) *Kashima Space Reserch Center, CRL*

Contact author: Alan R. Whitney, e-mail: awhitney@haystack.mit.edu

Abstract

In contrast to the first ~30 years of VLBI development, where highly specialized equipment for VLBI data acquisition was designed and built at great cost, the last few years are being driven more and more by taking advantage of rapidly developing technology in the computer and networking industry. This trend is only likely to accelerate, and VLBI must position itself to take maximum advantage of these technologies. Already, the transition from magnetic tapes to magnetic disks has been very rapid, and disks will almost certainly be the mainstay of VLBI data acquisition for the next few years. However, development of e-VLBI continues to be rapid and will accelerate. Already, international e-VLBI links of more than 500 Mbps have been demonstrated, with speeds in excess of 1-10 Gbps surely achievable in the near future. The advantages of real-time and near-real-time VLBI made possible by e-VLBI are significant, but major potential stumbling blocks are 'last-mile' connectivity for many telescopes and potentially high networking costs. The future of VLBI data acquisition and transport in the light of current and projected developments will be examined.

1. Introduction

Since the beginnings of VLBI in the late 1960s, a large segment of VLBI instrumentation development has been directed towards the development of specialized data systems to meet the extreme demands of both bandwidth and total data quantity that VLBI requires. Until recently, these systems have primarily been focused on magnetic tape as the only practical media. Beginning with modest data rates of <1 Mbps in 1967 recorded on 1/2" open-reel 2400-ft computer tapes at 800 bpi/track, several generations of specialized magnetic-tape-based data systems have evolved. In the past few years, however, with the rapid advance and broad commercialization of the computer industry, it is increasingly possible to take advantage of relatively inexpensive commodity technology as a basis for very high-performance VLBI data systems. An example is the recent development of magnetic-disk-based systems, such as the K5 [Ref 1] and Mark 5 [Ref 2] systems operating at 1024 Mbps, available for a tiny fraction of the cost of the tape-based systems they replace.

Electronic transmission of VLBI data, dubbed 'e-VLBI', is not new. As early as the mid-1970s, an experiment using satellite data transmission was successfully executed [Ref 3], but was not economically sustainable. In the late 1970s some VLBI data were transmitted via standard voice telephone lines at 1200 bps and successfully correlated [Ref 4], but this data transport mode was practical only for short tests. In the mid-1990s, dedicated fiber networks spanning limited geographic areas in Japan were successfully put into operation at data rates of 256 Mbps [Ref 5]. However, only in the last few years, with the advent of a global grid of high-speed fiber connections, has the possibility of transmitting a substantial amount of VLBI data become a practical possibility.

In this paper, we will examine the state-of-the-art in VLBI data systems and try to project to both the demands and the available technology in 2010 and beyond to meet these demands in the most cost effective and efficient manner.

2. VLBI Data Transport Demands in 2010

For continuing significant improvement in the geodetic VLBI technique over the next decade, it is clear that several things must happen. Among the likely changes:

- A global dedicated network of ~12-25 identical geodetic-VLBI stations, probably co-located with other space geodetic techniques (SLR, GPS among them), will be established.
- For both economic and scientific reasons, the VLBI antennas at these locations will be small and fast-moving. Antenna diameters in the range of 8-20 meters are a reasonable guess.
- In order to counter the burgeoning RFI problems encountered at some of todays VLBI stations, particularly at S-band, it is likely that a shift to higher observing frequencies will take place, perhaps to 8/15 GHz or maybe higher. Systems may even be available that are able to observe over extremely wide single bands from, say, 5 to 20 GHz.
- Due to smaller antennas and likely weaker source strengths at higher observing frequencies, observing bandwidths must be widened to re-gain the necessary SNR for precise geodetic observing. A reasonable guess is that aggregate data bandwidths that must be captured for correlation will be at least a few GHz wide, resulting in corresponding data rates of at least several Gbps/station.
- The duty cycle of observing will substantially increase at these dedicated stations, perhaps up to 50-75% averaged over a week.
- In order to operate efficiently and economically, these stations will be largely unattended by operators and must be remotely managed.

We will examine the possible options for data transport based on this likely scenario.

3. Modes of Operation

Though direct transmission of the data via e-VLBI to a correlator is clearly the most desirable from an efficiency point of view, there are a range of alternative data transport strategies that must be considered. Furthermore, the data transport strategy may evolve with time as technology permits or economics dictates, so the data transport system may need to be designed from the beginning with this evolution in mind. The range of possible data transport options is shown in Table 1, listed in order of least desirable to most desirable.

4. Magnetic Disk

The rapid advance of magnetic-disk technology over the past few years has seen magnetic disks literally burst onto the VLBI stage as performance and capacity rapidly increase and price per GB decrease. Still, we should assess the advantages and disadvantages of magnetic disks and try to project where the technology may be in 2010 and beyond. Some of the advantages and disadvantages are:

Table 1. Possible modes of data transport (in order from least to most desirable)

Situation at station	**Data transport mode**
No data link to correlator	Record, ship to correlator
Nearby high-speed POP with link to correlator	Record, transport to POP, transmit to correlator and record at correlator
'Slow' network connection to correlator	Use disk FIFO buffer - transmit at whatever speed is available; record at correlator. Sustainable observation duty cycle is constrained.
High-speed link at station, but not to all stations	Transmit to correlator and record
High-speed links to all stations	Transmit and correlate in real-time (no recording)

Advantages

- <u>Fast technology advance:</u> In terms of capacity, the technology advancement rate of disks over the past 10 years has outstripped the Moores Law advancement rate of semi-conductor technology by about 50%; this shows some signs of slowing, but many analysts attribute this more to market forces rather than technological advances. Nevertheless, advances in capacity are remarkable even over the past 3 years, moving single-disk capacity from ~120 MB in 2001 to 1 TB today (early 2004). Improvements in single-disk data rates have been much slower, but aggregation of multiple disks into single physical modules to increase aggregate data rates is both practical and economical.

- <u>Rapidly falling prices:</u> Price per GB has been dropping about 50% per year for the past 5 years. Though there is some evidence this rate may be slowing, this is still a much faster decline than any other competing media. Typical disk media costs have now dipped below $1/GB and are expected to drop to ~$0.50/GB over the next year.

- <u>Easy to take advantage of new technology:</u> Because disk drives connect to the system at a standard electrical interface, the technology used in the disk drive is invisible to the user and may advance and change radically with no impact on the design of the data system.

- <u>Very large market:</u> It is obvious that the vast market for disk drives is the driving force in the rapid technology advance and decrease in price. Currently, there are no obvious challengers to the domination of magnetic disks for large mass-market random-access storage systems.

Disadvantages

- <u>Shipping fragility:</u> Compared to magnetic tapes, magnetic disks are more susceptible to shipping damage due to the delicate nature of their internal mechanisms. However, experience has shown that susceptibility to damage is somewhat vendor dependent. It should be pointed out, however, that some of the disk-based VLBI data systems can continue to operate in the face of the loss of one or more drives with only slightly degraded performance. And, of course, not all data transport scenarios that involve local media require shipping the media (see Table 1).

- Limited data rates: Compared to magnetic tape, multiple-disk modules can easily support data rates to 1 Gbps. However, if date rates of the order of 10 Gbps or higher are required, even disks become problematic due to the large number necessary to support these high rates. For example, at least 30 disks of todays commodity variety, operating simultaneously, would be necessary to sustain operation at 10 Gbps; the practicalities and economics of such a situation need to be studied further.

5. Other Types of Recordable Media

Over the years we have seen many promises for alternative types of media, particularly optical-based media, but in practice these have not become contenders for VLBI data storage. For example, recordable optical disks are still more expensive than comparable magnetic-disk storage, especially re-writable optical media; some non-re-writable optical media is comparable in cost to magnetic disk cost, but data densities are rather now and the media costs would be recurring. Additionally, sustainable data rates on optical media are generally lower than for magnetic disks. Optical holographic storage has been long promised but has never become a commercial success.

In terms of recordable media, magnetic disks reign as king and show no hint that they will relinquish their crown over the next decade.

6. e-VLBI

e-VLBI, particularly with full real-time processing, is the ultimate solution for VLBI data transport; e-VLBI is rapidly coming of age, though it also brings its share of problems as well. Some of the advantages and disadvantages:

Advantages

- Potential for very high data rates: Since increasing data rate translates into increasing sensitivity for geodetic VLBI, the promise of very high data rates for e-VLBI is very enticing. This is particularly attractive and important if observations are done with small antennas. Global networks operating at 10 Gbps/wavelength/fiber are standard commercial practice today, with capability of up to ~100 wavelengths on a single fiber for an aggregate of ~1 Tb/sec/fiber.
- Rapid turnaround for results: e-VLBI, particularly real-time or near-real-time e-VLBI, has the potential for reducing the correlation processing delay to near zero and producing the final analyzed geodetic results in hours. This will help to meet the turnaround requirements specified in the IVS Working Group 2 for IVS Product Specification and Observing Programs.
- Lower or eliminate media costs: This is obvious, of course. In Table 1, each of the succeeding scenarios requires less recording of data at a station and hence a reduction of media cost, down to zero in the full 'real-time data transfer' scenario.
- Fully automated operations: The last three scenarios in Table 1 require no shipping of media and therefore allow for completely unattended operation of a station, helping to lower operational costs.
- Monitor station health: With the capability to transmit data rapidly to the correlator, it is possible to monitor the overall health on a comprehensive basis, as well as assist in the remote diagnosis of problems for assistance in repair.

- Enables distributed correlation: Though not practical today, distributed correlation using arrays of commodity PCs, perhaps geographically dispersed, is a possibility for the 2010 era. With e-VLBI, the data are easily dispersed to many geographically distributed sites. Experiments in distributed software correlation are now taking place in Japan, and though the performance is not now sufficient to accommodate the overall needs of geodetic VLBI, the continued improvement in commodity PC computing power may change the situation by 2010.

Disadvantages

- Last-mile connectivity: Though high-speed global networks are now a reality, the 'last-mile' connection to stations is a potentially expensive issue that must be faced before one can move to full real-time capability.

There is no doubt that e-VLBI, particularly real-time or near-real-time, offers many advantages. One-time last-mile connectivity costs and recurring fiber leasing costs are the primary issues to be resolved. Clearly, co-location of several space-geodetic techniques at each station is advantageous to help reduce these costs.

The cost of fiber data connections can be kept to a minimum by ownership or lease of dark fiber or dark wavelengths on fiber; in these cases, the owner is also responsible for terminal equipment, but is free to upgrade or replace this equipment with no additional costs associated with the fiber itself. In general, total communications-infrastructure costs are much lower for this approach compared to leasing configured services from a service provider.

7. Questions Still to be Answered

There are still a number of questions to be answered and issues to analyze to complete the VLBI2010 analysis of the data transport issue. Among such questions:1) Cost estimates for last-mile connections. 2) What are the technology options for the last-mile terminal equipment? 3) Cost-benefit analysis of various options in Table 1. 4) How can stations such as O'Higgins, which cannot be connected by fiber, be managed (satellite?)? 5) Are current VSI (H,S and E) specifications [Ref 6] adequate?

References

[1] Osaki, H, Advancement of Versatile Scientific Sampling Processor, CRL/Technology Development Center News, Serial No.21, Nov 2002; available http://www2.crl.go.jp/ka/radioastro/tdc/news_21/pdf/tdcnews_21.pdf.

[2] Mark 5 information available at http://web.haystack.mit.edu/mark5/Mark5.htm.

[3] Yen, J. L., K. I. Kellerman, B. Rayher. N. W. Broten, D. N. Fort, S. H. Knowles, W. B. Waltman, and G. W. Swenson, Jr., Real-Time, Very Long Baseline Interferometry Based on the Use of a Communications Satellite, Science, 198, 289-291, 1977.

[4] Levine, J. and A. Whitney, Mark III Real-Time Fringe-Detection System, Radio Interferometry Techniques for Geodesy, NASA Conference Publication 2115, 1979.

[5] Yoshino, T. et al, Keystone Project and VLBI real-time data processing, Proceeding of 4th APT Workshop, Sydney, Australia, 1995.

[6] VLBI Standard Hardware Interface information available at http://web.haystack.edu/vsi/index.html.

Yasuhiro Koyama et al.: Correlators in 2010 and Beyond, IVS 2004 General Meeting Proceedings, p.90–94
http://ivscc.gsfc.nasa.gov/publications/gm2004/koyama1

Correlators in 2010 and Beyond

Yasuhiro Koyama [1], *Tetsuro Kondo* [1], *William T. Petrachenko* [2], *Hans Hinteregger* [3], *Alan R. Whitney* [3]

[1] *Kashima Space Research Center, Communications Research Laboratory*
[2] *Geodetic Survey Division, Natural Resources Canada*
[3] *MIT Haystack Observatory*

Contact author: Yasuhiro Koyama, e-mail: koyama@crl.go.jp

Abstract

The current generation VLBI correlators have given us tremendous amounts of data products from regular IVS sessions. However, at the same time, it is also true that the capacity of the correlation processing is one of the limiting factors today which are restricting the number of stations and frequency of sessions to be performed. At present, at least three large scale correlators are under discussion for development. These projects are ALMA, SKA, and Extended VLA. All of these projects are seeking possibilities to enlarge current limitations in numbers of baselines and maximum speed of data rates and we have to learn a lot from these projects. On the other hand, the processing speed of the software correlators with distributed processing are getting faster and it seems it will become feasible to use software correlators for large scale VLBI processing by the year 2010. We would like to discuss various possibilities of correlators to be used for IVS sessions in 2010 and beyond.

1. Introduction

The major task of the "Correlation and Fringe Finding" subgroup for VLBI2010 is to consider next generation correlation processing for global scale VLBI sessions. For this purpose, we would like to start by reviewing currently operating correlator systems and near future correlator systems currently under planning or consideration. Then we would like to discuss the future strategies and scenarios of the correlator developments. Software correlation is in a primitive stage at present, but it will become feasible not far in the future and we would like to include the software correlator as one of the candidates of the future correlators. It is also considered as our task to consider the adequate method for fringe checking after observations and post correlation processing including determination of delay and delay rate from correlation results and appropriate methods for data archiving.

2. Current and Next Generation Correlators

Currently, various correlator systems are operationally used in geodetic, astrometric, and astronomical VLBI data processing. Table 1 lists some of the major existing correlator systems currently in operation. In these lists, Mark IV, K4, and S2 correlators are regularly used to process the IVS regular sessions at present. Availability of the correlators including the operational staffs and capability of the correlators sometimes becomes one of the limiting factors which restricts the frequency of observing sessions, number of stations in the session, and the observation mode, such as maximum data rate for each baseline. It has to be noted that the number of stations are the maximum number of the actual configuration and some of the correlators are capable to process more stations if additional play back units are connected to the correlators.

Table 1. Currently operational correlator systems.

Correlator	Location	Number of Stations	Maximum Data Rate (Mbps)	Maximum number of spectral points per IF channel	Reference
Mark IV	Haystack, USNO, JIVE, Bonn	16	1024	8192	[12]
K4	Kashima, Tsukuba	4	256	256	[7]
S2	Penticton	6	128	8192	[2]
VLBA	Socorro	24	512	1024	[1]
VSOP	Mitaka	10	1024	8192	[4]
GICO2	Kashima	4	2048	1024	[8]

All of the correlators listed in Table 1 have hardware correlator architectures. The K4 correlator is using FPGA (Field Programmable Gate Array) chips while the other correlators are are using specially designed custom correlation chips.

There are also several projects to develop next generation VLBI correlators. Korean VLBI Network and Chinese VLBI Network projects are currently planning to develop new correlator systems for their networks. Large scale correlator developments are considered in the LOFAR (Low Frequency Array), SKA (Square Kilometer Array), EVLA (Extended Very Large Array), and ALMA (Atacama Large Millimeter Array) projects. For the EVLA project, WIDAR (Wideband Interferometric Digital Architecture) design is proposed and developments will proceed in two stages [3]. During the first stage developments, 32 stations will be supported whereas the capacity of the correlator system will be expanded to accept 48 stations in the second stage developments. Sampling mode of 4096 Msps (sample per second), 3 bits per sample, eight 2 GHz bandwidth channels will be supported. For the ALMA project, maximum sampling rate will be 4000 MHz and the number of stations which can be processed at once will be 80 stations. An experimental single baseline correlator which can process 4000 MHz frequency band was developed to technically demonstrate the feasibility of the correlator [9].

3. Future Correlators

To define the detailed architecture of the future correlator systems, it is essential to define the observing mode and number of stations in the observing sessions. The cost of development and automation will also have to be considered. To consider actual design of the correlator, it is also very important to ensure compatibility among different data acquisition system. The lack of compatibility used to be the major obstacle which sometimes prevented inter-operability of different observing systems. To solve the problem, VLBI Standard Interface specifications were either defined or are under development for hardware, software, and data transport format [11]. The use of these standard specifications will be quite important in future correlator developments.

At present, efforts to develop software correlation programs are being pursued by various groups. The current capability seems still primitive to realize a large scale operational correlator. However, the maximum processing data rate of about 70 Mbps was achieved by using ordinary available single chip CPU and it seems promising that the capability will be dramatically improved [6]. Since capacity of a software correlator can be easily expanded by using distributed processing, software correlation will become one of the candidates for future correlator systems in 2010 and beyond. Software correlator has various advantages since it can be modified according to the observational requirements such as frequency resolution and pulsar gating. In principle, if maximum possible data rate is most important for high sensitivity, a custom chip LSI will be the most adequate choice whereas the software correlator and FPGA architectures will be more favorable if cost becomes the major issue.

There are other discussions to perform station based fringe stopping processing at the observing site. It will separate part of the correlation processing task to the data acquisition system at observing sites and hence will simplify the design of the correlator. On the other hand, it will fix the fringe rotation spatial reference point and therefore will limit the field of view for astronomical mapping purposes. Investigations will be necessary to figure out how it can contribute to develop a high speed simplified correlator system.

4. Operational Aspects of Correlation Processing

For fringe checking after observing sessions, data transfer of part of the observed data and correlation of these data are very effective to confirm the observations were successful. In the future beyond 2010, such e-VLBI fringe checking will become the usual practice. However, even in the future, there will be some stations which will not have high speed network connection such as at Syowa station in Antarctica and e-VLBI operation with these stations will be very difficult. In such a case, satellite communication will become an alternate method to transfer observed data for fringe checking.

For geodetic and astrometric VLBI sessions coordinated by IVS, Mark III format database files are created from correlator output data for S-band and X-band, at present. The software package CALC and SOLVE are used to perform initial data analysis and NGS data card format files are generated for data analysis by other software packages such as OCCAM. The Mark III format database files can only be handled on HP-UX operating system at present, and it is desired to develop standard data file format for data archiving which can be handled on any operating systems. Platform Independent VLBI Exchange (PIVEX) file format has been proposed for data archive [5]. The PIVEX format has been designed to be transportable to any operating platforms and it is expected to help developing software for data analysis on any operating systems. However, if we consider the situation if only part of the observing stations are connected with high speed Internet, these data will be correlated first and then the remaining baselines will be correlated later. In such cases, the database files have to be updated every time the correlation processing is performed. Then the analysis centers will have to retrieve the updated database files and repeat data analysis from the initial processing. In this case, current practice of using database files may not be the most appropriate way of data archiving. If we follow the similar mechanism of "data clearing house" commonly used by other fields such as Geographical Information System (GIS), we can archive the up-to-date database in the centralized data servers. Then the analysis centers will request necessary data set from the data servers according to their purpose of data analysis. If rapid UT1-UTC estimation is the purpose, the data for for the specific time period will be used. If the structure of a specific source have to be investigated, all the data obtained on the source will be retrieved. Also, the initial data processing such as ambiguity removal and bad data screening will be performed once and the results will be reflected in the original data set at the data servers. Then the initial data processing does not have to be repeated. If such a clearing house like mechanism is adopted, it can be expanded to centralize the control of distributed correlation processing. The data servers will allocate data to the distributed processors so that the computing resource will be effectively used for correlation processing. The processed data will be stored at the data servers and the analysis center will be able to estimate UT1-UTC on the fly even while the observing session is continuing.

5. Post Correlation Processing

Currently, all geodetic VLBI data processing uses delay and delay rate determined for each baseline. In this case, if an adequate signal to noise ratio was not obtained for a specific baseline, such data are not used for data analysis. In addition, correlation factors between these values are usually ignored. This is, however, a simplified approximation. If we consider the situation where we have raw observation data at each observing station $x_i(t))$ and we have to estimate delay τ_i and delay rate $\dot{\tau}_i$ at i-th station $(i \geq 2)$ with respect to reference station 1, the problem is to find the maximum likelihood set of τ_i and τ_i $(i \geq 2)$ by maximizing the following.

$$\max \sum_{i=2}^{n} \int_{t_0}^{t_1} x_1(t) x_i(t - \tau_i - \dot{\tau}_i(t - t_0))dt$$

The idea of global fringe fitting was discussed by [10] and the technique is now sometimes used in the astronomical VLBI data processing. It should also be possible to estimate correlation factors between τ_i and $\dot{\tau}_i$. To use these values, the database file structure has to be extended and the data analysis software also has to be modified. But it is will be a necessary direction of development especially as the number of observing stations in the session increases.

6. Summary

The future correlation processing and other related issues before data analysis were briefly reviewed and considered. Unless the observing mode and the size of the observing network is defined, it is impossible to specify detailed design of the future correlator systems. However, the important points would be to use standards such as VSI and PIVEX. The considerations of the use of global fringe fitting technique and correlation factors between delay and delay rate determinations may become a good opportunity to revisit long ignored aspects of VLBI data processing.

References

[1] Benson, J. M. (1995), The VLBA Correlator, in Very Long Baseline Interferometry and VLBA, ASP Conference Series, by J. A. Zensus, P. J. Diamond, and P. J. Napier (eds.), **82**, pp.117-131.

[2] Carlson, B. R., P. E. Dewdney, T. A. Burgess, R. V. Casorso, W. T. Petrachenko, and W. H. Cannon (1999), The S2 VLBI Correlator: A Correlator for Space VLBI and Geodetic Signal Processing, Pub. Astro. Soc. Pacific, **111**, pp.1025-1047.

[3] Carlson, B. R. and P. E. Dewdney (2003), VLBI Capabilities of the EVLA Correlator, in New Technologies in VLBI, by Y. C. Minh (ed.), ASP Conference Series, **306**, pp.271-286.

[4] Chikada, Y., N. Kawaguchi, M. Inoue, M. Morimoto, H. Kobayashi, S. Mattori, T. Nishimura, H. Hirabayashi, S. Okumura, S. Kuji, K. Sato, K. Asari, T. Sasao, and H. Kiuchi (1991), The VSOP Correlator, in Frontiers of VLBI, by H. Hirabayashi, N. Inoue, and H. Kobayashi (eds.) (University Academy Press, Tokyo), pp.79-84.

[5] Gontier A. and M. Feissel (2002), PIVEX: a Proposal for a Platform Independent VLBI Exchange Format, IVS 2002 General Meeting Proceedings, NASA/CP-2002-210002, pp.248-254.

[6] Kimura, M and J. Nakajima (2002), The Implementation of the PC-based Giga bit VLBI System, IVS CRL-TDC News, No.21, pp.31-33.

[7] Kiuchi, H., M. Imae, T. Kondo, M. Sekido, S. Hama, T. Hoshino, H. Uose, and T. Yamamoto (2000), Real-time VLBI System Using ATM Network, IEEE Trans. Geosci. Remote Sensing, **38**, pp.1290-1297.

[8] Koyama, Y., T. Kondo, J. Nakajima, M. Sekido, and M. Kimura (2003), VLBI Observation Systems Based on the VLBI Standard Interface Hardware (VSI-H) Specifications, in New Technologies in VLBI, by Y. C. Minh (ed.), ASP Conference Series, **306**, pp.135-144.

[9] Okumura, S. K., S. Iguchi, Y. Chikada, and M. Momose (2003), Recent Development of Digital Spectro-Correlators for Radio Interferometers - ALMA Second-Generation Correlator, in New Technologies in VLBI, by Y. C. Minh (ed.), ASP Conference Series, **306**, pp.259-270.

[10] Schwab, F. R. and W. D. Cotton (1983), Global Fringe Search Techniques for VLBI, Astron. J., **88**, pp.688-694.

[11] Whitney, A. R. (2001), VLBI Standard Interface Specification, IVS 2000 Annual Report, NASA/TP-2001-209979, pp.18-49.

[12] Whitney, A. R., R. Cappallo, and W. Aldrich, B. Anderson, A. Bos, J. Casse, J. Goodman, S. Parsley, S. Pogrebenko, R. Schilizzi, and D. Smythe (2004), Mark IV VLBI Correlator: Architecture and Algorithms, Radio Sci., **39**, RS1007, doi:10.1029/2002RS002820.

Harald Schuh: Report of the Subgroup "Data Analysis" of Working Group 3 VLBI2010 (Outline), IVS 2004 General Meeting Proceedings, p.95–96
http://ivscc.gsfc.nasa.gov/publications/gm2004/schuh1

Report of the Subgroup "Data Analysis" of Working Group 3 VLBI2010 (Outline)

Harald Schuh

Institute of Geodesy and Geophysics, University of Technology, Vienna
e-mail: harald.schuht@tuwien.ac.at

Abstract

By mid March 2004 the subgroup on data analysis of WG3 VLBI2010 has written a rather detailed report which will be finished in another 6 weeks. Thus, for these Proceedings the preliminary outline of the subgroup report is given to inform the IVS components about the present state of the work.

1. Geodetic and Astrometric Data Analysis

1.1. Data Analysis: Improved Models

- Loading corrections
- Antenna deformation
- Implementation of IAU Resolutions 2000 and IERS Conventions 2003
- Source structure effects
- Improved variance-covariance modeling of VLBI observations

1.2. Data Analysis: New Strategies

- Robust and Reliable VLBI Solutions
- Consistency of TRF, EOP and CRF
- Intra-VLBI Combinations of Complete Solutions
- Investigations of Differences in Analysis Software Packages
- Phase Solutions for All Baseline Lengths

1.3. Automation of the VLBI Data Analysis Procedure - Impacts, Requirements, and Concept

- Impacts of the Automation
- Requirements for the Automation
- Experiences from a research project on the automation of VLBI data analysis

2. Atmosphere, Ancillary Data and Models

2.1. Use of Numerical Weather Models

- New mapping functions
- Gradient models
- Ionospheric parameters

2.2. Long Term Perspectives Beyond 2010

2.3. Use of Other Instruments

- Microwave radiometry and GPS: independent techniques for atmospheric corrections
- Clock synchronisation

3. New Goals to be Aimed at by VLBI

3.1. ICRF

3.2. ITRF

3.3. Linking of Dynamical and Quasi-Inertial Reference Frames

3.4. Earth Orientation Parameters

3.5. Contribution to Climatology

3.6. Contribution to Relativity

4. New VLBI Configuration and Observing Systems

5. Goals and Tasks

5.1. Key Issues Before 2010

5.2. Visions After 2010

5.3. Feedback to Other Subgroups

6. References

Chopo Ma: Data Longevity Beyond 2010, IVS 2004 General Meeting Proceedings, p.97–99
http://ivscc.gsfc.nasa.gov/publications/gm2004/ma2

Data Longevity Beyond 2010

Chopo Ma

NASA Goddard Space Flight Center
e-mail: cma@virgo.gsfc.nasa.gov

Abstract

The current cache of S/X-band geodetic/astrometric VLBI data accumulated since 1979 is ~5 million observations and is increasing by ~300 000 observations per year. The long time interval and access to all such VLBI data for re-analysis have contributed to their usefulness for the terrestrial and celestial reference frames, Earth orientation parameters, tidal and nontidal loading, and troposphere. While data access and integrity have been maintained through the Mark III data base system as storage devices and media have evolved, past transitions have been major projects. A new format and retention concept to ensure eternal archiving and access should make use of self-documentation, generalized media, network connectivity and multiple redundancy. Similarly permanent organizations or sequences of organizations are also necessary.

1. Introduction

The size of the current dual frequency geodetic/astrometric data set is ~5 million delay and delay rate observables accumulated by various national and international observing programs since 1979. The data set is growing by ~300,000 observations a year, and the rate is likely to rise as technical developments such as the Mark 5 recorder and e-VLBI improve the efficiency of data acquisition and correlation. The usual forms for data distribution and archiving of geodetic/astrometric data are Mark III data base files and NGS card images, both developed in the 1970s. These data files are available at various IVS data centers in North America, Europe and Asia. In addition to VLBI data used directly for geodetic and astrometric analysis, most correlators retain their raw correlator output and some also archive the fringe results. Since one of the strengths of VLBI as a space geodetic and astrometric technique is the ability to re-analyze the entire data set with improved modeling and estimation, it is essential to maintain data access and integrity indefinitely. An analogy is perhaps astronomical plates, which have had utility far beyond the lifetimes and intentions of the original investigators. This paper will concentrate on the delay/delay rate observables with some mention of the much more voluminous and varied correlator and fringe output.

2. Content

Compared to the number of bits recorded at the VLBI stations, the data used directly for analysis is quite limited, no more than a few Gbytes in the most compact binary form. The fundamental information is the output of the fringe finding process: various delays, delay rate and fringe phase along with their uncertainties as well as baseline, source, time tag and observing frequencies. Other outputs include phase calibration from individual frequency channels and a quality flag. Some information comes from individual stations such as cable length calibration and weather data. To reduce duplicate effort some primitive analysis results have been retained in the

Mark III data base files such as ambiguity resolution, ionosphere calibration and editing. These entries are not strictly necessary and can be redone if necessary. Because of the data flow design of the Mark III analysis system, there is considerable other information in the data base file by the stage at which the primitive analysis results are included.

3. Format

The current Mark III and NGS formats have demonstrated their utility by their continued use but both are far from ideal. In particular the former holds much extraneous and redundant information while the latter lacks certain data and any flexibility. A new format is required that can make use of current computer speed, memory size and disk capacity while retaining and extending the desirable features of the current formats. The new format should be self-documenting in terms of data history, content and organization. It should be self-contained, not requiring information in other locations for data extraction. The self-documentation and self-containment could include embedding the relevant data extraction software within the data organization. The format must be expandable since new data types and dimensions are sure to arise. Although not as compact as binary, the fundamental format should be ASCII or another text type to allow examination and access at a primitive level if necessary.

4. Media

The media must provide two functions, on one hand active media for easy, efficient routine access and on the other passive media for physical security and integrity. For the foreseeable future the ready access medium is likely to be magnetic disks attached to computers or networks. This medium permits simple extension of the data set as more VLBI data become available and has sufficient capacity at low cost to keep the complete data set on line. Periodically the data set must be copied to media that can be physically removed and stored. Since the complete VLBI data set is not large and is unlikely to grow more rapidly than media capacity, the passive media copies will not be physically large or expensive. However, the history of information technology has demonstrated that such media evolve continually, sometimes leaving data stranded and unreadable. Although optical disks and solid state devices like flash memory may be the passive media for the intermediate future, hard copy, perhaps microscopic, might prove to be the most durable and secure. More important than the actual passive media are the regular archiving and cataloging of the complete data set.

5. Access

Easy, efficient access to the VLBI data set for both extension and retrieval is an essential element to ensure continuing use and improvement of the analysis results. On an everyday basis the data should be available via network from multiple, mirrored data repositories to assure fast, reliable retrieval. In addition to catalogs of the data holdings, metadatabases with such details as networks and sources should be maintained at the data repositories and at other relevant organizations. The VLBI data should also be included in larger data aggregations and any integrated space geodetic data system such as INDIGO (IERS, 2003).

6. Archiving

The archiving of the VLBI data set may present some particular difficulties because of the extended time frame during which the data will continue to be useful. At any given time, the existing data repositories must be responsible for backing up their active media, if only to prepare for the inevitable system crash. Provided the proper organization exits, the other data repositories can also assist. However, in parallel to this routine precaution complete archive copies on suitable passive media should be made on a regular schedule and distributed to other interested organizations such as the space geodesy services, geodetic agencies, astronomical observatories or the VLBI stations. Storage and cataloging of such archive copies can be very simple at these locations. The essential point is that these organizations should have a long term interest in the continued use of VLBI data even as some VLBI entities may cease their activities. By wide and continual distribution of the complete current data set, its longevity can outlast any individual component.

7. Correlator Data Management and Archiving

Several of the correlators that have processed geodetic/astrometric observations have retained both the correlator and fringe output. Because of the amount of data and absence of regular reprocessing, these data are not kept on active media and exist only at the original correlation facility. The data have migrated, sometimes incompletely, through various passive media as such media have evolved. Since the potential exists for refringing of the correlator output with better algorithms to decrease instrumental and ionosphere noise, such archives should be kept. However, the management of these correlator archives will probably remain with the correlators although catalogs of these data should be maintained along with the catalog of the analysis data.

References

[1] IERS, IERS Annual report 2002, p. 14, 2003.

R. Craig Walker: Future Directions on the VLBA, IVS 2004 General Meeting Proceedings, p.100–104
http://ivscc.gsfc.nasa.gov/publications/gm2004/walker

Future Directions on the VLBA

R. Craig Walker

National Radio Astronomy Observatory
e-mail: cwalker@nrao.edu

Abstract

Over the next few years, incremental improvements are expected on the VLBA. The Mark 5 recording system will be installed, raising the sustainable bandwidth by a factor of eight. Improvements in both receivers and optics should significantly improve the sensitivity at high frequencies. And, the VLBA may begin to contribute to the navigation of interplanetary spacecraft. But the big changes ahead for the VLBA relate to the Expanded VLA (EVLA) project, and especially the proposal to extend the resolution of the VLA by a factor of 10 by building eight new antennas and upgrading two VLBA antennas. These 10 antennas are referred to as the New Mexico Array (NMA). The correlator for the EVLA/NMA can also correlate VLBI data and will replace the current VLBA correlator, providing a significant increase in capability. Also the additional antennas will provide excellent, and much needed, short spacing coverage for the VLBA for improved imaging. The sharing of the correlator and some antennas will require a tight integration of the VLA and VLBA. In time, the VLBA may lose its separate identity and become the long baseline component of a single instrument that covers baselines from 25 m to 8600 km.

1. Introduction

The Very Long Baseline Array (VLBA) is a dedicated instrument for VLBI. It includes ten 25 m antennas that are used at frequencies between 327 MHz and 96 GHz. The antennas are operated remotely and are unattended most of the time. The VLBA also includes a 20 station correlator. Both the correlator and the stations are operated from the same room in the Array Operations Center (AOC) in Socorro, New Mexico. The AOC is also where much of the maintenance, software development, user support, and scientific staff for both the VLBA and the Very Large Array (VLA) are located.

The VLBA and VLA are run by the National Radio Astronomy Observatory (NRAO) which is a facility of the National Science Foundation, operated under cooperative agreement by Associated Universities, Inc. Observing time is allocated on the basis of refereed scientific proposals. Anyone, regardless of national or institutional affiliation, may propose for time.

Much of the geodetic/astrometric observing being done on the VLBA has been folded into the RDV projects for which all VLBA antennas and up to 10 other stations observe for 24 hours, 6 times per year. Because of the large number of baselines in these observations (up to 190), these projects are starting to contribute a significant fraction of the overall geodetic data base.

Plans for future enhancement of the VLBA fall into two categories. Over the next few years, improvements in recording systems and high frequency performance are expected. Spacecraft navigation may get added to the types of observations done on the array. There will also be ongoing improvments in software that should enhance usability but that won't be discussed here. The longer term outlook is dominated by the Expanded VLA project (EVLA) and especially the portion of that project that will add new antennas to extend VLA baselines to 350 km. Since those antennas are scattered across New Mexico, that portion of the project is called the New Mexico Array (NMA). The VLBA is expected to share the correlator and two antennas with the EVLA/NMA so tight integration of operations is required. The long range goal, although not part of any current proposal, is to upgrade the VLBA equipment to full EVLA standards and operate the EVLA/NMA/VLBA as one instrument with baselines from 25 m to 8600 km.

2. Near Term Projects

Perhaps the most important of the near term projects is to replace the VLBA tape system with the Mark 5 disk system. This replacement is well under way at other observatories, but is difficult for the VLBA because so many record and playback units (36) and so many disks are needed to sustain full time operation. The expected cost is around $3 million and an effort to find the necessary funds is underway.

For the VLBA, the Mark 5B system is required in order to reach 1 Gbps operation. With Mark 5A, the formatters limit the recorded bit rate to 512 Mbps and the correlator playback is limited to 256 Mbps per station input. The samplers, however, can generate 1 Gbps and the correlator could handle 512 Mbps per station (in a maximum of 8 baseband channels) after the deformatters. For 1 Gbps observations, 10 station data can be processed by using all 20 station inputs. Larger observations would would require 2 pass processing.

There is interest in improved high frequency performance because much of the interesting science being done on the VLBA is at high frequencies. The receivers at 22 and 43 GHz could be improved significantly by upgrading their amplifiers to current standards. This would not require major alterations to the receivers as long as no attempt is made to reach the very wide bandwidths of the EVLA receivers. As with Mark 5, funding for this project still needs to be identified.

In the last few years, receivers at 80-96 GHz have been installed on the 8 VLBA antennas where they are usable (St. Croix is too wet and the Brewster subreflector needs work). Funding for the receivers was supported to a significant degree by the Max-Planck-Institut für Radioastonomie. The VLBA antennas were specified to work well at 43 GHz with a goal of working at 86 GHz. The current efficiencies, before any post-construction surface adjustments, are near 50% at 43 GHz and 10-20% at 86 GHz. It should be possible to improve the 86 GHz efficiency by adjusting panels on the main reflectors and by improving the subreflector surfaces. A project is under way to do both.

The tactic adopted to improve the surfaces is to first work on the subreflector and then to adjust the main antenna panels based on holographic measurements. The fact that the subreflector is rotated to select the observing frequency band means that large subreflector errors cannot simply be compensated for by panel adjustments. One could end up improving one frequency at the expense of another. However using panel settings to compensate for small residual subreflector errors when the subreflector is at the 86 GHz position is probably acceptable because the other frequencies are not as sensitive to surface errors.

Adjustment of the subreflector surfaces requires filling and/or sanding and is best done off the antenna. The work is being done at the VLA on what at any given time is the spare subreflector. Once adjusted, that subreflector is mounted on the next antenna that will receive holographic measurements. That antenna's subreflector then becomes the spare and is adjusted in turn. The subreflector tuning process is done with the help of a Faro Arm, a device with an instrumented, jointed arm that can measure the position of a sensing head in 3 dimensional space with a repeatability of about 75 microns. With this arm, it is possible to iterate very rapidly between sanding and measuring. An adjusted subreflector was recently put on Pie Town but the benefit will not be clear until the main reflector panels are adjusted.

A holography system has been developed that can be mounted without disturbing the normal receivers and can be used at a variety of subreflector rotation positions. This system has a 12 GHz satellite receiver with a feed aimed at right angles to the normal feeds. There is a 45 degree reflector in the right place to deflect the beam to the subreflector. The whole assembly can be mounted above the normal feeds, and can be positioned at several locations around the feed circle. The reference horn is mounted on the back side of the antenna apex to minimize any effects from pointing shifts. By making measurements at multiple subreflector rotations, it is possible to partially separate subreflector and main antenna offsets. The data handling and correlation are handled in a PC. The whole system is portable. So far it has been under test at Pie Town and the first round of panel adjustments should happen soon.

There is a project, in cooperation with the JPL, to explore the use of the VLBA for spacecraft navigation. The value of VLBI observations to constrain the position of deep space probes has been demonstrated using the Delta-DOR technique on the DSN. But such observations require special setups and special signals from the spacecraft to provide the multiple tones needed to obtain a delay. Phase referencing techniques commonly used in VLBI astronomy could allow observations to be made without special signals and at any time that the transmitter is on. They would have no impact on normal communications activities with the satellite. It is likely that the observational data would be delivered to the navigators as total delays so that they can be treated like any other VLBI data. But those delays would be derived from the phases after phase referencing to a background source of known position has been used to remove any phase ambiguities. Such a capability would provide an additional, and perhaps paying, “customer” for the VLBA and aid some of the most publicly visible projects in all of astronomy.

3. The EVLA Connection

The EVLA project is a major upgrade to the VLA. There are two phases to the project. The first is already funded and under construction. That phase includes several items to improve the sensitivity and capability of the 28 current antennas. Most of the receivers will be replaced by new wide-band systems that, with 8 receivers, will provide continuous coverage between 1.0 and 50 GHz. The LO/IF system will break the signals from a receiver into 4 analog channels of 2 GHz each in each polarization for a total sampled bandwidth of 16 GHz. Each sample will be encoded with 3 bits to help with RFI tolerance (8 bits for narrower bandwidths) and sent to the correlator over optical fiber. The total bit rate from each antenna is 96 Gbps. The correlator will provide 16384 channels per baseline over all IFs in the wide band modes and more for narrower bandwidths. The correlator is being built at the Dominion Radio Astrophysical Observatory in Canada and is being funded by Canada. Mexico has also contributed financially to the EVLA project. In both cases, these are indirect contributions to the Atacama Large Millimeter Array, which is under construction by NRAO and partners from Europe and Japan. Much of the fiber has already been buried and the first antenna to be converted to EVLA electronics is nearly finished.

The EVLA “WIDAR” correlator has a design that can support VLBI correlation. And it is possible to use the inputs that would normally be allocated to one EVLA antenna to correlate 4 GHz from 2 antennas or 1 GHz from 4 antennas. The design also naturally comes in blocks of 8 stations. The phase 1 correlator will have 32 station inputs to have enough capacity to handle the 27 active VLA antennas. This leaves 5 unused station inputs that could be used for 10 VLBI stations at 4 GHz (16 Gbps with 2 bit samples) or 20 antennas at 1 GHz (4 Gbps). With these bandwidths and with the channelization capabilities of the new correlator, the extra stations have significantly greater capability than the current VLBA correlator. The plan is to shift to using the EVLA correlator for the VLBA and probably to shut down the current VLBA correlator.

The second phase of the EVLA project, which has not yet been funded, has two components, a new compact configuration and the NMA. The new configuration just requires construction of new pads and some rail. It is meant for use when observing very large sources. The NMA is a much more expensive component. The concept is to increase the resolution of the current VLA by a factor of 10 using 10 antennas in New Mexico with baselines of up to 350 km. Eight of those antennas will be new, probably 25 m antennas of the VLBA design. Two will be the existing VLBA antennas currently at Pie Town and Los Alamos. The Los Alamos antenna will be moved for reasons related to land use priorities at the Los Alamos National Lab and independent of the EVLA project. Both the Pie Town and Los Alamos antennas will have their electronics upgraded to EVLA standards.

The NMA antennas will have the same bandwidth and bit rate capabilities as the Phase 1 EVLA. This will require sending 96 Gbps per antenna over distances of several hundred kilometers. The current plan is to lease dark fibers from the local rural telephone companies and to have NRAO provide all the electronics, lasers etc. This appears to be cost effective at the rates that these subsidized companies are willing to charge. So far it has not proven possible to get anywhere near as good rates from the larger companies that don't benefit from the rural subsidies. While the rates are affordable for the EVLA project, scaling them up by mileage to what it would take to connect the VLBA suggests that this model for e-VLBI would not be viable without totally dominating the VLBA operating budget.

The NMA will require that the correlator be increased by another 8 stations to 40 total. The EVLA/NMA needs 37 leaving 3 which is adequate for 1 GHz VLBA observations. During VLBA observations that use at least the two VLBA antennas that are part of the NMA, there will be at least 5 extra correlator stations which would handle VLBA observations with 4 GHz bandwidth. These concepts of moving antenna inputs to the correlator between EVLA and VLBI playback and moving antennas between NMA and VLBA make it clear that operations of the EVLA/NMA and the VLBA need to be tightly integrated. The eventual hope is that the cost of long range data transission will come down sufficiently that all 45 antennas can be correlated in real time. Then there will be a single instrument capable of providing whatever combination of baselines between 25 m and 8600 km that the observers need. A correlator expansion may be required to facilitate this once high bit rates can be obtained from the VLBA.

Until real time signals can be sent from the VLBA and other VLBI antennas, all NMA antennas will be equipped with recording systems for VLBI. The recorders will be located at the correlator so that all required disk changes can be handled by a single operator and the antennas can run unattended.

There are 3 primary ways in which the NMA antennas will be used. When the VLA is in the largest, or "A" configuration, the NMA will usually be used as the outer EVLA antennas, extending the EVLA resolution and utilizing the short spacings and high sensitivity provided by the VLA. The NMA can be used alone for various types of observations for which its resolution is appropriate or for projects such as flux density monitoring that take advantage of the lack of the configuration changes that make such projects very hard on the VLA. Finally the NMA can be used to provide short spacings for VLBI observations with the VLBA or global arrays. The latter two modes will actually dominate simply because the VLA is likely to be in the A configuration less than half the time. Thus the NMA is expected to have a major impact on VLBI science.

4. The Geodesy/Astronomy Connection on the VLBA

The impacts of the VLBA on geodesy and astrometry can be seen in a number of other presentations at this meeting. The uniformity and sensitivity of the antennas, the careful design to insure phase stability, and the ability to support very large observations (up to 20 stations), has allowed the VLBA to produce some of the best available data. It has also allowed large surveys to be made to increase the number of sources with well determined positions. The expected upgrades will improve the sensitivity and hence the quality of the results. The high frequency capabilities and improvements make the VLBA the logical instrument on which to explore alternative frequencies for future geodetic VLBI.

The results from the geodesy community have, and will continue to have, a major impact on VLBA astronomy. Without high quality reference frames and geometric models, VLBI is limited to observing sources that can be detected with a fringe fit in a coherence time. With the well understood geometry provided by the geodesy community, it has been possible to use phase referencing on frequencies between 1 and 50 GHz. This allows observations of sources of less than 1 mJy that can be detected only with many hours of data on many baselines. It has increased the effective sensitivity of the VLBA by more than an order of magnitude. It also allows a variety of astrometric projects with significant impact, such as paralax measurements to pulsars. When last checked, about half of all VLBA observations used phase referencing.

The ongoing efforts by the geodetic community to improve their results have the potential to significantly improve astronomy results too. For example, the global ionospheric models provided by the GPS community are already proving to be valuable to improve VLBA phase referencing at least to 8 GHz and maybe higher and are in common use. We are also interested in GPS tropospheric results and in the efforts reported at this meeting to improve tropospheric models. We look forward to continuing fruitful interaction between the geodetic VLBI community represented by the IVS and the astronomical community that is the VLBA's main user base.

5. NRAO Web Sites

For more information about the NRAO, see the home page at http://www.nrao.edu.
For specific information on the VLBA, see http://www.aoc.nrao.edu/vlba/html/.
For EVLA information, see http://www.aoc.nrao.edu/evla.

Wolfgang Winkler et al.: VIEPROJ1 - A Students' VLBI Project, IVS 2004 General Meeting Proceedings, p.105–108
http://ivscc.gsfc.nasa.gov/publications/gm2004/winkler1

VIEPROJ1 - A Students' VLBI Project

Wolfgang Winkler, Boris Bogensberger, Wilfried Karel, Michael Kistenich, Gerold Pacher, Andrea Pany, Andreas Roncat, Gerhard Summer, Johannes Boehm, Thomas Hobiger, Robert Weber, Harald Schuh

IGG, Vienna University of Technology

Contact author: Harald Schuh, e-mail: `harald.schuh@tuwien.ac.at`

Abstract

The VLBI project VIEPROJ1 was planned and executed involving university students doing the main work in every step. It was part of the lecture (diploma course) "Auswertung geodaetischer Weltraumverfahren" (space geodetic techniques), within the curriculum of Vermessung und Geoinformation (geodesy and geoinformation) at the Vienna University of Technology. The lecture was held by Prof. Harald Schuh and Prof. Robert Weber.

1. Scheduling

After the date of the session had been fixed and the participating stations had been chosen, Dorothee Fischer from the University of Bonn advised the students how to make an appropriate schedule for a 3 hours VLBI session, using the SKED software (Fig. 1). The final schedule was produced by the students; the skyplots can be seen in Fig. 2.

Figure 1. Introduction to SKED: Dorothee Fischer from Bonn University explained the principles of scheduling.

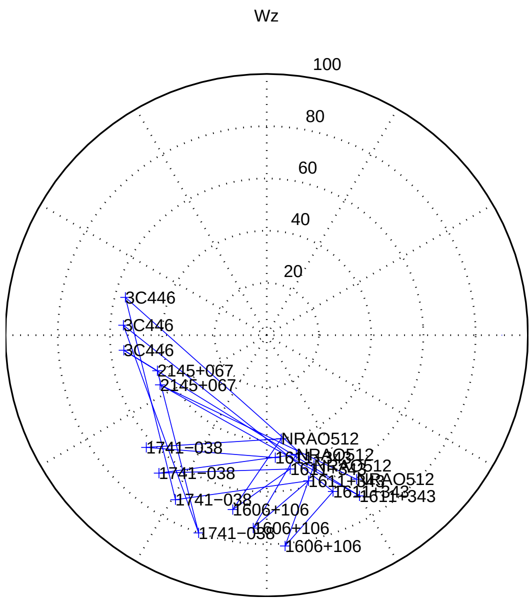

Skyplot for Wettzell

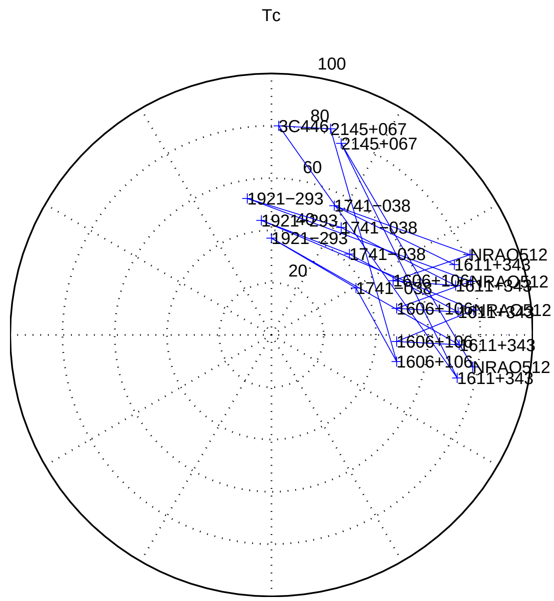

Skyplot for TIGO/Concepcion

Figure 2. Skyplots for the stations Wettzell and TIGO/Concepcion during the session.

2. Observation

On November 27, 2003 the radio telescopes of Wettzell, TIGO/Concepcion and O'Higgins observed about 20 different scans within 3 hours. Four Students visited the Fundamental Station Wettzell while the experiment took place (Fig. 3,4).

Figure 3. During the observation, TIGO was watched via webcam, and some students went to Wettzell. Left: Students are watching the TIGO antenna via webcam in a lecture room of the Vienna University of Technology. Right: Boris Bogensberger in front of the Wettzell antenna.

Figure 4. Gerhard Summer in the operators room.

3. Correlation

So far, the tapes from Wettzell and TIGO have been correlated at Bonn correlator. The tape from O'Higgins is still on its way there.

4. Analysis

The observed delays were analyzed with the OCCAM software (Titov et al., 2001 [2] at the Vienna University of Technology. Estimates for DUT1 and the station coordinates of TIGOCONC were calculated.

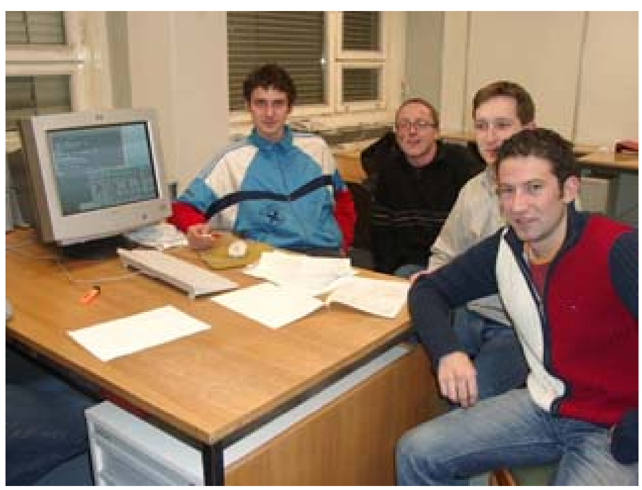

Figure 5. Students Pacher, Summer, Roncat and Winkler working with OCCAM.

5. Results

The following set-up was used to estimate the coordinates of TIGOCONC and DUT1:

- Vienna Mapping Function (VMF, Boehm and Schuh, 2004, [1])
- cutoff elevation angle 3°
- VLBI Terrestrial Reference Frame (VTRF)

Table 1. Estimated station coordinates of TICOCONC with formal errors in m.

x	149205410.89 ± 0.076
y	-488796089.96 ± 0.092
z	-380354133.09 ± 0.092

Table 2. Estimated DUT1 and deviation from IERS-C04.

DUT1	-0.3810 sec	0.3 msec

6. Acknowledgements

Without their participation the project wouldn't have been possible:

- Dorothee Fischer, University of Bonn
- Wolfgang Schlueter and his team in Wettzell (especially Mr. Kronschnabel)
- Hayo Hase and his team in Concepcion
- O'Higgins team
- Arno Mueskens and the correlator team in Bonn

References

[1] Boehm, J., and H. Schuh, Vienna Mapping Functions in VLBI analyses, Geophys. Res. Lett., 31, L01603, doi:10.1029/2003GL018984, 2004.

[2] Titov, O., V. Tesmer, and J. Boehm, OCCAM 5.0: User's Guide, In: AUSLIG Technical Notes, 7, 2001.

David L. Jauncey et al.: The Impact of Interstellar Scintillation on Astrometric VLBI, IVS 2004 General Meeting Proceedings, p.109–112
http://ivscc.gsfc.nasa.gov/publications/gm2004/jauncey

The Impact of Interstellar Scintillation on Astrometric VLBI

David L. Jauncey [1], James E. J. Lovell [1], Roopesh Ojha [1], Alan L. Fey [2], Yasuhiro Koyama [3], Hayley E. Bignall [4], Lucyna Kedziora-Chudczer [5], Jean-Pierre Macquart [6], Barney J. Rickett [7], Oleg Titov [8], Anastasios K. Tzioumis [1]

1) *Australia Telescope National Facility, CSIRO*
2) *US Naval Observatory*
3) *Kashima Space Research Centre, CRL*
4) *Joint Institute for VLBI in Europe*
5) *School of Physics, Sydney University*
6) *Kapteyn Astronomical Institute, University of Groningen*
7) *Department of Electrical and Computer Engineering, UCSD*
8) *Geoscience Australia*

Contact author: David L. Jauncey, e-mail: David.Jauncey@csiro.au

Abstract

We review the evidence demonstrating that interstellar scintillation (ISS) is the principal mechanism responsible for the intra-day variability (IDV) seen at cm wavelengths in many compact, flat-spectrum extragalactic radio sources. The presence of ISS in a radio source implies the presence of microarcsecond structure in the source. We examine the implications of such compact structure, and suggest that these ultra-compact radio scintillators may form a significant part of the next generation International Celestial Reference Frame (ICRF) sources because of their high level of compactness and positional stability.

1. Introduction

Over the last five years considerable evidence has accumulated to demonstrate unequivocally that ISS is the principal cause of the IDV seen at cm wavelengths in many compact, flat-spectrum extragalactic sources. Much of this evidence has come about through the discovery of three very rapidly varying IDV sources, PKS B0405−385 [1], J1819+3845 [2] and PKS B1257−385 [3]. The flux density of these sources changes so rapidly at 5 to 8 GHz that many *scints* of the quasi-periodic variations can be seen in a single 12-hour track.

The variability in these sources is sufficiently rapid that changes of 50% to 100% take place in time scales of an hour or less. This has allowed the detection of a significant time delay between the patterns of variability seen at widely separated radio telescopes. The first measured time delay was for PKS B0405−385 where, despite the poor geometry, a time delay of several minutes was measured at 4.8 and 8.6 GHz between the variability patterns seen at the VLA and the ATCA [4]. With more favourable geometry, Dennett-Thorpe & de Bruyn [5] tracked J1819+3845 with the VLA and Westerbork and saw not only a significant time delay, but were able to watch it change with the rotation of the Earth. Most recently, successful time delay measurements have been made at 4.8 and 8.6 GHz at several epochs for the rapid variable source PKS B1257−326 [6]. Such time delay measurements are only feasible for these extremely rapid variables. For these sources the observations of such a time delay establishes unequivocally an ISS origin for their rapid IDV.

The presence of time delays of order minutes implies a velocity of the interstellar medium (ISM) of order 30-40 kms^{-1} which is close to the speed of the Earth in its annual orbit around the sun. This coincidence implies the presence of an *annual cycle* in the variability characteristics of an IDV source if ISS is the mechanism responsible for the IDV. When the Earth is moving in the same direction as the ISM the relative speed is small and the variations will be slow. Six months later the Earth is moving in the opposite direction to the ISM, the relative speed is high and the variations will be much more rapid. This annual cycle, in the form of Earth Orbit Synthesis, is proving to be a powerful analysis tool for determining radio source structure at micro-arc-second resolution [7].

Such annual cycles have been found for a number of sources, B0917+624 [8] [9], PKS B1519−273 [10], and J1819+3845 [11], and it looks as though such behaviour may be widespread. The beautiful pattern of the annual cycle can be seen for the rapidly variable source PKS B1257−326 as determined by Bignall et al., [3]. Most recently an analysis of the 5 years of 2.3 GHz VLBI flux density measurements [12] derived from the Keystone Project [13] has revealed a strong annual cycle in the ITRF and ICRF source B0059+581 [16]. Despite large, overall flux density changes B0059+581 has repeatedly exhibited an annual cycle, firmly establishing an ISS origin for the IDV. B0059+581 was also found to exhibit ISS at 4.8 GHz in the recent MASIV VLA Survey [14].

The presence of such measured time delays and the presence of annual cycles in IDV sources establishes unequivocally that ISS is the principal cause of the IDV seen in many compact, flat-spectrum radio sources at cm wavelengths.

As is the case for optical scintillation in the atmosphere where *stars twinkle and planets do not*, interstellar scintillation at cm wavelengths selects those sources which house the most compact components which have microarcsecond sizes [15]. These scintillators are thus amongst the most compact known AGN, which is a good starting point for them to be high quality position reference sources.

2. The MASIV Survey: Finding More Scintillators

The number of known scintillators is small, however. We are therefore undertaking a large-scale, Micro-Arcsecond Scintillation-Induced Variability, MASIV, VLA survey of the northern sky at 4.9 GHz. Our objective is to construct a sample of 100 to 150 scintillating extragalactic sources with which to examine the microarcsecond structure and the parent populations of these sources and to probe the turbulent interstellar medium causing the scintillation. The first epoch of observations revealed variability on timescales ranging from hours to days in 85 of 710 compact flat-spectrum sources. The number of highly variable sources, those with rms flux density variations greater than 4% of the mean, increases with decreasing source flux density.

We have also completed follow-up 8.4 GHz VLBA observations of 75 low flux density scintillators from the first two epochs of the MASIV survey [17]. With these plus the existing data from the USNO radio reference frame image database, we can compare the milliarcsecond structures of the MASIV scintillators and non-scintillators. One striking point we find using several statistical measures, is that the scintillators are significantly more core-dominated than the non-scintillators. We find at 8.4 GHz with the VLBA [18] that 19 of the 75 low flux density scintillators are unresolved at a dynamic range of typically 200:1.

3. Are the Scintillators Good Radio Reference Frame Sources?

In order to be included in the radio reference frame a source should be strong at cm wavelengths, should be a point source with little or no structure at mas resolution, and its position should be stable on the sky.

With the advent of the Mark 5 VLBI recording systems with Gbs^{-1} data rates coming into widespread operation, the first criterion should be relatively easily satisfied by sources with flux densities in excess of $\sim$ 100 mJy. There are plenty of MASIV scintillators above 100 mJy.

The need for point sources is perhaps the most difficult criterion to fulfill. The presence of ISS demonstrates that the scintillators possess micro-arc-second components and are thus amongst the most compact known AGN. Our 8.4 GHz VLBA observations [17] [18] reveal that amongst flat-spectrum AGN, the scintillators are significantly more core-dominated. We find that 49% of the scintillators have in excess of 80% of their flux density in the core, compared with 10% of the non-scintillators. It is important to note that the scintillators and non-scintillators in our study were drawn from populations with identical spectral index distributions, so the only selection criterion separating the two classes is the presence or absence of scintillation.

Structural stability is a prime requirement for reference frame sources. While it is not possible to predict if any source will or will not be stable in the future, in many cases their past stability can be assessed. For example, B0059+581, which as noted above was found to be a strong, long lived scintillator, as was confirmed in MASIV, has weak mas structure. However, this structure has shown no variations over the 7 years that this source has been imaged in the Radio Reference Frame Image Database.

As might be expected B0059+581 also exhibits remarkable positional stability. In the analysis to select the most stable compact extragalactic sources, Feissel-Vernier [19] notes B0059+581 as one of the more stable reference frame sources. If we compare the class of MASIV scintillators with the class of ICRF defining sources for positional stability, based on the Feissel-Vernier data we find 67% of the scintillators have a positional stability index of 1 or 2, compared with 55% of the ICRF defining sources. We note that the defining sources have been preselected over a decade of VLBI observations. The scintillators as a class, on the other hand, with no selection criterion other than their scintillation, possess the better positional stability.

There are, however, a number of potential positional stability problems that might be expected with the scintillators as reference frame sources. For example, as the micro-arc-second component scintillates the flux density variability may produce position shifts due to refraction in the ISM. Such effects should be no more than the few micro-arc-seconds of the scattered component sizes. In addition, position shifts may be expected from the scintillation from possible *Christmas Tree* effects. While the scintillators are extremely compact at the milli-arc-second level, this may produce significant displacements depending on the overall milliarcsecond structure. These may be measurable and efforts should be made to do so.

4. Conclusions

In conclusion, we suggest that the IVS discuss selecting the additional sources for the next generation ICRF sources from the population of MASIV scintillating sources [20]. These sources possess a high level of compactness and positional stability. As such this makes them a potentially powerful population of sources to use to extend and improve the ICRF.

References

[1] Kedziora-Chudczer, L., D.L. Jauncey, M.H. Wieringa, M.A. Walker, G.D. Nicolson, J.E. Reynolds, A.K. Tzioumis, 1997, ApJ, 490, L9.

[2] Dennett-Thorpe, J., G. de Bruyn, 2000, ApJ, 529, L65.

[3] Bignall, H.E., D.L. Jauncey, J.E.J. Lovell, A.K. Tzioumis, L. Kedziora-Chudczer, J-P. Macquart, S.J. Tingay, D.P. Rayner, & R.W. Clay, 2003, ApJ, 585, 653.

[4] Jauncey, D.L., L. Kedziora-Chudczer, et al., In: Astrophysical Phenomena Revealed by Space VLBI, Proceedings of the VSOP Symposium, held at the Institute of Space and Astronautical Science, Sagamihara, Kanagawa, Japan, January 19 - 21, eds. H. Hirabayashi, P.G. Edwards, and D.W. Murphy, Published by the Institute of Space and Astronautical Science, 2000, 147

[5] Dennett-Thorpe, J., G. de Bruyn, 2002, Nature 415, 57.

[6] Jauncey, D.L., H.E. Bignall, J.E.J. Lovell, L. Kedziora-Chudczer, A.K. Tzioumis, J-P. Macquart, J-P., B.J. Rickett, In: Radio Astronomy at the Fringe, Eds., A.J. Zensus, E. Ros and Cohen, M.H., 2003, 199.

[7] Macquart, J-P., & D.L. Jauncey, 2002. A&A, 572, 786.

[8] 2001, ApJ, 550, L 11.

[9] Jauncey, D.L., J-P. Macquart, 2001, A&A, 370, L9.

[10] Jauncey, D.L., H.M. Johnston, H.E. Bignall, J.E.J. Lovell, L. Kedziora-Chidczer, A.K. Tzioumis, J-P. Macquart, 2003, Ap&SS, 288, 63

[11] Dennett-Thorpe, J., G. de Bruyn, 2001, Ap&SS, 278, 101.

[12] Koyama, Y., T. Kondo, & N. Kurihara, 2001, Radio Science, 36, 223.

[13] Yoshino, T., 1999, J. Comm. Res. Lab., 46.

[14] Lovell, J. E. J., D.L. Jauncey, H.E. Bignall, L. Kedziora-Chudczer, J-P. Macquart, B.J. Rickett, & A.K. Tzioumis, 2003, AJ, 126, 1699.

[15] Walker, M.A., 1998, MNRAS, 294, 307.

[16] Jauncey, D.L., J.E.J. Lovell, Y. Koyama, In preparation.

[17] Ojha, R., A.L. Fey, J.E.J. Lovell, D.L. Jauncey, & K.J. Johnston, 2004a, AJ, submitted.

[18] Ojha, R., A.L. Fey, D.L. Jauncey, J.E.J. Lovell, & K.J. Johnston, K.J., 2004b, ApJ, submitted.

[19] Feissel-Vernier, M., 2003, A&A, 403, 105.

[20] Jauncey, D.L., H.E. Bignall, J.E.J. Lovell, L. Kedziora-Chudczer, A.K. Tzioumis, J-P., Macquart, J-P., B.J. Rickett, In: New Technologies in VLBI, Ed., Y.C. Minh, 2003, 383.

Session 3

Network Stations, Operation Centers, Correlators

Page intentionally left blank

Arno Müskens et al.: Operational Experience with the Mark 5 Recording System at the Bonn and USNO Correlator,
IVS 2004 General Meeting Proceedings, p.115–119
http://ivscc.gsfc.nasa.gov/publications/gm2004/mueskens

Operational Experience with the Mark 5 Recording System at the Bonn and USNO Correlator

Arno Müskens [1], *Walter Alef* [2], *David Graham* [2], *Kerry Kingham* [3]

[1] *Geodätisches Institut der Universität Bonn*
[2] *Max-Planck-Institute for Radioastronomy*
[3] *U.S. Naval Observatory*
Contact author: Arno Müskens, e-mail: `mueskens@mpifr-bonn.mpg.de`

Abstract

We present a short overview of operations with the Mark 5 recoding system at the Bonn Correlator. Most IVS stations and many astronomy stations are equipped with the new Mark 5A units and recordings have been correlated in Bonn since 2002. We describe our experience with those recordings, the problems encountered, and their solutions.

1. Introduction

The Mark 5 VLBI data system is being developed as the first high-data-rate VLBI data system based on magnetic-disc technology. With sustained data rates of 1024 Mbit/s and storage limited only by the ever-increasing capacity of magnetic discs, the Mark 5 represents a radical departure from the traditional VLBI dependence on magnetic tape. The Mark 5A VLBI data system is about to become the most widespread recording system among the IVS community, and it has been defined as the new standard for the EVN. NRAO is actively seeking funding for the implementation of Mark 5 at the VLBA and its correlator.

The Mark 5 is based on a standard PC platform and uses a combination of COTS (commercial-off-the-shelf) and custom-designed interface cards. The heart of the system is a “StreamStor” disk interface card from Conduant Corporation that is specially designed for high-speed-real-time data collection and playback. Developed in cooperation with MIT Haystack, this rack mountable recorder features two hot-swappable 8-drive modules. The Mark 5 can record continuously by alternating between the two 8-pack modules. It can record and play back 8, 16, 32 or 64 tracks from a Mark IV or VLBA formatter with a maximum data rate of 1024 Mbit/s and 512 Mbit/s respectively. As such Mark 5A is a direct replacement for a Mark IV tape unit. Software, firmware, and hardware have been constantly improved by both Conduant Corporation and Haystack Observatory.

A new backplane which will accept both parallel and serial ATA disks is being developed by Conduant Corporation and should be available around summer 2004. NRAO will upgrade their tape tracking software “track” so that it will handle discs as well.

The advantages of the Mark 5 system are:

- robust operations, low maintenance cost,
- easily transportable,
- conformance to the VLBI Standard Interface (VSI) specifications, planned for Mark 5B,
- design based primarily on unmodified off-the-shelf subsystems and components,
- unattended operation limited by available disc sizes,
- cost for recording media (ATA disks) drops continuously,
- rapid random access to any data,
- instant synchronization on playback into the correlators,
- easily upgradable host platform,
- the data are written to all discs simultaneously in a "round-robin" fashion so that a single failing disc will not lead to the complete loss of one or more channels,
- data of a broken disc are replaced by a fill-pattern, which is recognized by the correlator,

Disadvantages:

- The disc modules have to be handled carefully,
- Some kinds of discs are more susceptible to damage in transport as the heads are parked on the disc platters,
- Disc packs must not be inserted into the Mark 5 unit with brute force as the 200-pin connector might get damaged
- The StreamStor card can hang occasionally.

Short history of Mark 5:

September 1999	Haystack Observatory white paper states the goals of a next generation 1 Gbit/s VLBI data system.
May 2000	Haystack Observatory proposed the development of a new high-data-rate VLBI data system based mostly on commercial-off-the-shelf (COTS) technology.
January 2001	COTS-VLBI interim report states discs should be future recording medium for VLBI.
March 2001	First Mark 5 demonstration system at 512 Mbit/s, built in two months. Upgrade plan to 1024 Mbps.
June 2001	Proposal for support of Mark 5 development to BKG, MPIfR and other agencies.
July 2002	First Mark 5P system received at Bonn correlator.
October 2002	Intensives started using Mark 5P.
December 2002	First two Mark 5A systems arrived at the Bonn correlator.
May 2003	First successful observation at 1 Gbit/s in the EVN with four telescopes.
September 2004	Eight Mark 5A systems are installed at the Bonn Correlator.

2. Bonn Correlator Status with Mark 5

Eight Mark 5A units have now been integrated into the correlator. As a default they are connected to the second head input of the station units (SU). In this setup all 32-track modes can be correlated with either tape or disc, changed using just a software switch. Single pass correlation of modes using up to 1 Gbit/s can be done, with simple re-cabling. Correlation with Mark 5 is now more or less standard and already more robust than correlation with tape drives. Various modes (including Mark III Mode C) have been correlated successfully with mixed disks and tape in a production mode. Roughly between 30% to 40% of all data correlated are now on Mark 5.

The Bonn correlator is awaiting its first IVS-R1 experiment which is a Mark 5 only recording. More experience and statistics in detailed form can be found in "Geodetic VLBI at Bonn Correlator" in this proceedings. Current and regularly updated correlator capabilities are listed at http://www.mpifr-bonn.mpg.de/EVN/MK4CORstatus.

3. USNO Correlator Status with Mark 5

Intensives started using Mark 5 with Mark 5P units in October, 2002. Initially, both tapes and discs were used to make sure experiments were successful. From November, 2002, Intensives were Mark 5 only. Today the Mark 5 Intensive processing factor is 1.0, which is better than the tape Intensive processing factor of 1.5. Reprocessing was cut from an average of one scan per experiment to one scan every four experiments. Very few failures occured in more than 200 Intensives. Some failed recordings and a few delayed processing runs were due to vacation of a critical person at a station and a correlator and to a Mark 5P to Mark 5A switchover. In addition two discs were lost in shipment but later found. Experience with our 24 hour experiments show that USNO has reduced the processing factor by 20% to 25% (2.5 to 2.0 and 2.0 to 1.5) and the reprocessing by almost 75%. We attribute this to converting two or three station to Mark 5 operation in the six or seven station experiments, which reduced the need for operator intervention.

4. Mark 5 Correlation Problems

Mark 5 8-packs have to be handled with care. After switching off an 8-pack the disc pack should not be removed from the Mark 5 before all discs have come to a stop, approximately 20 seconds. This is especially true for discs that park the heads on the platters. All disc-packs are uniquely identified with a "volume serial number" (VSN) both on the outside and electronically on the discs. At the correlator occasionally disc-packs are received where the VSN on the discs differs from that on the outside. As a result the modules cannot be identified properly by the operator or software. This can causes problems in tracking modules from station to correlator and creates delays at the correlator. It is not clear where this error happens. However, the stations are requested to check each disc-pack on arrival, and that includes a check of the VSN on the discs before recording.

At the correlators the disc-packs are also identified by the disc serial numbers. Unfortunately the observing logs created at each station during the observation sometimes contain wrong entries. This leads to further delays in correlation if not spotted while the observation is prepared for correlation. All Mark IV correlators have now similar experience with 24 hour experiments. Converting two to four stations to Mark 5A in the six to nine station experiments has reduced the processing factor by 20% to 25%.

5. Gbit/Sec Data Handling with the Mark 5A

5.1. Recording

Mark 5 terminals have been used at several EVN stations at 1 Gbit/s for test observations. Initial problems were encountered due to faulty or outdated firmware, faulty electronics and excessive cable lengths inside the Mark 5 units. After fixing these problems all units could record successfully artificial data generated internally by the Mark 5 unit.

In some cases data from the Mark IV formatters could not be recorded correctly. Apparently this was dependent on cable length between the Mark IV formatter and Mark 5 unit. A length of 0.5 m gave problems, cables of > 2 m similarly. A length of around 1.5 m seems OK. This might be due to bad impedance matching at the formatter output. These cables are also a potential source of RFI. Similary old cables that have been kicking around for many years and have been bent or creased and do not perform well at these high data rates. On the station side it is necessary to check both cables are the same length and routed neatly from the formatter to the Mark 5, and not strapped to any metal objects. These cables must be separated from video monitor cables and other sources of interference, as well as terminator boards plugged into the unused output connectors on the I/O panel on the back of the Mark 5 unit. The built in data checking commands "scan_check" and "track_check" provide an excellent indication of recording quality, unfortunately staff at some stations do not pay sufficient attention to these entries in the log. Dan Smythe has written some field system SNAP files that can be used to configure an acquisition system for 1024 Mbit/s and test its performance (see chk1024/vchk1024 commands).

5.2. Playback

Typically Mark 5 units are connected to the "upper" input connectors of the station unit, originally designed for the second head of tape drives. The single head of a tape unit is then connected to the "lower" input pair of the station unit. This enables easy software switching between tape and disc operation for each station unit. At 1 Gbit/s this is no longer possible, the connection between Mark 5 and station units must be changed to connect 64 tracks of the Mark 5 to the station unit. Correlation seems to be without problems, except for cases in which the online system already reports problems during the recording. Reports from the JIVE correlator indicate problems with data in which a LSB channel has been recorded without accompanying upper sideband channel. Also they reports problems with TRMS, which is visible in auto-correlation. A fix is being worked on. It is not clear if this affects all Mark IV correlations.

6. Mark 5B

The Mark 5B VLBI data system is now being developed by MIT Haystack Observatory in collaboration with other Institutions. It is expected that it will be deployed at the beginning of 2005. The Mark 5B will have a VSI-compliant interface and command set, and will be based on the same physical platform as the Mark 5A. The Mark 5B will bypass the formatter and connect directly to the output of the samplers (through a simple interface). This will allow a maximum data rate of 1024 Mbit/s also for VLBA record terminals. It will be compatible with the planned digital BBCs, which will have only VSI interfaces.

The Mark 5B will include simple Mark IV station unit capability, which will allow us to replace the bug-ridden station units which are the weakest points of the correlator. It will also allow a relatively inexpensive expansion of the number of stations at the existing Mark IV correlators. According to present planning the Mark 5B systems will not be able to play back Mark 5A recordings, while compatibility in the other direction is foreseen.

7. Conclusions

The Mark 5 system has been shown to make VLBI data recording and correlation significantly more robust and at the same time reduces the cost for maintenance and media drastically. Both geodetic and astronomical VLBI observing can soon profit from increased sensitivity provided by recording at data rates up to 1024 Mbit/s. The throughput can be higher than with tapes and should allow IVS to reach its ambituous plans for observing in the next few years.

References

[1] Müskens, A., Alef, W., in “International VLBI Service for Geodesy and Astrometry 2002 Annual Report”, eds. N. R. Vandenberg and K. D. Baver, NASA/TP-2002-210001, 2002.

[2] Withney, A., Mark 5 VLBI Data System Update, in “Proceedings of the 16th Working Meeting on European VLBI for Geodesy and Astrometry, held at Leipzig, May 9-10, 2003”, eds. W.‘Schwegmann and V. Thorandt, BKG Frankfurt/Leipzig

Alessandra Bertarini et al.: Overview of Geodetic Experiments at the Bonn Correlator, IVS 2004 General Meeting Proceedings, p.120–122
http://ivscc.gsfc.nasa.gov/publications/gm2004/bertarini

Overview of Geodetic Experiments at the Bonn Correlator

Alessandra Bertarini, Arno Müskens, Alexandra Höfer

Geodetic Institute, Bonn Unversity

Contact author: Alessandra Bertarini, e-mail: abertari@mpifr-bonn.mpg.de

Abstract

We present an overview of the Bonn correlator status during the years 2002 to 2003 showing the efficiency improvements achieved over that period giving particular emphasis to the geodetic experiments.

1. Introduction

The Bonn correlator is a facility founded by the Max-Plank Institute for Radioastronomy (MPIfR) and the Federal Agency for Cartography and Geodesy (BKG) and is operated in cooperation with the Geodetic Institute of Bonn University (GIUB). Every year about 25% of the geodetic experiments scheduled by IVS, the MPIFfR astronomical projects, and part of the coordinated millimeter VLBI array experiments are correlated in Bonn.

2. Correlator Time Allocation

The manpower present in Bonn to operate the correlator comprises two day-time operators and ten students who take over correlation during the night and weekends. They correlate for a maximum of 5840 h/y, divided equally between geodetic and astronomical experiments.

A script to log the time usage was written in 2002 and used during 2002 and 2003. The log shows that the correlator operated for about 4120 h in 2002 and 4600 h in 2003. As shown in figure 1, geodetic experiments in 2002 accounted for about 73% of the time used for production correlation, which is more than the equal division of time that was agreed. This led to an agreement between the GIUB and the MPIfR to pay for this extra time. The remaining time was divided between maintenance and idle time. Maintenance is counted only when it interrupts production correlation. Since production correlation continues to run in parallel for most of the maintenance procedures, maintenance causes only about 100 h/y of downtime. Idle time is counted when correlation is stopped, while waiting for tapes, setting up the correlator control files, fringe fitting and other causes.

A comparison between figure 1(a) and 1(b) shows clearly the improvements achieved during 2003. Geodetic experiments in 2003 accounted for about 57% of the time used for production correlation, nevertheless the number of correlated experiments increased from 42 (in 2002) to 46 (in 2003). The correlation time decreased principally thanks to three factors.

- The effort of Roger Cappallo who solved the so called *STC-error* timing problem involving the Delay Compensation Module (DCM). This led to a huge amount of recorrelation.
- The Track Recovery Module (TRM) byte slip, which caused a loss of fringes in the affected tracks, was solved by METRUM (contracted by JIVE).

- Introduction of Mark 5A helped to streamline correlation.

The idle time decreased principally thanks to the effort of the stations who helped reduce the shipping time, by preparing correct paperwork (e.g. customs declaration); and thanks to software development that streamlined the data processing.

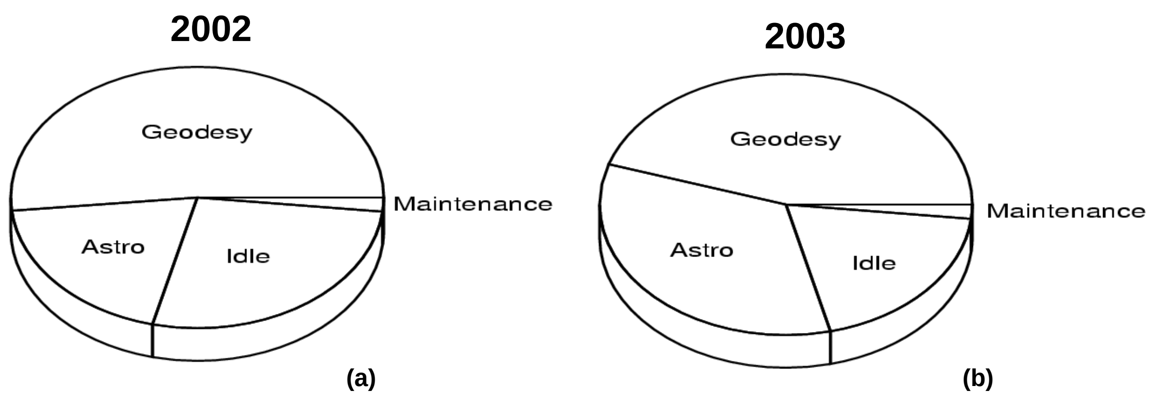

Figure 1. Pie charts describing the correlator time allocation in 2002 and 2003.

3. Processing Factor

The Processing Factor (PF) is defined to be the ratio between the hours spent correlating and the hours spent recording the data. In figure 2 the annual average of the PF calculated over all the experiments correlated in Bonn, has been plotted against the year in which the experiments were processed. This plot confirms the efficiency improvements described in the previous section.

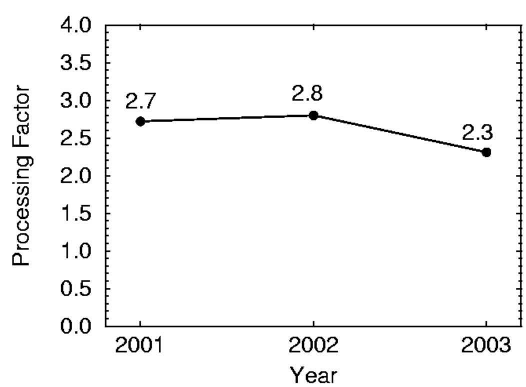

Figure 2. Annual averaged PF plotted against the year in which the experiments were processed.

We can attempt to predict how the PF will reduce with the continuing migration of stations to Mark 5A, using the experiment IVS-R1104 for a timing test. In R1104 there were 337 scans recorded in 24 hours by six stations. Of those six stations, four are equipped with Mark 5A recording system, which is the largest number of Mark 5A modules yet seen in Bonn in a single experiment. Of the 337 scans recorded, 151 were Mark 5A only and 186 had at least one tape.

Mark 5A is faster than tape because it does not need to peak, and so the scan setup time was measured to be about one minute shorter than the equivalent setup time when at least one tape is present. Had the 186 scans with tapes been Mark 5A only, we would have spared 186 minutes. That would have reduced the correlation time from 30.3 h to 27.2 h, leading to a 10% decrease in correlation time.

This 10% is an underestimate since we did not include the time lost due to tape slewing, and possible search for tracks, which vary from experiment to experiment. The PF will be further reduced due to the future plan of equipping all the stations with Mark 5 recording systems.

Further, we would like to reduce the idle time by parallelizing the fringe fitting process. This will reduce the waiting time between correlation and possible recorrelation.

4. Conclusion

Considering the nominal 2920 h/y of correlator time for geodesy, a decrease of 10% in the PF will allow correlation of more experiments than in the previous years. The Bonn correlator is ready to meet the IVS plan of increasing the number of experiments per year.

Robert M. Campbell: Recent Results from the EVN Mark IV Data Processor at JIVE, IVS 2004 General Meeting Proceedings, p.123–127
http://ivscc.gsfc.nasa.gov/publications/gm2004/campbell

Recent Results from the EVN Mark IV Data Processor at JIVE

Robert M. Campbell

Joint Institute for VLBI in Europe
e-mail: campbell@jive.nl

Abstract

Recent achievements at the EVN Mark IV data processor at JIVE include decreasing the read-out time for the whole correlator (32 Mark IV boards) to 0.25s, improving the end quality of user data (*e.g.,* excising TRM byte-slips, applying an improved 2-bit van Vleck correction), developing new astronomical capabilities (*e.g.,* oversampling), and strengthening liaison procedures with PIs (*e.g.,* through the new EVN archive facility). The move to Mark 5 and fiber-linked VLBI is well underway. 90% of the user experiments from the Oct/Nov'03 EVN session had at least one station recording onto disk, and three stations had moved over to all-disk recording in the Feb'04 session. Ftp fringe-tests have been included as a regular feature of EVN sessions, allowing for faster feedback to stations.

1. Background

A key item in the Mark IV upgrade of the EVN was the construction of the EVN Mark IV data processor at the Joint Institute for VLBI in Europe (JIVE). JIVE is hosted by ASTRON in Dwingeloo, the Netherlands, and is funded by science councils of a number of European countries. Special projects have been funded directly by the European Commission. The EVN Mark IV data processor [1], [2] was constructed in the context of the International Advanced Correlator Consortium through which the other Mark IV geodetic correlators were also built, with significant contributions, from European members, in hardware from CNR/IRA, control software from Jodrell Bank, and correlator software from ASTRON.

The first fringe on the EVN Mark IV data processor was seen on 21 July 1997 and its official inauguration took place on 22 October 1998. The "first science" resulting from data correlated on the EVN Mark IV data processor detected HI absorption against the counter-jet very close to the nucleus of NGC 4261 [3]. The first paper published in *Nature* based on EVN observations correlated at JIVE has also appeared [4], using OH mega-maser emission to study the kinematics and spatial structure of the circumnuclear torus in Mrk 231. The EVN Mark IV data processor now correlates the vast majority of astronomical EVN experiments, and about half of the global experiments. More information about the EVN and JIVE can be found at the websites www.evlbi.org and www.jive.nl .

2. Current Capabilities

Basic characteristics of the design of the EVN Mark IV data processor include: simultaneous correlation of up to 16 stations with 16 channels per station, each having a maximum sampling rate of 32 Ms/s (thus a total of 1 Gb/s per station for 2-bit recordings). The correlator houses 32 Mark IV boards. The principal science drivers behind the development of the data processor and associated software include the ability to handle continuum dual-polarization observations, spectral line experiments, and phase-reference mapping. Figure 1 shows the data playback units, the station units, the data distributor unit, and control computers. The correlator itself is housed in a separate room out of this view to the right.

Figure 1. A view of the main control space for the JIVE Mark IV Data Processor.

2.1. Features Snapshot

The EVN Mark IV data processor can currently correlate/provide:

- 1- and 2-bit sampling (all but a handful of experiments use 2-bit sampling).
- Mark III, Mark IV, VLBA, and Mark 5(A) recordings.
- sustained 512 Mb/s tape recordings or 1 Gb/s for Mark 5 recordings.
- parallel- and cross-polarization products as desired in dual-polarization observations.
- up to 2048 frequency points per baseline (see the discussion following equation 1 below).
- full-correlator integration times down to 0.25 s (half-correlator t_{int} down to 0.125 s).
- oversampling at 2 or 4 times the Nyquist frequency in order to provide subband bandwidths down to 500 kHz (the maximum Nyquist-sampled BW_{sb} is 16 MHz).
- multi-pass correlation (*e.g.,* for observations having >16 stations at any given time).

Capabilities whose development is still underway or not yet fully tested include pulsar gating, speed-up (playback at a bit-rate faster than that used in recording), and phase-cal extraction. Capabilities that are yet to come include sub-netting and recirculation (achieving greater equivalent correlator capacity for observations that don't use the maximum bandwidth per subband).

2.2. Correlator Capacity

The total correlator capacity can be expressed as:

$$N_{\text{sta}}^2 \cdot N_{\text{sb}} \cdot N_{\text{pol}} \cdot N_{\text{frq}} \leq 131072 \tag{1}$$

Here, N_{frq} is the number of frequency points per baseline/subband/polarization. N_{pol} is the number of polarizations wanted in the correlation (1, 2, or 4). N_{sb} represents the number of different subbands, counting lower- and upper-sidebands from the same BBC as distinct subbands. The value to use for $N_{\rm sta}$ is "granular" in multiples of 4: *e.g.,* if you have 5–8 stations, use "8". Independent of this equation, the maximum $(N_{\rm sb} \cdot N_{{\rm pol}_{\|}})$ is 16 (a station-unit limitation), and the maximum $N_{\rm frq}$ is 2048 (a single baseline/SB/pol must fit onto a single correlator board). All capabilities discussed in this report assume the use of local validity, which avoids problems ensuing from the Mark IV-format data-replacement headers correlating with each other in certain baseline-source geometries, but at the expense of a factor of two in $N_{\rm frq}$.

Table 1. Example configurations that would use the full correlator capacity (local validity)

$N_{\rm sta}$	$N_{\rm sb}$	$N_{\rm pol}$	$N_{\rm frq}$	comment
8	1	1	2048	EVN spectral-line
16	8	4	16	global cross-polarization mapping
16	14	1	32	Mark III/modeC-like (87.5% of the correlator)

2.3. Output Capacity

The minimum $t_{\rm int}$ for a configuration using the whole correlator is now 1/4 s; configurations that use no more than one-half of the correlator can achieve minimum $t_{\rm int}$ of 1/8 s. In the future, the Post-Correlator Integrator (PCI) will provide a minimum $t_{\rm int}$ for the whole correlator of 1/64 s.

These low integration times, together with the fine spectral resolution afforded by large $N_{\rm frq}$, will provide the possibility to map considerably wider fields of view through reduced bandwidth- and time-smearing effects in the *u*-*v* plane (see, *e.g.*, [5] §21.7.5). For example, the fields of view having ≤ 10% decrease in the response to a point source arising from each of these two effects are:

$$FoV_{\rm BW} \lesssim 49.''5\,\frac{1}{B}\,\frac{N_{\rm frq}}{BW_{\rm sb}}; \qquad FoV_{\rm time} \lesssim 18.''56\,\frac{\lambda}{B}\,\frac{1}{t_{\rm int}} \tag{2}$$

Here, B is the longest baseline length in units of 1000 km, λ is in cm, and $BW_{\rm sb}$ is in MHz. A primary goal of such wide-field correlations would be to map the entire primary beam of each antenna composing the array with only a single correlation pass. With the existing $N_{\rm frq}$ and $t_{\rm int}$ capabilities, we can already achieve this for a variety of observing configurations. More details can be found in `www.evlbi.org/user_guide/limit.html`. Of course, one drawback to such wide-field correlations is the rapid growth of the size of the FITS file seen by the user — at our current maximum, ~7 GB per hour of observation.

2.4. Recent Improvements

The following points represent some of the data-quality enhancements since the previous General Meeting not discussed elsewhere in this report:

- Positions of EVN stations that don't usually participate in geodetic campaigns have been significantly improved, in some cases with adjustments on the order of 5m [6]. In addition, a better tie between the Wb single-dish and array positions was determined, and an unrelated effect that introduced discrete phase jumps in $\rm Wb_{arr}$ (typically once per several hours) was detected and repaired during this process. The EVN performance in phase reference experiments has significantly improved following these improvements [7].

- We implemented a mechanism in the logic of the responsible station-unit boards to detect and repair TRM byte slips and to flag associated data, thus cutting down on the number of recorrelations required and streamlining the review process.
- The van Vleck correction for 2-bit data depends on the fraction of high- and low-magnitude bits within an integration, but this dependence was not being taken into account correctly. We now compensate for the observed "sampler statistics" in a post-correlation program.

3. Operational Overview

3.1. Correlation and Logistics

We operate the correlator 80 hours per week, from which time system testing and development must also come; typically 50–60 hours per week are production. After solving a few growing pains, we can include Mark 5 stations seamlessly in jobs. However, we will achieve the full efficiency gains from Mark 5 only when the last tape disappears, since a job will start only when the last station is ready (job-preparation time for tapes continues to be ~9 minutes). We currently have 6 Mark 5A units connected to station units for production correlation, with another 3 in house. The status of Mark 5 acquisition by EVN stations can be viewed via the Mark 5 link from the TOG section of the EVN web page. In the longer term, when stations upgrade to Mark 5B we will be able to move away from using local validity, effectively doubling the correlator capacity as described in equation 1 (the impact on the minimum t_{int} would be more complicated, depending on the stage of PCI development). Use of Mark 5B without the station units could also raise the possibility of correlating more than 16 stations at once.

3.2. Post-Correlation Data Review

Our main priority is always the quality of the data we provide to the EVN users. Our internal data review process, as illustrated in Figure 2, begins by transforming the lag-based correlator output into an AIPS++ Measurement Set (MS). From the MS, we can investigate slices of the correlation functions in both time and frequency/lag, allowing us to detect and diagnose various problems with the recorded data or the correlation itself, and to find any scans for which recorrelation would be profitable. We can also make various plots more suited to providing feedback to the stations rather than to the PI (*e.g.,* parity-error rates, sampler statistics). We apply various corrections to the correlated data at this stage (*e.g.,* the 2-bit van Vleck compensation), and flag subsets of the data for low weights and other known problems resulting in (uncorrectable) spurious correlation amplitudes and/or phases.

The last step converts the final MS into FITS format, usually written to a DAT tape. We send this to the PI, along with a summary of the correlation itself and various diagnostic plots. The FITS files can can be read into AIPS directly using `FITLD`. The EVN pipeline operates on the FITS data to create the first few AIPS `CL` tables (*e.g.*, T_{sys}-based amplitude calibration, off-source flagging, *etc.*), as well as to make make preliminary images of sources authorized by the PI. Plots, summaries, and pipeline results also go to the EVN archive, `www.jive.nl/archive/scripts/listarch.php`, followed after a 1-year proprietary period by the FITS files themselves.

Unless contacted by the PI to the contrary, we aim to release an experiment's tapes/disks four weeks after the PI is notified of the experiment's completion. To supplement the review products

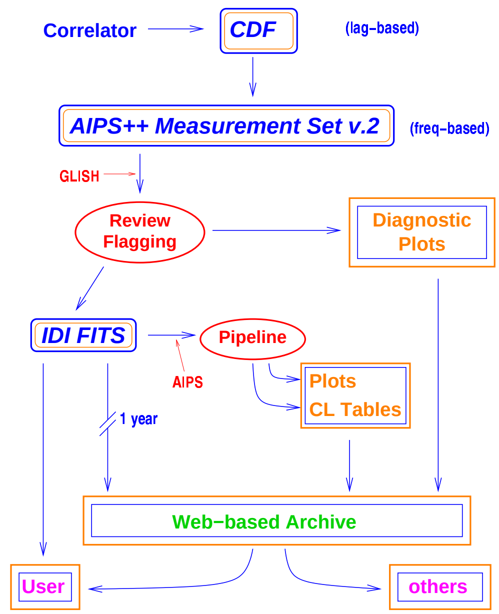

Figure 2. Post-correlation review process for an experiment.

mentioned above, the PI of course may also discuss the experiment/correlation with the responsible JIVE support scientist and/or arrange to visit JIVE for help in data reduction if desired. Specific programs exist to provide financial support for PIs from non-EVN European institutes and their collaborators in order to encourage visits to EVN institutes, including JIVE — see the "Access to the EVN" portion of the EVN web page: `www.evlbi.org/access/access.html`.

References

[1] Casse, J.L., "The European VLBI Network Mark IV Data Processor," in *Proceedings of the 4th EVN/JIVE Symposium*, eds. M.A. Garrett, R.M. Campbell, & L.I. Gurvits, *New Astron. Rev.*, **43**, 503–508, 1999.

[2] Schilizzi, R.T., Aldrich, W., Anderson, B., *et al.* "The EVN-Mark IV VLBI Data Processor," *Exper. Astron.*, **12**, 49–67, 2001.

[3] Van Langevelde, H.J., Pihlström, Y.M., Conway, J.E., *et al.* "A Thin HI Circumnuclear Disk in NGC4261", *Astron. & Ap.* **454**, L45–48, 2000.

[4] Klöckner, H.-R., Baan, W.A., & Garrett, M.A., "Investigation of the Obscuring Circumnuclear Torus in the Active Galaxy Mrk 231," *Nature*, **421**, 821–823, 2003.

[5] Wrobel, J.M., "VLBI Observing Strategies," in *VLBI and the VLBA*, eds. J.A. Zensus, P.J. Diamond, & P.J. Napier (ASP: San Francisco), 411–427, 1995.

[6] Charlot, P., Campbell, R.M., Alef, W., *et al.* "Improved Positions of Non-geodetic EVN Telescopes," in *Proceedings of the 6th EVN Symposium*, eds. E. Ros, R.W. Porcas, A.P. Lobanov, & J.A. Zensus, (MPIfR: Bonn), 9–12, 2002.

[7] Campbell, R.M. "Operational Issues of the Improved EVN Station Positions," in *Proceedings of the 6th EVN Symposium*, eds. E. Ros, R.W. Porcas, A.P. Lobanov, & J.A. Zensus, (MPIfR: Bonn), 37–40, 2002.

Andrey Finkelstein et al.: Some Results of the First Year of Participation of the Svetloe Observatory in IVS Observing Programs, IVS 2004 General Meeting Proceedings, p.128–132
http://ivscc.gsfc.nasa.gov/publications/gm2004/fink1

Some Results of the First Year of Participation of the Svetloe Observatory in IVS Observing Programs

Andrey Finkelstein, Valery Gratchev, Alexander Ipatov, Zinovy Malkin, Ismail Rahimov, Elena Skurikhina, Sergey Smolentsev

Institute of Applied Astronomy of Russian Academy of Sciences (IAA)

Contact author: Andrey Finkelstein, e-mail: `amf@quasar.ipa.nw.ru`

Abstract

Results of the first 16 geodetic VLBI sessions observed in 2003 at the Svetloe Radio Astronomical Observatory (SvRAO) of the Institute of Applied Astronomy (IAA) in the framework of the IVS observing programs are presented. Analysis of observations has been performed at the IAA using OCCAM/GROSS software. The processing of the observations allowed us to determine with high accuracy both the coordinates of the SvRAO and Earth orientation parameters. It is also shown that inclusion Svetloe observatory in the IVS network yields essential improvement of the accuracy of determination of the EOP. Obtained results show high quality of both observations and analysis made at the IAA.

1. Introduction

Svetloe Radio Astronomical Observatory (SvRAO) was founded by the Institute of Applied Astronomy (IAA) of the Russian Academy of Sciences (RAS) as the first station of the Russian VLBI network QUASAR. It is located in the Karelian Neck about 100 km towards North of St.Petersburg, and is primarily intended for regular observations in the framework of domestic and international VLBI programs [1, 2].

Until the end of 2002 SvRAO was equipped with only one terminal, Canadian S2, with Data Acquisition System developed at the IAA. Using this terminal, SvRAO participated in a number of VLBI programs in collaboration with other VLBI stations in China, Canada and Australia, also with the second IAA VLBI station, Zelenchukskaya, located in the North Caucasus.

In 2002, according to the Agreement between the RAS and NASA, a Mark IIIA terminal was installed at SvRAO, and since March 2003 the SvRAO started regular VLBI observations in the framework of the IVS astrometry and geodynamics programs. Being a result of nearly 15 years of efforts by the IAA, this is a major milestone for us.

2. VLBI Equipment of the SvRAO

The basic instrument of the SvRAO is a new generation fully steerable radio telescope with homology backup structure. The quasi-paraboloid main dish has a diameter of 32 m and focal length of 11.4 m, and the secondary mirror is an asymmetrical modified hyperboloid with diameter of 4 m. To be able to switch frequency band and provide multi-band observations quasi simultaneously, the input horns for different wavelengths are located above the circle of 3-meter diameter and fast switching is achieved by turning of the secondary mirror at certain angle around the radio telescope axis. To maintain simultaneous receiving at S and X bands in both orthogonal polarizations (to eliminate ionosphere effects), which is essential for realization of astrometric, geodynamical and geodetic programs, a special combined horn has been constructed.

The radio telescope is equipped with 5 low-noise cooled receivers with HEMT amplifiers for wavelengths 1.35, 3.5, 6.0, 13 and 18/21 cm for observations in the left and right circular polarizations. Micro-cryogenic closed circle refrigerators are used for the cooling of low noise amplifiers at 20 K. The working ranges of intermediate frequencies of the cryo electronic radiometers are 130–480 MHz and 130–890 MHz for X and S bands correspondingly. The noise temperature at the input of the cryostat is 15 K, and the total noise system temperatures are not higher than 50 K for S band and 70 K for X band at elevations above 20°. The signal from the radiometers is transmitted along phase stable coaxial lines connecting the focal cabin of the radio telescope with the Mark IIIA and S2 terminals located at the laboratory building.

The Svetloe VLBI site is provided with a qualitative system of time-frequency synchronization, consisting of 4 H-masers with long-time stability about $(3-5)\times 10^{-15}$. One H-maser operates constantly and each other can be switched on during one hour and will achieve all nominal technical parameters during 24 hours. The synchronization of the local time scale with Universal Time is realized with the use of GPS and GLONASS receivers with accuracy (30–50) ns.

The phase calibration system — generator of picosecond impulses includes two basic units: pulse generator of harmonics on semiconductor diode and circuit producing 1 MHz reference signal with rectangular wavefront from the harmonic signal with the frequency of 5 MHz provided by the H-maser. The measurement of the delay of 5 MHz reference signal in cable system is provided by phase comparator.

An automatic meteorological data system measures atmospheric pressure, direction and velocity of wind, temperature and humidity of air. These data are recorded in log-file of the media.

All systems of the radio telescope are united in general complex with the help of central computer with specialized software, permitting the automatic carrying out of observations in both VLBI and single dish modes. The basis of this software is the Mark IV Field System, v. 9.5.17. It was added by site-oriented interface developed at the IAA for control of the antenna, radiometers and registration terminals.

3. Observations and Results

The first regular IVS session at Svetloe was observed on March 6, 2003 [3]. In 2003 Svetloe participated in 21 IVS sessions — 16 R4 sessions (determination of EOP), 3 TRF sessions (improvement of the terrestrial reference frame), 2 EURO session (investigation of crustal deformations in Europe). Five R4 sessions (R4079, R4081, R4083, R4085, R4089) were correlated without Svetloe because of delay in tape delivering due to customs problems. In November 2003 Mark III BBC were transported to the USA for upgrade, and for this reason IVS sessions scheduled for the end of 2003 — the beginning of the 2004 were canceled. List of sessions observed at SvRAO in 2003 and related statistics are presented in Table 1.

During those 16 IVS sessions observed with the participation of SvRAO 33194 observations were obtained, 29197 of them are suitable for a scientific analysis. These observations were obtained at 22 VLBI stations, and 116 baselines of length from 99 km (DSS65–YEBES) to 12,496 km (DSS45–YEBES). Station statistics is presented in Table 2.

Scientific analysis of the observations has been performed at the IAA using OCCAM/GROSS software, and was primarily aimed to compute accurate coordinates of Svetloe radio telescope

Table 1. VLBI sessions observed at Svetloe in March–November 2003.

Session code	Date	Number of stations	Number of sources	Number of scans	Number of observations
R4061	MAR 06	8	36	313	2373
T2015	MAR 18	7	44	348	2079
R4063	MAR 20	8	34	332	2902
R4065	APR 03	8	44	322	2305
T2016	APR 08	7	38	231	1067
R4069	APR 29	8	47	340	2693
EURO68	MAY 06	9	53	324	5433
T2017	MAY 20	8	54	542	1985
R4073	MAY 29	8	54	399	2306
R4075	JUN 12	5	43	203	658
R4087	SEP 04	8	54	336	2322
EURO69	SEP 23	5	42	294	1807
R4091	OCT 02	6	46	279	1084
R4093	OCT 16	6	48	280	1065
R4095	OCT 30	7	48	256	1468
R4097	NOV 13	7	49	268	1647
Total		22	98	5067	33194

reference point and the EOP. Geocentric coordinates of the Svetloe radio telescope reference point obtained at the IAA are presented in Table 3.

For this computation coordinates of all stations except Svetloe were fixed to VTRF2003 values except coordinates of Gilmore Creek which was corrected for the jump in station position due to the earthquake that happened in November 2002. For comparison, VTRF2003 values, estimate obtained at the Main Astronomical Observatory (MAO), Ukraine (mao2003a.trf), and the latest GSFC estimate kindly provided by Daniel MacMillan (personal communication) are also included in the Table. All the solutions were obtained from processing of 10–11 observing sessions, except VTRF which is based only on one observing session R4061.

It is important that as a result of the IVS experiments Svetloe is now tied to 21 other globally distributed VLBI stations (Fig. 1). Estimates of the the baseline lengths including Svetloe are presented in Table 4.

Figure 1. Stations observed along with Svetloe.

Figure 2. Typical IVS R4 network in 2003.

Table 2. List of participating stations (D – distance from Svetloe, Nsess –number of sessions, Nobs – number of observations, Ngood – number of good observations, Nav – average number of good observations per session, Pg – percentage of good observations).

Station	Location	D	Nsess	Nobs	Ngood	Nav	Pg
ALGOPARK	Canada	6256	11	5784	5270	479	91.1
CRIMEA	Ukraine	1811	3	968	779	260	80.5
DSS45	Australia	11734	1	505	401	401	79.4
DSS65	Spain	3192	2	1725	1589	794	92.1
FORTLEZA	Brazil	8428	12	3809	3378	282	88.7
GGAO7108	USA	6767	2	91	47	24	51.6
GILCREEK	USA, Alaska	5854	6	4340	4113	686	94.8
KASHIM34	Japan	7174	1	608	513	513	84.4
KOKEE	USA, Hawaii	9561	11	4227	3797	345	89.8
MATERA	Italy	2374	12	8061	6581	548	81.6
MEDICINA	Italy	2140	2	2069	1771	886	85.6
NOTO	Italy	2809	1	1420	1227	1227	86.4
NYALES20	Norway, Spitsbergen	2133	11	8244	7511	683	91.1
ONSALA60	Sweden	1080	3	2690	2348	783	87.3
SESHAN25	China	6761	1	569	492	492	86.5
SVETLOE	Russia	—	16	8386	7369	461	87.9
TSUKUB32	Japan	7141	2	1321	1165	582	88.2
URUMQI	China	4127	2	1116	823	412	73.7
WESTFORD	USA	6269	1	283	204	204	72.1
WETTZELL	Germany	1655	13	8541	7720	594	90.4
YEBES	Spain	3130	2	1427	1100	550	77.1
YLOW7296	Canada	5807	1	204	196	196	96.1

Table 3. Svetloe coordinates at the epoch 2003.30 aligned to ITRF2000.

Analysis center	X, m	Y, m	Z, m
IAA	2730173.850 ±0.001	1562442.667 ±0.001	5529969.064 ±0.002
GSFC	.849 ±0.001	.666 ±0.001	.063 ±0.002
MAO	.838 ±0.002	.670 ±0.001	.070 ±0.003
VTRF	.850 ±0.003	.668 ±0.002	.071 ±0.006

It should be mentioned that in 2003 station Svetloe was included in the IVS network as tagged along station. i.e supplementary to the regular IVS R4 network. Figure 2 shows a typical configuration of the R4 network in 2003. One can see that Svetloe is located near other European stations, and thus does not strengthen substantially the network geometry. Nevertheless, we tried to estimate how it influences the accuracy of EOP results (the main goal of the IVS R4 program). Estimates of pole coordinates X_p, Y_p, $UT1$, and celestial pole offset X_c, Y_c were computed for each session both for whole network and for reduced network without Svetloe. Summary statistics for IVS R4 sessions is presented in Table 5.

Table 4. Baseline lengths from Svetloe to other stations (N — number of sessions).

Station	N	Length, m	Station	N	Length, m
ALGOPARK	11	6255567.6375 ± 0.0017	NOTO	1	2808545.4758 ± 0.0031
CRIMEA	2	1810877.6191 ± 0.0035	NYALES20	11	2133122.9974 ± 0.0008
DSS45	1	11734020.5515 ± 0.0170	ONSALA60	3	1079812.9398 ± 0.0012
DSS65	2	3192391.5692 ± 0.0022	SESHAN25	1	6760938.2664 ± 0.0104
FORTLEZA	12	8428008.6828 ± 0.0026	TSUKUB32	2	7140832.1567 ± 0.0042
GGAO7108	1	6767247.5683 ± 0.1347	URUMQI	2	4127151.1143 ± 0.0043
GILCREEK	6	5853689.1331 ± 0.0019	WESTFORD	1	6269171.0924 ± 0.0137
KASHIM34	1	7173755.4892 ± 0.0111	WETTZELL	13	1654774.8551 ± 0.0007
KOKEE	10	9561115.4073 ± 0.0029	YEBES	2	3129769.6030 ± 0.0043
MATERA	12	2373640.0972 ± 0.0009	YLOW7296	1	5807450.7281 ± 0.0165
MEDICINA	2	2139526.9604 ± 0.0024			

Table 5. EOP uncertainty (X_p, Y_p — pole coordinates, μas, $UT1$ — Universal Time, μs, X_c, Y_c — celestial pole offset, μas), and related statistics (σ_0 — post-fit rms, ps, C_{max} — maximum correlation between EOP) for IVS R4 sessions.

Network	$\sigma(X_p)$	$\sigma(Y_p)$	$\sigma(UT1)$	$\sigma(X_c)$	$\sigma(Y_c)$	σ_0	C_{max}
All stations	103	75	35	56	58	0.697	35
w/o Svetloe	113	79	41	58	61	0.730	37

Obtained results show that including Svetloe in the IVS network yields clear improvement in the quality of results. Hopefully, further participation of SvRAO in IVS programs as a regular station will allow us to realize more substantial progress in the accuracy of determination of EOP and TRF, and make a valuable contribution to geodesy and astrometry studies.

4. Acknowledgments

Authors wish to thank our colleagues Chopo Ma and Ed Himwich (Goddard Space Flight Center), and Brian Corey (Haystack observatory) for fruitful cooperation on VLBI technology and space geodesy being crowned with installation of the Mark IIIA terminal at the Svetloe observatory and its inclusion in the IVS network. We are also grateful to Dan MacMillan (Goddard Space Flight Center) for providing the latest GSFC estimates of Svetloe position.

References

[1] Finkelstein, A. M., 2001: Radiointerferometric Network QUASAR. Science in Russia, No. 5, 20–26.

[2] Finkelstein A., A. Ipatov, S. Smolentsev, 2004: Radio astronomy Observatories in Svetloe, Zelenchukskaya and Badary of VLBI network QUASAR. This issue.

[3] Finkelstein, A. M., A. V. Ipatov, S. G. Smolentsev, V. G. Grachev, I. A. Rahimov, Z. M. Malkin, 2003: Highly Accurate Determination of the Coordinates and the Earth's Rotation Parameters Involving the Svetloe VLBI Observatory. Astronomy Letters, 2003, **29**, No 10, 667–673.

Zhihan Qian et al.: Present Status and Future Plan on the Chinese VLBI Network, IVS 2004 General Meeting Proceedings, p.133–137
http://ivscc.gsfc.nasa.gov/publications/gm2004/qian

Present Status and Future Plan on the Chinese VLBI Network

Zhihan Qian [1], *Shuhua Ye* [1], *Xiaoyu Hong* [1], *Xiuzhong Zhang* [1], *Jin Zhang* [2], *Xizheng Zhang* [2], *Hongbo Zhang* [2]

[1] *Shanghai Astronomical Observatroy, CAS*
[2] *National Astronomical Observatories, CAS*
Contact author: Zhihan Qian, e-mail: qzh@center.shao.ac.cn

Abstract

At present, the Chinese VLBI Network (CVN) includes two fixed VLBI stations, named Sheshan (Seshan) Station and Nanshan (Urumqi) Station, respectively, and a mobile VLBI station as well as a two-station VLBI correlator of the VLBA style. Recently, the disk based recording terminals have been successfully developed for VLBI observations. For the future astronomical, geodetic and space scientific applications, especially, for the forthcoming Chinese Lunar Exploration Project, a 50m and a 40m radiotelescope, which will be located in Beijing and Kunming, respectively, are under manufacture and will be completed in 2005/2006. A new 5-station VLBI correlator with the capability of expansion to 10 or more stations is under design and also will be completed in 2005/2006.

1. Present Status

The construction of the Chinese VLBI Network (CVN) started early in 1980s. Up to date, two fixed VLBI stations, Sheshan Station, near Shanghai and Nanshan Station, near Urumqi and one mobile VLBI station as well as a two-station VLBI correlator were completed. Recently, the VLBI disk based recording terminals, named the CVN Disk-RT, were successfully developed for the VLBI observations.

1.1. Sheshan VLBI Station

The Sheshan VLBI Station, located in the Song Jiang County, south-west of Shanghai, eastern China, about 30 km from downtown Shanghai, was completed in 1987. The antenna is mounted on a building (see Figure 1). The S/X-, C-, and K-bands work at Cassegrain focus through a beam-waveguide system and the L-band works at the prime focus after turning over of the subreflector. Its location is: Longitude: 121.20°E, Latitude: 31.10°N. The ground height of the site above sea level is about 5 meters. The main specifications of the station are as follows:

- Antenna diameter: 25m
- Antenna type: Beam-waveguide Cassegrain system
- Antenna efficiency (S/X): 0.30/0.50
- System noise temperature (S/X): 100K/55K
- Recording System: Mark IV, S2 RT, CVN Disk-RT, and Mark 5 (available in 2004)
- Maser: Two SHAO-masers

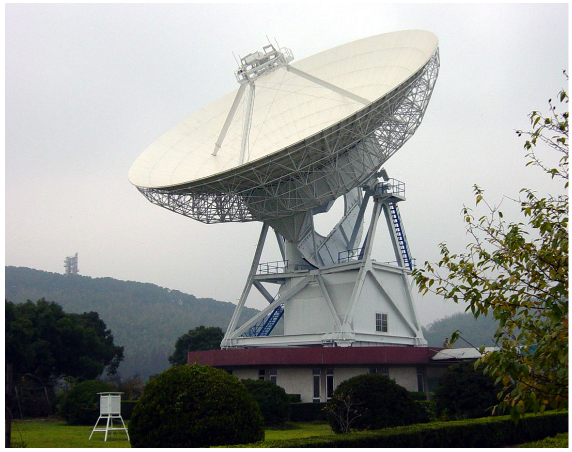

Figure 1. Sheshan 25m Radiotelescope

1.2. Nanshan VLBI Station

The Nanshan VLBI Station, located south-west of Urumqi, northwestern China, about 60 km from downtown Urumqi, was completed in 1994. Figure 2 shows the full view of the site. Its location is: Longitude: 87.18°E, Latitude: 43.47°N. The ground height of the site is about 2080 meters. The main specifications are as follows:

- Antenna diameter: 25m
- Antenna type: Cassegrain system
- Antenna efficiency (S/X): 0.50/0.54
- System noise temperature (S/X): 75K/45K
- Recording System: Mark IV, K4, CVN Disk-RT, and Mark 5 (available in 2004)
- Maser: Two SHAO-masers

Figure 2. A full view of Nanshan VLBI Station

1.3. Mobile VLBI Station

A mobile VLBI system was completed in 1999 and recently, it is located in the Yunnan Astronomical Observatory, NAO, CAS, about 10 km from downtown Kunming, southwestern China. Its antenna is mounted on a truck (in the middle of Figure 3), near a 10m radiotelescope which is used for solar observations (at the left of Figure 3). Its location is: Longitude: 102.80°E, Latitude: 25.02°N. The main specifications are as follows:

- Antenna diameter: 3m (Axis-offset)
- Antenna efficiency (S/X): 0.55/0.50
- System noise temperature (S/X): 120K/110K
- Recording System: S2 RT and CVN Disk-RT
- Maser: Two SHAO-masers

Figure 3. Mobile VLBI Station. It is located at the Yunnan Observatory. Its 3m antenna is on a truck and the VLBI terminal and hydrogen masers are in the right building (with white wall).

1.4. Disk Recording Terminal

Recently, The VLBI disk based recording terminals (CVN Disk-RTs) have been successfully developed for domestic VLBI observations. They have been demonstrated for both astronomical and spacecraft VLBI observations. The main specifications are as follows:

- Recording speed: 512Mb/s
- Playback speed: 256Mb/s
- Volume: 4X120GB (4 disks)
- Recording time: 16 hours (with the recording rate of 64 Mb/s)
- Format of input data: Mark IV

1.5. CVN Correlator

The CVN Correlator which is located at Shanghai Astronomical Observatory was completed in 2000 and its main specifications are as follows:

- Type: VLBA style, FX mode
- Station: Two
- Channel: 8/station
- Max. rate: 32 Mb/s/ch; 256 Mb/s/station
- Playback: P&G tape recorder and CVN Disk-RT
- Format of input: Mark IV and VLBA
- Format of output: FITS

2. Future Plan

For the astronomical, geodetic, and space scientific applications, especially, for the Chinese Lunar Exploration Project, two new VLBI stations equipped with a 50m and a 40m radiotelescopes, respectively, will be established in 2005/2006. For the first stage of the Chinese Lunar Exploration Project one important task of the CVN is the determination of the precise orbit of the lunar orbiter in cooperation with the Chinese Space Tracking Network. These two larger radiotelescopes also will be used for receiving scientific data from the lunar orbiter. A new 5-station VLBI correlator with the capability of real-time VLBI observations is under design and will be completed in 2006.

2.1. New VLBI Correlator

A new 5-station VLBI correlator with FX mode which possesses the capability of expansion to 10 or more stations is under manufacture and will be completed in 2005/2006. Its maximum data rate per station is 256 Mb/s with expansion to 1.0 Gb/s. Also, this correlator possesses the capability of data processing for real-time VLBI observations.

2.2. Miyun VLBI Station

A new VLBI station named Miyun Station with a 50m radiotelescope will be located nearby the existing Miyun Meter-wave Aperture Synthesis Radio Telescope in Miyun County, about 50 km from downtown Beijing. The 50m radiotelescope is under manufacture and will be installed at the site in late 2005. The model of the antenna is shown in Figure 4. The site location is: Longitude: 116.75°E; Latitude: 40.55°N. The main specifications of the station are as follows:

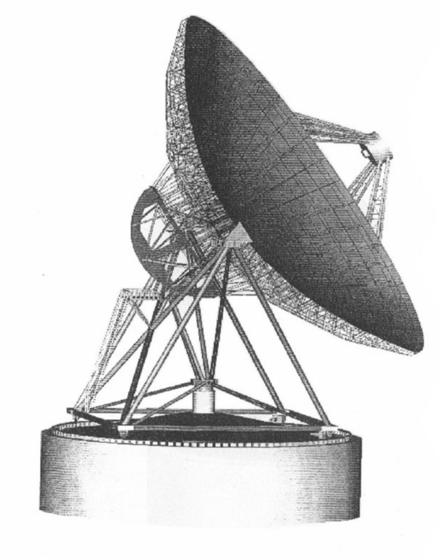

Figure 4. The model of 50m radiotelescope

- Antenna diameter: 50m (full panel for inner 30m and mesh from 30m to 50m)
- Antenna type: Prime feed
- Mount type: AZ-EL, with wheel-on-track machinery
- Bands: 92cm, 49cm, 18cm, 13/3.6 cm and 6cm
- Antenna efficiency (S/X): 0.50 at 13cm (50m); 0.48 at 3.6cm (inner 30m)
- Slew speed: AZ: $1.0°/s$; EL: $0.5°/s$
- Recording system: CVN Disk-RT and Mark 5
- Maser: SHAO-masers

2.3. Kunming VLBI Station

The Kunming VLBI Station will be equipped with a 40m radiotelescope. The selection of the site is under way. Probably, it will be located at the Yunnan Astronomical Observatory, NAO, CAS. The manufacture of the 40m radiotelescope has started. The designed structure is shown in Figure 5. The possible Location is: Longitude: 102.8°E, Latitude: 25.0°N. The 40m antenna will be installed at the site in late 2005. The main specifications of the station are as follows:

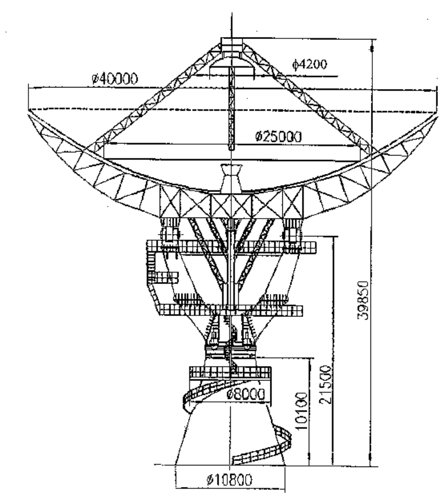

Figure 5. The designed structure of 40m radiotelescope

- Antenna diameter: 40m (full panel for Inner 25m and mesh from 25m to 40m)
- Antenna type: Cassegrain system
- Mount type: AZ-EL, concrete pedestal
- Bands: 13/3.6 cm and others (TBD)
- Antenna efficiency (S/X): 0.60 at 13cm; 0.40 at 3.6cm
- Slew speed: AZ: 1.0°/s; EL: 0.5°/s
- Recording system: CVN Disk-RT and Mark 5
- Maser: SHAO-masers

Shigeru Matsuzaka et al.: VLBI-GPS Co-location Results in Japan, IVS 2004 General Meeting Proceedings, p.138–142
http://ivscc.gsfc.nasa.gov/publications/gm2004/matsuzaka

VLBI-GPS Co-location Results in Japan

Shigeru Matsuzaka, Yoshimitsu Masaki, Hiromichi Tsuji, Kazuhiro Takashima, Takashi Tsutsumi, Yoshimasa Ishimoto, Morito Machida, Hirohito Wada, Shinobu Kurihara

Geographical Survey Institute

Contact author: Shigeru Matsuzaka, e-mail: `shigeru@gsi.go.jp`

Abstract

We present the results of our co-location surveys at two of our network VLBI sites and a preliminary comparison of VLBI and GPS solutions on a baseline between Tsukuba and Shintotsukawa. The comparison shows no systematic differences exceeding 10ppb between the two techniques. In addition we introduce a local hydrological effect on the vertical component of space geodetic measurements.

1. Introduction

Geographical Survey Institute (GSI) now operates and maintains 4 VLBI stations in Japan as well as 1,200 nationwide permanent GPS tracking array (GEONET: GPS Earth Observation NETwork), see Figure 1. Accurate tie information is indispensable for the maintenance of the high-precision terrestrial reference frame and it is true for our new geodetic system (JGD2000) as it is based on the fundamental network consisting of VLBI and GPS [2]. Co-location surveys at Tsukuba and Shintotsukawa VLBI sites show local ties are established at the mm-level between VLBI and GPS reference points and the comparison of baseline solutions indicates that there will not be relative systematic differences exceeding 10ppb between the two. As the precision of space geodetic measurement improves, we have to consider formerly negligible global/local effects that may contribute to the variation of solutions. We will show an example of local hydrological effect on the vertical component of positions and discuss its significance.

2. Local Tie and Transformation to Global Reference Frame

Local tie was established at each site between a GEONET point and the VLBI antenna by the method described in [5]. The standard error (north, east, up) in mm, of the determination was (0.5, 0.5, 1.0) for Tsukuba and (0.7, 0.8, 1.0) for Shintotsukawa. To transform the local relative vector to the ITRF system, we made GPS observations between the network and a direction maker 7-13km away from the site to determine the network's horizontal orientation and used the deflection of the vertical at the site. For the deflection of the vertical, we used the value obtained by astronomical observations at Tsukuba (1980-1983) and interpolated one from Japan's Geoid model (GSIGEO2000, [3]) at Shintotsukawa. The interpolation was compared with several sites with observed values and considered good enough for the transformation [4]. The relative vectors between GPS and VLBI are shown in Table 1.

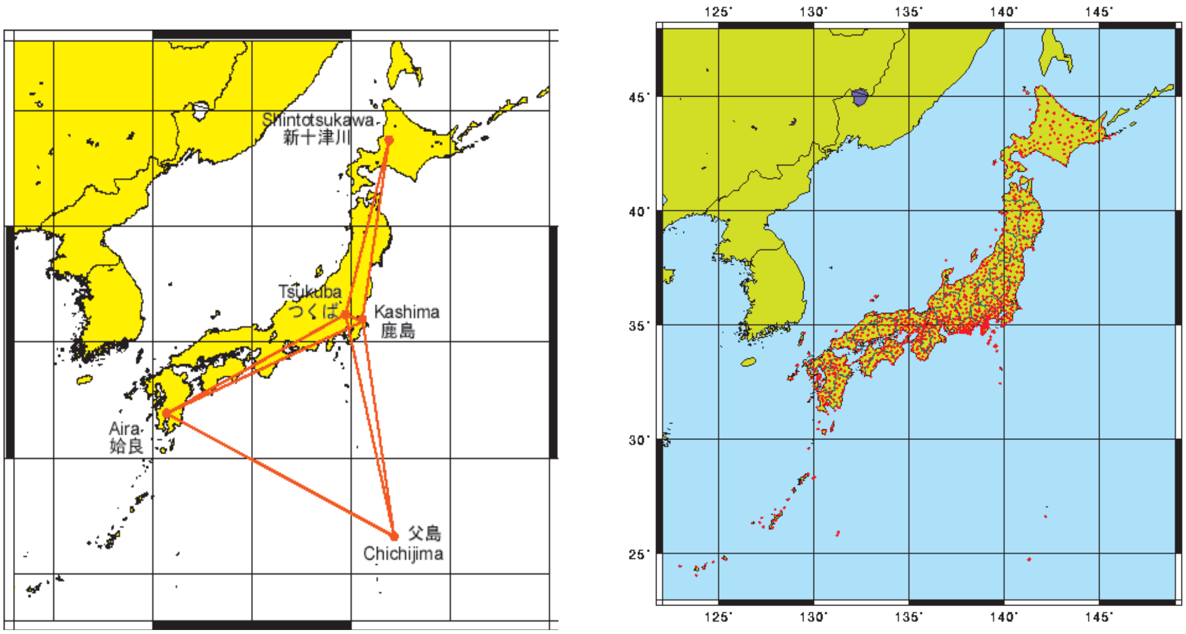

Figure 1. GSI's space geodetic networks, VLBI(left) and GEONET(right).

Table 1. Vectors from GPS to VLBI (ITRF2000, unit: m)

Vector	X	Y	Z	L
TSKB to 32m	-209.5453	29.7219	-216.8837	303.0366
942004 to 3.8m	6.5162	14.3860	-3.9314	16.2749

3. Comparison of VLBI and GPS Tme Series Solutions

Two sets of time series solutions were compared on one baseline. VLBI solutions were converted to the GPS baseline with simple vector additions as depicted in Figure 2. Analysis software was Calc/Solve for VLBI and Bernese for nationwide GPS network [1]. Figure 3 shows the two sets of solutions from 1995 to 2003 measurements for each component of the vector. No artificial offset between the two series was added. In horizontal components no systematic differences exceeding a few cm are seen. In contrast the vertical series differ by a few cm or more and we need to investigate what causes this discrepancy. Possible causes are, simple error of calculation, snow on GPS antenna, local effects such as by groundwater described in the next section, etc.

4. Local Effect on Vertical Position

For some time, an IGS site at GSI Tsukuba, TSKB has been known to show anomalous seasonal variation in height component. Recently the cause and mechanism of variation were revealed by Tobita et al.[7] and Munekane et al.[6]. We briefly introduce their results here. Time series (a) in

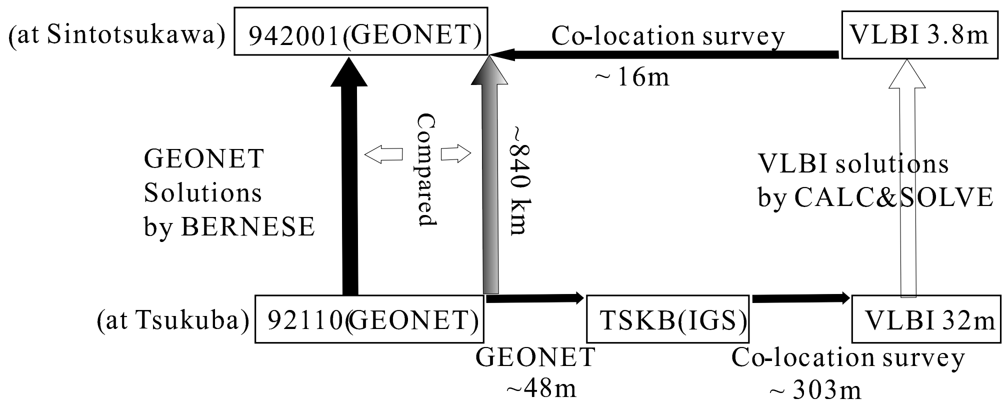

Figure 2. Comparison of VLBI and GPS, GEONET and VLBI+Local-tie solutions compared on the baseline (942001-92110).

Figure 4 shows the height variation for the past 8 years of TSKB. There is a strong correlation between the height change and groundwater level monitored at several deep wells at the site, see (b) and (c) in Figure 4. It was explained by the elastic deformation of water-contained layers and the cause of the water-level change was also investigated. The bottom graph in Figure 4 shows the relation of groundwater level and the amount of its extraction in a year. In the 4 months of summer, groundwater is used to irrigate the rice field in Tsukuba and corresponding to this, the level of water goes down and begins to come back in September.

5. Conclusion

An accurate local tie was established at 3 of 4 GSI VLBI sites in Japan. Co-location survey will be completed in 2004-5 if the remaining Chichijima site is co-located. Now that our domestic VLBI experiment has tripled its frequency (once per month in 2003) and time series solutions will be a reference for Japan's geodetic network by comparing and combining with daily GPS solutions. Investigation on smaller geophysical, meteorological and environmental effect on site positions becomes more important than ever as we further pursue the improvement of space geodetic observation. We will have to look into antenna thermal deformation, various loading effects and site specific environmental effect such as we introduced here.

References

[1] Hatanaka, Y., T. Iizuka, M. Sawada, A. Yamagiwa, Y. Kikuta, J. M. Johnson and C. Rocken, Improvement of the Analysis Strategy of GEONET, Bulletin of the Geographical Survey Institute, 49, 1-35, 2003.

[2] Imakiire, T., and M. Murakami, Establishment of the New Geodetic Reference Frame of Japan (JGD2000), In: International VLBI Service for Geodesy and Astrometry 2002 General Meeting Proceedings, NASA/CP-2002-210002, N. R. Vandenberg and K. D. Baver (eds.), 304-308, 2002.

[3] Kuroishi, Y., H. Ando and Y. Fukuda, A new hybrid geoid model for Japan, GSIGEO2000 derived from

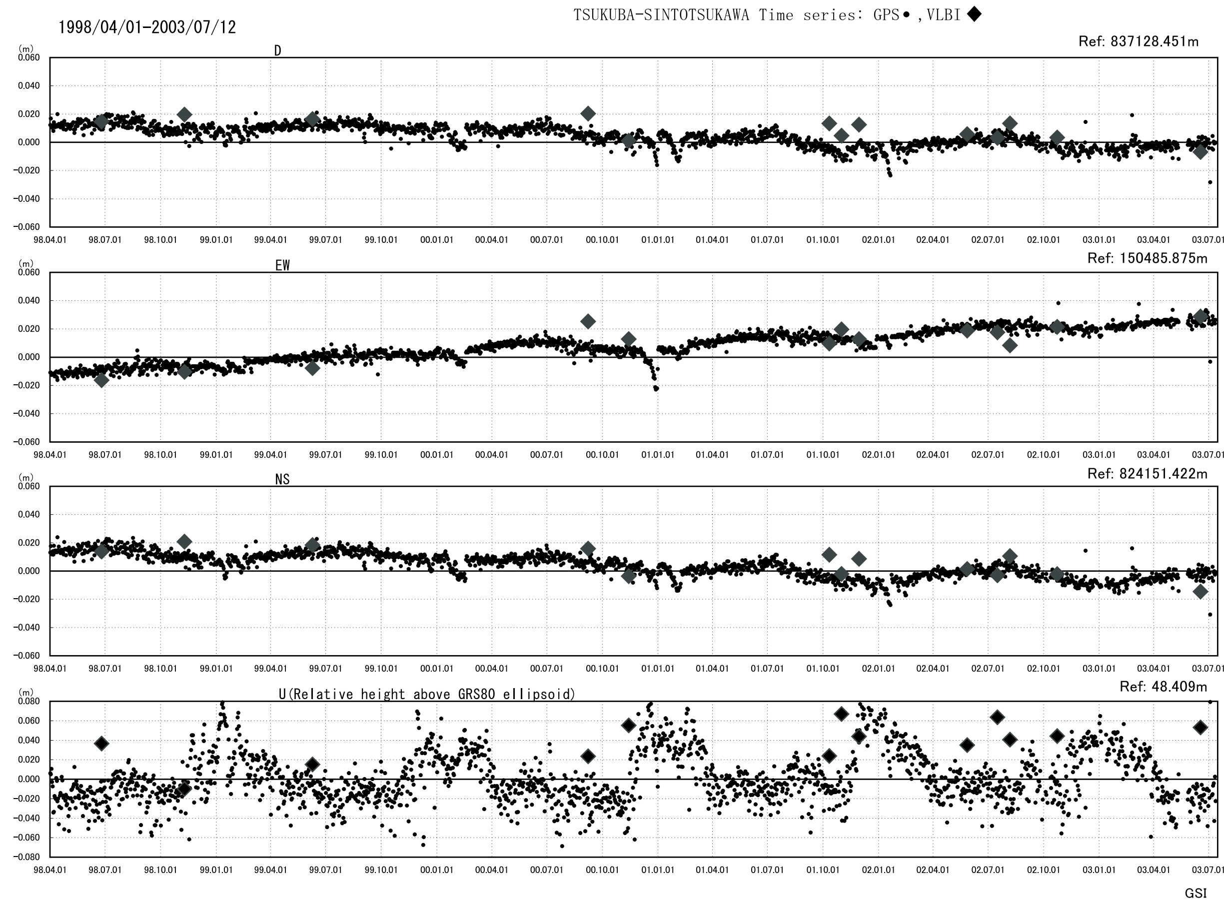

Figure 3. Time series solutions of baseline compoments, dot for GPS, diamond for VLBI.

the gravimetric geoid model, JGEOID2000 and the nationwide net of GPS at benchmarks, Journal of Geodesy 76, 428-436, Springer, 2002.

[4] Kuroishi, Y., private communication, 2003.

[5] Matsuzaka, S., Y. Hatanaka, K. Nemoto, Y. Fukuzaki, K. Kobayashi, K. Abe and T. Akiyama, VLBI-GPS Co-location Method at Geographical Survey Institute, In: International VLBI Service for Geodesy and Astrometry 2002 General Meeting Proceedings, NASA/CP-2002-210002, N. R. Vandenberg and K. D. Baver (eds.), 96-100, 2002.

[6] Munekane, H., M. Tobita and K. Takashima, Groundwater-induced vertical movements observed in Tsukuba, Japan, in preparation, 2004.

[7] Tobita, M., H. Munekane, M. Kaidzu, S. Matsuzaka, Y. Kuroishi, Y. Masaki and M. Kato, Seasonal variation of groundwater level and ground level around Tsukuba, J. Geod. Soc. Japan, in press, 2004.

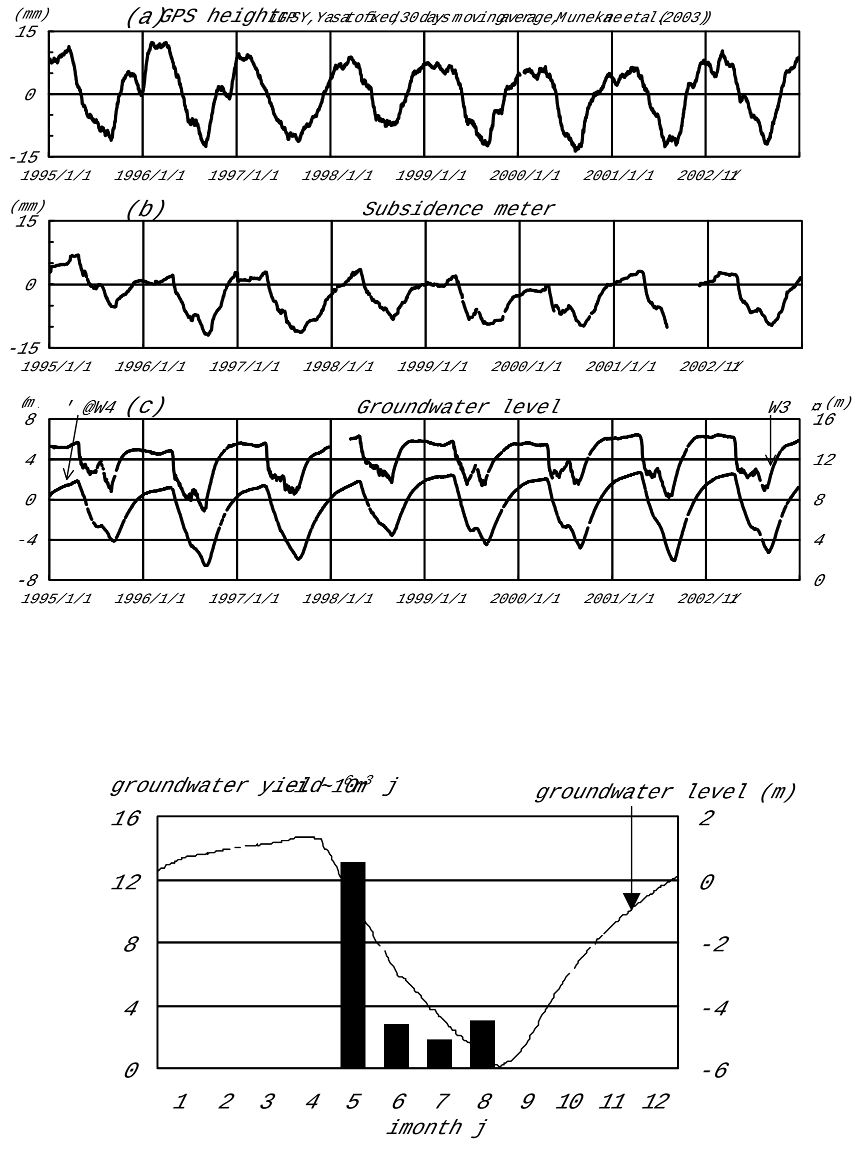

Figure 4. GPS height variation and relevant quantities, (a)GPS height, (b)Subsidence meter, (c)Groundwater level, bottom: Groundwater level vs. extracted amount, [6], [7].

Hayo Hase et al.: Projects at TIGO, IVS 2004 General Meeting Proceedings, p.143–145
http://ivscc.gsfc.nasa.gov/publications/gm2004/hase2

Projects at TIGO

Hayo Hase [1], Sergio Sobarzo [2], Cristobal Jara [2], Roberto Aedo [3], Gonzalo Remedi [3], Marcos Moreno [2], Gonzalo Hermosilla [2], Oscar Cifuentes [4]

1) *BKG - TIGO*
2) *Universidad de Concepción - TIGO*
3) *Universidad del Bío Bío - TIGO*
4) *Instituto Geográfico Militar - TIGO*

Contact author: Hayo Hase, e-mail: `hayo.hase@bkg.bund.de`

Abstract

The Transportable Integrated Geodetic Observatory (TIGO) has been operational in Concepción, Chile for two years. Recently we began several projects which will have some impact on the VLBI data production and analysis.

1. PROGEO

With respect to making a better academic and research use of the Geodetic Observatory TIGO the project partner *Universidad de Concepción* (UdeC) launched a *"Programme on the Science of Geodynamics and Geospace"* (PROGEO) in which several faculties try to develop cooperative research activities. A positive side effect is also the intention to found the first study career for geodesy in Chile along with PROGEO.

As the observatory is producing data, young scientists and students will have to learn how to use this geodetic data. The knowledge about how to do it is available in the international services. We would like to receive support from the international community. PROGEO opens the door for scientists to come to Concepción for giving presentations on related subjects or making courses with postgraduate students.

Please contact the director of PROGEO, Oscar Cifuentes, if you are interested in doing science or education together with us. Mailto: `oscar.cifuentes@tigo.cl`

2. eVLBI

In the TIGO eVLBI project we are preparing ourselves for the eVLBI age. PhD student Sergio Sobarzo is analyzing the network infrastructures to get connected to the correlators. TIGO is fortunate to have optical fibres of the university reaching its site. We have to learn how to interface our data and how to send them to its destination on the fastest route *without* blocking the usual university network traffic. This induces a second priority scheme for eVLBI data, which requires probably its own protocols.

The Chilean university network REUNA is interested and supportive of the eVLBI theme. In May 2004 at the coming national event on broadband communication "eVLBI" will be a theme. In 2005 REUNA hopes to provide Gbit-services to the universities. The link to the US and Europe will be the bottleneck for broadband data communication. However the Internet2 and AMPATH initiative in North-America and the European GEANT are looking to connect Latin America with more bandwidth to the northern hemisphere.

Some data transmissions via communication networks are planned for the near future in order to explore the possibilities and gain experiences in this subject.

3. Regional GPS Network

TIGO is located at the continental shelf of the South-American plate over a subduction zone. This requires careful interpretation of the geodynamical movements. We have to distinguish between continental, regional and local geodynamical movements. In order to do so, TIGO maintains a local survey network at the site, which also allows the determination of the space vectors between the IVS, ILRS, IGS reference markers. On the global level we are tied to other stations by the geodetic space methods and the measurements requested by the services. The gap of regional plate monitoring will be closed soon, when four GPS permanent receivers are being installed around TIGO at distances ranging from 15-50km at the sites Dichato, Faro Hualpen, Santa Juana and Quillón (fig. 1). The construction of the monuments is planned for March 2004.

Such a network at the coast of Chile permanently observed will allow also other research. The permanent stations can be used for weather forecast or determination of the water content in the lower atmosphere as well as a monitor device for ionospheric conditions which complement VLBI. The ionospheric research will be further complemented by Japanese-Chilean experiment with dedicated ionospheric antennas, of which one will be co-located at the TIGO observatory.

4. Vertical Datum

For the definition of a vertical datum a tide gauge will be installed at Dichato (a nice fishermen village) co-located with one of the four GPS receivers of the TIGO regional network (fig. 1). With permanent GPS observations between the tidegauge GPS monolith and the IGS site at TIGO the sealevel can be referred to TIGO (and its superconducting gravity meter).

5. Antenna Controller for Radiotelescope

We expect the installation of a new Antenna Control Unit for the TIGO radiotelescope in September/October 2004. This is a requirement because some spare parts are not available any more. With the upgrade we hope to extend the lifetime of TIGO by 10 years.

The interfacing to the Field System Software for VLBI operations requires some software programming.

6. Visitor Center

TIGO as an observatory is an attraction for students of university and schools of the region as well as for visiting professors at the university. A visitor center (which by its architecture also serves as a solar clock in contrast to TIGO's atomic clocks) was designed containing an auditorium for 120 persons and a hall for permanent interactive exhibitions. The concept allows us to perform star shows at night in the visitor center with an additional astronomical telescope. However the realization is still outstanding.

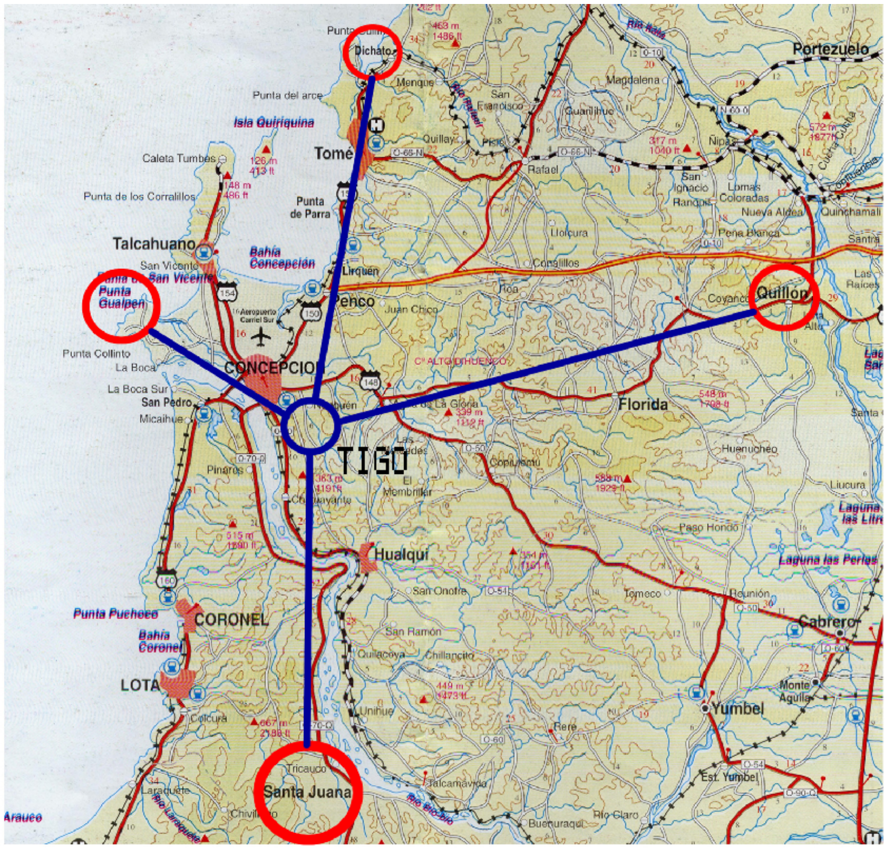

Figure 1. Map showing the locations of four intended sites for permanent GPS observations around TIGO. The upper point *Dichato* will co-locate the TIGO tide gauge. The baselines range from 15 to 50 km.

We are still looking for the funds and the telescope donation for this educative project in this developing country. Therefore the authors would like to invite the reader to support our idea and helping us in realizing this idea.

Maria Hennes et al.: New Technologies for the Real 3D Reference Point Determination, IVS 2004 General Meeting Proceedings, p.146–150
http://ivscc.gsfc.nasa.gov/publications/gm2004/hennes

New Technologies for the Real 3D Reference Point Determination

Maria Hennes, Cornelia Eschelbach

GIK, Geodetic Institute of the University of Karlsruhe, Germany

Contact author: Maria Hennes, e-mail: hennes@gik.uni-karlsruhe.de

Abstract

For local tie determination accuracy the reference point determination is required. This paper discusses the advantages of new cinematic measurement techniques such as robot tacheometers and laser trackers. Laser radar will be of advantage to detect reflector deformations.

1. Introduction

The availability of different space techniques on one observation site requires the establishment of local ties between the reference point of each observation method. Because sub-mm-accuracy is expected for space technologies in the near future, the positions of the reference points have to be determined with equal accuracy. In this contribution, new technologies for reference point determination in respect of the local tie realization and for deformation measurements of radio telescopes are presented, which, furthermore, aim at reducing the downtime of the telescope during local surveying.

According to the reference point definition the telescope's reference point as well as its defining elements are usually virtual, i.e. not materialized and not accessible. If a marker is mounted (e.g. magnetically) on the face surface of the elevation axis and the telescope is rotated azimuthally and vertically, in first approximation the marker's trajectories describe circles, which centers are dedicated to derive the reference point. For details see (Hennes et al, 2004 [6]; Eschelbach 2002 [2]). Efficiency of the trajectories determination can be achieved by the new technologies discussed below, which should replace the angular method.

2. Measurement Methods

2.1. Angular Method

The conventional method for reference point determination is the angular method using spatial intersection. The scale of the intersection network is derived from the local network, which connects the stations. Because the horizontal and vertical angles are measured with theodolites, this method is often referred to as theodolite method. For optimization of the network configurations see (Hennes et al, 2004 [6]). Because each target has to be observed from two stations and repositioning of the telescope is time-consuming and more inaccurate, it is highly recommended to observe the marker simultaneously from both stations. The observation data should be gathered in real-time using two electronic theodolites equipped with appropriate interfaces and connected to a central PC. At the same time, the data should be checked for gross errors by appropriate software, which solves the spatial intersection or even the least squares circle adjustment (i.e. IMKA

(GIK, Karlsruhe), or Axyz (Leica Geosystems AG Metrology Division, Unterentfelden, CH)). Furthermore, observing simultaneously from two stations gives more reasonable information on axis wobbling. If the elevation axis is not accessible for the marker adjustment process and therefore elevation circles have to be observed, the survey takes up to seven days, even if using two theodolites and two experienced observers.

2.2. Polar Method

The major advantage of polar measurement systems in comparison to theodolite measurement systems is that 3D positions (e.g. 3D coordinates) are determined in one step, because the polar measurements (distance and two angles) are measured (nearly) without delay. In respect of the observation schemes see (Hennes et al, 2004 [6]). Nowadays, most of these systems are able to track a moving target (reflector) and to determine the target coordinates quasi on-the-fly. Two instrument types have to be distinguished: robot tacheometers were developed primarily for plain survey and laser trackers are appropriate for industrial measurement tasks.

A robot tacheometer consists of a motorized theodolite equipped with an EDM and a target recognition unit usually based on video techniques. The implemented software controls the motion of the tacheometer's telescope and delivers approx. three (in the future nine) 3D coordinates per second at optimum. The position accuracy amounts to up to 0.3 mm depending on instrument type for a non-moving target and decreases with target velocity (down to some cm @ some m/s). It is highly recommended to correct the measured distances in respect of the addition constant, which is dependent on the angle-of-incidence, even if a 360° reflector is used (Favre, Hennes, 2000 [4]). Furthermore, the line-of-sight should be calibrated for near-range-use (Hennes, 2003 [5]). The system performance for special properties is presented in (Hennes, 2003 [5]; Krickel, 2004 [7]). Further details on tracking performance will be examined at the Geodetic Institute (University Karlsruhe, D) using our motion simulator.

From the first, laser trackers are constructed for fast high-accuracy tracking. The maximum data rate is 1000 Hz. The laser trackers of Leica Geosystems have the best reputations among the trackers offered, although other manufacturer's specifications seem slightly better in particular cases (see also Faro Technologies Inc., Lake Mary, FL, USA and API, Rockville, MD, USA). The Leica LTD-series is specified with an accuracy of 0.1 mm @ 10 m, if the target moves slowly; the accuracy improves by a factor of two, if the target is fixed.

These new technologies enable observations even if the VLBI telescope is moving. Hereby, the point uncertainty is negligible: For example, if the diameter of the elevation circle is 0.4 m and it is created within 10 minutes, the point uncertainty due to the target motion becomes 2 μm for a laser tracker assuming a data rate of 1000 Hz or 0.6 mm for a robot tacheometer operating with 3 Hz. The azimuthal angular speed must be reduced due to the larger diameter of the azimuth circle (e.g. 2.5 h @ 6 m diameter). That means that within very short observation times the required reference point accuracy can be easily obtained. The personal effort as well as the telescope's downtime time decrease dramatically. Although the reflector's orientation due to an angle-of-incidence-dependent offset (and therefore varying with the telescope's orientation) has to be taken into account in the calculation, this is no limiting factor, because Leica's new T-Products for the LTD 700 and 800 announced for 2004 will solve this problem. Examinations at our institute will check the properties of the LTD 500 (see figure 1) in combination with 360° reflectors on our motion simulator which are not specified up to now.

Figure 1. Laser radar Leica LR 200 (left) and laser tracker Leica LTD 500 (right).

2.3. Scanning

Scanning measurement systems should be preferred for the determination of the deformation of the telescope's reflector. The requirements can only be met by the so-called laser radar LR 200 (Leica Geosystems, see figure 1). The system works reflector-less and non-tactile. LR 200 reaches in the enhanced modus an accuracy of 10 μm producing a data rate of two measurements per second (Dold, 2002 [1]). Accuracy decreases with increasing data rate to 0.3 mm at 1000 Hz. For the definition of the six parameters of a surface patch in 10 m distance, the system needs approx. 1 s and achieves the required accuracy of 0.1 mm. The working range of the instrument covers typical main reflectors, if the sensor head (40 kg) is mounted close to the antenna focus. The sensor head may be tilted during the measuring process, so that measurements at each elevation are possible. For the determination of 1000 surface patches (panels), the survey should be done in less than one hour. If the laser radar is positioned externally, the connection of different stations can be achieved by scanning small spheres serving as fiducial points. Due to the fast data acquisition, the thermal deformation of the telescope elements can be determined.

2.4. Real-Time Capability and Performance

The surveying time should be taken into account with high priority, especially when considering methods for surveying the geometry of a radio telescope. All methods, which allow performing its original tasks during the surveying process, should be preferred. So, the application of the classic angular method will decrease in future, even if two connected theodolites with simultaneous data acquisition and real-time calculation are employed. With robot tacheometers and especially with laser trackers, the requirement of time-reducing survey methods can be met, because they are capable to track a fast moving target and, principally, even to determine circle segments for the reference point determination simultaneously with the ordinary VLBI operations. Furthermore, it must be guaranteed that the employed instruments were calibrated beforehand. This is related especially to the tracking components of the instruments. Moreover, an efficient solution for the angle-of-incident-dependent addition constant has to be integrated.

Although potential deformations occur significantly slower than the movements generating the circle paths, in most cases the angular method is too time-consuming to detect thermal deformations. The most efficient method would be the scanning method. If the panel structure has to be adjusted, the integrated "build and inspect" procedure of a laser tracker can be used most efficiently. Polar reference point determinations are capable to support the derivation of a model for describing thermal deformations based on temperature measurements of the basement.

3. Recent Results

3.1. Angular Measurement System

The conventional method based on angular measurements was tested in spring 2002 in a co-operation project between the Onsala Space Observatory, Chalmers University of Technology and the Geodetic Institute of University of Karlsruhe. For details see (Eschelbach, Haas, 2003 [3]) and (Eschelbach, 2002 [2]). The reference point's accuracy reached 0.3 mm (3D), and even the axis-offset could be determined to 6.0 mm $\pm$ 0.4 mm.

3.2. Performance of Polar Measurement Systems

A typical elevation circle (diameter 0.5 m) was simulated by mounting a reflector on a motion simulator. A Leica laser tracker LTD 500 was positioned in a short distance to the circle and close to the center normal vector. Within 10 s a full circle with approx. 1000 points (3D-coordinates) was measured. The rms-value of the measured points in relationship to the best-fitting circle was 0.02 mm; due to the high data number, its center position could be derived with an uncertainty of 1 μm. To analyze the quality of circle segments with real data, the same data was divided into six circle segments. The center coordinates calculated now separately differ up to 0.09 mm. Therefore, it is recommended to observe segments, which are as large as possible and complementary. The center coordinates' accuracy is approx. tenfold better than the manufacturer's specification for near range. Assigning this result to robot tacheometers capable to achieve point accuracy in slow motion of approx. 10 mm, a center point accuracy of 1 mm results, if the circle path is generated within more than 5 min. From this result, it can be assumed, that the required accuracy of the reference point can be achieved if several circles are observed. In respect of the geometry of the telescope, the effect of steep sights (i.e. station far from the circle center normal vector) has to be analyzed for both instrument types. Suitable procedures to avoid systematical effects have to be developed. Both will be done using our motion simulator.

4. Resume

In respect of the increasing accuracy of the VLBI techniques, the precise determination of the reference point location and of the geometric stability of VLBI telescopes becomes more and more important. The proposed strategies and results of contemporary engineering and industrial measurement systems such as theodolite measurement systems, robot tacheometers, laser trackers and laser radars demonstrate the potential of these systems and methods in respect of accuracy increase by new instrument developments, reliability increase by real-time computation and adjustment and last, but not least, by reducing the surveying time and therefore the downtime of the telescope. Especially recent developments such as embedded system control, simultaneous reduction of reflector-orientation based offsets and the application of laser radar can and will make a significant step to an efficient procedure for generating local ties. The control software for these technologies ensures an approved data management, so that deformation effects could be analyzed, compared with results of other sites and, at least, modeled in dependence of its interference parameters.

5. Acknowledgements

The authors want to thank Dr. R. Haas and his group at Onsala Space Observatory, Chalmers University of Technology, Sweden for enabling and supporting the measurements at the Onsala radio telescope. Furthermore, the authors are grateful for detailed discussion with several manufacturers.

References

[1] Dold, J., Autobauer setzen auf mobile Lasermesstechnik, Auto u. Elektronik, 45-48, 5/2002.

[2] Eschelbach, C., Determination of the IVS-reference point at the Onsala Space Observatory in a local reference frame, Diplomarbeit, Geod. Inst., Univ. Karlsruhe.

[3] Eschelbach, C., Haas, R., The IVS-Reference Point at Onsala - High End Solution for a Real 3D-Determination. In: Proc. 16th Working Meeting on European VLBI for Geodesy and Astrometry, eds. W. Schwegmann und V. Thorandt, Bundesamt für Kartographie und Geodäsie, Frankfurt/Leipzig, 109-118, 2003.

[4] Favre, C., Hennes, M., Zum Einfluss der geometrischen Ausrichtung von 360°-Reflektoren bei Messungen mit automatischer Zielerfassung, VPK 2/00, 72-78, 2000.

[5] Hennes, M., Systemeigenschaften von Robottachymetern im Nahbereich - Untersuchungen am Beispiel von Leica-Instrumenten, FuB, 300-310, 2003.

[6] Hennes, M., Haas, R., Eschelbach, C., Industriemesssysteme zur Qualitätssteigerung von VLBI-Ergebnissen, Paper to Kurs f. Ingenieurvermessung, Zürich, March, 15-19, 12 pages, 2004.

[7] Krickel, B., Leistungskriterien zur Qualitätskontrolle von Robottachymetern, Thesis Geod. Inst. Univ. Bonn, in press, 2004.

Seiji Manabe et al.: Status and Plan of Geodetic and Astrometric Observations with VERA, IVS 2004 General Meeting Proceedings, p.151–155
http://ivscc.gsfc.nasa.gov/publications/gm2004/manabe

Status and Plan of Geodetic and Astrometric Observations with VERA

Seiji Manabe, Yoshiaki Tamura, Takkaki Jike, Koji Horiai, VERA Team

National Astronomical Observatory of Japan

Contact author: Seiji Manabe, e-mail: `manabe@miz.nao.ac.jp`

Abstract

The construction of VERA (VLBI Exploration of Radio Astrometry) was completed in 2002 and scientific and system-checking observations are regularly done. In the recent two years since the previous IVS General Meeting there are two important progresses. One is that VERA's promising capability in the phase compensation was demonstrated by using a real observation. The other is that phase referenced maps are obtained with good but not sufficient positional accuracy. There have been some geodetic observations by participating in the Geographic Survey Institute (GSI)'s domestic observations on a once-a-month basis and link of Mizusawa station to the Tsukuba 32m antenna was obtained. Current status and some future plans of VERA are briefly reviewed.

1. Introduction

VERA is a Japanese domestic VLBI network consisting of Mizusawa, Iriki, Ogasawara and Ishigakijima stations. The construction of the four stations was completed at the end of March, 2002. Each station is equipped with a 20m radio telescope and VLBI backends.

The primary scientific goal of VERA is to reveal structure and dynamics of our Galaxy by determinig 3-dimensional force field and mass distribution. Galactic maser sources are used as dynamical probes, positions and velocities of which can be precisely determined by phase referenced VLBI relative to extragalactic radio sources. The distance is measured as a classical annual trigonometric parallax. The target accuracy in the annual parallax determination is 10μas. With this accuracy the distance to annual parallax of an object at a distance of Dkpc is given by D%.

In order for realizing this accuracy it is necessary to remove the effect of atmospheric fluctuation which is the largest error source in conventional VLBI. One of the methods to remove this effect is the phase referenced VLBI observation of two closely separated objects. VERA is equipped with a dual beam receiving system which enables observations of two objects simultaneously.

In this paper some recent progresses and current status of geodetic and astrometric observations will be described. Some future plans will also be presented.

2. Progress in the Recent Two Years

2.1. Proof of Capability of the Phase Compensation

VERA's enormous capability in phase compensation was first shown by Honma *et al.* (2002). Fig. 1 shows the observed fringe phases of the two strong maser souces, W49N and OH43.8-0.1 separated by 0.65°, and the differences between them for Mizusawa-Iriki baseline (1300km). The constant biases are subtracted from the individual phases. It is seen that the fringe phases change almost in parallel (indistinguishable in the figure) and the differences are much smaller than the

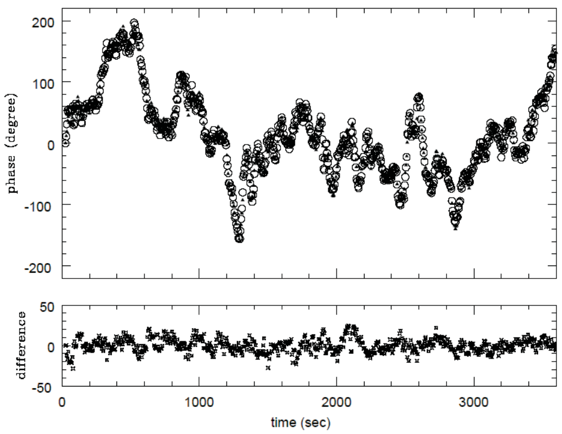

Figure 1. Top: observed fringe phases of W51N (open circle) and OH43.8-01 (triangle). Bottom: differential fringe phases. (Honma *et al.*, 2003)

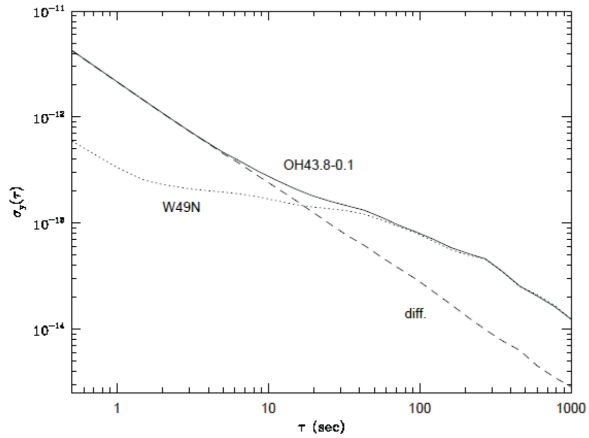

Figure 2. Allan standard deviations of the observed and differential fringe phases (Honma *et al.*, 2003)

variations of the individual fringe phases. The randomness of the differential fringe phases is confirmed in Fig. 2 which shows Allan standard deviations of the original and differential fringe phases. The linearity of the differential fringe phase proves that the spectrum is white and there remains no dominant systematic errors.

2.2. Phase-Referenced Maps of QSOs and Astrometric Precision

Fig. 3 shows the first phase referenced maps of 3C345 with respect to NRAO512 (Rioja *et al.*, 2003, private communication). Comparing the detailed map obtained by VLBA, it is seen that the overall features are recovered although fine structures are not resovled because of the small number of the stations and the short lengths of the baselines. The S/N ratio of the phase referenced map is almost the same as that of the non-phase referenced self-calibrated map.

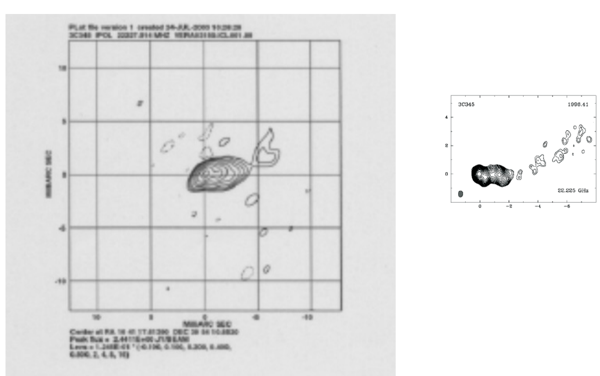

Figure 3. Left: map of 3C345 with reference to NRAO512 obtained with VERA. Right: map of 3C345 otained with VLBA.

In order to see the reliability of observation, maps of NRAO512 at three different epochs are compared in Fig. 4. The beam shape of the right map is fairly elongated because only Mizusawa, Iriki and Ishigakijima which are almost collinearly located participated in the observation. The positions of the brightness peaks coincide with the accuracy of 0.1mas which is better than that of HIPPARCOS by almost one order of magnitude although it is an order larger than the target accuracy.

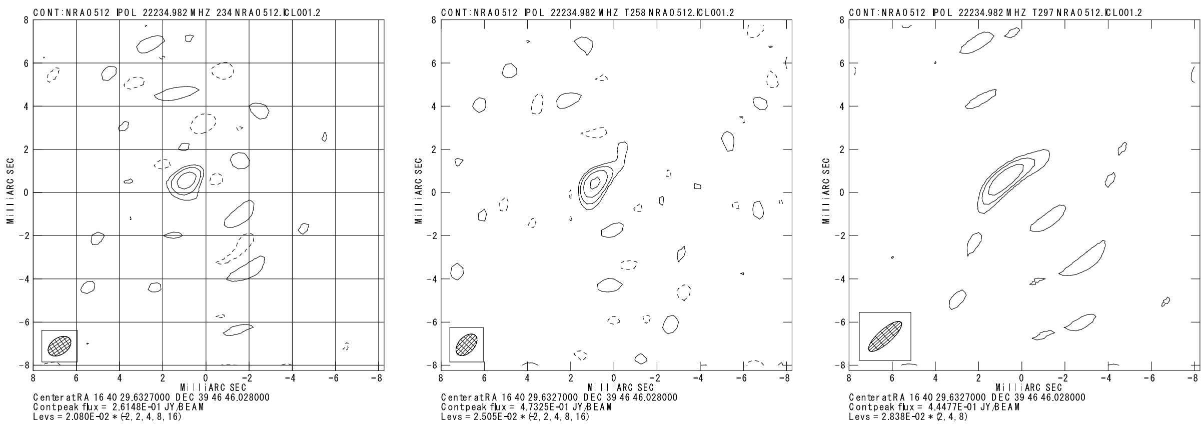

Figure 4. Phase referenced maps of NRAO512 with respect to 3C345 on doy 234, 258 and 297 in 2003.

3. Status of the Geodetic Observations

Very high accuracy of antenna positions is crucial to realize the target accuracy of radio source positions. For determining annual parallaxes with accuracy of 10μas a few mm is required for annual component in the antenna positions. Geodetic observation can be regarded as one of the calibration processes of VERA in this respect. However, if the target accuracy, say 2mm, is achieved in the antenna positions, the data series will be a wealth of geophysical information.

The simultaneous receiving system in S and X bands are installed at all four stations of VERA for conventional geodetic observations. The general features of this system are described in Tamura et al.(2002). The other frequency bands, namely K and Q, are expected to be usable in the future. The most important point of the VERA geodetic observing system is that only Mizusawa station has a data aquisition system compatible with K4 and other three stations have only DIR2000 DAS. No station has currently compatibility with Mark IV or Mark 5. Therefore, the three stations except for Mizusawa cannot directly be linked to the international VLBI network.

3.1. VERA Internal Geodetic Observations

The baseline of the observation strategy is that DIR2000 DAS is used for geodetic observations among the VERA network. The data are recorded on magnetic tapes and correlated at the Mitaka correlation center. The recording rate is 1Gbps. It is planned that in order for determining the antenna positions with sufficient accuracy considerable observation time, say 60-80 24-hour observing sessions per year, will be allocated for geodetic observations until characteristics of antenna position variations become clearly understood.

Experimental observations for very short time have been tried and fringes have been detected by using DIR2000 DAS. However, full 24-hour geodetic observations have not yet be tried because of insufficient stability of the observation system. They will be tried this year.

The observed data are correlated with the Mitaka correlator and raw visibilities are stored in the form of CODA File System. Then, they are bandwidth synthesized to obtain group delays and phase delay rates. These data are analysed to derive geodetic information by using the software developed at NAOJ. Some improvements of the software, in particular GUI, is under way.

3.2. International Link via the Tsukuba 32m Antenna of GSI

As describe above, only Mizusawa station is equipped with the K4 system and coordinates of the other stations have to be determined relative to those of Mizusawa. Therefore, in order to link VERA station positions to an international frame, for example ITRF, it is necessary to link Mizusawa to an international frame. This is realized by determining Mizusawa's position relative to the Tsukuba 32m antenna of GSI. Mizusawa participates in the GSI's domestic observation programs once a month and some results with internal precisions of 5-10mm have been obtained. However, since the number of successful observations is limited up to now, the international link is not yet considered to be strong enough.

3.3. Domestic Network

In addition to VERA three VLBI stations have been established at universities. They are Yamaguchi (32m), Gifu (11m) and Tomakomai (11m). The former two have strong interests in geodetic observations. Mizusawa made an experimental observation with Gifu and it was the first successful observation in the S and X bands for Mizusawa. Gifu is linked to GSI and Mitaka via an optical fiber network and performing regular observations with GSI. Geodetic as well as astrometric observations with VERA are expected for these radio telescopes in the near future.

4. Astrometry and Contribution to CRF

VERA is a dedicated instrument for astrometry and expected to be able to determine star positions very accurately. However, this does not mean that positions of VERA's main target sources, which are Galactic masers sources, are accurate in the sense of absolute coordinate determination. This is also the case when relative positions of two QSOs separated closely are determined. It is logically possible to construct a global reference frame by weaving a net of relative positions of extragalactic objects. However, a global reference frame is only realizable after covering the whole sky with this method and required resources may be too large to share observation time with maser astrometry. Therefore, VERA is not an outstanding instrument for constructing a global reference frame such as ICRF. However, the phase referenced VLBI by VERA may be useful for checking accuracy of a position catalogue by determining relative positions of some numbers of pairs of QSOs included in catalogues. The result shown in Fig. 4 can be considered to be a first step for contribution to CRF.

5. Future Plans

The most urgently needed task for VERA's geodetic observations is to stabilize the VERA system, in particular DIR2000 DAS. In addition a K5 DAS has to be installed at least at Mizusawa in order to keep the compatibility with the GSI 32m whose K4 DAS will be abandoned in 2005. Improvement of the analysis software is also an urgently needed task.

There is strong radio interference in the S-band from cellular phone at Mizusawa. The interfering noise is filtered out and the S-band is usable at least for VLBI. However, it is foreseen that we have to abandon the S-band in coming several years. In order to shift to the higher frequencies, the possibility of experiments in X- and K-bands with K-bands used for ionospheric correction are being investigated. Phase referenced astrometry of QSO pairs in K- and Q-bands mentioned in the previous section is also planned.

In the further future a new large correlator must be constructed to replace the Mitaka FX correlator which was built 10 years ago.

VERA will be used as main ground telescope to track lunar orbiters in the RISE project which aims to determine a precise and detailed gravity map of both the near and far sides of the Moon. VERA is expected to improve orbital accuracy near the lunar limbs. The rocket is scheduled to be launched in 2005 and the main observation period is in 2006.

Korea is constructing the Korean VLBI Network (KVN) consiting of three stations. If VERA and KVN are used, the coverage in the *uv* plane will be greatly improved, since VERA lacks short baselines and KVN is fairly compact. KVN's antennas do not have dual-beam capability. However, their high slew speed will make it possible to perform phase referencing by fast switching of antenna directions. It is strongly desired and expected that VERA and KVN closely cooperate in the future.

References

[1] Honma, M., *et al.*, First Fringe Detection with VERA's Dual-Beam System and Its Phase-Referencing Capability, Publ. Astron. Soc. Japan 55, ppL57-L60, 2003.

[2] Tamura, Y. and VERA Group, Geodetic Observation System in VERA, IVS 2002 General Meeting Proc., pp167-170, 2002.

Young Chol Minh et al.: Present Status of the KVN Construction Project, IVS 2004 General Meeting Proceedings, p.156–160
http://ivscc.gsfc.nasa.gov/publications/gm2004/minh

Present Status of the KVN Construction Project

Young Chol Minh, Hyun-Goo Kim, Seog-Tae Han, Duk-Gyoo Roh

Radio Astronomy Division, Korea Astronomy Observatory

Contact author: Young Chol Minh, e-mail: minh@trao.re.kr

Abstract

Korea's new VLBI project to construct the Korean VLBI Network (KVN) started in 2001, as a 7 year project which is fully funded by our government. We plan to build 3 new 20-m high-precision radio telescopes in 3 places in Korea, which will be used for VLBI observations exclusively. The 2/8, 22, 43, 86, ∼100, and ∼150 GHz HEMT receivers will be installed for astronomical, geodetic, and earth science VLBI research, but millimeter-wave VLBI will ultimately be the main goal/focus of KVN.

For the front-ends, we are going to install a multi-channel receiver system which employs perforated plate filters within a quasi-optical beam transportation system. This receiver system will give reliable phase calibrations for mm-VLBI as well as enable simultaneous multi-frequency band observations. We have completed the design of the KVN DAS system of 2 Gsps sampling rate, which will use 4 data streams to meet the multi-channel requirement. The hard-disk type new Mark 5 will be used as the main recorder of KVN. We plan to develop a new correlator for KVN, but this is still in the planning phase.

1. Background

The first radio astronomical project of Korea Astronomy Observatory (KAO) was the construction of the 14-m millimeter wave radio telescope at Daejeon, Korea, which was completed about 15 years ago. With the completion (construction) of this radome-enclosed 14-m radio telescope, the Taeduk Radio Astronomy Observatory (TRAO) was inaugurated as a branch of KAO. At present, a dual-channel (100/150 GHz) SIS receiver is being used, which was made by our engineering team, and we are preparing a multi-channel (15-beam) receiver (made by FCRAO) to be installed in our 14-m telescope. Our main research subjects are studies of interstellar molecular clouds and the physical and chemical processes in dense clouds. In particular, the SiO masers, star-forming regions, and interstellar molecular processes have been the major focus of our radio astronomy group.

Although we have been managing our millimeter-wave telescope and receiver systems successfully so far, our radio group has not yet been involved in any VLBI activities, mainly because of our millimeter-wave single-dish facility. Only recently (from 2001) have we started VLBI experiments, in millimeter wavelengths, with the Nobeyama VLBI group of Japan – with encouraging success.

After the 14-m radio telescope project, KAO concentrated its efforts mainly on the construction of optical telescopes. By the completion of the optical telescope project a few years ago, our radio group submitted a proposal for this Korean VLBI Network (KVN) construction project to our government, which was finally approved in 2000.

2. Scientific Goals of KVN

The KVN will be the first VLBI facility in Korea, which will be used for VLBI studies in astronomy, geodesy, earth science, etc. The general VLBI research targets will also be targets

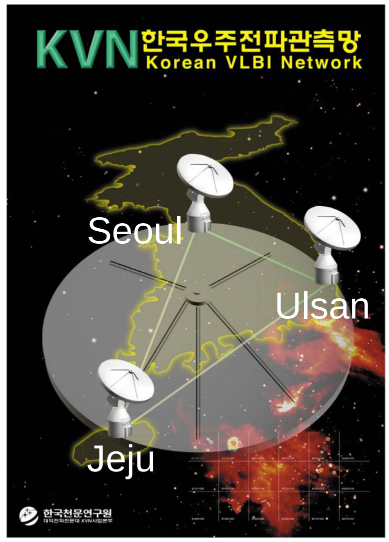

Figure 1. Three locations of the KVN observatory sites in Korea – Seoul, Ulsan, and Jeju – are indicated.

for KVN, within the KVN limitations. However, the KVN will be constructed as an advanced millimeter-wave (up to ~150 GHz) VLBI network. Since millimeter-wave VLBI is still in the developing stages around the world, we expect that our KVN will play an important role in promoting millimeter-wave VLBI research activities.

Because of the existing 14-m millimeter-wave telescope facility, the research activities of the present radio astronomy group of KAO are concentrated on interstellar molecular cloud studies. Therefore, one of our main KVN projects will be spectral-line observations focused on the interstellar molecular processes at millimeter wavelengths. At the same time, we are strengthening our VLBI group by increasing its members in high-energy astrophysics and AGN-related research fields, in order to promote research activities in various VLBI subjects.

In geodetic studies, most of the research work will be led by the geodetic society groups in Korea. Since the tectonic movement of the Korean peninsula, including several important fault plane movements, has never been measured, the monitoring of these movements will be an important national project which will be carried out with KVN. KVN will also participate actively in international campaigns for geodetic measurements.

3. Outline of the Project

In 2001, KVN started a 7 year project to construct the first VLBI facilities in Korea, which include 3 new radio telescopes and VLBI receiving systems to be dedicated exclusively to VLBI observations.

3.1. KVN Sites

The three KVN observatory sites, Yonsei University at Seoul, University of Ulsan at Ulsan, and Tamna University at Jeju, have been selected from among the many universities and institutes who wanted to invite our telescopes. Fig. 1 shows the location of these three KVN sites. The

Table 1. Site parameters of the three KVN observatories.

KVN	Longitude	Latitude		Distance (km)		
Observatory	(° ′ ″E)	(° ′ ″N)	Yonsei	Ulsan	Tamna	TRAO
Yonsei (Seoul)	126 56 35	37 33 44	-	305.2	477.7	135.1
Ulsan (Ulsan)	129 15 04	35 32 33	305.2	-	358.5	194.2
Tamna (Jeju)	126 27 43	33 17 18	477.7	358.5	-	356.0
TRAO (Daejeon)	127 22 19	36 23 53	135.1	194.2	356.0	-

maximum baseline length is about 450 km in the north-south direction, and the site parameters are summarized in Table 1. The site preparation work has already started at all three places. In Fig. 2, we show an example of the UV coverage and the synthesized beam shape for the three KVN antennas, including the existing 14-m radio telescope at TRAO, Daejeon. These 4 antennas will be connected using the optical fiber information networks in Korea, partly for e-VLBI, and partly for the real-time operations of KVN.

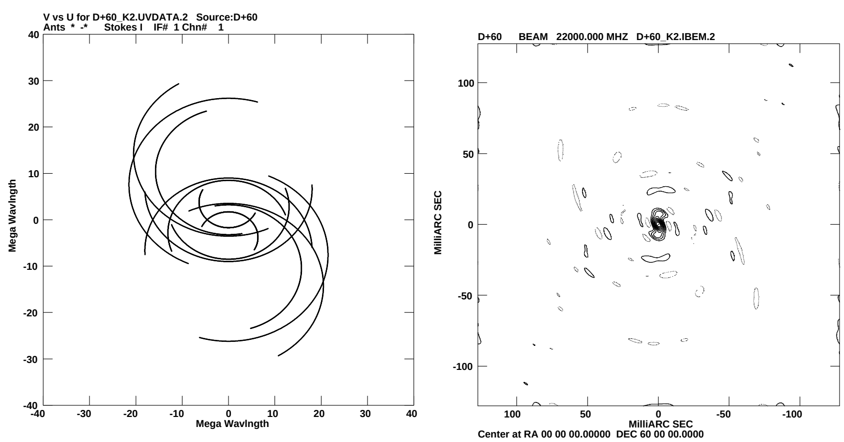

Figure 2. An example of the UV coverage and synthesized beam shape, for a source at 60° declination, for the three KVN antennas and the 14-m TRAO telescope at Daejeon.

3.2. Antennas

We plan to build 3 new high-precision Cassegrain type radio telescopes each of 20-m diameter, having reasonable efficiencies at frequencies above 100 GHz (total rms ≤ 150 μm). The slewing speed will be about 3°/sec in both AZ and EL. The requested wind speed tolerance is about 10 (20) m/s for precision (limited) observations, and 90 m/s for survival. We plan to start the foundation construction in 2004, and the antenna installations in 2005.

3.3. RF Receivers

For the KVN front-ends, several cryogenic HEMT receivers will be installed at the Cassegrain focus for 2/8, 22, 43, 86, ~100 and ~150 GHz operations. The 2/8 GHz receiver will be mainly for

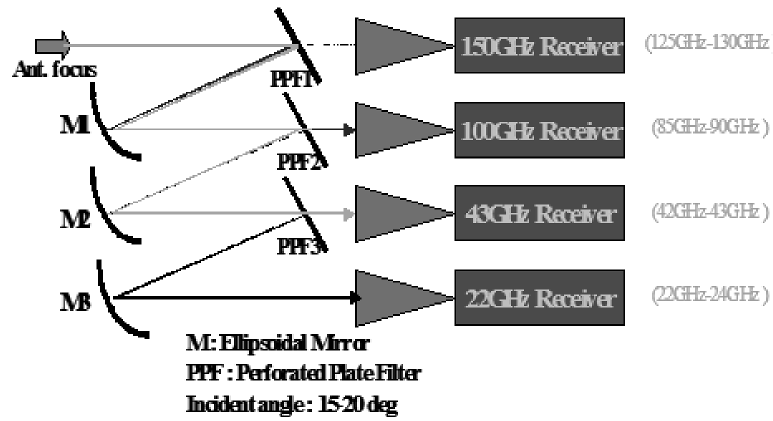

Figure 3. Design of the KVN quasi-optical beam transportation system using the PPFs.

Table 2. KVN receiver specifications.

Freq. Band	S Band	X Band	K Band	Q Band
Freq. Range	2.2~2.8 GHz	8~9 GHz	21.5~23.5 GHz	42~44 GHz
Rx Noise	<25 K	<25 K	<30 K	<50 K
1st IF / BW	2.5G/600MHz	8.5G/1GHz	8.5G/2GHz	8.5G/2GHz
IF Power	-20 dBm	-20 dBm	-20 dBm	-20 dBm
Polarization	LCP/RCP	LCP/RCP	LCP/RCP	LCP/RCP

geodetic observations. The 22/43 GHz receiver will be installed first, to set up the antennas and for the initial VLBI observations. Since our main goal will be mm-VLBI, the 86, ~100 and ~150 GHz receivers will be installed as soon as the full test of the KVN system is completed. Some parameters of the 'first' receivers are summarized in Table 2.

For KVN, which is designed for mm-VLBI, we plan to adopt a multi-channel quasi-optical beam transportation system which can be used for phase calibration in millimeter and sub-millimeter-wave VLBI, without losing observing time, and without the necessity to look for reference sources. In addition, this method enables us to observe several frequencies simultaneously.

Fig. 3 shows an initial design of the KVN beam transporting system employing frequency-selective surfaces – perforated plate filters (PPFs) [2]. The lowest 22 GHz band can be used as a phase-calibration reference for the higher frequency band observations, made toward the same source at the same time. Although there are some limitations [3], this multi-channel idea would give very reliable phase corrections in mm-VLBI.

3.4. KVN DAS and Recorder

We are developing the KVN data acquisition system (KVNDAS). Fig. 4 shows the configuration of KVNDAS. For our multi-channel receiver system, and to cover at least 1 GHz bandwidth, we employ four high-speed samplers which can be operated at 2 Gsps and 4 bits per sample. These four data streams of 8 Gbps will be transported via optical fibers to the operation building, and

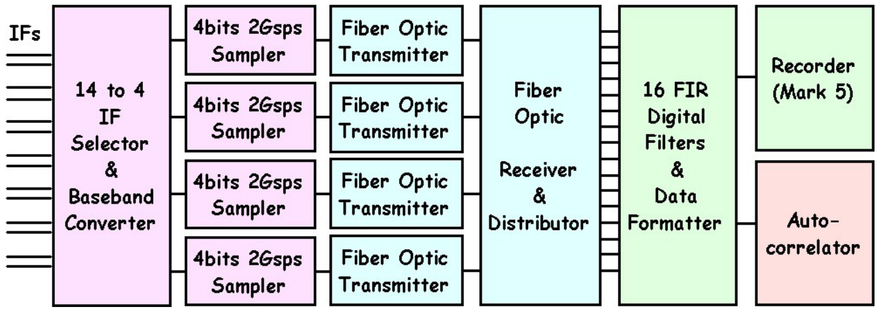

Figure 4. Schematic of the KVN DAS System.

then distributed among sixteen FIR digital filters. With these filters, we can choose a passband whose center frequency is arbitrarily programmable in the 1 GHz-wide input bandwidth, and then resample the filtered data at 2 bits per sample. These resampled data streams are then formatted and sent to the recorder. We will also prepare an autocorrelator for single-dish operation and total-power measurements.

As for the KVN recorder, we plan to use the new Mark 5 recorder [4]. KVN is involved in the development consortium for the Mark 5, led by Haystack Observatory of MIT. The characteristics of the Mark 5, which has a 1 Gbps rate using a standard PC and 16 hard disks with a VSI interface, are well explained in the Haystack web site. We plan to reproduce the Mark 5s for KVN.

We have just started the design of the new KVN correlator; this project is in the very first planning stages, at present.

4. Conclusion

The construction of KVN is underway as scheduled. The KVN is the first VLBI facility in Korea, which will be used for astronomical, geodetic, and earth science studies. It is our wish that KVN will be one of the best VLBI systems in the world, and we will actively participate in various VLBI programs after the completion of this project.

We hope that KVN will play a central role in promoting the VLBI research work of Korean societies and international collaborations, through the KVN Research Center which will be built in Seoul. Various support and manpower exchange programs to stimulate VLBI activities will be organized by the KVN project. Finally, for the success of the KVN project, it must be essential for us to collaborate with, and get many suggestions and support from, the leading institutes in VLBI research around the world.

References

[1] Alef, Y., et al., In: New Technologies in VLBI, Y. C. Minh (ed.), ASP Conf. Series 306, 75, 2003.

[2] Goldsmith, P. F., Quasioptical systems, IEEE Press., 1998.

[3] Sasao, T., In: New Technologies in VLBI, Y. C. Minh (ed.), ASP Conf. Series 306, 53, 2003.

[4] Whitney, A. R., In: New Technologies in VLBI, Y. C. Minh (ed.), ASP Conf. Series 306, 123, 2003.

Andrey Finkelstein et al.: Radio Astronomy Observatories Svetloe, Zelenchukskaya and Badary of VLBI Network QUASAR, IVS 2004 General Meeting Proceedings, p.161–165
http://ivscc.gsfc.nasa.gov/publications/gm2004/finkel

Radio Astronomy Observatories Svetloe, Zelenchukskaya and Badary of VLBI Network QUASAR

Andrey Finkelstein, Alexander Ipatov, Sergey Smolentsev

Institute of Applied Astronomy of Russian Academy of Sciences

Contact author: Andrey Finkelstein, e-mail: amf@ipa.nw.ru

Abstract

The paper presents common description and the current status of the observatories of the Russian VLBI network QUASAR.

1. Intrduction

The QUASAR project, which is carried out under the guidance of the Russian Academy of Sciences, involves creation of the full time operating VLBI network, consisting of 3 radio astronomy observatories. The observatories are located at Svetloe, Leningrad region; Zelenchukskaya, Republic of Karachaevo-Cherkessia, and Badary, Republic of Buryatia, and linked by connecting channels with the processing center, located at the Institute of Applied Astronomy (IAA), St. Petersburg (Fig. 1). At present 2 observatories — at Svetloe (1998) and Zelenchukskaya (2000) are operating both in single dish and VLBI mode. Observatory at Badary site is under installation and testing the hardware (Fig. 2).

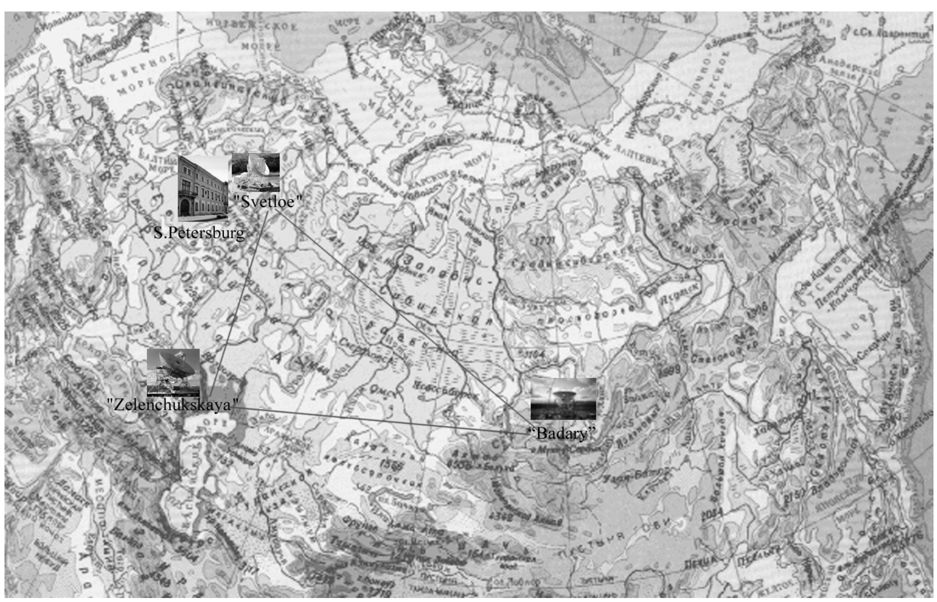

Figure 1. Geometry of the QUASAR VLBI network

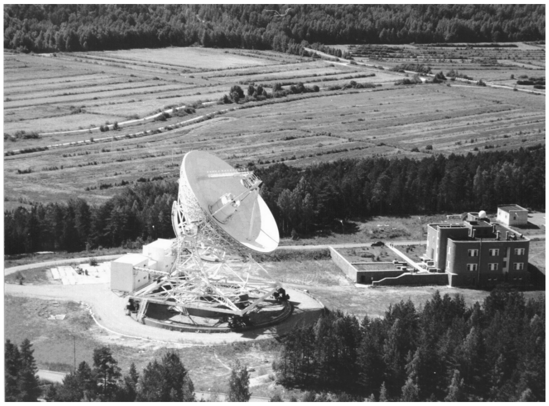

Observatory Svetloe
$\varphi = 60°32', \lambda = 29°47'$

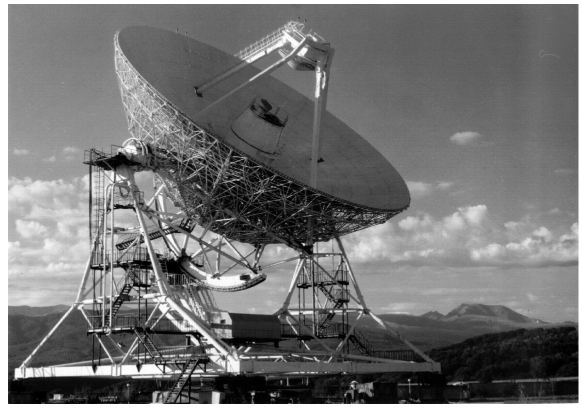

Observatory Zelenchukskaya
$\varphi = 43°47', \lambda = 41°34'$

Observatory Badary
$\varphi = 51°46', \lambda = 102°14'$

Figure 2. Observatories of the QUASAR VLBI network

2. Observatories Equipment

The main element of the observatories is the 32 m radio telescope for centimeteric wave length, which was designed for the Quasar project, since fundamental astrometry and geodesy tasks had special requirements for construction and dynamic qualities of this high-precision geodesic instrument (Table 1). The radiotelescope was constructed according to the Cassegrainian antenna, with the main quasi-parabolic mirror with a focus length of 11.4 meter, and with the additional mirror, which is a modified hyperboloid with a diameter of 4 meters. The only difference between these 3 telescopes is that the radio telescopes in Zelenchukskaya and Badary do not have an azimuth cabin, and the main hardware and cooling system compressors are installed in the special cabin for wire loop and in the special cabin near the angle engines respectively.

At present the telescopes are provided with HEMT radiometers for bandwidths 1.35, 2.45, 3.5, 6.0, 13 and 18/21 cm (Fig. 3), which allows production of simultaneous receiving of two orthogonal polarization. To maintain simultaneous receiving at 3.5 and 13 cm bandwidth in both orthogonal polarization (to eliminate ionosphere influence), that are the basic for fundamental astrometry and geodesy research, a combined horn has been constructed.

Table 1. Main dish parameters

dish diameter	32 m
subreflector diameter	4 m
Type	Cassegren
reflector form	quasiparaboloid
subreflector form	quasihyperboloid
focus	11.4 m
installation	azimuthal
azimuth turn limit	± 270 deg
elevation turn limit	$-5 \div 95$ deg
azimuth speed high/low	1.5°/s / $1.5'$/s
elevation speed high/low	0.8°/s / $1.0'$/s
surface quality	0.5 mm
pointing RMS	$10''$

Table 2. Parameters of the feed system (see Fig. 4)

Wavelength, cm	Horn number, i	Zi, mm	Ri, mm	Li, mm
1.35	1	4128	1333	131
2.6	2	4274	1302	280
6.2	3	4592	1234	605
13/3.5	4	5858	965	1900
18	5	6103	913	2150

To switch wavelengths and to be able to provide multi-bandwidth observations quasi simultaneously, the Cassegrainian antenna with an asymmetrical secondary mirror and additional focuses located not on the axis of the main mirror, but at some circle with center located at this axis is constructed. Input horns of different wavelength are located above this circle, and switching of the wavelength is achieved by turning the secondary mirror to a certain angle (Fig. 4., Table 2)

For achieving noise temperatures of the radio telescope-radiometer system not higher than 50 K, low-noise amplifiers (LNA) at all bandwidths, and some input lines, are cooled by a special micro-cryogenic closed cycle refrigerator to a temperature of 20 K (hydrogen level). Fig. 5 shows that at elevation angles above 20 degrees, noise temperatures of the systems at Svetloe and Zelenchukskaya do not exceed 50 K. Low noise temperature is one of the main features of the radio telescope, and the first measurements have shown that noise parameters of the radio telescopes of a Quasar network demonstrate higher quality compared to other radio telescopes involved in VLBI programs.

Each observatory is provided with the systems of frequency-time synchronization, consisting of 4 hydrogen maser standards with very high metrology qualities: $\sigma_{1s} = 10^{-13}$, $\sigma_{1000s} = 3 \times 10^{-15}$. This system also includes devices of the preliminary time synchronization using the navigation systems GLONASS and GPS, enabling synchronization of the separated scales of the atomic time with an error up to 100 ns.

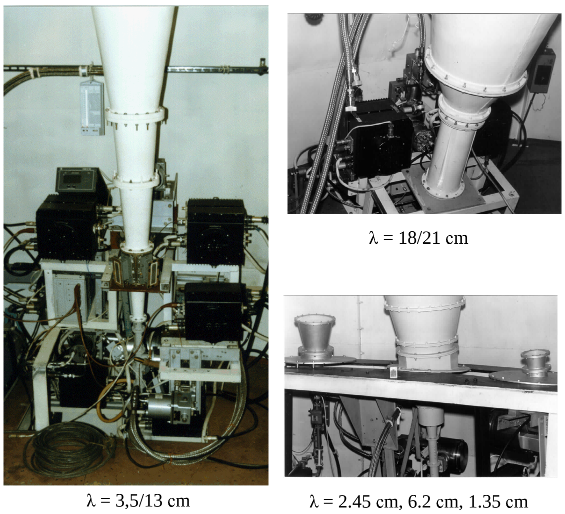

Figure 3. QUASAR — network radiometers

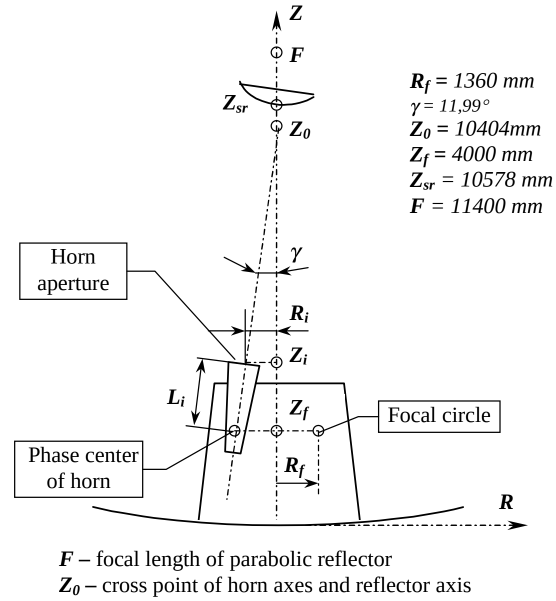

Figure 4. Schema of feeds arrangement

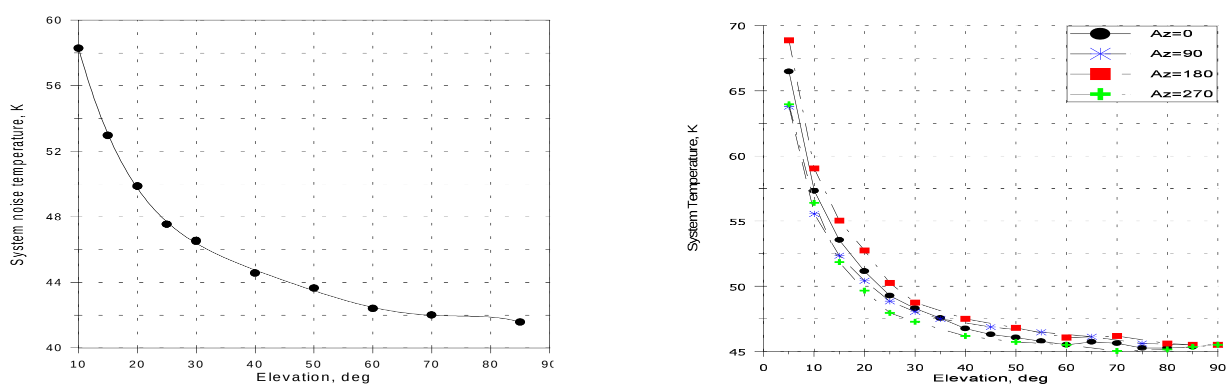

a) b)

Figure 5. System noise temperatures at X-band Svetloe (a) and Zelenchukskaya (b)

Figure 6. Video converters, developed in the IAA RAS

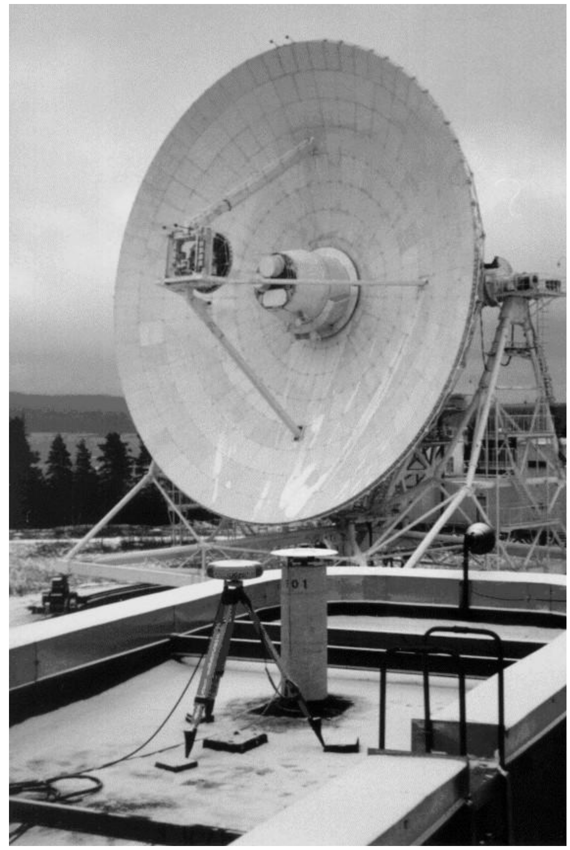

Figure 7. GPS, GLONASS Antennas on 32-m Antenna background

For registration, the Canadian system S2 is used with converters developed at the IAA (Fig. 6).

All the hardware of the Quasar network observatories — the radio telescope, receivers, systems of frequency-time synchronization and registration of signals on to magnetic tapes, are coordinated through the central computer, which is installed with a programming system — FS 9.0, which was adjusted for operating the hardware designed in Russia. Therefore, the radio telescopes of the Quasar system are capable of receiving data for observations from the international VLBI networks.

Electric power of the observatories is provided by two lines from different electric power stations, constant energy systems, diesel electric generators and batteries.

The Observatories Svetloe and Zelenchukskaya are supplied with geodetic GPS receivers — Turbo Roque (Zelenchukskaya) and Trimble 4000SST (Svetloe) (Fig. 7) and automatic meteorology stations, measuring temperature, pressure, humidity and the wind power.

Each observatory has a highly developed local geodesy network (Smolentsev S., Ivanov D., Malkin Z. Svetloe Radio Astronomical Observatory. 2000 IVS Annual Report, 123–126), fixed by geodesy pillars and supported by regular measurement according to methods of classical and space geodesy.

Igor Molotov et al.: VLBI Status of the Bear Lakes Radio Astronomy Station, IVS 2004 General Meeting Proceedings, p.166–169
http://ivscc.gsfc.nasa.gov/publications/gm2004/molotov

VLBI Status of the Bear Lakes Radio Astronomy Station

Igor Molotov [1], Yuri Gorshenkov [2], Alexander Stepanov [1], Alexander Dementiev [3], Gino Tuccari [4], Valerii Saurin [2], Alexis Zinoviev [5]

1) *RAS, Bear Lakes Radio Astronomy Station, Central Astronomical Observatory at Pulkovo*
2) *Special Research Bureau of Moscow Power Engineering Institute*
3) *Radiophysical Research Institute*
4) *INAF-IRA, Italian National Astrophysical Institute-RadioAstronomy Institute*
5) *Astro Space Center of P.N. Lebedev Physical Institute*

Contact author: Igor Molotov, e-mail: `molotov@kiam1.rssi.ru`

Abstract

The Bear Lakes Radio Astronomy Station (BLRAS) based on a 64-m dish antenna near Moscow was organized by Pulkovo Astronomy Observatory and Special Research Bureau in the end of 2002. The joint efforts of few institutions under INTAS IA-01-02 project allowed refurbishing the RT-64 construction and scientific infrastructure: modernizing the pointing system, adjusting two H-masers, upgrading GPS time service, repairing the building and rooms, painting the antenna. The apparatus rooms were connected to Internet by optical cable with possibility to transfer up to 500 Mb/s. Currently RT-64 has receivers at three frequency bands: 0.327 GHz, 1.665 GHz and 5 GHz. Three new receivers (0.61 GHz, 2.3 GHz and 8.4 GHz) are in production. The VLBI complex includes a BBC of 8 MHz bandwidth, sampler, S2 system and Mark II terminal. The elaboration of the 128 MHz 8-channel BBC was interrupted due to stopping the INTAS IA-01-02 financing. This circumstance also cancelled our plans about purchasing the FS computer and Mark 5 terminal.

The INTAS-01-0669 support allowed installing new VLBR terminal designed in Noto. This terminal records the VLBI data on PC-discs and then translates them in Internet for e-VLBI processing. BLRAS participated in two sessions of the Low Frequency VLBI Network (LFVN): at 1.665 GHz with S2 terminal for the investigations of the AGN, stars, OH-masers and solar wind; and at 5 GHz with both Mark II and VLBR terminals for the accurate radiolocation of Mars, 2000 PH 5 asteroid and high-orbit space debris. In the next year, we would like to obtain the large bandwidth BBC to participate in S2 geodetic VLBI and to support the LFVN activities. The works were partially supported also by RFBR 02-02-17568 and RFBR-02-02-39023 grants.

1. Bear Lakes VLBI Station Background and Programs

The unique fully steerable 64-m dish radio telescope was constructed at Bear Lakes near Moscow, Russia in 1979 and put into operation in 1983. This was the first large antenna of the former Soviet Union and it was fruitfully used for goals astronomy, deep space communication, space navigation and education of students of Moscow Power Engineering Institute over a very long time period.

The 64-m antenna was constructed by the Special Research Bureau of the Moscow Power Engineering Institute. It has a quasi-parabolic axially symmetric Gregory mirror system with subreflector of 6-m diameter and multi-band feedhorn system. The dish is equipped with a system for the phase compensation of gravitational deformation by means of a programmed subreflector movement. Rotation angles: + 220 degrees in azimuth, 1-89 degrees in elevation; guidance velocities: from 1.5 arcsec/s to 0.75 arcmin/s along two coordinates and object tracking accuracy about

15 arcsec. Effective area was about 2000 square meters at wavelength 18 cm with the possibility in principle for the main mirror to operate up to 1.35 cm.

It was a part of the Russian Deep Space Tracking Network which controlled all Russian deep space missions of Martian and Venusian programs and received the telemetry information from these spacecraft (i.e. it received the signals with Venusian surface panorama), participated in differential VLBI measurements of the Venus Atmosphere Dynamics Balloons in VEGA Project. Some part of antenna's time was spent for radio astronomy research under activity of few NIS scientific institutes. As part of radio interferometer "Orion", Bear Lakes participated in differential VLBI measurements of deep space and high-apogee mission spacecraft trajectories, fulfilled a series of VLBI experiments with USA DSN antennas, participated in a series of geodetic NIS VLBI observations and had episodic collaboration with European and Global VLBI Network with Mark II recording terminal. In fact, Bear Lakes RT-64 was the informal center of collective use for many scientific institutes of the NIS. But lack of modern radio astronomy equipment due to absence of specialized financing for this goal was limiting this activity. Nevertheless, Bear Lakes always demonstrated excellent and stable performances in the time of VLBI experiments (best of all other NIS antennas).

Figure 1. Bear Lakes RT-64.

The observations were carried out at 18 cm wavelength mostly. In 1996, Bear Lakes RT-64 joined the project of Low Frequency VLBI Network (LFVN) that has the purpose to arrange international VLBI cooperation with participation of former Soviet Union antennas.

The trial observations with Canadian S2 recording system (up to 128 Mbit/sec) were arranged between Bear Lakes and Tidbinbilla in June 1996 with a S2 baseline of 11538 km. But the RT-64 was equipped with S2 terminal on permanent basis in 1998 only. The base band converter (single channel of 2, 4 or 8 MHz) and sampler (S2 interface) were produced. The Bear Lakes RT-64 participated in five S2 observation sessions under LFVN project and a few VSOP experiments at 18-cm wavelength in 1998-2000.

In 2000, the 6-cm cooled receiver was installed at Bear Lakes RT-64 under LFVN program of VLBI radar searching for the near Earth asteroids, the Earth group planets and space debris. RT-64 participated in four VLBR sessions in 2001-2003.

In 2002, September 26, the agreement between Special Research Bureau of Moscow Power Engineering Institute and Central Astronomical Observatory at Pulkovo (CAO) of Russian Academy of Sciences was signed to establish the Bear Lakes Radio Astronomy Station (BLRAS) as a branch of CAO.

Figure 2. Recording terminals, base band converter, sampler, synthesizers, rubidium frequency standard, oscilloscopes, gauge of frequency, gauge of time intervals, spectrum analyzer, power supplies, paper recorder.

Since this time, all radio astronomical works at Bear Lakes RT-64 are carried out under BLRAS activities. During 2003 the program of the Bear Lakes VLBI site modernization was started:

- both H-masers were repaired and adjusted in GNIPI, N. Novgorod;
- "Thunderbolt GPS Disciplined Clock" with time precision down to 20 ns was purchased and incorporated in time and frequency service of antenna site;
- Internet access was organized by optical cable connection to the antenna building. The maximum possible speed is 500 Mbit/s (current 100 Mbit/s due to interface card);
- near real time VLBI terminal (NRTVT) was installed and tested in trial e-VLBI experiment on baseline with Noto in July 2003;
- the production of 49 cm, 13/3.6 cm receivers and two-channel radiometer will be finished in February 2004;
- repairing the antenna building and rooms was arranged during 2003;
- painting the antenna constructions and main mirror was started in summer;

- the works on the verification and rehabilitation of antenna constructions and mechanisms have been carried out.

The observations at 1.665 GHz that were carried out in January 2003, after long interruption (previous 18-cm experiment was in December of 2000), fixed the strong increasing of interferences in this frequency band that may be explained by close erecting of tower for mobile telephone connection "Combelga". There are no serious interferences at 5 GHz band. The investigations of S/X bands will be arranged in April after installation of the S/X band receivers.

The next e-VLBI experiment using NRTVT on baseline with Noto is scheduled for April 2004 (it is planned to test also NRTV terminals of Evpatoria RT-70 and Simeiz RT-22). The next VLBR session is scheduled for July 23-29, 2004 (the program includes asteroid 2000PH5, Mars, Venus and space debris). An astrophysical VLBI experiment (6-cm, 13-cm) is planned in November 2004.

Alexandr Volvach et al.: Single Dish Flux Density Monitoring of Geodetic VLBI Sources, IVS 2004 General Meeting Proceedings, p.170–174
http://ivscc.gsfc.nasa.gov/publications/gm2004/volvach

Single Dish Flux Density Monitoring of Geodetic VLBI Sources

Alexandr Volvach [1], *Larisa Volvach* [1], *Yuri Y. Kovalev** [2]

[1)] *Radio Astronomy Laboratory, Crimean Astrophysical Observatory*
[2)] *National Radio Astronomy Observatory*
Contact author: Alexandr Volvach, e-mail: volvach@crao.crimea.ua

Abstract

First campaign of single dish flux density measurements of sources used in geodetic VLBI experiments was carried out at the Simeiz radio telescope. Results of observations at 2.3, 5, and 8.4 GHz are presented and compared with RATAN–600 data.

1. Introduction

Since many compact sources have varying flux, it is important to monitor their correlated flux density in order to schedule geodetic VLBI sessions successfully. For majority of the sources there is a strong correlation between variation of total and correlated flux density [1], therefore single dish measurements can be used for prediction of correlated flux changes. Accompanied with estimates of the correlated flux density derived from analysis of geodetic VLBI observations and with maps produced from analysis of RDV experiments, these time series will provide important information for understanding the physics of these active galactic nuclei.

2. Goals of the Project

The Crimean Astrophysical Observatory has launched an initiative to monitor total flux density of the sources used for geodetic VLBI programs.

Our goal is to provide regular single dish flux density measurements at 2.3, 5, and 8.4 GHz of 104 out of 114 sources from the "geodetic list–2003" visible at the Simeiz radio telescope. Parameters of the instrument are given in Table 1. These sources are scheduled in more than 85% of all geodetic VLBI observations. Each source is observed at least once per month, although many strong sources from this list are scheduled more frequently.

3. Method of Observations and Results

The first campaign was successfully carried out at the Simeiz radio telescope at 2.3, 5, and 8.4 GHz during November 28 — December 11, 2003.

We used a new 5 GHz receiver with the low noise HEMT amplifier (LNA), cooled to a temperature of 15 K and a new dual-band 2.3 and 8 GHz receiver with uncooled LNA. The receivers have been installed in the primary focus of the antenna. Table 2 shows parameters of the receivers and the system equivalent flux density (SEFD).

* also at Astro Space Center of P.N. Lebedev Physical Institute, Moscow, Russia

Table 1. The antenna parameters of the Simeiz station.

Diameter D	22 m
Surface tolerance (root mean square)	0.25 mm
Wavelength limit	2 mm
Feed System	Cassegrian or primary focus
Focal length F	9.525 m
Focal ratio F/D	0.43
Effective focal length for Cassegrian system	134.5 m
Mounting	Alt-Az
Pointing accuracy	10 arcsec
Maximum rotation rate,	1.5 deg/sec
Maximum tracking rate	150 arcsec/sec
Working range in Azimuth (0 to South)	[−270°, +270°]
Working range in Elevation	0° – 85°

Table 2. Receivers performance and SEFD of the Simeiz antenna.

Band	Band, GHz	T_{sys}, K	$T_{receiver}$, K	SEFD, Jy
S	2.1 – 2.5	100	40	1100
C	4.6 – 5.2	35	5	400
X	8.2 – 8.7	80	50	1200

The source antenna temperature was measured by the standard ON–OFF method. Before performing the measurements of each source, we determined the local pointing correction by scanning strong sources. The radio telescope was then pointed alternately on the sources and on the five beam width distance off the source. The source antenna temperature was defined as the difference between the radiometer responses averaged during 10 sec at two different antenna positions. Depending on the intensity of the emission from sources, we made a series of 20–60 measurements and then calculated the mean signal power and the root mean square error of the mean. Four sources, 3C 274, 3C 353, DR–21, NGC 7027, were observed each hour in order to derive gain curves used for calibration. Their flux densities are given by Baars et al. [2] and Ott et al. [3] and form a "standard scale".

Results of flux density measurements at 2, 5 and 8 GHz are presented in Table 3.

We plan to repeat these observations every three months. Each observing campaign at three frequencies takes in total approximately 10 days.

4. Comparison with Other Measurements

We have compared our measurements with 2.3, 3.9, and 7.7 GHz data collected by the Russian 600 meter ring radio telescope RATAN–600 in the second half of 2003 (mainly in October, 2003) in a framework of an ongoing monitoring project with well defined and checked calibration scale (see description of the program, observations and data reduction procedure in Kovalev et al. [4]). Results of the flux density comparison are presented in Figure 1.

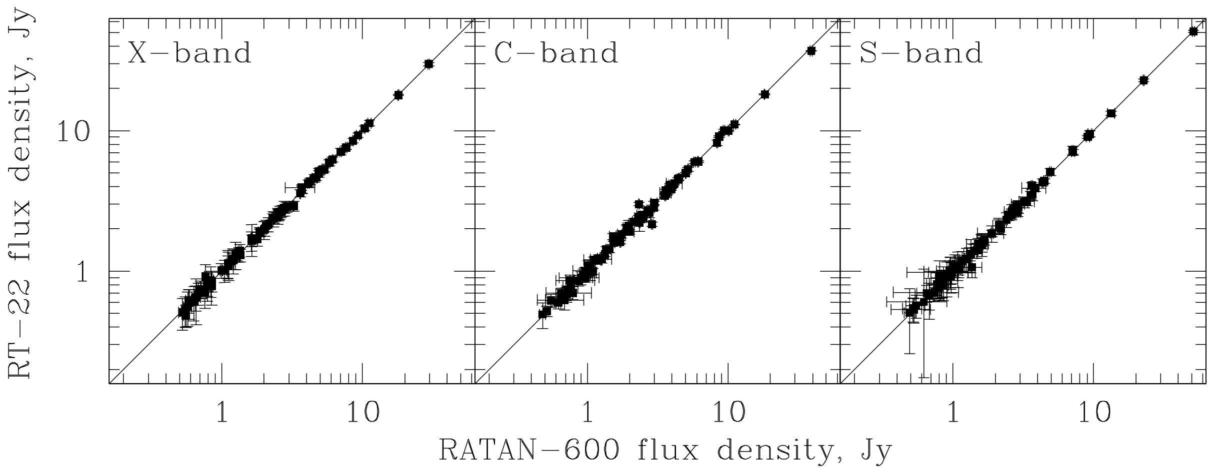

Figure 1. Results of comparison of flux densities measured by RT–22 and RATAN–600 with 1σ error bars.

There is good agreement between the data. A scatter around the line of equality is explained mainly by differences in RT–22 and RATAN–600 bands and by the fact that the sources are variable, but the observations were not strictly simultaneous. We conclude that monitoring observations of the geodetic VLBI sources can be successfully performed by the Simeiz radio telescope RT–22. We expect that further refinement of the methods of observations and data reduction will allow us to reduce random errors of the total flux density measurements.

Acknowledgments. Authors thank I. Srepka for maintenance of the receivers at the station, A. Shevchenko and P. Koseko for their efforts in observations. We are grateful to L. Petrov for useful discussions. RATAN–600 observations were supported in part by the RBFR grant 01–02–16812 and the Russian ministry for science and technology under a subcontract. Y. Kovalev is a Karl Jansky postdoctoral fellow of the National Radio Astronomy Observatory.

References

[1] Kovalev, Y.Y., Kovalev, Yu.A., & Nizhelsky, N.A., In: Future Directions in High Resolution Astronomy, ASP Conf. Ser., in press, 2004.

[2] Baars, J.W.M., Genzel, R., Pauliny-Toth, I.I.K., & Witzel, A., A&A, 61, 99–106, 1977.

[3] Ott, M., Witzel, A., Quirrenbach, A., Krichbaum, T.P., Standke, K.J., Schalinski, C.J., & Hummel, C.A., A&A, 284, 331–339, 1994.

[4] Kovalev, Y.Y., Nizhelsky, N.A., Kovalev, Yu.A., Berlin, A.B., Zhekanis, G.V., Mingaliev, M.G., & Bogdantsov, A.V., A&AS, 139, 545–554, 1999.

Table 3. Results of RT–22 observations of the geodetic VLBI sources in December 2003.

IVS name	IAU name	$S_{8\,\mathrm{GHz}}$, Jy	$S_{5\,\mathrm{GHz}}$, Jy	$S_{2.3\,\mathrm{GHz}}$, Jy
0003−066	0003−066	3.94 ± 0.17	3.05 ± 0.08	2.63 ± 0.17
0048−097	0048−097	0.91 ± 0.19	0.86 ± 0.07	0.76 ± 0.12
0059+581	0059+581	3.80 ± 0.25	3.82 ± 0.05	3.13 ± 0.20
0106+013	0106+013	2.90 ± 0.23	3.44 ± 0.08	3.46 ± 0.23
0111+021	0111+021	0.61 ± 0.11	0.59 ± 0.05	0.53 ± 0.10
0119+041	0119+041	1.01 ± 0.12	0.96 ± 0.08	1.06 ± 0.30
0119+115	0119+115	1.70 ± 0.43	1.59 ± 0.04	1.06 ± 0.16
0201+113	0201+113	0.78 ± 0.21	0.97 ± 0.04	1.03 ± 0.16
0202+149	0202+149	2.00 ± 0.24	2.15 ± 0.08	4.07 ± 0.20
0229+131	0229+131	1.69 ± 0.19	2.04 ± 0.04	1.63 ± 0.19
0235+164	0235+164	1.29 ± 0.13	1.60 ± 0.04	1.85 ± 0.09
3C 84	0316+413	17.96 ± 0.15	18.17 ± 0.19	22.82 ± 0.44
CTA 26	0336−019	2.60 ± 0.19	2.82 ± 0.09	2.89 ± 0.21
NRAO 150	0355+508	5.90 ± 0.29	3.74 ± 0.09	2.77 ± 0.12
0434−188	0434−188	0.84 ± 0.13	0.99 ± 0.05	1.10 ± 0.20
0454−234	0454−234	3.58 ± 0.21	3.60 ± 0.08	2.67 ± 0.19
0458−020	0458−020	1.17 ± 0.15	1.21 ± 0.05	1.17 ± 0.20
0528+134	0528+134	2.86 ± 0.22	2.70 ± 0.08	2.32 ± 0.27
0552+398	0552+398	4.93 ± 0.27	4.99 ± 0.06	3.00 ± 0.16
0556+238	0556+238	0.60 ± 0.16	0.69 ± 0.07	0.98 ± 0.16
0607−157	0607−157	4.65 ± 0.24	4.09 ± 0.08	2.64 ± 0.33
0642+449	0642+449	4.23 ± 0.23	3.00 ± 0.07	0.99 ± 0.18
0656+082	0656+082	0.53 ± 0.12	0.62 ± 0.09	0.80 ± 0.16
0727−115	0727−115	5.10 ± 0.26	4.50 ± 0.10	3.50 ± 0.32
0743+259	0743+259	0.48 ± 0.08	0.69 ± 0.09	1.01 ± 0.28
0804+499	0804+499	0.65 ± 0.13	0.70 ± 0.06	0.79 ± 0.14
0805+410	0805+410	0.80 ± 0.09	0.61 ± 0.06	0.70 ± 0.09
0808+019	0808+019	0.74 ± 0.10	0.68 ± 0.06	0.69 ± 0.09
0823+033	0823+033	1.31 ± 0.29	1.19 ± 0.07	1.00 ± 0.15
OJ 287	0851+202	2.60 ± 0.19	2.04 ± 0.09	1.54 ± 0.27
4C 39.25	0923+392	10.41 ± 0.39	9.07 ± 0.10	5.08 ± 0.29
OK 290	0953+254	0.86 ± 0.21	0.94 ± 0.09	1.00 ± 0.26
0955+476	0955+476	1.87 ± 0.12	1.70 ± 0.06	1.10 ± 0.12
1034−293	1034−293	1.14 ± 0.26	1.00 ± 0.05	0.67 ± 0.21
1101+384	1101+384	0.55 ± 0.15	0.52 ± 0.04	0.84 ± 0.22
1124−186	1124−186	1.64 ± 0.26	1.42 ± 0.07	1.07 ± 0.20
1128+385	1128+385	1.40 ± 0.14	1.20 ± 0.05	0.60 ± 0.43
1156+295	1156+295	1.90 ± 0.13	1.90 ± 0.06	1.85 ± 0.24

Table 4. Results of RT–22 observations of the geodetic VLBI sources in December 2003.

IVS name	IAU name	$S_{8\,\mathrm{GHz}}$, Jy	$S_{5\,\mathrm{GHz}}$, Jy	$S_{2.3\,\mathrm{GHz}}$, Jy
1219+044	1219+044	0.69 ± 0.12	0.77 ± 0.07	0.67 ± 0.14
3C 273B	1226+023	29.80 ± 0.73	37.01 ± 0.21	50.98 ± 0.90
1300+580	1300+580	0.78 ± 0.12	0.85 ± 0.07	0.54 ± 0.10
1302−102	1302−102	0.50 ± 0.12	0.70 ± 0.07	1.00 ± 0.24
1308+326	1308+326	2.40 ± 0.22	2.00 ± 0.10	1.09 ± 0.15
1334−127	1334−127	3.80 ± 0.22	3.70 ± 0.22	2.85 ± 0.22
1351−018	1351−018	0.78 ± 0.17	0.90 ± 0.07	0.98 ± 0.17
OQ 208	1404+286	2.14 ± 0.24	2.21 ± 0.29	1.66 ± 0.12
1418+546	1418+546	1.01 ± 0.18	1.02 ± 0.17	0.83 ± 0.18
1519−273	1519−273	2.51 ± 0.23	2.09 ± 0.21	1.56 ± 0.14
1606+106	1606+106	1.97 ± 0.29	2.40 ± 0.15	2.59 ± 0.18
1611+343	1611+343	5.31 ± 0.23	4.57 ± 0.11	4.39 ± 0.15
1622−253	1622−253	4.57 ± 0.27	4.20 ± 0.08	2.51 ± 0.14
NRAO 512	1638+398	1.09 ± 0.19	1.21 ± 0.07	1.32 ± 0.35
3C 345	1641+399	7.58 ± 0.25	8.19 ± 0.37	9.04 ± 0.20
DA 426	1652+398	1.65 ± 0.15	1.68 ± 0.12	1.39 ± 0.15
1726+455	1726+455	1.22 ± 0.19	1.10 ± 0.09	1.08 ± 0.19
1739+522	1739+522	1.29 ± 0.11	1.23 ± 0.07	1.09 ± 0.13
1741−038	1741−038	6.21 ± 0.25	5.32 ± 0.17	4.30 ± 0.25
1745+624	1745+624	0.73 ± 0.09	0.67 ± 0.07	0.56 ± 0.10
1749+096	1749+096	2.60 ± 0.28	1.76 ± 0.08	1.22 ± 0.23
1908−201	1908−201	2.35 ± 0.29	2.35 ± 0.07	2.13 ± 0.18
1920−211	1920−211	2.43 ± 0.28	2.60 ± 0.20	3.09 ± 0.27
1921−293	1921−293	11.32 ± 0.55	10.04 ± 0.23	9.50 ± 0.46
1923+210	1923+210	2.40 ± 0.15	1.82 ± 0.10	1.41 ± 0.17
1958−179	1958−179	2.69 ± 0.24	2.24 ± 0.11	1.32 ± 0.14
2113+293	2113+293	0.59 ± 0.14	0.49 ± 0.10	0.50 ± 0.24
2121+053	2121+053	2.53 ± 0.18	2.47 ± 0.07	2.01 ± 0.20
2126−158	2126−158	1.31 ± 0.15	1.31 ± 0.04	0.92 ± 0.22
2128−123	2128−123	4.35 ± 0.23	4.02 ± 0.14	2.88 ± 0.29
2134+00	2134+000	8.49 ± 0.31	10.01 ± 0.08	7.08 ± 0.29
2136+141	2136+141	2.76 ± 0.19	2.43 ± 0.06	1.57 ± 0.20
2145+067	2145+067	7.10 ± 0.37	5.98 ± 0.13	3.91 ± 0.21
2149+056	2149+056	0.69 ± 0.15	0.89 ± 0.09	0.90 ± 0.28
2201+315	2201+315	2.80 ± 0.34	2.50 ± 0.05	2.10 ± 0.27
2209+236	2209+236	0.65 ± 0.23	0.89 ± 0.05	1.27 ± 0.27
3C 446	2223−052	5.30 ± 0.22	6.00 ± 0.07	7.20 ± 0.55
2234+282	2234+282	1.19 ± 0.24	1.42 ± 0.07	1.50 ± 0.29
2243−123	2243−123	2.10 ± 0.20	2.35 ± 0.14	2.48 ± 0.18
3C 454.3	2251+158	9.29 ± 0.31	11.08 ± 0.05	13.29 ± 0.47
2255−282	2255−282	5.01 ± 0.26	3.43 ± 0.05	2.70 ± 0.37
2318+049	2318+049	1.11 ± 0.25	1.06 ± 0.09	0.90 ± 0.25
2356+385	2356+385	0.45 ± 0.13	0.56 ± 0.10	0.43 ± 0.09

Session 4

New Technology Developments in VLBI

Page intentionally left blank

Alan R. Whitney: The Mark 5B VLBI Data System, IVS 2004 General Meeting Proceedings, p.177–181
http://ivscc.gsfc.nasa.gov/publications/gm2004/whitney1

The Mark 5B VLBI Data System

Alan R. Whitney

MIT Haystack Observatory

e-mail: awhitney@haystack.mit.edu

Abstract

The Mark 5B VLBI data system is now being developed at MIT Haystack Observatory. It is based on the same physical platform and uses the same disk-modules as the Mark 5A; it also supports the same maximum data rate of 1024 Mbps. However, the Mark 5B will incorporate a VSI standard interface and command set. This will allow 8-BBC VLBA systems to bypass the existing VLBA formatter and connect directly to the output of VLBA samplers (through a simple interface) at a maximum data rate of 1024 Mbps. For 14-BBC systems with Mark IV formatters, the Mark 5B will allow connection of all 14 BBCs to two Mark 5Bs for a total aggregate data rate of 1792 Mbps. In addition, the Mark 5B is being designed to support all critical functionality of the Mark IV Station Unit so that the Mark 5B may played back directly to the Mark IV correlator through a simple interface. Prototype Mark 5B systems are expected to be available mid-to-late 2004.

1. Mark 5 VLBI Data System

Incorporating primarily low-cost PC-based components, the Mark 5 system [Ref 1] supports data rates up to 1024 Mbps, recording to an array of inexpensive removable IDE/ATA disks. The general goals of the Mark 5 system are:

- Low cost
- Based primarily on unmodified COTS components
- Modular, easily upgradeable
- Robust operation, low maintenance cost
- Easy transportability
- Conformance to VSI specification [Refs 2,3]
- Compatibility with existing VLBI systems during transition
- Flexibility to support e-VLBI
- Minimum of 1 Gbps data rate
- 24-hour unattended operation at 1 Gbps

All but the last goal are clearly achievable with today's technology; 24-hour unattended operation at 1 Gbps is expected to arrive within ~2 years with continued development in high-capacity disk technology.

2. Mark 5 Development Program

The Mark 5 system is being developed in two stages:

1. Mark 5A: The Mark 5A system, in use since late 2002, is intended as a direct replacement for a Mark IV or VLBA magnetic-tape transport at either a station or correlators. It records 8, 16, 32 or 64 tracks from a Mark IV/VLBA formatter, and plays back in the same Mark IV/VLBA format. As such, the Mark 5A is a direct replacement for a Mark IV tape unit at 1024 Mbps and VLBA tape unit at 512 Mbps. Approximately 80 Mark 5A systems have been deployed to stations and correlators around the world.

2. Mark 5B: The Mark 5B is a VSI-compliant system with capability up to 1024 Mbps; no external formatter is necessary, though access to a VSI interface is required. The Mark 5B is expected to be deployed in late 2004.

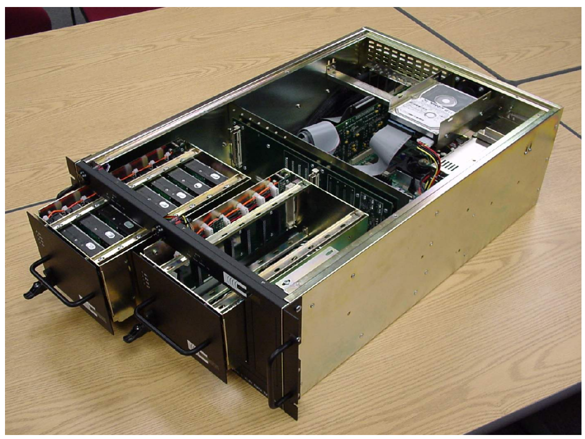

Figure 1. A photograph of the prototype Mark 5A system with its two removable '8-pack' disk modules; the Mark 5B will look the same. A Mark 5A system may be upgraded to a Mark 5B system simply by replacing a Input/Output PCI board in the host PC.

3. Characteristics of the Mark 5B Data System

The Mark 5B system has the following characteristics:

- Uses the same chassis and disk packs as the Mark 5A
- Implements the VLBI Interface Standards (VSI-H, VSI-S and VSI-E)
- Maximum record/playback data-rate is 1024 Mbps (same as Mark 5A)
- Requires new Mark 5B I/O card, currently under design
- Eliminates the need for an external formatter (but requires mating VSI interfaces)
- With a 14-BBC Mark IV or VLBA system, up to 1792 Mbps can be recorded with two parallel Mark 5B systems

- Mark IV Station Unit capabilities are being designed into the Mark 5B so that Mark 5B systems can be connected to Mark IV correlators without the use of a Mark IV Station Unit.
- Built-in phase-cal extraction and state-counting during recording and playback
- Xilinx FPGA design will be updateable via software download from PC; Mark 5A FPGA requires programming from a separate external source

4. Reliability Features

Several features exist in Mark 5 systems to ensure data integrity and continuity in the face of failing or failed data disks:

1. If a disk becomes slow or fails during recording, the recording load is dynamically adjusted among the disks within a module so that no data are lost.
2. If a disk fails or is missing during playback, the Mark 5 will fill any data gaps with a user-specified data pattern that can be detected and cause the data to be invalidated at the correlators.

5. Station Unit Emulation Capability

The Mark IV Station Unit acts as the interface between data from Mark IV/VLBA tape-format data (from either tape or Mark 5A disk systems) and the Mark IV correlator proper. It has several functions:

- Delays the data according to a fifth-order spline polynomial supplied to the Station Unit before presentation of the data to the correlator proper
- Inserts headers into the data stream with model information used by the correlator proper
- Extracts up to two phase-calibration signals from each channel
- Counts state statistics to aid in post-correlation correlation-coefficient normalization

This functionality is being built into the Mark 5B to allow the Mark 5B to connect to a Mark IV correlator without the use of a standard Mark IV Station Unit. The implementation of these functions is aided by an on-board 256 MB memory which will allow dynamic changes in the data-delay at intervals specified by the controlling delay model.

6. Compatibility with Mark 5A

The Mark 5B is being designed so that disk modules recorded on a Mark 5B can be played back on a Mark 5A unit. The playback format on the Mark 5A unit will be in VLBA track format; a list of supported 'compatibility modes' is given in Table 1. Existing Mark 5A units will need to be upgraded to support this compatibility path. This compatibility mode will allow data recorded on Mark 5B systems to be correlated on existing Mark 5A correlators during the transition period to Mark 5B.

Table 1. "VLBA-compatible" modes - Mark 5B disks played on Mark 5A system

#Active DIM Input Bit-streams	Fanout ratio to VLBA-format tracks	#output VLBA tracks
32	1	32
32	2	64
16	1	16
16	2	32
8	1	8
8	2	16
4	1	4
4	2	8
2	2	4

7. VSI Interfaces to Existing Mark IV and VLBA Systems

In order to use the Mark 5B with existing VLBA or Mark IV systems, a VSI interface providing sampled data, clock and 1 pps must be available for connection to the Mark 5B. These interfaces are also being developed at Haystack Observatory as part of the Mark 5B development project:

- VLBA systems (8 BBCs with VLBA formatter): An interface based on the Metsahovi VSI-C converter board will be used. The VSI connector will carry the 2-bit USB and LSB samples from BBCs 1 to 8.
- Mark IV systems (with existing Mark IV formatter): The interface will use the existing samplers, plus 32 MHz and 1pps synthesizers in the Mark IV formatter chassis, and will add a communications and control board. It will support two data modes:

  1. 'Astronomy' mode: 2-bit USB/LSB from BBCs 1 to 8 on VSI output 1; 2-bit USB/LSB from BBCs 9 to 16 on VSI ouput 2; max recording rate 2048 Mbps with two parallel Mark 5B systems
  2. 'Geodetic' mode: 2-bit USB from BBCs 1 to 14 and 2-bit LSB from BBCs 1 and 8

8. Interface to Mark IV Correlator

A Correlator Interface Board (CIM) is necessary to convert the VSI-format output of the Mark 5B system into the form necessary for input into the Mark IV correlator. The CIM will be housed in a separate chassis and connect to the VSI-output connector of the Mark 5B.

9. Summary

The Mark 5B system is the second in the line of Mark 5 VLBI data systems and the first to implement the VSI standard. Built on the same platform as the Mark 5A, the Mark 5B offers both a simple migration path for existing Mark 5A users and an inexpensive VSI-compatible VLBI data system for new installations. In addition, a Mark 5B/Mark 5A compatibility path has been established to ease in the transition from Mark 5A to Mark 5B. The Mark 5 system is being developed with support from BKG, JPL, KVN, MPI, NASA, JIVE, NRAO and USNO.

References

[1] Whitney, A.R., et. al., "Mark 5", Available from http://web.haystack.mit.edu/mark5/Mark5.htm.

[2] Whitney, A.R., "VLBI Standard Hardware Interface Specification -VSI-H," August 2000, Revision 1.0, Available from http://dopey.haystack.edu/vsi/index.html.

[3] Whitney, A.R., "VLBI Standard Software Interface Specification - VSI-S," February 2003, Revision 1.0 Available at http://dopey.haystack.edu/vsi/index.html.

Jouko Ritakari et al.: Gbit/s VLBI and eVLBI with Off-The-Shelf Components, IVS 2004 General Meeting Proceedings, p.182–185
http://ivscc.gsfc.nasa.gov/publications/gm2004/ritakari

Gbit/s VLBI and eVLBI with Off-The-Shelf Components

Jouko Ritakari, Ari Mujunen

Metsähovi Radio Observatory

Contact author: Jouko Ritakari, e-mail: Jouko.Ritakari@hut.fi

Abstract

Metsähovi Radio Observatory has pioneered in the use of off-the-shelf microcomputers in VLBI. During the years 2001 and 2002 MRO developed a hard-disk based data acquisition and playback terminal for VLBI. The recording system is VSI-H compatible and uses off-the-shelf microcomputers with unmodified Linux operating system. Only minimal hardware and software development were needed. One data acquisition terminal can record at 512 Mbit/s speed, but the system is designed to be easily scalable to multi-gigabit per second speeds. The system is compatible with most of the standards used in VLBI, it can record data from the ADS-1000 Gbit/s sampler developed in CRL, VLBA samplers, VLBA formatter, Mark IV formatter and S2. K4 compatibility has been designed but not yet tested. It must be emphasized that the MRO data acquisition terminal is not a prototype but a mass-produced product. Boards for 60 data acquisition terminals have been produced in August 2002 and 17 terminals have been deployed to nine radio telescopes so far. During the years 2002 and 2003 Metsähovi made several 1 Gbit/s and 2 Gbit/s VLBI observations with Kashima station at 22 GHz frequency. These observations used the ADS-1000 sampler and were correlated with a high-speed software correlator at Kashima. In May 2003 Metsähovi and Jodrell Bank Observatory succeeded in the first European 1 Gbit/s Mark 5-style VLBI experiment. Data was recorded in MRO-designed hard disk recorders, transferred to JIVE via Internet and played back to the correlator with Mark 5 terminals. During the second half of 2003 the MRO team has concentrated in evaluating the new reliable UDP-based protocols for eVLBI. Several candidates have been found. Initial tests using these protocols are very promising and demonstrate the advantages of having the data in normal Linux files.

1. Basic Ideas

The MRO data acquisition system was built to test the idea that VLBI data can be treated like any normal data. It can be captured with normal microcomputers, stored in normal files and transferred with standard networking tools. Correlation is nothing special, it is only computing.

2. Equipment

Two printed circuit boards were developed for the MRO data acquisition system: the VSIB data acquisition board for the microcomputer and the VSIC stand-alone universal converter board.

Both of the boards have been mass-produced in August 2002. The firmware and software have been frozen in 2002 and are fully operational with no known errors.

2.1. The VSIB Data Acquisition Board

The VSIB data acquisition board is the core of the MRO system. The VSIC is one of the first VSI-H standard compatible data acquisition systems.

When the design was started in mid-2001, design goal for one microcomputer was 256 Mbit/s recording speed and 600 GB capacity (same as in one Mark IV thin tape). During the design work we found out that the performance was even better than expected: one microcomputer could reliably record data at 512 Mbit/s and the capacity with the new 320 GB hard disks is 1.2 TB.

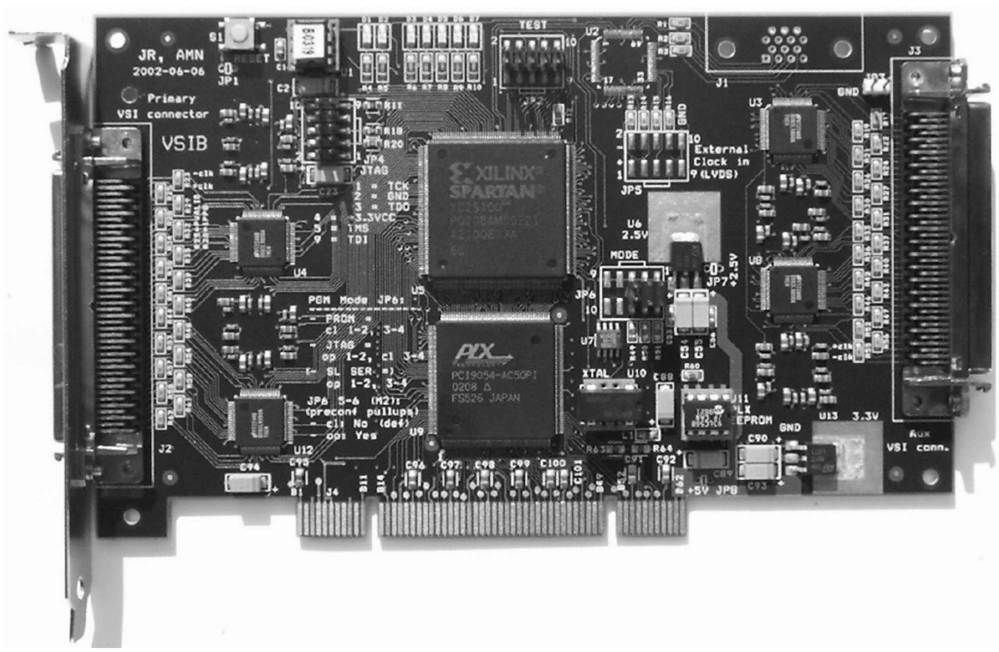

Figure 1. The VSIB Data Acquisition Board

2.2. The VSIC Universal Converter

The VSIC universal converter board is a byproduct of the development project. Originally the development project was divided in two parts: Metsähovi was designiung the data acquisition part and JIVE was developing the Mark IV to VSI converter, the data distributor.

When the VSIB design was completed it became clear that an interim solution was needed for testing the VSIB. Minimum requirements were a test vector generator and 32-track Mark IV formatter interface. During the design of the VSIC it became apparent that VLBI used lots of different cabling standards that all used 40-wire twisted pair flat cables and differential signalling. It was possible to design a universal converter to convert anything to the VSI-H standard.

The VSIC was designed very quickly, in two weeks of time. It supports the following standards:

- VLBA samplers
- VLBA formatter output, both data raplacement and non-replacement modes
- Mark IV formatter outputs, heads 1 and 2
- S2 DAS (with an adapter cable)
- K4 (design complete, not tested yet)

Additionally the VSIC converter board can operate as a test vector generator either in ramp signal mode or in the VSI mode.

3. Compatibility with Other Systems Used in VLBI

The MRO system is directly compatible with all the VSI-H compliant devices, for example the ADS-1000 Gbit/s sampler developed in Communications Research Laboratory.

With the VSIC converter the MRO system can record data from most of the legacy interfaces.

Data formats are compatible with the Mark 5A system, data recorded with the MRO system can be played back with a Mark 5A.

4. Experiments with the MRO System

The MRO system has been used in a series of successful eVLBI experiments and several world records have been achieved:

- 12-Jul-2002 First fringes with MRO system between Westerbork and Jodrell Bank at 256 Mbit/s
- 24..26-Sep-2002 iGrid eVLBI demo at 256 Mbit/s
- 16-Oct-2002 First Kashima - Metsähovi 1 Gbit/s experiment [1]
- 5..14-Feb-2003 Second Kashima - Metsähovi 1 Gbit/s experiment
- 12-Mar-2003 First European 1 Gbit/s experiment Metsähovi - Jodrell Bank
- 17-Jun-2003 First Kashima - Metsähovi 2Gbit/s experiment [2]

The 1 Gbit/s and 2 Gbit/s experiments between Metsähovi and Kashima used direct IF sampling with the ADS-1000 Gigabit Sampler. Data was correlated in CRL Kashima with a high-speed software correlator.

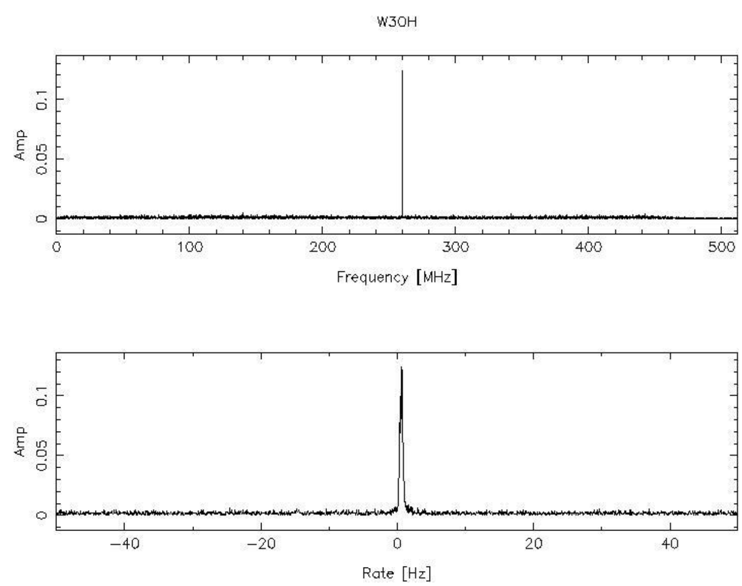

Figure 2. 1Gbps Fringe Metsähovi - Kashima

The 1 Gbit/s experiment between Metsähovi and Jodrell Bank recorded data from Mark IV formatter in Mark 5A compatible format. Data was transferred to JIVE correlator via Internet and was played back to the correlator with Mark 5A terminals.

5. Future: Off-The-Shelf eVLBI

The off-the-shelf approach has proved to be very powerful, standard Unix tools can be used to manipulate or transfer the data if it is stored in normal Unix files.

Our next area of interest will be data communications protocols for eVLBI. At this moment the international Internet trunk lines are fast enough for real eVLBI work, but the protocols have serious drawbacks: TCP is too slow for high-speed long-delay networks and transfer with UDP is unreliable.

Several solutions have been proposed: Use of jumbo frames, use of several TCP streams in parallel, use of RTP protocol.

Fortunately the telecom industry is solving the same problems. We have made a quick survey and located several promising new protocols that can be used in eVLBI:

- UDT (UDP Data Transfer) [3]
- Sabul (Simple Available Bandwidth Utilization Library)
- Tsunami
- FOBS
- RBUDP (Reliable Blast UDP) [4]
- GTP (Group Transfer Protocol)

These protocols are either reliable UDP variants or combinations of UDP protocol used for transmitting the data and TCP protocol used for control.[5] The Linux source code of most of these protocols is available in Internet.

References

[1] Y. Koyama, T. Kondo, J. Nakajima, M. Kimura, H. Uose, S. Iwamura, International e-VLBI Experiments, In: IVS CRL Technology Development Center News, No.21, pp.23, November 2002.

[2] M. Kimura, J. Nakajima, J. Ritakari, A. Mujunen, First detection of 2-Gbps wideband fringes between two PCbased VLBI systems, In: IVS CRL Technology Development Center News, No.22, pp.5, June 2003.

[3] R. Grossman, Y. Gu, Introduction to SABUL/UDT, http://www.ncne.org/training/techs/2003/0803/presentations/pptfiles/0803-grossman1.ppt

[4] E. He, J. Leigh, O. Yu,T. DeFanti Reliable Blast UDP: Predictable High Performance Bulk Data Transfer, http://www.evl.uic.edu/cavern/papers/cluster2002.pdf

[5] R. Wu, A. Chien, Evaluation Of Rate Based Transport Protocols For Lambda-Grids, http://dsd.lbl.gov/DIDC/PFLDnet2004/papers/Wu.pdf

Tetsuro Kondo et al.: Current Status of Software Correlators Developed at Kashima Space Research Center, IVS 2004 General Meeting Proceedings, p.186–190
http://ivscc.gsfc.nasa.gov/publications/gm2004/kondo

Current Status of Software Correlators Developed at Kashima Space Research Center

Tetsuro Kondo, Moritaka Kimura, Yasuhiro Koyama, Hiro Osaki

Kashima Space Research Center, Communications Research Laboratory (will be National Institute of Information and Communications Technology from April 1, 2004)

Contact author: Tetsuro Kondo, e-mail: `kondo@crl.go.jp`

Abstract

We have been developing two types of software correlators run on a PC. One type aims at obtaining the correlation data compatible with those processed by the hardware correlator for geodetic use, and the other is an ultra high-speed software correlator for processing gigabit VLBI data. At present time the processing speed on a PC is about 10 Mbps for the former one and 90 Mbps for the latter one. We are now developing the distributed processing technique for further speedup to realize real-time correlation in the e-VLBI system.

1. Introduction

Raw data of the Mark I, world's first digital VLBI system developed in the U.S. in 1960s, were correlated by a computing program (software correlator). It took 90 minutes by using the main frame computer IBM360/50 to process 144 Mbits data [1]. It was equivalent to a data processing rate of 26.7 kbps. In 1980s Kashima VLBI group also developed a software correlator named CCC (Cross Correlation in a Computer) run on a minicomputer of HP1000 series [2]. It took 150 minutes to process 16 Mbits data by using a minicomputer HP1000/A900, and this corresponded to 1.8 kbps. The CCC was used in the actual fringe test of a domestic VLBI conducted in 1985, and we could successfully get fringes. However, it was not practical for the reason that not only data processing but also data transmission took too much time. We had to wait for progress in both computing speed and data transmission speed to put a software correlator to practical use. Thereafter personal computers (PC) have shown continuous improvement in performance. Indeed, the computing speed of a recent PC is much faster than that of the workstations and minicomputers of ten years ago, and the use of a software correlator for VLBI data processing becomes realistic. Therefore we have been developing a software correlator again since 1999. Actually a software correlator with sufficient processing speed was developed and demonstrated that it could be used for a routine processing. We are also developing the distributed processing technique for further speedup to realize real-time correlation in the e-VLBI system. In this paper, we will report the current status of our software correlator.

2. Software Correlators

There are two types of correlators (Figure 1). One is an XF type and the other is an FX type. The XF type correlator multiplies each time-domain data directly to obtain a cross correlation while the FX type first Fourier transforms into the frequency domain and then multiplies two frequency domain data to obtain a cross spectrum.

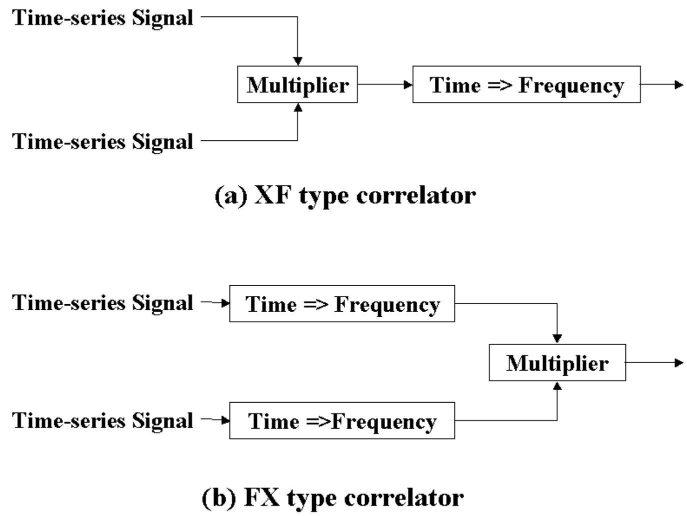

Figure 1. Two types of correlators.

2.1. XF-Type Software Correlator

The CCC was an XF-type software correlator developed by Kashima VLBI group in the 1980s for a fringe test [2]. It was developed by using the FORTRAN language on an HP-1000/45F minicomputer and was migrated to an HP-1000/A900 later. It took 150 minutes to process 16 Mbits data (i.e., equivalent to a processing speed of 1.8 kbps) by using the HP1000/A900. Therefore, we thought that it was unrealistic to use routine correlation processing. However we tested the CCC for a prompt fringe check at a Japanese domestic VLBI experiment conducted on the Kashima-Miyazaki baseline in 1986. Distance is about 1000 km, and usually it took a few days to ship a magnetic tape from Miyazaki to Kashima. To obtain the prompt result of fringe test, we sent raw data over telephone line using a 1200 bps modem. It took 1 hour and 21 minutes to transfer 4 Mbit data, and then data were correlated using the CCC. Finally we could successfully detect fringes only in 10 hours from when an observation was ended. This was an extremely short turn around time at that time. However telephone cost was very expensive at that time in Japan, so that we never tried this e-VLBI again. The CCC was also used in the first Canada-Japan VLBI experiment using a wave-front clock technique conducted in 1990. Raw data observed at Algonquin were recorded on floppy disks and brought back to Kashima. Then the CCC was executed to get fringes. If we had enough budget for international phone communications, we could carry out an international e-VLBI at that time. As mentioned above the CCC was successfully used for some experiments, but computing power of mini-computer at that time was insufficient to use a software correlator for routine processing of VLBI data.

Now ten years have passed, and PCs showed a drastic improvement in performance during this period. The use of software correlator thus becomes realistic, therefore we started the development of software correlator again. We have developed the PC-based VLBI data-acquisition terminal named K5 dedicated to transmitting the data through the Internet since 1999 [3]. A software correlator was planned to be used in correlation processing from the beginning of K5 development, and the software correlator dedicated to geodetic use (K5 software correlator) based on the CCC has been developed by using the C language for K5 data processing. Since the K5 software correlator aims at obtaining the correlation data compatible with those processed by the hardware correlator (i.e., not only correlation processing but also extraction of phase calibration signals is implemented), a bandwidth-synthesizing program can handle correlated data directly to get a precise observed delay.

We carried out a benchmark test of K5 software correlator for various kinds of CPUs. Results are summarized in Figure 2. Clock frequency is taken as a parameter expressing CPU power. Time required to correlate 1 sec period data of 4 ch 8 MHz-1bit sampling data (corresponding to 32 Mbits) was measured. Data used are 4-ch data, so that processing time of 4 sec (denoted by a dotted line) represents the border for real-time processing for 1 ch data. We can see that the fastest one exceeds processing speed of 10 Mbps.

We have already processed 24-hour session data by using the software correlator, and it was confirmed that geodetic results obtained by the software correlator gave results that coincide well with those obtained by the hardware correlator.

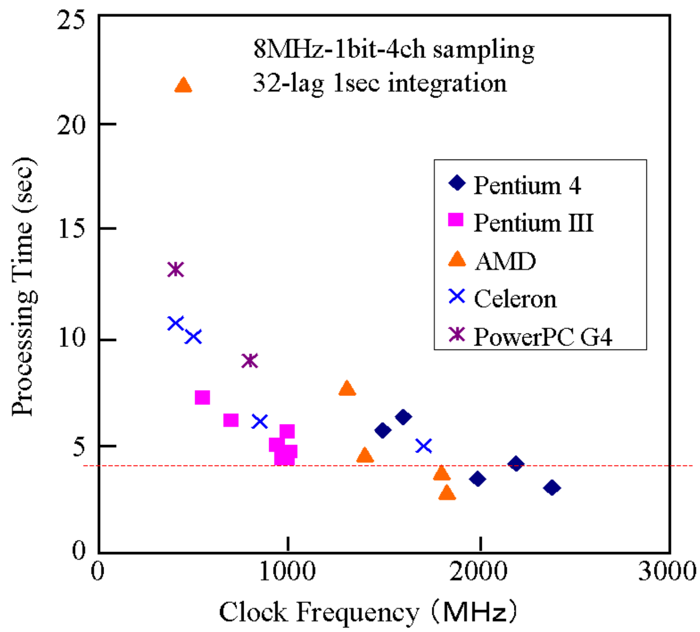

Figure 2. Benchmark test results of K5 geodetic software-correlator.

2.2. FX-Type Software Correlator

We have also developed an FX-type software correlator specializing in processing speed to process gigabit VLBI system data mostly for an astronomical use [5]. In order to maximize the performance of CPU, various kinds of optimizations, such as an effective use of multi-processors and utilization of SIMD (Single Instruction Multiple Data) technology for parallel processing, were taken into the development. An assembler language program was also used partially to improve the performance.

Figure 3 shows results of performance test of the K5 FX software correlator using a PC equipped with dual AMD Athlon 1.8GHz processors. Throughput was measured for different lags, and reached about 90 Msps (it corresponds to the processing speed of 90 Mbps when 1 bit sampling are adopted) for lag numbers from 512 to 8192. The size of cache memory of CPU affected the performance at large number of lags, resulted in the performance loss. Multi-baseline correlations with multi-PCs are also planned to achieve further speed up of processing. By the use of the latest and fastest four PCs, it is possible to process 1Gbps data in real time.

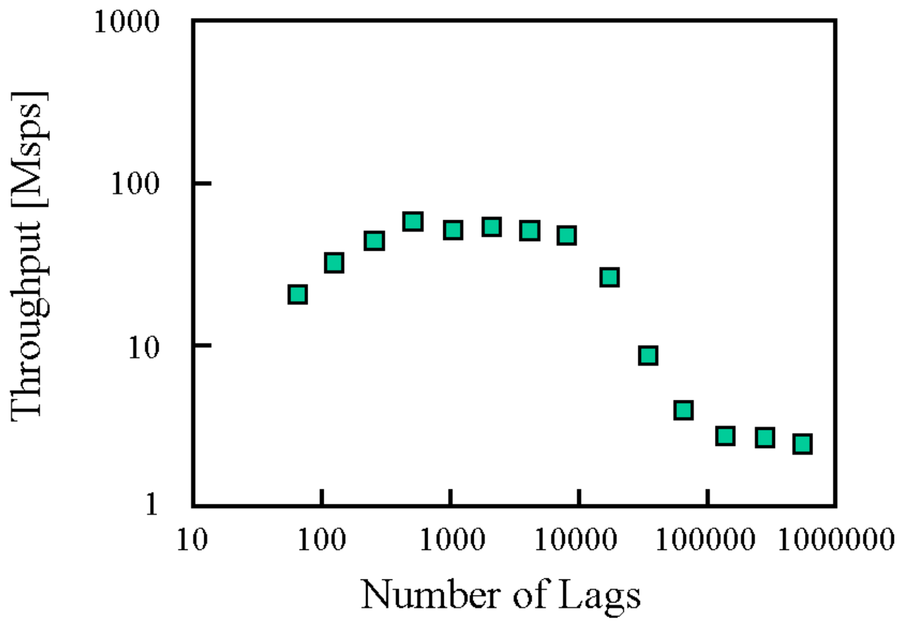

Figure 3. Performance evaluation results of K5 gigabit software-correlators.

3. Distributed Correlation Processing

We are developing a distributed processing system to increase total processing speed. Figure 4 shows one of ideas of distributed processing system to realize real-time processing using a number of PCs where each PC is incapable of real-time processing. Raw data are divided into a number of short-segmented data, e.g., 1 sec period data. A PC (leftmost PC in the figure) correlates the first pair of segmented data (labeled 00 in the figure). After this processing, the PC processes next available pair of segmented data (labeled 06 in the figure). Second (from the leftmost in the figure) PC first correlates the second pair of segmented data (labeled 01), and then correlates next available pair of segmented data (labeled 07). In this way the use of a number of PCs allows us to correlate raw data in real-time even though each PC has no capability of real-time processing. In order to realize this idea, we are developing a distributed processing system consisting of a server PC and client PCs like SETI@home. We named the system VLBI@home after SETI@home and are testing the system at our office (for details see the separate paper in this proceedings [6]).

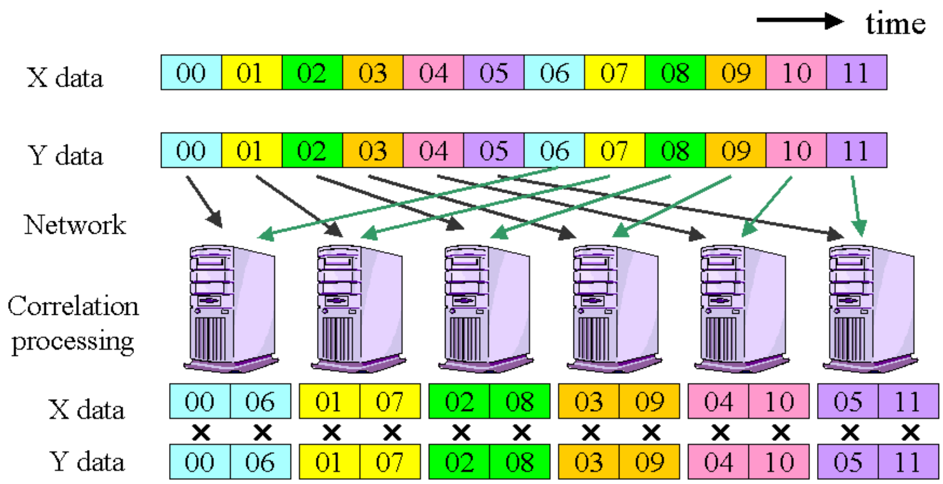

Figure 4. A principle of distributed correlation processing.

4. Conclusion

It is said that the performance of PC will improve by doubling every two years and it will last at least about ten years from now. If it is true, we can expect the improvement of processing speed of a software correlator without any special improvement of software itself. Actually a software correlator run on a recent PC begins to have a practical processing speed to carry out routine correlation processing. A network-distributed processing system is also being developed to achieve further speedup. We think that a part of routine correlation processing carried out by a hardware correlator will be taken over by a software correlator in the future.

References

[1] Bare, C., B.G. Clark, K.I. Kellermann, M.H. Cohen, and D.L. Jauncey, Interfrometer experiment with independent local oscillators, *Science*, 157, 189–191, 1967.

[2] Kondo,T., J. Amagai, H. Kiuchi, and M. Tokumaru, Cross-correlation processing in a computer for VLBI fringe tests, *J. Commun. Res. Lab.*, Vol.38, No.3, 503–512, 1991.

[3] Kondo, T., Y. Koyama, M. Sekido, J. Nakajima, H. Okubo, H. Osaki, S. Nakagawa, and Y. Ichikawa, Development of the new real-time VLBI technique using the Internet Protocol, *Technical Development Center News CRL*, No.17, 22–24, 2000.

[4] Koyama, Y., T. Kondo, H. Osaki, K. Takashima, K. Sorai, H. Takaba, and K. Fujisawa, Evaluation of the K5 system in geodetic VLBI experiments, *Technical Development Center News CRL*, No.23, 26–30, 2003.

[5] Kimura, M. and J. Nakajima, The implementation of the PC based giga bit VLBI system, *Technical Development Center News CRL*, No.22, 31–33, 2002.

[6] Takeuchi, H., T. Kondo, Y. Koyama, and J. Nakajima, VLBI@home – VLBI correlator by GRID computing system, *IVS 2004 General Meeting Proceedings*, 2004 (this issue).

Stephen T. Lowe: Softc: an Operational Software Correlator, IVS 2004 General Meeting Proceedings, p.191–194
http://ivscc.gsfc.nasa.gov/publications/gm2004/lowe

Softc: an Operational Software Correlator

Stephen T. Lowe

Jet Propulsion Laboratory / California Institute of Technology
e-mail: steve.lowe@jpl.nasa.gov

Abstract

Softc has been used operationally for spacecraft navigation at JPL for over 2 years and will be JPL's Mark 5 correlator next year. Softc was written to be as close to an ideal correlator as possible, making approximations only below 10^{-13} seconds. The program can correlate real USB, real LSB, or complex I/Q data sampled with 1, 2, 4, or 8-bit resolution, and was developed with strong debugging tools that made final debugging relatively quick. Softc's algorithms and program structure are fully documented. Timing tests on a recent Intel CPU show Softc processes 8 lags of 1-bit sampled data at 10 MSamples/sec, independent of sample rate.

1. Introduction

Level-one VLBI processing has traditionally required state-of-the-art processing power and data bandwidths that could only be implemented using custom electronic hardware and data storage equipment. These devices, correlators, often took many years to design and build followed by at least a year of use to excise the more obvious processing problems. This long development time also ensured that by the time a correlator was debugged and in a stable operational mode its equipment was obsolete. Because there was no other processing option, the VLBI community has endured high costs associated with these devices. These costs include many millions of dollars for development, on the order of $1M annually to pay for the ongoing debugging, capability improvements, and maintenance, a trained operator staff, and the infrastructure costs of the correlator room such as leasing, power, and air conditioning. Data storage and transport has used custom tape technology, but this is also expensive, and as the technology has been pushed to higher densities, tape drive/head maintenance costs have increased. Finally, some indirect correlator costs include lack of flexibility for novel experimental setups, lack of transparent processing algorithms, lack of repeatable output due to tape playback errors, and downtime for maintenance, testing, and modifications.

It has been known for some time that all the disadvantages of the traditional correlator noted above could be eliminated if efficient data handling could be moved from tape to disk, and general-purpose computers could meet the processing requirements. Until recently, neither of these conditions could be met adequately, but interestingly it now appears the crossover points for both of these competing technologies, custom tape vs. disk, and custom hardware vs. general-purpose computer, is in the recent past [1]. Both the recent Mark 5 disk format and software correlators such as Softc take advantage of huge commercial R&D budgets worldwide. These are cases of custom VLBI hardware capabilities being overtaken by commercial products developed with enormous resources compared to those in the VLBI community. By extrapolation we are likely to experience other paradigm shifts soon in the remaining custom VLBI hardware, namely station electronics. We are also beginning to see how all these changes are significantly altering the optimum values of VLBI system parameters. For example, it will be more efficient to have smaller antennas with higher bandwidths, and reliability should increase with the improved hardware, disk storage, and real-time fringe verification.

2. History

In 1995 JPL began to decommission its Delta-Differenced One-way Range (DeltaDOR) spacecraft navigation system. The decommissioning process was to mothball the DeltaDOR capability, eliminate its near real-time Block I hardware correlator, and after a short time cease DeltaDOR funding. At around this same time, test programs were written to assess software correlation speed and to find fringes in old Block I quasar data. These tests showed the Block I bandwidths were low enough that it could be replaced with a software correlator. Since there was no other choice to preserve this capability, a project to replace the Block I with a software correlator began in 1996. This task was essentially completed but since this was a mothballing effort and DeltaDOR was not necessary for any mission, the program, called Softc, was never used. This was probably fortunate as the program, by design, exactly duplicated the Block I processing including its many approximations and flaws. In 1998, the RadioAstron project agreed to fund further development of Softc as a debugging tool for their project. This opportunity was used to essentially start over and build a true software correlator with all its intrinsic advantages without being constrained to a hardware correlator's shortcomings. Unfortunately, this effort was canceled in 1999 just as full code testing began. Softc then remained complete but unused and untested until 2001 when the mis-navigation and demise of Mars Climate Orbiter prompted JPL to resurrect the DeltaDOR navigation technique. Softc underwent full-code testing using geodetic experiments and DeltaDOR passes of Mars Global Surveyor, in orbit at the time, and Mars Odyssey, which was on its way to Mars at the time. Softc's first critical use was the successful Mars Odyssey orbit insertion in Oct 2001. Softc has also been used to successfully navigate both Mars Exploration Rover missions, Deep Space 1, Europe's Mars Express, and Japan's Nozomi and Muses-C (Hayabusa) missions.

3. Capabilities

Softc was designed to be as close as possible to an ideal correlator, where ideal refers to processing accuracy; no compromise in accuracy greater than 10^{-13} sec was made to increase performance (or for any other reason). Softc can correlate 1, 2, 4, and 8-bit sampled data, upper, lower or double (I/Q) sideband data, and data using either of two sample encoding schemes. Softc is quite portable, as it was developed on a little-endian Alpha running VMS, it works operationally on a large endian machine running Solaris, and has been tested on little-endian Intel machines running Linux. It produces identical output on these machines with no code modifications, even with different C compilers.

Softc was designed to process essentially any VLBI data. To do this and remain independent of the hardware and post-correlation software interfaces, Softc has its own input and output data formats. These formats were designed to be as simple as possible, but a translation program is needed to convert the sampled data into Softc's format, and another program is needed to translate from Softc's output to the desired post-correlation format. It is also possible to place these translators inside Softc; this has been done on the output side for our DeltaDOR effort and will likely be done for Softc's input in the future.

4. Code Debugging

One of the greatest hurdles in developing a VLBI correlator is the elimination of processing errors and inaccuracies. It is common for hardware correlator developers to spend years tracking down reasonably significant bugs. Also common are correlator users finding new, consequential errors long after all known problems were eliminated. An important limitation for correlator developers has been the lack of good debugging tools. For this reason, a significant effort, perhaps 40% of Softc's development, went into the creation of a full Monte Carlo data generator. This generator creates simulated VLBI data that can then be processed by Softc. In this way, the expected results can be calculated exactly a priori, and any deviations from these results indicate problems with the correlator.

The Softc Monte Carlo can simulate data in two ways. The first is an engineering mode where data can be generated with user selected delays, delay rates, fractional sample offsets, etc. This mode was very useful in the initial stages of debugging, as the implied geometric models were quite simple and covered a much greater parameter space than could be achieved by Earth-based station models. For example, data can be generated having a constant geometric fringe rate many times that possible for any Earth-based experiment; Softc's performance under these extreme conditions is a good check that fringe-frequency related calculations are done correctly.

The second Monte Carlo mode simulates data using the correlator model. Correlating this simulated data with Softc using the same model should result in no residual delays or phases, and tests Softc in its usual processing mode. The power of this type of test was confirmed when data were simulated using the Block I correlator model for an old experiment. When the Block I processed the simulated data, the residual delay was not zero, but a constant 1-sample delay. In other words, it appears the Block I had always reported delays with a constant 1-sample delay error, and this problem was never found throughout the life of the correlator, but was found immediately with this Monte Carlo test. Softc has passed a large number of extensive Monte Carlo tests, and this, combined with the fact that few calculational approximations are made, gives great confidence that any remaining processing errors are either insignificantly small or easily corrected.

Other tools were also created to find errors early in Softc's development. Because Softc was originally created to correlate 1 and 2-bit sampled data, the core processing routines perform extensive bit-level manipulations. Several test driver programs were developed for each bit-manipulation routine to check its function. Although these drivers are not part of the run-time portion of Softc, they should be considered part of the code package in the same way the Monte Carlo is part of Softc. These programs were designed to test the bit-manipulation routines under the most extreme conditions, and a significant effort went into trying to find processing errors in the core routines. The results of these tests were that the core routines, which perform the bulk of the processing, could be considered essentially bug-free. This made full-code debugging much easier because when a strange problem was seen in the results, many of the most perverse explanations one might imagine could be dropped from consideration.

In full code testing we found the unresolved errors to be dominated by modeling errors. The Monte Carlo cannot detect such problems because the same bad model both generates and correlates the data, or in other words, Softc cannot assess what is or is not a realistic model. For example, the first significant problem found turned out to be a sign error in the troposphere model. The Monte Carlo did not detect this (and could not possibly have done so), so only full code testing of real data could find these types of errors.

5. Future Directions at JPL

We recently obtained a new 18-CPU Beowulf computer and are currently porting Softc, Fit (our post-correlation software), and Modest (our parameter estimation software) onto this machine. We plan to interface this to two Mark 5 recorders by Jan 2004 and this will be JPL's VLBI correlator. Work is in progress to update Fit and to add additional Softc capabilities so we should have a clean, modern software system in early 2004. Timing tests on this system show Softc can process 8 lags of 10 MHz sampled real USB single-bit data in real time, and that the processing time is roughly linear with sampling rates from 1 to 100 MHz.

We are canceling the development of our 4-station hardware correlator, which is now essentially complete. There is nothing wrong with this correlator other than it is a *hardware* correlator with all its intrinsic disadvantages. Walking away from our hardware correlator now puts us on a path with a future and will likely save significant money. Because the economics of this decision are probably common to other institutions, we may not see another 4-station hardware correlator being developed anywhere. The economics may also favor replacing larger correlators even now, but the community probably needs to go up the software correlator learning curve beginning with the smaller systems.

Work is under way to obtain an open software license for Softc so that others can benefit from this program. Softc and its algorithms are documented [2] and that report should be publicly available very soon.

6. Summary

Softc was created to be as accurate as possible, capable of processing essentially any VLBI data, pass strong debugging tests, have a simple user interface, have no platform dependencies, and be written modularly in the most common programming language. It has been used operationally for spacecraft navigation for over 2 years and will be JPL's Mark 5 correlator next year.

References

[1] See Whitney, R., "Mark 5 Disk-Based Gbps VLBI Data System," MIT Haystack Observatory, http://web.haystack.mit.edu/mark5/software.html for more on the tape vs. disk issue.

[2] Lowe, S., "Softc: a Software VLBI Correlator," JPL Report, in press.

Valery Gratchev: New Correlator PARSEC, IVS 2004 General Meeting Proceedings, p.195–199
http://ivscc.gsfc.nasa.gov/publications/gm2004/gratchev

New Correlator PARSEC

Valery Gratchev

Institute of Applied Astronomy

e-mail: `gratch@isida.ipa.rssi.ru`

Abstract

The Institute of Applied Astronomy is developing Altera FPGA-based scalable correlator PARSEC with Mark IV specification. We have developed the prototype correlator MicroPARSEC. PCI-bus correlator board MicroPARSEC has standard office PC board format.

1. PARSEC Correlator

The Institute of Applied Astronomy is developing Altera FPGA-based scalable correlator PARSEC with Mark IV specification. The correlator unit uses PCI-bus correlator boards, standard CompactPCI hardware with single board Intel Pentium control computer and standard Linux operating system (Figure 1). We have estimated that it is possible to provide 4-station and 16-channel 1 or 2-bit data processing by using single correlator unit with Mark 5 VSI compatible playback system for VLBI and e-VLBI.

Figure 1. The prototype of Altera FPGA-based scalable correlator PARSEC with Mark IV specification.

2. MicroPARSEC Prototype Correlator

We have developed the prototype correlator MicroPARSEC. PCI-bus correlator board MicroPARSEC (Figure 2) has the following features:
– standard office PC board format,
– single board supports 2 cross-correlation 64 lags channels for one baseline,
– input data rate up to 64 Msamples/sec/channel, 1 or 2 bit sampling,
– integrated input data rate to 512 Mbit/s,
– the board can be connected directly to Canadian S2-RT or S2-PT.
The features of the IAA correlators are summarized in Table 1.

Table 1. Comparison of the correlators at the IAA

	TISS-1M	**MicroPARSEC**	**PARSEC**
Year of production	1993	2003	2004
Data input format	Mark III	S2/VSI	S2/VSI
Number of channels	30	2	16
Number of lags	8	64	64
Processing rate/ch	4 Mbps	64 Mbps	64 Mbps
Sample bit	1 bit	1 or 2 bit	1 or 2 bit
Phase resolution in fringe rotation	32 bit	32 bir	32 bit
Phase cal detect	1 Hz ÷ 1 MHz	1 Hz ÷ 4 MHz	1 Hz ÷ 4 MHz
Accumulation counter	24 it	30 bit	30 bit
Parameter period	5ms ÷ 1s	50ms ÷ 50s	50ms ÷ 50s
Pulsar gate	No	Yes	Yes
Main logic	Standard logic 1C	FPGA	FPGA
Data transfer	S2	S2/Mark 5B	S2/Mark 5B
Baselines	3	1	6

We have produced and tested four prototype correlator boards. For a first test we repeated processing data of S2 VLBI observation with 2 MHz video band at Svetloe-Zelenchukskaja baseline, which had been recorded in January 2002 at 8 GHz in S2 mode, and compared with correlator TISS-1M output data (Figure 3). The same data processing was made for 2 MHz video band at the sample rate of 32 Mbps (Figure 4).

MicroPARSEC may be used as scalable spectrum analyzer for station phase cal extraction and other different system diagnostic and/or spectral line real time observation data processing in single dish mode on our radio telescopes in Svetloe, Zelenchukskaya and Badary. The features of the IAA spectral analyzer are summarized in Table 2.

For a test of MicroPARSEC spectrum analyzer we processed spectral line observation, which have been recorded at Svetloe observatory in December 2003 at 18 cm and 1.35 cm in S2 single dish mode. The results are demonstrated at Figure 5 and 6. The spectral resolution of 1 kHz was achieved for the sample rate of 32 Mbps and 2 MHz video band.

We are going to start volume production in order of the correlator board MicroPARSEC for standard office PC with standard Windows 98/2000/XP operating system and special control and monitor program developed in IAA.

The S2/Mark III correlator and new correlator PARSEC are located at and staffed by the Institute of Applied Astronomy in Saint-Petersburg, Russia. The correlators are sponsored and

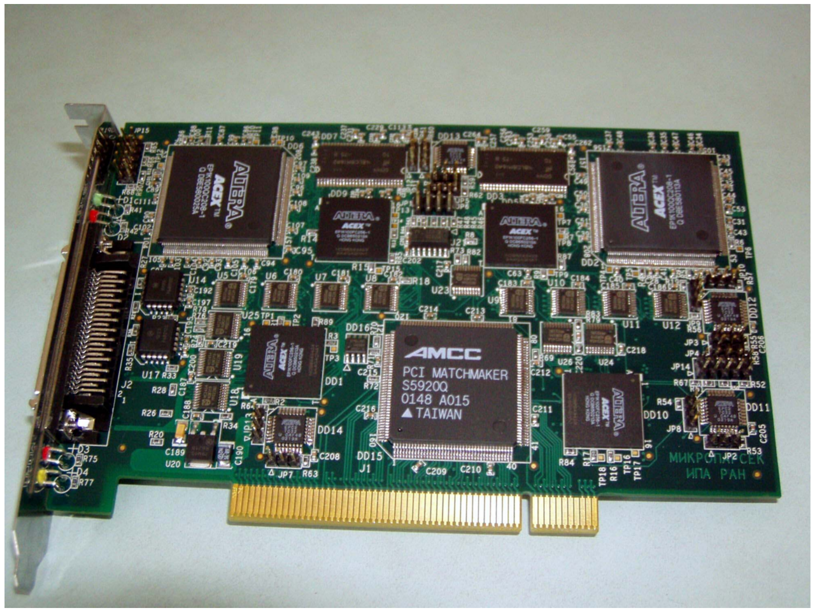

Figure 2. PCI-bus correlator board MicroPARSEC.

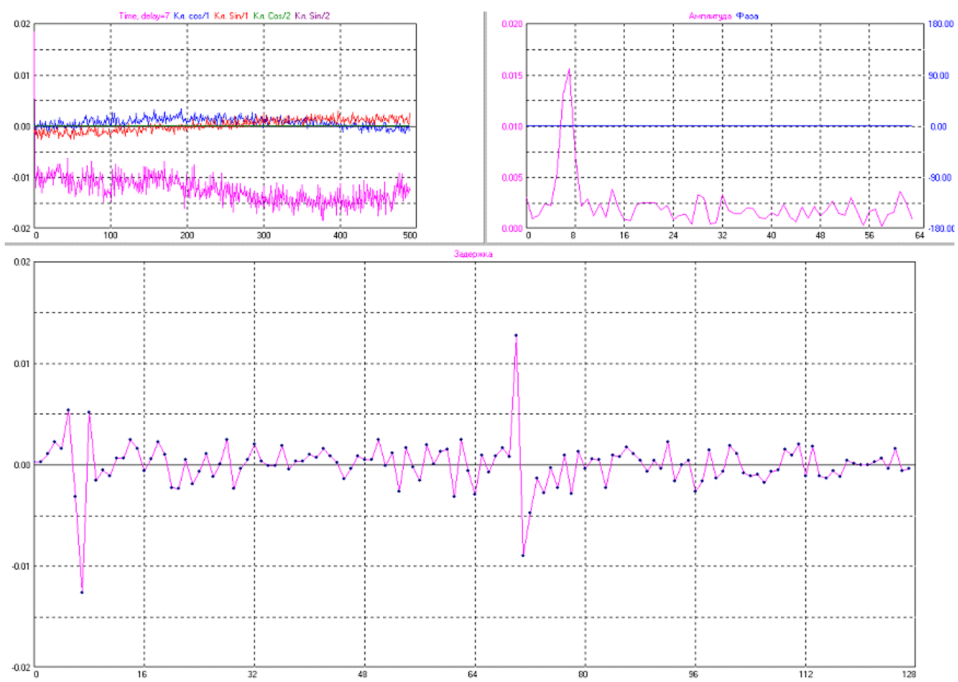

Figure 3. Output data of the MicroPARSEC at the 4 Mbit/s.

funded by the Russian Academy of Sciences, by the Russians Foundations of Basic Reserch and by the Russian Ministry of Sciences and Technologies. Dedicated to processing geodetic, astrometric

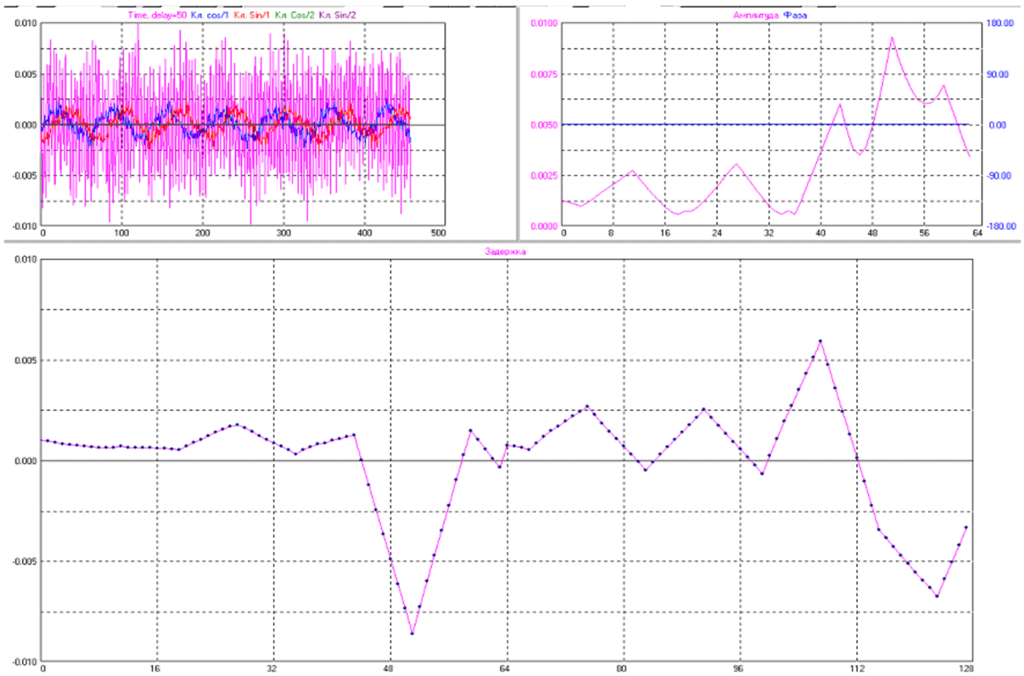

Figure 4. Output data of the MicroPARSEC at the 32 Mbit/s.

and astrophisic VLBI observations, the general role of the correlators are an operational processor for VLBI observation in Russia.

Table 2. The IAA spectrum analyzer specification

Parameter	MicroPARSEC spectrum analyser
Number of input ECL 1 bit/2bit signals	1-16/1-8
Processing rate	64 Mbps
Number of real lags	256
Number of multiplexing lags:	
for 16 MHz video band	512
for 8 MHz	1024
for 2 MHz	4096
for 125 kHz	65536
Spectral real time resolution:	
for 32 MHz video band (minimum)	250 kHz
for 125 kHz video band (maximum)	3.81 Hz
Sample bit	1 bit or 2 bit
Accumulation time	from 50 ms up to 10 s
Accumulation counter	30 bit

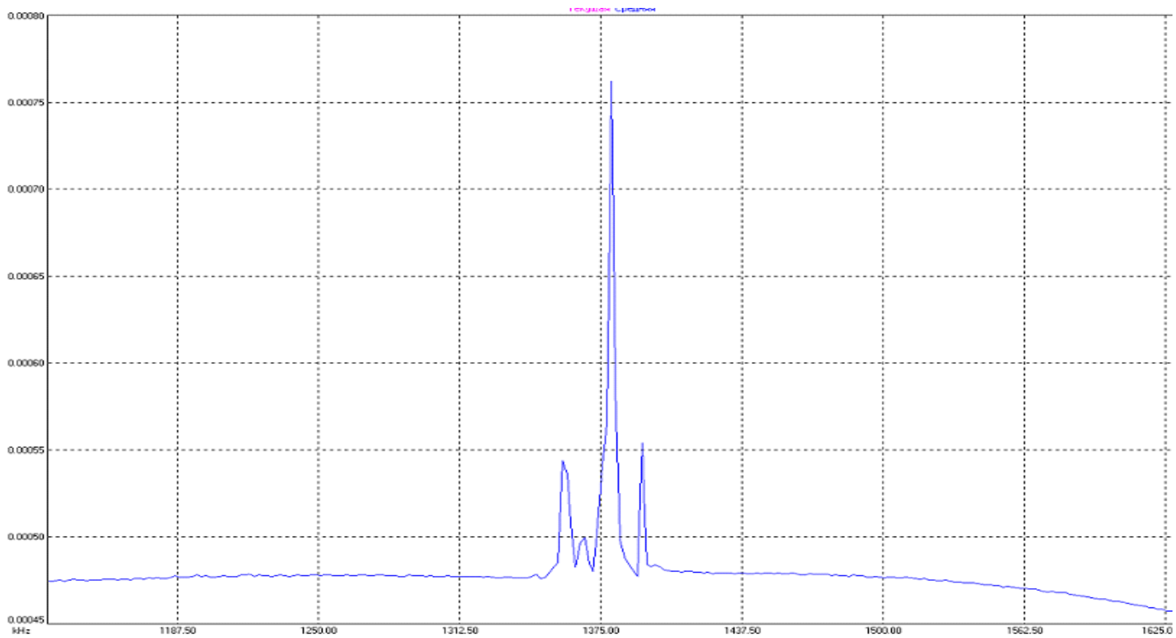

Figure 5. Spectrum of W3OH radio source at the wavelength of 18 cm.

Figure 6. Spectrum of W49 radio source at the wavelength of 1.35cm.

Hiroshi Takeuchi et al.: VLBI@home – VLBI Correlator by GRID Computing System, IVS 2004 General Meeting Proceedings, p.200–204
http://ivscc.gsfc.nasa.gov/publications/gm2004/takeuchi

VLBI@home – VLBI Correlator by GRID Computing System

Hiroshi Takeuchi, Tetsuro Kondo, Yasuhiro Koyama, Junichi Nakajima

Kashima Space Research Center, National Institute of Information and Communications Technology, Japan

Contact author: Hiroshi Takeuchi, e-mail: ht@crl.go.jp

Abstract

Kashima VLBI group have been developing a VLBI software correlator system using GRID computing technology. Like SETI@home, client/server model is used in the system and screensaver-type correlator program runs only when the client PC is idle. No expensive dedicated hardware correlator is necessary, but standard personal computers in observatories provide CPU resources. Using software correlator system, the type of a correlation process is selectable (e.g. XF or FX, geodetic purpose or astronomical purpose) and correlation processes can be easily repeated, changing various kind of correlation parameters (e.g. integration time, phase center of the map, number of lags, FFT size). Current processing speed of the system has reached 70 Mbps by using sixteen low-cost PCs. The processing speed has been improving day by day, by means of algorithm improvements for the correlation program and installations of high-speed network equipments. This paper describes the configuration of the system in detail and reports on a first experimental result of GRID computing in VLBI.

1. Introduction

In conventional VLBI systems, received radio signal at observing stations have been recorded to magnetic tapes and hardware correlators have been used for data processing. In the meantime, recent developments of personal computers enable us to use standard PC system for the VLBI data analysis. We have developed K5 VLBI system (see [1],[2]) in which raw VLBI data are transferred through the Internet and geodetic correlation analyses are made by software programs. K5 has been used in various experiments, such as spacecraft positioning observations, a multiple baseline geodetic experiment in which five VLBI stations paticipated, and e-VLBI observations between Kashima and Westford observatory to determine UT1-UTC within 24 hours. Since the K5 system is connected to the Internet directly, we can construct the low cost and high performance VLBI analysis system using GRID computing technology. To improve performance of the software correlator program, we have been developing a client/server type distributed computing system like SETI@home (see [3]).

Client/server-type distributed computing system is characterized by having the following three features. First, a large amount of data is divided in small units and transferred to client PCs. Second, sent data are processed by the PCs. And third, the result data are sent back to the server. This type of system generally works well when the network speed is faster than the processing speed in client PCs. At present, XF-type K5 software correlator which is used for geodesy have a capability to process 4 Mbps data in real time when it runs on a PC equipped with a Pentium3 1GHz. Thus, distributed computing method has the potential to increase the software correlation speed if the 10 Mbps, 100 Mbps or more high speed network environments are equipped.

2. Overview of the System

In the present system, raw VLBI data are divided into appropriate short-time period data and each segmented data is assigned to each PC. In the case of multi-baseline observations, all the data received at the same moment at different stations are gathered into one client to minimize data transmission costs. As shown in Figure 1, system consists of following components: control server that controls whole system, database server that stores processing conditions of VLBI data and statistics of each client PC, FTP servers at each VLBI station that transmit observed raw data to clients, and a lot of clients by which VLBI data are correlated. When a screensaver-type client software (a screenshot is shown in Figure 3) activates, it ask the control server about filenames of the data to be processed and IP addresses of observed VLBI stations. The client downloads the data from the FTP servers and correlates the data. Resulting data and related information such as download time and correlation time are reported to the database server via the control server.

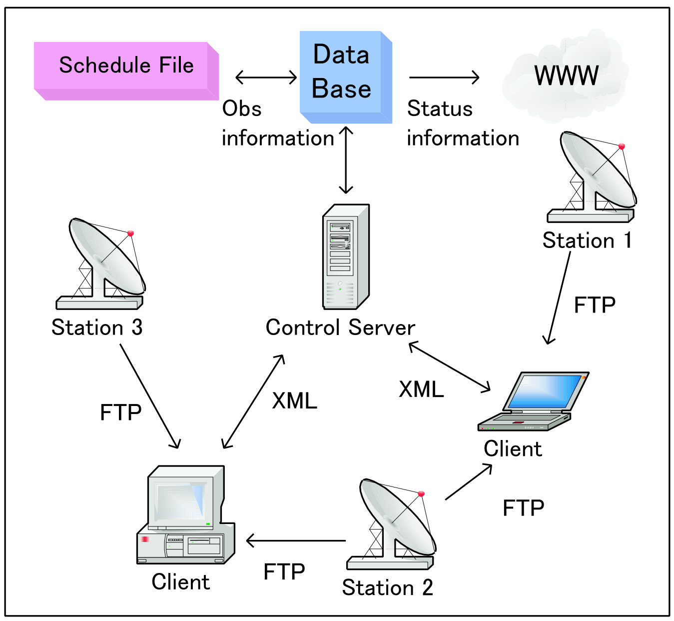

Figure 1. Schematic diagram of the whole system. It consists of a controlserver, a databese server, FTP servers at each VLBI stations, and a number of client PCs.

3. Detailed Structure of Control Server and Client Program

A schematic diagram of a control server is shown in Figure 2. In the server program, file information of each segmented data are stored in a C++ structure (see the right-hand side of Figure 2). Structures relevant to unprocessed segments are listed in a queue (upper queue in Figure 2). Referring to the database server, new structure is added to this queue in real-time. If a client connects to the server, information in the structure at the forefront of the queue is transmitted and the structure is transferred to another queue in which information of processing segments are listed (lower queue in Figure 2). When the correlation process in the client finished, it is reported to the server and relative structure is deleted from the second queue. Finally, reported information is stored in the database server. If a client connects to the control server while the first queue is empty, file information is transmitted from the second queue so as not to remain unprocessed data.

In client PCs, VLBI data transfer is realized by a built-in FTP-client function in the screen-saver type client program. A multi-thread simultaneous downloading from different VLBI stations is possible and it has resume capability, which will restart interrupted downloads. Correlation process is performed by the external correlator program, cor.exe (see [4]). In a socket connection between a control server and a client PC, all information is represented in XML format.

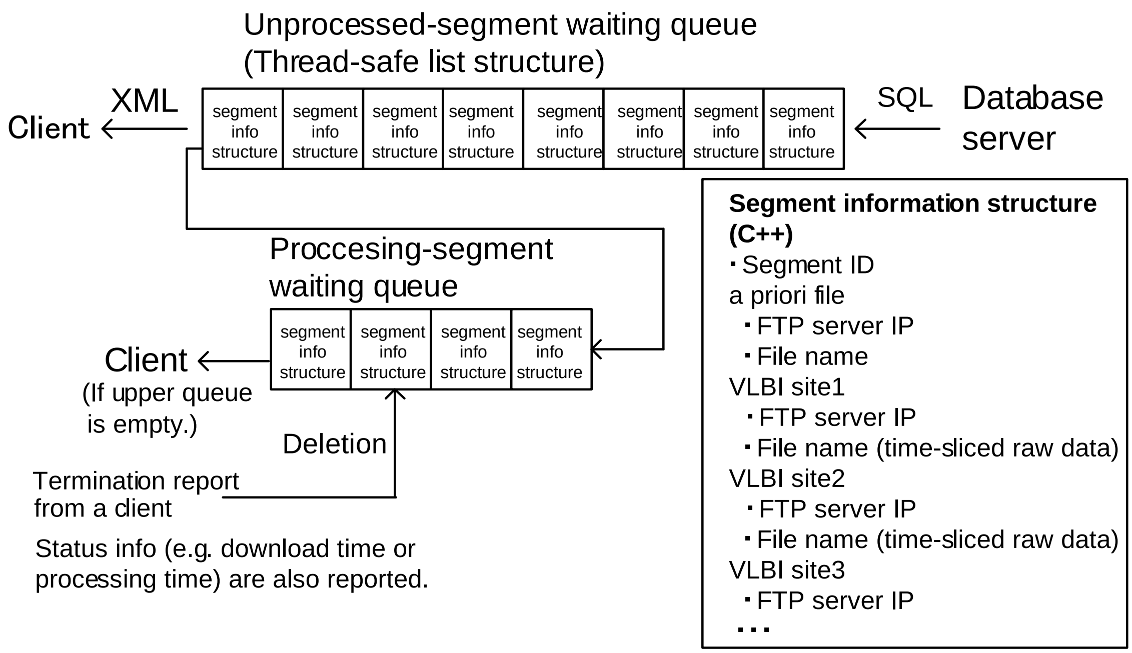

Figure 2. Schematic diagram of a control server, in which file information of a segmented VLBI data is represented in a C++ structure.

4. System Bottleneck Detection

There are three factors which can become a bottleneck of the system: data processing rates of clients, network speed, and data transfer rates of FTP servers. These three factors can be monitored using statistical data stored in the database server. Data processing rates of clients can be calculated from recorded correlation times. A typical value of the rate using a 1CPU PC is 2 to 12 Mbps. If this factor becomes a system bottleneck, it is necessary to increase the number of clients or to improve the algorithm of correlation programs. The statistics of download time in each client is used to evaluate the network performance. A typical network speed is 10 Mbps to several Gbps. The network speeds around FTP servers determine the total performance of the system. If it is not enough compared to a total data processing rate of the clients, it becomes a bottleneck of the system. The data transfer rate of a FTP server is limited by the access speed of hard disks. A typical value is 200 Mbps for random accesses and 1 Gbps for sequential accesses. If it becomes a bottleneck of the system, FTP mirroring is effective and Ramdisk can be used for real-time observations. Eliminating these factors, overall system performance can be increased up to 10 Gbps, the highest network rate we can use at this time.

Figure 3. Screenshot of screensaver-type client program downloading two VLBI raw data simultaneously. Two data are cross-correlated by a XF-type software correlator and result data are sent back to a server.

5. New Features as a GRID Computing System

In the case of existing GRID system like SETI@home, unanalyzed original data are always stored in one location. On the other hand, VLBI raw data are stored in multiple locations in nature, and each client PC must download the data from separated data storages. Additionally, in the case of multi-baseline observations, analyzed raw data are reusable on the other PC for the analysis of different baselines. Because of these unique features, there are some new possibilities as a distributed computing system as follows:

- Allocate different set of FTP servers to each client in order to optimize total network transmission cost.
- Multicast data transmissions from a VLBI station to multiple client PCs.
- Reuse of the analyzed VLBI raw data by P2P (peer-to-peer) data transmissions between clients.

Basically, all the data taken at the same moment at different VLBI stations should be gathered into one PC to minimize data transmission costs. However, if the number of observation stations (N) is increased, data processing time in one PC is increased on the order of N^2 and it may become impossible to analyze all baselines by one PC. The above methods are effective to distribute a segmented data to multiple PCs in such a case.

6. Current Status of the System and Future Plans

The overall performance of the system for a 32-lag XF-type correlation is 70 Mbps using sixteen standard PCs in our observatory. We are planning to perform a 64 Mbps real-time experiment. In this year, we will improve the network capacity and file server performances to achieve 1 Gbps using a large number of PCs. In future, all the information concerning VLBI experiments shall be integrated in a database (see Figure 1) for the easy management of VLBI experiments. The concrete proposal of such kind of database system is shown in [5]. We expect that distributed computing method will become a key technology for VLBI analysis in the next decade. Various type of distributed computing methods have also suggested (see [6],[7] for details) besides this system.

References

[1] Kondo, T., Technology Development Center at CRL, In: International VLBI Service for Geodesy and Astrometry 2002 Annual Report, NASA/TP–2003-211619, N. R. Vandenberg and K. D. Baver (eds.), 297–300, 2003.

[2] Koyama, Y., T. Kondo, H. Osaki, K. Takashima, K. Sorai, H. Takaba, K. Fujisawa, Evaluation of the K5 system in geodetic VLBI experiments, In: IVS CRL Technology Development Center News, No.23, 26–30, 2003.

[3] SETI@home web page
`http://setiathome.ssl.berkeley.edu/`

[4] Kondo, T., Y. Koyama, H. Osaki, Current Status of the K5 Software Correlator for Geodetic VLBI, In: IVS CRL Technology Development Center News, No.23, 18–20, 2003.

[5] Takashima, K., Total VLBI data management system using database server -The organizer for VLBI@home-, In: IVS CRL Technology Development Center News, No.23, 21–22, 2003.

[6] Kondo, T., M. Kimura, Y. Koyama, H. Osaki, Current Status of Software Correlators Developed at Kashima Space Research Center, In: IVS 2004 General Meeting Proceedings, NASA/CP–2004-212255, N. R. Vandenberg and K. D. Baver (eds.), ?–?, 2004.

[7] Kimura, M., J. Nakajima, The implementation of the PC based Giga bit VLBI system, In: IVS CRL Technology Development Center News, No.21, 31–33, 2002.

Stephen Parsley: eVLBI Research in the European VLBI Network, IVS 2004 General Meeting Proceedings, p.205–209
http://ivscc.gsfc.nasa.gov/publications/gm2004/parsley

eVLBI Research in the European VLBI Network

Stephen Parsley

Joint Institute for VLBI in Europe
e-mail: parsley@jive.nl

Abstract

Multi-gigabit connections are now available in most European countries via National Research and Education Networks (NRENs) and across Europe via GÉANT. The EVN Data Processor at JIVE, and a growing number of telescopes, now have high bandwidth connections to these networks. With the support of DANTÉ and a consortium of NRENs, the European VLBI Network (EVN) is currently involved in a Proof-of-Concept project to connect up to six European telescopes directly to the EVN data processor. The project will explore the feasibility of achieving real-time eVLBI using shared IP across the production, research and education (R&E) networks.

1. Introduction

In January 2003 a meeting was convened in Amsterdam to discuss the technical details of a Proof-of-Concept project to connect up to six European telescopes directly to the EVN data processor at JIVE. The meeting was set up and chaired by DANTÉ, operators of GÉANT, the pan-European R&E network. This followed a series of meetings between DANTÉ and the EVN leading to approval for such a project from the NREN Policy Committee (NREN-PC). The meeting was attended by technical representatives from JIVE, six EVN telescopes, six European NRENs and other networking experts.

Information was exchanged and agreements were reached about the targets of the project and a time-plan was formulated. For each group the objectives agreed upon were as follows:

- For the EVN:
  - Feasibility of eVLBI: Costs, timescales, logistics.
  - Standards: Protocols, parameter tuning, procedures at telescope and correlator.
  - New Capabilities: Higher data rates, improved reliability, quicker response.
- For the NRENs:
  - To see significant network usage with multiple Gbit streams converging on JIVE.
  - Up to 5 telescope sites supported (6 including Westerbork).
  - Must be seen to enable new science.
  - Support will be best effort IP service limited resilience.

2. Project Status

The project has progressed largely according to plan. In the EVN, deployment of Mark 5 has provided a uniform interface to telescopes, correlator and the networks. Disk recording enables various eVLBI tests to be performed on and off-line without disruption to normal operations and, in some cases, ahead of the provision of a high bandwidth connection. The DWDM connection to JIVE has been upgraded to six Gigabit Ethernet lines and connections into the Netherlands were upgraded to 10 Gb/s well ahead of schedule. Progress with local connections to telescopes has been slower but toward the end of 2003 1 Gb/s connections to Westerbork and Onsala came on line. With Jodrell Bank's existing 150 Mb/s connection these three stations were able to take part in a series of eVLBI tests. Through these tests and some laboratory work at JIVE, good progress has been made with understanding the network interface and configuration issues, and the evaluation of optimum data transfer parameters.

3. Milestones

- May 2003: First use of FTP for VLBI session fringe checks.
- September 2003: Mark 5 - Mark 5 data transfer between Bologna and JIVE.
- October 2003: First light on Westerbork Gigabit connection.
- November 2003: International baseline, eVLBI fringes, only 15 minutes after observation.
- November 2003: Onsala Space Observatory connected at 1 Gb/s.
- January 2004: First European eVLBI image (see Figure 1).

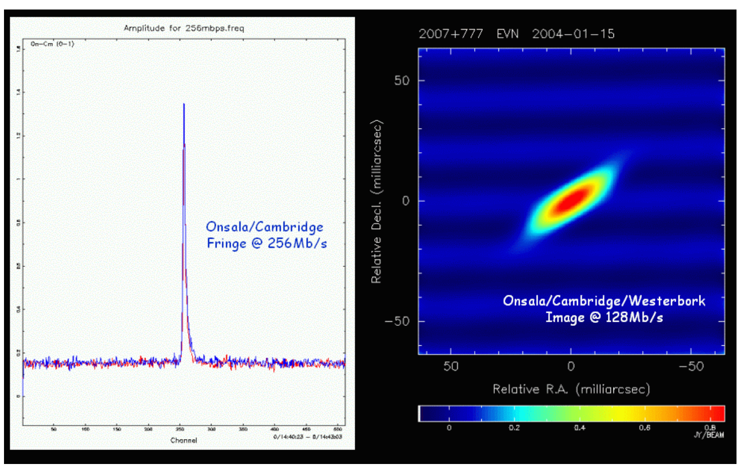

Figure 1. First European eVLBI Image

4. eVLBI Facilities at JIVE

Mark 5 is now used exclusively for eVLBI experiments at JIVE. A Cisco 15252 DWDM unit, connecting to one fibre pair from Amsterdam, provides six Gigabit Ethernet lines, using LX Optics, expandable to up to sixteen lines. A dedicated line from Westerbork has also been installed that is completely isolated from other network elements. A number of experimental environments are provided by these facilities with varying levels of isolation from external network elements and competing traffic.

5. Tests and Results

The built-in transfer processes of the Mark 5 (in2net, net2disk etc.) have been used in different combinations for tests involving various levels of disk buffering. Some tests were also performed using TCP and UDP based network performance monitoring programmes. The results of these tests are collected in Table 1. A number of questions arise from these results that are the subject of ongoing investigation:

Table 1. Test Results (J indicates jumbo-frames)

	Memory-Memory		Disk2net2Disk		In2net2Disk	In2net2Out
	UDP	TCP	UDP	TCP	TCP	TCP
Bench - patch cable		960Mb/s (J)	250Mb/s	544Mb/s		
JIVE-AMS-JIVE	500Mb/s	360Mb/s	341Mb/s (J)	456Mb/s (J)		
Wb-JIVE	867Mb/s	680Mb/s	249Mb/s (J)	378Mb/s (J)	256Mb/s	
Bologna-JIVE	670Mb/s	128Mb/s		307Mb/s		
Onsala-JIVE				177Mb/s	256Mb/s	
JIVE-Haystack	612Mb/s			71Mb/s		
Jb (150Mb link)-JIVE					64Mb/s	64Mb/s

- Why are data rates lower when disk access is involved? What can be done to improve this?
- JIVE-Amsterdam-JIVE and Westerbork-JIVE connections are private lines, with no competing traffic. Why are they slower than via a patch cable on the bench?
- When the underlying protocol for Mark 5 disk-disk transfers is changed from TCP to UDP the data rate goes down. How can this happen?
- Data rates across the European networks vary by a factor of two. Is this typical?

The data rates detailed in Table 1 where achieved after a lengthy investigation to find the optimum values for various parameters. Results of this investigation are given in Table 2. So far the underlying logic of these numbers is not well understood.

Table 2. Parameter Settings (Disk2net2Disk, TCP)

recv/send (Bytes)	socbuf (Bytes)	data rate (Mb/s)
268320	134160	331
	268320	421
	536640	425
	1073280	412
2097152	1048576	522
	2097152	509
	3145728	496
	3997696	453
4194304	1048576	521
	2097152	544
	3145728	506
	3997696	524

In an effort to move the enquiry forward JIVE is currently upgrading two Mark 5 units with Intel(R), SE7501BR2, server grade motherboards. This will confirm or otherwise that some of the performance limitations are a function of the underlying PC hardware. Installation of the new motherboard was moderately easy and operation as a normal Mark 5 unit has been confirmed.

6. Correlator Developments for Real-Time

In a real time system data will arrive at the correlator with some delay comprising a network delay and an instrumental delay caused by various bus/memory/peripheral manoeuvres within the interface units. Within Europe the network delay is in the range 10-30 ms. If other delays are known and stable, the correlator time reference can be synchronised, with a suitable delay, to UT. The existing input buffer will be able to absorb differential delays across the networks. To achieve this both hardware and software modifications are required at the correlator and this is the subject of one package of work at JIVE. If delays are unpredictable it may be necessary to provide a bigger buffer, and if this is done the synchronisation requirement can be relaxed. The Mark 5 has a 512 MByte buffer in the output path which, at the highest data rate, holds up to four seconds of data; more than enough for our needs. Tests are currently under way at JIVE to characterise the performance of Mark 5 in these direct-to-network modes. Of interest are the data rates achievable and the behaviour of the servo mechanism.

7. Forward Planning

In January 2004 NREN and EVN representatives met again to review progress one year on. The overall conclusion was that the project is largely on schedule. Developments for real-time operation are seen as the next priority. Plans are in place to achieve multiple telescope real-time operation by mid-2004. There are good prospects for a Gigabit connection to Torun on this timescale. Other telescopes, including Jodrell Bank and Medicina, do not expect to get a connection until the end of 2004 but DANTÉ and the NRENS are now willing to continue support for another year. In the coming three months attempts will be made to understand/remove Mark 5 data rate limitations and to develop the use of UDP for higher rates. Higher rate tests between Bologna and JIVE, using UDP, are also planned. Within six months further tests between Wb, On & Jb should be possible as link speeds improve and more NREN PoP JIVE tests will be staged to push larger data volumes across the European networks.

The meeting agreed that the original goal of six telescopes in real-time at 1 Gb/s was unrealistic. Many stations are unlikely to get more than one Gigabit Ethernet connection, and Gigabit Ethernet is actually limited to something less than 1 Gb/s. The existing VLBI system with Mark 5 is also restricted to fixed octaves— 64 Mb/s, 128 Mb/s, 256 Mb/s, 512 Mb/s, 1 Gb/s.

The revised goals agreed are real-time eVLBI at 512 Mb/s with at least three telescopes participating. Non real-time tests will be performed to maximise network loading up to the limits of Mark 5 and Gigabit Ethernet.

8. Conclusions and Acknowledgements

For the practitioners of VLBI the benefits of a real-time system are clear. Meanwhile the NRENs recognise VLBI as a genuine high-demand application, that can already source very large data flows from all corners of Europe. The big-science image of VLBI is also very welcome to the administrators and policy makers who need eye-catching publicity to maintain the profile of their product.

There are many practical difficulties however underlying these superficial enthusiasms. The astronomical community is, understandably, reluctant to commit heavily from very limited funds for local loop connections. During the normal VLBI session, eVLBI tests are an unwelcome distraction to already busy operations staff. Outside the sessions coordinated reservation of expensive telescope time can be difficult to achieve. At the same time the limited service afforded by the networks compounds any problem. No special tuning of the network for VLBI traffic is provided and technical problems have to take their place in the normal service queue, at a low level of priority.

For the above reasons the success of the project depends on the drive, effort and cooperation of individuals in both communities who are willing to work a little outside the normal parameters of their jobs. The experience of the first year of the project tells us that real progress only begins when real data starts to flow across real networks; and the key to this is to have telescopes connected directly to the network. When this begins to happen technical problems can be identified and engaged, and identifiable progress can be made. The following roll-call identifies some of the individuals and organisations who have made the progress achieved so far possible:

- European (R&E) networks: GARR, NORDUnet, SUNET, SURFnet, UKERNA, DANTÉ
- At the telescopes:
  - Michael Lindqvist, Michael Olberg: Onsala Space Observatory
  - Paul Burgess, Ralph Spencer: Jodrell Bank Observatory
  - Tony Foley, Hanno Holties: Westerbork Synthesis Radio Telescope
  - Giuseppe Maccaferri: Istituto di Radioastronomia, Medicina
- At JIVE/ASTRON:
  - Cormac Reynolds, Schedules
  - Arpad Szomoru, technical co-ordination
  - Sergei Pogrebenko, science advisor and software correlator
  - Klaas Stuurwold, network facilities and NREN liaison.
- Richard Hughes-Jones of UoM for network performance measurement software.
- The Haystack Mark 5 team for the Mark 5 itself and helpful support.
- Onsala and Westerbork Observatories management and staff for providing the high-bandwidth links to their telescopes that have got this project off the ground.

References

[1] Hughes-Jones, R., Parsley, S., Spencer, R., High Data Rate Transmission in High Resolution Radio Astronomy vlbiGRID FGCS:- iGRID2002 conference special issue, 2002

[2] Parsley, S.M., VLBI Participation in Next-Generation Network Development, eVBLI Workshop, Haystack Observatory, 2002

[3] S.M. Parsley, P. Burgess, R. Hughes-Jones, A. Mujunen, S. Pogrebenko, J. Ritakari, R. Spencer, A. Szomoru, H. Verkouter, eEVN, ASP Conference Series, New Technologies in VLBI, 2002

Zheng Weimin et al.: e-VLBI Progress of the Chinese VLBI Network, IVS 2004 General Meeting Proceedings, p.210–214
http://ivscc.gsfc.nasa.gov/publications/gm2004/zheng

e-VLBI Progress of the Chinese VLBI Network

Zheng Weimin, Zhang Xiuzhong, Shu Fengchun

Shanghai Astronomical Observatory, Chinese Academy of Sciences

Contact author: Zheng Weimin, e-mail: zhwm@center.shao.ac.cn

Abstract

At present the Chinese VLBI Network (CVN) contains two fixed stations, one mobile station and the 2-station Shanghai correlator. The PC-based VLBI data acquisition terminal and playback unit named CVN harddisk system was developed at Shanghai Astronomical Observatory recently. The CVN harddisk systems were installed at Sheshan station, Urumuqi station and Shanghai Observatory, and several e-VLBI test observations were completed in 2003. Now the Shanghai correlator is able to correlate the data from the tape or the harddisk. Based on the CVN harddisk system, research on the software correlator was also carried out. The prototype software correlator was successfully used in the station fringe check, satellite fringe search and data processing. When processing the satellite observation data, the hardware Shanghai correlator can produce the group delay & delay rate, guided by the software correlator. The CVN will be updated to a realtime VLBI network, including 4 stations and 2 realtime 5-station correlators (hardware & software), which will be applied to the Chinese Lunar satellite navigation, as well as the geodetic and astronomical observations in the future. Researches on the digital BBC and formatter have been carried out.

1. Introduction

Nowadays, the Chinese VLBI Network (CVN) contains three radio VLBI stations and one correlator. The Sheshan station is near Shanghai and the Nanshan is near Urumqi. The diameter of each antenna is 25 meter. They are also members of the European VLBI Network (EVN) and the International VLBI Service for Geodesy and Astrometry (IVS). The third one located in Kunming, southwest China, is a mobile VLBI station with a 3-meter antenna and a S-2 VLBI recorder [1]. The 2-station Shanghai correlator is placed at Shanghai Observatory. Since 2002, Shanghai Observatory has carried out the researches on the e-VLBI, and has achieved several results. The PC-based VLBI data acquisition terminal and playback unit named CVN harddisk system was developed and placed at the Nanshan, Sheshan station and the Shanghai Correlator last year. Besides, we have begun to develop some e-VLBI techniques like software correlator and digital Base Band Converter (DBBC), etc. Several observations based on the CVN harddisk system were successful. In addition, the software correlator processed the data, too. We will expand the CVN to a new 4-station realtime VLBI network with realtime correlators in 3 years, which will be used in the Chinese first lunar satellite navigation, as well as geodesy and astrometry.

2. CVN PC-Based VLBI Data Record and Playback Harddisk System

Since 2002, the VLBI Laboratory of Shanghai Astronomical Observatory has begun to develop the PC-based VLBI data record & playback system named CVN harddisk system. The main target of this system was that we needed a low cost and reliable harddisk system to replace the expensive and unreliable tape playback unit made by Penny & Giles Company. In order to make it, we decided to use, as far as possible, the ordinary industrial PCs with off-the-shelf Components. Another reason was that, although there were several harddisk systems like Mark 5, K5 and PCEVN, none of them was compatible with the Shanghai correlator (VLBA model). Thereby, we had to design the record interface and the playback interface compatible with the Mark IV formatter and the Shanghai correlator.

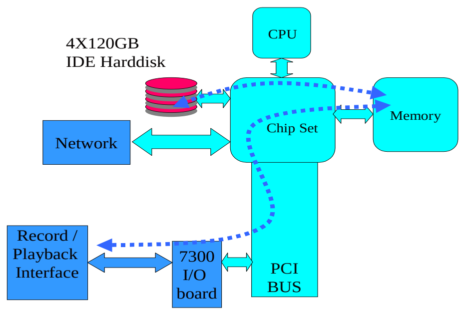

Figure 1. Structure of the CVN harddisk system.

Figure 2. CVN harddisk system play-back unit (upper) with plackback inter-face (lower).

Figure 1 shows the structure of the CVN harddisk system. The hardware platform is an ADLINK NuPRO-841 mainboard. We selected ADLINK PCI-7300B, an ultra-high speed digital IO board as the input and output interface. This board is a 32-channel, 40 MHz PCI data IO board, and the maximum IO speed reaches 80 MB/s. The operation system is Debin Linux. Data are stored in the normal Linux files. To increase the record and playback speed, four 120 GB harddisks are mounted on one CVN unit, and data are recorded in (or read from) the four harddisk simultaneously. The control software is self-developed.

Figure 3. CVN harddisk system (left) with the record interface.

With the record and playback interface, as shown in figure 2 and figure 3, the CVN system is compatible with both the Mark IV formatter and the Shanghai correlator. The total cost of one CVN harddisk unit is only \$ 3000.

In the record mode, the data and the corresponding clock signals from the Mark IV VLBI formatter are changed from the ECL level to the TTL level by the record interface, and then received by the PCI-7300B IO board. The record interface is able to decode the Mark IV format and display the UTC, track information etc. The harddisk system can check the data quality by software before recording. The data are recorded only if there are no parity or frame errors.

The playback interface receives the control and monitor commands from the correlator through RS232 and MCB ports, and adjusts the output data speed accordingly. Therefore, from the view of the correlator, there is no difference between this harddisk playback system and a P&G tape playback unit.

The recording speed of one CVN harddisk unit is 288 Mbps (32 track@9 Mhz), and the maximum recording speed is up to 576 Mbps (32 track@9 Mhz). With four 120 GB disks, one unit can record 7 hours, when the data clock is 4.5 MHz, which is equivalent to the 80 ips tape speed. The playback rate is up to 288 Mbps (32 track@9 Mhz).

The milestones of CVN system are:

Mar 2003: Successful record testing at Sheshan station

Apr 2003: Disk-disk & disk-tape playback test

May 2003: First fringe demonstrated between Nanshan and Sheshan

May 2003: First successful e-VLBI fringe test between Nanshan and Sheshan (disk-internet-disk, FTP).

3. Software Correlator

Since the cost performance of the commercial computer increases wonderfully recently, it seems that there is a tendency of using software instead of hardware correlator in the VLBI data pre-processing. Because the CVN harddisk system stored data in the normal Linux files, we began to develop the software correlator prototype (Matlab version). At the beginning, this software was used to check fringe.

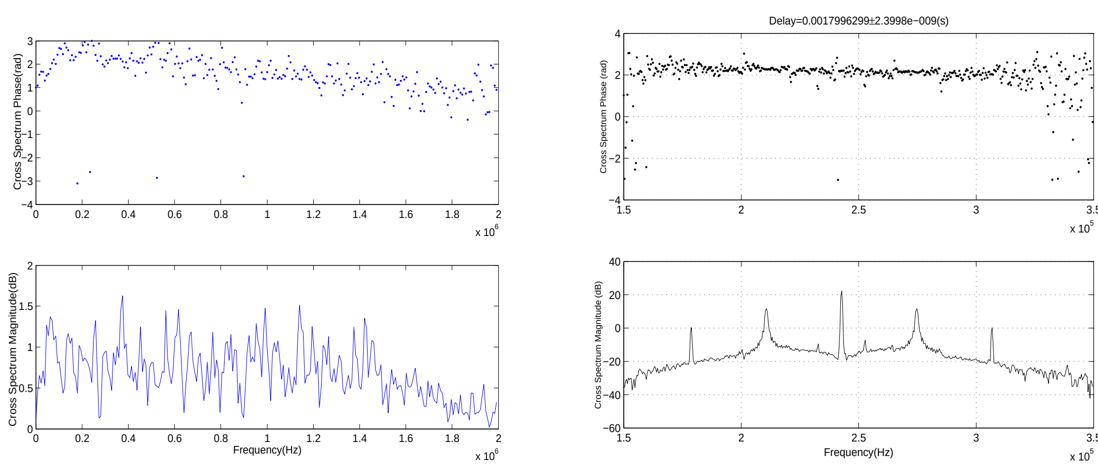

Figure 4. Fringe check by software correlator, phase (upper) and amplitude (lower) spectra, DA193 (left), satellite telemetry signal (right).

In fringe check observations, we chose two kinds of radio source. One was a strong extragalactic source, like DA193. Another source was the GEO satellite downlink telemetry signal. Due to the high SNR satellite signals, the software correlator was able to use 8 MByte VLBI data transmitted from each station through ftp to find legible fringe (Figure 4), and the corresponding observation time was as short as only 0.5 second. When observing DA193, the observing time was about 30 seconds, and the corresponding data was 500 MByte. Figure 4 shows the fringe of one track.

The software correlator was used to search fringe in the satellite observations. Last year we tried several satellite VLBI observations to study how to use VLBI to track the Chinese lunar satellite in the near future. We observed the downlink telemetry signals which most satellites had. Because the satellite orbit accuracy we got was bad, there were big error of the delay and delay rate model calculated from such orbit data. So there was not any fringe when we used the Shanghai (hardware) correlator to process the data. For this reason, we decided to apply the software correlator for fringe search firstly. The spectra of the satellite telemetry signals are quite different from those of the wideband extragalactic sources. The telemetry signal is a narrow band signal with a strong carrier wave in the center of the spectrum domain, as well as several tones (Figure 4). The software correlator calculated the frequency difference of the carrier wave received by two stations firstly, which was the Differential One-way Doppler (DOD) or the fringe rate. Then the DOD value was used to stop the fringe; finally, it correlated the signals and found out the group delay. According the group delay and the fringe rate found by the software correlator, the Shanghai correlator completed the correlation of satellite signals.

The precision of the DOD is only several mHz, while the group delay are less than 10 nanoseconds, when the integration time of the software correlator is 0.5 second. Considering the bandwidth of the telemetry signal is only 200 kHz, the software correlator's results are favorable, and therefore the software correlator is applied to calculate the delay & DOD individually. The software correlator also found the Nanshan station local oscillator frequency shift (about 100 Hz).

When observing the Geospace Double Star, which is a spin stabilization satellite with a 4-second spin period, the software correlator's results show the satellite spin effect on the fluctuation of the group delay and DOD (Figure 3). We will try to remove the effect which affects the precision of the delay and delay rate.

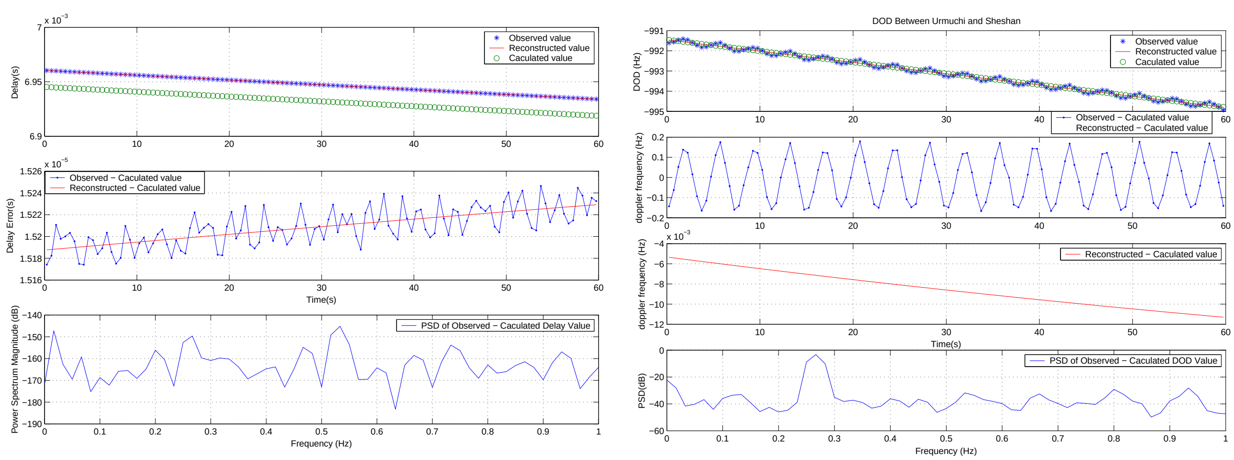

Figure 5. Satellite's spin effect on the delay (left) and DOD (right).

4. Observation and e-VLBI Data Transmission Experiment

Two CVN harddisk systems were placed at the Nanshan station and the Sheshan station last year. We have successfully made dozens of observations of wideband extragalactic source, satellite and maser by the harddisk system. Differential VLBI mode was tested in the satellite observation for preparation of the lunar satellite navigation.

Among these observations, we tried several e-VLBI data transmission experiments. After the observation, the Nanshan station transmitted the data from the local harddisks to the ones located at the Shanghai observatory through domestic ISDN or the Internet for the hardware and software correlator to correlate. At the same time, the disks at Sheshan were taken to Shanghai observatory by car.

Although the domestic network speed is only about 50 KB/s, these experiments still show the possibility of the e-VLBI of CVN, especially for the fringe check. It is inspiring that the network speed will increase a lot in the near future for the lunar project. e-VLBI or even realtime VLBI is doable at that time.

5. Realtime VLBI in the Chinese Lunar Project

China will launch its first lunar satellite in three years. Realtime VLBI will be used in the satellite navigation. For these reasons, two new big antennas will be built and added into the CVN in two years. One is a 50 m antenna which will be placed at Miyun, suburb of Beijing, another is a 40 m antenna, which will be placed at Kunming. The Shanghai observatory will build two 5-station realtime correlators, one is a hardware correlator, and another is software one. All these four stations and the correlators will be connected by high-speed optical fiber network. The software correlator will be the backup of the hardware correlator. Because in the lunar project the data speed is much lower compared with the astronomical observations, realtime, multiple station software correlator is doable.

The VLBI Laboratory of Shanghai observatory is developing the new equipment, which will be used in the realtime CVN, like formatter and DBBC. The prototypes of the formatter and DBBC have been finished and successful experiments were completed at the end of 2003.

The 3-station observation and e-VLBI test and data process will be completed.

6. Acknowledgements

The authors gratefully acknowledge the support of K. C. Wong Education Foundation, Hong Kong. The authors also appreciate the great help of Cheng Zhong, Zhu Renjie, Lu Chunmei, Xiang Ying, Xu Zhijun and Li Yuanfei, the members of the VLBI laboratory of Shanghai Observatory.

References

[1] Zhang, XZ,. Zheng, WM,. Shu, FC, Hang, ZY,. Xiang, Y., CVN Correlator and its Future, New Technologies in VLBI, Astronomical Society of the Pacific Conference Series Volumes, Vol. 306, 287–300, 2003.

David Lapsley: A Practical Approach to e-VLBI over Long Fast Networks, IVS 2004 General Meeting Proceedings, p.215–219
http://ivscc.gsfc.nasa.gov/publications/gm2004/lapsley

A Practical Approach to e-VLBI over Long Fast Networks

David Lapsley

MIT, Haystack Observatory

e-mail: dlapsley@haystack.mit.edu

Abstract

Modern VLBI experiments demand transfers of up to several terabytes per day, and though modern research and education networks have backbone bandwidths of up to 10 Gbps and should be easily able to handle this load, at this speed, traditional transport options (TCP/UDP) do not perform/behave well. Many enhancements have been proposed to TCP, in particular, to improve its performance in high speed networks, however, they are not yet widely deployed. In the interim, advanced application layer transport protocols offer an alternative, easily deployable and effective solution.

In this paper, we discuss some of these protocols and look at the results of some tests using these protocols. Some of these protocols are still experimental, so they should be used/deployed only after extensive reliability and fairness testing. However, they do provide a relatively easy and efficient way in which to improve data transport rates across high speed, long round trip time networks.

1. Introduction

In order to realize the benefits of e-VLBI, data must be transported in an efficient manner at high bandwidths. However, the rate of evolution of the core backbone speeds has far exceeded the rate of evolution of the traditional network transport protocols used to support applications such as the File Transfer Protocol (ftp), scp, world wide web etc. As such, many scientists that are trying to transport large amounts of data over a wide area face a number of issues in order to realize their goal. In this paper, we describe some of the e-VLBI experiments that have been performed to date, the issues that are currently being faced by e-VLBI practitioners and some of the alternative solutions that are available for alleviating these issues. Finally, we conclude with a comment on the suitability of these alternatives for e-VLBI data transport.

The two most common transmission protocols in use today are: (1) the Transmission Control Protocol (TCP): which provides congestion avoidance and control, guaranteed, in-order data delivery and is typically used for data applications that can tolerate delay but not loss (e.g. ftp) and (2) the User Datagram Protocol (UDP): which is a light-weight datagram protocol that does not provide any form of congestion avoidance or control, does not guarantee data delivery and is typically used for real-time applications that can tolerate data loss, but not delay (e.g. audio conferencing/internet telephony).

Both protocols have their advantages and limitations. The limitations are somewhat exacerbated on networks that have high bandwidths and long round trip times (which is typical for e-VLBI). In particular, TCP throughput can suffer significantly under these circumstances. UDP on the other hand is not really useful for sustained high bandwidth data flows across shared, wide area networks as it does not provide any sort of reliability mechanism.

A number of enhancements to this layer have been proposed. These include application layer transport protocols such as the Simple Available Bandwidth Utilization Library (SABUL – which is also known as the User Datagram Transport (UDT) protocol) [3], Tsunami [1] and Reliable

Blast UDP (RBUDP) [2]. These all transport data using UDP channels that have an extra layer of reliability and congestion avoidance and control added. Many enhancements to the traditional TCP stack have been proposed: Low et al.'s Fast AQM TCP [4], Floyd's High Speed TCP (HSTCP) [6], Kelly's Scalable TCP (STCP) and Kitabi's XCP [7]. These are all implemented at the kernel layer inside the operating system.

2. e-VLBI Experiments to Date

The material in this paper is based on practical experience obtained from the co-ordination and running of many e-VLBI experiments. In this section, we provide a brief summary of the experiments in which MIT Haystack Observatory has participated.

In October, 2002 a sustained disc-to-disc transfer of 788 Mbps was achieved between Mark 5s at the NASA Goddard Geophysical and Astronomical Observatory in Maryland and the correlator at Haystack Observatory in Westford, Massachusetts. Data was simultaneously transferred from the Westford telescope to the correlator [8]. This is the highest rate e-VLBI experiment to date.

Since that time, there have been many experiments between the US and Japan in support of geodetic experiments. In June of 2003 an entire Intensive experiment was transferred from the Communications Research Laboratory (CRL) antenna in Kashima, Japan to Haystack. The data was recorded using the K5 format and then converted to the Mark 5 format for correlation on the Mark IV correlator at Haystack. The entire 40 GB dataset was transferred in 51 minutes, with the first correlation results available in under an hour. The average transfer rate was 107 Mbps. At the same time, data from the Westford antenna was transferred to Japan, where it was converted to K5 format and correlated using the CRL software correlator. An estimate of the UT1-UTC offset was obtained in under 24 hours. This was the first time this had been achieved.

Since that time, several e-VLBI transfers have been performed between Japan and the US as part of the International VLBI Service's (IVS) "T-" series and "CRF-" series experiments. In particular, e-VLBI has been used to transport some of the data for the following experiments: CRF22, CRF23, T2023, T2024 and T2026. This series of experiments has been quite important in paving the way for the "operationalization" of e-VLBI data transfers. Special software and procedures have been developed to support these types of experiments.

In addition to e-VLBI experiments, network protocol testing has been performed to determine the efficacy of various protocols for the transfer of e-VLBI data. At an International e-VLBI demonstration at the Internet2 Fall Member's Meeting in October 2003 data rates of 644 Mbps and 400 Mbps between the US and Japan were obtained using FAST TCP [4] and HSTCP [6] respectively. Since that time, rates in excess of 900 Mbps have been achieved on slightly lossy links using high speed protocols such as Tsunami [1] and UDT [3].

These experiments have provided invaluable experience in how to efficiently transport e-VLBI data across national and international wide area high speed research networks.

3. e-VLBI Data Transport Issues

TCP is used for the majority of Internet data transfers. It includes a congestion control mechanism that ensures that users competing for network resources share those resources in a manner that is in some sense fair, without driving the network into congestion collapse. TCP is used by applications such as ftp, scp and the world wide web to create data connections and reliably transport data across the network. The fundamental algorithms underlying TCP were designed roughly 20 years ago by Van Jacobson. At this time, the bandwidth and size of networks was much less than today. In current high speed networks, bandwidths of 10 Gbps are not uncommon in the network backbone, with round trip times ranging up to 100s of milliseconds. In this environment, TCP throughput can be severely impacted by packet loss. The famous Mathis equation [5] relates a TCP connection's bandwidth (BW) to its mean segment size (MSS $\equiv$ packet size), round trip time (RTT) and the packet loss probability (p):

$$BW = \frac{MSS}{RTT}\sqrt{\frac{C}{p}} \tag{1}$$

Where C is a constant that is commonly chosen as 1.5 and BW is in bytes/second.

To gain insight into how sensitive TCP throughput is to packet loss at high speed, consider a concrete example (often used by Sally Floyd): a TCP connection with MSS=1500 bytes, RTT=100 ms and a desired BW of 10 Gbps. This requires a packet loss rate of at most one drop in every 5,000,000,000 packets. This is at most one drop every 1.67 hours and is simply not realistic in present day shared networks.

UDP is a light-weight packet protocol that does not have any congestion control implemented. It was originally intended to support real-time protocols that were loss-insensitive, but delay sensitive. UDP does not react to packet loss, but will allow an application to transmit data as fast as it wants, without regard for the amount of available bandwidth in the network, nor the UDP packet loss rate. UDP can provide high throughput, but is unreliable. Sustained high rate UDP flows can also impact other network users, and/or look like Denial of Service attacks to network administrators. This can result in a UDP flow being shut down as a results of a user complaint or network administrator concern.

The two traditional transport protocols, TCP and UDP, both have limitations when it comes to the transport of sustained, high bandwidth data flows across shared, high speed networks. In the next section, we will look at some alternatives that can be used in place of these protocols to achieve enhanced data throughput.

4. e-VLBI Data Transport Alternatives

There are basically two different approaches to enhancing the throughput of data transmission across high speed wide area networks:

- **Application Layer Protocols**: such as Tsunami and SABUL/UDT. These are implemented as user space applications that implement rate-based flow control and reliability on top of a UDP layer. These are easy to deploy and use but may be overly aggressive.
- **Enhancements to TCP**: such as FAST and HSTCP. These are implemented in kernel space and are high performance enhancements to TCP. Typically, they require a special kernel or kernel patch to be applied. They are slightly more complicated to install and use, but are a much better alternative in the long term. The major advantage they have is that once the kernel is in place, no adjustments are required to the application software.

In this paper, we investigate the performance of Tsunami and SABUL/UDT.

Tsunami is a rate-based ftp-like application. It uses two connections: a TCP connection for the transfer of control information between the client and server and a UDP connection for the transfer of data. The rate at which data is transmitted into the network is controlled by varying the inter-packet delay. This value is varied according to an algorithm that monitors the packet loss rate and adjusts the transmission rate based on this.

UDT (formerly SABUL) also uses rate-based flow control. However, UDT is a C++ library rather than an application. UDT uses just one UDP connection (as opposed to Tsunami's two connections). Both control and data are transported over the UDT connection. In a similar fashion to Tsunami, the rate at which data is transmitted into the network is controlled by varying the inter-packet delay according to the packet loss rate.

Several tests were done using Tsunami and UDT between a performance node in Tokyo[1] (that was connected at 1 Gbps to the Asia Pacific Advanced Network (APAN) backbone) and a performance server at MIT Haystack Observatory. The bottleneck link capacity was 1 Gbps (the access rate at each end), with a round trip time of $\sim$ 170 ms. At the time these results were taken, TCP performance between these two nodes was quite poor, averaging much less than 100 Mbps. This was due to intermittent packet loss on the end to end path. The results are presented in the following section.

5. Test Results

Figure 1(a) shows the throughput versus offered load for the Tsunami protocol. The dotted line represents the memory to memory throughput from Japan to the USA. Throughput increases linearly with offered load until $\sim$ 800 Mbps at which time the overall system throughput falls off. This could be due to either network or host processing/throughput limitations. The dashed line represents the disc-to-disc performance with a high speed server at the receiver end (dual Intel Xeon 2.4 Ghz with fast SCSI discs and RAID5). In this case the throughput plateaus at $\sim$ 370 Mbps. This is equal to the disc read throughput limitation on the sender side. The solid line represents the disc-to-disc throughput, where the receiving node is a slower machine (1 GHz Pentium III, with SCSI discs, but without RAID). In this case, the overall system throughput peaks at $\sim$ 280 Mbps and then plateaus at a much lower value of $\sim$ 180 Mbps. This is due to losses at the receiver (for these systems the disc read rate at the sender was higher than the disc write rate at the receiver. Thus the receiver was not able to keep up with the traffic stream from the receiver above 280 Mbps, it's internal buffers filled up and then discarded traffic resulting in an overall decrease in system throughput.

Figure 1(b) shows the throughput for a number of separate UDT trials. The solid line represents memory to memory tests from Japan to the US. Average throughput across the 5 trials was 545 Mbps, with a maximum throughput of $\sim$ 650 Mbps and a minimum of $\sim$ 300 Mbps. The dashed line represents disc-to-disc throughput from Japan to the US. The average throughput across these trials was 356 Mbps. In this case, the disc I/O throughput is the system bottleneck.

6. Conclusions

Modern research and education networks have backbone bandwidths of up to 10 Gbps. At these speeds, traditional transport options (TCP/UDP) do not perform/behave well. Many enhancements have been proposed to TCP, in particular, to improve its performance in high speed

[1] This server was kindly made available by Communications Research Laboratory

networks, however, they are not yet widely deployed. In the interim, advanced application layer transport protocols offer an alternative, easily deployable and effective solution.

In this paper, we have discussed some of these protocols and looked at the results of some tests using these protocols. Some of these protocols are still experimental, so they should be used/deployed only after extensive reliability and fairness testing. However, they do provide a relatively easy and efficient way in which to improve data transport rates across high speed, long round trip time networks.

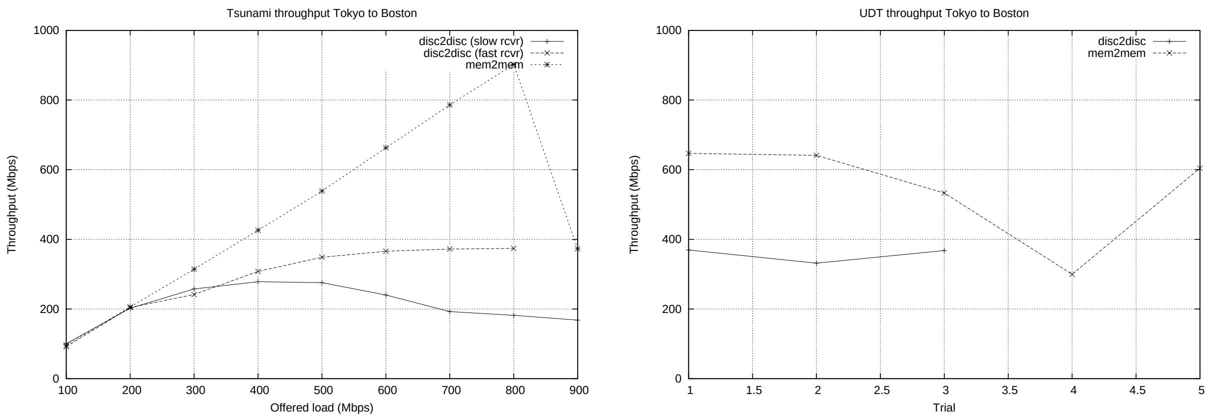

(a) Tsunami Throughput (b) UDT Throughput

Figure 1. Test results

References

[1] Meiss, M., S. Wallace, "Tsunami", Available from http://www.indiana.edu/~anml/anmlresearch.html.

[2] He, E., J. Leigh, O. Yu, T. A. DeFanti, "Reliable Blast UDP : Predictable High Performance Bulk Data Transfer", IEEE Cluster Computing 2002, Chicago, Illinois, Sept, 2002.

[3] "DataSpace", http://sourceforge.net/projects/dataspace/

[4] Jin, C., D. Wei, S. H. Low, G. Buhrmaster, J. Bunn, D. H. Choe, R. L. A. Cottrell, J. C. Doyle, W. Feng, O. Martin, H. Newman, F. Paganini, S. Ravot, S. Singh, "FAST TCP: From Theory to Experiments". submitted for publication, April 1, 2003

[5] Mathis, M., J. Semke, J. Mahdavi, T. Ott, "The Macroscopic Behavior of the TCP Congestion Avoidance Algorithm", Computer Communication Review, volume 27, number3, July 1997.

[6] Floyd, S., "HighSpeed TCP for Large Congestion Windows", RFC3649, Experimental, December 2003.

[7] Kelly, T., "Scalable TCP: Improving Performance in Highspeed Wide Area Networks", Submitted for publication, December 2002.

[8] Whitney, A., et. al, "The Gbps e-VLBI Demonstration Project", February 2003. Available at ftp://web.haystack.edu/pub/e−vlbi/demo_report.pdf

Yasuhiro Koyama et al.: Geodetic VLBI Experiments with the K5 System, IVS 2004 General Meeting Proceedings, p.220–224
http://ivscc.gsfc.nasa.gov/publications/gm2004/koyama2

Geodetic VLBI Experiments with the K5 System

Yasuhiro Koyama [1], Tetsuro Kondo [1], Hiro Osaki [1], Masaki Hirabaru [2], Kazuhiro Takashima [3], Kazuo Sorai [4], Hiroshi Takaba [5], Kenta Fujisawa [6], David Lapsley [7], Kevin Dudevoir [7], Alan Whitney [7]

1) *Kashima Space Research Center, Communications Research Laboratory*

2) *Communications Research Laboratory*

3) *Geographical Survey Institute*

4) *Hokkaido University*

5) *Gifu University*

6) *Yamaguchi University*

7) *Haystack Observatory, Massachusetts Institute of Technology*

Contact author: Yasuhiro Koyama, e-mail: koyama@crl.go.jp

Abstract

At Kashima Space Research Center of Communications Research Laboratory, developments of the K5 VLBI system have been continuing based on conventional PC systems to realize e-VLBI observations and data processing over the Internet. By using the prototype models of the K5 system, various geodetic VLBI experiments have been performed and the results were evaluated to investigate the performance and the function of the K5 system. In the two domestic geodetic VLBI experiments, the results from the K5 system were compared with the results from the K4 system and it was confirmed that the K5 system is performing as expected. A series of short e-VLBI sessions was performed by using the Mark 5 system at Westford station and the K5 system at Kashima station to demonstrate rapid turn around UT1-UTC estimation from international e-VLBI. Since October 2003, all IVS sessions in which Kashima 34-m station participated were recorded by the VLBA recorder as well as by the K5 system in parallel, and the K5 data files were transferred to MIT Haystack Observatory after converting the format of K5 data files to the Mark 5 data format. The data were then recorded to Mark 5 disk units for correlation processing. These procedures will become first and important steps towards the routine e-VLBI operations in the IVS sessions in the future.

1. Introduction

After the prototype models of the K5 system were developed, the K5 system is beginning to be used for various VLBI observations such as the precise orbit determination of the spacecrafts Nozomi and Geotail [1] and the demonstration of international e-VLBI observations [2]. Therefore, it is very important to ensure that there is no problem with the performance of the K5 system by comparing the results from the K5 system with the results from the conventional VLBI systems such as the K4 system. For this purpose, two domestic geodetic VLBI sessions were carried out to evaluate the performance and functions of the K5 system. The compared results from these two VLBI sessions will be presented in this report. Then, the recent activities of using K5 system in the international geodetic VLBI sessions will also be introduced.

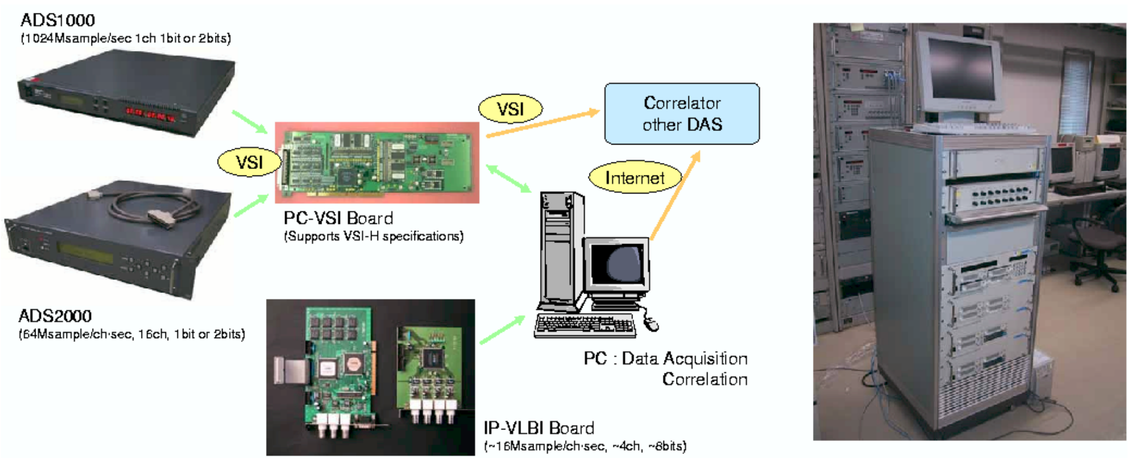

Figure 1. Concept of the entire K5 system (left) and the picture of the prototype model (right).

2. K5 System

The K5 system is designed to perform real-time and near-real-time VLBI observations and correlation processing using Internet Protocol over commonly used shared network lines. Various components are being developed to realize the target goal in various sampling modes and speeds. The entire system will cover various combination of sampling rates, number of channels, and number of sampling bits by selecting subset of the available systems shown in Figure 1. The K5 system is characterized by the use of conventional PC systems and the IP based shared network such as Internet. The data correlation can be performed by hardware correlators which support VSI-H specifications as well as by using the software correlator programs. In a similar fashion, the K4 system is characterized by the use of magnetic cassette tape recorders with rotary-heads and the dedicated network based on ATM (Asynchronous Transfer Mode).

For observations with relatively low data sampling rates, the output signal of the base-band converters are sampled with the IP-VLBI board and the sampled data are directly processed with the PC system to which the IP-VLBI board is installed. All the conventional geodetic VLBI modes of total data rate up to 512 Mbps with 16 channels can be covered. The prototype model of the K5 system (also shown in Figure 1, which is called Versatile Scientific Sampling Processor (VSSP), is a realization of the K5 system's concept by using this configuration. It consists of four UNIX PC systems. Each UNIX PC system has one IP-VLBI board. Because the IP-VLBI board supports various sampling modes, it has many possibilities to be used not only for VLBI observations but also for various other scientific researches which require precise timing information in the data. A signal distributor unit for 1 PPS and 10 MHz signals and 16-channel base-band signal variable amplifier unit are mounted in the upper part of the rack. The monitor and the keyboard on the top of the rack are connected to the four PC systems by using a four-way switch. Each PC system is equipped with four removable hard disk drives of the data capacity of 120 GBytes each. The sampled data can be transferred to the network by using TCP/IP or can be recorded to internal hard disks as ordinary data files. The maximum recording speed of 512 Mbps has been achieved with the current configuration.

To process the data sampled with the K5 system, software correlation programs are also under development. The software correlation programs receive data from K5 systems over the Internet and then calculate cross correlation functions. It can also read data files on internal hard disks after transferring the data. These capabilities allow us to transfer observed data in real-time if the connecting network is fast enough, and in near real-time if data buffering is required. Since easily re-writable software programs and general PC systems are used, the processing capacity and the function of the correlator can be easily expanded and upgraded.

3. Evaluation of K5 System in Geodetic VLBI Experiments

Two geodetic VLBI sessions were performed with domestic baselines in Japan by using K5 and K4 systems to evaluate the performance and functions of the K5 system. The first session was performed using two 11-m antennas at Kashima and Koganei from January 31 to February 1, 2003. The second session was performed using the opportunity of a domestic regular geodetic VLBI session coordinated by Geographical Survey Institute (GSI). The session, which is called JD0306, was performed for 24 hours from July 16, 2003. As a regular domestic experiment, four VLBI stations operated by GSI at Tsukuba (32-m), Shintotsukawa (3.8-m), Chichijima (10-m), and Aira (10-m) participated with the K4 systems. At Tsukuba station, K5 system was used in addition to the K4 system. By using the same observing schedule, Kashima (11-m), Tomakomai (11-m), and Gifu (11-m) stations participated in the session by using both K5 and K4 systems. In addition, Yamaguchi (32-m) station participated in the session by using K5 system only in X-band.

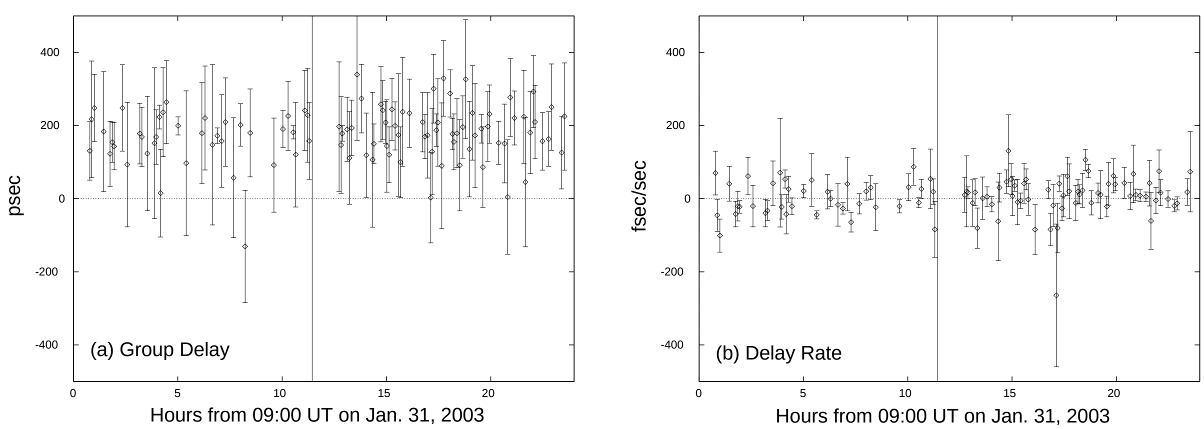

Figure 2. Difference of (a) group delay and (b) delay rate obtained from K4 and K5 systems.

In both sessions, the data files recorded with the K5 system were processed by the software correlation programs and the K4 observation tapes were processed by using the K4 hardware correlator at Kashima and Tsukuba. Both data were then analyzed by CALC and SOLVE softwares developed by Goddard Space Flight Center of National Aeronautics and Space Administration. Figure 2 shows the difference of group delay and delay rate determined by K5 and K4 systems. The constant offset seen in the group delay comparison can be absorbed as a part of the clock difference estimated through the data analysis processing and therefore it does not cause any problem in the data analysis. The RMS of the difference is calculated as 72.7 psec for group delay and 118 fsec/sec for delay rate. Table 1 compares the baseline lengths estimated from the data obtained with K5 and K4 systems. Since the K5 system at Kashima and Gifu stations stopped

Table 1. Comparison of baseline lengths estimated from the data obtained with K4 and K5 systems.

Exp.	Baseline	System	No. of valid data	Baseline Length (mm)	RMS Residual Delay (psec)	Rate (fsec/sec)
1	Kashima-Koganei	K4	112	109099657.0 ± 6.7	76	136
		K5	159	109099641.2 ± 3.2	33	92
2	Tsukuba-Kashima	K4	176	53811894.9 ± 2.1	53	158
		K5	130	53811891.6 ± 3.1	81	121
	Tsukuba-Gifu	K4	184	311067474.0 ± 2.9	98	189
		K5	55	311067483.3 ± 4.0	58	136
	Tsukuba-Tomakomai	K4	124	740526116.3 ± 4.4	103	165
		K5	169	740526119.4 ± 5.1	103	146
	Kashima-Gifu	K4	174	358799168.6 ± 2.8	72	191
		K5	48	358799174.7 ± 4.5	92	144
	Kashima-Tomakomai	K4	171	749810979.9 ± 4.4	115	125
		K5	108	749810985.5 ± 5.5	106	143
	Gifu-Tomakomai	K4	154	902668931.2 ± 4.8	135	125
		K5	49	902668930.6 ± 6.1	116	138

recording for about six hours and 12 hours respectively during the observations, and the number of valid data for Tsukuba-Kashima and Tsukuba-Gifu baselines are fewer than the data from the K4 system. From these comparisons, it can be concluded that the estimated baseline lengths are consistent with each other within 2 times the estimated uncertainties. In addition, the comparison of the RMS residuals of group delay and delay rate suggests the performance of the K5 system is comparable with the K4 system.

4. International Geodetic VLBI Experiments

In 2003, a series of test e-VLBI sessions were performed with the Kashima-Westford baseline. The 34-m antenna VLBI station at Kashima and the 18-m antenna station at Westford were used for the observations. At the Kashima station, the K5 system was used to record the observed data. At the Westford station, the Mark 5 system developed by Haystack Observatory was used to record the observed data. The observed data were recorded to internal hard disks at each site and transferred to Kashima and Haystack Observatory after the observations by using FTP. For this purpose, a software program was used to extract the data from the Mark 5. At Haystack Observatory, file format of the K5 data files was converted and recorded to the Mark 5 system. After the conversion, data recorded at Kashima and at Westford were processed for cross correlation processing using the Mark IV correlator at Haystack Observatory. At Kashima, the Mark 5 data files were converted to K5 file format and then correlation processing was done by using the software correlation programs. The observations were performed with 14 channels (8 for X-band and 6 for S-band) and 2 MHz for each channel.

After the data processing, CALC and SOLVE software were used to perform data analysis. In the estimation process, positions of both Kashima and Westford stations were fixed to the ITRF2000 reference frame and UT1-UTC was estimated along with the clock offset, its rate, and the atmospheric zenith delay. From the 2-hour session performed on March 25, 2003, UT1-UTC was estimated with uncertainty of 23.9 microseconds, which is comparable to the results from intensive sessions. From the 2-hour session performed on June 27, 2003, the UT1-UTC was estimated within 21 hours and 20 minutes after the last observation in the session finished. For this session, file transfer speed reached 107 Mbps in the direction from Kashima to Haystack Observatory. The opposite direction was not as fast, but the speed was about 45 Mbps. Thus the rapid estimation of the EOP in less than one day was successfully demonstrated by the international e-VLBI observations and data analysis.

Since October 2003, four IVS VLBI sessions were performed including the Kashima 34-m antenna station. The K5 system was used to record observed data along with the VLBA data recorder. The data recorded with the K5 system were transferred to Haystack Observatory using the high speed research network. The K5 data files were converted to the Mark 5 file format either at Kashima before the file transfer or at Haystack Observatory after the file transfer. Then the data were recorded to the Mark 5 disk units and shipped to correlator sites. These are the first but important trials to introduce e-VLBI in the routine sessions coordinated by IVS.

5. Conclusions

The results from two geodetic VLBI experiments between K4 and K5 VLBI systems were compared to ensure that the K5 VLBI system has expected capability and performance similar or better than the K4 VLBI system. The results from two different systems are consistent with each other considering the estimated error. From these comparisons, it can be concluded that there is no problem in using the K5 VLBI system for precise VLBI observations. By using K5 system at Kashima station and Mark 5 system at Westford station, fast turn around UT1-UTC estimation from e-VLBI within a day has been successfully demonstrated. We expect we can further shorten the turn-around time by upgrading the network and using distributed software correlator system. Since October 2004, all IVS sessions in which Kashima 34-m station participated were recorded by the K5 system and we are planning to extend the e-VLBI operation to other IVS observing stations.

6. Acknowledgements

The authors would like to express sincere appreciation to many members of Geographical Survey Institute, Hokkaido University, Gifu University, Yamaguchi University, Communications Research Laboratory, Haystack Observatory, and other participating institutes of the Abilene, Super-SINET and TransPAC networks who supported VLBI sessions described in this report.

References

[1] Kondo, T., Y. Koyama, R. Ichikawa, M. Sekido, and H. Osaki, Quasi Real-time Positioning of Spacecrafts Using the Internet VLBI System, Proceedings of the IAG G02 Symposium in the 23rd. IUGG General Assembly, Sapporo Japan, July 2003 (*in printing*).

[2] Koyama, Y., T. Kondo, H. Osaki, A. Whitney, and K. Dudevoir, Rapid turn around EOP measurements by VLBI over the Internet, Proceedings of the IAG G02 Symposium in the 23rd. IUGG General Assembly, Sapporo Japan, July 2003 (*in printing*).

Gino Tuccari et al.: A Near Real Time e-Radar/VLBI Network, IVS 2004 General Meeting Proceedings, p.225–228
http://ivscc.gsfc.nasa.gov/publications/gm2004/tuccari1

A Near Real Time e-Radar/VLBI Network

Gino Tuccari [1], Igor Molotov [2], Salvatore Buttaccio [1], Gaetano Nicotra [1], Alexander Dementiev [3], Alexander Konovalenko [4], Alexis Zinoviev [5], Yuri Gorshenkov [6], Xiang Liu [7], Xiaou Hong [8], Alexander Volvach [9]

[1] *INAF-IRA, Italian National Astrophysical Institute-RadioAstronomy Institute*
[2] *RAS, Bear Lakes Radio Astronomy Station, Central Astronomical Observatory at Pulkovo*
[3] *Radiophysical Research Institute*
[4] *Institute of Radio Astronomy*
[5] *Astro Space Center of P.N. Lebedev Physical Institute*
[6] *Special Research Bureau of Moscow Power Engineering Institute*
[7] *Urumqi Astronomical Observatory*
[8] *Shanghai Astronomical Observatory*
[9] *Radio Astronomy Laboratory of CAO*

Contact author: Gino Tuccari, e-mail: g.tuccari@ira.cnr.it

Abstract

A narrow band e-VLBI system is in development as a part of the LFVN (Low Frequency VLBI Network) activity taking advantages of the relatively small portion of band necessary in a certain class of radioastronomy observations.

Data are acquired using a simple dedicate terminal and recorded on disk. The maximum recorded signal band is 48 MHz wide, flexibly scalable up to few kilohertz and then with the concrete possibility to transfer the full amount or portion of it in near real time to a correlation point, using the standard Internet connection, when narrow band acquisitions are appropriate. Radar, spectral lines, low frequency, spacecraft navigation observations could benefit from this inexpensive solution in those stations where large antennas and sensitive receivers are available, and where is still missing the possibility to be supplied with standard VLBI terminals, giving then yet the possibility to perform radio astronomy research. The terminal is at present placed in Noto (Italy), Bear Lakes (Russia), Urumqi (China) and a few other stations, Simeiz (Crimea), Seshan (China), Evpatoria (Ukraine), will get a terminal in the first months of 2004.

A mixed software/dsp correlator is also in development in Noto, based on a shared computing strategy, allowing to improve auto- and cross-correlation performance adding a number of PCs equipped with a dedicated DSP board to improve the correlation capability. During the VLBR03.1 radar session in July 2003, the VLBI data from Noto and Bear Lakes were successfully translated to Noto and processed for detecting the spectrum of the echo signals. This work was supported by INTAS 01-0669, INTAS IA-01-02, RFBR 02-02-17568 and RFBR-02-02-39023 grants.

1. NRTV Acquisition Terminal

The Near Real Time VLBI terminal is a system conceived to get a portion of data coming from a receiver and translate such information through the network in order to have it available for further processing, being auto or cross-correlation. Mainly the system has been thought of for stations having no VLBI equipment at all, so that the first section, as optional, is planned with a digital base-band converter able to process the receiver IF in a way that further acquisition and recording is possible.

The maximum bandwidth is 48 MHz wide, so limited for meeting the actual capability of the internet connection. Indeed main criteria in the development have been to get an inexpensive system with the possibility to transfer data through the standard network. For narrow band the transfer could be almost real time, while for wider bands the data transfer can be realized during the observations intervals and afterwards, saving anyway the long time and cost needed to transfer real disks. Of course this last solution is still possible in case of very bad connection, that anyway is going to be improved everywhere in the radiotelescope sites worldwide.

Figure 1. The entire acquisition terminal is shown: from the left side, an external Firewire/USB2 disk, NRTV Box, a commercial PCI board.

The IF band to be recorded is down-converted using a standard or custom analog base-band converter as available in the radiotelescope. Such down conversion could be possible using a fully digital converter in development and kept available for those stations having no interferometric base-band converter at all. In such case the IF band of interest has to be shifted in the region 80-128 MHz, or 128-166 MHz, and the portion of band to be acquired is then translated to base band (0-48 MHz). Such bandwidth can be decreased so to get: 32-16-8-4-2-1-0.5-0.25-0.125 MHz. The narrower the band the less time needed to transfer data through the network, so the real useful band has to chosen considering the type of observation. For example in case of Radar-VLBI experiments, the Doppler shifted echo carrier reflected by the target body is to be detected, so that a narrow band is particularly efficient. Spectral line emissions observations similarly to the radar ones can benefit by the narrow band selection. In case of continuous emission the wider the band the better the sensitivity, so data transfer takes a longer time due to the network bottleneck.

Baseband converted bands, both in the analog or in the digital domain are then fed into the NRTV Box, where they are assembled in a very simple format with 1 or 2 bit representation, and then sent to a PC ATA disk where they are stored. Access to the recorded data can immediately

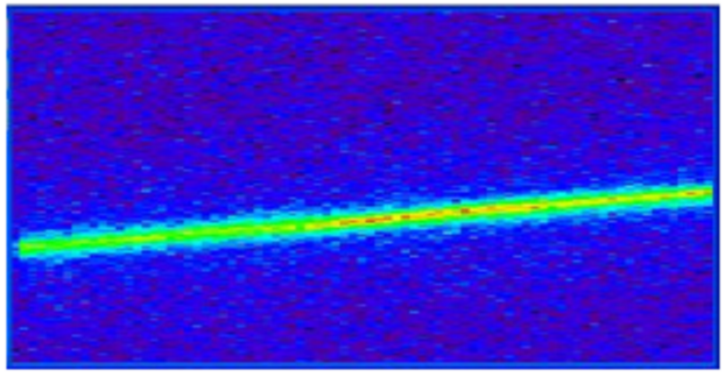

Figure 2. The spectra in time show the echo of the radar signal transmitted by Evpatoria, reflected by Mars, received in Noto. Frequency carrier was 5010.024 MHz, receiving LO was 5010.000 MHz. Vertical axis 238037,11-262329,11 Hz, horizontal axis day 207/208-time 2304-0025

be realized in order to transfer data after writing, in samples for data analysis, or in full for data processing. The control software supports data acquisition by means of manual, time triggered, custom scheduling, or Field System interface.

Data sent through the network are collected in a correlation point where a first analysis is done immediately after the observation. This is particularly useful to recognize possible problems in the receiving system or in case of Radar observations, for detecting transmitter failures in the pointing or emitted power. Autocorrelation is then performed with data coming from the different stations.

A software system is used to perform the correlation process, and this instrument is widely upgradable, being done with more PCs working in parallel in network. Time sharing is possible processing different slots of recorded time with different computers. This correlator is going to be increased as soon as more machines will be available in the cluster, during their down time.

The NRTV system is expected to be used in conjunction with other systems and correlators, in particular in that situations when a quick process is worth to be considered.

2. Low Frequency VLBI Network Project

The LFVN project was started in 1996, having the purpose to arrange the international VLBI cooperation with participation of former Soviet Union radio telescopes. During the project 18 VLBI experiments were carried out using various combinations of radio telescopes and correlators in Canada, China, Urumqi, England, India, Italy, Japan, Latvia, Poland, Russia, South Africa, Ukraine, and USA.

Main directions of LFVN activity are:

- Learning the VLBI radar method, combination of classic radar and VLBI: study of short-periodic variation of proper rotation for the Earth group planets, improving the orbits of asteroids crossing the Earth orbit, measuring the space debris population at geo-stationary and high-elliptic orbits;

- Developing new methods of the solar investigations: mapping the solar wind irregularities, measuring the spatially-temporary structure of solar spikes;
- Mastering the near-real time differential VLBI technique for determining the satellite and deep space mission coordinates;
- Traditional VLBI astronomic observations as AGN and OH-maser imaging and investigation of active stars and stellar coronae structures.

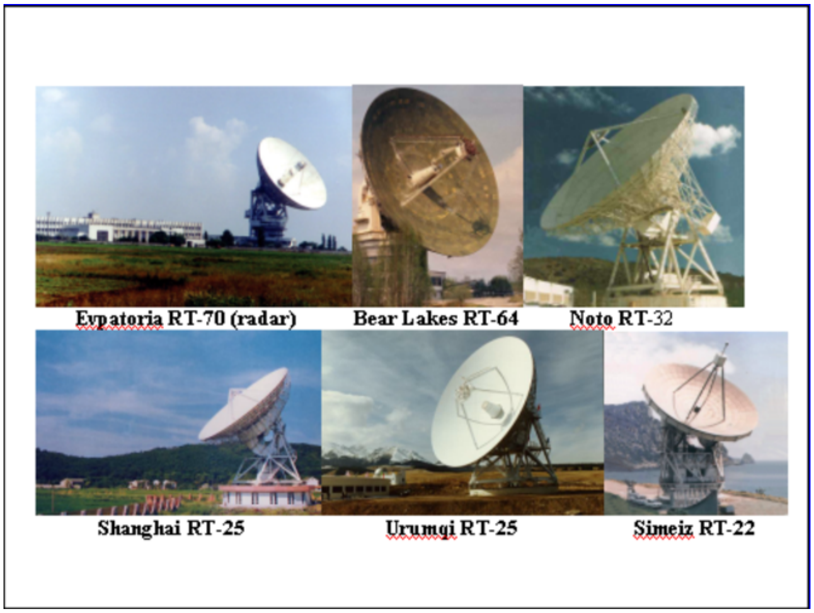

Figure 3. Some Radiotelescopes involved in the LFVN Project

3. Acknowledgements

This work was supported by INTAS 01-0669, INTAS IA-01-02, RFBR 02-02-17568 and RFBR-02-02-39023 grants.

References

[1] Molotov, I.E., Likhachev, S.F., et al. Low Frequency VLBI Project. IAU Publ. 199, 492-493, 2002a.

[2] Tuccari, G., Molotov, I., Buttaccio, S., et al. Radar VLBI activity with participation of Noto. Proceedings of the Sixth European VLBI Network Symposium. MPIfR, Bonn, pp. 45-47, 2002.

[3] Molotov, I.E., Konovalenko A. et al. Radar interferometer measurements of space debris using the Evpatoria RT-70 transmitter. Advances in Space Research. 2004 COSPAR. Published by Elsevier Ltd, in press.

Seog-Tae Han et al.: The Multi-Channel Millimeter Wave Receiver for VLBI, IVS 2004 General Meeting Proceedings, p.229–233
http://ivscc.gsfc.nasa.gov/publications/gm2004/han1

The Multi-Channel Millimeter Wave Receiver for VLBI

Seog-Tae Han, Do-Heung Je, Duk-Gyoo Roh, Sek-O Wi, Se-Jin Oh, Min-Gyu Song, Chang-Hoon Lee, Kwang-Dong Kim

KVN, Radio Astronomy Division, Korea Astronomy Observatory

Contact author: Seog-Tae Han, e-mail: sthan@trao.re.kr

Abstract

The most important thing in millimeter and sub-millimeter wave VLBI is how to calibrate the variations in the phase of an electromagnetic wave propagating through the troposphere. A lot of techniques for calibrating the phase fluctuations due to troposphere have been well proposed and demonstrated [1][2][3]. The millimeter wave multi-channel receivers system which can be used for phase calibration in millimeter and sub-millimeter wave VLBI observation are proposed. In this paper, a conceptual multi-channel receiver system and a quasi-optical filters which could be used in this receiver are described.

1. Introduction

In the past few decades centimeter VLBI observation has been extensively carried out in world wide radio astronomy observatories. However, recently it has been moving toward to millimeter wave and sub-millimeter waves VLBI observation.

The problems for the millimeter-wave and sub-millimeter waves VLBI observation could be categorized as 1) phase stability and noise of receiver system due to local oscillators, transmission lines and their components, 2) those of receiver noise temperatures are much higher than that of centimeter receivers, 3) atmospheric phase fluctuation due to a water vapor in troposphere which influences on the deterioration of the sensitivity and imaging capability. Both phase stability and receiver noise temperature of such millimeter and sub-millimeter receivers have been intensively well developed since last decade. It could be solved by advanced high technologies in such fields. However, the remain problem in millimeter and sub-millimeter wave VLBI is how to calibrate the variations in the phase of an electromagnetic wave propagating through the troposphere. A lot of techniques for calibrating the phase fluctuations due to troposphere, such as fast frequency switching, paired cluster antenna, rapid system temperature measurement, dual beam antennas and multi-frequency feed system have been well proposed and demonstrated [1][2][3].

In this paper, the multi-channel receivers system which can be used for phase calibration in millimeter and sub-millimeter wave VLBI are proposed.

2. Conceptual Configuration of Multi-Channel Receiver

The phase calibration by using the multi-channel receiver system is based on the phase contributions by a given amount of water vapor increasing linearly with frequency, that is, the troposphere is non-dispersive [3]. It was demonstrated that the tropospheric phase fluctuation in millimeter wave can be calibrated by centimeter wave observation results [2]. It clearly shows that not only phase calibration can be done by using the proposed multi-channel receiver system, but also validity of the non-dispersive model of the troposphere is well verified.

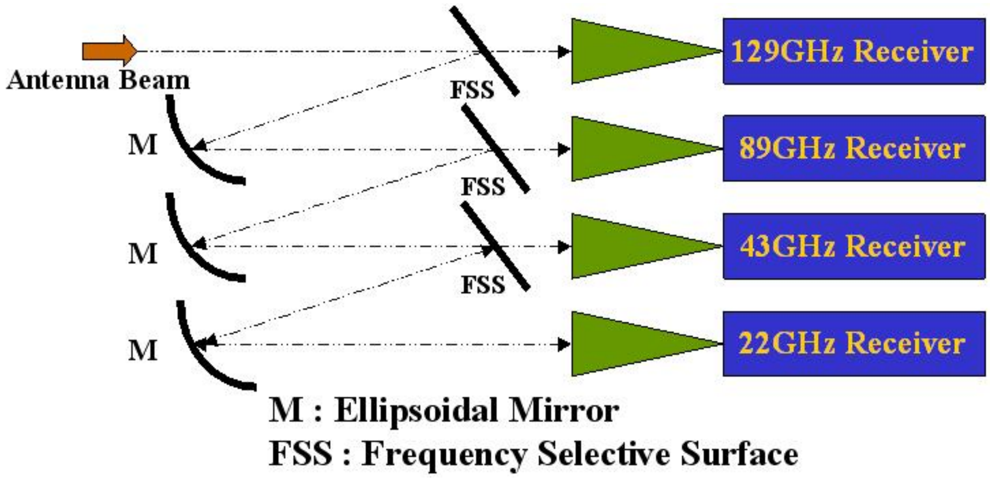

Figure 1. Multi-channel receiver system

The multi-channel receiver system is shown in figure 1. This system could employ a sequence of frequency-selective surface or perforated plate filter. The latter offer very good high-pass filter characteristics but are restricted to modest angles of incidence [4]. The bands of interest are 23 GHz, 43 GHz, 86 GHz and 129 GHz bands. The perforated plate filters are arranged so that 129 GHz band is encountered first by the beam coming from the antenna, and is transmitted to its feed horn. Lower frequency bands are reflected by first perforated plate filter and the beam transformed by ellipsoidal mirrors, sent to the 86 GHz band feed horn, and so on. Nevertheless the simultaneous observations for all bands by using this system can be done. Therefore 23 GHz band phase of source can be used for calibrating the phase of the same source of higher frequency bands observed at the same time.

The 129 GHz band interacts with the smallest number of optical components as shown in figure 1. It means that quasi-optical losses and antenna pointing errors could be minimized. The most important thing in this system is the properties of the perforated plate filter which have low transmission and reflection losses, low pass-band ripple, low cross polarization and wide pass bandwidth. Even 230 GHz band receiver and higher bands can be used in this system, if a good performance of perforated plate filter in these frequency bands could be made.

3. Quasi-Optical Filter for Multi-Channel Receiver

3.1. Perforated Filter as a High Pass Filter

The side view of perforated filter is shown in figure 2. A perfect conductor has several thousand array perforated holes with same given diameter. The number of holes is determined by the actual size of Gaussian beam at its location. The perfect conductor hole acts as a circular waveguide which has a high pass filter characteristic intrinsically. Therefore cut-off frequency of filter could be easily made by changing of diameter of perforated hole. As shown in figure 2, to make better performance of pass band ripple and losses, the impedance matching layer with dielectric material has been used both side of perfect conductor as well as holes filled with dielectric material.

Theoretical evaluation results by using CST [5] are shown in figure 3. A performance of filters

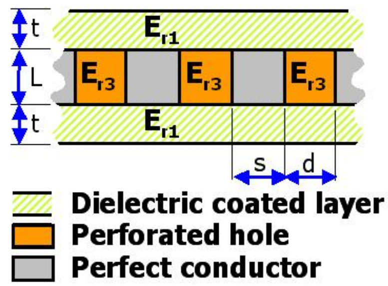

Figure 2. Perforated plate filter

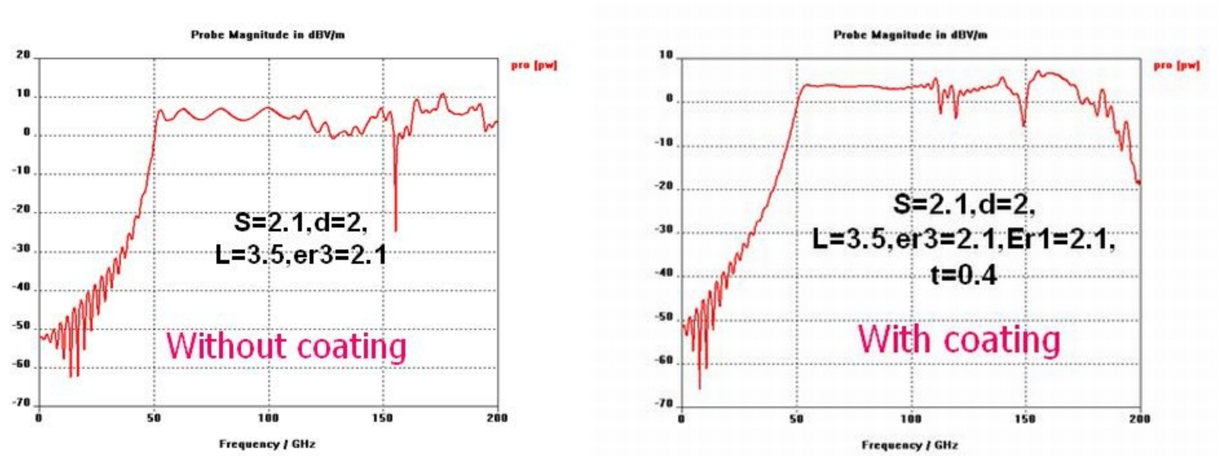

Figure 3. High pass filter characteristic, (a)without coating, (b)with coating

compared with coating layer with dielectric material and without coating layer is significantly different. It means that the filter should have such a impedance matching layer.

3.2. Metal Mesh Filter as a Low Pass Filter

The low pass filter with metal mesh grid which could be used on the multi-channel receiver and its performance are shown in figures 4 and 5, respectively. It has been developed by QMC & Thomas Keating, England. The cut-off frequency of low pass filter can be determined by changing a gird space and its diameter. The pass band ripple and rejection band as well as losses are good enough to be used in multi-channel receiver for quasi-optics.

4. Quasi-Optical System for Multi-Channel Receiver

The quasi-optical system for multi-channel receiver is shown in figure 6. All quasi-optical filters are located at Gaussian beam waist to minimize their sizes. The 22 GHz and 43 GHz band signals are transmitted, 86 GHz and 129 GHz band signals are reflected by the first low pass filter which is located at cassegrain focus. The reflected signals of 22 GHz and 43 GHz are re-collimated by an ellipsoidal mirror 3, then go to the low pass filter 2. Reflected signal of 43 GHz and transmitted

Figure 4. Low pass filter

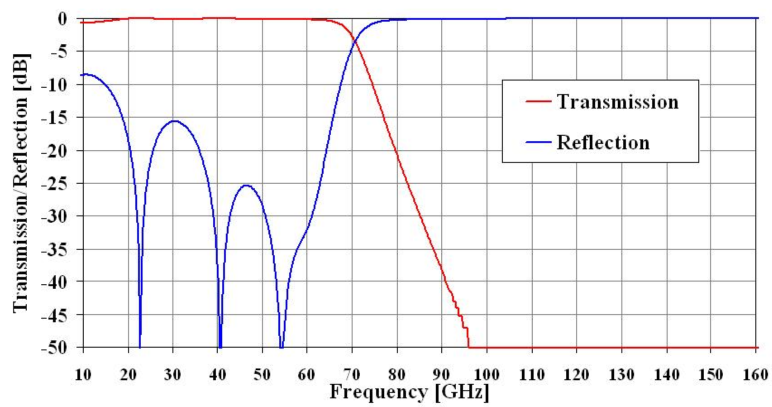

Figure 5. Low pass filter characteristic

signal of 22 GHz by the low pass filter 2 propagate through their own beam passages, and finally reach each feed horns. The 86 GHz and 129 GHz signals reflected by low pass filter 1 are re-collimated by ellipsoidal mirror 1, then go to their own feed horns through the low pass filter 3, respectively.

To minimize the losses at quasi-optical components, the beam selective system is chosen as shown in figure 6. For instance, we want to make observation 43 GHz and 86 GHz signals simultaneously, the beam selective system of LPF1 should be positioned at PPF, that of LPF2 is positioned at metal flat mirror, that of LPF3 should be positioned free space, respectively. All kinds of observational frequency channel modes can be done by combination of three set of the beam selective system.

5. Discussion

We expect that an insertion and a cross polarization losses at quasi-optics system would be absolutely dominated by quasi-optical filters and ellipsoidal mirrors. For better performance of

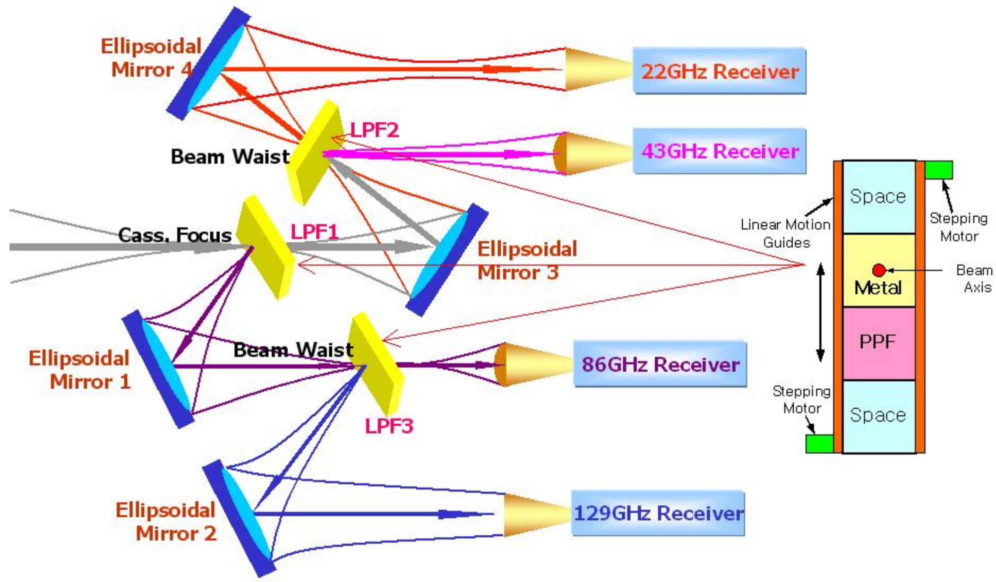

Figure 6. Quasi-optical circuit for multi-channel receiver

this system in term of losses, the further research of quasi-optical filter and mirrors should be required, and also be verified their properties by using special measurement system.

In addition, the pointing accuracy and aperture efficiency of antenna for each channel should be considered, because the proposed quasi-optical circuit is very complicated.

References

[1] Alef, W. et al., 2003, New Technologies in VLBI ASP conference series

[2] Asaki, Y. et al., 1998, Radio Science, 33, 1297

[3] Sasao, T., 2002, New Technologies in VLBI ASP conference series

[4] Goldsmith, P. F., 1998, Quasioptical systems, IEEE Press.

[5] CST Microwave Studio, http://www.cst-world.com

Gino Tuccari: DBBC - a Wide Band Digital Base Band Converter, IVS 2004 General Meeting Proceedings, p.234–237
http://ivscc.gsfc.nasa.gov/publications/gm2004/tuccari3

DBBC - a Wide Band Digital Base Band Converter

Gino Tuccari

INAF-IRA, Italian National Astrophysical Institute-RadioAstronomy Institute
e-mail: g.tuccari@ira.cnr.it

Abstract

It is presented a description of a project to develop a fully digital backend system to replace the presently used terminals. The need for such replacement is well known and motivated by the necessity to both renew an obsolete system whose components replacement is every day more difficult, and for achieving better performance making use of the more predictable digital techniques. Field Programmable Gate Array (FPGA) components show continuous increasing performance in terms of gate density and working frequency, giving a real opportunity to take advantages within a concept of fully upgrading methodology. Then, if what could now be developed to accomplish the transition between recording systems and the application of the VSI interfacing standard, is realized in the present, still the same hardware environment can serve different needs in the near future, with the data transport and correlator evolution. This development is producing some prototypes for testing the performance of different architectures taking into account theoretical achievable performance and the actual features. Two samples with preliminary configurations are placed in Noto and Effelsberg; development and testing are indeed performed in the field.

1. Introduction

The introduction of a new backend system in the VLBI system has been widely discussed during the last years, due to different reasons, some looking at the past, others to the future. Indeed the technologies used in the VLBI terminal now adopted, have been developed in the decades 70s and 80s of the past century, and so, now maintenance and performance are strongly affected by their obsolescence. More, data acquisition has been recently deeply upgraded with new disk based recording systems, greatly improving reliability and performance, while e-VLBI is becoming reality, as it can be seen in numerous experiments, proving and preparing the VLBI world to this huge leap.

Meanwhile 'Digital Radio' technologies are becoming familiar within new telecommunication developments, where frequency conversion is required, so that implies an effort is to be done for understanding if commercial technology is now ready for the VLBI needed performance, at a cost for which also a new generation of radio telescopes, now with a lack of VLBI terminals, could greatly get benefits.

All these considerations, as well as others related, imposed the need for such a development. A new backend hardware to be economically convenient, flexible, able to improve the performance, needs to be completely reviewed, trying to keep apart choices or solutions adopted in the past, mostly imposed by the limitations and necessities coming with the tape recording. Such critical reconsideration can greatly furnish benefits in terms of costs and performance.

A new class of commercially available devices is present on the market, fully programmable, giving the possibility to structure a system flexible to be adapted for different needs with different solutions. This aspect seems to be very promising for supporting also in a future evolutions in the correlators and in the data transfer methods.

2. Project Overview

The main idea behind this project is to replace the existing terminal with a complete and compact system to be used with any VSI compliant recorder or data transport. Moreover the cost has to be limited making use of commercially available components.

Hardware programmability is a feature in order to optimize the architecture to the needed performance, because different performance involve different number of gates necessary to perform the required functionality. Under this assumptions, maximum input and output data rates are the limitation and they have to be set so to satisfy the present and for reasonable future necessities.

The new development needs to be fully compatible with the existing terminals and correlators in order to require a minimum effort to be introduced in the stations and no modification at the correlator side, still maintaining the possibility to be upgraded for wider bands correlators. The upgrades, on the other hand have to be mostly software in order to avoid and modify any hardware part, for cost savings and simplification in the operations, so that programmable hardware is planned as main component.

The entire project is based on a flexible architecture, composed of one or more FPGA boards as computation elements, placed in a mixed cascaded/parallel structure, so to guarantee a parallel usage of data input and a shared parallel output data flow. For such a reason the upgrade could also in principle be possible in hardware replacing or adding compatible modules for different or modified performance, even if this is strongly limited by the software programmability.

In the DBBC project a single unit is composed of four IF input in the range 0-] 00 or 00-9 0 MHz, with each of them feeding a 1i0s, GHz sampler. Then four polarizations or bands are available for a single group of output channels selection. In other words, a group of . s or g, channels is able to handle a shared combination of channels coming from the four bands.

Multiple architecture can be used taking the advantage to adopt fully re-configurable FPGA Core Modules, where one of such modules is an autonomous board populated with an appropriate number of gates, fed by one of the input IF, and sharing the output data bus. More narrow or few wide channels per module can be assigned, maintaining the maximum number of gates provided by the Core Module. Modular realization for possible cascaded processing is provided, that implies the use of one or more Core Modules for achieving more gates number and then more processing capability. The input bus is cascaded, with very low skew, between modules for the same band.

An analog monitor, produced by DA conversion, has been added for testing purposes, in order to be able to evaluate with a common spectrum analyzer the different channels' content and performance. This has been proved particularly useful in order to adopt standard equipment normally in use in our radio-telescopes.

Field System support is required to configure the different modules and allow standard settings, and still getting total power measurements and any other information the converter is able to produce. A partial FPGA configuration approach is used so to optimize the configuration time.

Different configurations can be supported to obtain similar, but not identical, functionalities, such as SSB down converter, wide band parallel FIR, poly-phase FIR/FFT. The more flexibilities, the more number of gates and cost. The possibility to independently tune different channels, and to have them filtered at different bandwidth, while it is an obvious feature in the analog implementation, is not the same in the digital implementation, so that different solutions can be more convenient. The project anyway allows us to implement different architectures, and to change them at convenience.

A Core Module can handle a maximum input bandwidth of 10 Gbit/s and a maximum output bandwidth of , i09g Gbit/s. The two high rate buses are named HIS and HSO respectively, and a further Control/Configuration bus, HSCC, adopts PCI-X (or . GIO(1x) if available during the development time).

Different modules with different number of gates are supported for different functionalities and costs, making use of a standard board populated with a flexible number of chips. A module with s, Mgates can handle up to , independent narrow band LSB&USB channels (preliminary), or , wide band channels (ex. 1x 1s, sxs g, , D1s8 MHz) (preliminary).

3. Digital Down Converter Configuration

Different architectures can be used in the Core Modules, having different performance and behaviors. One possible configuration is the DDC digital down converter in the classical implementation meaning. In such a solution a direct conversion is typically performed between high data rate sampled IF band and lower data rate base band. One or two channels are generated for each converter, as in the analog implementation. Important differences, greatly improving the performance are anyway present: local oscillator is a Numerically Controlled Oscillator (NCO), mixer is complex as Look Up Table multiplier, low-pass band filters are Finite Impulse Response (FIR). Decimation circuitry is adopted because of the high ratio between IF and output data rate and is performed with multirate/multistage FIR.

Digital Total Power (DTP) measurement at IF and at base band level is adopted, Rescaling/Gain Control (RGC) is adopted for dynamic range control and final data representation.

Narrow bandwidth typically adopted is defined for this project in the range: 1g, 8, , , s, 1 MHz, having still possibility to filter with narrower bandwidth. Such solution directly affects the tuning step size. Still, the finer tuning capability, the more resource needed, with consequent number of gates involved and cost increasing.

Wide bandwidths are defined as 1s, s g, 1s8, g, , . s MHz and are generated at fixed tuning bases. So for example the 1s MHz band is in the range 0 - 1s, or 1s - 10s, MHz IF band; s g MHz band is defined as 0-s g/s g- 1s, or 1s-7g8/7g8-10s, MHz, and so on.

Output data rate is . s MHz at present in order to be able and fit with the standard, now adopted VSI-H data rate, but g, and 1s8 MHz are available. Data output configuration for wide bands is conceived in a multiplexing fashion.

4. Development Issues

The development will pass through two prototype levels, each of them characterized by testing with real observations. The first level includes two systems with an environment including A/D, FPGAs, D/A, etc., that have been assembled and named 'DbbcProt A', placed in IRA (Noto) and 'DbbcProt B' placed in MPI (Bonn, Effelsberg). Development and on field testing between units are linked together, including correlation phases, in order to keep under control effects on the real data.

A modified version of the EVN Mark IV formatter with digital input is used in the first phase of development, while afterwards a VSI interface will be used. At the end of the development period four functionally complete prototypes of second generation will be delivered to stations for a more complete testing. Such final prototypes will be able to include VSI-E interfacing capabilities, through an optional high speed network connection.

References

[1] Ferr 24 3 6 5tal F 5ter2 and F lterbank2 for VLBI3
Pre2ented at the Sympo2 um of the Internat onal VLBI Serv ce for Geode2y and A2trometry "New Technolo6 5e2 5n VLBI" 4held n Gyeon6-ju4Korea45-8 November 2002

[2 Tuccar 4G3 evelopment of a 6 5tal ba2e Band Converter (BBC): Ba2 c Element2 and 5n 5tary Re2u5t23 "New Techno5o6 e2 5n VLBI" 4A P Conference Ser e24Vol306 42003 ed3 Y3 C M nh (San Franc 2co: ASP) 4pp3177-192

Hans Hinteregger: Low-Cost Wideband Digital Back-Ends for LOFAR⇒e-VLBI⇒SKA , IVS 2004 General Meeting Proceedings, p.238–242
http://ivscc.gsfc.nasa.gov/publications/gm2004/hinteregger

Low-Cost Wideband Digital Back-Ends for LOFAR⇒e-VLBI⇒SKA

Hans Hinteregger

MIT, Haystack Observatory

e-mail: hhinteregger@haystack.mit.edu

Abstract

Virtually all next-generation radio astronomy applications could be economically served by a new wideband Digital Back-End (DBE) with a common block diagram, which consists basically of

1. High-speed analog-to-digital converters (A/Ds) sampling wide baseband (or higher-Nyquist-zone-filtered) analog input signals,
2. One or more stages of polyphase/FFT filter-bank, for the desired spectral resolution of output channels, and a
3. High-speed serial transceiver for selected data transport to storage and/or correlation processor.

Design of wideband DBEs is outlined, with examples of modern low-cost components: high speed A/Ds, field programmable gate arrays (FPGAs), and 0.1-10 Gb/s serial transceivers now available. For example, a dual input 512 Msample/sec DBE with 64-channel filter banks thought suitable for (e-)VLBI could be built for about $300.

1. Introduction

A paradigm shift to DBEs in radio astronomy is under way. Projects like Australia Telescope Compact Array (ATCA)[1] and Allen Telescope Array (ATA) in USA, are developing and beginning to test FPGA-based polyphase-FFT filter banks. DBEs promise greatly improved performance (aggregate bandwidth, spectral resolution, isolation, stability), essential flexibility for a wide range of experimental and operational requirements, and much lower replication, maintenance, and update costs, than traditional (now obsolescent and increasingly difficult to maintain) analog back ends. In this paper I stress feasibility of low-cost generic DBE building blocks. Study of low-cost feasibility was prompted by evident needs of both high performance and low cost in large arrays of (many thousands of) receiving elements, in particular, for LOFAR and SKA in the near and longer term respectively. This study also suggests that simple DBE building blocks should now be developed for timely, low-cost modernization of (e-)VLBI back-ends for service in the decade from 2005 to 2015. Suggested attributes of a DBE building block are:

1. **Low-cost** $500 max. (doesn't include NRE amortization)
2. **Wideband** Dual 256 MHz wide analog inputs, from 1^{st}, 2^{nd}, or 3^{rd} Nyquist zone filters, to be sampled at 512 MS/s.
3. **Digital** Polyphase-FFT filter banks (1 or 2 stages) after A/D, selection of output bands, requantization for transport, VSI-E over Ethernet formatting, etc.

[1] The influence of Dick Ferris of CSIRO ATNF on the author is gratefully acknowledged.

4. **Mini-module** 1-10 Gb/s out, "independent" parallel subsystem, 6-10 in^2, 6 W.

5. **Simple** KISS (keep it simple, stupid), or else!

To limit NRE and increase reliability it is important to minimize complexity.

For VLBI for example, I would suggest implementing only 16- or 64-channel single sideband (SSB) filter-banks for 32 16-MHz-wide or 128 4-MHz-wide outputs respectively. The former requires only half the FFT hardware resource or flow-through processing time per sample of the latter.

Also, not clearly necessary in DBE is an additional digital down converter (DDC), which is a digital quadrature mixer driven by a numerically controlled digital oscillator. The addition of a DDC could enable local Doppler compensation which may ease future distributed e-VLBI processing in PCs. If, after careful consideration, such a DDC is justified, a separate dedicated commercial DDC chip or custom FPGA version can be added.

It is important to keep DBE forward and backward compatible, as well as simple. Example 1, forward compatibility: Provide for multiple and wider IF bands and aggregate bandwidth scalability with parallel DBE mini-modules. Support wider IFs with 1^{st}, 2^{nd}, 3^{rd} Nyquist zone filters in front of parallel sampler A/Ds. Example 2, backward compatibility: Support VSI-H parallel I/O port as well as VSI-E over 1 or 10 gigabit Ethernet serial port.

2. DBE: 3 Parts, 2 Easy, 1 Hard

2.1. Part 1 (easy): Pair of Commercial-Off-The-Shelf (COTS) A/Ds

A leading candidate is MAX105, a dual 6-bit 800 MS/s-rated chip. Cost is $36.

Note, each A/D is preceded by an analog bandpass filter limiting the signal to the 1^{st}, 2^{nd}, or 3^{rd} Nyquist zone. These filters are not "formally" part of the DBE but could be physically mounted on-board. Cost is about $20 per filter in large quantities.

Table 1 lists some COTS A/Ds in order of increasing maximum sample rate along with resolution (bits/sample), cost, and power consumption parameters. MAX105 is by far the most affordable converter rated near GS/s. Its 6-bit resolution gives MAX105 an interference-to-signal ratio (ISR) of 27 dB [4], more than adequate for most radio astronomy applications, including even LOFAR in radio-quiet Western Australia. If needed, higher interference tolerance (6 dB per added effective bit of resolution), and better linearity (increase of spur free dynamic range, SFDR, from 50 to 70 dB, for example, with MAX1121) can be obtained, but at a much lower maximum sampling rate.

2.2. Part 3 (easy): Standard COTS Pluggable Transceiver, SFP or XFP

SFP (Small Form-factor Pluggable) transceivers are produced in high volume and available in many versions for:

1. Multimode fiber at 850 nm for 600 m short reach,

2. Cat5 copper for 100 m very short reach, and

3. Single-mode fiber for intermediate, long, and extended reaches from 10 to 120 km.

4. CWDM (coarse wavelength division multiplexed), for up to 16 wavelengths with 20 nm spacing from 1310 to 1610 nm have been available for 2 years.

5. DWDM (dense wavelength division multiplexed), for up to 44 wavelengths with 0.8 nm spacing, all within the C-band that can be amplified with erbium doped fiber amplifier (EDFA), have just been introduced by multiple vendors and now claim to be priced competitively with CWDM.

Plug-compatible SFP choices range from under $75 to over $750 in cost depending primarily on reach and CWDM or DWDM capability. Copper SFPs typically autonegotiate 10/100/1000 Mb/s Ethernet. Multi-rate fiber SFPs typically autotune from 0.155 to 2.7 Gb/s, OC-3 to OC-48 with forward error correction (FEC).

XFP (X=10 Gb/s small Form Pluggable, similar to SFP) transceivers are intended for 2.5 to 10.8 Gb/s operation. Non-WDM 1310 nm products for 10 and 40 km reach, costing $500 and $1500 respectively, have been introduced. Finisar demonstrated a C-band (15xx nm) DWDM XFP early in 2003. XFP is aimed at the next generation of high volume low-cost applications. The product line and its markets are expected to mature within 3 years, by which time 10 Gb/s XFP pricing should be comparable to today's 2.5 Gb/s SFP. XFP has a serial electronic interface called XFI which can be driven from a dedicated $100 Xilinx interface chip or directly from a Xilinx Virtex 2 Pro X series FPGA. This just introduced X series increases speed limit of dedicated high-speed serial ports from 3.2 to 10.8 Gb/s.

Note that candidate FPGA chips mentioned below, XC2VP20 (or VP20X), have 8 dedicated serial I/O ports which provide "glueless" physical-coding-sublayer (PCS) interfaces to SFP (or XFP) transceivers.

2.3. Part 2: FPGA(s) are Multi-Functional, NRE-Intensive, Hard Part of DBE

Replication cost of the FPGA part can be kept low enough if design adheres to KISS discipline. Adequate resources for design, technical review, detailed oversight, and rigorous testing must be provided. Proven efficient intellectual-property (ip) cores can be used where appropriate. Note, the author does not have the experience to here credibly estimate the cost of NRE including design tools and "learning curve".

2.4. Figure 1 Illustrates 3-Part and Miscellaneous DBE Cost Breakdown

Some plausible configuration options are shown. For example, 2 FPGAs could be used to support a dual 1024-point filter bank at 512 MS/s. The simplest option shown, with (a) dual A/D chip, (b) single $100 FPGA (qty. 50,000), and (c) short reach transceiver, should cost ~$250 in sufficiently high volume, and is thought to be suitable for (e-)VLBI.

3. Selection and Functions of FPGAs

3.1. Xilinx Virtex II Pro Strawman: Midsize XC2VP20-5, $100, Qty. 50,000 in 4Q04

This chip was chosen as conservative low-cost reference platform, thought to be big, versatile, and fast enough to accommodate at least the simplest envisioned combinations of primary and secondary DBE functions outlined below.

More complex DBEs with, for example, much larger, faster, or multi-stage filter banks, could be accommodated by adding one (or possibly more) identical (or at least identically packaged)

FPGAs to a mini-module PCB with layout that accepts at least 1 "extra" FPGA.

The resources of the VP20 include 20,880 logic cells, 88 dedicated 18-bit multipliers, 88 blocks of 18 Kb RAM, 8 serial "rocket I/Os", and 2 PowerPC CPUs.

3.2. Primary Function: Polyphase and FFT Filter-Banks [1,2]

A 64-point complex FFT can be computed in half real time, using a proven 64/256/1024-point Xilinx ip-core that uses 12 of 88 multipliers and one quarter of both the RAM and logic cell resources. If the chip is clocked at 128 MHz, 2 cores (<1/2 chip) could therefore keep up with complex or dual-real data sampled at 512 MS/s. A dedicated 16-point FFT would take less than half the 64-point resources.

The polyphase front-end of the filter bank – which is needed to improve adjacent output channel rejection from only 13 dB for FFT alone to > 50 dB for an appropriate effective 8-tap FIR in front of each FFT input – should not need more than 32 of the remaining 64 multipliers.

3.3. Secondary Functions

The remaining DBE functions of the FPGA are:

1. Dual 2-way demultiplexed LVDS A/D interface, input clocked at 256 MHz.
2. Selection of filter-bank output channels for transmission.
3. Requantization (compression to 1, 2, or 3 bits) of selected output channels.
4. VSI-H and VSI-E formatting of selected data for transmission.
5. Transceiver interface with or without gigE media-access-control (MAC).
6. Miscellaneous clock, time, monitor, control, and housekeeping.

Though detailed resource requirements for these functions have not yet been estimated, they should all fit, given some effort to make efficient use of remaining resources, the 2 embedded general purpose CPUs in particular.

MAC is needed if the transceiver must be able to connect directly to an Ethernet switch or router, but not if the transceiver is connected indirectly via a locally-controlled protocol-and-format-blind high-speed serial cross-point 'system' switch to an Ethernet formatting device. A simple gigE MAC ip-core uses less than 10% of a VP20.

4. Bottom Line

A Digital Back-End (DBE) building block (mini-module) can now be designed to:

- Cost about \$300 for VLBI, about \$500 for LOFAR
- Convert two 256-MHz- wide baseband (or higher Nyquist zone) inputs to 32 16-MHz-wide or 128 4-MHz-wide output channels for VLBI (but LOFAR needs '2^{nd} stage' filter-bank)
- Select and format arbitrary subsets of these channels for transmission using VSI-E over Ethernet serial protocol or VSI-H parallel intermediate interface.
- Be an independent parallel subsystem, managed through its serial receiver via either an Ethernet or "system" switch as described above.

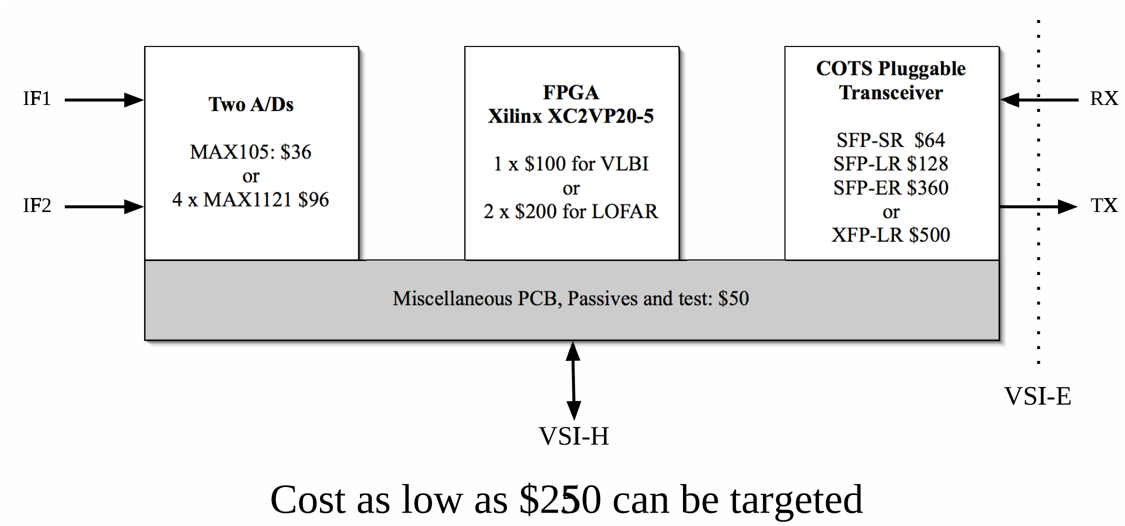

Figure 1. DBE Mini-module

Table 1. COTS A/Ds

Description	Gsamples/ second	bits/ sample	$	Watts
AD9430	0.21	12	108	1.2
MAX1124	0.25	10	50	0.5
MAX1121	**0.25**	**8**	**24**	**0.4**
$\frac{1}{2}$**MAX105[3]**	**0.8**	**6**	**18**	**1.3**
MAX104	1.0	8	400	5.2
MAX108	1.5	8	600	5.2

References

[1] Ferris, R., High Speed Samplers and Digital Filters, June 2003 presentation.

[2] Crochiere, R. E., Rabiner, L. R., Multi-rate Digital Signal Processing, Prentice Hall 1983.

[3] Hinteregger, H. F., Summary of Initial Tests of MAX105, Haystack LOFAR Memo #16, 2 February 2004.

[4] Hinteregger, H. F., Speed, Resolution and Linearity of A/Ds for LOFAR, Haystack LOFAR Memo #15, 2 February 2004.

Alexander Ipatov et al.: The Data Acquisition System Developed for Quasar Network, IVS 2004 General Meeting Proceedings, p.243–247
http://ivscc.gsfc.nasa.gov/publications/gm2004/ipatov

The Data Acquisition System Developed for Quasar Network

Alexander Ipatov, Nikolay Koltsov, Leonid Fedotov

Institute of Applied Astronomy Russian Academy of Sciences

Contact author: Alexander Ipatov, *e-mail:* avi@ipa.nw.ru

Abstract

The new data acquisition system developed at IAA RAS is described. This system contains 8 base band converters (BBC) for both (lower and upper) side bands. Input IF is from 100 MHz to 1000 MHz. Bandwidths are 0.25 MHz, 2 MHz, 8 MHz or 16 MHz. There are two-bit samplers and 32 MHz clock and 1 PPS synchronizers. There are detectors for IF and video signals control in BBC channels. There are narrow bandwidth channels to select a phase calibration signal. The DAS is controlled by computer with Mark IV Field System software.

In 2003 the IAA Technology Development Center (TDC) finished designing of the data acquisition system (DAS) for the S2-RT recording terminal. This DAS includes main module and up to 3 added modules. Each of modules contains distributor for 2 input IF signals (100–1000 MHz), 2 base band converters, control unit and power-supply unit (fig. 1).

The input signal distributor has two channels, each of which contains a 100–1000 MHz input band-pass filter, a controlled attenuator, a low-noise amplifier, a power divider (splitter) and an electronic switch (fig. 1). The gain irregularity of the entire amplification path is reduced to 1.3 dB in the 100–1000 MHz frequency range. But it is <0.2 dB in any 32-MHz part of the frequency range, which is quite acceptable for VLBI. The amplitude characteristic of the distributor channel is linear in a dynamic range of 33 dB, but the acceptable level of input signals can be additionally increased by a least 18 dB using the controllable attenuator. The dynamic range of the input signals is in good agreement with the levels of the intermediate-frequency signals that arrive from the radio astronomy receiver outputs.

The DAS may include from 2 up to 8 BBCs. The BBC consists of 2 cassettes: the BBC itself and a Local Oscillator (LO) with a control instruction decoder. The first cassette includes an amplifier-preselector and an image-rejection mixer board and 2 identical video amplifier boards with signal samplers. The amplifier-preselector has a gain of 20 dB and wide dynamic range. The low intrinsic noise level (noise factor < 3 dB) makes it possible to operate at a signal-noise temperature/intrinsic amplifier noise temperature ratio of > 30 dB, which virtually excludes any influence of the latter factor. In this case, a sufficient dynamic range margin of > 30 dB also remains. The irregularity of the frequency response in the 100–1000 MHz range is 1–1.5 dB, and is < 0.2 dB in any 32-MHz part of the frequency range. The preselector filters are set to attenuate spurious signals up to 33 dB. This spurious signals are formed in mixers at the LO voltage harmonics. SSBM includes U2794 integrated circuit and five-stage phase-shifting video amplifiers. This guarantees a image rejection of > 23 dB and a corresponding sensitivity loss due to the image channel noise of $< 0.5\%$. In practice, the channel decoupling is > 26 dB in most cases (fig. 2).

The video amplifier board contains switchable filters with passbands of 0.25, 2, 8 and 16 MHz and 2-bit signal sampler. In the central part of the passband the irregularity of the frequency response is 0.3 dB, while the nonlinearity of the phase-frequency characteristics is less than 2 degrees. The slope of the edges of the frequency response is 30 dB/octave. These parameters where confirmed during tests by radio instruments and the correlation processing of data from observations of actual noise signals. The high quality of the samplers has been confirmed by their prolonged operation as components of the Kvazar complex's radio telescopes VLBI equipment. LO cassette contains one hybrid-strip board, which incorporates 2 controllable self-excited oscillators with a digital phase-locked loop, an output frequency divider with switchable filters, a synchronism indicator and a control-code decoder. Root-mean-squares of LO phase noises were reduced to 1.2 degrees (fig. 3) for reducing the phase coherence loss to less then 0.34%. This fully corresponds to the requirements imposed on terminals of the Mark IV - Mark 5 class.

Main DAS module contains the digital signals level meter to control input IF signals and video signals. Added modules contain only video signals level meter. The measurement error of these levels is 0.1%. Main DAS module also contains the 32 MHz clock with 1 PPS synchronizer for S2-RT and filters for selection of the harmonic phase calibration signals.

The DAS is controlled by a microprocessor connected to the radio telescope's central computer, or by the operator's individual PC through an RS-232 interface. The system's software is compatible with the package of the Mark IV Field System observation programs that are widely used in international observing practice.

Parameters of this DAS are showed in table 1.

Table 1. Parameters of the new DAS

Intermediate frequency range	100–1000 MHz
Number of IF inputs	2
Number of modules	from 1 up to 4
Number of base band converters	from 2 up to 8
Connection of base band converters to IF inputs	electronic switch
Sidebands	upper and lower
Image rejection	more then 26 dB
Bandwidths	0.25; 2; 8 and 16 MHz
Number of digitizer bits	2
IF attenuator's range on distributor inputs	0–18 dB
IF attenuator's range on base band converter's input	0–15 dB
Attenuation step	1 dB
Error of signal level measure	0.1%
Phase noise of local oscillator	less then 1.2 degree rms
Clock Frequency for signal's record	32 MHz
Number of two-bits output streams	up to 16
Max Total Output Data Rate	1 Gbit/s
Module Dimension	300 × 445 × 465 mm

First module of new DAS was tested in the Svetloe and Zelenchukskaya observatories. In 2003 DAS of 4 modules (8 BBCs) for the S2-RT recording terminal was produced (fig. 4). Now it is being tuned and tested by IAA TDC. We are planning to install new DAS at the Badary observatory in summer or in autumn 2004.

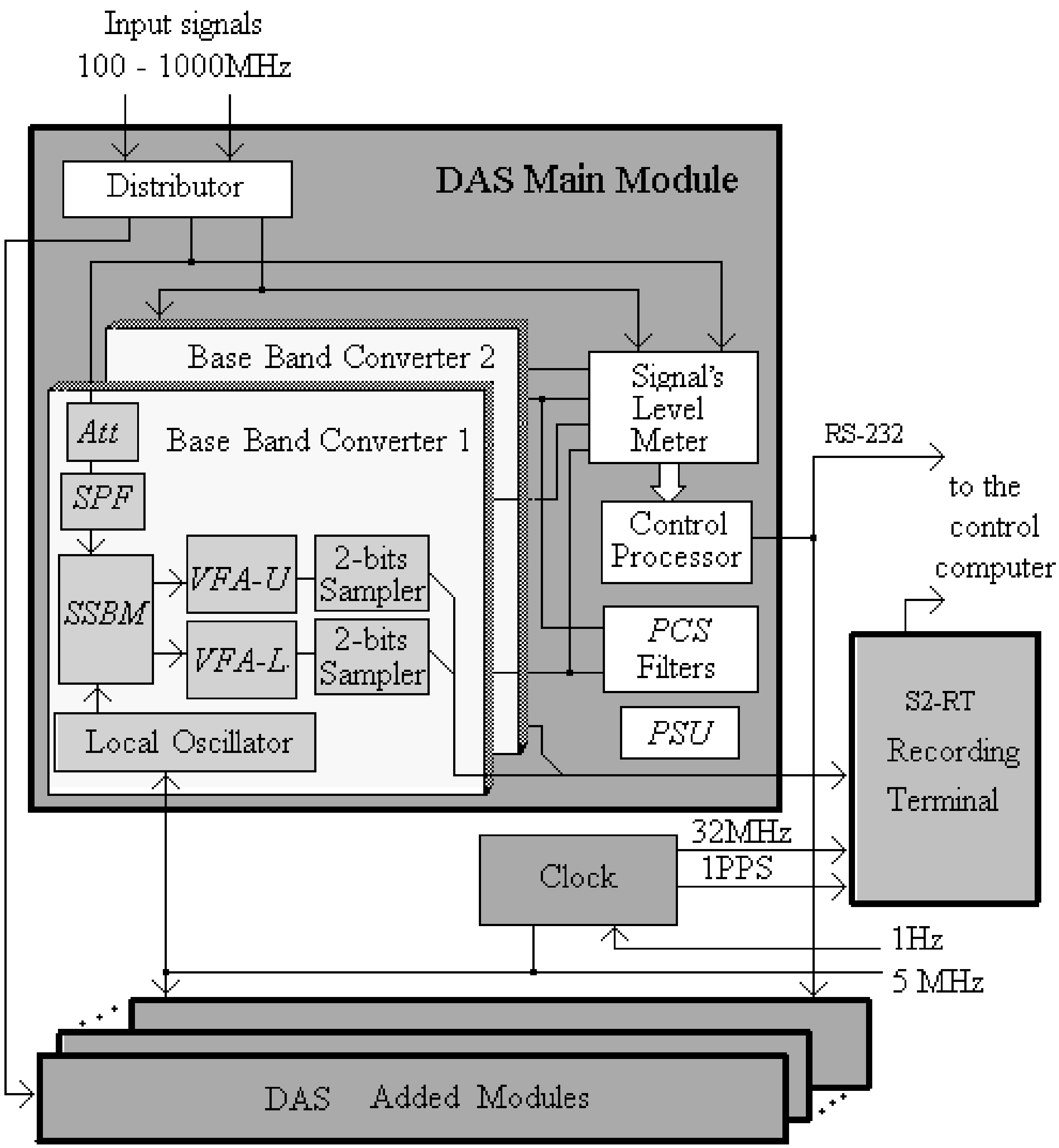

Figure 1. Blok diagram of the data-acquisition and record system: *Att* — controlled attenuator, *SPF* — switchable preselector filtres, *SSBM* — single side band mixer, $VFA-U$ — video frequensy amplifier for upper-side-band signal, $VFA-L$ — video frequensy amplifier for lower-side-band signal, *PCS* Filters — filter for phase calibration signal, *PSU* — power-supply unit.

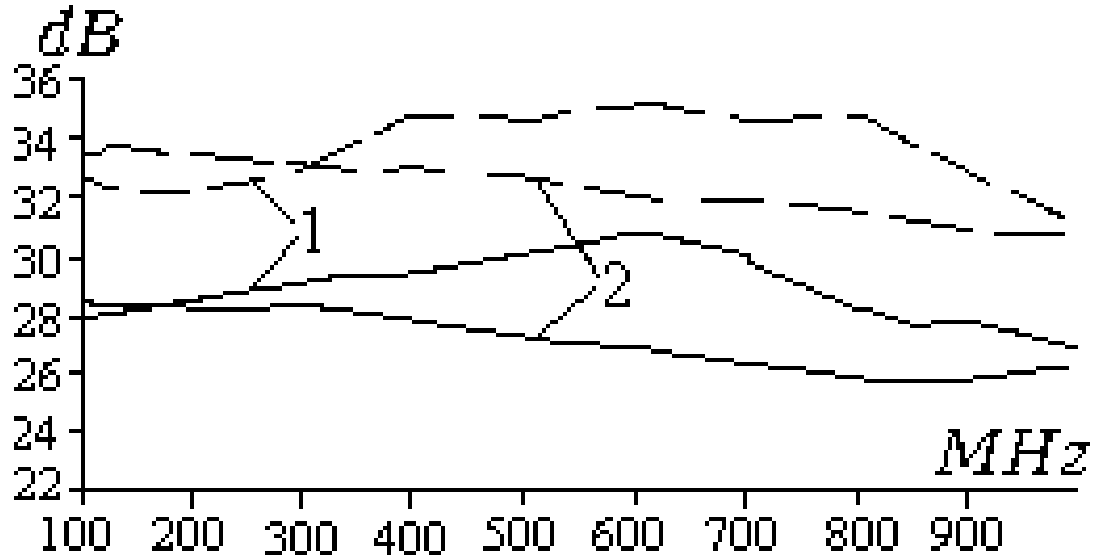

Figure 2. Experimental curves of image rejection for the reception of signals in the upper (1) and lower (2) side bands by two BBCs.

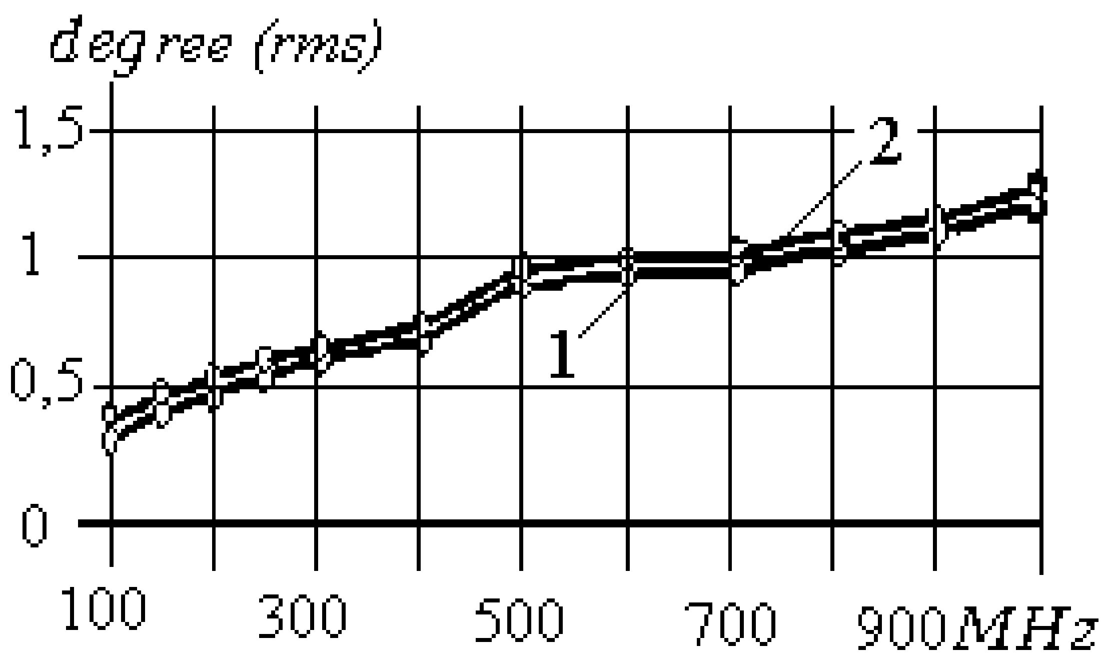

Figure 3. Measured phase noise of the LO in bands 0.01–2 MHz (1) and 0.01–16 MHz (2).

Figure 4. 8-chanel DAS with S2-Rt recoding terminal: **1, 2, 3, 4** — DAS modules; **5** — control PC; **6** — oscilloscope for phase calibration signal monitorng; **7, 8, 9** — S2-RT modules.

Duk-Gyoo Roh et al.: A Design of Data Acquisition System for Korean VLBI Network, IVS 2004 General Meeting Proceedings, p.248–252
http://ivscc.gsfc.nasa.gov/publications/gm2004/roh

A Design of Data Acquisition System for Korean VLBI Network

Duk-Gyoo Roh [1], *Kwang-Dong Kim* [1], *Se-Jin Oh* [1], *Hyun-Soo Chung* [1], *Han-Kyu Choi* [2]

[1]) *KVN, Radio Astronomy Division, Korea Astronomy Observatory*
[2]) *CubeX Co. Ltd.*
Contact author: Duk-Gyoo Roh, e-mail: `dgroh@trao.re.kr`

Abstract

Korean VLBI Network is under construction and will be capable to observe several frequency bands simultaneously. We are developing the KVN data acquisition system for our multi-channel receiver system. To cover 1 GHz bandwidth, we employ four high speed samplers, which can be operated at 2 Gsps and 4 bits per sample. These four data streams of 8 Gbps each will be transported via optical fibers to the operation building, and then distributed among sixteen FIR digital filters. With these filters, we can choose one of predefined passbands whose center frequency is arbitrarily programmable in the 1 GHz-wide input bandwidth, and then resample the filtered data at 2 bits per sample. These resampled data streams are then formatted and sent to the recorder. We plan to use the new Mark 5 recorder. KVN is involved in the development consortium for Mark 5, which is led by Haystack Observatory of MIT.

1. Introduction

Most of current VLBI systems in the world are based on the narrow-bandwidth multi-channel data acquisition systems because of the historical reasons on samplers and recorder characteristics. With the progress of the techniques on digital signal processing, it becomes possible to sample a wider bandwidth signal directly, and to record them up to 1 Gbps recording speed. Thus new type of VLBI systems that are based on the wide-bandwidth single-channel data acquisition system has shown up. However these progresses make that more and more VLBI stations are not compatible to each other since the different data acquisition systems.

Korean VLBI System (KVN) is under construction [1], and we are designing our data acquisition system in these circumstances. We are willing to build a unique data acquisition system which takes many benefits of the digital data processing, but which is compatible to existing VLBI observation modes. We will employ the high speed sampler and FIR digital filters.

With minimizing the analog IF processing, we can get more stable frequency and phase characteristics. Since there is one set of bandpass filter and baseband converter in analog IF stage, the single whole passband is digitized by a high speed sampler at once, there are no phase offsets between each channel. And also it becomes possible to change the passband characteristics by controlling the programmable filter coefficients. It can be used for both of the narrow-bandwidth multi-channel observation and the wide-bandwidth single-channel observation with the same equipment. It is possible to build several equipments with same characteristics, and is easy for maintenance and upgrade.

In this paper, a design of the KVN Data Acquisition System is proposed. Figure 1 is the conceptional block diagram of KVN data acquisition system.

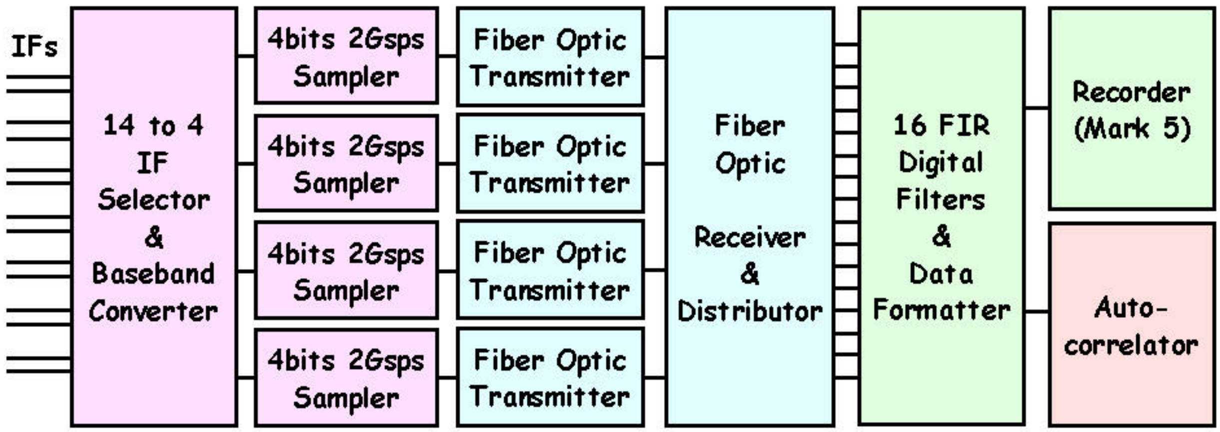

Figure 1. Block diagram of KVN Data Acquisition System

2. IF Processing Unit

KVN data acquisition system is designed to be suitable for the simultaneous multi frequency observation, such as phase compensation of the millimeter VLBI observation. Our multi-channel receiver system [2] will have two setups, which are the 2 and 8 GHz configuration mainly for geodetic observation and 22, 43, 86 and 129 GHz configuration for astronomical observation. Each of the receivers will provide both the left hand and right hand polarization IFs.

The IF selector consists of eight 2-to-1 IF switches and four 8-to-1 IF switches, to select four IFs among sixteen IF input ports. Each of the IF signals has the center frequency 8.5 GHz and the bandwidth 2GHz, and is converted to the baseband of center frequency 1.5 GHz and 1 GHz bandwidth. Finally these four baseband signals are fed into four high speed samplers respectively for digitization.

With this IF processing unit we can configure our receiver system as simultaneous four frequency band observation, simultaneous two frequency band observation with dual polarizations, and so on. For single dish operation, it has not only the IF blanking capability, but also the Doppler tracking capability via fine control of LO while baseband conversion.

3. High Speed Sampler and Optical Transmission

Each of baseband signals is sampled with the high speed sampler that is operated at 2 GHz for 1 GHz bandwidth. The sampler is under developing by combining two 1 GHz base samplers with a special clock-shifted clocking unit. Figure 2 is the schematic of the high speed sampler, model CXS-2048. The sampler has several modes of quantization, and we will use the 4 bits quantization as system default, in order to reduce the signal losses in the second sampling at the final stage of digital filtering. The sampler is controlled via 10/100 based Ethernet, and has self-diagnostics within itself.

The four data streams of 8 Gbps for each IF are serialized and transmitted to digital filter in the operation building apart about 100 meters, using the 10 Gbps optical transmitter and single mode optical fiber. We are considering to include the analog optical links for test and maintenance purpose, if possible.

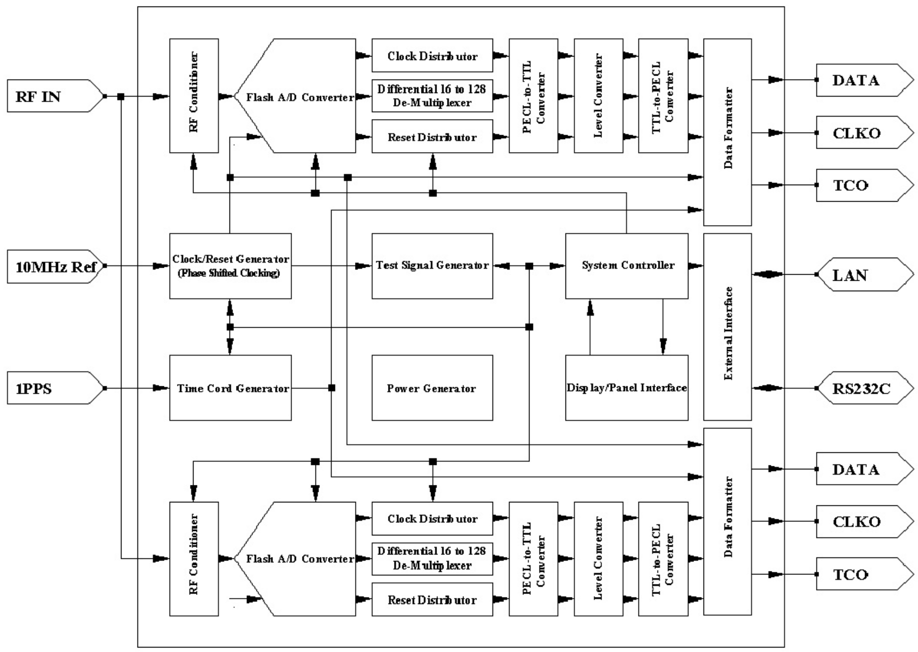

Figure 2. Schematic of High Speed Sampler CXS-2048

At the operation building, these data streams are divided into sixteen streams each as in optical form, and are distributed into every input module of digital filters. With this original idea in data distribution, we can reduce the complexity and difficulty of data feeding in electrical form.

4. Digital Filters

Digital filter is one of the most highlighted parts of KVN data acquisition system with the high speed sampler. The structure of digital filter for KVN data acquisition system is shown in figure 3. It consists of sixteen identical FIR filter cards with associated optical input modules and the station cards, which is used to build up the output data stream to the recorder and the autocorrelator. At the input module, one data stream is selected among the four data streams, and is converted back to electrical signal.

Each FIR digital filter card is used to calculate tap weighted multiplying with configurable tap size from 64 to 2,048 in maximum to generate the 2-bits wide output data streams from 1 to 16 in 32 MHz data rate. It can be operated in the data rate of maximum 2,048 Msps. Final data output is conformed to VSI-H specification, and is sent to the recorder. We will use the hard disc type data recorder Mark 5. KVN is involved in the development consortium for Mark 5, which is led by Haystack Observatory of MIT.

This digital filter is programmable to support the variety of observational needs from the narrow-bandwidth multi-channel observation to the wide-bandwidth single-channel observation. One can choose one of the predefined passbands whose center frequency is arbitrarily programmable in the 1 GHz-wide input bandwidth, and then resample the filtered data at 2 bits per sample for recording. The most common operation modes are shown in the Table 1. The fundamental 1/4

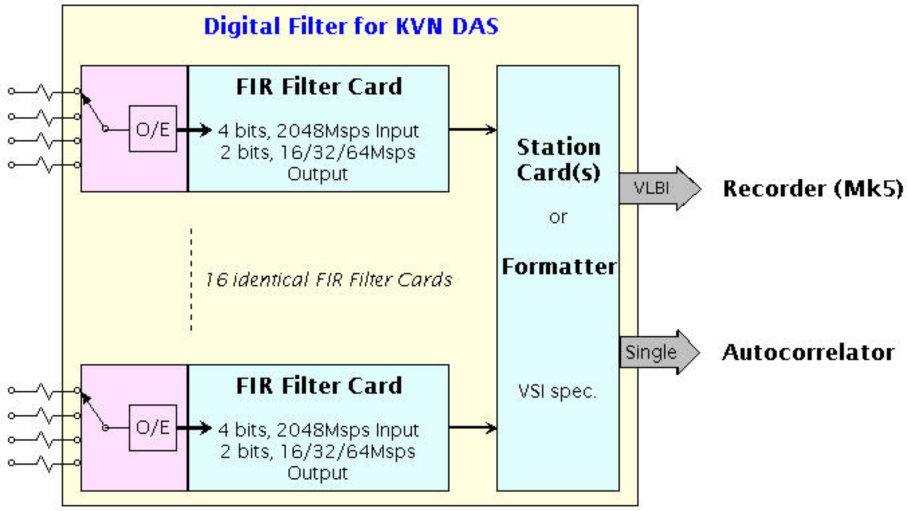

Figure 3. Structure of Digital Filter for KVN Data Acquisition System

band mode is the wide-bandwidth single-channel configuration, which is for mainly astronomical continuum observation. With these 1/64 band mode and 1/128 band mode, we can setup the digital filters to be compatible to the currently existing narrow-bandwidth multi-channel data acquisition systems. The most common operation mode is 1/64 band for 16 MHz bandwidth. The 1/128 band mode for 8 MHz bandwidth is a degraded operation mode for geodetic observation. Part of the output data will be used to keep the compatibility to the current existing recording format of the geodetic observation. One of the simulation results is shown in figure 4, which is for basic 1/64 band mode of this digital filter card.

Table 1. Operational Modes of Digital Filter Card

Mode / Bandwidth	# of Taps	Input Format	Output Format	# of 32 MHz Outputs
1/4 Band / 256 MHz	128	4 bits × 64 @ 32 MHz	2 bits, 512 Msps	16
1/8 Band / 128 MHz	256	4 bits × 64 @ 32 MHz	2 bits, 256 Msps	8
1/16 Band / 64 MHz	512	4 bits × 64 @ 32 MHz	2 bits, 128 Msps	4
1/32 Band / 32 MHz	1,024	4 bits × 64 @ 32 MHz	2 bits, 64 Msps	2
1/64 Band / 16 MHz	2,048	4 bits × 64 @ 32 MHz	2 bits, 32 Msps	1
1/128 Band / 8 MHz	2,048	4 bits × 64 @ 32 MHz	2 bits, 16 Msps	1

5. Summary

We present a design of the KVN Data Acquisition System, which consists of the high speed samplers, optical data transmission, and FIR digital filters. It is suitable to observe up to four independent IFs simultaneously for the cases of phase referencing observation which is critical for mm-VLBI, multi-transition study, dual polarization study etc. It covers 1 GHz bandwidth each

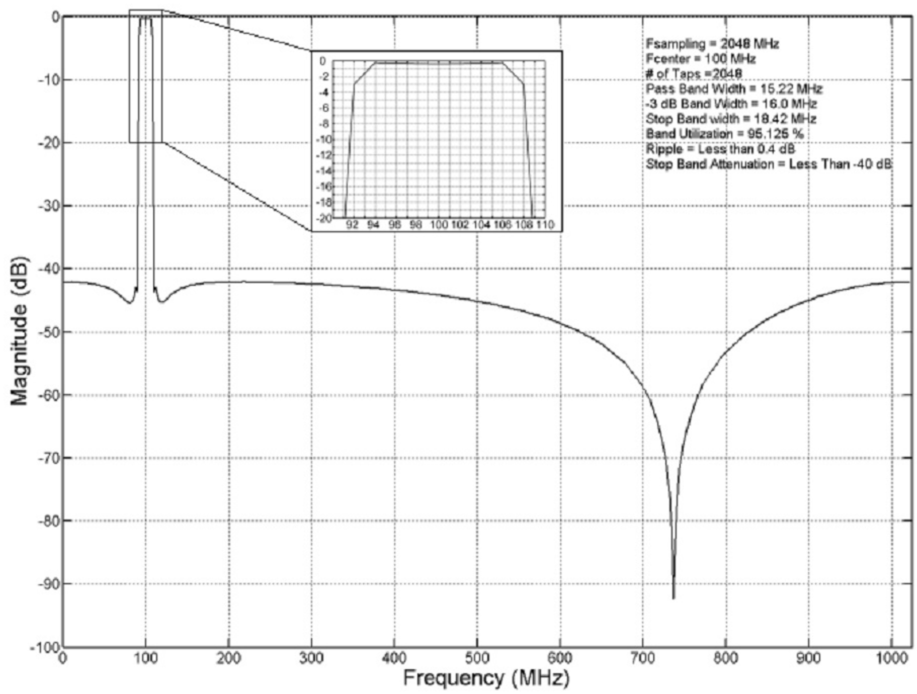

Figure 4. A simulation result of 16MHz bandpass characteristics

for four IFs. With the current limitation of data recording speed, it can be used to record a 256 MHz bandwidth in 2 bits per sample. But we can hopefully observe more than 1 GHz bandwidth in near future.

The KVN Data Acquisition System is very flexible to be used in variety of observational modes, and is capable of operations in the narrow-bandwidth multi-channel observation and the wide-bandwidth single-channel observation. It includes many original ideas for the high speed data streams and for the flexible mode configuration. With a wideband multi-channel receiver system of KVN, this unique high-speed and flexible data acquisition system is ideal for the phase compensation technique of the multi-frequency observation, which is essential for the mm-wave VLBI.

References

[1] Minh, Y. C. et al., IVS 2004 General Meeting Proceedings, edited by N. R. Vandenberg and K. D. Baver, NASA/CP-2004-212255

[2] Han, S.-T. et al., IVS 2004 General Meeting Proceedings, edited by N. R. Vandenberg and K. D. Baver, NASA/CP-2004-212255

Ryuichi Ichikawa et al.: An Evaluation of VLBI Observations for the Deep Space Tracking of the Interplanetary Spacecrafts, IVS 2004 General Meeting Proceedings, p.253–257
http://ivscc.gsfc.nasa.gov/publications/gm2004/ichikawa

An Evaluation of VLBI Observations for the Deep Space Tracking of the Interplanetary Spacecrafts

Ryuichi Ichikawa [1], Mamoru Sekido [1], Hiroo Ohsaki [1], Yasuhiro Koyama [1], Tetsuro Kondo [1], Takafumi Ohnishi [2], Makoto Yoshikawa [3], Wayne Cannon [4], Alexander Novikov [5], Mario Bérubé [6], NOZOMI DVLBI Group [7]

1) *Kashima Space Research Center, Communications Research Laboratory*
2) *Space Solutions Department, Advanced Science Solutions Group, Fujitsu Limited*
3) *Institute of Space and Astronautical Science, Japan Aerospace Exploration Agency*
4) *Space Geodynamics Laboratory/York University*
5) *Space Geodynamics Laboratory*
6) *Natural Resources Canada*
7) *JAXA, GSI, NAO, Hokkaido Uni., Gifu Univ., Yamaguchi Univ.*

Contact author: Ryuichi Ichikawa, e-mail: richi@crl.go.jp

Abstract

We performed more than 30 VLBI experiments for the two Japanese spacecraft NOZOMI and HAYABUSA from September 2002 until June 2003 using nine VLBI antennas in Japan. Algonquin 46-m of Natural Resources Canada also participate in several experiments. The final group delay products obtained from the VLBI experiments were available with approximately 30 hours latency. These group delays are consistent with the NOZOMI orbit using range and range rate observables. However, the rms scatter between them are relatively large up to several tens of nanoseconds due to the low signal to noise ratio of the NOZOMI signals. We also perform another VLBI experiments for HAYABUSA in order to establish the positioning technology for the interplanetary spacecrafts in realtime.

1. Introduction

Precise spacecraft positions (5-10 nrad) can be obtained with differential spacecraft-quasar VLBI (DVLBI) observations that directly measure the angular position of the spacecraft relative to nearby quasars. We performed more than 30 VLBI experiments for the two Japan's spacecrafts, NOZOMI and HAYABUSA from September 2002 until November 2003 [see Ichikawa et al., 2003 [1] and Sekido et al., 2003 [2] in detail]. These VLBI experiments are aimed to establish the positioning technology for the interplanetary spacecrafts in realtime. In this paper we describe the preliminary results of the VLBI experiments and future plans.

2. NOZOMI VLBI Experiments

2.1. NOZOMI Mission Sequence

NOZOMI, which means "Hope" in Japanese, is Japan's first Mars probe developed and launched by the Institute of Space and Astronautical Science (ISAS). NOZOMI was originally scheduled to reach its destination in October 1998, but an earlier Earth swingby failed to give it sufficient speed, forcing a drastic rescheduling of its flight plan. According to the new trajectory strategy, NOZOMI's arrival at Mars is scheduled early in 2004 through two additional earth swingbys in December 2002 and June 2003.

Our main concern was to determine the NOZOMI orbit just before the second earth swingby on June 19, 2003. It was significantly important to get the timing to maneuver the NOZOMI before the swingby. ISAS scientists were afraid that the range and range rate (R&RR) orbit determination might not be available because it was difficult to point the high-gain antenna mounted on the spacecraft toward the earth during the period between two swingby events. So we started to support the orbit determination of the NOZOMI using VLBI technique since September 2002.

2.2. VLBI Experiments

We use nine VLBI antennas in Japan to perform the VLBI experiments at X-band. Algonquin 46-m of Natural Resources Canada (NRCan) also participate in several experiments in collaboration with the Space Geodynamics Laboratory (SGL) of CRESTech. We equipped the state of the art "K5 VLBI system" to these stations as shown in Figure 1. The K5 system is the multiple PC-based VLBI system equipped with a PCI-bus Versatile Scientific Sampling Processor (VSSP) board on the FreeBSD and Linux operating system. The K5 system includes the original software packages which are data sampling and acquisition, real-time IP data transmission, and correlation analysis. For the purpose of analyzing the VLBI observables we are developing the specific VLBI delay model for finite distance radio source. The model is already implemented in the VLBI software package. The package will include the VLBI observation scheduling to take account of the passage of the spacecraft near the quasar line of sight and the propagation delay estimating for the ionosphere and the neutral atmosphere.

We detected fringes of NOZOMI range signal for several baselines using software correlation in spite of weak and narrow-bandwidth signal. In addition, we also detected phase delay fringes using updated correlation software [Sekido et al., 2004[3]]. The final products obtained from the NOZOMI VLBI experiments were available with approximately 30 hours latency as shown in Figure 1.

The several tens of gigabytes data sets were acquired at each station on the K5 system within 3-5 hours VLBI experiment. After the completion of each VLBI experiment, the data sets at Usuda, Gifu, and Koganei were transferred to the Kashima using a high-speed optical fiber network on TCP/IP protocol in less than 3 hours. Correlation processing was completed at Kashima about 10-15 hours later. The estimation of clock parameter based on the quasar group delays was completed at Kashima 1 hour later. On the other hand, the removable data hard disks at other stations (Tomakomai, Tsukuba, Yamaguchi, and Algonquin) were mailed to Kashima. Thus, the latency to product the group delays using these station data were up to several days.

2.3. Results

The NOZOMI positions were estimated based on the obtained group and phase delays (see in detail Sekido et al.[2004][3]). These positions were compared with the NOZOMI orbit using range and range rate (R&RR) observables. Preliminary results using group delay observables demonstrate that the VLBI delay residuals agree with R&RR observables. However, according to the comparisons of the residual group delays, the rms scatter between the R&RR results and group delays are relatively large up to several tens nanoseconds as shown in Figure 2. We consider these large scatters are caused by low signal to noise ratio of the NOZOMI VLBI group delays.

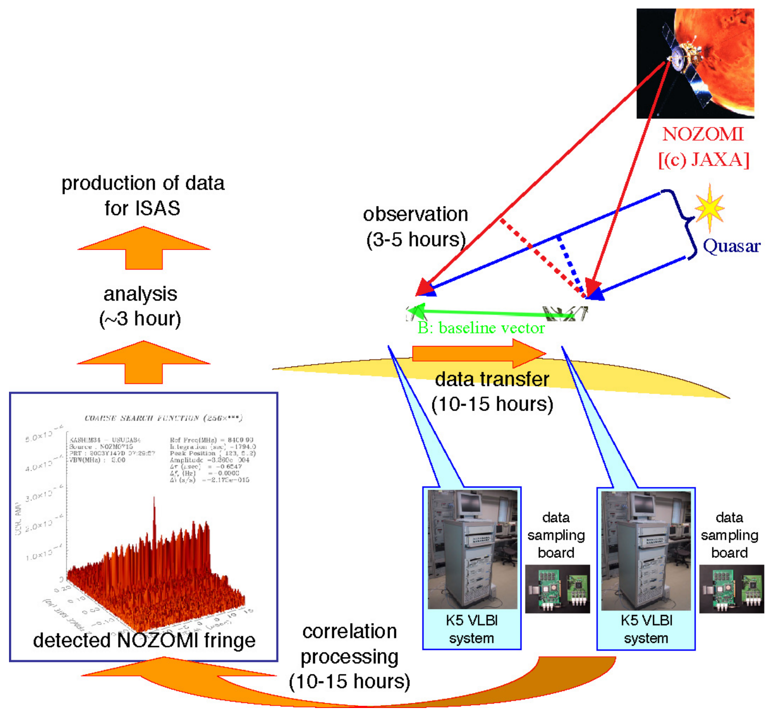

Figure 1. Schematic image showing NOZOMI VLBI data flow and analysis

The estimated position based on the phase delays are well consistent with the R&RR results. In particular, the declinations determined by phase delay signals are identical with those obtained by R&RR values.

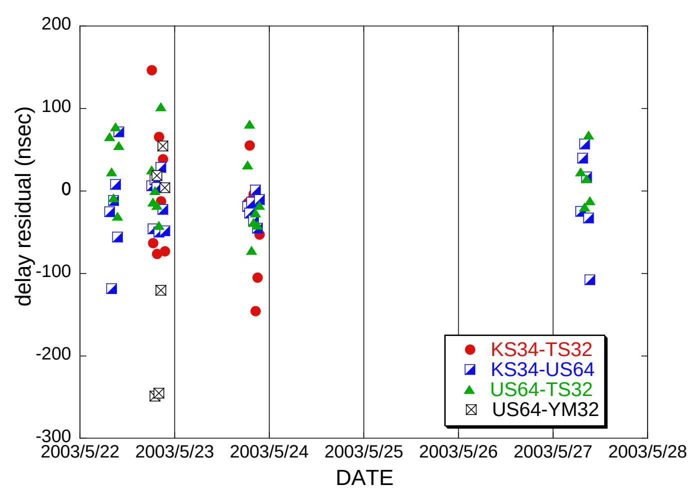

Figure 2. Residual delays between determined position using R&RR data by ISAS and VLBI group delay observables

Eventually, we provided 15 DVLBI group delay data sets to ISAS to support the orbit determination at the end of May 2003. On the other hand, ISAS scientists have fortunately succeeded to determine the NOZOMI orbit using R&RR observables at the end of May 2003. The NOZOMI completed its final Earth swingby operation on June 19 2003. NOZOMI passed within 11,000 km of the Earth in a manuever.

3. HAYABUSA VLBI Experiments

NOZOMI VLBI experiments are insufficient to develop the VLBI tracking technique due to some problems such as signal weakness, narrow band width and so on. Thus, we perform another VLBI experiments. The one of the candidate targets is HAYABUSA, which was developed to investigate asteroids. HAYABUSA, which means “Falcon” in Japanese, was launched on May 9 2003, and has been flying steadily towards an asteroid named “Itokawa”, after the late Dr. Hideo Itokawa, the father of Japan’s space development program. HAYABUSA is traveling through space using an ion engine. It will orbit the asteroid, land on it, and bring back a sample from its surface [JAXA, 2003][4].

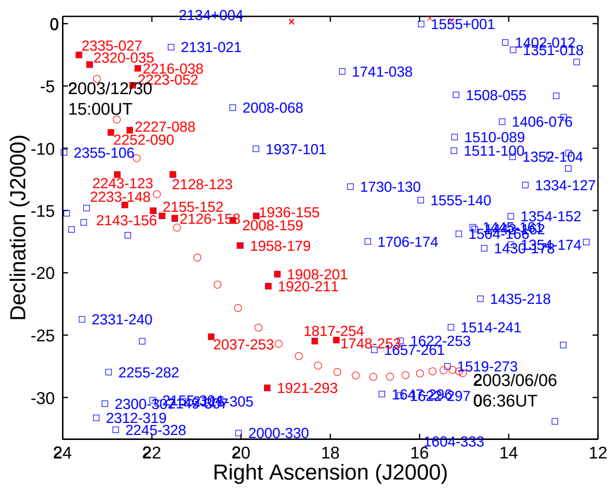

Figure 3. Trajectory of the HAYABUSA spacecraft(circles) and nearby radio sources(solid squares) from September 1 to December 31 2003.

First, we evaluated the signal intensities of the candidate quasars to perform the differential VLBI experiments. We selected 24 quasars from the ICRF catalog considering the HAYABUSA trajectory during September 1 to December 31, 2003. The separation angles between the HAYABUSA and the quasars are less than 5 degrees at each epoch. A source geometry of the HAYABUSA spacecraft and nearby quasars are illustrated in Figure 3. The first HAYABUSA VLBI experiment was successfully carried out November 26, 2003. Figure 4 shows two examples of group delay fringes of HAYABUSA range and telemetry signals for the Kashima-Usuda baseline. We are now evaluating the obtained HAYABUSA group delays by comparing with the R&RR results.

4. Planed Activities

We have to carry out additional works to achieve our final goal as follows:

- Improvement of the analysis software for spacecraft positioning using phase delay observables

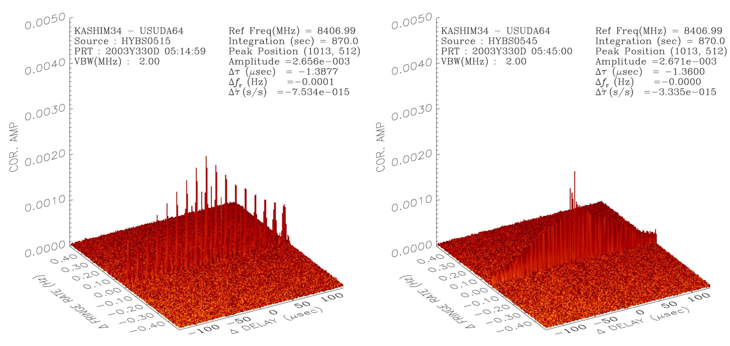

Figure 4. Detected HAYABUSA group delay fringes for the Kashima 34m – Usuda 64m baseline on November 26, 2003. (left: range signal, right: telemetry signal)

- Improvement of the finite distance VLBI model to expand its capability in a positioning of the low earth orbit satellites
- Improvement of processing speed and efficiency for the VLBI data correlation using multi-processor and high speed network
- Development of the differential VLBI software package such as the antenna tracking for the spacecraft, the automatic scheduling of the VLBI observation, the propagation delay estimation, and so on
- Validation of the NOZOMI VLBI experiments by comparing with R&RR data obtained by ISAS.

References

[1] Ichikawa et al., An evaluation of VLBI observations for the positioning of the NOZOMI Spacecraft and the future direction in research and development of the deep space tracking using VLBI, IVS CRL/TDC News, No.23, pp 31-33, 2003.

[2] Sekido et al., VLBI Application for Spacecraft Navigation (NOZOMI) -follow-up on Model and Analysis, IVS CRL/TDC News, No.23, pp 34-35, 2003.

[3] Sekido et al., VLBI Observation for Spacecraft Navigation (NOZOMI) Data Processing and Analysis Status Report, IVS 2004 General Meeting Proceedings, this issue, 2004.

[4] JAXA web site, http://www.muses-c.isas.jaxa.jp/English/index.html, 2003.

Mamoru Sekido et al.: VLBI Observation for Spacecraft Navigation (NOZOMI) - Data Processing and Analysis Status Report, IVS 2004 General Meeting Proceedings, p.258–262
http://ivscc.gsfc.nasa.gov/publications/gm2004/sekido1

VLBI Observation for Spacecraft Navigation (NOZOMI) - Data Processing and Analysis Status Report

Mamoru Sekido [1], Ryuichi Ichikawa [1], Hiro Osaki [1], Tetsuro Kondo [1], Yasuhiro Koyama [1], Makoto Yoshikawa [2], Takafumi Ohnishi [3], Wayne Cannon [4], Alexander Novikov [4], Mario Bérubé [5], NOZOMI VLBI Group [6]

1) *Kashima Space Research Center/CRL*
2) *Institute of Space and Astronautical Sciences/JAXA*
3) *Advanced Science Solutions Group/Fujitsu Limited*
4) *Space Geodynamics Laboratory/CRESTech*
5) *Geodetic Survey Division/Natural Resources Canada*
6) *CRL, ISAS, NAOJ, GSI, Gifu Univ., Yamaguchi Univ., and Hokkaido Univ.*

Contact author: Mamoru Sekido, e-mail: sekido@crl.go.jp

Abstract

We started investigation and development of VLBI application for orbit determination. Under the collaboration of Japanese VLBI community and Canadian VLBI team, a series of VLBI observation was performed for spacecraft NOZOMI, which was Japanese first Mars mission. PC-based data acquisition system and software correlator was used for observation and data reduction. Relativistic VLBI delay model for finite distance radio source and analysis software package were developed for this project. We are taking approach with group delay and phase delay in parallel. Current accuracy of delay measurements are order of several tens of nanoseconds and a ten picoseconds for group delay and phase delay, respectively. Preliminary result of estimated spacecraft coordinates are obtained.

1. Introduction

Range and Range rate (R&RR) measurements, which have been traditionally used for Spacecraft navigation in deep space, has sensitivity in direction of the line of sight (LoS). Complimentarily, VLBI is sensitive in direction perpendicular to the LoS. Thus joint use of these two techniques is expected to enhance the precision of spacecraft navigation. And JPL/NASA has been using this technique sometimes for planetary missions since 1980s. Requirement of navigation accuracy is increasing in recent and in future space missions for precise landing and orbiting other planets and for saving energy for orbit correction. Due to these reasons, Japanese space agency JAXA, CRL (NICT from April 2004), and NAOJ have started collaboration on VLBI application for spacecraft navigation. In 2003, first Japanese Mars mission "NOZOMI" was planned to do two earth swingbys for changing its orbit to Mars. During the period between two swingbys (Dec. 2002 and Jun. 2003), a series of VLBI observations were performed for the spacecraft by wide support of Japanese VLBI community across different institutes and Universities, and Canadian VLBI team (SGL/CRESTech, NRCan, and CSA). Detail of the VLBI observation of NOZOMI is described in the other article of this issue [3]. Currently CRL is doing analysis of celestial coordinates (α, δ) estimation of spacecraft (hereafter Spacecraft (SC) Astrometry) as one of the steps for spacecraft navigation.

2. Tasks to be Done for Spacecraft Astrometry

VLBI observation for spacecraft in the solar system is different from normal VLBI in some points. Firstly curvature of wavefront have to be taken into account in the delay model, which was ignored in standard VLBI model [1]. As second point, the signal from spacecraft is normally narrow band signal as wide as a few MHz. Thus group delay resolution is in order of a nanosecond in best case. To achieve high angular resolution with group delay observable, intercontinental baseline is inevitable. As another choice, phase delay has potential of 3 - 4 order better delay resolution than group delay if ambiguity problems can be solved. We are taking both approaches in parallel for the SC astrometry.

2.1. Finite Distance VLBI Model

VLBI delay model named “consensus model” [1] is used as standard VLBI delay model in world wide VLBI community. However this model assumes the radio source is at infinite distance and ignoring curvature of wavefront, which have to be taken into account when radio source is closer than 30 light years [10]. Sovers & Jacobs [10] discussed the curvature effect of finite distance radio source. Fukushima [2] proposed useful expression of VLBI delay model for finite distance radio source. However, alternative formula corresponding to the consensus model was not presented in those papers. Moyer [7] has derived an expression of VLBI delay model for finite distance radio source with solution of light time equation. Although, iterative computation is needed to solve the light time equation. Since we intended to use the CALC9 as the base of a priori computation software, then author has developed a formula for finite distance radio source[8].

$$\begin{aligned}\tau_2 - \tau_1 \quad &= (1+\beta_{02})^{-1} \\ &\left\{ \Delta t_g - \frac{\vec{\mathbf{K}} \cdot \vec{\mathbf{b}}}{c} \left[1 - (1+\gamma)U - \frac{V_e^2 + 2\vec{\mathbf{V}}_e \cdot \vec{\mathbf{w}}_2}{2c^2} \right] - \frac{\vec{\mathbf{V}}_e \cdot \vec{\mathbf{b}}}{c^2} \left(1 + \beta_{02} - \frac{\vec{\mathbf{K}} \cdot (\vec{\mathbf{V}}_e + 2\vec{\mathbf{w}}_2)}{2c} \right) \right\},\end{aligned} \tag{1}$$

where $\beta_{02} = \widehat{\vec{\mathbf{R}}}_{02} \cdot \frac{\vec{\mathbf{V}}_2}{c}$, $\vec{\mathbf{K}} = \frac{\vec{\mathbf{R}}_{02} + \vec{\mathbf{R}}_{01}}{R_{02}+R_{01}}$, and $\vec{\mathbf{R}}_{\mathrm{ij}} = \vec{\mathbf{X}}_{\mathrm{i}} - \vec{\mathbf{X}}_{\mathrm{j}}$. Indexes 0,1,2 indicate respectively radio source, station1, and 2. Variables of large capital indicate quantities in frame of Solar System Barycenter (SSB), and small ones are those in geocentric reference frame. $\vec{\mathbf{V}}_2$ and $\vec{\mathbf{w}}_2$ are velocity vector of station 2 in SSB frame and geocentric frame, respectively. This formula has precision of less than five picoseconds for the radio source beyond 10^9 m from observer.

2.2. Data Processing and Analysis System

IP-sampler system [4][5] was used for data acquisition. The data were sampled at 4 MHz with 2 bit quantization per channel. The PC-based data acquisition system has some advantages for spacecraft observation. Since sampled data is directly stored in hard disk of personal computer, it is suitable for data transfer through the Internet and for processing with software correlator, which has wider flexibility than hardware correlator. Additionally one data channel is enough for sampling narrow band signal from the spacecraft. Quasars were also observed at the beginning and end of experiments for calibration of clock parameters. Quasar data were sampled in four data channels, for improving signal to noise ratio (SNR) and for getting higher delay resolution by using bandwidth synthesis technique.

Since we are taking both approaches using group delay and phase delay, two sorts of software correlator were used to derive those observables. Group delay was derived by the same correlation software used in K5 system, and phase delay was derived by another correlation software for line spectrum signal.

A priori delay, delay rate, and partial derivatives were computed by modified version of 'CALC9', which was originally developed by GSFC/NASA and we modified it for our purpose (hereafter we call it 'CALC9M'). New VLBI delay model of finite distance radio source mentioned above section was implemented in this software[1].

From observables (O) derived by correlation processing and a priori values (C) computed with 'CALC9M', residuals (O-C) were computed and analyzed by least square parameter fitting with partial derivatives. Least square analysis package was also developed for this project.

3. Least-Square Analysis Results

3.1. Group Delay

Post fit residual plots of group delay and delay rate of VLBI observation of NOZOMI are displayed in figure 1. The post fit residuals of group delay were scattered in range of several tens

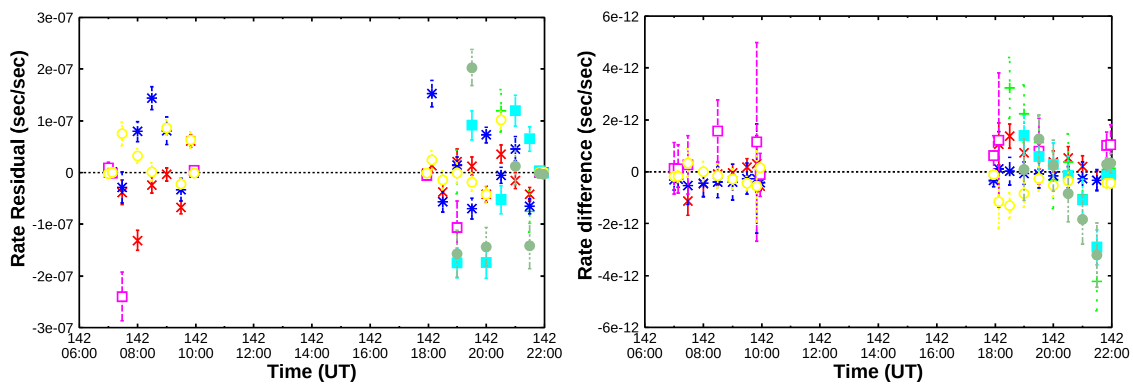

Figure 1. Post fit residual of group delay (left) and delay rate (right) in nz142 (2003/5/22) VLBI experiment. Some Quasars were observed at the beginning and end of sessions.

of nanoseconds. This seems to be current accuracy of group delay measurement, since scattering range of closure delay data was in the same order. The reasons of this large error of group delay observable will be due to low SNR and narrow bandwidth of signal from the spacecraft. The disadvantage of low SNR can be overcomed if correlation is taken with signal itself, which is transmitted from the spacecraft. This technique is used by JPL/NASA.

3.2. Phase Delay

Phase delay can be used as an observable if fringe phases between scans can be connected without ambiguity for a long time interval. Since we took conservative observation strategy in NOZOMI observation, namely tracking the NOZOMI continuously for a long time, phase connec-

[1]The delay model expressed by formula (1) is derived from framework of TCB, however JPL ephemeris and spacecraft orbit is usually given in TDB frame. Thus another modified version of formula (1) (Sekido & Fukushima 2004) was actually implemented in 'CALC9M'

tion between scans were not so difficult in this case as far as fringes are detected with enough SNR. Phase delay was extracted by line-spectrum software correlator. Figure 2 shows an example of closure of phase delay among Kashima, Usuda, and Tsukuba stations after the phase connection. It demonstrates phase connection is performed successfully without any ambiguity jump, where three scans are included in the time span of the figure. The closure plot indicates that the delay measurement accuracy is around a few tens of picoseconds. Figure 3 shows preliminary result of phase delay analysis. Left panel is post-fit residual plot of phase delays on several baselines and right one indicates coordinates of NOZOMI estimated with phase delay measurements. The right panel indicates the VLBI solutions converge to a certain points as the number of baselines data sets increases. Declination of the VLBI solution almost coincides with that of orbit determination (OD) by ISAS with R&RR measurements. Although, there is a large offset in right ascension between two sort of measurements. We need further check of software to make practically reliable output.

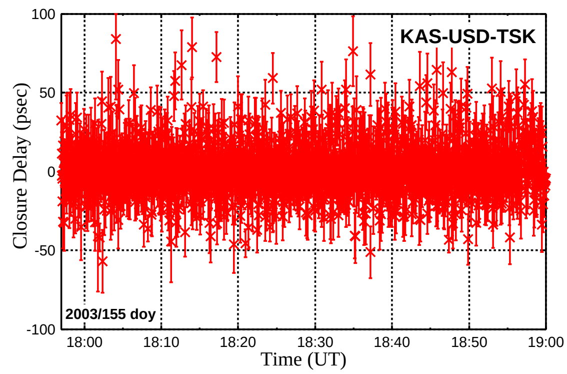

Figure 2. Closure of phase delay among Kashima, Usuda, and Tsukuba stations.

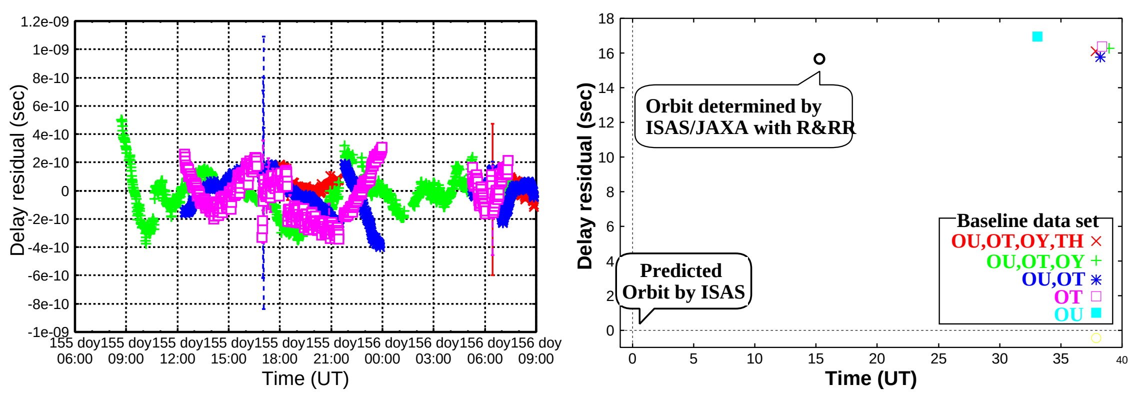

Figure 3. Post-fit residual of phase delay (left) and celestial coordinates of NOZOMI estimated from VLBI phase delay measurements in nz155 (2003/6/4) VLBI observation (right). Origin of the plot is the predicted orbit of NOZOMI. ○ mark indicates the coordinates determined by R&RR measurement by ISAS. Other marks are estimated coordinates of NOZOMI by VLBI phase delay observation with different baselines data sets. Each characters “O”, “U”, “T”, “Y”, “K”, and “H” represents VLBI stations Kashima 34m, Usuda 64m, Gifu 11m, Yamaguchi 32m, and Hokkaido 11m, respectively.

4. Acknowledgments

We thanks to VLBI group of GSFC/NASA for permission of modification and using CALC9 for our purpose. We also thanks the Canadian Space Agency for supporting the operation of Algonquin observatory for the NOZOMI observation.

References

[1] Eubanks, T. M. A Consensus Model for Relativistic Effects in Geodetic VLBI., Proc. of the USNO workshop on Relativistic Models for Use in Space Geodesy: 60-82, 1991.

[2] Fukushima, T. Lunar VLBI observation model. A&A 291, 320-323, 1994.

[3] Ichikawa R., M. Sekido, H. Osaki, Y. Koyama, T. Kondo, T. Ohnishi, M. Yoshikawa, W. Cannon, A. Novokov, M. Bérubé, and NOZOMI DVLBI group, An Evaluation of VLBI Observations for the Deep Space Tracking of the Interplanetary Spacecrafts, IVS 2004 General Meeting Proceedings, edited by N. R. Vandenberg and K. D. Baver, NASA/CP-2004-212255, 2004.

[4] Kondo, T., Y. Koyama, M. Sekido, J. Nakajima, H. Ohkubo, H. Osaki, S. Nakagawa, and Y. Ichikawa, Development of the new realtime VLBI technique using the Internet Protocol, IVS CRL-TDC News No. 17, 22-24, 2000.

[5] Kondo, T., Y. Koyama, J. Nakajima, M. Sekido, R. Ichikawa, E. Kawai, H. Ohkubo, H. Osaki, M. Kimura, Y. Ichikawa, and GALAXY Team, Real-time Gigabit VLBI System and Internet VLBI System, In: International VLBI Service for Geodesy and Astrometry 2002 General Meeting Proceedings, NASA/CP–2002-210002, N. R. Vandenberg and K. D. Baver (eds.), 142-146, 2002.

[6] McCarthy, D. D. and G. Petit, IERS Conventions 2003, IERS Technical Note No. 32., 2003.

[7] Moyer, T. D., Formulation for Observed and Computed Values of Deep Space Network Data Types for Navigation, JPL Monograph 2 (JPL Publication 00-7) 2000.

[8] Sekido, M., & T. Fukushima, Relativistic VLBI delay model for finite distance radio source, Proceedings of IUGG 2003 in Sapporo, Special issued of J. of Geodesy, in Press.

[9] Sekido, M., & T. Fukushima, VLBI Delay model for Finite distance distance radio source in TCB and TDB frame, to be submitted.

[10] Sovers, O. J. & C. S. Jacobs, Observation Model and Parameter Partials for the JPL VLBI Parameter Estimation Software "MODEST"-1996. JPL Publication 83-39, Rev. 6: 6–8, 1996.

Session 5

Analysis Strategies and Software

Page intentionally left blank

David Gordon: CALC: The Next Upgrade, IVS 2004 General Meeting Proceedings, p.265–266
http://ivscc.gsfc.nasa.gov/publications/gm2004/gordon2

CALC: The Next Upgrade

David Gordon

Raytheon ITSS/NASA Goddard Space Flight Center
e-mail: dgg@leo.gsfc.nasa.gov

1. What is Calc?

Calc is a Fortran program that calculates theoretical VLBI delays and rates. It first computes a solid body rotation matrix which translates a set of site coordinates from the terrestrial reference frame (TRF) into the celestial reference frame (CRF). It then computes corrections to the transformed site coordinates for various effects such as the solid Earth tides, ocean loading, and pole tide, and further computes the a priori delay effects of the atmospheres and antenna axis offsets. It then computes the theoretical delays and rates using a model which includes relativistic effects. Calc also computes numerous partial derivatives of the delays and rates with respect to certain interesting effects, such as nutation, pole position, UT1, the atmosphere, site positions, and source positions, which can be used later in Solve analysis.

2. Calc History

Calc dates back to 1975, when it was derived from program VLBI-3, which was originally written by Doug Robertson and brought to GSFC. Calc originally ran on an IBM360 computer. It has been updated and expanded many times since, mostly at the GSFC analysis center. The current version (versions 9.12 and 9.13) was designed for compliance with the IERS Conventions (1966) [1]. The next upgrade, version 10, will be modified to comply with the latest IERS Conventions (2003) [2].

3. Calc Usage

There have been two primary usages of Calc over the years. First, it has been used for geodetic/astrometric analysis as part of the Calc/Solve analysis sytem. Calc/Solve is currently used at nine IVS Analysis Centers, where it runs on HP Unix workstations. Second, it has been used for generating the correlator delay models at most of the world's VLBI correlators. Correlators currently using Calc include the three Mark IV correlators, and the VLBA, DRAO, JIVE, and ATNF correlators.

4. Calc Upgrade Plan

The largest part of the current Calc upgrade involves converting the TRF-to-CRF transformation to use the non-rotating origin method, replacing the classical equinox-based method. The new transformation will be a combination of a) a precession/nutation matrix based on the IAU2000A expansion (using X and Y positions of the celestial ephemeris pole (CIP) in the geocentric reference system (GSRS), b) a polar motion matrix, which will include short period ocean tidal and nutation terms, and c) a diurnal spin matrix using the Earth Rotation Angle, which is linear with time. Calc will also compute the first and second time derivatives of this rotation matrix, and its partial derivatives with respect to X and Y nutation, UT1-TAI, and x and y pole positions.

Calc will also compute a classical, equinox-based transformation, as outlined in the IERS Conventions (2003) [2]. This will be used to compute partial derivatives of the delays and rates with respect to the classical nutation offsets, delta epsilon and delta psi.

Updates to other Calc modules will be made as necessary. Some minor changes in the solid Earth tide computation will be made, and an option to use a frequency domain computation may be included. The previous ocean loading model will be retained, but an option to use an alternate model (by L. Petrov) may be added. The pole tide model will be modified to remove the mean pole offsets, as provided by the IERS. An antenna thermal deformation model will be added. And the DE/LE405 JPL Ephemeris will be used.

Several antennas have fixed axes which are tilted slightly from their design specifications. Notably, Pie Town's fixed (vertical) axis currently tilts $\sim$4 arc-minutes to the SSW, and is increasing at a rate of $\sim$.3 arc-minutes/year (though not at a constant rate since $\sim$1991.). A few other antennas have smaller tilts that appear to be constant. Unless corrected for, the tilt at Pie Town can produce errors as high as $\pm$9 psec in the axis offset correction. Therefore, a correction for antenna axis tilts will be put into the axis offset model.

5. Timetable

Much of the upgrade work on Calc has already been completed. We expect to finish the code by the end of Spring or early Summer 2004. Modifications to Solve will then be necessary. We hope to begin using Calc 10 operationally before the end of 2004.

References

[1] McCarthy, D., IERS Technical Note 21, IERS Conventions (1996), 1996.

[2] McCarthy, D., G. Petit, IERS Technical Note 32, IERS Conventions (2003), 2003.

Oleg Titov et al.: OCCAM v.6.0 Software for VLBI Data Analysis, IVS 2004 General Meeting Proceedings, p.267–271
http://ivscc.gsfc.nasa.gov/publications/gm2004/titov1

OCCAM v.6.0 Software for VLBI Data Analysis

Oleg Titov [1], *Volker Tesmer* [2], *Johannes Boehm* [3]

[1]) *Geoscience Australia*

[2]) *DGFI, Deutsches Geodätisches Forschungsinstitut*

[3]) *IGG, Vienna University of Technology*

Contact author: Oleg Titov, e-mail: `olegtitov@ga.gov.au`

Abstract

The OCCAM VLBI software package, originally developed in the beginning of the 80s, has been maintained by different scientists from different countries and agencies. The current version 6.0 of OCCAM is a powerful tool with new models and strategies to accomplish several tasks in astrometry and geodesy. For example, new mapping functions based on numerical weather models have been implemented in the software. Three options for the adjustment (least squares collocation, least squares method and Kalman Filtering) are available. A short description of the strategies is presented as well as results of their application.

1. Introduction

OCCAM is a transportable, freely distributed software package for VLBI data analysis which is based on NGS cards. The version 6.0 is an enhancement of the previous OCCAM version 5.0 [11]. Currently, it is in use on different platforms (PC, HP, LINUX). All codes are generally available for check and update.

2. Data Reduction

All reductions correspond to the IERS Conventions 2003 except the IAU 2000 recommendations, which have not been implemented yet.

- Three mapping functions (NMF [5], VMF [1], IMF [6]) are available for data analysis.
- Positions and velocities of the Sun, Earth and Moon are calculated using new ephemerides DE405/LE405.
- Nutation models IAU1980 and MHB2000 are available optionally.
- Subdiurnal EOP variations can be calculated using the Eanes [2] or Gipson [4] models.
- Atmospheric loading corrections are used from Petrov and Boy ([7]).
- The antenna thermal deformations are computed as described by the Skurikhina model [8], which is developed from the official IERS (2000) model [14].
- OCCAM 6.0 supports three options for the calculation of the geometric delay (IERS 1992 [12], IERS 1996 [13] and the IAU 1997 models).

3. Adjustment

The adjustment can be carried out using three different methods: Kalman Filter (KF), least squares method (LSM) and least-squares collocation method (LSCM):

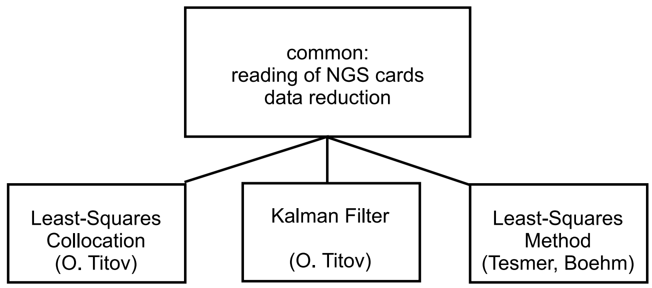

Figure 1. After the data reduction, there are three different options for the adustment strategy: O. Titov takes care of the Kalman Filter and the least-squares collocation method, J. Boehm and V. Tesmer are in charge of the classical least-squares method.

- The Kalman Filter option is used for operational EOP service. All five EOP and the first derivatives of the pole components and UT1-UTC are estimated on a daily basis as well as VLBI station coordinates. To solve the system of normal equations for daily TRF estimates, NNT and NNR constraints are applied. A random walk model is used for the stochastic parameters clock offset and wet delay. Clock rates and wet gradients are treated as constant parameters, but sometimes, the clock rate is treated as stochastic in case of the maser instabilities.
- The LSM treats the tropospheric parameters (zenith delay and horizontal gradients), as well as the clocks as piece-wise linear functions on segments from 20 minutes to 4 hours. This option is currently used to evaluate the EOP and the TRF in a global sense, but not yet operationally.
- The LSCM allows a global adjustment of the VLBI data with which a consistent solution of the CRF, TRF and EOP can be obtained. All parameters are subdivided into three groups: global (constant for the full period of observations), daily or 'arc' (constant for 24-hour session) and stochastic (variable from scan to scan). The wet delays and gradients and clock offsets are treated here as stochastic parameters with an apriori mathematical expectation and a covariance matrix. A three-group parametrical model is used as described by [9]. The covariance functions for the clock offsets and the wet delays are calculated in accordance with [10]. We used WVR data by Haas (see [3]) to build up the covariance function for the wet gradients. Having the a priori covariance, the full covariance matrix is calculated for each VLBI session. It takes into account the correlations between observables inside the 24-hour session. The algorithm also permits estimation of all of the stochastic parameters with a time resolution corresponding to the rate of VLBI data performance (5-10 minutes). Unfortunately, the time for the full matrix inversion increases in proportion N^3 (where N is the number of observations), wherefore the LSCM requires too much computing time and RAM memory.

4. OCCAM 6.0 - Results

Using the LSCM option, a CRF solution can be built up. The catalogue AUS2003b has recently been submitted to the IVS database. It includes updated coordinates for 682 radiosources from 2985 sessions over a 24-year period (1980-2003). The median accuracy of the catalogue is ~0.2 mas. The weighted rms of the solution is 22 psec. All the radiosource positions are treated as global parameters, therefore, the approach needs to be updated to take into account apparent proper motion caused by different effects.

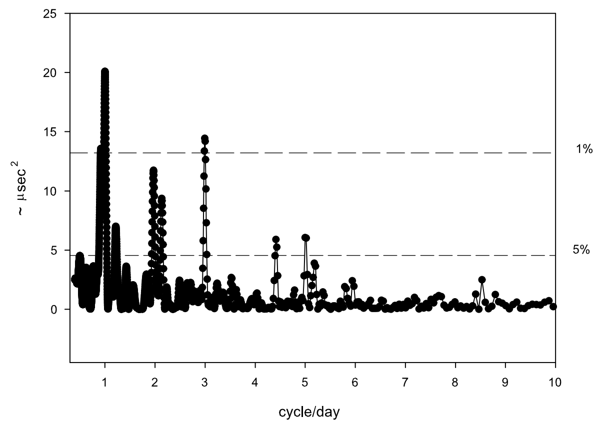

Figure 2. PSD of the UT1-UTC variations (CONT02). Model by Eanes [2] has been extracted.

A time series of the station coordinates is also available from the LSCM solution. An additional least squares adjustment gives station coordinates and velocities for a selected reference epoch. The velocities of 52 VLBI sites have been estimated in frame of the AUS2003b solution. The results are in close agreement with those of other VLBI and GPS studies. Nonetheless, some non-linear effects (mostly of seasonal character) in the station position time series with amplitude up to 1 cm have been found.

Table 1. The list of signal significant at the 5% level in the UT1-UTC variation spectrum from CONT02 campaign

Frequency of signal (cycle/day)	**Period (day)**	**Relation of the amplitude to the 5% criteria level**
5.0	0.2	2.1
4.425	0.226	2.0
3.0	0.334	3.1
2.137	0.468	2.5
1.969	0.508	2.8
1.217	0.822	2.2
1.0	1.0	3.7
0.919	1.088	3.0
0.5	2.0	1.8

LSCM-estimated Earth orientation parameters with high time resolution were analysed to compute spectra of the variations with periods less than 24 hours. Fig. 2 shows the spectrum of UT1-UTC variations from the two-week CONT02 VLBI campaign, which provides 15 days of continuous VLBI observations of eight participating stations. As the Eanes model (2000) [2] has been removed from the time series, the plot present the deviations from the model. Some signals with frequencies around 1 and 3 cycles/day are significant on the 1% level; more signals are significant on the 5% level (see Table 1). Some of the signals are not predicted by any model. Therefore, confirmation of them from analysis of independent time series is essential. An interpretation of the signals still has to be done.

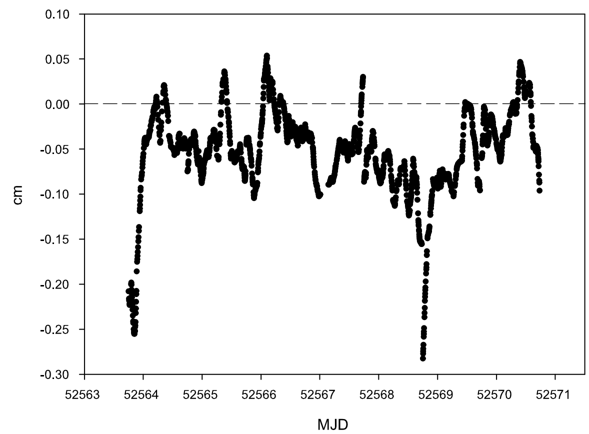

Figure 3. Variations of the north troposphere gradient for the Onsala VLBI site from the CONT02 campaign.

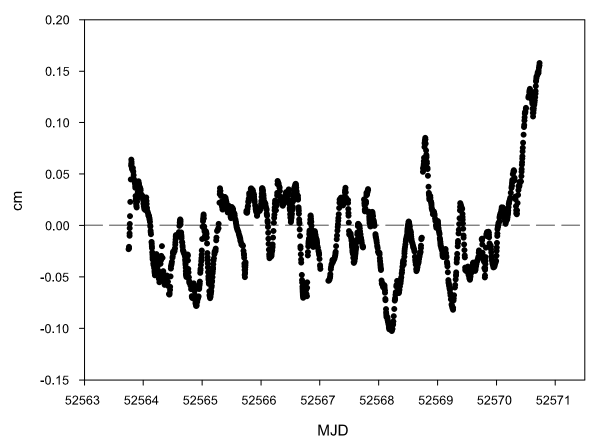

Figure 4. Variations of the east troposphere gradients for the Onsala VLBI site from the CONT02 campaign.

Time series of the wet troposphere delays and gradients have been calculated also. Figures 3,4 show variations of the troposphere gradients for the Onsala VLBI site during the first week of the CONT02 campaign.

5. Plans

- Implementation of the IAU Resolutions 2000;
- Complete SINEX output from the classical least-squares method including the CRF;
- Global solution by least squares method;
- Comparison of global solutions by LSM and LSCM;
- Development for Space VLBI data analysis (RadioAstron, VSOP-2).

References

[1] Boehm, J., and H. Schuh, Vienna Mapping Functions in VLBI analyses, Geophys. Res. Lett., 31, L01603, doi:10.1029/2003GL018984, 2004.

[2] Eanes, R., personal communication

[3] Haas, R., personal communication

[4] Gipson, J., Very Long Baseline Interferometry Determination of neglected tidal terms in high-frequency Earth Orientation Variation, In: JGR, 101, 28051–28064, 1996.

[5] Niell, A.E., Global mapping functions for the atmosphere delay at radio wavelengths, JGR, Vol. 101, No. B2, 3227-3246, 1996.

[6] Niell, A.E., Preliminary evaluation of atmospheric mapping functions based on numerical weather models, Phys. Chem. Earth, 26, 475-480, 2001.

[7] Petrov, L., J.-P. Boy, Study of the atmosphere pressure loading signal in VLBI observations, In: JGR, 109, 1–13, 2004.

[8] Skurikhina, E., On Computation of Antenna Thermal Deformation in VLBI Data Processing, In: Proc. 15th Working Meeting on European VLBI for Geodesy and Astrometry, D. Behrend and A. Rius (eds.), Barselona, 124–130, 2001.

[9] Titov, O., Estimation of Subdiurnal Tidal Terms in UT1-UTC from VLBI Data Analysis, In: IERS Technical Notes 28, B. Kolaczek, H. Schuh and D. Gambis (eds.), Paris Observatory, 11–14, 2000.

[10] Titov, O., H. Schuh, Short-periods in Earth Rotation seen in VLBI Data analysed by least-squares collocation technique, In: IERS Technical Notes 28, B. Kolaczek, H. Schuh and D. Gambis (eds.), Paris Observatory, 11–14, 2000.

[11] Titov, O., V. Tesmer, J. Boehm. OCCAM 5.0: User's Guide, In: AUSLIG Technical Notes, 7, 2001.

[12] IERS Conventions 1992, D. McCarthy (ed.), Paris Observatory, 1992.

[13] IERS Conventions 1996, D. McCarthy (ed.), Paris Observatory, 1996.

[14] IERS Conventions 2000, D. McCarthy (ed.), Paris Observatory, 2000.

Ojars J. Sovers et al.: MODEST: a Tool for Geodesy and Astrometry, IVS 2004 General Meeting Proceedings, p.272–276
http://ivscc.gsfc.nasa.gov/publications/gm2004/sovers

MODEST: a Tool for Geodesy and Astrometry

Ojars J. Sovers [1], *Christopher S. Jacobs* [2], *Gabor E. Lanyi* [2]

[1] *RSA Systems/Jet Propulsion Laboratory*

[2] *Jet Propulsion Laboratory*

Contact author: Ojars J. Sovers, e-mail: `ojars@rsasys.com`

Abstract

Features of the JPL VLBI modeling and estimation software "MODEST" are reviewed. Its main advantages include thoroughly documented model physics, portability, and detailed error modeling. Two unique models are included: modeling of source structure and modeling of both spatial and temporal correlations in tropospheric delay noise. History of the code parallels the development of the astrometric and geodetic VLBI technique and the software retains many of the models implemented during its advancement. The code has been traceably maintained since the early 1980s, and will continue to be updated with recent IERS standards. Scripts are being developed to facilitate user-friendly data processing in the era of e-VLBI.

1. Introduction

The final step in analysis of radiometric Very Long Baseline Interferometric (VLBI) data is the determination of best estimates of physical parameters from the observables: the delays of wavefront arrival times and their time rates of change. Software for carrying out this procedure normally consists of two programs: modeling and parameter estimation. The code developed and used by the Jet Propulsion Laboratory combines these two functions and is known by the acronym "MODEST" (for MODel and ESTimate). This paper gives an overview of the features of MODEST that may be of interest to the general VLBI community. We include a brief history of the initial development and evolution since the 1970s, and enumerate some features that appear to be unique to its current version. During the past two decades, several detailed comparisons have been carried out with other analysis codes in order to validate correct implementation of commonly accepted modeling standards, as well as to determine the possible level of uncertainty introduced by alternate choices in analyses of identical data. Portability of the code to a wide range of computers using varied operating systems has been demonstrated. Finally, reasonably complete documentation of MODEST has been maintained over the years. This includes a user manual, periodic publication of a modeling algorithm description [6], and a 1998 review paper of the physics of VLBI modeling [5].

2. History

The JPL VLBI code originated in the 1970s when Fanselow, Thomas, Williams and collaborators set out to identify and code physical models pertinent to quantitative description of radiometric VLBI measurements. The time was ripe to take advantage of the potential of highly stable clocks and large antennas at gigahertz frequencies to provide unprecedented accuracy in determining an inertial celestial reference frame and positioning points on the Earth's surface. Initially the analysis code was developed for single baseline experiments using the Deep Space Network (DSN) antennas. Its first incarnation, named Masterfit, was on IBM System 360 computers at Caltech, using the Fortran-66 language with 9-track magnetic tapes and punch cards as storage devices and I/O media.

A major step forward was stimulated by the introduction of relatively small and inexpensive computing equipment in the late 1970s. Availability of individual VAX computers for small groups of researchers provided convenient platforms for data analyses. At this point the MODEST code already comprised several tens of thousands of source lines, and it was realized that maintainability and traceability would be indispensable requirements for its future evolution. For easier code readability, a structured Fortran preprocessor had been used in the IBM version, and was retained in the migration to VAXes. This facilitated code modularity and anticipated many features which are now available in standard Fortran. During this era, VLBI analyses were already complicated and voluminous enough to benefit from ever-increasing computer speed and storage capacity. Estimation of thousands of parameters from tens of thousands of observables demanded a large fraction of available disk storage and many hours of CPU time.

The next major step in the evolution of VLBI data analyses was the advent of ever cheaper personal computers with Unix-based operating systems in the 1990s. The consequence for MODEST was the development of portable code utilizing the advantages of the features of advanced Fortran compilers. Improvements in computer speed and storage capacity have paralleled the growth of the VLBI data base during the past two decades. Hundreds of thousands of parameters are now determined from millions of observations in elapsed times of order 24 hours on gigahertz-CPU machines.

Recent important applications of MODEST have included updates of the celestial and terrestrial reference frames (source positions and DSN station locations). These results were used in VLBI-assisted navigation of the Mars '03 landers. Anticipated future developments include software correlation and post-processing VLBI data, feeding automated scripts for MODEST analyses.

3. Portability

As mentioned in the previous section, MODEST code was reworked to make it compliant with modern Fortran compilers during the 1990s. It was subsequently found to be fully portable to many computers then in common use. The VMS operating system, however, requires platform-specific compilation to provide for the specification of record sizes in units of 4-byte words rather than bytes. By early 2004 the platforms on which MODEST has been successfully implemented include a variety of Intel PCs with Linux systems, Hewlett-Packard, Sun, and Digital Unix systems, as well as the venerable Alpha running under VMS. MODEST also currently compiles on Macintoshes with OS X operating systems. After some minor linking problems are resolved, it will be functional on all current versions of Unix-like operating systems.

Future improvements are expected to focus on making the code more readable and therefore more easily maintainable. The advanced features of Fortran 90/95 should improve program modularity and dynamic memory allocation. The resulting code is expected to remain fully portable as various Fortran compilers become more standardized.

4. Unique Features

While VLBI analysis packages are generally quite similar in their capabilities, several features appear to be implemented only in MODEST code. These may be categorized in two general classes: observable weighting and modeling. Most simply, weighting is employed in the presence of unidentified systematic errors in VLBI observables that are manifested as normalized χ^2 values which depart from 1. Traditionally, added noise σ_{CON} is introduced in order to force $\chi^2_\nu \approx 1$. This uniform white noise is the same for all observations in a given subset. MODEST has three additional categories of added noise, applied to different data subsets in order to discriminate between different systematic errors. They target varied error sources: σ_{STN} is particular to the observing station and accounts for instrumental errors; σ_{SRC} is particular to the source and accounts for source structure problems; and σ_{TRP} is particular to the tropospheric delay and downweights observations at low elevation angles. Such added noise contributions may be either empirically adjusted, or chosen on general principles for a conjectured model of the particular hypothetical systematic error.

Another aspect of observable weighting goes beyond the above-mentioned noise sources to address one of the presently dominant VLBI error sources, namely the troposphere. The standard troposphere model maps zenith delays to the elevation of each observation and estimates them at frequent intervals. A MODEST option employs a parameterized turbulent atmospheric flow model [8] to calculate an observable covariance matrix for all observations within an experiment. This matrix is based on physical parameters such as troposphere height, wind velocity, and saturation scale describing the turbulent flow. In contrast to Kalman filtering, it accounts for spatial as well as temporal correlations between observations. If desired, this covariance matrix can supplement the customary troposphere model. For single-baseline DSN data the troposphere covariance formulation is found to reduce baseline length scatter substantially.

In the unique model category, maps may be available for the spatial structure of a source's radio emission. MODEST is capable of accepting models of such extended distributions, parameterized as Gaussian components. Delay corrections based on such maps [1] can replace the standard point-source model, and have been demonstrated to produce modeling improvements amounting to several mm [4].

A final non-standard capability of the MODEST code is to "restart" parameter estimation runs. If details of the least-squares parameter estimation have been saved for a given fit, more data may be added to resume the least squares estimates starting with the previous results. This may facilitate operational aspects of large fits, and is especially useful in combining raw observables from different space geodetic techniques. For example, it was used in an early determination of the precession constant from a combination of VLBI and lunar laser ranging measurements [2].

Finally, it should be mentioned that MODEST has a plethora of modeling options. For example the current version offers a choice of nine tropospheric mapping functions and 13 nutation models, to name but two categories. Such versatility makes it a very powerful tool.

5. Operational Characteristics

To illustrate some practical aspects of maintaining and running MODEST code, we summarize some pertinent measures of size, time, and storage space requirements. The source code consists of approximately 50000 lines, 30000 of which are non-comment. Internal memory requirements of the executable are less than 1 Gbyte. With the exception of the Solar System ephemeris, all auxiliary input files (*e.g.* UT1 and polar motion, ocean loading, etc.) are in ASCII format. The observable ("FIT") file can be either ASCII or binary (to save space for global data sets). Its contents are limited to information required for analyses; all other post-correlation results are archived separately.

Single-experiment analyses are essentially instantaneous on GHz-speed machines. Logistical considerations are only important for large global solutions. A solution estimating 700 source coordinate pairs and 400000 other parameters from 3.3 million observation pairs (EST step) requires approximately 36 hours on a 2.2-GHz dual processor XEON machine. It uses a 64-MB solution specifications file (2.4 million lines), an 8-GB regress file, 25 GB scratch space, and produces 12 GB of output. Modeling the observations (MOD step) requires 9 hours to produce the regress data set from a 300-MB raw observable file.

Numerous auxiliary programs are associated with MODEST processing. They include codes to generate the complex solution specification file for large fits, to optimize parameters for troposphere covariance matrices, to print and plot various classes of estimated parameters, and to perform comparisons of radio source catalogs. The total lines of code in such software exceed the size of MODEST itself by approximately a factor of 2.

6. Traceability, Documentation, and Verification

Starting in the early VAX days, automated procedures were developed to keep track of software changes at each new version of the code. Differences of program modules are archived along with narratives of the reasons for the changes. Much of this history is also preserved in the code itself in the form of comment lines. In principle, any of the hundreds of versions of MODEST and Masterfit that were operational during the past quarter century can be reinstated, and any particular data processing run can be reproduced, given availability of the raw input data. In late 2003 numbered versions reached 417. Together with several hundred versions of the predecessor Masterfit, there is a long archived history of traceable, time-stamped changes of the code over the past two decades. Many outdated models (*e.g.* Woolard nutation) remain available for historical purposes.

It appears that the MODEST software is perhaps the most thoroughly documented VLBI analysis program in common use today. This documentation consists of two parts: an "operator manual", and algorithm definition. The operator manual is a 50-page long description of the contents of all input and output files required to run MODEST. It is embedded in the main module, and is thus never separated from the code itself. Algorithm documentation includes periodically updated modeling descriptions in the form of a JPL Report, initially published in 1983 and now in its 7th (1996) version [6], which is now somewhat outdated. These practically oriented reports have a more intimate connection to the software than does the 60-page 1998 review paper describing the detailed physics of the VLBI model [5].

In order to gain assurance that VLBI modeling and parameter estimation are performed correctly, several detailed comparisons with other software were carried out over the years. On the modeling side, the first was a comparison with the Goddard Space Flight Center software CALC in 1982 [7] and again in 1997. Comparisons with the Paris Observatory's GLORIA and the satellite geodetic code GINS [3] were done in 1997 and 2000, respectively. It was concluded that the codes agree to close to a picosecond for the important aspects of the model. Stronger conclusions were prohibited only by the inability to make models exactly equivalent. Parameter estimates present a more difficult problem, but recent comparisons of global source position results between MODEST and CALC/SOLVE were found to agree at the 100 microarc second (15-ps) level. This is most likely a consequence of editing and parameterization choices by different analysts.

7. Conclusion

The JPL VLBI analysis software MODEST has evolved during the past three decades to keep pace with improvements of physical models as well as with advances in computing hardware. It offers several unique options for data weighting and modeling, and retains all models used during its evolution. Documentation is currently probably the most complete among contemporary VLBI analysis packages. Discrepancies with independent software are at the picosecond level for model details. Comparisons of the results of parameter estimates (which also test effects of editing choices by different analysts) similarly show agreement at the 15-ps level. In this era of easily available, cheap and fast computing power, MODEST has proved to be portable to numerous platforms.

8. Acknowledgments

Masterfit and MODEST development over the years profited from the efforts of people (too many to name individually) in the Tracking Systems and Applications section at JPL. They analyzed, coded, and tested the numerous parts of the VLBI model, as well as exposed deficiencies and improved the efficiency of the code.

References

[1] Charlot, P., Radio-Source Structure in Astrometric and Geodetic Very Long Baseline Interferometry, *Astron. J.* **99**, pp. 1309–1326, 1990.

[2] Charlot, P., O.J. Sovers, J.G. Williams, and XX Newhall, Precession and Nutation from Joint Analysis of Radio Interferometric and Lunar Laser Ranging Observations, *Astron. J.*, **109**, pp. 418–427, 1995.

[3] Meyer, U., P. Charlot, and R. Biancale, GINS: A New Multi-technique Software for VLBI Analysis, in *IVS 2000 General Meeting Proceedings*, N.R. Vandenberg and K.D. Baver (Eds.) (NASA/CP-2000-209893, Hanover, MD), pp. 324–328 (2000).

[4] Sovers, O.J., P. Charlot, A.L. Fey, and D. Gordon, Structure Corrections in Modeling VLBI Delays for RDV Data, in *IVS 2002 General Meeting Proceedings*, N.R. Vandenberg and K.D. Baver (Eds.) (NASA/CP-2002-210002, Hanover, MD), pp. 243–247 (2002).

[5] Sovers, O.J., J.L. Fanselow, and C.S. Jacobs, Astrometry and Geodesy with Radio Interferometry: Experiments, Models, Results, *Rev. Mod. Phys.* **70**, pp. 1393–1454, 1998.

[6] Sovers, O.J. and C.S. Jacobs, Observation Model and Parameter Partials for the JPL VLBI Parameter Estimation Software "MODEST" – 1996, JPL Report 83-39, Rev. 6, 151 pp., 1996; Fanselow, J.L, Observation Model and Parameter Partials for the JPL VLBI Parameter Estimation Software "MASTERFIT – V 1.0", JPL Report 83-39, 54 pp., 1983.

[7] Sovers, O.J. and C Ma, Comparison of GSFC and JPL VLBI Modeling Software: Benchmark, *NASA JPL TDA Progress Report* 42-83, pp. 101–112, 1985.

[8] Treuhaft, R.N. and G.E. Lanyi, The Effect of the Dynamic Wet Troposphere on Radio Interferometric Measurements, *Radio Science* **22**, pp. 251–265, 1987.

Johannes Boehm et al.: Vienna Mapping Functions in VLBI Analyses, IVS 2004 General Meeting Proceedings, p.277–281
http://ivscc.gsfc.nasa.gov/publications/gm2004/boehm1

Vienna Mapping Functions in VLBI Analyses

Johannes Boehm, Harald Schuh

IGG, Vienna University of Technology
Contact author: Johannes Boehm, e-mail: johannes.boehm@tuwien.ac.at

Abstract

In recent years numerical weather models (NWM) have been applied to improve mapping functions which are used for tropospheric delay modeling in VLBI and GPS data analyses. The Vienna Mapping Functions VMF (Boehm and Schuh, 2004, [1]) are based on direct raytracing through NWM, and allow exploitation of the full information provided in the NWM. On the other hand, the Isobaric Mapping Functions IMF (Niell, 2001, [4]) use intermediate parameters calculated from the NWM. In this study, pressure level data from the ECMWF (European Centre for Medium-Range Weather Forecasts) are applied to determine the coefficients of the VMF and the IMF. Used for the analyses of IVS-R1 and IVS-R4 VLBI sessions, both mapping functions improve the repeatability of baseline lengths (by ∼10% for IVS-R1 and ∼5% for IVS-R4) compared to the Niell Mapping Functions NMF (Niell, 1996, [3]).

1. Introduction

Raytracing through radiosonde data has often been applied to develop and validate mapping functions which are needed for tropospheric modeling in VLBI and GPS data analyses. For example, the Niell Mapping Functions NMF (Niell, 1996, [3]), which require station height, station latitude and day of the year as input parameters, were developed using radiosonde data over a wide range of latitudes. In recent years, much effort has been put into the development of mapping functions based on data from numerical weather models. Niell (2001, [4]) proposed the Isobaric Mapping Functions (IMF) which apply as input parameters the height of the 200 mbar pressure level (z200) and the ratio of the wet path delay along a straight line at 3.3° elevation and zenith delay (smfw3). The equations relating these two parameters to the coefficients of the continued fraction form (see Eq. 1) are based on raytracing through radiosonde data. The tilting of the 200 mbar pressure level also provides information for the correction of hydrostatic north-south and east-west gradients before estimating the remaining wet gradients.

$$mf_{h,w} = \frac{1 + \cfrac{a}{1 + \cfrac{b}{1 + c}}}{sin(e) + \cfrac{a}{sin(e) + \cfrac{b}{sin(e) + c}}} \tag{1}$$

When working on the implementation of these mapping functions with pressure level data from the ECMWF, it became evident that the NWM could be exploited more rigorously by discarding intermediate parameters like z200 and smfw3. The main idea behind the Vienna Mapping Functions VMF is to directly use the raytracing through the NWM instead of taking intermediate steps.

2. Determination of the Vienna Mapping Functions (VMF)

The continued fraction form for the hydrostatic and wet mapping function for an elevation angle e is shown in Eq. 1. This form is also used in the NMF (Niell, 1996, [3]) and in the IMF (Niell, 2001, [4]). Three coefficients a, b and c are sufficient to map zenith delays down to elevations of 3°. In the case of VMF, these coefficients are determined from raytracing through NWM.

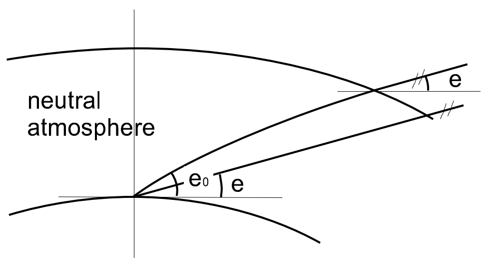

Figure 1. Raytracing through NWM

Input parameters for the raytracing program are an initial elevation angle e_0, and values for height, temperature and water vapor pressure at distinct pressure levels in the neutral atmosphere (e.g. 15 levels from 1000 to 10 hPa total pressure). The raytracing yields the outgoing (vacuum) elevation angle e, and the values for the hydrostatic and the wet mapping function. The hydrostatic mapping function includes the geometric bending effect.

Instead of raytracing at 10 different elevation angles from 90° to 3.3° elevation and estimating the coefficients a, b and c in a least-squares adjustment (rigorous approach VMF(rig), Boehm and Schuh, 2004, [1]), the fast approach VMF(fast) requires the raytracing for only one initial elevation angle of 3.3° (see Fig. 1). This yields one value for the hydrostatic mapping function, one value for the wet mapping function, and the vacuum elevation angle e (~3°). Then, pre-defined formulas are used for the b_h, c_h, b_w, and c_w coefficients, and the coefficients a_h, a_w can be determined by simply inverting the continued fraction form (Eq. 1). To check the quality of VMF(fast), the values of the mapping functions have been compared to VMF(rig) for CONT02, a continuous 15-day VLBI campaign with eight stations in October 2002. For an elevation angle of 5° the RMS differences are about 5 mm for the hydrostatic and 1 mm for the wet part when the hydrostatic and wet zenith delays are assumed to be 2000 mm and 200 mm, respectively. This would imply that the corresponding error in the station height is less than 2 mm when the cutoff elevation angle is set to 5°. Moreover, the RMS differences vanish at about 3° because VMF(fast) is tuned for this elevation angle, and above 5° elevation the RMS differences are also decreasing rapidly.

3. Validation of the VMF

Improved mapping functions are expected to improve geodetic accuracies. Good measures for the quality of geodetic results are the "baseline length repeatability" and the difference in baseline length when changing the cutoff elevation angle ("elevation angle cutoff test"). For the geodetic VLBI analysis, the classical least-squares method of the OCCAM 5.1 VLBI software package (Titov et al., 2001, [6]) is used. Free network solutions with a minimum of squared station coordinate residuals are calculated for the 24h sessions with five Earth orientation parameters being estimated (nutation, dUT1 and pole coordinates). Atmospheric loading parameters are obtained from Petrov and Boy (2004, [5]), and total gradient offsets are estimated every 6 hours using the model by Davis et al. (1993, [2]).

Baseline length repeatabilities are determined for CONT02 (2002, October 16-31), and for all IVS-R1 and IVS-R4 sessions from January 2002 till August, 2003. For the following investigations all baselines which include the station TIGO/Concepcion (Chile) are excluded, because due to the small antenna dish (6 m diameter), the low SNR does not allow a reliable validation of the tropospheric mapping functions. Also, the baselines with station Gilmore Creek (Alaska, U.S.A.) are not considered before the Earthquake on November 3, 2002. The cutoff elevation angle was set to 5°. Approximately 70% - 80% of the baselines got improved repeatabilities with the new mapping functions IMF and VMF compared to NMF. The mean relative improvement is ~5% for IVS-R4 and CONT02, and it is even ~10% for IVS-R1 (Boehm and Schuh, 2004, [1]), mainly due to the enormous improvement for baselines with station Tsukuba (Japan) (Fig. 2) which does not take part in IVS-R4 and CONT02.

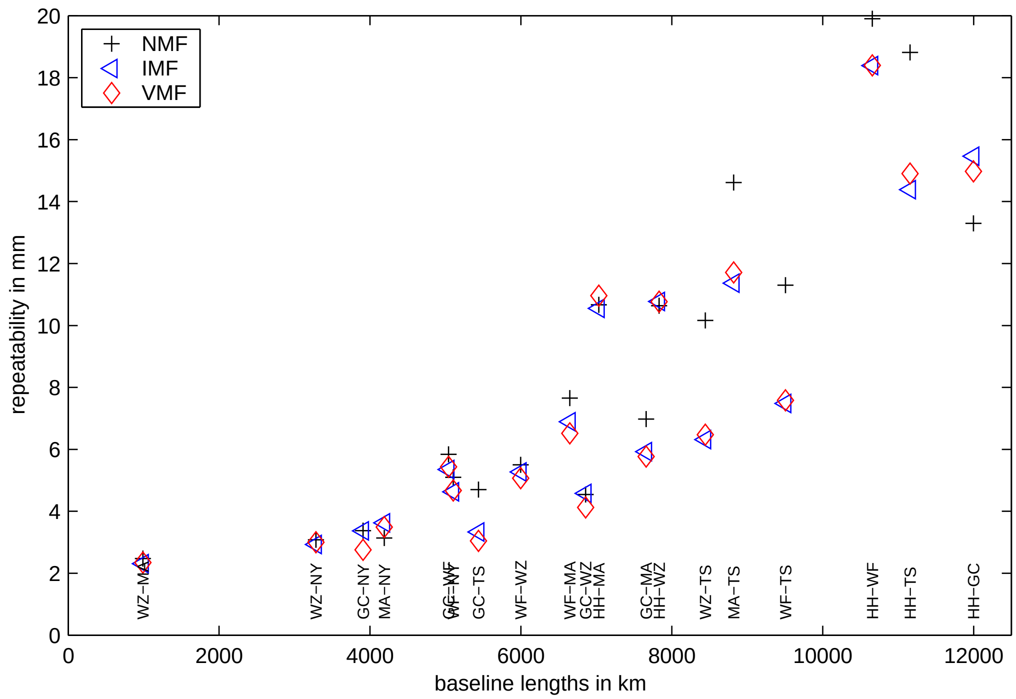

Figure 2. Baseline length repeatabilities for IVS-R1. Especially, the repeatabilities for all baselines with station Tsukuba (TS) in Japan are improved considerably. The repeatabilities are approximately the same for VMF and IMF.

Fig. 3 shows the hydrostatic and wet mapping functions for VMF and NMF at station Tsukuba (Japan). There is a significant bias between the hydrostatic mapping functions, which is caused by the fact that NMF is based on radiosonde data in the U.S.A. (Niell, 1996, [3]) and Tsukuba does not fit into this latitude-dependent model.

Another measure of the quality of mapping functions can be obtained by elevation angle cutoff tests. These tests show how baseline lengths change when the cutoff elevation angle is varied. They are a good measure for the absolute accuracy of the mapping functions, because they reveal systematic errors in the mapping functions as the baseline lengths will be influenced when the cutoff angle is changed. Supposing that NMF and VMF yield almost identical results when the

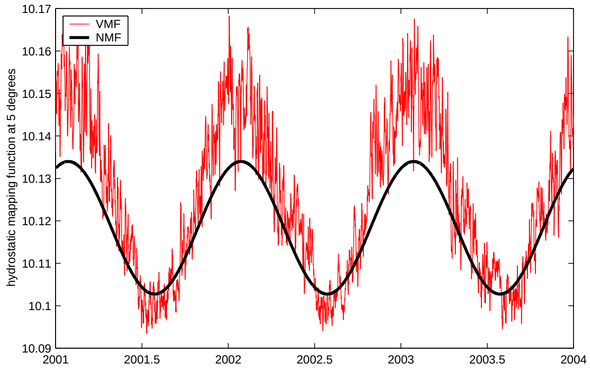

Hydrostatic mapping functions at 5° elevation for NMF and VMF. The time series are biased significantly, which again biases the station heights by ∼−3mm (see Tab. 1).

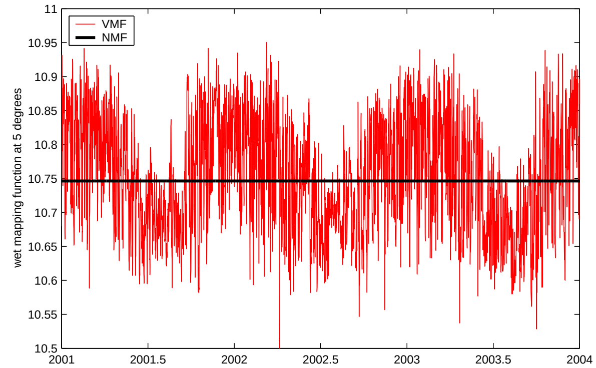

Wet mapping functions at 5° elevation for NMF and VMF. NMF does not account for seasonal variations.

Figure 3. Mapping functions at station Tsukuba for NMF and VMF. Unlikely to NMF, the Vienna Mapping Functions (as well as IMF) are able to model variations with periods down to 6 hours.

cutoff elevation angle is set to 10°, the elevation angle cutoff test can be taken to determine station height changes when using VMF (or IMF) instead of NMF for 5° cutoff (see Table 1). These results are confirmed by the rule of thumb saying that the station height error is ∼1/3 of the mapping function error for the lowest observations.

Table 1. Changes in mean station heights in mm for IVS-R1 and IVS-R4 when using VMF or IMF instead of NMF. These results are derived from elevation angle cutoff tests.

	gc	wz	ny	ma	wf	ts	hh	ft	kk	ap	sh
IVS-R1	+1.9	+0.4	+1.0	-1.0	-1.7	-3.0	-0.5				
IVS-R4	+1.8	-0.3	+0.6	-0.9				-0.6	-1.1	-0.3	-1.0

4. Mapping Function Parameters Provided by IGG

The Institute of Geodesy and Geophysics (IGG) of the Vienna University of Technology gets regular access to data from the ECMWF (European Centre for Medium-Range Weather Forecasts). Derived parameters which are necessary to determine IMF and VMF for non-commercial purposes have been provided to the scientific community since September 2003. Table 2 gives an overview of the ECMWF datasets which are used for these computations. The parameters for IMF (z200 and smfw3) are provided on a global grid with a resolution of 2.5° x 2.0°. The coefficients a_h, a_w for the hydrostatic and wet part of VMF(fast) are determined for all geodetic VLBI stations. This list will be extended to other selected sites, e.g. the IGS (International GPS Service) stations in near future. All parameters are given every six hours and they can be found at the webpage http://www.hg.tuwien.ac.at/∼ecmwf.

Table 2. Specification of the ECMWF datasets which are used for the computation of IMF and VMF(fast)

<table>
<tr><th></th><th>IMF</th><th>VMF(fast)</th></tr>
<tr><td>doy 1 in 1979 -
doy 365 in 2001</td><td colspan="2">2.5° x 2.0° ERA-40 Re-Analysis
pressure level dataset (15 levels from 1000 to 10 hPa)</td></tr>
<tr><td>doy 1 in 2002 -
doy 238 in 2003</td><td colspan="2">2.5° x 2.0° operational
pressure level dataset (15 levels from 1000 to 10 hPa)</td></tr>
<tr><td>doy 239 in 2003 -
now</td><td>2.5° x 2.0° operational
pressure level dataset (15 levels)</td><td>~0.3° operational
pressure level dataset (21 levels)</td></tr>
</table>

5. Conclusions and Outlook

Recent mapping functions such as IMF and VMF based on data from numerical weather models like ECMWF provide better repeatabilities of baseline lengths. There is a mean improvement of 5% to 10% versus results obtained by NMF, but further investigations remain to be done. Especially, the quality of the mapping functions at certain stations has to be evaluated by means of nearby radiosonde data or different numerical weather models, and a closer look needs to be taken at systematic effects revealed by elevation angle cutoff tests. So far, baseline length repeatabilities are not significantly better with VMF compared to IMF, although VMF exploits the NWM more rigorously. But as the time series get longer, one might speculate that the advantages of VMF become visible, since starting with doy 239 in 2003 the vertical and horizontal resolution of the ECMWF data has increased significantly (to 21 levels and down to 0.3°, respectively), and the quality of ECMWF data will improve steadily in the future.

References

[1] Boehm, J., and H. Schuh, Vienna Mapping Functions in VLBI analyses, Geophys. Res. Lett., 31, L01603, doi:10.1029/2003GL018984, 2004.

[2] Davis, J.L., G. Elgered, A.E. Niell, C.E. Kuehn, Ground-based measurement of gradients in the “wet” radio refractivity of air, Radio Science, Vol. 28, No. 6, 1003-1018, 1993.

[3] Niell, A.E., Global mapping functions for the atmosphere delay at radio wavelengths, JGR, Vol. 101, No. B2, 3227-3246, 1996.

[4] Niell, A.E., Preliminary evaluation of atmospheric mapping functions based on numerical weather models, Phys. Chem. Earth, 26, 475-480, 2001.

[5] Petrov, L., and J.P. Boy, Study of the atmospheric pressure loading signal in VLBI observations, submitted to JGR, 2004.

[6] Titov, O., V. Tesmer, and J. Boehm, Occam Version 5.0 Software User Guide, Auslig Technical Report 7, 2001.

Volkmar Thorandt et al.: Residual Plotting and Ambiguity Resolution (REPA), IVS 2004 General Meeting Proceedings, p.282–286
http://ivscc.gsfc.nasa.gov/publications/gm2004/thorandt

Residual Plotting and Ambiguity Resolution (REPA)

Volkmar Thorandt, Gerald Engelhardt

Bundesamt für Kartographie und Geodäsie

Contact author: Volkmar Thorandt, e-mail: volkmar.thorandt@bkg.bund.de

Abstract

Some elements of the Calc/Solve software have been identified which badly needed re-programming for migration of the package to LINUX operating system. One of these elements is the interactive graphics tool CNPLT. The program REPA is an interactive graphics tool which replaces CNPLT and can be used for visualization of observations and residuals, manual ambiguity resolution, and other interactions for a given VLBI experiment. As of now program versions on the basis of FORTRAN77 and FORTRAN90 are running on HP workstations.

1. General Idea

REPA is based on the open PGPLOT software and on the DiaGI/MultiDiaGI layer which is a comprehensive set of graphic tools based on PGPLOT (Petrov, L. (2003)). REPA is a module of the Calc/Solve analysis software package and can be used either in standalone mode or it can be started from interactive Solve. The main idea is a three level structure as shown in figure 1.

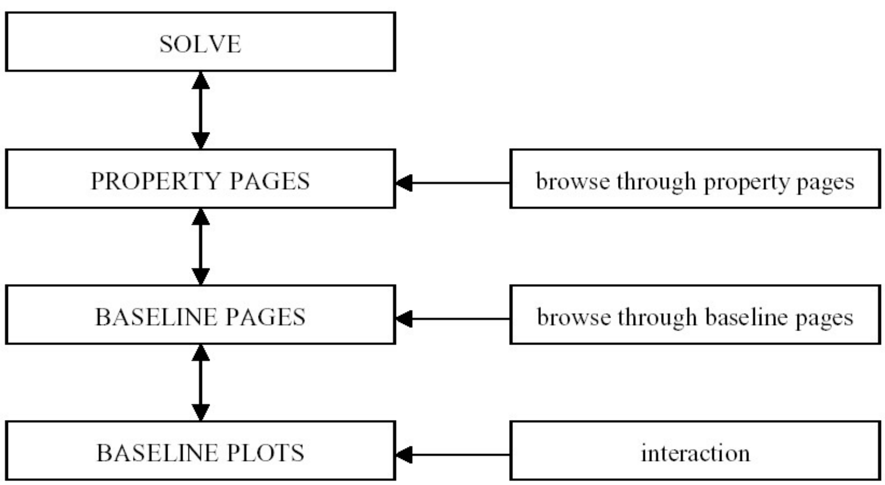

Figure 1. Three Level Structure.

The main features of the program are:

- **suppress/recover observations**
  single observations, groups of observations in a single baseline
- **resolve/reset ambiguities**
  single observations, groups of observations in a single baseline, all ambiguities of a database in one step

- **plotting of different database characteristics**
  group delays vs. time, elevation and azimuth; rates vs. time; SNR vs. elevation; phase delays vs. time; cable calibrations vs. time; ionospheric corrections vs. time; meteorological data (temperature, pressure, humidity) vs. time

2. First Level - Property Pages

Here the analyst can choose one of the available so-called Properties. Properties are different kinds of observations and residuals which can be displayed and changed interactively, depending on the kind of data. In the current version of REPA three Property Pages are included. First Property Page is shown in figure 2.

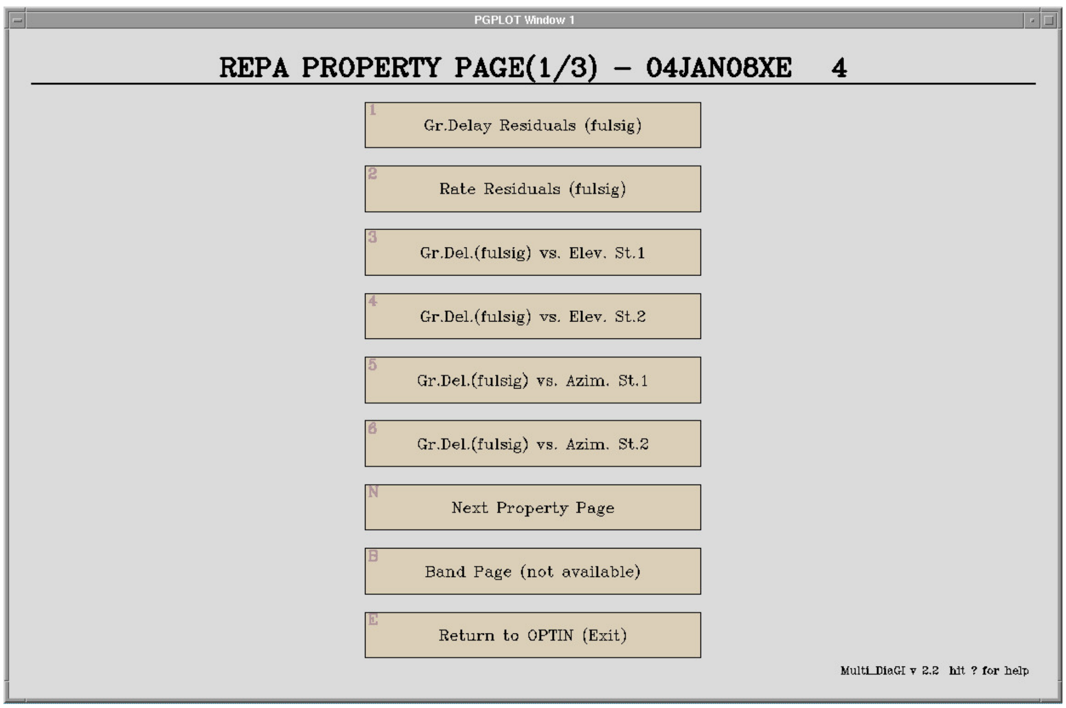

Figure 2. First Level - Property Pages.

3. Second Level - Baseline Pages

Small plots of all baselines are displayed in MultiDiaGI plots (figure 3). The user can browse through all Baseline Pages to find the baseline which has to be treated. A set of different buttons is located on the right hand side of the Baseline Pages. Here it is possible to browse through the Baseline Pages (if there are more than one), to change or to reload experiment bands, and to work on the ambiguities. By pressing the reset ambiguities button all ambiguities can be set back to the original state. The solve ambiguities button causes the ambiguity resolution for all baselines of the loaded experiment in one step. To make it easier to evaluate the result of this action the program writes some information about it to the terminal similar to the example in the table below:

Table 1. Screen output for ambiguity resolution.

Baseline	CALCULATED	THEORETICALLY
GILCREEK HARTRAO	37	46 IDP
GILCREEK MATERA	-15	-19 IDP
GILCREEK TIGOCONC	-61	-61 IDP
GILCREEK WESTFORD	-52	-46 IDP
GILCREEK WETTZELL	63	56 IDP
HARTRAO MATERA	-45	-65
HARTRAO TIGOCONC	-109	-107
HARTRAO WESTFORD	-86	-93
HARTRAO WETTZELL	33	10
MATERA TIGOCONC	-48	-42
MATERA WESTFORD	-37	-28
MATERA WETTZELL	77	74
TIGOCONC WESTFORD	22	15
TIGOCONC WETTZELL	137	117
WESTFORD WETTZELL	115	102

Weighted Mean Residuals (WM) in nanoseconds, IDP: independent baselines

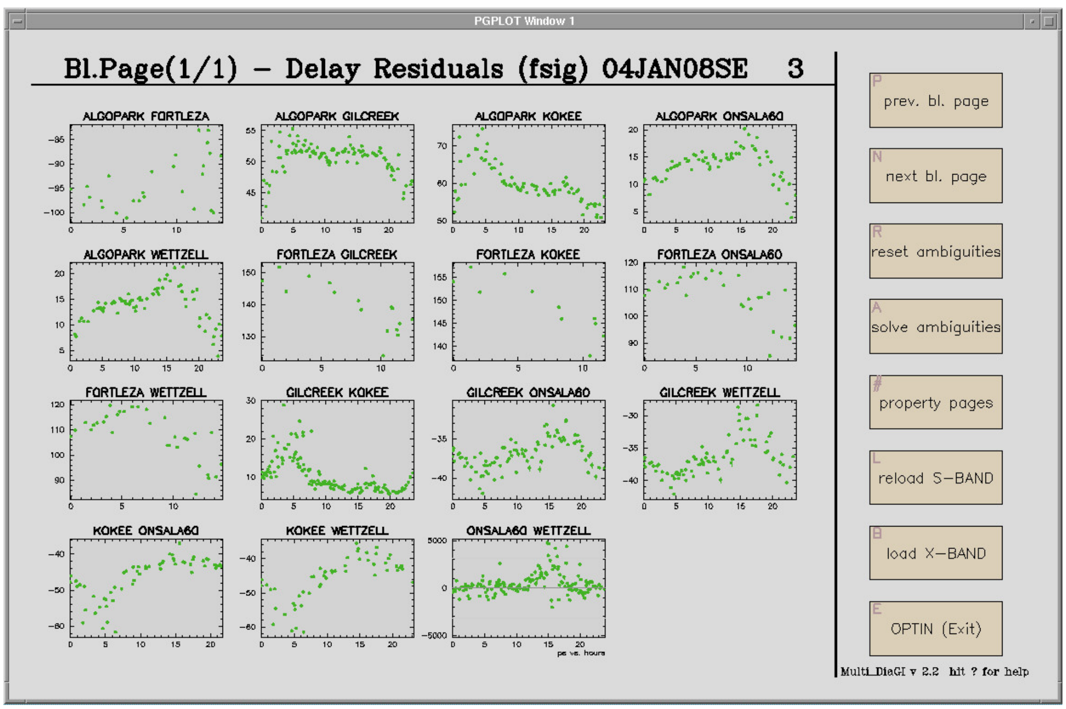

Figure 3. Second Level - Baseline Pages.

4. Third Level - Baseline Plots

All observations of the chosen baseline are displayed in the Baseline Plot as shown in figure 4. The plot consists of the observation plot area with axes and inscriptions, the user function line, the headline, the bottom line(s), one or two (for more than 50 sources) source name columns, and status labels.

Depending on the chosen property there are different sets of user functions available which are displayed in the user function line and can be chosen by left mouse clicks on the buttons. This action causes the binding of the chosen user function(s) to the mouse button(s). The analyst has the following user functions at his disposal:

- **get information on observations**
- **suppress/recover single observation**
- **suppress/recover observation groups**
- **ambiguity shift for single observations**
- **ambiguity resolution of observation groups**
- **reset ambiguities to original status**
- **connect observations with the same source**
- **browse through baseline plots**
- **change plot area**

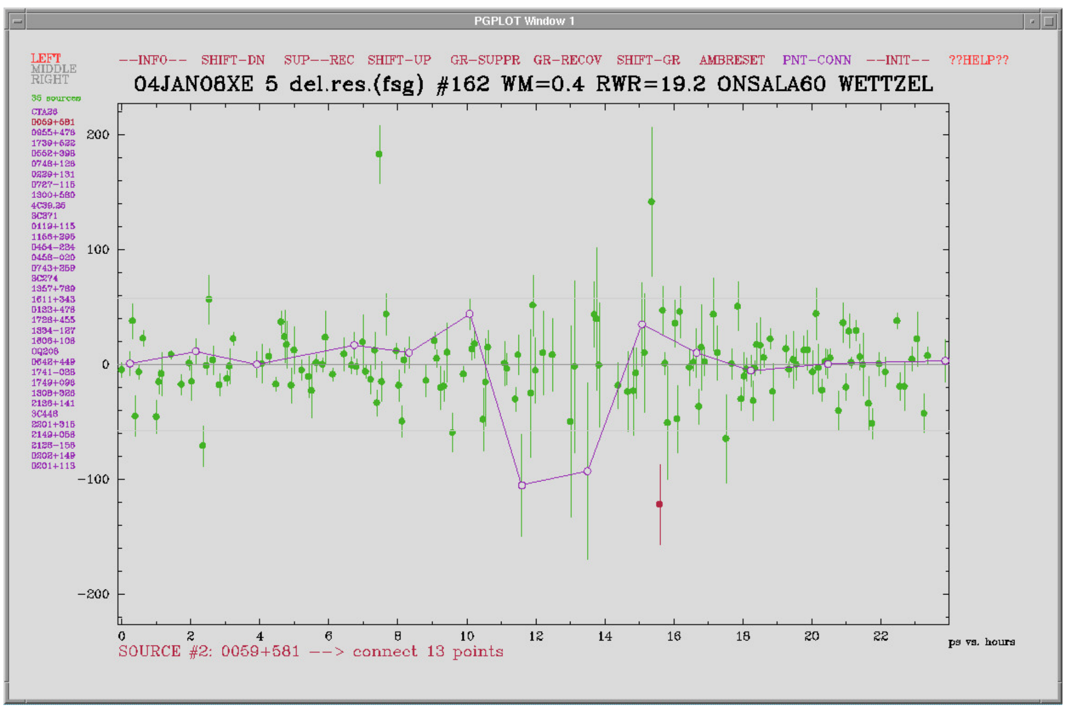

Figure 4. Third Level - Baseline Pages.

5. Future Plans

Together with the whole Calc/Solve package the program REPA will be ported to the LINUX operating system.

References

[1] Thorandt, V., Engelhardt, G., Residual Plotting and Ambiguity Resolution (REPA), In: Proceedings of the 16th Working Meeting on European VLBI for Geodesy and Astrometry, held at Leipzig, May 09-10, 2003, edited by W. Schwegmann and V. Thorandt, Bundesamt für Kartographie und Geodäsie, Frankfurt/Leipzig, 2003.

[2] Petrov, L., Release of Mark 5 VLBI Analysis Software Calc/Solve from Sep. 25, 2003 (web-reference: http://gemini.gsfc.nasa.gov/solve).

Wolfgang Schwegmann: An Embedded Expert System for the Automation of VLBI Data Analysis: Concept, Implementation and Results, IVS 2004 General Meeting Proceedings, p.287–291
http://ivscc.gsfc.nasa.gov/publications/gm2004/schwegmann2

An Embedded Expert System for the Automation of VLBI Data Analysis: Concept, Implementation and Results

Wolfgang Schwegmann

Bundesamt für Kartographie und Geodäsie (BKG)
e-mail: `wolfgang.schwegmann@bkg.bund.de`

Abstract

The delay between the observation and the availability of results is an important disadvantage of geodetic VLBI compared to other geodetic space techniques. One reason is the complicated and highly interactive analysis procedure, requiring well-founded expertise. While advances in e-VLBI technology promise to considerably cut the latency, automatic VLBI analysis tools have still to be developed to obtain VLBI results in near real-time. In this paper the concept, implementation and first results of an embedded expert system for the automation of the entire VLBI analysis procedure are presented.

1. Introduction

Geodetic VLBI data analysis is a very complex process and needs a lot of manual interactions. It is very time consuming because most tasks require a comprehensive knowledge of the whole procedure of the data analysis and the analyst needs a lot of experience and knowledge for solving the complex problems within the data analysis. Thus, an automation of the whole VLBI data analysis procedure would be very useful. It allows one to close the gap between the time of observation and the availability of results, i.e. a quicker turnaround can be achieved. The costs of operations will decrease, because the analysts will be relieved from their routine burdens. Thus, they can spent more time to improve the modelling or to investigate instrumental errors. The management of the data analysis will be much easier, because it is based on an explicitly modelled standard procedure that is performed by automatic programs. Last but not least, the results of the data analysis are much more consistent and reliable, because the same analysis strategy is going to be used and all steps of the analysis procedure are perfomed in the same way.

To achieve the automation, knowledge-based methods from the field of research of artificial intelligence are used. An *Intelligent Assistant for Data Analysis in VLBI* (IADA) is developed as an embedded expert system. Expert systems are software systems that are designed to reproduce the special knowledge and the expert's capability of reasoning within a narrow application area. By applying the explicitly modelled expert's knowledge such systems are able to solve complex problems. The term "embedded" is of particular interest, because embedding expert systems in the existing data processing environment is critical for the success of such a system. Embedding IADA in the Mark IV data analysis software CALC/SOLVE by building a powerful interface guarantees the automation of the whole VLBI analysis procedure.

Two consecutive steps are necessary to develop an expert system for the automation of the VLBI data analysis procedure: A so-called *Structured Model*, describing the tasks to be solved during the data analysis and the knowledge necessary to do that, has to be built. This model has to be implemented, i.e. the knowledge has to be formally represented within the expert system and an interface has to be developed to use it in conjunction with the existing analysis software.

2. Concept of IADA

The concept of IADA is based on the so-called *Structured Model of the VLBI Data Analysis Procedure*. This model describes the course of the VLBI data analysis and represents the knowledge necessary within the single steps of the analysis. For a successful automation it is important to model all the required knowledge in a structured and formal way. Thereto, the processing strategy of the data analysis has to be characterized by several steps that are performed one by one. Each step represents a major task within the data analysis and is subdivided into several substeps to describe the current task in more detail (cf. figure 1). Each substep has to be characterized by the following items:

- *Tasks*: The tasks of the current substep of the analysis procedure.
- *Parameterization*: Every task demands a special parameterization that depends on the results of previous steps of the analysis.
- *Models*: The models to be used.
- *Approach*: The approach to perform the tasks.
- *Evaluation criteria* (quality control): to evaluate the results of the current step of the data analysis.
- *Error sources*: To list all possible faults that can cause unsatisfactory results.
- *Trouble-shooting*: Methods to correct for faults; they are assigned to an error source.

Moreover, the *Structured Model* has to define the generic tasks to be solved during the automatic data analysis. Some tasks can be processed by the existing software while other tasks have to be handled by the expert system. The process flow between IADA and SOLVE and the several tasks that are performed by IADA are shown in figure 2.

The user interface for the usage of IADA is realized in SOLVE (cf. section 3). Thus, the analyst is able to call IADA for an automatic data analysis from within his usual software environment. The user interface allows the analyst to select a specific step and substep of the analysis procedure. For this substep IADA can be called in order to perform it automatically, to check the current parameterization, to evaluate the results of the analysis, to recover possible problems and to find solutions to solve the problems. From the user interface the analyst invokes the interface that handles the data and information flow between SOLVE and IADA.

For step 1, 2 and 3 of figure 1 the interface calls external programs (GETDB, XCALC, XLOG). These programs are independent modules within the Mark IV data analysis system and can be run in automatic or in interactive mode. They can be used independently from IADA as well as in conjunction with the expert system. In the latter case IADA is responsible for the control of the process flow, i.e. to call the programs when necessary and to check the results. GETDB, XCALC and XLOG are described in more detail in [2].

For the steps 4 to 8 (cf. figure 1) IADA is going to be used and according to figure 2 the following tasks are passed through: During the *Preparation* IADA specifies all information necessary to perform the current substep. The respective data are collected by the interface and included into the knowledge base of the expert system during the *Initialization*. Based on this information conclusions are drawn that are important for the next steps of the analysis (*Deduction*). Then the parameterization is being reviewed during the *Control*. Corrections to remove possible errors in the

<table>
<tr><th>Step</th><th>Substep</th></tr>
<tr><td>1 DownloadDB</td><td>1.1 X-Band |
S-Band |
X+S Band</td></tr>
<tr><td>2 Calc</td><td>2.1 X-Band |
S-Band |
X+S Band</td></tr>
<tr><td>3 LogFiles</td><td>3.1 Xlog</td></tr>
<tr><td>4 DataLoading</td><td>4.1 X-Band |
S-Band |
X+S Band</td></tr>
<tr><td>5 InitialSolution</td><td>5.1 InitialSettings
5.2 AprioriClock
5.3 AmbiguitySolution
5.4 EvaluateResults</td></tr>
<tr><td>6 IntermediarySolution</td><td>6.1 InitialSettings
6.2 OutlierElimination
6.3 EvaluateResults</td></tr>
<tr><td>7 FinalSolution</td><td>7.1 InitialSettings
7.2 OutlierElimination
7.3 ExamineSolution
7.4 FinalOutlierElimination
7.5 CheckCableCal
7.6 FinalParameterization
7.7 EvaluateResults</td></tr>
<tr><td>8 DatabaseUpdate</td><td>8.1 WebDoku
8.2 DBUpdate</td></tr>
</table>

Figure 1. Steps and substeps of the VLBI analysis procedure.

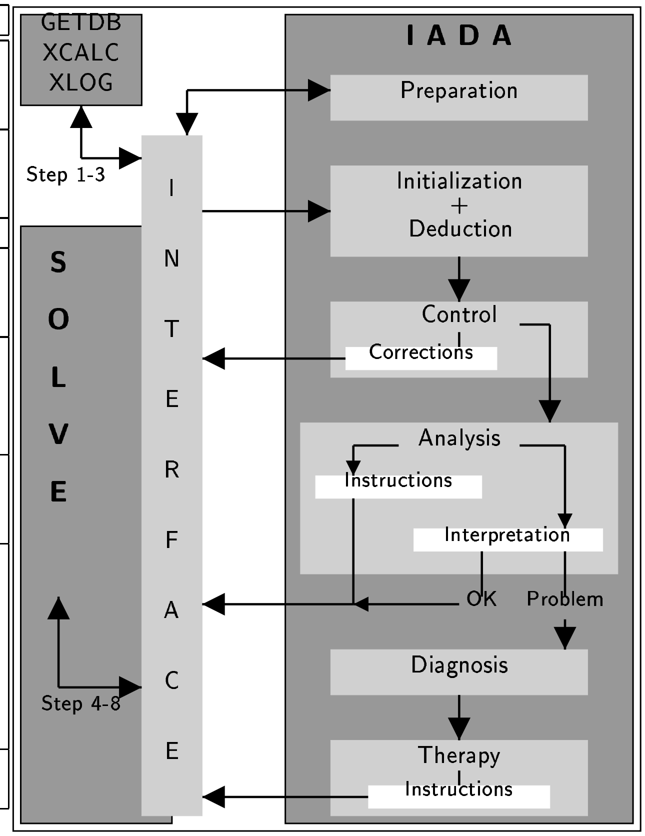

Figure 2. Process flow within IADA and SOLVE for each single substep.

parameterization are passed back to SOLVE and the analysis is continued with the *Initialization*. The actual tasks of the substep are performed during the *Analysis*, i.e. the instructions to be realized in SOLVE are going to be determined with respect to the current analysis situation or the current situation is going to be evaluated. If the result of this interpretation does not recover any problems the analysis is going to be continued with the next step or substep. Otherwise the *Diagnosis* is going to be started in order to find possible error sources for the actual problem. If symptoms of a well known problem can be identified methods to solve the problem are derived and the corresponding instructions are passed back to SOLVE (*Therapy*). Afterwards the current substep is going to be analyzed in IADA again.

3. Implementation of IADA

The Implementation of IADA requires two steps: During the so-called *Knowledge Representation* the *Structured Model of the VLBI Data Analysis Procedure* has to be transformed and stored in the knowledge base of the expert system. The problem of how to represent the knowledge of the VLBI data analysis procedure has already been described in [1]. In addition, a user interface has to be developed as well as an interface to exchange data and information between the existing software and the expert system. Both interfaces have been implemented within the existing analysis software, i.e. within the Mark IV data analysis system. The interface between SOLVE and IADA allows use of the existing software in conjunction with the expert system by applying the appropriate program for the different tasks of the VLBI data analysis. In principle IADA is responsible for the control of the data analysis process, for the evaluation of analysis results and for the detection and solution of problems (cf. figure 2). On the other hand the number crunching, the setting of parameters, the plotting of residuals, etc. is done further on in SOLVE.

A schematic representation of the embedded expert system for the automation of the VLBI data analysis is shown in figure 3. The main components are the existing SOLVE software package and the expert system (IADA). Some modules within SOLVE have been modified in order to allow an automatic data processing (dashed boxes). The boxes with a grey background are new automatic modules: GAMBSOL allows resolution of group delay ambiguities, CBREAK finds clock breaks, OUTLIER is an algorithm for outlier detection, IADAO is the user-interface for IADA and INTF is the interface to exchange data, information and commands between SOLVE and IADA.

IADAO allows the analyst to specify all information necessary for the automatic data analysis, e.g. database name, current step and substep of the analysis, application of IADA in interactive or automatic mode, and so on (cf. figure 4). This includes several configuration settings to control the automatic analysis (cf. figure 5). It can be specified, for example, whether to generate a comprehensive report in the form of web pages including several plots and protocol files. Beneath IADA the interface INTF is the most important component of the system. It consists of two main modules: `Solve->Iada` extracts on request of IADA all necessary information from the *work files* for further processing in IADA; `Iada->Solve` reads the results and instructions from IADA, makes appropriate changes in the *work files* and calls the appropriate programs to perform the instructions given by IADA.

4. Results

The embedded expert system has been applied to analyze 50 INTENSIVE sessions and 30 24 h experiments. All INTENSIVE sessions could be processed automatically and the results as well as an example of comprehensive web report are given in [2]. In the case of the 24 h experiments 70% of all experiments could be processed automatically. Most of the problems of the remaining 30% arose due to problems in solving the group delay ambiguities. However, in some cases the data could not be processed correctly because of a lack of knowledge in the expert system. This proves that expert systems can never replace a human expert because it is not possible to completely implement the expert's knowledge and problem solving strategies in an expert system. Nevertheless, IADA has shown that an embedded expert system can be used to automate the entire VLBI data analysis procedure in about 70% of the investigated 24 h experiments.

References

[1] Schwegmann, W., Automation of the VLBI Data Analysis, In: Measurement of Vertical Crustal Motion in Europe, TMR Network FMRX-CT96-0071 Scientific Report 1996-2001, J. Campbell, A. Nothnagel and R. Haas (eds.), ISBN 92-894-0763-8, 140–145, 2002.

[2] Schwegmann, W., G. Engelhardt, V. Thorandt, Towards an Operational Automatic VLBI Data Analysis Tool for INTENSIVE sessions, In: *2004 General Meeting Proceedings*, edited by N.R. Vandenberg and K.D. Baver, NASA/CP-2004-212255, this volume, 2004.

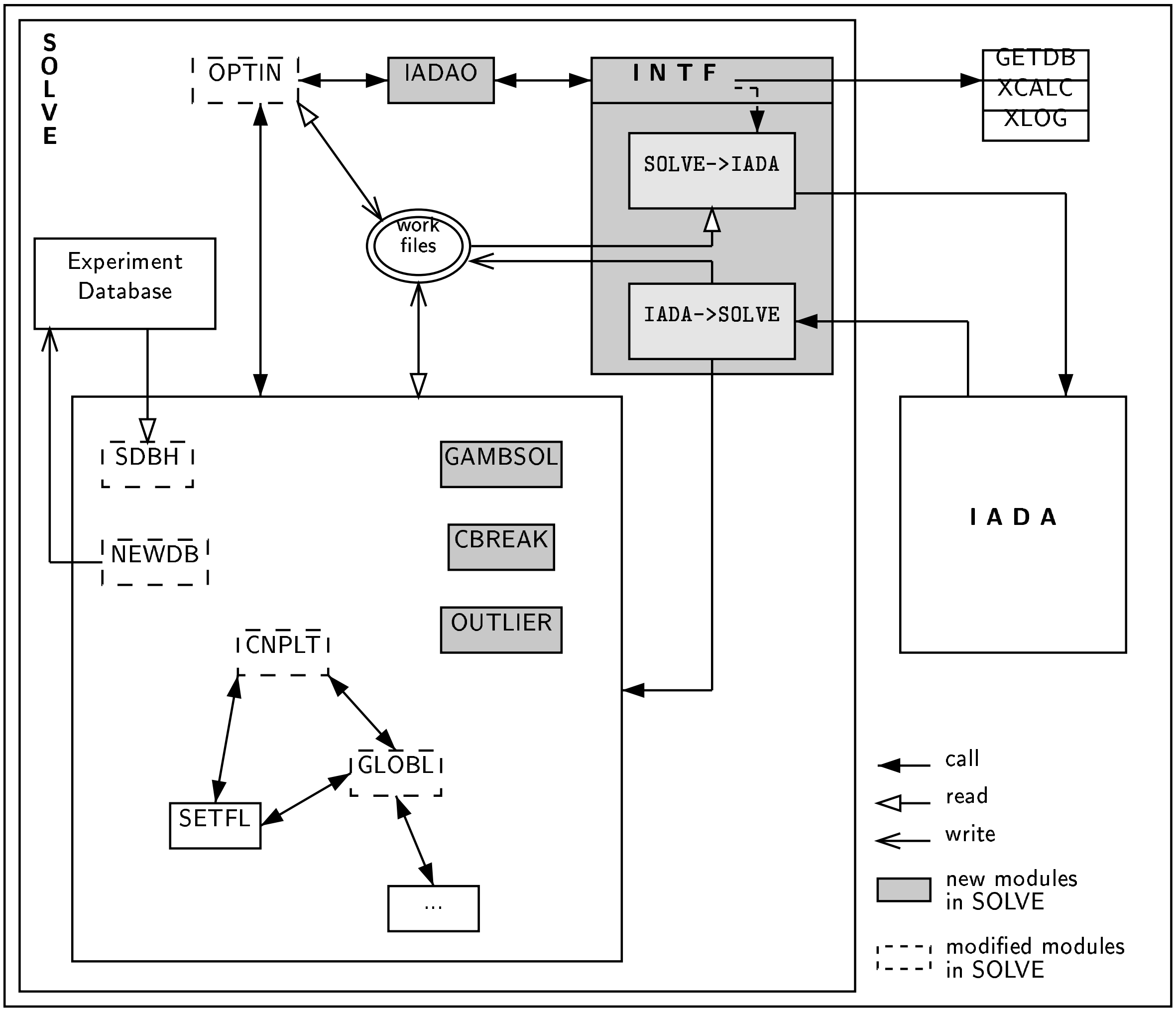

Figure 3. Schematic diagram of the embedded expert system for the automation of the VLBI data analysis.

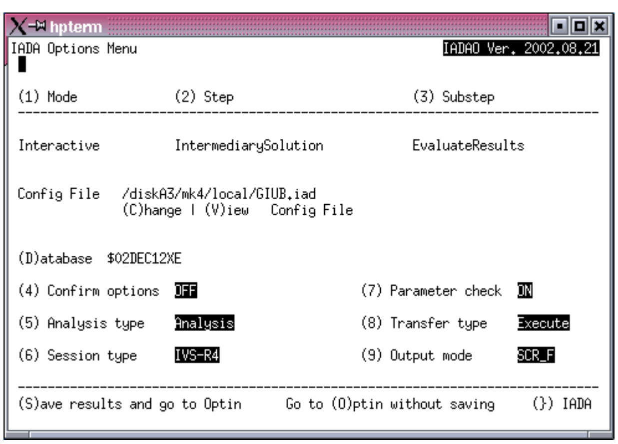

Figure 4. IADAO: The user-interface of IADA.

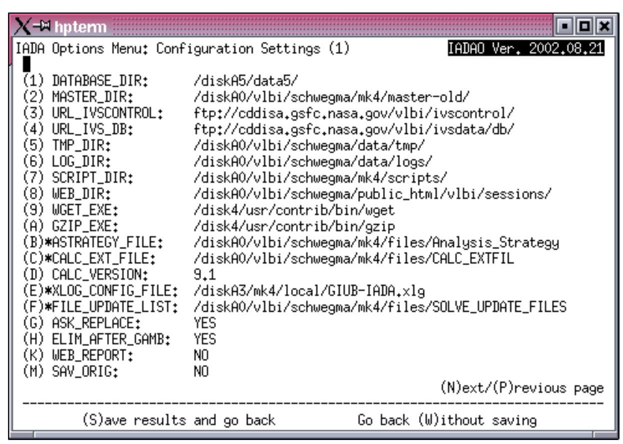

Figure 5. IADAO: Configuration settings.

Wolfgang Schwegmann et al.: Towards an Operational Automatic VLBI Data Analysis Tool for INTENSIVE Sessions
, IVS 2004 General Meeting Proceedings, p.292–295
http://ivscc.gsfc.nasa.gov/publications/gm2004/schwegmann1

Towards an Operational Automatic VLBI Data Analysis Tool for INTENSIVE Sessions

Wolfgang Schwegmann, Gerald Engelhardt, Volkmar Thorandt

Bundesamt für Kartographie und Geodäsie (BKG)

Contact author: Wolfgang Schwegmann, e-mail: `wolfgang.schwegmann@bkg.bund.de`

Abstract

Currently the delay between the time of observation and availability of UT1 results from the INTENSIVE sessions is 2-5 days. Advances in e-VLBI technology promise to considerably shorten the latency resulting from the shipment of the tapes or discs from the VLBI stations to the correlators. To avoid the additonal delay caused by the standard VLBI data analysis procedure the existing highly interactive analysis tools have to be automated to guarantee the availablity of VLBI results in near real time.

Thus, an automatic VLBI data analysis tool is being developed by the VLBI group of the Federal Agency for Cartography and Geodesy (BKG). It is realized as a new tool within the Mark IV data analysis software CALC/SOLVE and based on a software system for the automation of any geodetic VLBI experiment. The system reads a database with correlator output, sets appropriate parameterization, eliminates outliers, solves the LSQ problem and generates a detailed report on the data analysis. The time needed to generate UT1 results starting from the correlator output is less than 10 minutes. 50 INTENSIVE experiments have been analysed and the results are comparable to the *EOP-I* products available at the IVS data centers.

1. Introduction

The delay between the time of observation and the availability of results is an important disadvantage of geodetic VLBI compared to other geodetic space techniques. One reason is the complicated and highly interactive analysis procedure, requiring well-founded expertise. While advances in e-VLBI promise to considerably cut the latency, automatic VLBI analysis tools still have to be developed to obtain VLBI results in near real-time.

Thus, an automatic VLBI data analysis tool for the operational analysis of INTENSIVE sessions is being developed by the VLBI group of the Federal Agency for Cartography and Geodesy (BKG). It is based on an experimental software package called IADA (Intelligent Assistant for VLBI Data Analysis [1]). IADA has been realized as an embedded *Expert System*[1] within the Mark IV data analysis software CALC/SOLVE and can be used to perform the whole VLBI data analysis procedure automatically. Based on IADA the tool for the automation of INTENSIVE sessions has been built as an additional module within SOLVE. This module is able to automate the analysis of INTENSIVE sessions without the use of an Expert System because the analysis of INTENSIVE sessions is less complicated than the analysis of 24-h sessions.

[1]Expert Systems are software systems to model the knowledge of qualified experts for a particular domain and to use this knowledge for solving a complex problem within this domain.

2. The Automatic VLBI Data Analysis Tool

The components of the Mark IV data analysis system have been extended in order to allow an automatic processing. New modules have been developed and existing modules in SOLVE have been modified. The system executes the following operations automatically:

1. download a database from a ftp-server and import it into the catalogue system (program GET_DB, cf. figure 1);
2. run CALC, i.e. build the CALC control file, check all input data, start CALC and check the results (program XCALC, cf. figure 2);
3. download log-files, extract and check calibration data, save the data into calibration files and include the data into the database by calling program DBEDIT (program XLOG, cf. figure 3 and 4);
4. load the database into scratch files;
5. set a priori clock model;
6. resolve group delay ambiguities;
7. set parameterization;
8. find preliminary solution;
9. eliminate outliers;
10. find final solution;
11. generate detailed report on the data analysis (cf. figure 5)

The automatic data analysis is controlled by a new module within SOLVE. This module calls the appropriate program or SOLVE module for each of the above steps. To perform the automatic data analysis the analyst only has to specify the experiment name to be analysed and a configuration file containing all information necessary for the automatic data analysis.

3. Results and Outlook

The new tool for the automatic VLBI data analysis has been used to analyse 50 INTENSIVE sessions between September 2002 and April 2003. All experiments could be processed automatically without any problems with an average processing time of about 10 minutes. The results have been compared to those from the *EOP-I* products of the IVS Analysis Centers (BKG, GSFC, IAA, SPU) available at the IVS Data Center. Figure 6 shows the differences from each series to the average of all series. The results of the automatic tool (IADA) are comparable to those of the IVS Analysis Centers.

To use the new tool for an operational automatic VLBI data analysis some tasks have still to be solved. After loading the databases into the scratch files an initial quality control has to be done and at the end of the analysis methods of quality control have to be developed. As soon as these tasks have been solved an operational automatic VLBI data analysis of INTENSIVE sessions will be possible.

References

[1] Schwegmann, W., Automation of the VLBI Data Analysis, In: Measurement of Vertical Crustal Motion in Europe, TMR Network FMRX-CT96-0071 Scientific Report 1996-2001, J. Campbell, A. Nothnagel and R. Haas (eds.), ISBN 92-894-0763-8, 140–145, 2002.

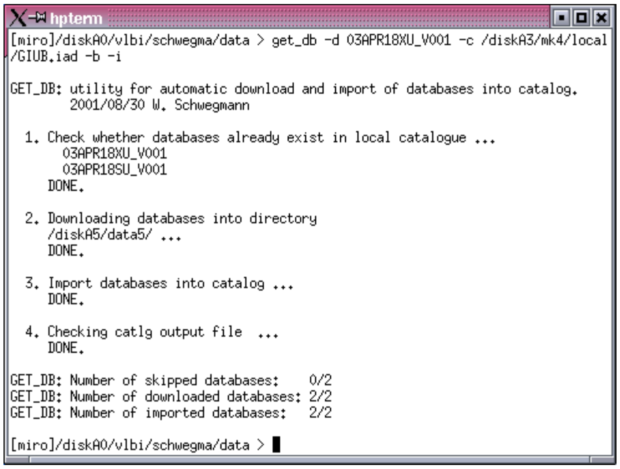

Figure 1. Program GET_DB.

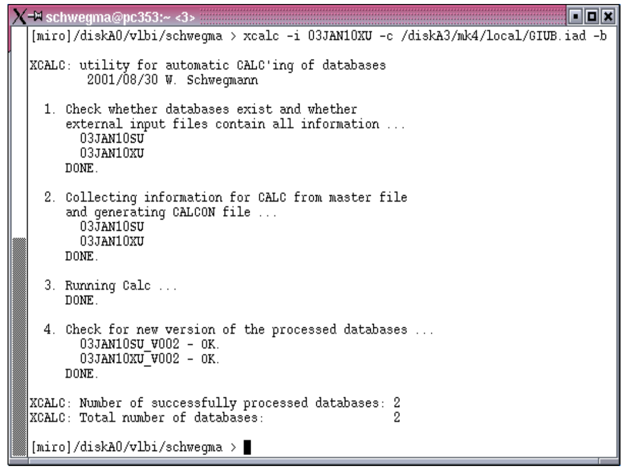

Figure 2. Program XCALC.

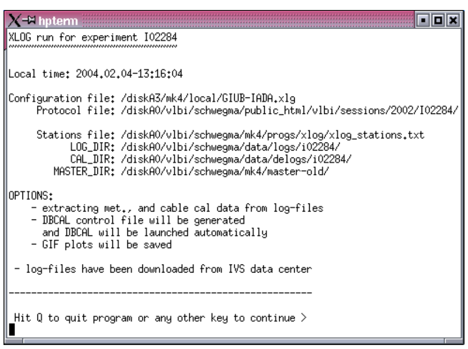

Figure 3. Program XLOG – initialization window.

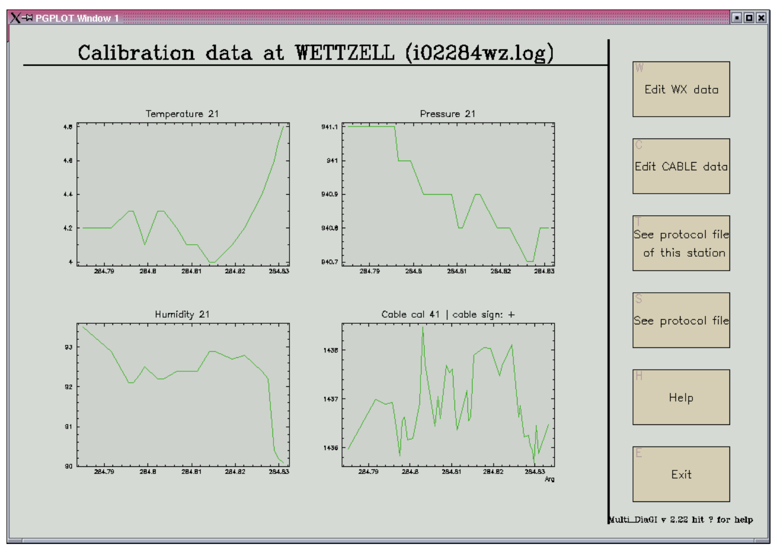

Figure 4. Program XLOG – data manipulation window.

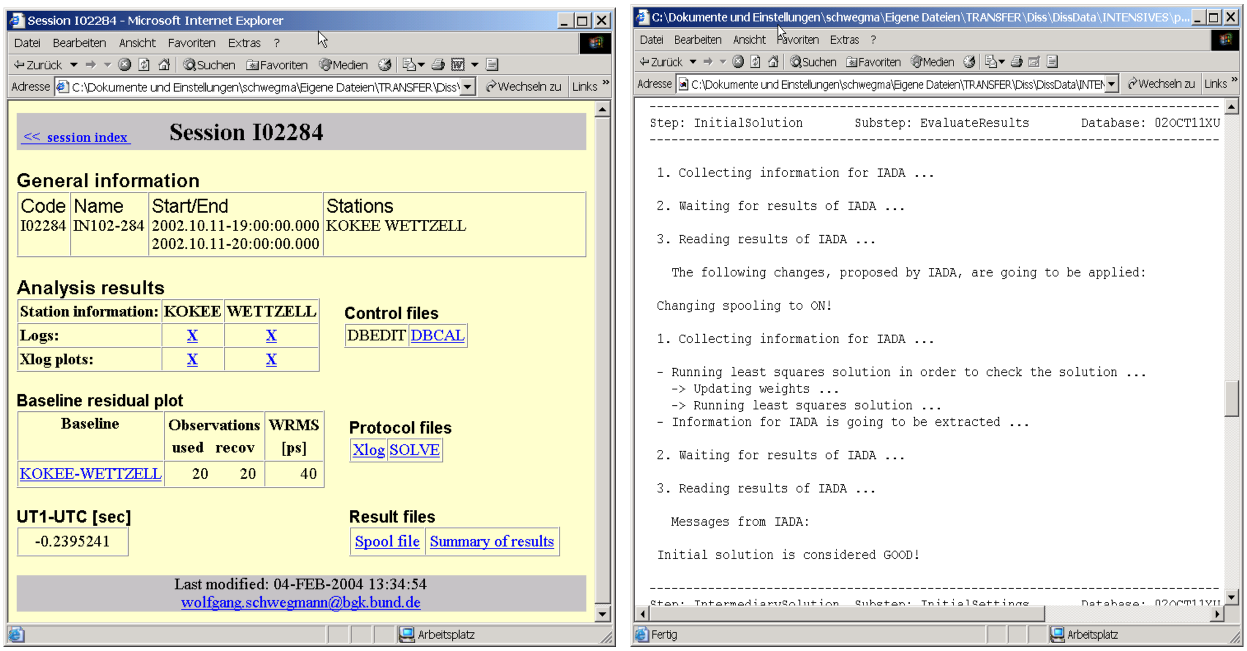

Figure 5. *Left:* Web-Site with detailed information on the data analysis; from this site all results of the analysis as well as several protocol files and plots can be viewed. *Right:* Protocol file containing all information with respect to the automatic data analysis.

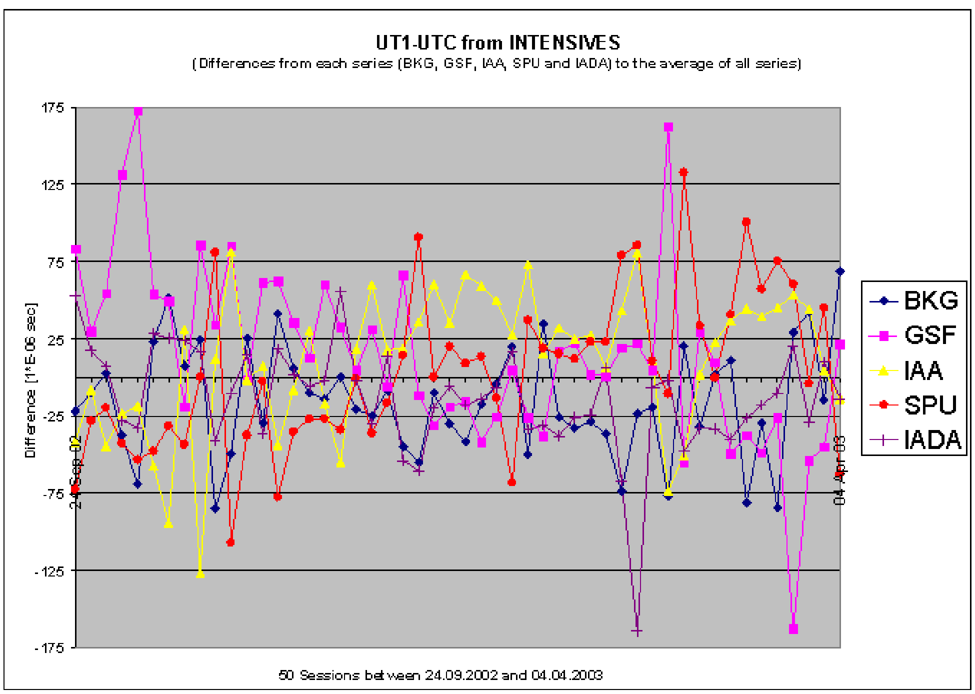

Figure 6. Results of the analysis of 50 INTENSIVE sessions obtained by the new automatic tool (IADA) compared to the EOP-I series of the IVS Analysis Centers.

Volker Tesmer et al.: An Advanced Stochastic Model for VLBI Observations and its Application to VLBI Data Analysis, IVS 2004 General Meeting Proceedings, p.296–300
http://ivscc.gsfc.nasa.gov/publications/gm2004/tesmer1

An Advanced Stochastic Model for VLBI Observations and its Application to VLBI Data Analysis

Volker Tesmer, Hansjörg Kutterer

DGFI, Deutsches Geodätisches Forschungsinstitut

Contact author: Volker Tesmer, e-mail: tesmer@dgfi.badw.de

Abstract

Further refinements of the functional representation of the geometric-physical properties of the VLBI observations mostly need big efforts and are not possible with any precision. Although the stochastic model is an important part of the VLBI observation equations, the stochastic properties of VLBI observations have not been studied in detail so far. The idea is to interpret discrepancies between the functional model and the observations as variances of the observations. In particular, the characterisation of station and elevation dependent influences is of limited precision. Remaining influences can be modelled by specific stochastic properties of the observations. This paper focusses on the application of a refined stochastic model of the observations to the estimation of VLBI parameters.

1. Refinement of the Traditional Stochastic Model of VLBI Observations

The traditional stochastic VLBI model $\mathbf{\Sigma}_{yy}$ consists of a factor σ_0^2 to describe the common variance level and the cofactor matrix $\mathbf{Q}$ of all observations. $\mathbf{Q}$ is composed of the variances σ_i^2 of the n observations (i=1,2,...,n), derived from the correlation process (approximated by the SNR, see [3]) and a constant σ_{const}^2 to consider quasi-random deficiencies in the functional model:

$$\mathbf{\Sigma}_{yy} = \sigma_0^2\mathbf{Q} = \sigma_0^2 \; (\; diag(\sigma_1^2, \sigma_2^2, ..., \sigma_n^2) + \sigma_{const}^2 \;) \; . \tag{1}$$

Deficits of the traditional stochastic VLBI model are to be expected in station, elevation and source dependent parts of the observations' variances. Additionally, the value of the additive constant is usually only roughly known. VLBI observations are also correlated with each other (caused by the correlation process, due to deficits of the tropospheric modelling and deficits of the modelling of the station coordinates). This has been neglected so far. Until now, their values were not determined by means of rigorous methods (for details see [4] or [5]).

The refined stochastic model (eq. 2) is in contrast to the traditional stochastic model (eq. 1) more differentiating, because it allows us to describe more than just one stochastic quantity (σ_0^2 to describe the common variance level of all observations):

$$\mathbf{\Sigma}_{yy} = \theta_1\mathbf{V}_1 + \theta_2\mathbf{V}_2 + ... + \theta_k\mathbf{V}_k \; = \; \textstyle\sum_{m=1}^{k} \theta_m \mathbf{V}_m \; . \tag{2}$$

If, e.g., θ_1 shall describe the common variance level only for the observations i=1 and i=2, the corresponding matrix must simply be chosen to be $\mathbf{V}_1 = diag(\sigma_1^2, \sigma_2^2, 0, ..., 0)$. An additive constant for all observations (e.g. called θ_2) can be characterised with $\mathbf{V}_2$ being an identity matrix. θ_3 can represent a correlation coefficient of the observations i=1 and i=2 if $\mathbf{V}_3$ is an empty matrix except the elements $\mathbf{V}_3(1,2) = \mathbf{V}_3(2,1) = \sqrt{(\sigma_1^2 \cdot \sigma_2^2)}$.

2. Estimated Variance Components of the Refined of the Stochastic Model

The components of the type according to section 1 were determined by means of a Minimum Norm Quadratic Unbiased Estimation (MINQUE) as described in [1, p. 246f] or [2, p. 303f]. For all assumed deficits of the traditional stochastic model, corresponding components could be estimated. Concerning the correlations between observations it was found that in present solutions VLBI observations can be considered as almost uncorrelated (a largest value of 0.2 was detected due to the correlation process).

In contrast, some of the deficits of the variances of the traditional stochastic model (especially the station and elevation dependent parts) were found to be very significant and clear. Therefore the refined stochastic model was chosen to consist of the following parts (values and their formal errors see table 1, graphically displayed in figure 1):

$$\begin{aligned}\mathbf{\Sigma}_{yy} &= \theta_{var\ level}\mathbf{V}_{var\ level} \\ &+ \theta_{additive}\mathbf{V}_{additive} \\ &+ \sum_{j=1}^{47}\theta_{station^A\ j}\mathbf{V}_{station^A\ j} + \sum_{j=1}^{47}\theta_{station^B\ j}\mathbf{V}_{station^B\ j} \\ &+ \sum_{m=1}^{8}\theta_{elev^A\ m}\mathbf{V}_{elev^A\ m} + \sum_{m=1}^{8}\theta_{elev^B\ m}\mathbf{V}_{elev^B\ m} \quad .\end{aligned} \tag{3}$$

Table 1. 57 components for the refined stochastic model of VLBI observations.

type of θ	**est.**	**value θ**	**type of θ**	**est.**	**value θ**	**type of θ**	**est.**	**value θ**
var level	0.395	± 0.0011	PIETOWN	0.145	± 0.0093	FORTLEZA	0.145	± 0.0049
additive	0.206	± 0.0012	NRAO 140	0.281	± 0.0463	MK-VLBA	0.309	± 0.0132
WESTFORD	0.168	± 0.0034	DSS45	0.120	± 0.0168	OV-VLBA	0.193	± 0.0126
HRAS 085	0.459	± 0.0084	NRAO85 3	0.238	± 0.0058	CRIMEA	0.351	± 0.0140
MOJAVE12	0.190	± 0.0051	NOTO	0.209	± 0.0085	NYALES20	0.174	± 0.0046
RICHMOND	0.312	± 0.0056	HOBART26	0.270	± 0.0135	NRAO20	0.103	± 0.0047
WETTZELL	0.062	± 0.0032	KASHIM34	0.352	± 0.0222	YEBES	0.265	± 0.0150
ONSALA60	0.149	± 0.0048	MATERA	0.157	± 0.0052	URUMQI	0.023	± 0.0167
KASHIMA	0.321	± 0.0091	LA-VLBA	0.075	± 0.0064	TSUKUB32	0.081	± 0.0108
HATCREEK	0.432	± 0.0226	EFLSBERG	-0.079	± 0.0159	$\varepsilon = 5° - 8°$	1.213	± 0.0111
OVRO130	0.235	± 0.0252	FD-VLBA	-0.183	± 0.0051	$\varepsilon = 8° - 11°$	0.769	± 0.0074
HAYSTACK	0.350	± 0.0181	SANTIA12	0.304	± 0.0194	$\varepsilon = 11° - 15°$	0.570	± 0.0056
KAUAI	0.322	± 0.0067	KP-VLBA	0.399	± 0.0136	$\varepsilon = 15° - 20°$	0.396	± 0.0045
GILCREEK	0.072	± 0.0032	NL-VLBA	0.306	± 0.0112	$\varepsilon = 20° - 30°$	0.249	± 0.0031
KWAJAL26	0.338	± 0.0252	HN-VLBA	0.569	± 0.0187	$\varepsilon = 30° - 45°$	0.103	± 0.0026
ALGOPARK	0.067	± 0.0051	OHIGGINS	0.401	± 0.0432	$\varepsilon = 45° - 65°$	0.034	± 0.0024
HARTRAO	0.205	± 0.0084	BR-VLBA	-0.071	± 0.0073	$\varepsilon = 65° - 90°$	(0)	(± 0)
MEDICINA	0.076	± 0.0059	DSS15	0.023	± 0.0154			
SESHAN25	0.319	± 0.0140	KOKEE	0.160	± 0.0040			
DSS65	0.097	± 0.0090	SC-VLBA	0.948	± 0.0178			

In earlier investigations (e.g. [4] or [5]), some of the estimated variance components were doubtful or not representative, respectively. Most of them were not determined from a sufficiently large number of observations, like the components for most of the VLBA telescopes, YEBES and EFLSBERG, as well as the components for the observations below 5° elevation. Here, the observations of additional sessions were added to the analysis (now 2211 sessions instead of 2124) and the observations below 5° were strictly removed from the analysed data sets. As a consequence, all of the 57 components can be considered as stable and reliable estimates (see also section 4).

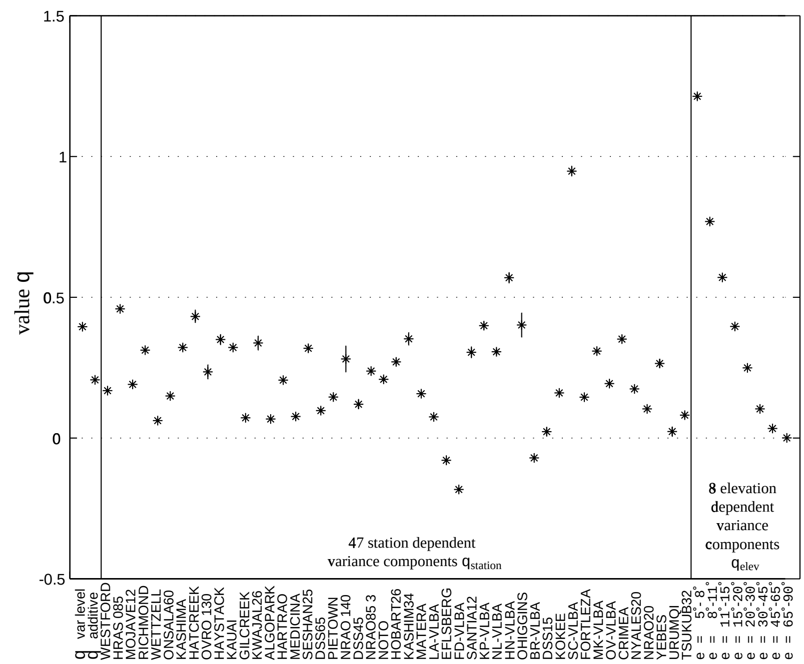

Figure 1. 57 components for the refined stochastic model of VLBI observations.

3. Indirect Influence of the Refined Stochastic Model on Parameter Estimations

When applying the refined stochastic model to parameter estimations, care has to be taken regarding indirect effects which are mainly connected with (for details see [4]):

- the weights and the respective impact of the pseudo observations for the constraints of auxiliary clock and tropospheric parameters,
- the power of outlier tests which compare observations' residuals with their formal errors,
- influence of observations under very low elevations, which can decisively affect the variances of the tropospheric parameters as well as their covariances with station positions, the EOP and the parameters of the station clocks.

The following readjustments yielded optimum efficiency of the refined stochastic model with respect to improved parameter estimations:

- change the weights of the constraints for:
  - 1 h rates of the PWLF for the tropospheric ZD from 15 mm/h to 10 mm/h,
  - 1 h rates of the PWLF for the clocks from 40 mm/h to 30 mm/h,
  - 24 h gradient offsets from 0.3 mm to 0.5 mm,
- change the criterion for outlier rejection from 3 σ to 3.5 σ,
- change the cut off angle from 8° to 5°.

4. Important Aspects Concerning the Applicability to VLBI Sessions

The estimated components were tested in several ways concerning their stability (w.r.t. time dependencies, dependencies due to network configurations, etc.). It could very clearly be shown, that they represent all VLBI data used at DGFI (more than 2000 sessions between 1984 and 2001).

As the traditional stochastic model of the observations is suspected to have deficiencies which are at least partially due to functionally not ascertainable differences between the functional model and the observations, it is assumed that the estimated components are dependent on the functional model used. However, investigations showed clearly that the results of a MINQUE are quite insensitive to slight changes in the parameterisation like fixing or estimating station positions. Significant changes could only be created artificially like e.g. by upweighting pseudo-observations in the solutions by the factor 100 (pseudo-observations are by default used to stabilise auxiliary troposphere and clock parameters by constraining them to the value zero with a certain empirically derived variance). This indicates clearly that the estimated components can be applied to all standard VLBI solutions.

Because of (partially large) dependencies between estimated components, it is not recommended to restrict the model to parts of the set of components. This means that always all six components (one for the variance level, one for the additive part, two for the telescopes and two for the elevations) have to be applied according to eq. 3. If not, the derived variance-covariance matrix $\boldsymbol{\Sigma}_{yy}$ might be distorted or even meaningless.

5. Application of the Refined Stochastic Model

One of the major motivations for the investigations concerning the stochastic model of the observations was to improve VLBI solutions. In the following sections 5.1 and 5.2, two different solution setups are described, which are mostly suitable for such tests.

5.1. Repeatability of Estimated Station Positions of the Refinements

For 2211 sessions between 1984 and 2001, station positions were computed session by session. The datum for each single session was NNR (no-net-rotation) and NNT (no-net-translation) w.r.t. a solution for station positions and velocities, computed from all these 2211 sessions in order to avoid systematic discrepancies which could distort the results. As all knowledge concerning the time dependent physical behaviour of the station positions was modelled a priori, it is assumed that the smaller (or less significant, respectively) the residual position estimates are, the better is the modelling of the corresponding observations.

Table 2. Repeatability of estimated station positions, determined from 2211 sessions.

	$\frac{\mathbf{RMS_{new}}}{\mathbf{RMS_{old}}}$	$\frac{\mathbf{WRMS_{new}}}{\mathbf{WRMS_{old}}}$
latitute	95.9 %	97.4 %
longitude	95.8 %	96.6 %
radial	96.8 %	99.9 %

The results indicate very clearly that the estimated parameters improve in the meaning as described before. In contrast to the preliminary results presented in [4], most of the results also became more realistic concerning their formal errors (except the radial components).

5.2. Similarity of EOP from Simultaneous NEOS-A and CORE-A Sessions

134 of the VLBI sessions stored at DGFI were carried out simultaneously by the two independently observing NEOS-A and CORE-A networks (start and end time of the respective schedules differed less than 15 minutes). Daily EOP were computed for each single session, fixing the TRF

to a solution for station positions and velocities (as mentioned in the last section) to avoid systematic differences due to inhomogenities of the TRF. For this test it is assumed that the better the modelling of the observations is, the smaller (or less significant, respectively) are the differences between the estimated corrections to the EOP determined from the two networks.

Table 3. Similarity of EOP from 67 pairs of simultaneous NEOS-A and CORE-A sessions.

	$\frac{\mathbf{RMS_{new}}}{\mathbf{RMS_{old}}}$	$\frac{\mathbf{WRMS_{new}}}{\mathbf{WRMS_{old}}}$
$\mathbf{X_P}$	99.2 %	98.6 %
$\mathbf{Y_P}$	88.0 %	87.2 %
ΔUT1	95.4 %	94.0 %
PSI	83.6 %	88.7 %
EPS	99.8 %	98.8 %

Similar to the results presented in the last section, the estimated parameters improve. Nevertheless, the refinements of the stochastic model do not influence all EOP the same way, which has not yet been fully understood. Maybe this is due to the small number of data points (67 only), whereby these estimates represent a certain network and/or observing geometry only.

6. Conclusions and Outlook

The presented results demonstrate very clearly that the largest deficiencies of the traditional stochastic model are found in its station and elevation dependent attributes. Another result was that in present solutions, VLBI observations can be considered as almost uncorrelated. Refinements of the stochastic model can be applied to almost all standard VLBI solutions, no matter if the primary target parameters are the EOP or station positions. Furthermore, it became very clear that standard VLBI solutions can be improved using the refined stochastic model. Even further improvements of this approach could be achieved by a more sophisticated description of stochastical properties of VLBI observations such as a function which models a station-wise elevation dependent weighting. But, one has to consider that further progress in the functional modelling of the VLBI observations (like, e.g., an improved description of the tropospheric influences) may affect the corresponding stochastic attributes significantly.

This research has made use of the IVS VLBI observation data. It was partially supported by the German research association “Deutsche Forschungsgemeinschaft (DFG)”, contract (DR 143/11-1).

References

[1] Koch, K.-R.: Parameter Estimation and Hypothesis Testing in Linear Models. Springer, Berlin, New York, 1999

[2] Rao, C.: Linear Statistical Inference and its Applications. John Wiley & Sons, New York, 1973

[3] Schuh, H., J. Campbell: VLBI in Geodynamical Investigations. Acta Geod. Geophys. Hung., Vol. 29 (3-4) 397-420, 2000

[4] Tesmer, V.: Refinement of the Stochastic VLBI Model: First Results. In: W. Schwegmann, V. Thorandt (eds): Proceedings of the 16^{th} Working Meeting on European VLBI for Geodesy and Astrometry, Bundesamt für Kartographie und Geodäsie, Frankfurt/Leipzig, 207-218, 2003

[5] Tesmer, V.: Das stochastische Modell bei der VLBI-Auswertung. Verlag der Bayerischen Akademie der Wissenschaften, Reihe C, Heft Nr. 573, München, in press, 2004

Hansjörg Kutterer: Reliability Measures for Geodetic VLBI Products, IVS 2004 General Meeting Proceedings, p.301–305
http://ivscc.gsfc.nasa.gov/publications/gm2004/kutterer

Reliability Measures for Geodetic VLBI Products

Hansjörg Kutterer

Deutsches Geodätisches Forschungsinstitut (DGFI)
e-mail: kutterer@dgfi.badw.de

Abstract

The reliability of geodetic VLBI products depends essentially on the checkability of the observation data and the reference frame points. In statistics, reliability has two meanings. The first one deals with the detectability of incomplete or incorrect parts of the model by means of statistical hypothesis tests (internal reliability). The second one studies the impact of non-detectable model errors on the estimated parameters (external reliability). In this paper the theoretical background of reliability is shortly reviewed. The focus lies on its application to the estimation procedure with respect to possible errors in the reference frame. The potential influence of non-detectable errors in the station and source coordinates on VLBI products is presented and discussed based on the data from the CONT02 campaign.

1. Theoretical Background

Precision and reliability are quality issues of their own right. Whereas precision measures such as formal errors or error ellipses, respectively, can already be computed from minimum observation configurations, reliability measures are only meaningful in the case of sufficient partial redundancy. In other words, each observation must be checkable by at least some other observations. Such a check is based on a statistical hypothesis test.

Two different forms of reliability can be distinguished. On the one hand, internal reliability describes the detectability of errors in the data and is quantified by means of, e.g., the marginally detectable blunder in a hypothesis test with a certain Type I error probability α. The associated probability for successful blunder detection is the test power $1 - \beta$ with β the Type II error probability. On the other hand, external reliability means the maximum influence of a non-detected blunder on the parameters of interest. For details see [1] or [2].

In VLBI data three types of data are of interest: the original delay observations, the parameter soft constraints in terms of pseudo-observations, and hard constraints for datum definition in terms of condition equations. In this paper only the third type is considered as the focus lies on possible outliers in the (terrestrial or celestial) reference frame positions. The terrestrial datum components are defined by means of a NNT (No Net Translation) and a NNR (No Net Rotation) condition with respect to the ITRF2000. The celestial datum components are defined by means of a NNR condition with respect to the ICRF.

The basic test idea is that the datum definition should be identical (in a statistical meaning) for each arbitrarily chosen set of datum points. Hence, the estimated parameters based on a datum definition using all stations and sources should be approximately the same as those derived from a datum definition when, e.g., one arbitrary datum point is discarded. In the following this is briefly described in mathematical terms.

The datum defining condition equation for the parameter updates $\mathbf{\Delta x}$ reads as

$$\mathbf{G}\ \mathbf{\Delta x} = \mathbf{0}. \qquad (1)$$

The constraint matrix $\mathbf{G}$ is represented in transposed form point by point as

$$\mathbf{G}^T = \begin{bmatrix} \mathbf{G}_1^T & \mathbf{G}_2^T & \ldots & \mathbf{G}_n^T \end{bmatrix}. \tag{2}$$

with

$$\mathbf{G}_i = \begin{bmatrix} \mathbf{G}_{terr,NNT,i} & \mathbf{G}_{terr,NNR,i} & \mathbf{G}_{cel,NNR,i} \end{bmatrix}. \tag{3}$$

In case of terrestrial datum points (stations) it is

$$\mathbf{G}_{terr,NNT,i} = \begin{bmatrix} 1 & 0 & 0 \\ 0 & 1 & 0 \\ 0 & 0 & 1 \end{bmatrix}, \quad \mathbf{G}_{terr,NNR,i} = \begin{bmatrix} 0 & -z_i & y_i \\ z_i & 0 & -x_i \\ -y_i & x_i & 0 \end{bmatrix}, \quad \mathbf{G}_{cel,NNR,i} = \mathbf{0} \tag{4}$$

and in case of celestial datum points (radio sources)

$$\mathbf{G}_{terr,NNT,i} = \mathbf{0}, \quad \mathbf{G}_{terr,NNR,i} = \mathbf{0}, \quad \mathbf{G}_{cel,NNR,i} = \begin{bmatrix} \cos(RA)\cdot\sin(DE) & -\sin(RA) \\ \sin(RA)\cdot\sin(DE) & \cos(RA) \\ \cos(DE) & 0 \end{bmatrix}. \tag{5}$$

The remaining entries are all equal to 0. The definition of two different geodetic datums based on the same set of reference points can be described by

$$\mathbf{G}_1 = \mathbf{P}_1\mathbf{G}, \quad \mathbf{G}_2 = \mathbf{P}_2\mathbf{G} \tag{6}$$

where $\mathbf{P}_1$ and $\mathbf{P}_2$ denote two selection matrices, i.e., diagonal matrices with entries 1 on the main diagonal for datum point coordinates and 0 for all other parameters. The parameter differences and their cofactor matrix, respectively, are then given by

$$\mathbf{w} = (\mathbf{S}_2 - \mathbf{S}_1)\Delta\mathbf{x}, \quad \mathbf{Q}_{\mathbf{ww}} = (\mathbf{S}_2 - \mathbf{S}_1)\ \mathbf{Q}_{\mathbf{xx}}\ (\mathbf{S}_2 - \mathbf{S}_1)^T. \tag{7}$$

with $\mathbf{Q}_{\mathbf{xx}}$ the cofactor matrix of $\mathbf{\Delta x}$ and the matrices $\mathbf{S}_1$ and $\mathbf{S}_2$ for the projection of $\mathbf{\Delta x}$ into the two different datums

$$\mathbf{S}_1 = \mathbf{I} - \mathbf{G}\left(\mathbf{G}^T\mathbf{P}_1\mathbf{G}\right)^{-1}\mathbf{G}^T\mathbf{P}_1, \quad \mathbf{S}_2 = \mathbf{I} - \mathbf{G}\left(\mathbf{G}^T\mathbf{P}_2\mathbf{G}\right)^{-1}\mathbf{G}^T\mathbf{P}_2. \tag{8}$$

A proper test statistic for the significance of the parameter difference is given by

$$T = \frac{1}{\sigma^2}\mathbf{w}^T\mathbf{Q}_{\mathbf{ww}}^{-}\mathbf{w} \sim \begin{cases} \chi^2_{3,\lambda}, & \text{for terrestrial stations} \\ \chi^2_{2,\lambda}, & \text{for radio sources} \end{cases} \tag{9}$$

with the formal variance factor σ^2, the superscript "-" denoting a reflexive generalized inverse and with the non-centrality parameter $\lambda = \lambda(\alpha, \beta)$ which is characterized by

$$\lambda \quad \begin{cases} = 0 & |H_0 : E(\mathbf{w}) = \mathbf{0} \\ > 0 & |H_a : E(\mathbf{w}) \neq \mathbf{0} \end{cases} \tag{10}$$

Here H_0 denotes the null hypothesis ("identical datum by $\mathbf{G}_1$ and $\mathbf{G}_2$") and H_a the alternative hypothesis ("non-identical datum").

The results presented in the following sections were derived from 14 days (October 17-30, 2002) of the CONT02 campaign. For the computations a preliminary extension of the software package OCCAM 6.0 (see [3]) was used permitting the estimation of source coordinates. The source and station coordinates were estimated from the normal equations system which was accumulated over the complete campaign. All other parameters were removed in advance in a rigorous way.

2. Influence of Datum Point Selection

2.1. Station Effects

In a first scenario the terrestrial stations are tested according to Eq. (9). Two datum definitions are compared. The first datum is defined by the coordinates of all stations. The second datum is defined by taking all points but one as datum points. Hence, the greater the value of the test statistics, the less compatible is the estimated position of this point and its reference frame position. If all values are small or at least on the same level, the null hypothesis seems to be quite likely. A clear hint regarding a lacking compatibility is given if there is a particular test value significantly greater than the others.

The results are shown in figure 1. If all eight stations which participated in the CONT02 campaign are selected as datum points, the test statistic values presented in the back row are obtained (dark grey). There is a clear indication of ONSALA60 and a minor indication of GILCREEK. In a next step ONSALA60 is discarded in advance so that it does not influence the reference datum. The corresponding values are given in the front row (light gray). Note that GILCREEK is not indicated any longer. The situation looks now quite homogeneous. Obviously the ITRF 2000 position and the estimated position of ONSALA60 during the CONT02 campaign do not agree well. Taking some reference frame noise level into account the positions of the other stations are rather consistent.

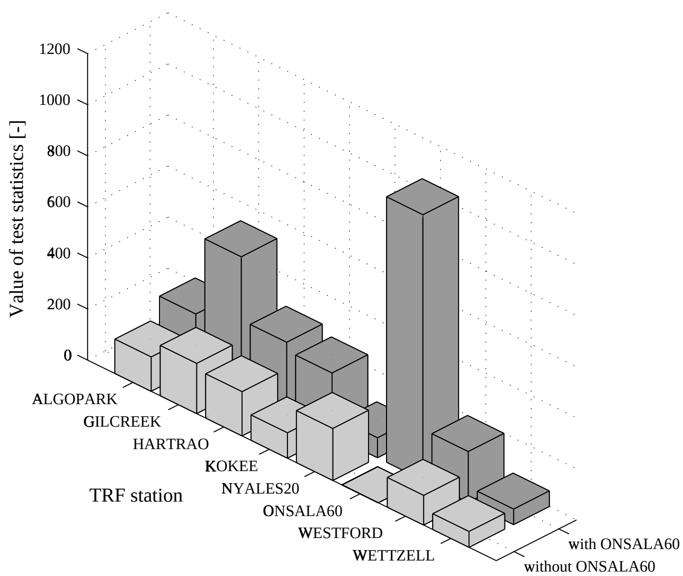

Figure 1. Test statistic values if the respective station is discarded from the datum definition. If ONSALA60 is discarded before testing, the values of the other stations are reduced and homogenized significantly.

The most important results concerning possible discrepancies between the estimated and the reference positions are the following. The coordinate uncertainty induced by the datum point selection is about 2 mm, the biases detectable by the test according to Eq. (9) (considering $\lambda = 10.90$ derived from $\alpha = 0.05$ and $\beta = 0.2$) are less than 3.6 mm on average and less than 10.7 mm at maximum. Hence, the datum point selection for the CONT02 is rather uncritical for the estimated station positions.

2.2. Radio Source Effects

In a second scenario the radio source positions are tested as it was outlined in Section 2.1. Again, the initial datum was defined using all sources. Afterwards, one particular source was discarded from the definition of the datum. This was done in turn for all sources. The values of the test statistics are presented in figure 2. It can clearly be seen that some of the sources have significantly larger values than the others. Again, this points to discrepancies between the estimated and the reference positions.

Reliability ellipses (see figure 3) can be calculated based on the test statistics according to Eq. (9) in order to assess the detectable errors in a reference point position. These ellipses represent the locus of an erroneous position which can be detected with $\beta = 0.2$ when testing with $\alpha = 0.05$ according to Eq. (9). The smaller the ellipses, the higher is the reliability. Significant semimajor axes indicate directions with low reliability. Hence, the sources with mean declination are rather reliable whereas the others reveal some deficiencies. Note that the size and orientation of the ellipses is mainly caused by the session configuration and scheduling. There is no clear assignment of the reliability measures to the ICRF classes ("defining", "candidate", "others").

The coordinate uncertainty of the radio sources induced by the datum point selection is about 10 μas, the biases detectable by the test according to Eq. (9) (considering $\lambda = 9.63$ derived from $\alpha = 0.05$ and $\beta = 0.2$) are less than 0.24 μas on average and less than 3 mas at maximum. Hence, the datum point selection for the CONT02 is mostly uncritical for the estimated source positions. Note that there isn't any impact on the estimated station positions and vice versa.

2.3. EOP Effects

In order to assess the influence of possibly erroneous datum point positions on the EOP, the reference datum was defined using all stations and all sources. An alternative datum was defined by discarding the station ONSALA60 and the radio sources 0106+013 and 4C39.25 which were indicated by the tests. The effect of the two different datums on the EOP turned out to be mainly a constant offset. For the pole coordinates -14 μas (x-component) and +45 μas (y-component) were found. The offset in Universal Time (ΔUT1) yielded +13 ms. In case of nutation the offset in obliquity was stable (+4 μas) whereas the values of the offset in longitude varied about an average value of -10 μas. Although these effects are rather small, they indicate the possible amount of biases in the parameters due to typical inconsistencies in the reference frames.

3. Conclusions

Proper reliability measures for VLBI products can be derived in a rigorous way using statistical test theory as background. The reliability analysis of the CONT02 campaign is well-suited for the illustration of the procedure but the presented results must not be overrated. They are certainly capable to give some background for the interpretation of the CONT02 results. For a thorough assessment of station and source coordinates it is rather recommended to assess a large number of different VLBI sessions in the outlined way.

At present, there is one open question concerning methodology which will soon be solved: the presented reliability measures are relative as an absolute accuracy level was not yet introduced. For this purpose the test statistic according to Eq. (9) needs to be extended in order to handle empirical variances in a statistically proper way. This will be solved soon.

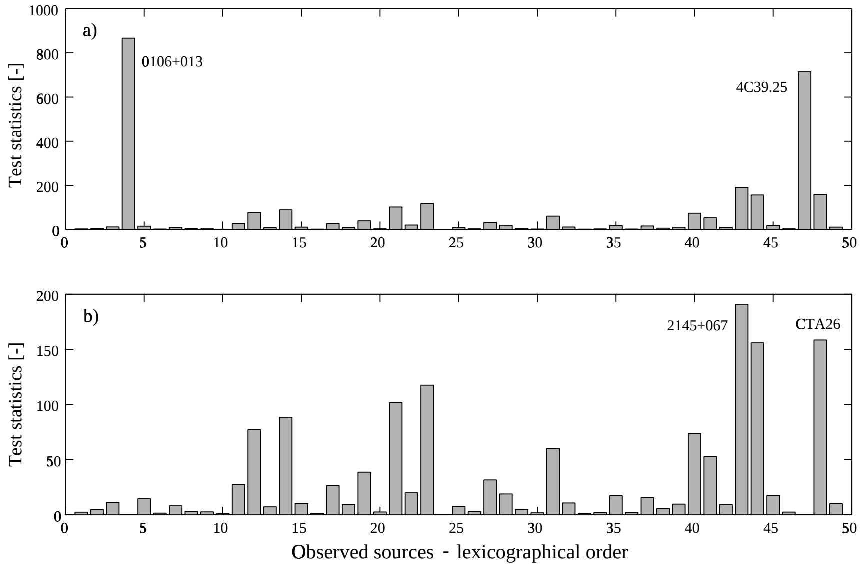

Figure 2. Test statistic values if the respective radio source is discarded from the datum definition. Note the different ranges on the y-axis. Some sources with significant test values are named. a) Datum defined using all radio sources. b) Datum defined as in a), but without the sources 0106+013 and 4C39.25.

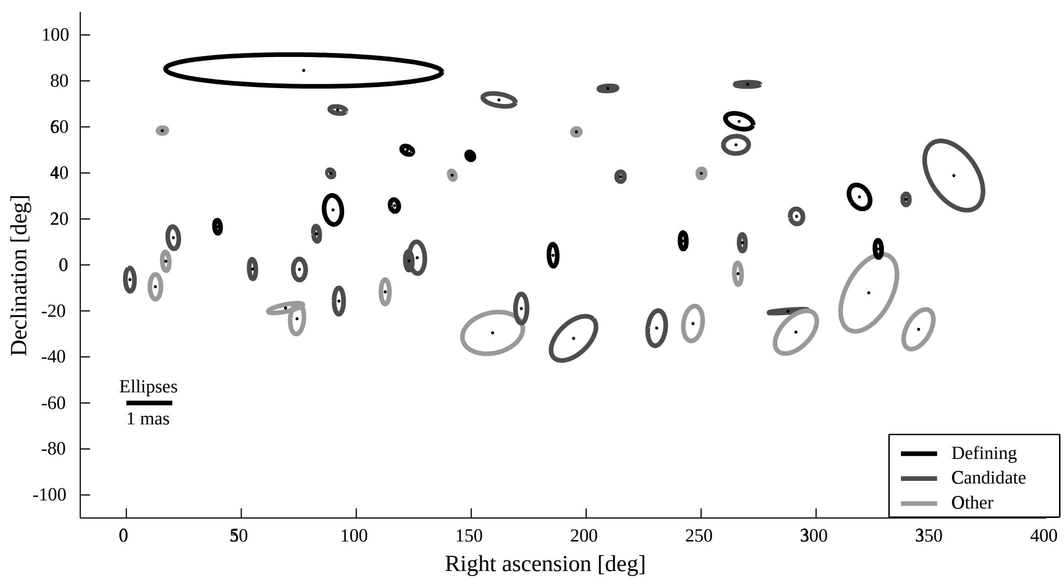

Figure 3. Reliability ellipses for the estimated radio source positions (Legend: ICRF classification).

References

[1] Baarda, W., A testing procedure for use in geodetic networks, Publications on Geodesy, Vol. 2, No. 5, Netherlands Geodetic Commission, Delft, 1968.

[2] Koch, K.R., Parameter Estimation and Hypothesis Testing in Linear Models, Springer, Berlin, 1999.

[3] Titov, O., J. Boehm, V. Tesmer, OCCAM v.6.0 software for VLBI data analysis, In: IVS 2004 General Meeting Proceedings, edited by N. R. Vandenberg and K. D. Baver, NASA/CP-2004-212255.

Thomas Hobiger et al.: Modelling Vertical Total Electron Content from VLBI Observations, IVS 2004 General Meeting Proceedings, p.306–310
http://ivscc.gsfc.nasa.gov/publications/gm2004/hobiger2

Modelling Vertical Total Electron Content from VLBI Observations

Thomas Hobiger, Harald Schuh

Institute of Geodesy and Geophysics, University of Technology, Vienna
Contact author: Thomas Hobiger, e-mail: thobiger@mars.hg.tuwien.ac.at

Abstract

The vertical total electron content (VTEC) can be understood as the sum of electrons in a column ranging in zenith direction from the ground through the ionosphere with a footprint size of one square meter. Although VLBI is a differential technique it is possible to derive absolute TEC values for each station from VLBI observations as shown in prior papers and presentations. At the Institute of Geodesy and Geophysics, Vienna, investigations of the functional and stochastical model have been made. An approach dealing with trigonometric functions that allows direct conclusions on amplitudes and phases of the sub-daily periods is presented. Other strategies using piece-wise linear functions and an extended piece-wise linear approach with adaptive interval widths are shown, too. The usage of kernel functions, in this case of Gaussian type, as a very general approach for modelling the ionosphere, is illustrated. The weights of a delay observable used for the stochastical model should also consider the zenith distance on each station and a corresponding weighting function is applied.

1. Theory

VLBI observations are performed at two different frequencies (X- and S-band) in order to correct for the ionospheric delay. This information can be used to model the ionosphere above each station, although only the differences between the two stations are measured. Instrumental offsets at each station bias these measurements (eq. 1).

$$\tau_{model}(t) = \tau_{ion,1}(t) - \tau_{ion,2}(t) + \tau_{offset,1} - \tau_{offset,2} \tag{1}$$

The ionospheric delay $\tau_{ion,i}(t)$ at X-band over station i at time t can be modeled by equation (2) with an appropriate mapping function (eq. 3) (e.g., Schaer 1999, [1]).

$$\tau_{ion,i}(t) = \frac{1.34 \cdot 10^{-7}}{f_x^2} \cdot M_f(\varepsilon_i) \cdot VTEC_i(t) \tag{2}$$

$$M_f(\varepsilon_i) = \frac{1}{\cos\left\{\arcsin\left[\frac{R\cos\varepsilon_i}{R+h}\right]\right\}} \tag{3}$$

VTEC represents the vertical total electron content at the intersection point of the ray path in zenith direction with the infinitesimally thin ionospheric layer assumed to be at height h (=450 km) (fig. 1), R is the mean radius of the Earth, ε_i is the elevation angle at station i and f_x the effective ionospheric frequency at X-band.

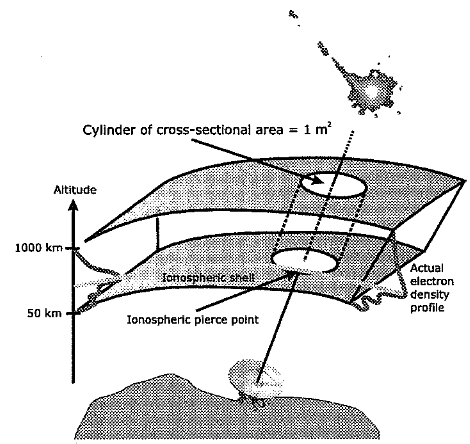

Figure 1. Modelling the ionosphere by means of VLBI

2. Functional Model

Three different approaches for modelling the VTEC have been investigated.

- Fourier components (eq. 4), first used by Kondo (1991), [2]
- piece-wise linear function (PLF) with adaptive interval lengths (eq. 5), 8 observations per interval
- Kernel-functions (eq.6)

$$VTEC_{FOURIER,i}(t) = a_{i0} + \sum_{k=1}^{4}\left[a_{ik}\cos\left(\frac{kt\pi}{12}\right) + b_{ik}\sin\left(\frac{kt\pi}{12}\right)\right] + c_i t \qquad (4)$$

$$VTEC_{PLF,i}(t) = offset_i + rate_{i,1}(t_1 - t_0) + rate_{i,2}(t_2 - t_1) + \ldots + rate_{i,n}(t_n - t) \qquad t \leq t_n \quad (5)$$

$$VTEC_{KERNEL,i}(t) = \sum_{i=1}^{n_{max}} A_i \cdot KF_i(t) \qquad KF_i(t) = \exp(-C^2 \cdot (t - t_i)^2) \qquad (6)$$

The different functional models are compared for the IVS-R4 session of Sept. 4th, 2003. VTEC values derived for station Fortaleza are shown in the left plot of figure 2 (Fourier-approach), center plot of figure 2 (PLF-approach), and right plot of figure 2 (Kernel-approach) in comparison to the official IGS combined solution (from [4]). The absolute correlation coefficients $|r_{ik}|$ between all unknown parameters of the above-mentioned IVS-R4 session are plotted in figure 3 according to the different modelling strategies.

The differences for all IVS-R4 stations between the individual VLBI approaches and the IGS solution during the 24h IVS-R4 session were analyzed, too (figure 4 and table 1).

3. Stochastical Model

A stochastical model was developed, that takes the different elevation angles ($\varepsilon_1, \varepsilon_2$) on each station into account (eq. 7 and 8). Taking this function to the i-th power allows increasing the weight

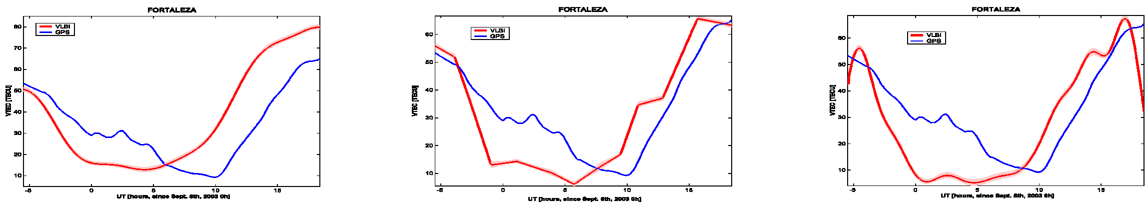

Figure 2. VLBI results for station Fortaleza from the Fourier (left), PLF (central) and Kernel (right) approach compared to the IGS solution.

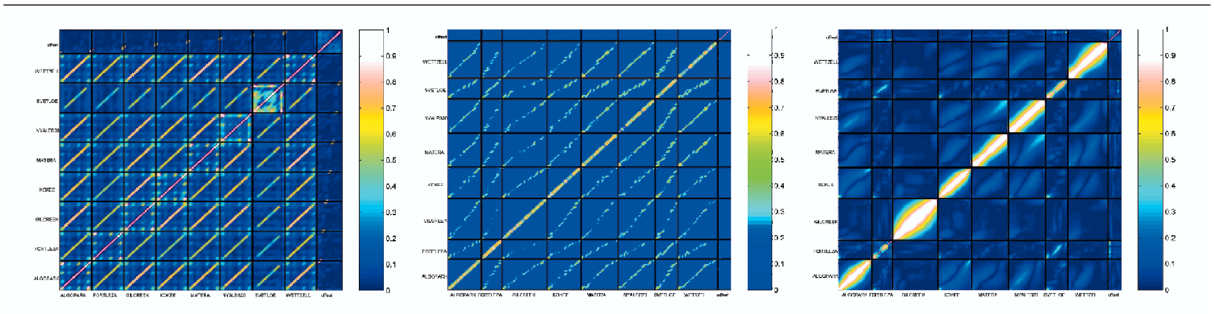

Figure 3. Absolute correlation coefficients between all unknown parameters for the Fourier (left), PLF (central) and Kernel (right) approach.

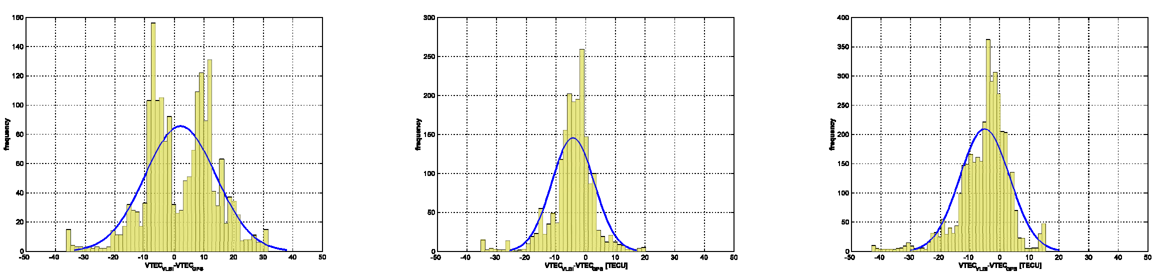

Figure 4. Histogram of the differences between VLBI and GPS (IGS) for the Fourier (left), PLF (central) and Kernel (right) approach.

Table 1. Mean differences of various VLBI approaches to GPS during the IVS-R4 session of Sept. 4th, 2003

VLBI (Fourier-approach) minus GPS:	2 TECU	± 12 TECU
VLBI (PLF-approach) minus GPS:	-4 TECU	± 8 TECU
VLBI (Kernel-approach) minus GPS:	-5 TECU	± 10 TECU

either on low or on high elevation observations depending on the value of i (figure 5). Varying values of i and applying the PLF-approach for the IVS-R4 session of Sept. 4th, 2003 yields different results for the a posteriori sigma (σ_0), of the mean differences to GPS ($\overline{\Delta VTEC_{VLBI-GPS}}$) and the r.m.s ($\sigma\left(\Delta VTEC_{VLBI-GPS}\right)$) as shown in table 2. For $i = +4$ the a posteriori σ_0 is close to 1 (indicates that weights were chosen correctly, see Koch, 1997, [3]) and that the r.m.s. VLBI - GPS reaches the smallest value. However, when using $i = +4$ the mean difference to GPS is rather big (-4.95 TECU) which can be explained by the reduced ability to separate the instrumental offsets from the ionospheric parameters due to downweighting of elevation observations.

$$M_f(\varepsilon) = \frac{1}{\cos\left\{\arcsin\left[\frac{R\cos\varepsilon}{R+h}\right]\right\}} = \frac{1}{\sqrt{1-\left(\frac{R}{R+h}\cos\varepsilon\right)^2}} \tag{7}$$

$$w^i(\varepsilon_1,\varepsilon_1) = \left(\frac{M_f(90^\circ)}{\sqrt{\frac{1}{2}\left[M_f(\varepsilon_1)\right]^2+\frac{1}{2}\left[M_f(\varepsilon_2)\right]^2}}\right)^i = \tag{8}$$

$$= \left(\frac{2\cdot\left[1-\left(\frac{R}{R+h}\right)^2\cos^2\varepsilon_1\right]\cdot\left[1-\left(\frac{R}{R+h}\right)^2\cos^2\varepsilon_2\right]}{2-\left(\frac{R}{R+h}\right)^2\left(\cos^2\varepsilon_1+\cos^2\varepsilon_2\right)}\right)^{i/2}$$

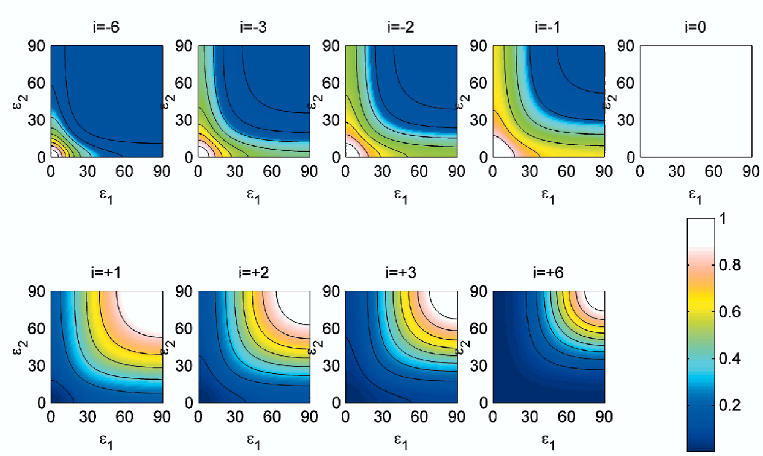

Figure 5. Weighting of VLBI measurements as a function of elevations (ε_1,ε_2), normalized to maximum.

4. Conclusions

It is possible to derive ionospheric parameters in terms of vertical total electron content exclusively from VLBI data, i.e. without any external information. Comparisons with GPS show

Table 2. Impact of different weighting of PLF-approach on a posteriori sigma (σ_0), on the mean difference to GPS $\overline{\Delta VTEC}_{VLBI-GPS}$), and on the r.m.s ($\sigma\left(\Delta VTEC_{VLBI-GPS}\right)$)

i	-6	-4	-3	-2	-1	0	1	2	3	4	6
σ_0	18,05	10,12	7,27	5,33	4,08	3,05	2,27	1,71	1,28	1,01	0,61
$\overline{\Delta VTEC}_{VLBI-GPS}$	-4,83	-4,81	-4,79	-4,72	-4,63	-4,58	-4,62	-4,72	-4,99	-4,95	-4,93
$\sigma\left(\Delta VTEC_{VLBI-GPS}\right)$	7,91	7,89	7,88	7,95	7,88	7,91	7,89	7,81	7,64	7,49	7,48

differences of up to a few TEC units. The piece-wise linear model and the weighting function shown in eq.(8) are recommended.

5. Acknowledgements

Research project P16136-N06 “Investigation of the ionosphere by geodetic VLBI” is funded by the Austrian Science Fund (FWF).

References

[1] Schaer, S., Mapping and Predicting the Earths Ionosphere Using the Global Positioning System, Inaugural Dissertation der Philosophisch-naturwissenschaftlichen Fakultaet der Universitaet Bern, Bern, 1999

[2] Kondo T., Application of VLBI data to measurements of ionospheric total electron content, Journal of the Communications Research Laboratory, Vol. 38, No. 3, 613-622, Tokyo, Japan, 1991

[3] Koch, K.-R., Parameter Estimation and Hypothesis Testing in Linear Models, Springer, Berlin, 1997

[4] `http://igscb.jpl.nasa.gov/components/dcnav/cddis_products_ionex.html`

Volker Tesmer et al.: Simultaneous Estimation of a TRF, the EOP and a CRF, IVS 2004 General Meeting Proceedings, p.311–314
http://ivscc.gsfc.nasa.gov/publications/gm2004/tesmer2

Simultaneous Estimation of a TRF, the EOP and a CRF

Volker Tesmer, Hansjörg Kutterer, Hermann Drewes

Deutsches Geodätisches Forschungsinstitut (DGFI)

Contact author: Volker Tesmer, e-mail: tesmer@dgfi.badw.de

Abstract

The paper presents first results of a DGFI VLBI solution with simultaneous estimation of station positions and velocities, celestial coordinates of the radio sources and Earth orientation parameters. The datum is realised by NNT and NNR conditions for the terrestrial (ITRF2000) and NNR for the celestial reference (ICRF-Ext1) frame. Using minimum datum conditions, biases can be avoided which are due to fixed reference frames or other relevant parameters of the observation equations.

1. Solution Description

For 2211 sessions between 1984 and 2001, normal equations were set up with the VLBI software OCCAM 6.0 ([6] and [7]), including a total of 47 telescopes observing 589 sources. The auxiliary parameters (for troposphere and clocks) were reduced for each session. All normal equations were accumulated to one equation system with the DGFI software DOGS-CS (as described in [5]). The datum of the solution was realised by NNT and NNR conditions for 26 telescope positions and velocities w.r.t. ITRF2000 ([1]) and NNR of 549 sources w.r.t. ICRF-Ext1 ([2] and [3]).

2. Estimated Source Coordinates

The estimated source coordinates agree well with the ICRF-Ext1: for 549 sources, the quadratic mean of the deviations is smaller than 2 mas (Fig. 1 and 3). There are almost no significant biases w.r.t. ICRF-Ext1 (Fig. 2). Although some weakly determined parameters are highly correlated, no large correlations were found between TRF and CRF related parameters.

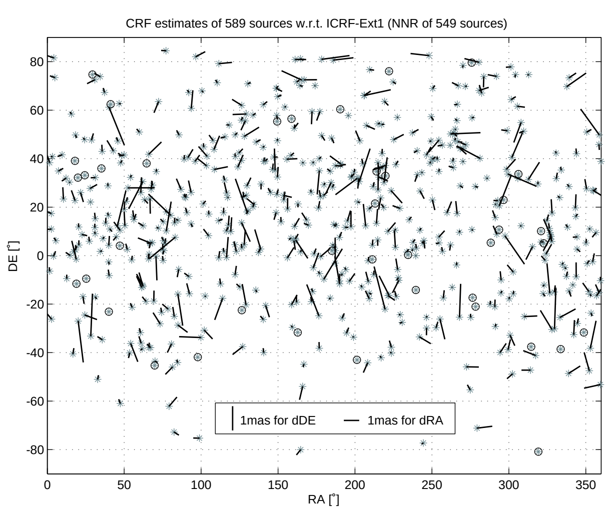

Figure 1: Estimates dDE, dRA of the solution (in black, units see legend). Only estimates for the 549 sources with sqrt(dDE²+dRA²) < 2mas are shown. They were used as identical points for the NNR conditions w.r.t. ICRF-Ext1. The 40 sources not used for the datum realisation are surrounded by circles.

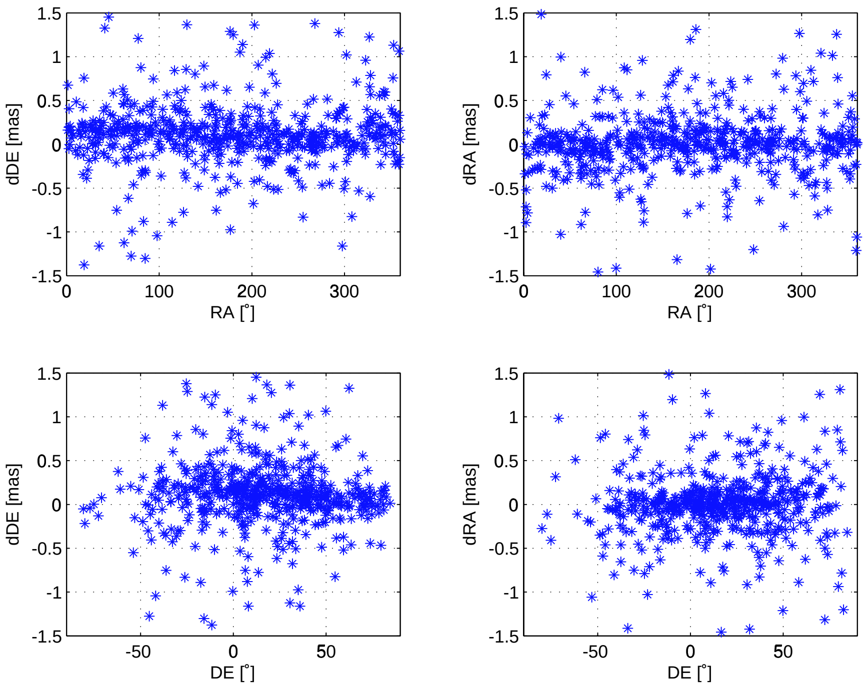

Figure 2: Estimates dDE and dRA of the source positions w.r.t. ICRF-Ext1, plotted vs. the a priori values of right ascension (RA) and declination (DE). No significant biases were found except small systematics for dDE vs. DE.

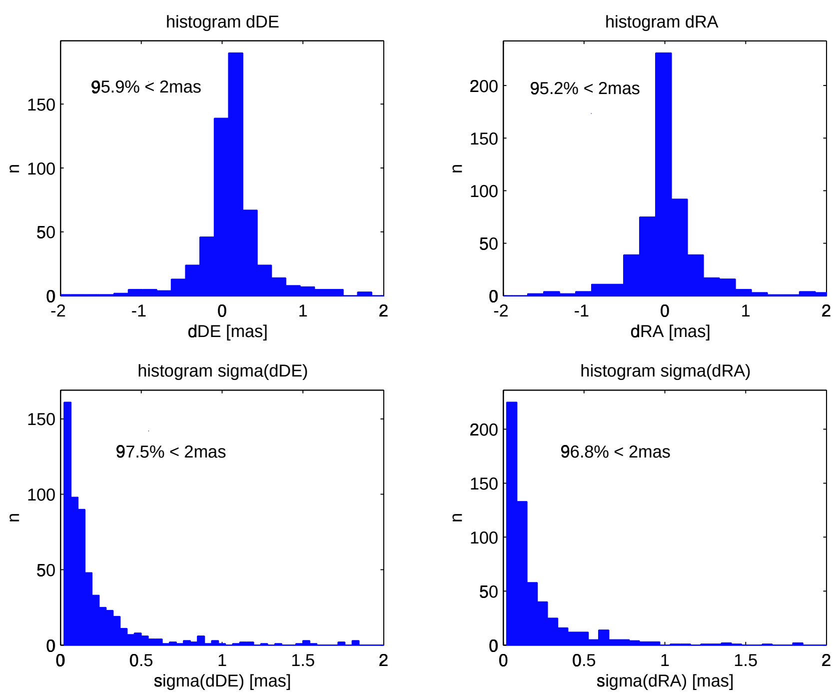

Figure 3: Histograms of the estimates dDE and dRA and the corresponding formal errors for all 589 sources. More than 95% of the estimates are smaller than 2 mas.

3. Influence of Fixing the CRF to ICRF-Ext1 on an Estimated TRF

As shown in figure 4, the estimated station positions of a TRF depend on the handling of the source coordinates in the solution: Two solutions were computed, one estimating the source positions simultaneously (solution setup 1) and another fixing the CRF on the values given in ICRF-Ext1 (solution setup 2). This change affects the coordinates of the telescopes very slightly (almost always < 2 mm) but apparently in a systematic way. One reason for such a bias might be that no horizontal atmospheric gradients were estimated for the determination of the ICRF (e.g., as seen by [4]). Furthermore, the inhomogeneous distribution of the stations and/or the sources could have a significant influence. But, as the estimated source positions are not correlated (< 0.2) with the station positions, this remains unexplained so far and needs to be further investigated.

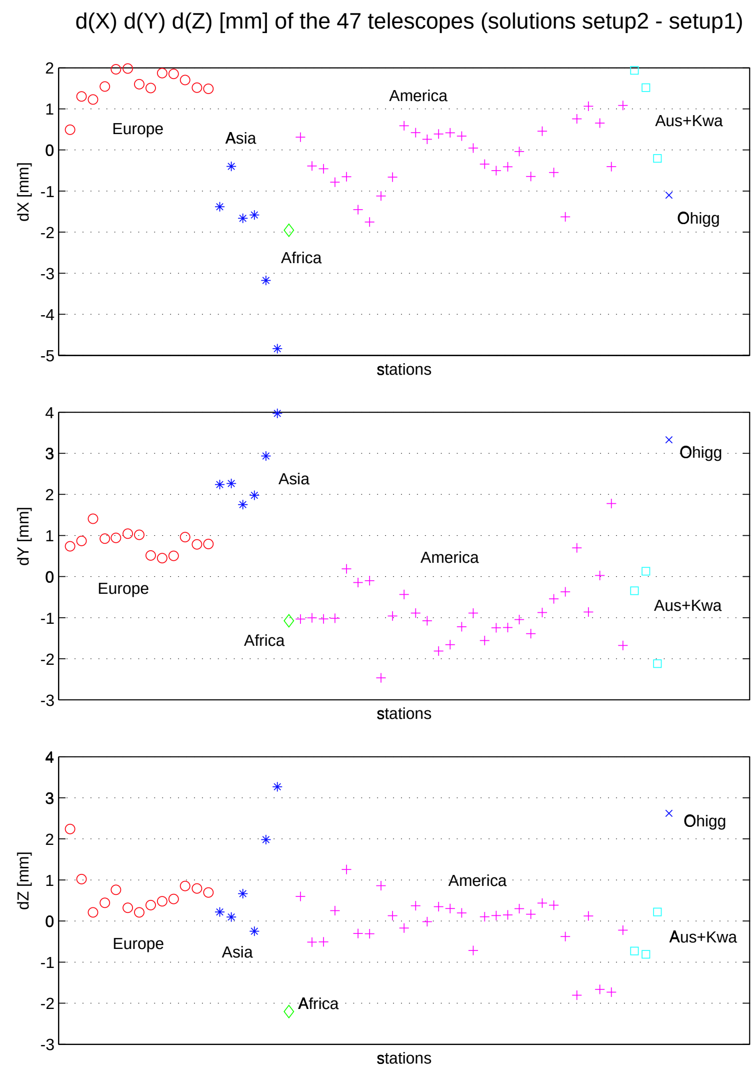

Figure 4: Differences between the cartesian components dX, dY and dZ, of the station positions, estimated with two different solution setups:

- setup 1 TRF and CRF estimated,
- setup 2 TRF estimated with CRF fixed to ICRF-Ext1.

4. Conclusions

At DGFI, a VLBI solution with a TRF, the EOP and a CRF being estimated simultaneously can very well be established applying a non-biasing NNR and NNT datum for the TRF and NNR for the CRF. In these first results, small effects in the TRF estimates due to fixing the ICRF-Ext1, as well as a small but maybe systematic deviation of the declination source coordinate estimates (dDE) is found, depending on the declination (DE) itself. This will be studied in more detail.

This research has made use of the IVS VLBI observation data. It was partially supported by the German research association "Deutsche Forschungsgemeinschaft (DFG)", contract (DR 143/11-1).

References

[1] Altamimi, Z.: ITRF2000: A new Release of the International Terrestrial Reference Frame for Earth Science Applications, J. of Geoph. Res., Vol. 107, B10, 2214, 10.1029/2001JB000561, 2002

[2] Ma, C., M. Feissel (eds): Definition and Realisation of the International Celestial Reference System by Astrometry of Extragalactic Objects. IERS Technical Note 23, Paris, 1997

[3] Ma, C., F. Arias, M. Eubanks, L. Fey, A.-M. Gontier, C. Jacobs, O.J. Sovers, B. Archinal, P. Charlot: The International Celestial Reference Frame as Realized by Very Long Baseline Interferometry. The Astronomical J. 166, 516-546, 1998

[4] MacMillan, D., C. Ma: Atmospheric Gradients and the VLBI Terrestrial and Celestial Reference Frames. Geoph. Res. Letters, Vol. 24, No. 4, 453-456, 1997

[5] Tesmer, V.: VLBI solution DGFI01R01 Based on Least- Squares Estimation Using OCCAM 5.0 and DOGSCS. In: Vandenberg, N., K. Baver (eds): IVS 2002 General Meeting Proc., NASA/CP-2002-210002, 295- 299, 2002

[6] Titov, O., V. Tesmer, J. Böhm: OCCAM 5.0 Users Guide. AUSLIG Technical Reports 7, AUSLIG, Canberra, 2001

[7] Titov, O., V. Tesmer, J. Böhm: OCCAMv.6.0 software for VLBI data analysis. In: Vandenberg, N., K. Baver (eds): IVS 2004 General Meeting Proc., NASA/CP-2004-212255, to be published in this issue, 2004

V.S. Gubanov et al.: Project: Global Analysis of 1979-2004 VLBI Data, IVS 2004 General Meeting Proceedings, p.315–319
http://ivscc.gsfc.nasa.gov/publications/gm2004/gubanov

Project: Global Analysis of 1979-2004 VLBI Data

V.S. Gubanov [1], *Yu.L. Rusinov* [1], *I.F. Surkis* [1], *S.L. Kurdubov* [2], *C.Y. Shabun* [2]

[1] *Institute of Applied Astronomy*
[2] *St.-Petersburg State University*
Contact author: V.S. Gubanov, *e-mail:* `gubanov@quasar.ipa.nw.ru`

Abstract

New software IAA RAS QUASAR is prepared for the analysis of practically all VLBI observations over the period of 1979-2004. The general purpose is improvement of reference systems ICRF, ITRF and EOP. Main features are explained and some results are demonstrated.

1. Introduction

First version of software QUASAR with usage global collocation technique was developed in 1998-2000 by V.S. Gubanov and I.F. Surkis with collaboration by Yu.L. Rusinov. Further development goes on by I.A. Verestchagina and students of SPb State University C.Ya. Shabun and S.L. Kurdubov. At present package QUASAR is a multipurpose system which can make mass processing of VLBI observations in different modes and purposes. It features the opportunity of use of various estimation techniques for the intraday stochastic component of UT1, tropospheric wet-delay and local clock time-scale variations. The following techniques based on parametric, stochastic and dynamic modeling will be used in QUASAR: a) multi-group least-squares (MGLS), b) moving least-squares filter (MLSF), c) global least-squares collocation (GLSC), d) recursive Kalman filter of random walk (KFRW) and e) recursive two-dimension Kalman filter (TDKF). More detail presentation of these techniques is carried out in [1]–[4], but their testing and comparison are continued. For this reason the presented below applications are related to GLSC as a basic technique of software QUASAR.

2. Preparation of QUASAR VLBI Database

All available data were sorted by programs and prepared for processing in compact format. The following procedures are executed: a) relative clock trends are reduced to standard quadratic model, b) super-series of programs CONT, VLBA and Bb023 are shared by some sub-series with observation numbers does not exceed 2000 [1]. After this all observations were processed by GLSC techniques, the EOP corrections and all stochastic signals were estimated in reference frames ICRF-Ext.1, ITRF2000 and EOP(IERS)C04.

3. Covariance of Signals

Obtained signal estimates were used for auto-covariance function calculations. These functions normalized to dispersion and averaged on 50 most active stations for wet- and clock-signals and on years for UT1-signal are presented in Figs. 1–3. The light gray curves show common average functions. These functions were modeled by positive-definite parametric function. Averaged dispersions of wet- and clock-signals are taking into account independently for every station and season of observation.

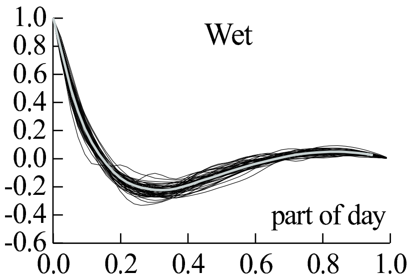

Fig. 1

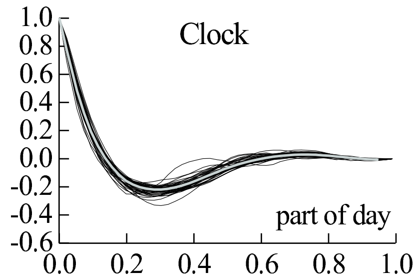

Fig. 2

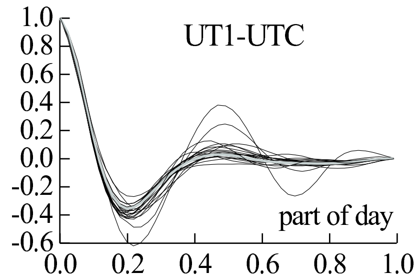

Fig. 3

4. Joint Determination of EOP and ITRF Corrections

In processing long series of observations the EOP trends are convenient for representing as polynomial expansions the coefficients of which are common for all series. The random EOP corrections are determined for every series. It is useful to determine stations coordinates for every session in order to investigate their high frequency variations. At Figs. 4–5 and 6–8 results of these determinations using NEOS-A observation data on 2001–2002 are shown.

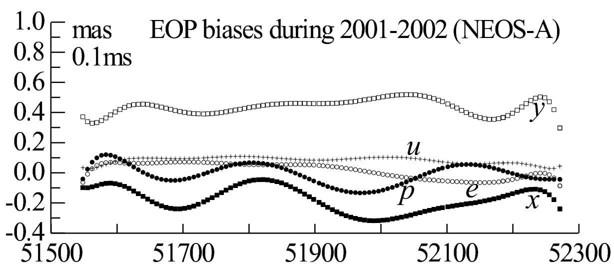

Fig. 4

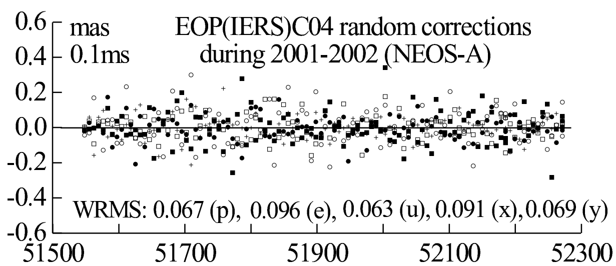

Fig. 5

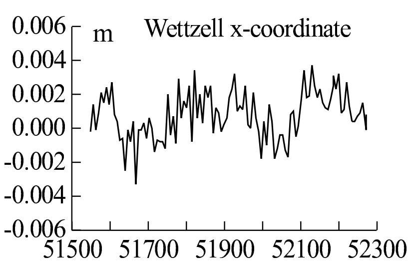

Fig. 6

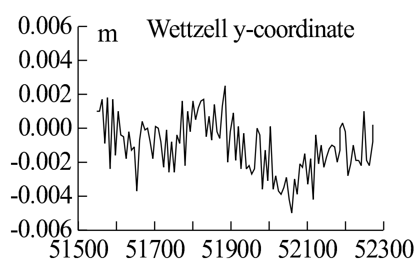

Fig. 7

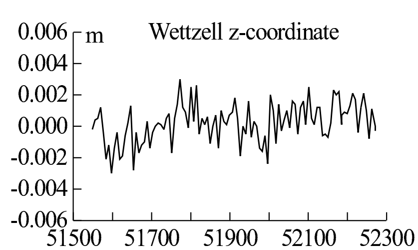

Fig. 8

5. Super-Sessions Analysis

Least-squares collocation demands the inverse for every daily series with observation number N one covariance $N \times N$-matrix, and the mass processing of near 5000 daily sessions obtained on 1979-2000 became very difficult because it demands some iterations. For this reason all super-sessions with $N > 2000$ was shared on some sub-sessions with $N < 2000$. The super-sessions with $2000 < N < 4000$ (program CONT etc.) was shared according to "time principle" by two sub-series such as odd moments of observations relates to 1st sub-series and even - to 2nd sub-series (option 1). For example, at Fig. 9 the total wet-component of tropospheric path delay in zenith for station Onsala obtained by GLSC-analysis of 7 super-series 940119-940125 (CONT-94) shared by option 1 is shown with the comparison of synchronous WVR measurements.

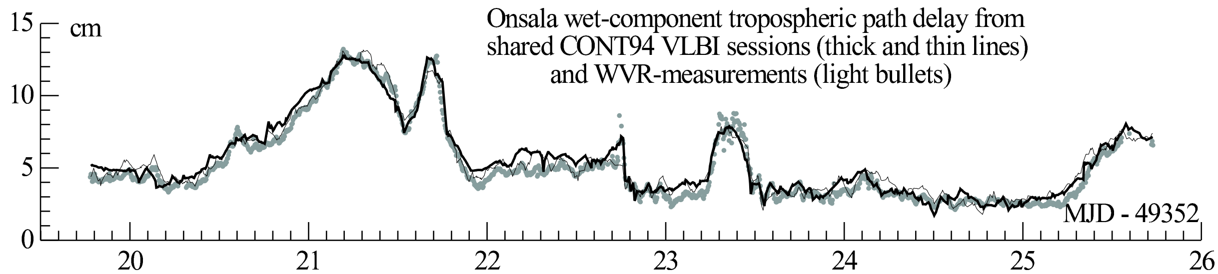

Fig. 9

The more complicated problem is sharing of VLBA and Bb023 super-sessions which contain up to 34000 observations. In this case option 1 cannot be used and sharing according to "base-principle" (option 2) was applied. All set of bases were shared by some subsets, everything of them make independent configuration quite optimal for all parameters and signals. Results of this option application are demonstrated below using example of super-session VLBA-02.03.06 contained more than 21.5 thousands of observations at 18 stations. This session was shared by 17 sub-sessions, which may be processed by GLSC both independent and combined. The results of combined solution of these sub-sessions — corrections of radio-sources coordinates (Fig. 10), coordinates all 18 stations (Fig. 11), and EOP (Fig. 12) — are shown. The radio source and station coordinates corrections was obtained under some constraints that is guarantees their unbias relative to reference systems ICRF-Ext.1 and ITRF2000.

All sub-sessions of 2nd type are independent because they do not contain the same bases, but the same station can be contained in more than one sub-session then some estimates of one signal for this station can be obtained. In the agreement of these estimates among themselves it is possible to conclude about its reliability. For example, at Figs. 13-18 estimations of wet- and clock-signals for three selected stations are shown. These signals obtained from independent processing all sub-sessions of one super-session VLBA-020306. Too excessive noise of clock-signal estimates pays attention to itself, therefore there is additional filtering needed.

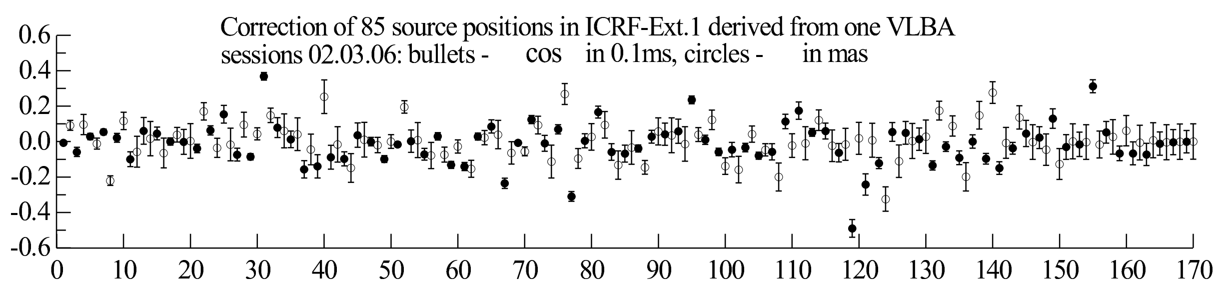

Fig. 10

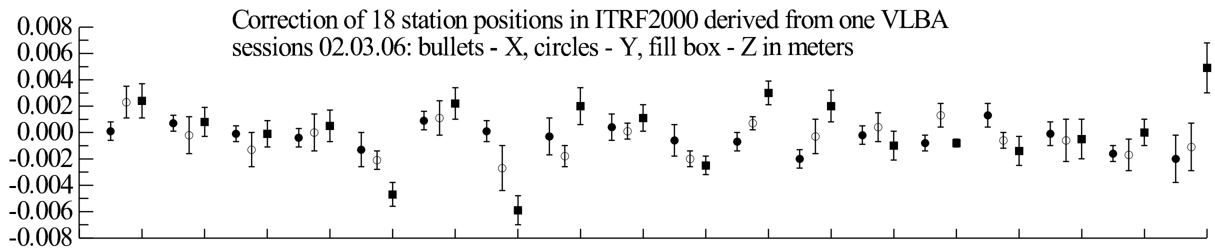

Fig. 11

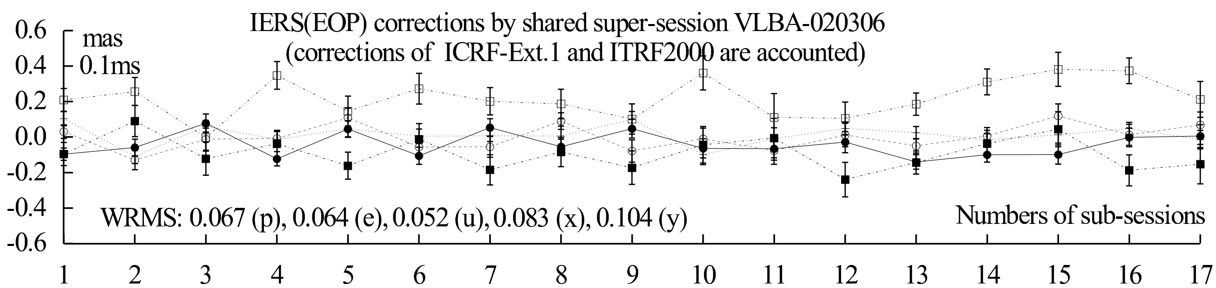

Fig. 12

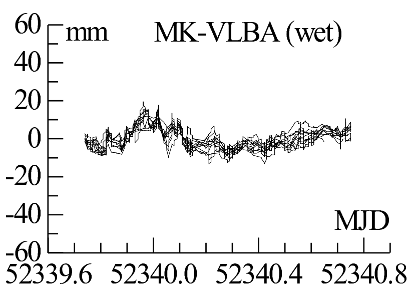

Fig. 13

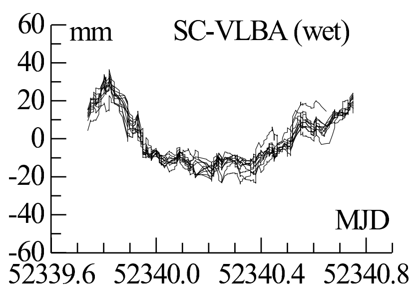

Fig. 14

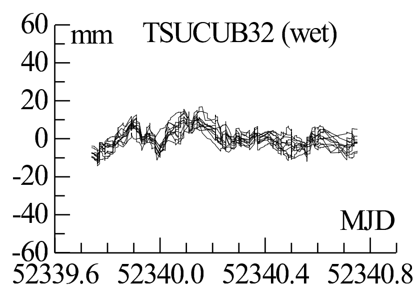

Fig. 15

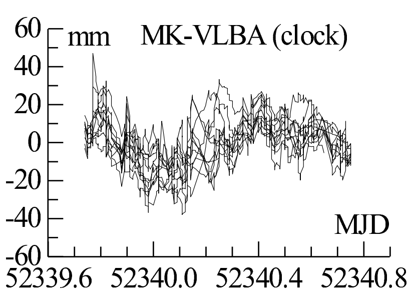

Fig. 16

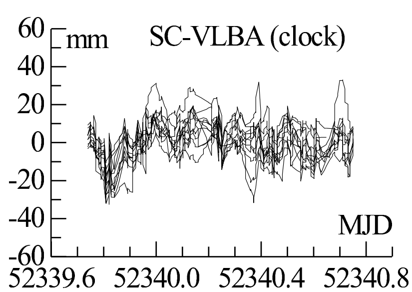

Fig. 17

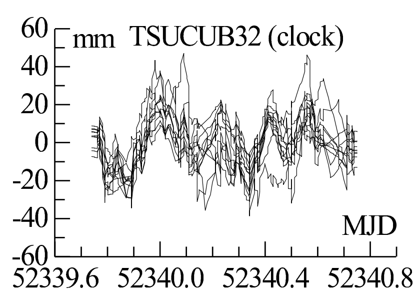

Fig. 18

At Fig. 19 the residuals of the one VLBA-020306 sub-session are shown. Its RMS is 3 mm, that more less than summary RMS of geometric and ionospheric delays errors. In the result for the majority of sessions χ^2-criterion is less than 1. This is the fact that the estimates of clock-signals and errors of observations has 100 percent correlation and the latter penetrates into clock-signals as white noise. This noise has to be filtered in order that χ^2-criterion was valid. After solution of this problem GLSC-technique will be ready for mass processing of VLBI observations with serious scientific purposes.

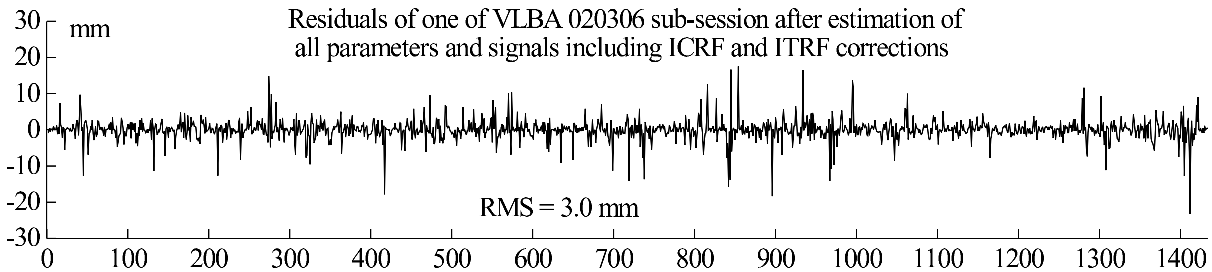

Fig. 19

6. Conclusion

At present there is full confidence that in first half of 2004 software QUASAR will be ready for mass processing of VLBI observations during 1979–2003 by least squares collocation and up to the end of year first results will be obtained. Up to this time at least one alternative technique of stochastic analysis mentioned in introduction will be verified and entered into practice.

7. Acknowledgements

Authors are grateful to the Russian Foundation of Basic Research for financial support of this project (grant No. 03-02-17591).

References

[1] Gubanov V.S., Project: Global Analysis of 1979-2004 VLBI Data, Proc. of Journées-2003, St.-Petersburg, 24–27 Sept., 2003. SPb, IAA RAS, 2004 (in press).

[2] Gubanov V.S., Generalized Least-Squares. Theory and Application in Astrometry. SPb, Science, 1997 (in Russian).

[3] Gubanov V.S., Advanced Methods of Astrometrical Data Analysis. Proc. of IAA RAS, No. 6, “Astrometry and Celestial Mechanics”. SPb, IAA RAS, 2001, pp.102–113 (in Russian).

[4] Gubanov V.S., Kozlova I.A. and Surkis I.F., Processing of VLBI Observations: Software QUASAR. II. The Data Analysis Techniques. Communications of IAA RAS, No. 142. SPb, IAA RAS, 2002, pp.1–36 (in Russian).

Zinovy Malkin: Towards IVS Analysis Conventions, IVS 2004 General Meeting Proceedings, p.320–323
http://ivscc.gsfc.nasa.gov/publications/gm2004/malk2

Towards IVS Analysis Conventions

Zinovy Malkin

Institute of Applied Astronomy of Russian Academy of Sciences (IAA)
e-mail: malkin@quasar.ipa.nw.ru

Abstract

One of the main goals of the IVS is to provide a supreme quality of the IVS products, such as EOP, TRF, CRF, etc. To achieve this, a comparison and combination of the products contributed by the IVS Analysis Centers is needed to understand and mitigate systematic errors of individual solutions and derive the final IVS combined product of the best quality. However, some inconsistencies in models and processing strategy used in various Analysis Centers still exist, which sometimes makes comparison and combination of their results more difficult than desirable. Moreover, this can lead to errors in the combined products, difficulties in geophysical interpretations, and inconsistency of the IVS products with other IERS techniques. So, IVS Analysis Conventions are definitely needed. In this paper some steps to establish such Conventions are proposed. They include standardization of some models used in analysis and other topics.

1. Introduction

One of the main goals of the IVS is to provide a supreme quality of the IVS products, such as EOP, TRF, CRF, etc. To achieve this, a comparison and combination of the products contributed by the IVS Analysis Centers (ACs) is needed to understand and mitigate systematic errors of individual solutions and derive the final IVS combined product of the best quality. However, some inconsistencies in models and processing strategy used at the IVS ACs still exist, which sometimes makes comparison and combination of their results more difficult then desirable. Moreover, this can lead to systematic errors in the combined IVS products, and inconsistency of the IVS products with other IERS techniques. So, IVS Analysis Conventions are definitely needed.

In this paper some steps to establish such Conventions are proposed. They include standardization of some models used in analysis and other topics. Evidently, the proposals made in this paper can be separated into three groups w.r.t. feasibility of realization:

1. No substantial change in analysis procedures or software update is needed.
2. No substantial change in analysis procedures is needed, but software update is required.
3. Change in analysis procedures is required. Evidently, this requires more detailed consideration in the IVS analysis community.

This paper is intended to continue a discussion on the standardization of analysis procedure at the IVS ACs started at the 4th IVS Analysis Workshop in April 2003, and understand where such a standardization is meaningful.

2. Database Version Numbering

The problem is that the correlator and analysis teams creating the databases often save the database version number after re-processing. There are many such examples of re-fringing, re-editing, adding new data or info, etc. when database name is not changed. This resulted in difficulties in automated update of institutional archives, and possible inconsistencies in results obtained in different AC using databases with different content.

Proposal: Change DB version number in case of ANY update.

Another issue related to the database numbering is a "final" version number. Mostly it is 4, but sometimes it is 3. As a consequence, one is not always sure which database is ready for scientific analysis.

Proposal: Establish a standard of the content of a database versions 1-4 (if it does not exist; I cannot find it, however).

3. EOP Format

There are three problems with the current EOP submissions.

1. Different ACs report EOP at different epochs—some use UTC as required by the IVS and IERS combination centers, some use TDB, which is inconsistency in epochs at the level of $TDB - UTC \approx 0.0007^d$, which is much greater than accuracy of reported EOP epochs ($0.00001 -$ -0.000001^d).

Proposal: Use UTC for the EOP epochs in accordance with the IERS and IVS requirements.

2. At least two ACs (GSF and IAA) compute two kinds of EOP series obtained from the analysis of the 24h VLBI sessions. The first one contains sessions for which all five EOP are estimated, the second one contains only nutation estimates, mainly for sessions with poor geometry. Mixing these data in single file seems to be not convenient, and may be confusing.

Proposal: Include in the EOPS files only sessions for which all the EOP are estimated. Implement the third IVS EOP file type, in addition to EOPI and EOPS, which may be named as EOPN to with only meaningful nutation estimates.

3. Sometimes, during the analysis of the VLBI results, it is essential to know which stations participating in the session (and listed in the master file) were actually used for computation. There would be no problem in case of reporting the EOP results in the SINEX format, but with existing IERS/IVS EOP format, it is impossible to get such information if a participating station was excluded from the analysis.

Proposal: Include a station list in the EOP line, preferably in the last field for convenience of a processing.

We, at the IAA AC, include the station list in the master file format at the end of a EOP line (see *e.g.* the files iaao0307.eopi and iaao0307.eops in the IVS archive), and found this very convenient for some kind of analysis. Besides, we put the clock reference station in the beginning of the list, which also seems to be useful.

4. Station Positions and Eccentricities

It seems to be important to achieve agreement about handling station eccentricities and irregular changes in station positions in a uniform way to avoid possible confusions. It seems reasonable to use an eccentricity only for the stations whose observations are related to the geodetic mark or other point different of axes intersection. One well known example is TSUKUB32. In such a case, introducing a jump in the station position seems to be preferable to avoid an inconsistency with the ITRF.

Proposal: Use eccentricity for “M” DOMES only, for other events/jumps use change in coordinates and, when necessary, velocity (*e.g.* for GILCREEK after the earthquake).

5. Models

It seems evident that all AC should submit their results to the combination centers using the same geophysical models. If this is not the case, inevitably systematic differences between the solutions obtained in different ACs will (and do) exist which is difficult to account for during comparison and combination. Evidently, models used for VLBI data analysis should be consistent with other space geodesy techniques to avoid systematic differences between them, which may (and do) give rise to errors of the final IVS and IERS products.

Recently, Goddard and Vienna teams accomplished a hard and important work on computation and distribution of data related to modelling atmospheric loading and mapping function. The provided files are convenient enough for easy implementing of these models in an analysis software, and all ACs should be encouraged to do that as soon as possible (although, strictly speaking, after an approval of the IVS Analysis Coordinator; in particular one of two computed mapping functions should be recommended).

Moreover, it seems reasonable to have a single procedure and data files (to eliminate the computational efforts, simplify file downloading and implementation in analysis software) for computation and distribution of all atmosphere related models (loading, mapping function, gradients, ..., something else?), if feasible.

However, some models still need to be standardized. Ocean loading, hydrology, antenna deformations, rotational deformations of the Earth, etc., influence mainly on the estimates of station coordinates. Using different models of the daily and subdaily EOP variations leads to an inconsistency in the nutation series.

Let us consider some examples of inconsistencies in used models and possible consequences for scientific analysis. Also let us keep in mind that modern geodetic analysis does try to achieve an mm level of accuracy.

1. Using numerical atmospheric loading and mapping function models using direct processing of numerical weather data proves its benefit. As a result, we may expect that more and more centers will compute those models for space geodesy data processing. However, it would be useful for proper interpretation of results to compare the results computed at the various centers. For instance, a brief comparison of the three atmospheric loading models computed at the GSFC, OSO and JPL shows disagreement in both height and horizontal components at a level of several millimeters for individual epochs and up to 1 mm in the amplitude of seasonal components. Even larger effects can be seen when using different values of the reference pressure and/or topography models

2. A preliminary results of the just started IVS Pilot Project on baseline length show the systematic differences between individual solutions at a level of several millimeters [1]. It can be easily seen that that may result from inconsistencies (which really exist) in ACs' processing strategy. Most evident of those are the following.

- Different handling (or ignoring) of the antenna thermal deformation, including using different reference temperatures, may lead to biases and seasonal terms at a level of 2-3 mm [2].

- Using different mapping functions leads to scale differences of about several tenths ppb, *i.e.* about 0.2–0.4 mm/Mm in the baseline length [3].
- Using different relativistic models (*e.g.* IERS 1992 and 2003) leads to the scale difference in the baseline length $L_G \approx$ 0.7 ppb, *i.e.* 0.7 mm/Mm.
- Using different models for polar tide, more precisely different model for mean pole (zero values vs. IERS recommended actual mean pole coordinates) leads to the difference in the baseline length more than 15 mm for recent epochs and baselines located in different hemispheres.

Evidently, proper comparison, combination and interpretation of the baseline length series at a millimeter level of accuracy is impossible without a correction of individual series for the differences in the individual ACs' models.

Proposal: All models used for the VLBI analysis should be considered, and ways for their standardization should be discussed.

Evidently, this topic is difficult to agree. Moreover, improvement of the models is an natural task for all ACs. Nevertheless, it seems to be necessary to find a way to combine ACs' interests with the IVS ones. A possible strategy is to use the same conventional models for submission of the results to the IVS and IERS, and use extended/improved models for other scientific investigations. Here we consider the TRF and CRF realization as a part of model.

In any case, a special investigation of the impact of differences in the models used in the ACs on the final result seems to be extremely important (many results of such studies are known, but many points yet have to be clarified).

6. Conclusion

Of course, not all topics related to the subject of this paper are considered here. As mentioned above, this is only an attempt to activate a discussion. However, it seems extremely important to solve the problems raised here, in the first place related to the unification of models and/or careful investigation of their impact on the IVS and IERS products. Results of such investigations can be then used to mitigate the systematic errors in combined products, especially taking into account that nowadays they prevail in the differences between the solutions obtained in different ACs.

Probably the problems of developing IVS Analysis Conventions should be considered in the framework of the IVS WG 3 on VLBI2010, and/or a special IVS Pilot Project should be initiated.

References

[1] Nothnagel, A., 2004, this issue.

[2] Skurikhina, E., 2004, Ph.D. Thesis. — in Russian.

[3] Niell, A., and L. Petrov, 2003, Using a Numerical Weather model to improve Geodesy. Proc. The State of GPS Vertical Positioning Precision, Luxembourg, April 2003.

Gerald Engelhardt et al.: Activities of the IVS Analysis Center at BKG in 2003, IVS 2004 General Meeting Proceedings, p.324–328
http://ivscc.gsfc.nasa.gov/publications/gm2004/engelhardt

Activities of the IVS Analysis Center at BKG in 2003

Gerald Engelhardt, Volkmar Thorandt, Dieter Ullrich

Bundesamt für Kartographie und Geodäsie

Contact author: Gerald Engelhardt, e-mail: gerald.engelhardt@bkg.bund.de

Abstract

The main analysis activities at the International VLBI Service (IVS) Analysis Center at BKG can be divided into the processing of the correlator output, the producing of two Earth Orientation Parameter (EOP) time series for submission to the IVS, the regular submissions of tropospheric parameters for the IVS-R1 and IVS-R4 sessions, and the generating of daily SINEX (Solution INdependent EXchange format) files for the IVS.

For the IVS products Terrestrial Reference Frame (TRF) and Celestial Reference Frame (CRF) quarterly updated solutions are computed. The main features of these works are explained and some results are compared to the official IERS (International Earth Rotation and Reference Systems Service) products.

A UT1 time series derived from about 1-hour measurements of the baseline TSUKUBA-WETTZELL was generated and first results of the data processing were compared with the results of the official BKG UT1 time series derived from data of the baseline KOKEE-WETTZELL. The measurements of the new station TIGOCONC (Conception, Chile) have been used in the processing for about 1.6 years. So first velocity information about this station could be estimated from the station coordinate series. The use of unstable sources identified by Martine Feissel-Vernier [1] was tested and comparisons were made with the results of the routinely used procedure for the EOP determination of the BKG VLBI group.

1. General Information

The IVS Analysis Center at BKG is responsible for the computation of EOP time series, quarterly updated global solutions for the TRF and CRF, the estimation of tropospheric parameters of the IVS-R1 and IVS-R4 sessions, and the generating of daily SINEX files.

The VLBI group at BKG continued the generation of calibrated databases for the sessions correlated at the MPIfR (Max-Planck-Institut für Radioastronomie)/BKG Mark 5 Astro/Geo Correlator at Bonn (e.g. R1, T2, OHIG, EURO) and submitted them to the IVS Data Centers for distribution. After the preprocessing only one global solution is computed for the extraction of the EOP, tropospheric parameters, TRF, and CRF. The producing of the UT1 time series for intensive observations and the generating of daily SINEX files are based on independent session solutions.

At BKG the Mark 5 VLBI data analysis software system Calc/Solve, release of September 25, 2003 [2], is currently used for VLBI data processing. In addition, the older Mark IV version, release of May 15, 2003 and an independent program environment for the Calc/Solve software are available. The latter is used for the data and product handling outside of Calc/Solve. The Mark IV Calc/Solve software under Fortran77 is installed on a HP9000/280/1 workstation with an HP-UX10.20 operating system and the Mark 5 software under Fortran90 on another HP workstation with an HP-UX11.00 operating system.

2. Data Analysis for the IVS

2.1. BKG Time Series bkg00006

The currently generated EOP time series bkg00006 is extracted from a global solution with 24 hours VLBI sessions from 1984 on. Altogether 2902 sessions were processed. The main parameter types in this solution are globally estimated station coordinates and velocities together with radio source positions. Minimal constraints for the datum definition are applied to get zero net rotation and net translation for 26 selected station positions and velocities with respect to the VTRF2003 [5] and zero net rotation for 212 defining sources with respect to ICRF-Ext.1 [3]. The station coordinates of the stations TIGOCONC (Chile) and SVETLOE (Russia) are estimated as local parameters in each session.

2.2. BKG Time Series bkgint03

The UT1 time series bkgint03 from intensive observation sessions of the baseline KOKEE-WETTZELL each with a duration of about 1 hour is generated with fixed TRF (VTRF2003) and fixed CRF derived from the global BKG solution for EOP determination. The estimated parameter types are only UT1, station clock, and zenith troposphere. Currently altogether 1088 UT1 intensive sessions were analysed for the period between 1999.01.01 and 2004.01.26.

2.3. Quarterly Updated Solutions

For the IVS products TRF and CRF quarterly updated solutions are estimated. There are no differences in the solution strategy compared to the continuously computed EOP time series bkg00006. The results are formatted to IERS format for the radio source positions and SINEX format, version 2.1 for the station coordinates and velocities.

2.4. Tropospheric Parameters

The VLBI group of BKG has started regular submissions of tropospheric parameters to the IVS (wet and total zenith delays, horizontal gradients) for all IVS-R1 and IVS-R4 sessions since January 1, 2002. The tropospheric parameters are directly extracted and transformed into SINEX for tropospheric estimates from the results of the standard global solution for the EOP time series bkg00006. In future the submission of a long time series of tropospheric parameters from 1984 on is planned.

2.5. Daily SINEX Files

The VLBI group of BKG has started regular submissions of daily SINEX files as base solutions for the planned IVS time series of baseline lengths and for combination techniques. In addition to the global solutions independent session solutions are computed for the parameter types station coordinates, EOP, and nutation parameters.

3. Special Computations

Besides the routine data analysis for the IVS special computations with respect to a new UT1 time series, station data of TIGOCONC, and unstable radio sources were made.

3.1. UT1 Time Series from 1-Hour Data TSUKUBA-WETTZELL

A new UT1 time series from intensive observation sessions based on K4 technology of the baseline TSUKUBA-WETTZELL each with a time span of about 1 hour was generated. Altogether 20 sessions from 2002.07.01 to 2002.12.19 and 28 sessions from 2003.04.12 to 2003.12.20 were analyzed. The processing strategy was identical to the routine computations of the UT1 time series bkgint03. The results are listed in Table 1.

Table 1. Results of the new UT1 intensive series TSUKUBA-WETTZELL in comparison with the standard UT1 intensive series KOKEE-WETTZELL

Topic	Data based on K4 technology TSUKUBA-WETTZELL	bkgint03 KOKEE-WETTZELL
Number of observations 2002.07.01-2003.12.20	48	270 resp. 51 (∗)
WRMS derived from the differences to C04 in UT1-UTC	19.3 μs	12.8 μs resp. 11.4 μs
Mean formal standard deviation from Solve in UT1-UTC	8.6 μs	15.6 μs resp. 12.1 μs

(∗) only epochs from data TSUKUBA-WETTZELL, range of about half a day

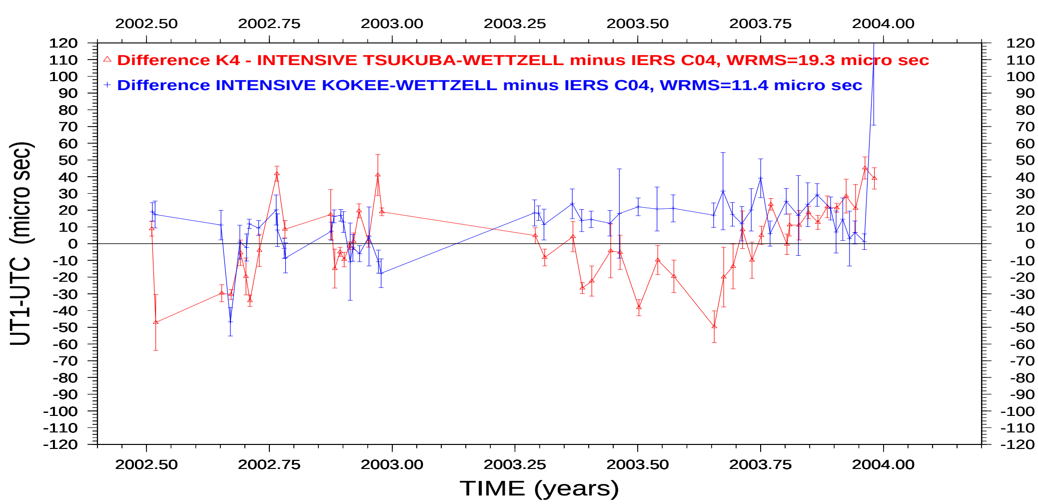

Figure 1. Residuals of TSUKUBA-WETTZELL and KOKEE-WETTZELL UT1-UTC intensive series w.r.t. IERS C04

It can be stated that the new UT1 time series from TSUKUBA-WETTZELL data shows more scatter w.r.t. IERS CO4 series [4] although the mean formal standard deviation of UT1-UTC from Solve is better than the one from the standard series bkgint03 (see Figure 1). Nevertheless the new series is compatible to the series from KOKEE-WETTZELL data and can be used to control it.

3.2. Results from 1.6 Years Data of Station TIGOCONC (Chile)

At the new transportable fundamental station for geodesy in South America TIGOCONC located near of Conception in Chile VLBI data has been observed since May 13, 2002. In the global BKG solution for the extraction of the EOP (bkg00006) coordinate series of TIGOCONC were determined from 2002.05.13 to 2004.01.05. By using a straight-line model for fitting the TIGOCONC coordinate series, useful velocity information about the North, East, and Up component of station TIGOCONC could be estimated. The results are listed in Table 2.

Table 2. Station velocities of TIGOCONC derived from 1.6 years coordinate series in comparison with the global estimated velocities of SANTIA12

Solution from bkg00006	Station velocity mm/year	Standard deviation mm/year	WRMS mm
TIGOCONC N-component	13.7	1.9	13.0
TIGOCONC E-component	27.7	1.3	8.1
TIGOCONC U-component	9.0	4.4	21.0
SANTIA12 N-component	15.4	0.5	
SANTIA12 E-component	19.3	0.4	
SANTIA12 U-component	4.6	1.3	

On closer inspection of the standard deviations the estimated velocity information of station TIGOCONC are all significant. The station velocities of station SANTIA12 only 462 km north of TIGOCONC on the same South American plate make possible a plausibility control of the estimated velocities of TIGOCONC. The largest difference is 8 mm/year in the East component and could be explained by the fact that both stations are located on the plate boundary.

The accuracy (WRMS) derived from a straight-line model for fitting the session-wise determined baseline lengths from each baseline with TIGOCONC, also called baseline length repeatability, is about 2 ppb.

3.3. Test of Unstable Radio Sources

Test basis for the analysis of unstable radio sources was the paper by Martine Feissel-Vernier [1], table 6 with 162 unstable radio sources and stability criterion 3 or 4 included in it. In a first approximation the analysis strategy was set to a linear rate estimation in right ascension and declination of 162 unstable sources. So 162 unstable radio source positions were estimated as global parameters with their proper motions together with the no-net-rotation condition of sources w.r.t. ICRF-Ext.1 for 81 stable defining sources marked in the ICRF-Ext.1 catalogue in contrast to the routine global solution (bkg00006). The results prove that about 41 percent of the investigated sources show significant source proper motion with an amount of more than a triple standard deviation of proper motion (Table 3).

Table 3. Results of the linear rate estimation of unstable radio sources

	Source motion more than $3\times$ standard deviation	Source motion more than $2\times$ standard deviation
No. of sources for RA+DEC	24	32
No. of sources for RA or DEC	42	61
Total	66	93
(including defining sources)	(19)	(34)

An example for the estimation of source proper motions is the defining source 2145+067 (1814 sessions from 1984-2003 with 67881 observations) with a right ascension velocity of -28 $\pm$ 0.9 $\mu as/year$ and a declination velocity of 12 $\pm$ 1.3 $\mu as/year$.

To study the effect of modelling of source proper motion with respect to the estimated EOP a comparison was made with IERS C04. Bias and WRMS derived from the differences to C04 are only slightly changed compared to the EOP from the standard global solution bkg00006. But the biases relative to C04 for the nutation parameters dPsi and dEps are more changed compared to polar motion parameters and UT1-UTC.

3.4. Outlook

The VLBI group at BKG will continue the refining of the solution strategy for series bkg00006. Topics for this are the estimation of axis offsets, the use of a new atmosphere model based on the VMF (Vienna Mapping Functions), and the handling of unstable radio source positions. Other works are the continuation of the UT1 time series from 1 hour data TSUKUBA-WETTZELL and the extension of the graphics module REPA [6].

References

[1] Feissel-Vernier M. (2003): Selecting stable extragalactic compact radio sources from the permanent astrogeodetic VLBI program, In: Astronomy and Astrophysics manuscript no. MS3523, 2003/03/10.

[2] GSFC, NASA (2003): Release of Mark 5 VLBI Analysis Software Calc/Solve from Sep. 25, 2003 (web-reference: http://gemini.gsfc.nasa.gov/solve).

[3] ICRF-Ext.1 (http://hpiers.obspm.fr/webiers/results/Icrf)

[4] IERS C04 EOP (http://hpiers.obspm.fr/eop-pc)

[5] Nothnagel A.(2003): VTRF2003: A Conventional VLBI Terrestrial Reference Frame, In: Proceedings of the 16th Working Meeting on European VLBI for Geodesy and Astrometry, held at Leipzig, May 09-10, 2003, edited by W. Schwegmann and V. Thorandt, Bundesamt für Kartographie und Geodäsie, Frankfurt/Leipzig, 2003.

[6] Thorandt V., Engelhardt G. (2003): Residual Plotting and Ambiguity Resolution (REPA), In: Proceedings of the 16th Working Meeting on European VLBI for Geodesy and Astrometry, held at Leipzig, May 09-10, 2003, edited by W. Schwegmann and V. Thorandt, Bundesamt für Kartographie und Geodäsie, Frankfurt/Leipzig, 2003.

David M. Hall et al.: VLBI Analysis at the U.S. Naval Observatory, IVS 2004 General Meeting Proceedings, p.329–333
http://ivscc.gsfc.nasa.gov/publications/gm2004/hall1

VLBI Analysis at the U.S. Naval Observatory

David M. Hall, David A. Boboltz, Alan L. Fey, Kerry A. Kingham

U.S. Naval Observatory

Contact author: David M. Hall, e-mail: dmh@usno.navy.mil

Abstract

The United States Naval Observatory (USNO) is currently producing a periodic global Terrestrial Reference Frame (TRF) solution updated twice a week using the IVS-R4 and IVS-R1 experiments. The USNO analysis center is responsible for the daily solutions and submission of the IVS-R4 and CRF experiment databases to the IVS. Here we present the results of our VLBI analysis with comparisons to other EOP series.Additional information regarding VLBI analysis at the USNO and the periodic solutions can be found at http://rorf.usno.navy.mil/vlbi/.

1. Analysis Center Activities 2003

- Continued analyzing weekly IVS-R4 and IVS-R1 VLBI sessions for use in internal USNO global solutions.
- Continued producing periodic global TRF solutions for use in estimating Earth orientation parameters.Global TRF solutions (USNO 2003a and USNO 2003b) can be found at: http://rorf.usno.navy.mil/solutions/.
- Compared EOP-S estimates obtained from the periodic TRF solutions to those obtained from the GSFC quarterly solutions and with the IERS-C04 time series.
- Assumed scheduling, analysis, and IVS data submission responsibilities for all CRF experiments, which are designed to densify the ICRF in the Southern Hemisphere. For 2003 this includes CRF-17 to CRF-24.
- Began producing periodic global CRF solutions designed to reproduce and extend the current generation ICRF.
- In collaboration with the group at the Australia Telescope National Facility (ATNF), conducted six 24-hr astrometric observing sessions, CRF-MS7 and CRF-DS5 to CRF-DS9, for the explicit purpose of densifying the ICRF in the Southern Hemisphere.

2. USNO 2003b Global Solution

- The Batch SOLVE solution used all available multi-baseline VLBI observations at 8.4 GHz (X-band) and 2.2 GHz (S-band) from 3 August, 1979 through 6 September, 2003.
- This included a total of 3045 diurnal sessions and 3,531,109 measurements of group delay.
- The Earth Orientation parameters: X and Y pole positions and rates, UT1 angle and rate, and daily offsets in nutation (longitude and obliquity) were estimated for each session separately.

- Positions of 485 sources were estimated as global parameters.
- Positions for an additional 251 sources sources were estimated independently as local parameters (arc-sources).
- Of these 251 sources, 147 were treated as arc-sources due to weighted RMS position errors > 1.5 or chi-square per degree of freedom > 2.5 in either right ascension or declination as determined in the USNO CRF2003b solution.
- The remaining 104 arc-sources had fewer that 40 observations or were observed in only one experiment.
- A total of 114 sources were eliminated due to bad data or insufficient number of observations.
- Positions of 129 stations and velocities for 118 of those stations were estimated as global parameters.
- Shown below are plots from the USNO 2003b solution. Clockwise from upper left are the experiment rms delays and rates, X vs. Y pole position, nutation offsets as a function of time, and pole position and UT angle as a function of time.

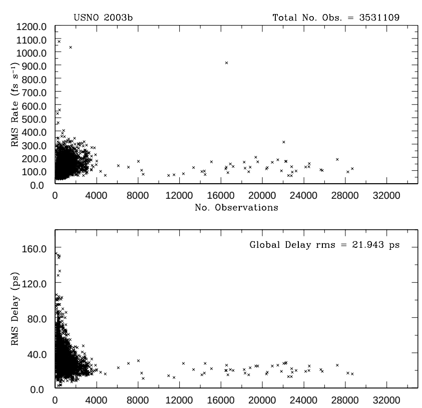

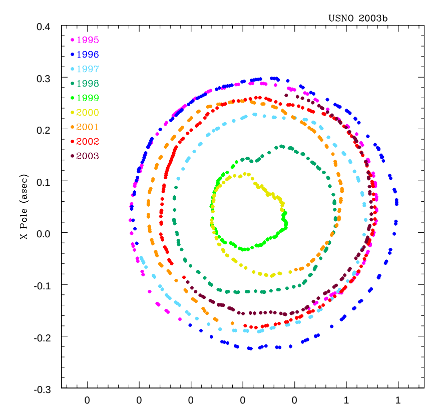

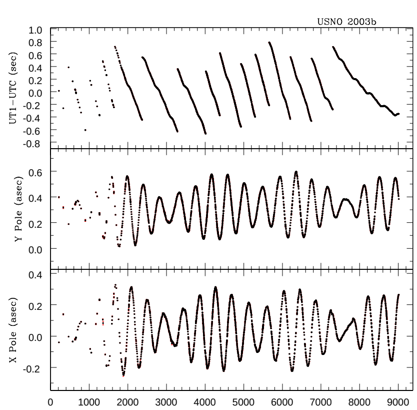

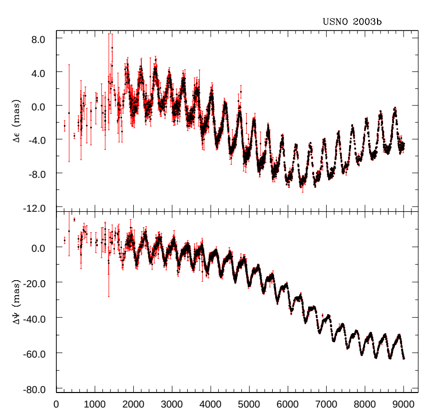

3. Comparison with IERS-C04

- Shown here is a comparison of the EOP estimates from the USNO 2003b solution with the IERS C04 time series from 1979 to 2003.
- Plotted are the differences for pole position, UT angle, and nutation offset.
- A weighted least-squares linear fit to the differences and the weighted rms are shown on each plot.

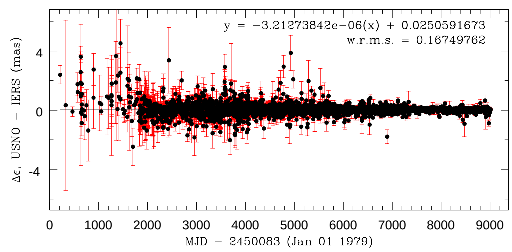

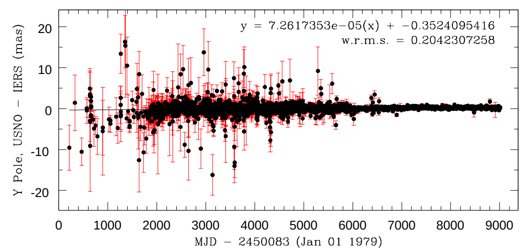

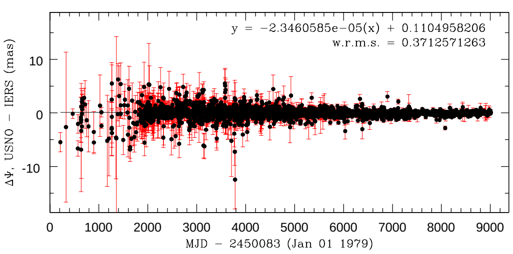

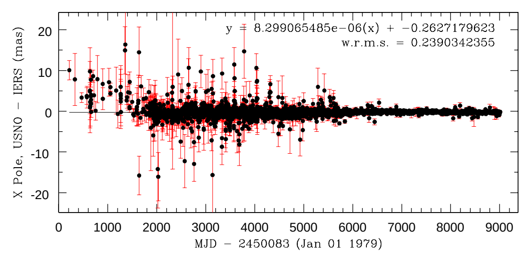

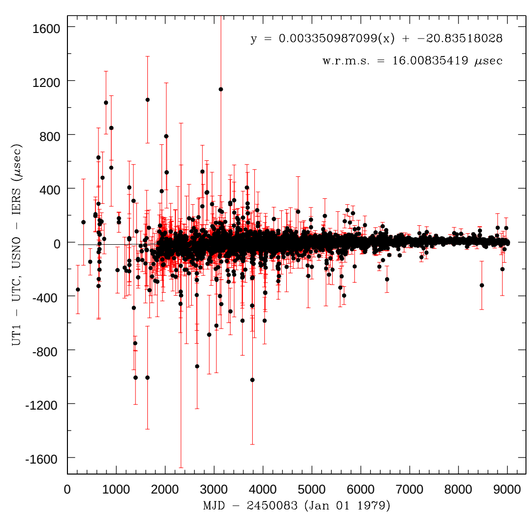

4. Comparison with GSFC 2003c

- Shown here is a comparison of the EOP estimates derived from the USNO 2003b solution with those derived from the GSFC 2003c solution from 1979 to 2001.
- Plotted are the differences for pole position, UT angle, and nutation offset.
- A weighted least-squares linear fit to the differences and the weighted rms are shown on each plot.

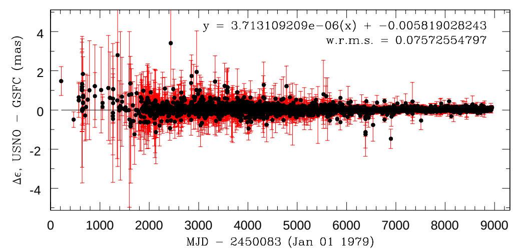

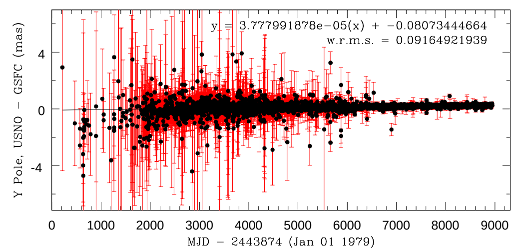

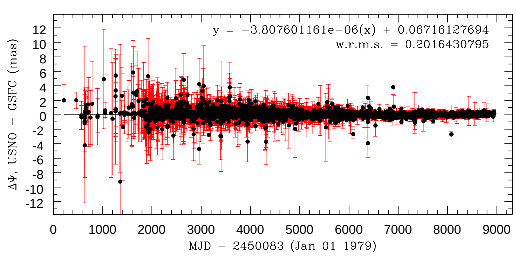

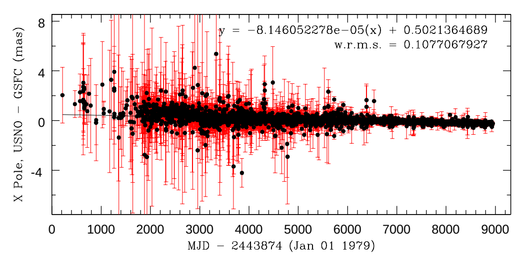

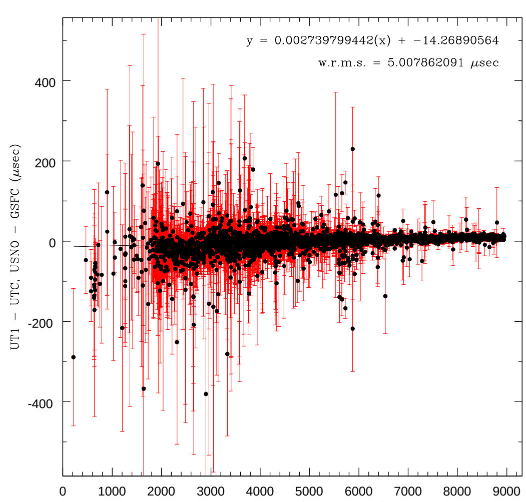

5. Future Plans

- Continue processing of weekly IVS-R4 and IVS-R1 experiments for use in internal USNO global solutions.
- Continue analysis and database submission for all IVS-CRF experiments.
- Continue production of periodic global TRF solutions and submission of EOP-S estimates to the IVS updated bi-weekly with IVS-R1 and IVS-R4 experiments.
- Continue production of periodic global CRF solutions.
- Make additional astrometric observations in the Southern Hemisphere in collaboration with ATNF partners.

Page intentionally left blank

Session 6

Results and Geodetic/Geophysical/Astrometric Interpretation

Page intentionally left blank

Chopo Ma: Refinement of the ICRF, IVS 2004 General Meeting Proceedings, p.337–340
http://ivscc.gsfc.nasa.gov/publications/gm2004/ma1

Refinement of the ICRF

Chopo Ma

NASA Goddard Space Flight Center
e-mail: cma@virgo.gsfc.nasa.gov

Abstract

Since the ICRF was generated in 1995, VLBI modeling and estimation, data quality, source position stability analysis, and supporting observational programs have improved markedly. There are developing and potential applications in the areas of space navigation, Earth orientation monitoring and optical astrometry from space that would benefit from a refined ICRF with enhanced accuracy, stability and spatial distribution. The convergence of analysis, focused observations, and astrometric needs should drive the production of a new realization in the next few years.

1. Introduction

The ICRF (International Celestial Reference Frame) is the first realization of the ICRS (International Celestial Reference System) at radio frequencies and consists of 212 defining sources whose positions are independent of the equator, equinox, ecliptic and epoch but consistent with the previous stellar and dynamical realizations within their respective errors. The accuracy of individual positions has a floor of 0.25 milliarcseconds based on an extensive error analysis while the orientation stability of the axes is $\sim$20 microarcseconds. Initially the ICRF positions of 608 sources were estimated (Ma et al., 1998). While the ICRF did not come into official use until 1 January 1998, the catalog positions were used before that date to orient and stabilize the HIPPARCOS catalog, the ICRS realization at optical frequencies. Since then the radio positions have been improved for non-defining sources and the catalog extended by 109 sources in ICRF-Ext.1 and ICRF-Ext.2 (Fey et al., submitted) using newer data from conventional geodetic/astrometric sessions along with $\sim$1200 sources from a series of VLBA sessions devoted to the VLBA Calibrator Survey (Beaseley et al., 2002).

2. Considerations for Generating the Next ICRF

The process for introducing and adopting the ICRF was detailed and lengthy. A firm theoretical framework, sufficient observational data, established VLBI analysis, an expectation of order of magnitude improvement over the stellar celestial reference frame, and preparation of the astronomical community were all important in a smooth transition from FK5 to ICRF. The rationales for the next radio realization are rather different and the process may be less formally structured.

One rationale and a prerequisite is useful improvement in the intrinsic quality of a new realization. The limitations of the ICRF are the error floor (related to modeling, estimation, and data imperfections), the defining sources (too sparse, unevenly distributed spatially, insufficiently stable in retrospect), and data distribution (overall sparseness of sources and particular deficiency in the southern hemisphere). Each of these weaknesses can be significantly ameliorated by developments since 1995 and expected changes in analysis and CRF observing in the next few years.

There are two areas that would directly benefit by a more accurate and stable realization. Spacecraft navigation using differential VLBI relative to a nearby ICRF object is now a standard technique in the NASA solar system exploration program and is also planned for the Japanese and Chinese lunar probes. This measurement type is dependent on the accuracy of ICRF positions as well as ICRF objects in the relevant parts of the sky. The second area is VLBI monitoring of Earth orientation parameters, particularly precession/nutation and UT1. These measurements will continue to be the unique domain of VLBI. Enhanced stability and accuracy are needed to detect the small, variable effects of deep structures of the Earth.

A prospective development in optical astrometry, the GAIA mission, may prove to be the most stringent requirement for the radio realization. Expected to be launched within a decade, GAIA is projected to achieve 10 microarcsecond precision for brighter quasars. To achieve the best optical-radio registration and to insure the highest accuracy for the transfer from radio to optical realizations, the radio CRF must be pushed to the limit. A particular VLBI observing effort may be needed for the common sources since the current ICRF sources are generally weaker than desirable in the optical band.

The process for adopting the ICRF was quite formal, culminating in an IAU resolution at the IAU General Assembly at Kyoto in 1997. Since then the responsibility for the maintenance of the ICRS has been given to the IERS (International Earth Rotation and Reference Systems Service) while the IVS has operational responsibility for the VLBI realization. The IAG (International Association of Geodesy) is forming a working group in Subcommission 1.4 Interaction of Celestial and Terrestrial Reference Frames to investigate the systematic errors in the ICRF because of the impact on Earth orientation parameters and indirectly on the satellite celestial reference frames. While the work for the ICRF was accomplished within an IAU working group, the work for the next VLBI realization may be more loosely coordinated or placed under a different organization. The process for preparing the astronomical community and for formal adoption remains to be decided.

3. Areas of Refinement

There are four main areas in which the VLBI realization of the ICRS can be improved: analysis, data, defining sources, and observing programs.

Since 1995 considerable progress has occurred in VLBI modeling and estimation. New analysis software has been developed (Titov et al., this volume; Tesmer et al., this volume). The largest source of errors is probably the troposphere, so improved troposphere mapping functions that use weather model information such as the IMF (Isobaric Mapping Function) (Niell, 2002) and the VMF (Vienna Mapping Function) (Boehm et al, this volume) and better gradient estimation should reduce systematic errors and temporal noise. Refined loading models for ocean, atmosphere and hydrology effects should permit the unified solution for CRF, TRF and EOP to exploit the unique capability of VLBI. In constrast, the ICRF analysis estimated station positions for each session to reduce contamination from the TRF. However, analysis methods to properly model nonlinear station motions as well as apparent sources motions and other instabilities need to be tested and compared. Treating unstable sources as arc parameters as was done for the ICRF may unnecessarily weaken the results. It should be noted that the ICRF-Ext.1 and ICRF-Ext.2 analysis were consistent with the analysis for the ICRF.

The ICRF used all available geodetic/astrometric VLBI data from 1979 to 1995.6. The sources observed, the number of sources and observations in each session, the network sizes and geometries, and the sensitivity of the VLBI equipment evolved over the period and have continued to improve since then. Instead of ~15 sources with a network of 3-4 stations producing several hundred observations in the earliest years, the most extensive modern sessions use 20 stations and up to 80 sources resulting in several tens of thousands of observations. In addition, Gontier et al. (2001) showed that the stability of the CRF improved noticeably around 1990. Consequently the next realization probably will discard early sessions as well as those unsuitable for astrometry. Figure 1 shows that the 792 sources observed since 1990 in conventional geodetic/astrometric sessions cover the sky with reasonable uniformity. It will remain true, however, that the bulk of the data will come from geodetic sessions, ~200 "geodetic" sources most frequently observed, and the northern hemisphere. Sessions using the VLBA together with up to 10 other stations will contribute a significant fraction of the total observations.

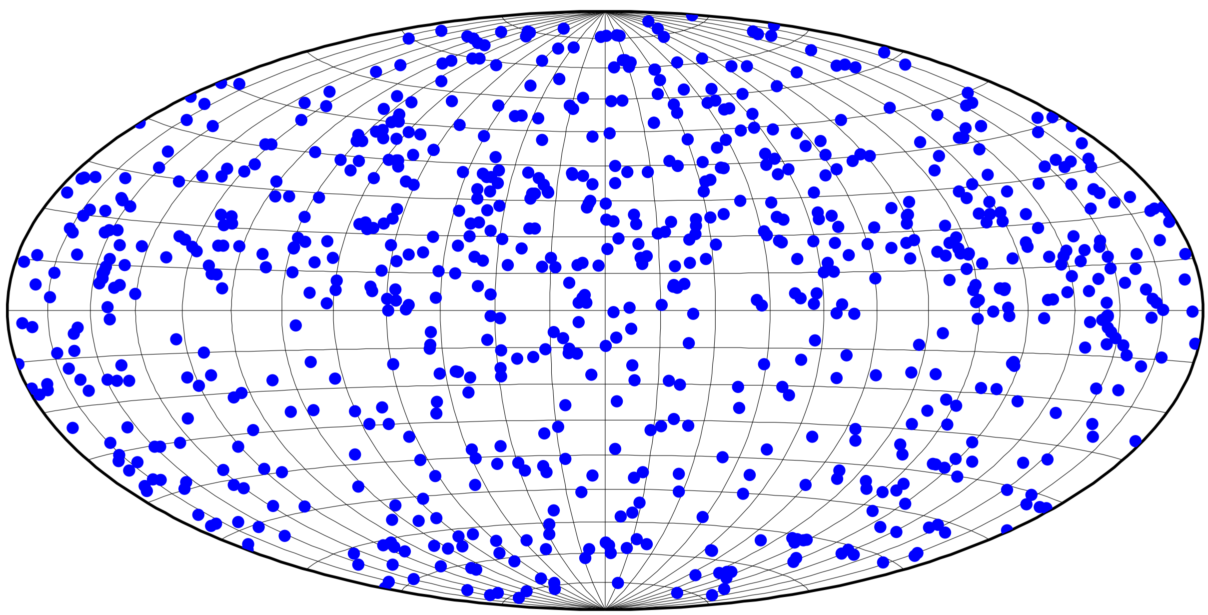

Figure 1. 792 sources observed since 1990.

The positions of the 212 defining sources are the formal realization of the ICRS called the ICRF. These sources were chosen with the best information available in 1995 based largely on number of observations and position stability. However, the distribution of the data over sources and over the sky was extremely nonuniform with most of the observations from fewer than 100 "geodetic" sources used in the regularly scheduled geodetic sessions in the northern hemisphere. In order to have over two hundred defining sources with somewhat more extensive and uniform sky distribution, the selection criteria could not be too severe. Even so, less than 30% of the defining sources are in the south. On the other hand, some frequently observed sources were not selected as defining sources because they had sufficient data to detect anomalous behavior. Recent analysis by Feissel-Vernier (2003) looking at annual VLBI source position time series from 1990 to 2002 and using very different criteria from the ICRF identified a different set of sufficiently observed sources with stable positions. A number of ICRF defining sources failed these stability criteria. It is clear that the next realization should reexamine the defining sources and ensure that the data set is robust enough to make a new selection.

While the Feissel-Vernier analysis showed that better defining sources can now be found, the number and distribution of such sources still leaves something to be desired. In the planned IVS observing program the vast majority of the sessions are primarily geodetic in nature. The VLBA sessions contribute to both geodesy and astrometry by design. Recognizing the data deficiencies, the astrometric sessions will concentrate on the southern hemisphere, particularly to provide sufficient temporal coverage to identify stable sources. In addition, a small fraction of each geodetic session will be allocated to observing stable and potentially stable sources to accumulate data more rapidly for time series analysis and estimation of apparent proper motion. Potentially stable sources are those whose current time series have insufficient data to establish stability but do not show disqualifying motions or scatter. Over the next few years these observing efforts should significantly augment the potential defining sources for the next realization.

4. Summary

The next VLBI realization of the ICRS, perhaps to be designated ICRF-200x, will differ significantly from the ICRF. It will utilize the state of the art VLBI analysis as of the end epoch 200x, correcting known systematic errors in the ICRF and reunifying the CRF, TRF and EOP. The data set will most likely include only astrometrically relevant data from 1990 to 200x. The defining sources will be more extensive and uniformly distributed than those of the ICRF, relying on the geodetic data augmented by recent directed astrometric observations for stable sources and the southern hemisphere.

References

[1] Beaseley, A.J. et al., The VLBA Calibrator Survey - VCS1, Ap J Sup 141, 13, 2002.

[2] Boehm, J. and Schuh, H., Vienna mapping functions in VLBI analysis, this volume, 2004.

[3] Fey, A.L. et al., The ICRF. Extension and revision: Positions of 109 additional sources, submitted to Astron. J.

[4] Gontier, A.-M., Le Bail, K. and Feissel, M., Stability of the extragalactic VLBI reference frame, A&A 375, 661, 2001.

[5] Feissel-Vernier, M., Selecting stable extragalactic compact radio sources from the permanent astro-geodetic VLBI program, A&A 403, 105, 2003.

[6] Ma, C. et al., The ICRF as realized by VLBI, Astron J 116, 516, 1998.

[7] Niell, A.E., Improved atmospheric mapping functions for VLBI and GPS, Earth Planets Space 52, 699, 2000.

[8] Tesmer, V., Kutterer, H. and Drewes, H., Simultaneous estimation of a TRF, the EOP and a CRF from VLBI observations - first DGFI results using OCCAM, this volume, 2004.

[9] Titov, O., Tesmer, V. and Boehm, J., OCCAM v.6.0 software for VLBI data analysis, this volume, 2004.

Alan L. Fey: Status of the International Celestial Reference Frame, IVS 2004 General Meeting Proceedings, p.341–345
http://ivscc.gsfc.nasa.gov/publications/gm2004/fey1

Status of the International Celestial Reference Frame

Alan L. Fey

U.S. Naval Observatory

e-mail: afey@usno.navy.mil

Abstract

There have been two extensions (updates) of the ICRF since its initial definition in 1998. The primary objectives of extending the ICRF were to provide positions for the 109 extragalactic radio sources observed since the definition of the ICRF and to refine the positions of candidate and other sources using additional observations. A secondary objective was to monitor sources to ascertain whether they continue to be suitable for use in the ICRF. Positions of the ICRF defining sources have remained unchanged. Improved positions and errors for the candidate and other sources were estimated and reflect the changes in the data set and the analysis. The 109 new sources were added with ICRF coordinates. A brief overview of the current observing programs contributing to the maintenance and extension of the ICRF will also be presented.

1. Introduction

At the XXIII General Assembly of the International Astronomical Union (IAU) held on 20 August 1997 in Kyoto, Japan, the International Celestial Reference Frame (ICRF) [1] was adopted as the fundamental celestial reference frame. As a consequence, the definitions of the axes of the celestial reference system are no longer related to the equator or the ecliptic but have been superseded by the defining coordinates of the ICRF. The ICRF is currently defined by the radio positions of 212 extragalactic objects obtained using the technique of Very Long Baseline Interferometry (VLBI) at frequencies of 2.3 and 8.4 GHz over the past 20+ years. The ICRF has now replaced the FK5 optical catalog as the fundamental frame and is the realization of the International Celestial Reference System (ICRS) [2] at radio wavelengths. The HIPPARCOS catalog [3] is the realization of the ICRS at optical wavelengths [4].

2. A Brief ICRF Time Line

- 1988: The IAU sets up working groups to establish a new reference frame.
- 1991: The IAU establishes the theoretical basis for a new reference frame.
- 1994: The IAU defines the ensemble of fiducial points for a new reference frame as extragalactic objects.
- 1995: A sub-group of the IAU Working Group on Reference Frames is tasked to construct a new reference frame based on VLBI observations of quasars.
- 1997: The IAU establishes the ICRS and adopts the ICRF.
- 1998: On January 1st, the ICRF replaces the FK5 optical catalog as the fundamental celestial reference frame.

- 1999: The first extension of the ICRF, ICRF-Ext.1, is completed adding 59 new radio sources with ICRF coordinates.
- 2002: The second extension of the ICRF, ICRF-Ext.2, is completed adding 50 new radio sources with ICRF coordinates.

3. The ICRF

The ICRF is currently defined by the radio positions of 212 extragalactic objects. The radio positions are based upon a general solution for all applicable dual frequency 2.3 GHz and 8.4 GHz Mark III VLBI data available through the middle of 1995 consisting of 1.6 million pairs of group delay and phase delay rate observations. The positional accuracy of the ICRF sources is better than about 1 mas in both coordinates. The ICRF "defining" sources set the direction of the ICRS axes and were chosen based on their observing histories and the stability and accuracy of their position estimates. In addition to the 212 defining sources, positions for 294 less observed "candidate" sources along with 102 less suitable "other" sources were also given by [1] to densify the frame. The final orientation of the frame axes was obtained by a rotation of the positions into the system of the International Celestial Reference System (ICRS) [2] and is consistent with the FK5 J2000.0 optical system, within the limits of the latter system accuracy. The sky distribution of the 608 ICRF sources is shown in Figure 1. The sky distribution of the ICRF Defining sources is shown in Figure 2.

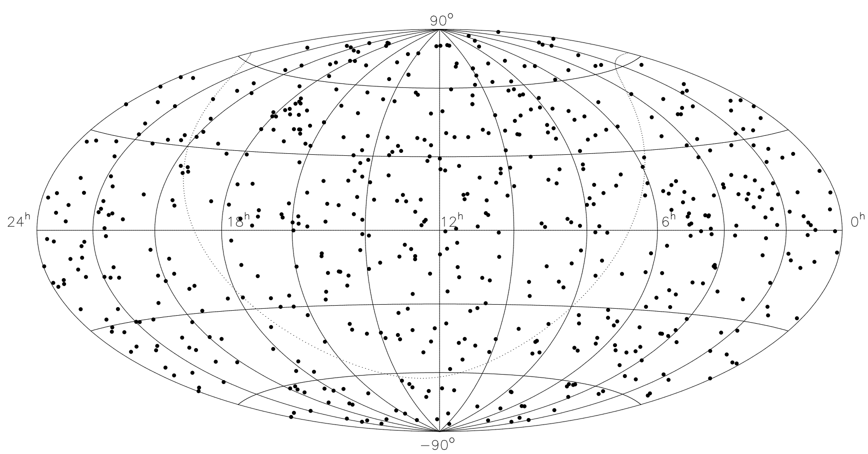

Figure 1. Distribution of the 608 ICRF sources on an Aitoff equal-area projection of the celestial sphere. The dotted line represents the Galactic equator.

4. ICRF-Ext.1

The primary objectives of extending the ICRF were to provide positions for extragalactic radio sources observed since the definition of the ICRF and to refine the positions of candidate and other sources using additional observations. A secondary objective was to monitor sources to ascertain whether they continue to be suitable for use in the ICRF.

The data added to the ICRF in ICRF-Ext.1 [5] spanned December 1994 through April 1999

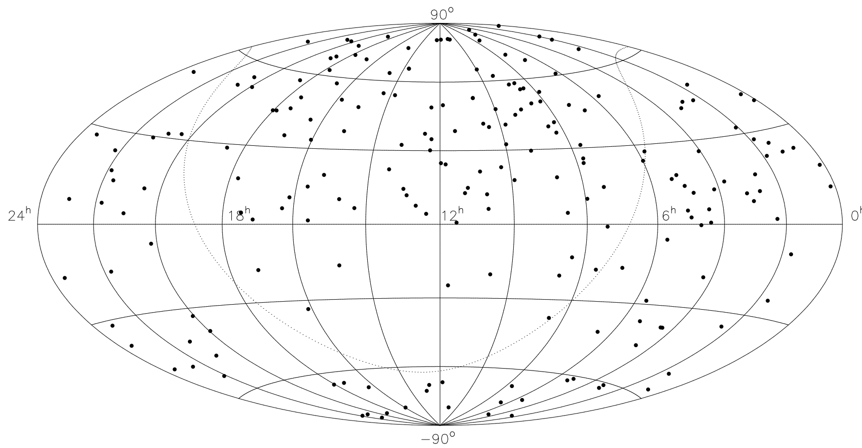

Figure 2. Distribution of the 212 ICRF Defining sources on an Aitoff equal-area projection of the celestial sphere. The dotted line represents the Galactic equator.

and were obtained from both geodetic and astrometric observing programs. Approximately 0.6 million new observations from 461 sessions were added. There were 59 new sources. The positions and errors for the defining sources were unchanged from the ICRF. Improved positions and errors for the candidate and other sources were estimated and reflect the changes in the data set and the analysis. (While the coordinates of individual sources may change to better match the available observations, the IAU recommendation adopting the ICRF states that any updates of the ICRF will keep the same coordinate axes by means of a statistical no-net-rotation condition.) The 59 new sources were added with ICRF coordinates. The distribution on the sky of the new sources is shown in Figure 3.

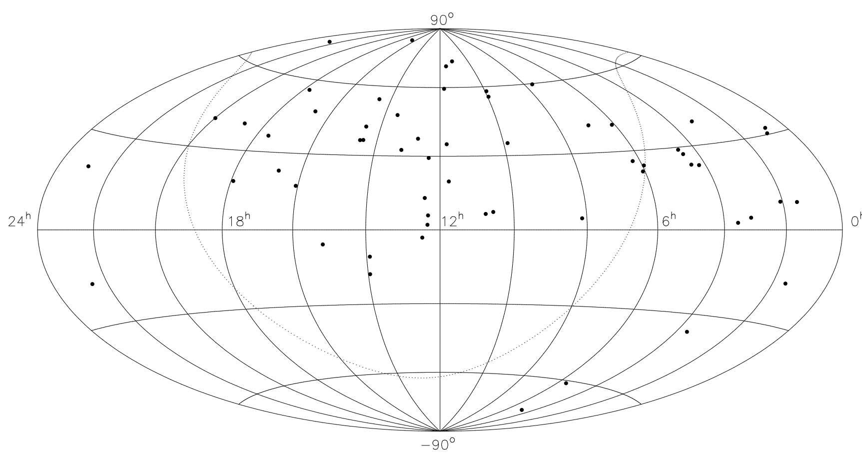

Figure 3. Distribution of 59 new sources in ICRF-Ext.1 on an Aitoff equal-area projection of the celestial sphere. The dotted line represents the Galactic equator.

5. ICRF-Ext.2

The data added to the ICRF in ICRF-Ext.2 [6] spanned May 1999 through May 2002 and were obtained from both geodetic and astrometric observing programs. Approximately 1.2 million new observations from approximately 400 sessions were added. There were 50 new sources. The positions and errors for the defining sources were unchanged from the ICRF. Improved positions and errors for the candidate and other sources were estimated and reflect the changes in the data set and the analysis. The 50 new sources were added with ICRF coordinates. The distribution on the sky of the new sources is shown in Figure 4.

ICRF-Ext.2 marks a milestone in that it utilizes all available Very Long Baseline Array (VLBA) RDV data. The VLBA RDV data is obtained through a collaborative program of geodetic and astrometric research between the U.S. Naval Observatory (USNO), the Goddard Space Flight Center (GSFC) and the National Radio Astronomy Observatory (NRAO). A total of over 652 000 delay observations (almost 20% of all available observations!) from 30 VLBA geodesy/astrometry sessions were included in the ICRF-Ext.2 solution.

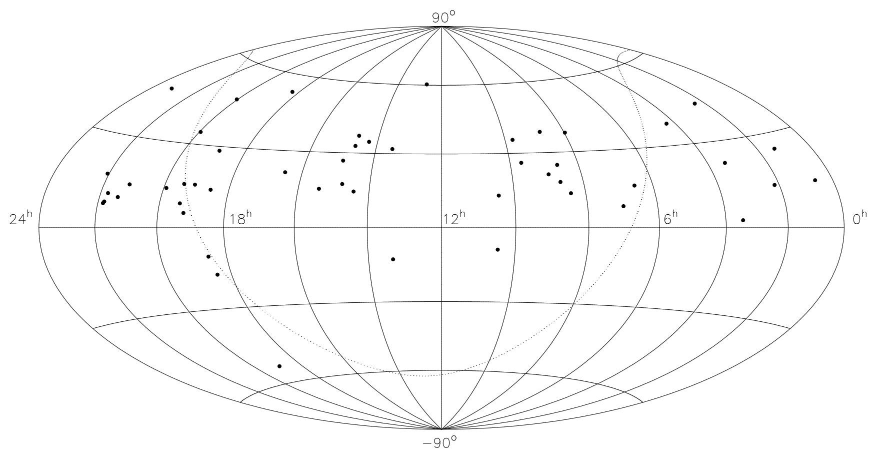

Figure 4. Distribution of 50 new sources in ICRF-Ext.2 on an Aitoff equal-area projection of the celestial sphere. The dotted line represents the Galactic equator.

6. ICRF Maintenance

The IAU has charged the International Earth Rotation and Reference Systems Service (IERS) with the maintenance of the ICRF. Maintenance activities are run jointly by the IERS ICRS Product Center and the International VLBI Service (IVS).

The IERS ICRS Product Center is directly responsible for the maintenance of the ICRS and ICRF. The Center is run jointly by the Observatoire de Paris and the USNO. More information can be obtained from the Product Center Web page at `http://www.iers.org/iers/pc/icrs/`.

The IVS is an international collaboration of organizations which operate or support VLBI. The IVS provides a service which supports geodetic and astrometric work on reference systems, Earth science research, and operational activities. Many of the observing programs for maintenance of the ICRF are coordinated by the IVS. More information about the IVS can be obtained from the IVS Web page at `http://ivscc.gsfc.nasa.gov/`.

6.1. Observing Programs for ICRF Maintenance

The following observing programs are among those that contribute astrometric data for maintenance of the ICRF.

- **IVS CRF Experiments:** These 24^{hr} duration VLBI experiments, coordinated by the IVS, concentrate primarily on observation of southern hemisphere ICRF sources for monitoring and to increase the sky density of ICRF defining sources.
- **VLBA RDV Experiments:** These 24^{hr} duration VLBI experiments are part of a collaborative program of geodetic and astrometric research between the USNO, GSFC and NRAO. VLBA RDV experiments concentrate primarily on observation of northern hemisphere ICRF sources ($\delta > -30°$). Intrinsic source structure information is also obtained from these experiments.
- **IVS Geodetic/Astrometric Experiments:** These 24^{hr} duration VLBI experiments, coordinated by the IVS, concentrate primarily on observation of sources for geodetic purposes and for Earth Orientation Parameter estimation but are also useful for astrometric purposes.
- **VLBA Calibrator Surveys:** These 24^{hr} duration VLBI experiments are part of a joint NRAO/GSFC program to expand both the list of high quality geodetic sources and the list of phase reference calibrators for imaging.
- **EVN Experiments:** These 24^{hr} duration VLBI experiments are part of a Bordeaux Observatory program to expand the list of ICRF defining sources in the northern hemisphere using the European VLBI Network (EVN).
- **LBA:** These 24^{hr} duration VLBI experiments using the Australia Telescope National Facility (ATNF) Long Baseline Array (LBA) are part of a joint USNO/ ATNF program to expand the list of ICRF defining sources in the southern hemisphere. Intrinsic source structure information is also obtained from these experiments. Astrometric results for 22 sources are now available [7].

References

[1] Ma, C., et al. 1998: "The International Celestial Reference Frame as Realized by Very Long Baseline Interferometry," AJ, 116, 516

[2] Arias, E. F., Charlot, P., Feissel, M., & Lestrade, J. –F. 1995: "The extragalactic reference system of the International Earth Rotation Service, ICRS." A&A, 303, 604

[3] Perryman, M. A. C., et al. 1997: "The HIPPARCOS Catalogue," A&A, 323, 49

[4] Kovalevsky, J., et al. 1997: "The HIPPARCOS catalogue as a realisation of the extragalactic reference system," A&A, 323, 620

[5] 1998 IERS Annual report, 1999: "First extension of the ICRF, ICRF-Ext.1," Chapter VI, D. Gambis (ed), Observatoire de Paris, p. 87-114.

[6] Fey, A. L., et al. 2004: "Second Extension of the International Celestial Reference Frame, ICRF-Ext.2," AJ, submitted

[7] Fey, A. L., et al. 2004: "Accurate Astrometry of 22 Southern Hemisphere Radio Sources," AJ, accepted for publication

Martine Feissel-Vernier: Stability of the VLBI-Derived Celestial Reference Frame, IVS 2004 General Meeting Proceedings, p.346–350
http://ivscc.gsfc.nasa.gov/publications/gm2004/vernier

Stability of the VLBI-Derived Celestial Reference Frame

Martine Feissel-Vernier

Observatoire de Paris/SYRTE and Institut Géographique National/LAREG
e-mail: feissel@ensg.ign.fr

Abstract

We present background information of a paper [5] that investigated several stable source selection processes and proposed a list of 199 stable sources that could be used for a future improvement of the ICRF. Their expected performance in maintening the direction of the ICRF axes (± 6 μas) is better by a factor of four or five than that of the current 212 ICRF defining sources.

1. The Observations

The data analysis in this study is based on the time series of coordinates of 707 radio source derived by Alan Fey (USNO) using 3.6 millions of observations accumulated in various international programs up to May 2002. The observations consist of time series derived from a set of three analyses of the existing VLBI observing sessions. Each analysis results in time series of coordinates per session for one third of the sources ("arc" sources), the coordinates of the other sources being treated as "global", i.e. they are assumed to stay fixed in time and are estimated globally. Each analysis includes a no-net-rotation (NNR) condition with respect to the ICRF based on a part of the ICRF *defining sources* [7] . To avoid inconsistencies that are due to the NNR condition realization in the three analyses, and that can reach the level of 50 microarcseconds (μas), we consider here for each source the time series of its coordinates differences with their global weighted mean.

2. Apparent Motion of Sources

When observed at the current level of precision (a fraction of milliarcsecond, mas), no object is really pointlike. Most of the known activity of quasars takes the form of jets, i.e., aligned emissive structures that cause an apparent motion of the observed phase center. As a result, most objects exhibit time variations of their position in some preferred direction.

We illustrate in figure 1 the 1984-2002 time evolution of the positions of four sources in local equatorial frames. See [6] for more detail on the apparent motion of these sources.

3. The Stable Sources Selection Scheme

Stable sources were selected from the 1989.5-2002.4 data in a two-step process, as follows.

1. A first selection is made on the basis of continuity criteria for one-year weighted average coordinates. The preselection conditions are the following ones.

   (a) Length of observation period longer than five years.

   (b) Not less than two observations of the source in a given session.

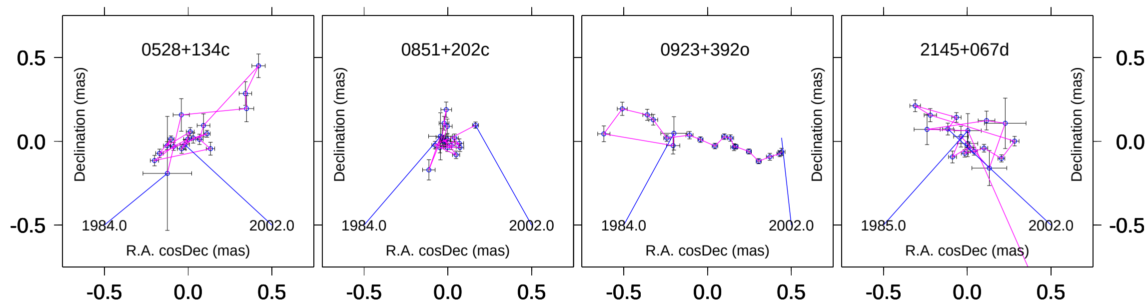

Figure 1. Observed motion of four radio sources over 1984-2002 (yearly averages). Similar plots for 362 well observed sources are available at http://hpiers.obspm.fr/icrs-pc/icrf/time-series.html.

(c) One-year average coordinates based on at least three observations.

(d) Not more than three successive years with no results, conditions (b) and (c) being met.

(e) At least half of the one-year averages available over the source observation time span.

This first screening kept 362 sources for the years centered at 1990.0 through 2002.0. These include 67% of the defining sources, 44% of the candidates and 85% of the others.

2. The time series of yearly values of $\alpha \cos\delta$ and δ of the preselected sources are then analysed in order to derive

   (a) the linear drift (least squares estimation) and the normalized drift. The latter is the absolute value of the linear drift divided by its formal uncertainty;

   (b) the Allan standard deviation [1] for a one-year sampling time. The Allan variance of a time series x_i with N items and sampling time τ is defined as:

$$\sigma_A^2(\tau) = \frac{1}{2N} \sum_i (x_{i+1} - x_i)^2$$

For each local coordinate ($\alpha \cos\delta$ and δ), two partial indices are defined (see Table 1). The partial stability indices range from 1 (most stable) through 3 (least stable), with a rejection value (10) associated to very large drifts or standard deviations.

4. Relationship of the Stable Sources with the ICRF Source Qualifications

The **partial stability indices** for each of the 362 sources investigated (drift, Allan variance and normalized drift) can be compared with two existing ICRF qualifiers:

- the source status: defining, candidate or other, and
- the source structure index [3] in the X band. Structure index values 1 and 2 indicate very good and good astrometric suitability, values 3 and 4 poor and very poor suitability.

The comparisons are plotted in figures 2 and 3. The sources considered as stable are those inside the lower left rectangles. The plots show only partial agreement of the ICRF qualifiers with the stability criteria.

Table 1. Partial stability criteria.

Statistics	Threshold	Partial index
Allan Standard deviation (AlSd)		
	AlSd $\leq$ 100 μas	1
	100 μas $\leq$ AlSd $\leq$ 200 μas	2
	200 μas $\leq$ AlSd $\leq$ 300 μas	3
	AlSd $\geq$ 300 μas	10
|Drift| (Vel)		
	Vel $\leq$ 10 μas/year	1
	Vel $\geq$ 50 μas/year	10
|Normalized drift| (Nvl)		
	Nvl $\leq$ 1	1
	1 $\leq$ Nvl $\leq$ 3	2
	Nvl $\geq$ 3	3

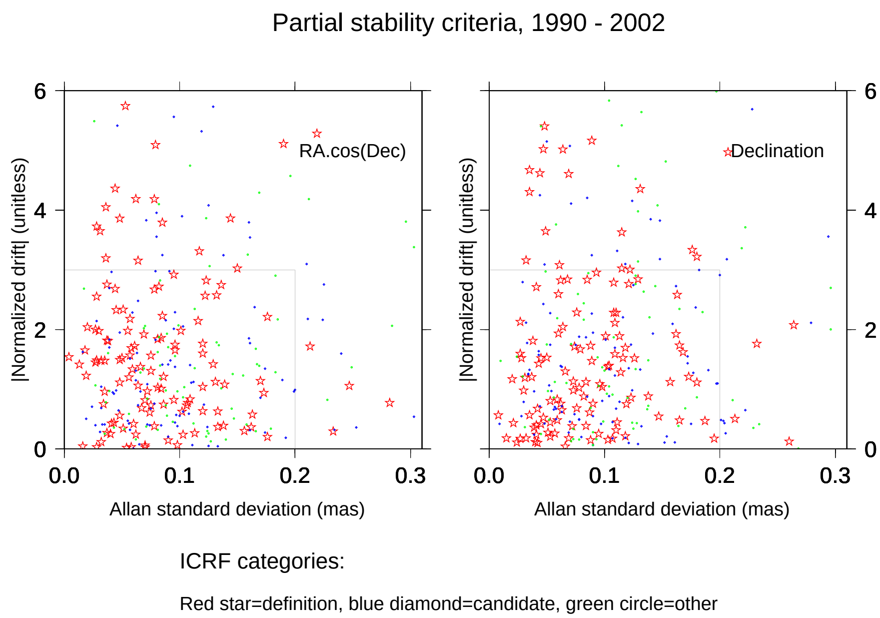

Figure 2. Relationship of the ICRF source status with the partial stability index

Table 2 gives the relationship of the **global stability index** with the ICRF qualifiers. Sources with global stability indices 1 and 2 are considered as stable. Although a number of defining sources get small partial stability indices, some of them are clearly detected as unstable. The candidate sources are globally in the same situation. Conversely, a number of "other" sources, i.e. considered as having questionable stability in the ICRF work, are detected as stable. Compared to the ICRF selection, the proposed scheme rescues a number of sources that are in fact efficient for maintaining the ICRF axes directions [2]. For what concerns the source stability indices, 80% of the stable sources have a good structure index (1 or 2), while the ratio is also large for the unstable sources (64%). Altogether, 61% of the well observed sources with a good structure index

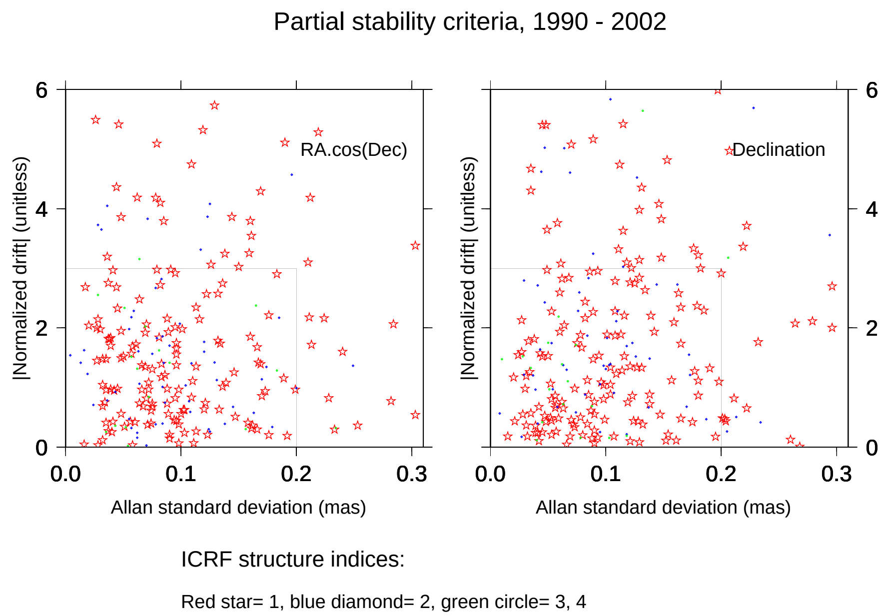

Figure 3. Relationship of the source structure index with the partial stability index

are detected as stable, and 39% are detected as unstable. This finding is of interest in the context of studying the dynamics of the quasars' activity.

Table 2. Stability index and ICRF source qualifiers.

Stab. index	Source status Def.	Can.	Oth.	Structure index 1	2	3-4	Stab. index	Source status Def.	Can.	Oth.	Structure index 1	2	3-4
Stable							Unstable						
1	33	26	15	46	11	7	3	2	1	4	6	2	0
2	48	42	34	76	26	6	4	58	61	34	70	26	13

5. Testing Source Selections

Out of the 362 preselected sources the stability scheme described in section 3 produces 199 stable sources, a number to be compared to the 212 defining sources in the ICRF. To test their efficiency for maintaining the direction of the axes of the celestial reference frame, we consider the 13 yearly differential reference frames (1990.0 - 2002.0) that are formed by the set of stable sources observed in each year and we compute the series of yearly differential rotation angles A_1, A_2, A_3 around the axes of the equatorial coordinate system for the 13 years. Table 3 lists efficiency estimates for the stable sources and for the ICRF defining sources. These estimates are

- the average standard deviation of the series of A_1, A_2, A_3, that characterizes the scattering of the series of yearly rotation angles, and
- their Allan standard deviations for one-year and four-year sampling times, that characterize

their stability in time. Note that if the time series of the rotation angles have white noise, the four-year Allan standard deviation will be equal to half (square root of one fourth in sampling time) the one-year one. In the case of flicker noise, both values will be equal.

The estimated efficiency of the ICRF defining sources is lower than that of the proposed selection by nearly a factor of three for the one-year estimates and a factor of five in the longer term. In addition, the axis stability spectrum is nearly white noise in the case of the stable sources, while it is degraded to flicker noise in the case of the defining sources.

Table 3. Stability of rotation angles of yearly reference frames relative to the 1990-2002 mean frame.

Source selection scheme	Nb of sources kept	Std dev. μas	Allan Std dev. 1 year μas	4 years μas
Stable	199	10.8	9.4	5.9
ICRF Defining	212	25.6	26.0	27.6

6. Discussion

When compared to the current ICRF defining sources, the selection scheme developed in [5] achieves improved time stability of yearly reference frames (6 μas vs 28 μas) , which implies improved internal consistency.

This has consequences in astrometric applications, but it may also have bearings in the geophysical interpretation of the Earth's orientation in inertial space. As an example, Dehant et al. [4] have shown that source instabilities perturb precession and long term nutation determinations at the level of tens of μas, a level comparable to that of the discrepancy of VLBI results with the precession constant or the 18.6-year nutation component in the IAU2000 Nutation model.

Finally, we recommend that the set of selected stable sources be considered in the scheduling of repeated VLBI sessions for Earth rotation, geodesy and astrometry, as well as in any future improvement of the International Celestial Reference Frame.

References

[1] D.W. Allan, 1966, Proc. IEEE 54, 221

[2] E.F. Arias, S. Bouquillon, 2003, A&A, In press

[3] P. Charlot, 2004, This volume

[4] V. Dehant, M. Feissel-Vernier, O. de Viron, C. Ma, M. Yseboot, C. Bizouard, 2002, JGRB, 108, 2275

[5] M. Feissel-Vernier, 2003, A&A, 403, 105

[6] M. Feissel-Vernier, 2004, in IERS Technical Note in preparation (J. Souchay ed.)

[7] C. Ma, E.F. Arias, T.M. Eubanks, A.L. Fey, A.-M. Gontier, C.S. Jacobs, O.J. Sovers, B.A. Archinal, P. Charlot, 1998, AJ 116, 516

David Gordon: VLBA Impact on Geodesy and Astrometry, IVS 2004 General Meeting Proceedings, p.351–355
http://ivscc.gsfc.nasa.gov/publications/gm2004/gordon1

VLBA Impact on Geodesy and Astrometry

David Gordon

Raytheon ITSS/NASA Goddard Space Flight Center
e-mail: dgg@leo.gsfc.nasa.gov

Abstract

Large global solutions with and without VLBA sessions are compared to assess the impact of the VLBA. VLBA sessions comprise ~30% of all the normal geodetic/astrometric VLBI observations, and are found to make significant improvements in the TRF and CRF and to contribute significantly to the measurement of the long period nutation terms.

1. Introduction

Geodetic usage of the VLBA began in 1989, with the inclusion of Pie Town in occasional Mark III sessions. Increasing geodetic/astrometric use continued for several years, as more antennas became available. These early sessions were all correlated at the Haystack or USNO Mark III correlators. Beginning in 1995, geo/astro sessions using the full VLBA plus a few Mark III stations were started, along with their correlation on the new VLBA correlator. In 1997, the RDV sessions were begun, consisting of 6 yearly sessions, using the full VLBA and up to ten Mark IV stations. Early on in their usage, the VLBA antennas were recognized for their greater sensitivity and phase stability. Though not routinely done, the 8 continental US VLBA stations could be phase connected in nearly all of the RDV and earlier sessions. The geo/astro community now has nearly 9 years of full VLBA and VLBA-correlated sessions, In view of its recognized high quality, it seems like a good time to take an objective look at what contribution the VLBA has made to the gedetic/astrometric programs. To make this analysis, a Solve global solution was run to match the latest GSFC quarterly solution, but with all effects of the VLBA removed. This meant removing all RDV and most earlier VLBA sessions. For some of the earliest sessions, with just one or two VLBA stations and several Mark III stations, we just excluded the VLBA sites. The VLBA Calibrator Sessions (VCS1 and VCS2) [1] [2] were not included in either solution. The basic statistics of the two solutions, with and without the VLBA, are shown below in Table 1. The VLBA sessions represent about 30% of all the normal geodetic/astrometric VLBI observations, but less obvious is their effect on the terrestrial and celestial reference frames.

Table 1. Solution Statistics with/without the VLBA

	Without VLBA	With VLBA
No. Observations (millions)	2.98	4.28
No. Sources	879	910
No. Stations	138	148
No. Baselines	1044	1327

2. Impact on the Terrestrial Reference Frame

At first glance, it seems that the VLBA represents only a small fraction of the 148 VLBI stations in the TRF, but most of these are inactive sites. In reality, the VLBA represents nearly 30% of the active geo/astro VLBI sites, and they are among the most accurately determined sites, greatly adding to the stability of the TRF in the North America, Caribbean, and Pacific regions. Further, use of the VLBA with other worldwide Mark III/IV sites has greatly strengthened the worldwide TRF. Baselines with a VLBA antenna at one or both ends show an average repeatability of 0.8 parts-per-billion, compared to 1.5 ppb for all baselines. In Table 2, we list the horizontal site position and velocity formal errors from the two solutions for the VLBA and the 14 Mark IV stations used in VLBA sessions. Participation in VLBA sessions has improved the TRF positions and velocities for most of these Mark IV sites by typically 10-40%. Standing out anomolously are GGAO, which has been used almost exclusively in the RDVs, so its improvement is much more dramatic; and TIGO which has been used in only the last few RDVs, so it shows little improvement yet.

3. Impact on the Celestial Reference Frame

Though the regular VLBA sessions add only 31 additional sources, they greatly improve the source position determinations for most sources between -30 and +90 degrees declination. Figures 1 and 2 show the distribution of right ascension and declination uncertainties for all sources north of -30 degrees. Inclusion of the VLBA sessions results in a dramatically narrower distribution of errors. But we need to ask whether this improvement is just the result of the increased number of observations. If the VLBA data were equivalent in quality to the Mark III/IV data, then we would expect the source formal errors to decrease at a rate proportional to the square root of the number of observations. But if the quality is greater, then the formal errors should decrease faster. For 484 sources with more than 10 Mark III/IV observations, we find the average square root (giving all sources equal weight) of the ratio of the number of observations (Mark III/IV+VLBA divided by Mark III/IV-only) to be 1.946. This compares to average ratios of the formal errors (Mark III/IV-only divided by Mark III/IV+VLBA) of 2.184 in Declination and 2.673 in R.A. Thus, the implication is that the VLBA source data is higher in quality than the Mark III/IV data, most significantly in R.A. This can be attributed to the improved geometry of the RDV sessions, particularly in longitude, and the greater sensitivity and phase stability of the VLBA systems.

If we include the 12 VLBA calibrator sessions from VCS1 and VCS2 [1] [2], then the total number of geodetic/astrometric sources increases to 2290, a 150% increase. This increases the number of sources known to better than 1 n-radian from 615 to 2011, and there is now at least one well known calibrator within 4 degrees of any target source over 90% of the sky north of -40 degreees declination. This is, of course, most significant for radio astronomy phase referencing, where nearby calibrators are needed. Most of the new sources are too weak for the regular Mark IV 24-hr and 1-hr Intensive sessions, but undoubtably, many will contribute towards the next definition of the ITRF.

Table 2. Horizontal Site Formal Errors

	Position With/Without VLBA (mm)	Velocity With/Without VLBA (mm/yr)
GGAO7108	.41 / 2.6	.12 / .71
GILCREEK	.25 / .36	.03 / .04
HARTRAO	.58 / .68	.13 / .15
KOKEE	.40 / .60	.06 / .09
MATERA	.34 / .42	.06 / .07
MEDICINA	.36 / .46	.07 / .08
NOTO	.37 / .45	.08 / .09
NRAO20	.24 / .40	.07 / .09
NYALES20	.29 / .37	.04 / .04
ONSALA60	.31 / .39	.05 / .06
TIGOCONC	8.7 / 9.2	1.30 /1.43
TSUKUB32	.62 / .73	.12 / .13
WESTFORD	.23 / .38	.03 / .05
WETTZELL	.31 / .40	.05 / .06
BR-VLBA	.22 / —	.03 / —
FD-VLBA	.24 / —	.04 / —
HN-VLBA	.24 / —	.04 / —
KP-VLBA	.25 / —	.04 / —
LA-VLBA	.23 / —	.03 / —
MK-VLBA	.42 / —	.07 / —
NL-VLBA	.22 / —	.03 / —
OV-VLBA	.24 / —	.04 / —
PIE TOWN	.24 / —	.03 / —
SC-VLBA	.36 / —	.07 / —

4. Impact on EOP/Nutation

Table 3 shows the relative performance of the current session types in EOP and nutation, taken from a recent GSFC EOP submission. It can be seen that the RDVs produce the most accurate determination of all five Earth orientation parameters. With only 6 sessions per year though, the usefulness of the greater precision in UT1 and pole positions is limited. One of the greatest strengths of the VLBA/RDV sessions lies in the nutation measurements, where high frequency is not needed. The RDV nutations are over twice as precise as in the regular weekly (R1 and R4) or monthly (R&D) sessions. This makes them ideal for studying and monitoring the longer term nutation components, such as the free core nutation and possibly the free inner core nutation.

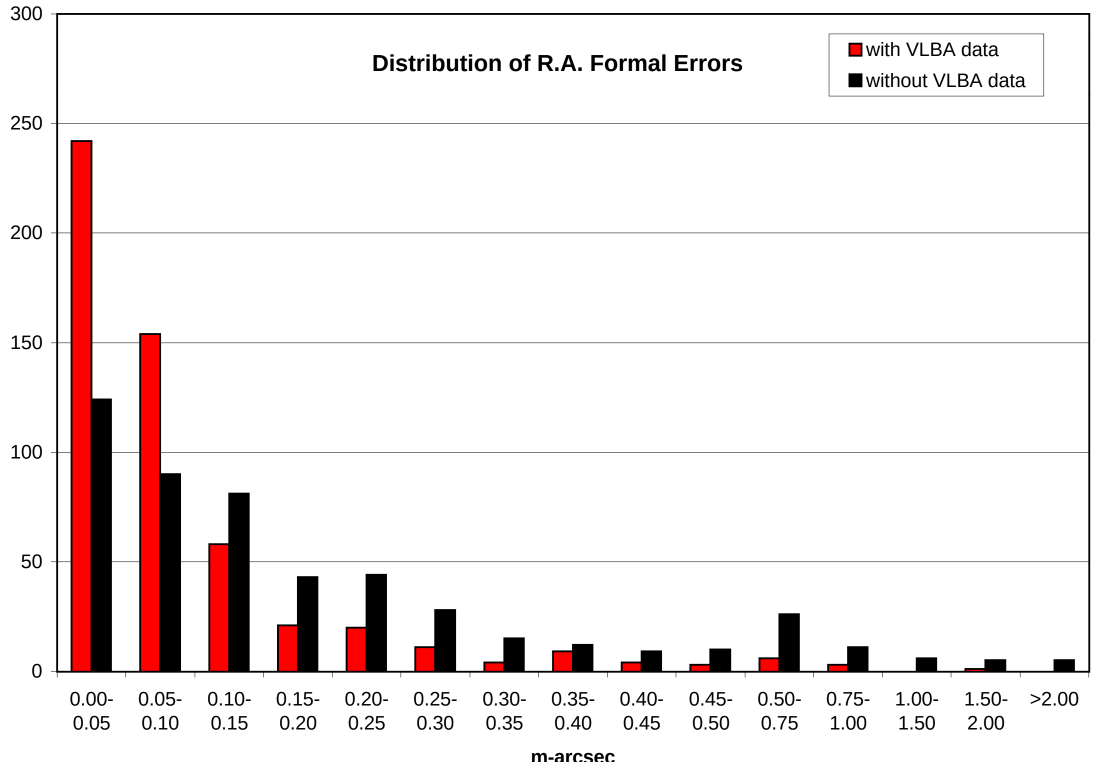

Figure 1. Distribution of formal errors in Right Ascension for the two solutions for all sources between -30 and +90 degrees declination.

Table 3. EOP/Nutation Formal Errors

	No.	Xpole	Ypole	UT1	Psi	Eps
		μasec	μasec	μsec	μasec	μasec
RDV	41	29.9	30.7	1.59	59.1	24.0
R1	103	56.5	56.5	2.00	125.0	51.3
R4	102	85.7	70.8	2.95	169.7	68.2
R&D	16	70.9	66.9	2.57	147.3	61.8
Cont02	14	49.2	39.4	1.75	95.5	40.8

5. K/Q Session Contributions

Four K/Q sessions and one K-band survey session have been run on the VLBA over the last two years to begin building up a higher frequency reference frame. This frame will be needed in the near future for more precise spacecraft navigation at Ka band. A K/Q collaboration group is currently working on building up the basic catalog, investigating systematic effects, and selecting ecliptic sources for the next round of Mars missions. The VLBA has been invaluable in this effort, and it is unlikely that it could be undertaken at this time without the VLBA. Also, because of the

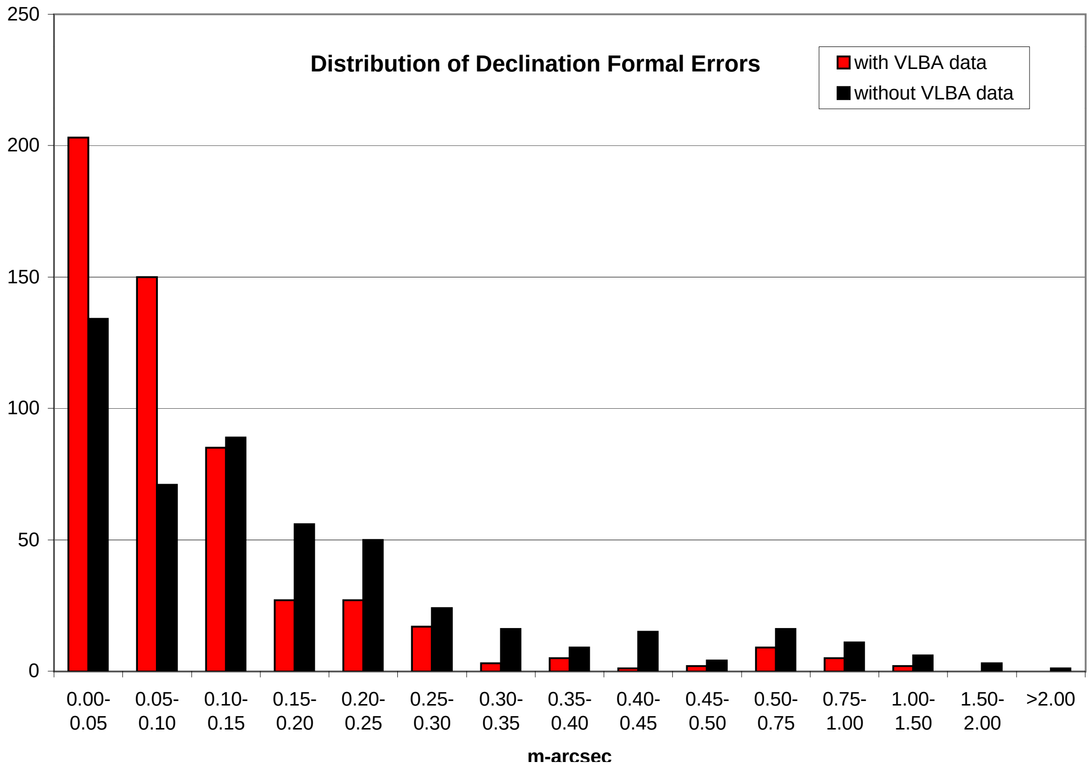

Figure 2. Distribution of formal errors in Declination for the two solutions for all sources between -30 and +90 degrees declination.

increasing interference at S-band, attempts are underway to establish a Ka/X geodetic frequency standard [3] as an alternate or replacement for X/S.

References

[1] Beasley, A.J., D. Gordon, A.B. Peck, L. Petrov, D.S. MacMillan, E.B. Fomalont, C. Ma, The VLBA Calibrator Survey–VCS1, Ap. J. Supplement, 141, 13–21, 2002.

[2] Fomalont, E.B., L. Petrov, D.S. MacMillan, D. Gordon, C. Ma, The Second VLBA Calibrator Survey: VCS2, Ap. J., 126, 2562–2566, 2003.

[3] Jacobs, C., G. Lanyi, C. Naudet, Standard Observing Bands: Is Now the Time To Replace S/X with X/Ka?, this volume, 2004.

Alan L. Fey et al.: VLBI Astrometry of 22 Southern Hemisphere Radio Sources, IVS 2004 General Meeting Proceedings, p.356–360
http://ivscc.gsfc.nasa.gov/publications/gm2004/fey2

VLBI Astrometry of 22 Southern Hemisphere Radio Sources

Alan L. Fey [1], *Roopesh Ojha* [2], *David L. Jauncey* [2], *Kenneth J. Johnston* [1], *John E. Reynolds* [2], *James E. J. Lovell* [2], *Anastasios K. Tzioumis* [2], *Jonathan F. H. Quick* [3], *George D. Nicolson* [3], *Simon P. Ellingsen* [4], *Peter M. McCulloch* [4], *Yasuhiro Koyama* [5]

1) *U.S. Naval Observatory*
2) *Australia Telescope National Facility*
3) *Hartebeesthoek Radio Astronomy Observatory*
4) *University of Tasmania*
5) *Kashima Space Research Center / Communications Research Laboratory*

Contact author: Alan L. Fey, e-mail: `afey@usno.navy.mil`

Abstract

Milliarcsecond accurate radio positions for 22 Southern Hemisphere extragalactic sources are reported. These positions are derived from Mark III Very Long Baseline Interferometry observations made between 2003 February and 2003 August. The results presented here supplement an ongoing project to increase the sky density of Southern Hemisphere sources in order to better define the International Celestial Reference Frame and to provide additional phase reference sources with accurate positions for use in astrophysical observations. The positions for all 22 sources are south of $\delta = -30°$ (positions for ten of the sources are south of $\delta = -60°$) and represent the largest group of new milliarcsecond accurate astrometric positions for sources in this declination range since the initial definition of the ICRF. The reported positions have average formal uncertainties of 0.5 milliarcseconds in right ascension and 0.6 milliarcseconds in declination.

1. Introduction

The United States Naval Observatory (USNO) and the Australia Telescope National Facility (ATNF) are leading a collaboration in a continuing Very Long Baseline Interferometry (VLBI) research program in Southern Hemisphere astrometry and source imaging. The goals of this program are to increase the sky density of International Celestial Reference Frame (ICRF) sources in the Southern Hemisphere by adding new sources with milliarcsecond accurate positions and to image all Southern Hemisphere ICRF sources at least twice for structure monitoring. Initial results of the precise astrometry are reported here. Results of the imaging will be reported elsewhere.

Despite its significance and stated accuracy, the ICRF suffers from a deficit of sources [1], particularly in the Southern Hemisphere. Of the 212 ICRF defining sources, less than about 30% are in the Southern Hemisphere. This non-uniform distribution between the northern and southern sky is due primarily to the fact that most VLBI arrays are physically located in the Northern Hemisphere. As a result, astrometric/geodetic observations have historically concentrated on Northern Hemisphere sources.

There have been two extensions/updates [2, 3] of the ICRF since its initial definition by [1]. One of the primary objectives of extending the ICRF was to provide positions for extragalactic radio sources observed since the ICRF was defined. However, because the new observations concentrated primarily on Northern Hemisphere sources, only four of the 109 new sources reported by [2, 3] have positions south of $\delta = -30°$.

To increase the sky density of Southern Hemisphere sources in the ICRF, we have initiated a program of dedicated Southern Hemisphere VLBI observations with the specific intent of obtaining accurate positions for new Southern Hemisphere sources, i.e., sources not previously reported with coordinates in the ICRF. In this paper, we use astrometric VLBI data obtained between 2003 February and 2003 August to estimate milliarcsecond accurate positions for 22 new Southern Hemisphere sources. Positions for these new sources are reported in the frame of the ICRF.

2. Observations

In order to identify new extragalactic radio sources to be added to the ICRF, survey observations of selected Australia Telescope Compact Array calibrator sources were interspersed among our VLBI imaging observations. The survey observations were made at a frequency of 8.4 GHz and used the S2 VLBI recording system. Candidate sources were selected based on positive detection on baselines either between Australia and South Africa or between Australia and Hawaii. A total of 29 possible astrometric targets were identified. Dedicated astrometric Mark III VLBI observations were scheduled on 2003 February 5 using a VLBI array consisting of the 64 meter antenna at Parkes, Australia (PARKES), the 26 meter antenna at Hobart, Tasmania (HOBART), the 34 meter antenna at Kashima, Japan and the 20 meter antenna at Kokee Park, HI. Observations on 2003 May 20 used an array consisting of the 26 meter antenna at Hartebeesthoek, South Africa (HART), HOBART and PARKES. Observations on 2003 August 9 and 2003 August 20 used an array consisting of HART and the 70 meter Deep Space Network antenna at Tidbinbilla, Australia. All observations were correlated at the Washington Correlator.

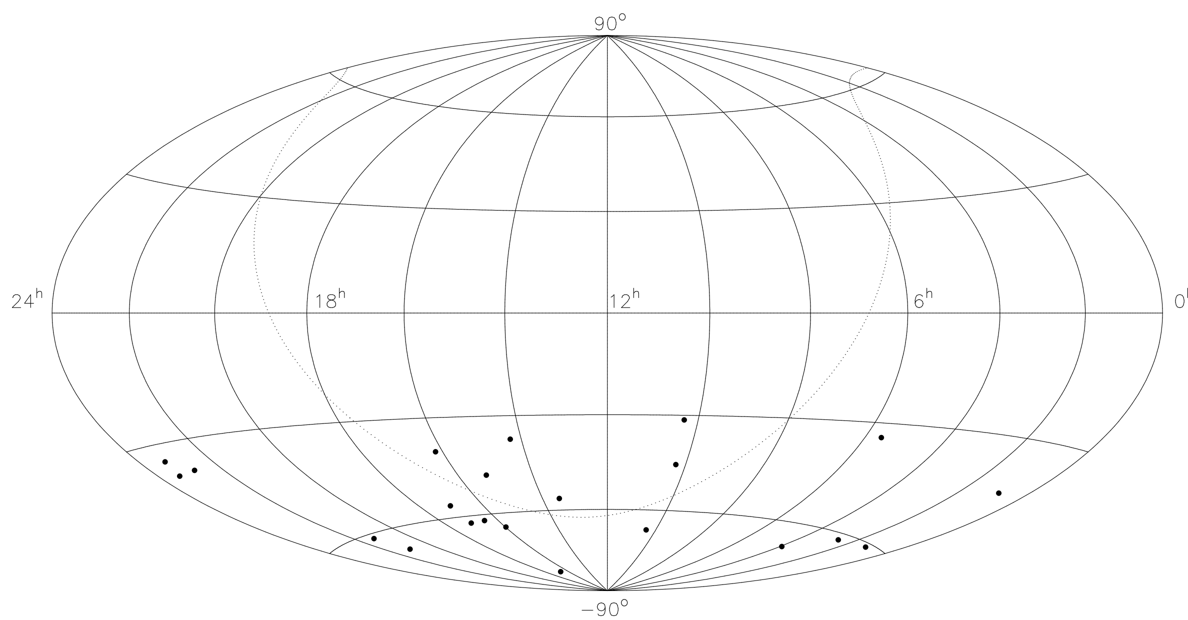

Figure 1. Distribution of sources on an Aitoff equal-area projection of the celestial sphere. The dotted line represents the Galactic equator.

3. Analysis

Accurate astrometric positions were estimated at the USNO using the Goddard Space Flight Center analysis system consisting of the astrometric and geodetic VLBI reduction software CALC and SOLVE. The radio positions reported here are based upon a general solution similar to that for the ICRF and its extensions except that all applicable dual frequency 2.3 GHz and 8.4 GHz Mark III VLBI data available through the end of 2003 August, including the four dedicated experiments described in Section (3), were used. This data set consisted of 3 899 468 group delay measurements from 3 562 24-hour observing sessions. Similar to the ICRF solution, the primary geodetic parameters, the station positions, were estimated separately for each session in the solution. The weighting of the data followed the ICRF solution. The solution described here differed from that of the ICRF and extension solutions in that the delay rate observable was not used, only the group delay observable was used. Additionally, the troposphere was modeled using the NMF mapping function. The post-fit weighted root-mean-square residuals of the final solution were 22.23 ps for delay with a reduced χ^2_ν of 0.923. Additional information on the analysis can be found in [4].

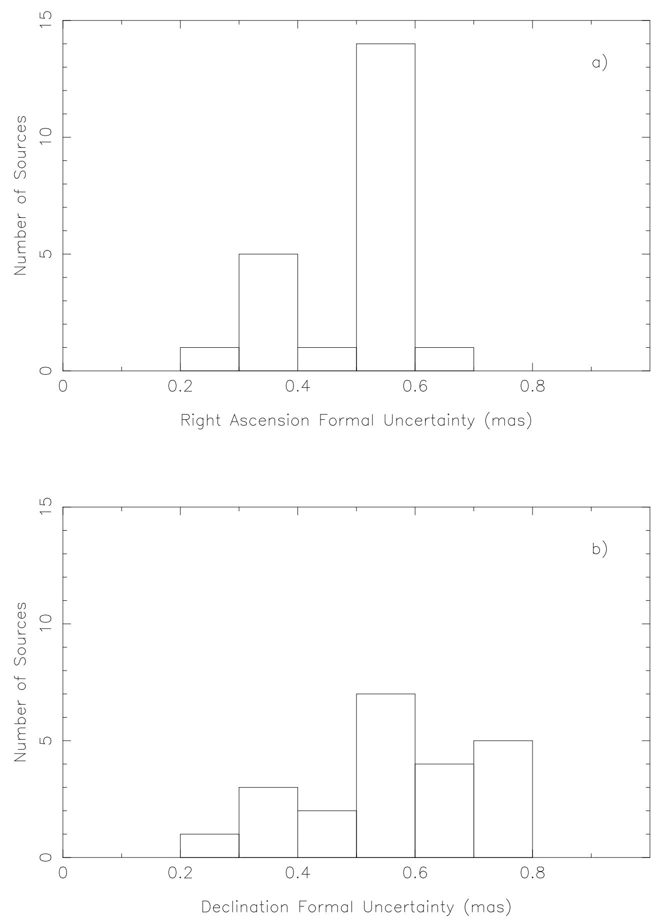

Figure 2. Distribution of position formal uncertainty in a) Right Ascension and b) Declination.

Table 1. Optical Identification of Sources

Source	**ID**	m_v.	z
PKS 0048–427	Q	19.98	1.749
PKS 0107–610	Q	21.4	
PKS 0235–618	Q	17.8	
PKS 0355–669	Q	18.7	
PKS 0534–340	G	18.3	0.684
PKS 1012–448			
PKS 1016–311	Q	17.58	0.794
PKS 1022–665			
PKS 1325–558			
PKS 1412–368	G	22.5	
PKS 1511–476			
PKS 1554–643	G	17.0	
PKS 1606–398	Q	20.9	0.518
PKS 1624–617			
PKS 1633–810	Q	18.0	
PKS 1657–562			
PKS 1659–621			
PKS 2102–659	G	21.0	
PKS 2117–614			
PKS 2244–372	Q	19.0	2.252
PKS 2314–340	Q	18.5	3.1
PKS 2321–375	Q	18.9	0.37

4. Results

The primary result obtained from the least-squares solution is the set of invariant source positions and their formal uncertainties. Of the initial 29 sources, no successful observations (group delay measurements) were obtained for the source PKS 0201–440. The sources PKS 1045–620, PKS 1109–567, PKS 1505–496, PKS 1600–489, PKS 1646–506 and PKS 2205–636 had too few successful observations to be useful at the present time. The remaining 22 sources were observed with 10 or more successful observations obtained during at least two or more 24-hour observing sessions. Positions for these sources are listed in [4]. The distribution on the sky of the new sources is shown in Figure 1. Note that the positions for all 22 sources are south of $\delta = -30°$. Additionally, the positions for ten of the sources are south of $\delta = -60°$. The distribution of the position formal uncertainties is shown in Figure 2. The formal uncertainties of the positions were *not inflated* as was done for the ICRF and its extensions. The estimated positions have average formal uncertainties of 0.5 milliarcseconds in right ascension and 0.6 milliarcseconds in declination.

Optical information including identification, visual magnitude and redshift (where known) for all 22 sources are listed in Table 1.

References

[1] Ma, C., et al. 1998: "The International Celestial Reference Frame as Realized by Very Long Baseline Interferometry," AJ, 116, 516

[2] 1998 IERS Annual report, 1999: "First extension of the ICRF, ICRF-Ext.1," Chapter VI, D. Gambis (ed), Observatoire de Paris, p. 87-114.

[3] Fey, A. L., et al. 2004: "Second Extension of the International Celestial Reference Frame, ICRF-Ext.2," AJ, submitted

[4] Fey, A. L., et al. 2004: "Accurate Astrometry of 22 Southern Hemisphere Radio Sources," AJ, accepted for publication

David A. Boboltz et al.: Extending the ICRF to Higher Radio Frequencies – Imaging and Source Structure, IVS 2004 General Meeting Proceedings, p.361–365
http://ivscc.gsfc.nasa.gov/publications/gm2004/boboltz

Extending the ICRF to Higher Radio Frequencies – Imaging and Source Structure

David A. Boboltz [1], Alan L. Fey [1], Patrick Charlot [2], Edward B. Fomalont [3], Gabor E. Lanyi [4], Liwei D. Zhang [4], KQ VLBI Survey Collaboration [5]

1) *U.S. Naval Observatory*

2) *Bordeaux Observatory*

3) *National Radio Astronomy Observatory*

4) *Jet Propulsion Laboratory, California Institute of Technology*

5) *Multiple Institutions*

Contact author: David A. Boboltz, e-mail: dboboltz@usno.navy.mil

Abstract

We present imaging results and source structure analysis of extragalactic radio sources observed using the Very Long Baseline Array (VLBA) at 24 GHz and 43 GHz as part of an ongoing NASA, USNO, NRAO and Bordeaux Observatory collaboration to extend the International Celestial Reference Frame (ICRF) to higher radio frequencies. The K/Q-band image database now includes images of 108 sources at 43 GHz (Q-band) and images of 230 sources at 24 GHz (K-band). Preliminary analysis of the observations taken to date shows that the sources are generally more compact as one goes from the ICRF frequency of 8.4 GHz to 24 GHz. This result is consistent with the standard theory of compact extragalactic radio sources and suggests that reference frames defined at these higher radio frequencies will be less susceptible to the effects of intrinsic source structure than those defined at lower frequencies.

1. Introduction

The K/Q-band VLBI Survey is part of an ongoing NASA, USNO, NRAO and Bordeaux Observatory collaboration to extend the International Celestial Reference Frame (ICRF) to higher radio frequencies [1]. The long term goals of this program are a) to develop higher frequency reference frames for improved deep space navigation, b) to extend the VLBA calibrator catalog at 24 and 43 GHz, c) to provide the benefit of the ICRF catalog to new applications at these higher frequencies and d) to study source structure variation at 24 and 43 GHz in order to improve astrometric accuracy. Here we describe the production of the K/Q-band image database and provide some preliminary results on extragalactic source structure at higher frequencies from the analysis of the image data.

2. Observations

Observations for the K/Q-band VLBI Survey were made using the 10 stations of the VLBA at K-band (24 GHz) and Q-band (43-GHz) under experiment names BR079 and BL115. Table 1 summarizes program observations recorded to date. All observations were taken using short duration "snapshots" over a number of different hour angles in order to maximize the u-v plane coverage. Data were recorded using eight 8-MHz bands. The data were correlated at the NRAO correlator in Socorro, NM. For the first two experiments BR079A and BR079B the same 65 ICRF sources were observed in order to test the repeatability of the observations. Experiment BR079C observed 67 ICRF sources with 24 of those overlapping sources from previous experiments. Experiment BL115A was a K-band only experiment designed to search for additional high-frequency sources. Experiment BL115B was again a K/Q-band experiment in which 70 sources were observed with roughly 1/3 of the sources overlapping with previous experiments.

Table 1. Summary of K/Q-band VLBI observations.

Experiment Code	Observation Date	Observing Band(s)	No. of Sources Observed	No. of Sources Imaged	Notes
BR079A	15-May-02	K and Q	65	65	65 ICRF sources
BR079B	25-Aug-02	K and Q	65	65	Same 65 sources as BR079B
BR079C	26-Dec-02	K and Q	67	67	24 sources overlapping BR079A,B
BL115A	22-May-03	K only	249	184	122 new sources
BL115B	13-Sep-03	K and Q	70	N/A	Partially imaged

3. Data Reduction and Imaging

Data from the K/Q-band VLBI program were calibrated using the Astronomical Image Processing System (AIPS) which is maintained by the National Radio Astronomy Observatory (NRAO). An initial amplitude calibration was performed using the system temperature measurements recorded during the observations and the VLBA antenna gains supplied by NRAO. To correct the residual delays and rates, a fringe-fit was performed within AIPS. Post fringe-fit data reduction was accomplished using the Caltech DIFMAP software package. The data were self-calibrated and imaged using the hybrid mapping technique to correct for any residual amplitude and phase errors in an automated iterative process. Images and visibility data for sources at K- and Q-band may be obtained at the USNO Radio Reference Frame Image Database **http://www.usno.navy.mil/RRFID**.

4. Results

4.1. Source Compactness

One of the primary goals of the imaging part of the K/Q-band VLBI program is the determination of source structure and its effect on astrometry at higher frequencies. A useful indicator of the degree to which a source may be considered compact is the ratio of the source core flux density to the total flux density in the image or the source compactness. By this indicator, a point-like source, one in which all of the flux was contained in the core, would have a ratio of 1.0. Source compactness (core/total flux density) can be determined using either the CLEAN components from the images themselves or Gaussian model fits to the features in the image. In the case of Gaussian models, the core is defined as the model component fit to the image feature with the smallest angular size, and the total flux density is defined as the sum of the flux densities from all Gaussian components. For the CLEAN components case, the core is defined as the sum of the CLEAN components within one synthesized beam, and the total flux density is defined as the sum of all positive CLEAN component flux densities in the image.

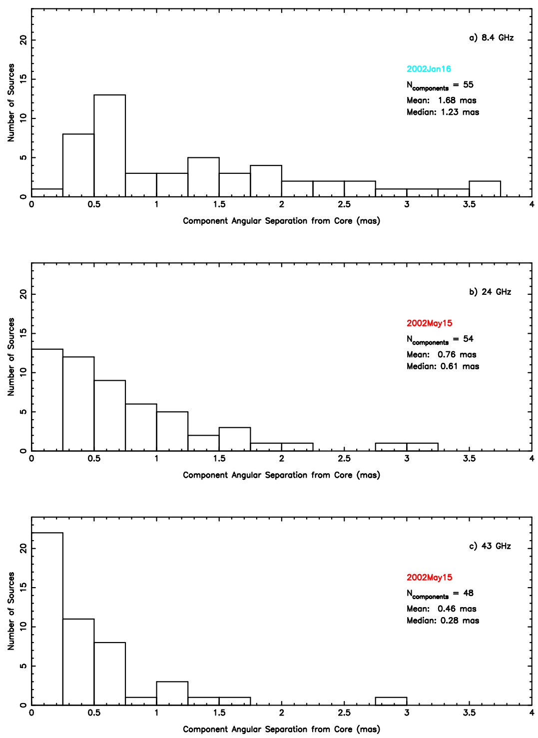

Figure 1. Distribution of Gaussian component angular separation from the core for the 28 sources common to K/Q-band experiment BR079A and VLBA X-band data observed January 16, 2002.

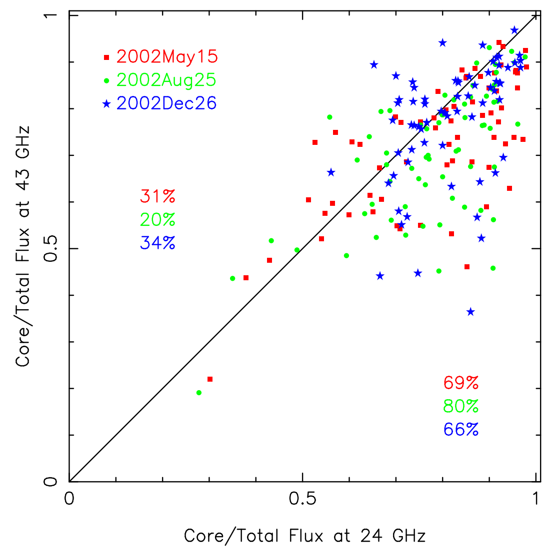

Figure 2. Comparison of the core/total flux as derived from the CLEAN components for the 108 sources observed at 24 GHz and 43 GHz in experiments BR079A, B and C

Figures 1–4 demonstrate the various ways in which the Gaussian/CLEAN components and the source compactness can be utilized. Figure 1 shows a histogram of angular separations of the Gaussian components from the core component for the K/Q-band experiment BR079A. This figure demonstrates the trend toward smaller source angular extents with increasing observing frequency. However, a comparison of the source compactness at 24 and 43 GHz (Figure 2), indicates that even though the total angular extent of the source is smaller at higher frequencies, the sources are really no more compact at Q-band than at K-band. Figure 2 plots data from three experiments, BR079A-C. In this figure sources more compact at K-band lie below the diagonal line while sources more compact at Q-band lie above the line. The results are consistent for all three K/Q-band experiments analyzed thus far.

Shown in Figures 3 and 4 are the results from our K-band only survey (BL115A). Figure 3 plots a histogram of the source compactness. Figure 4 plots this source compactness as a function of source flux density. Preliminary results indicate that weaker sources appear to be more compact than their higher flux counterparts. This trend, however, could be a selection effect in the data and further investigation is required.

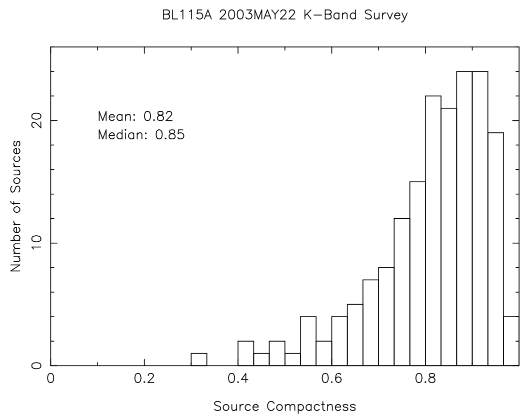

Figure 3. Histogram showing the source compactness (core/total flux) for the 184 sources observed at 24 GHz in experiment BL115A.

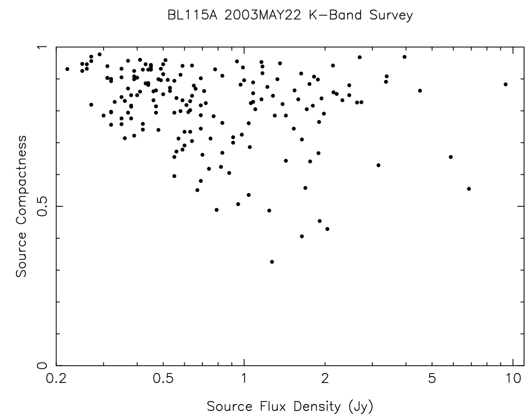

Figure 4. Source compactness (core/total flux) vs. source total flux density for the 184 sources observed at 24 GHz in experiment BL115A.

4.2. Structure Index

A second indicator of source quality is the "structure index" developed by Fey and Charlot [2, 3]. The structure index is defined as the median value of the corrections to the VLBI delay observables due to the source structure as measured in the image. Sources can be categorized by structure index with 1 and 2 indicating compact structure desirable for astrometry/geodesy, 3 being marginal, and 4 being unacceptable for use in astrometric/geodetic VLBI. Figures 5 and 6 compare structure index results from our K/Q-band observations with previously recorded X-band ICRF observations. In Figure 5, histograms showing the structure index at a) X-band, b) K-band, and c) Q-band are plotted. The K- and Q-band results are for the 65 ICRF sources from experiment BR079A, while the X-band results are from a nearby (in time) VLBA experiment with 28 ICRF sources overlapping BR079A. The results show a significant increase in the number of good (structure index of 1 or 2) sources from X-band, ~86%, to K-band, ~97%. There was no improvement in structure index from K-band to Q-band for this experiment. Figure 6 compares histograms of the source structure indices at X-band and K-band for 156 ICRF sources observed in experiments BR079A-C and BL115A. The X-band structure indices were derived from previous VLBA experiments. At X-band approximately 83% of the sources have structure indices of 1 or 2, while at K-band this number increases to ~95%. This improvement in source structure at higher frequencies should translate to increased astrometric accuracy for the source positions and ultimately for a reference frame based on high-frequency radio observations.

References

[1] Jacobs, C. S., et al. 2003, The International Celestial Reference System: Maintenance and Future Realization, 25th meeting of the IAU, Joint Discussion 16, 22 July 2003, Sydney, Australia, 16,

[2] Fey, A. L. & Charlot, P. 1997, ApJS, 111, 95.

[3] Fey, A. L. & Charlot, P. 2000, ApJS, 128, 17

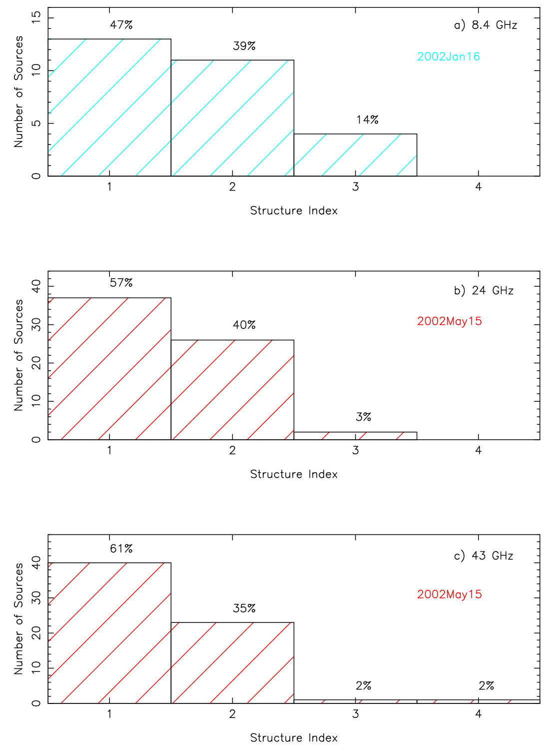

Figure 5. Distribution of structure indices for 28 ICRF sources at a) 8.4 GHz, and for 65 ICRF sources at b) 24 GHz, and c) 43 GHz. The 65 sources at 24 and 43 GHz are from BR079A observed 15 May, 2002. The 28 overlapping sources at 8.4 GHz are from a VLBA experiment conducted on 16 January 2002. Note the shift toward lower values as the observational frequency increases.

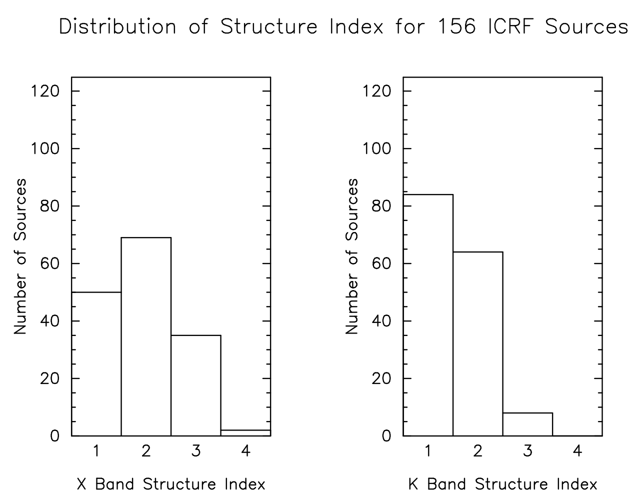

Figure 6. Distribution of structure indices for ICRF sources at 8.4 GHz (left panel) and 24 GHz (right panel). K-band structure indices are from experiments BR079A-C and BL115A. Note the shift toward lower structure indices from X-band to K-band.

Nicole Capitaine et al.: The VLBI Contribution to Precession (Present and Future), IVS 2004 General Meeting Proceedings, p.366–370
http://ivscc.gsfc.nasa.gov/publications/gm2004/capitaine

The VLBI Contribution to Precession (Present and Future)

Nicole Capitaine [1], *Patrick Wallace* [2]

[1] *SYRTE/Observatoire de Paris*
[2] *HMNAO/Rutherford Appleton Laboratory*
Contact author: Nicole Capitaine, e-mail: `capitaine@syrte.obspm.fr`

Abstract

In this paper, we emphasize the potential of VLBI for providing the actual position of the pole in the celestial reference system and consequently the precession of the equator and we recall the main characteristics of the IAU 2000 precession and its link to observations. Then, we investigate the possible present and future role of VLBI observations in identifying a replacement for the precession component of IAU 2000, with improved dynamical consistency. We compare the properties and accuracies of the high precision 2003 solutions for precession and describe tests of the solutions against VLBI observations. We conclude by providing what is required from VLBI in the future in order that it can, at the present level of accuracy, discriminate between various precession models.

1. Introduction

The IAU 2000 precession-nutation model [14] was adopted by the IAU and implemented in the IERS Conventions 2003 [12]. The precession component of the IAU 2000 model consists simply of VLBI estimated corrections to the precession rates in longitude and obliquity of the IAU 1976 precession [13]. This represents a significant improvement of the previous precession but further improvements are necessary to improve the dynamical consistency of the model. The possible VLBI contribution to this next stage of improvement has to be investigated.

2. Present Contribution of VLBI to Precession

2.1. The Treatment of Precession

The classical treatment of precession uses the ecliptic as an intermediary in the terrestrial to celestial transformation. This mixes two different phenomena, namely (i) the precession of the ecliptic due to planetary perturbations and (ii) the precession of the equator. Moreover, for historical reasons, precession is considered separately from nutation. The classical representation which is used in the current VLBI procedures thus uses a large number of parameters for precession and nutation and refers to the equinox, the motion of which has to be modeled.

The adoption of the ICRS as the international celestial reference system by the IAU since 1998 made it possible to refer the Earth orientation parameters to a geocentric celestial reference system (GCRS) that verifies the kinematical condition of absence of global rotation with respect to quasars and the realization of which is independent from precession-nutation models. This has been associated with a revision and improvement of concepts regarding the Earth's orientation in space [11], [6], that has been recommended in the IAU 2000 resolutions. This clearly separates the two precession phenomena, considers the combination of precession and nutation of the equator as being the motion of the equator in space and avoids possible systematic errors [18]. More details can be found in [4], and [5] (Figures 3 and 4).

2.2. Positioning the CIP in Space

VLBI currently provides estimated pole offsets that contain both the discrepancies in the precession-nutation model which is used in the VLBI procedure and the pole offset at epoch between the model and the GCRS (see for example Figure 6 in [5]). This means that VLBI provides the actual position of the pole in the GCRS, which shows the potential of VLBI for obtaining the precession of the equator. The current accuracy is of the order of a few hundred microarcseconds.

It should be noted that the GCRS x, y-coordinates of the CIP unit vector used in the new representation provide directly where the pole is in the sky, which corresponds to what VLBI actually determines.

2.3. The IAU 2000 Precession-Nutation

The IAU 2000A Precession-Nutation model was adopted by IAU 2000 Resolution B1.6 to replace the IAU 1976 Precession and the IAU 1980 Theory of Nutation (IAU 2000A for 0.2 mas level and IAU 2000B, its shorter version, for 1 mas level). The nutation series was generated by the convolution of the MHB 2000 transfer function [14] with the rigid-Earth nutation series REN-2000 [17]. It is based upon basic Earth parameters estimated from VLBI observations, including the Earth's dynamical flattening, H. The resulting nutation series includes 678 lunisolar terms and 687 planetary terms and provides the direction of the celestial pole in the GCRS with an observed accuracy of 0.2 mas. Due to the definition of the Celestial Intermediate Pole (CIP), the diurnal and semi-diurnal terms in nutation are considered as variations of polar motion [5]. The Free Core Nutation (FCN), which cannot be predicted rigorously, is not included in the IAU 2000A model, and sets a fundamental "noise level" of a fraction of 1 mas if IAU 2000A is used as it is.

The precession component of the IAU 2000 model is provided by corrections to the IAU 1976 precession of $-0.29965''/c$ in longitude and $-0.02524''/c$ in obliquity and is associated with VLBI estimates for celestial pole offsets at J2000 of $\delta\psi_0 = -41.775$ mas and $\delta\epsilon_0 = -6.8192$ mas.

2.4. The IAU 2000 Expressions for X, Y and GST

IAU 2000A expressions for the x, y-coordinates of the CIP unit vector in the GCRS have been developed [6] which include precession, nutation, coupling between precession and nutation and frame biases, the polynomial part of these expressions being for the precession of the equator [8].

The "Earth Rotation Angle" (ERA) along the equator of the CIP between the Celestial Ephemeris Origin (CEO) and the Terrestrial Ephemeris Origin (TEO) is provided (IAU 2000 Resolution B1.8) by a conventional linear expression of UT1 [11]. Greenwich sidereal time (GST) which refers to the equinox, is the sum of the ERA and the accumulated precession and nutation along the moving equator, from epoch to the date t. It can be written as the sum of a polynomial part, GMST, mainly due to precession and a periodic part, the "complete equation of the equinoxes". The IAU 2000 expression for GST [7] is consistent with the IAU 2000A precession-nutation and with the expressions for ERA(UT1) and the GCRS position of the CEO [6].

3. Further Improvements in Precession

3.1. High Precision Precession Models

The IAU 2000 precession, which consists only of VLBI MHB-estimated corrections to the precession rates in longitude and obliquity of the IAU 1976 precession, suffers from a lack of dynamical consistency. Expressions for the precession of the equator should strictly be (i) solutions of the dynamical equations for the Earth's rotation and (ii) referred to an improved ecliptic precession.

New precession models have recently been developed that are compatible with IAU 2000 with improved dynamical consistency:

- the B03 model by Bretagnon *et al.* [3] based on the analytical VSOP87 ecliptic [1], on the SMART 97 nutation theory for a rigid Earth [2] and on the MHB precession rate in longitude,

- the F03 model by Fukushima [10] based on an ecliptic fitted to the JPL numerical ephemerides DE405 [16] on a 600-yr interval, on the SF01 nutation theory [15] and on a quadratic fit to VLBI.

- the P03 model by Capitaine *et al.* [8] that is decribed in the next section.

An IAU Division I WG on "Precession and the Ecliptic" was established at the 2003 GA (Chair: J. Hilton) to recommend a new model.

3.2. The P03 Precession

The P03 ecliptic precession [8] has been derived both from the analytical solution VSOP87 and a fit to the JPL numerical ephemeris DE406 [16] over a 2000-yr interval. It has been evaluated as being the most accurate available model by comparing the various solutions to the best numerical ephemerides and by investigating the deficiencies in the other models [9] .

The P03 integration constants have been derived from (i) theoretical contributions to precession rates for a non-rigid Earth model from [14] and [19], (ii) MHB estimates [14] and (iii) corrections for perturbing effects on the observed quantities [9]. For example the precession in longitude has been shown not to be, as generally considered, the "observed" quantity but its projection parallel to the equator on a conventional ecliptic with the obliquity used in the current VLBI software (*i.e.* the IAU 1976 value). The P03 precession of the equator has been obtained by solving the dynamical precession equations, with an improved ecliptic and updated MHB integration constants.

The polynomial difference between the P03 and IAU 2000 expressions for X and Y are in μas, with t expressed in Julian centuries of TT since J2000 TT [8]:

$$dX = 155t - 2564t^2 + 2t^3 + 54t^4 \;; \quad dY = -514t - 24t^2 + 58t^3 - 1t^4 - 1t^5.$$

3.3. Checks Against VLBI Data

Checks of the precession models against VLBI data (GSFC series from 1980 to 2003) have been performed using the X and Y expressions. Figures 1 and 2 show plots corresponding to the X coordinate (*i.e.* $\Delta\psi \sin\epsilon$). These checks show that: (i) the IAU 2000A precession-nutation model gives a much better fit to the data than IAU 1976/1980, (ii) the VLBI data before 1990 are excessively noisy, (iii) the FCN should be corrected to avoid systematic errors, but no model exists since 2000, and (iv) VLBI cannot at present allow us to discriminate between the models.

The numerical estimates resulting from quadratic fits (with a RMS of 374 μas for X and 416 μas for Y) are the following where c_0, c_1, c_2 are for the constant, linear and quadratic terms respectively and c_{ij} is for the correlation coefficient between the i and j terms:

(i) $X_{IAU2000A}$: $c_0 = (\ 1 \pm 10)\ \mu$as; $c_1 = (-1368 \pm 304)\ \mu$as; $c_2 = (-11414 \pm 2579)\ \mu$as; $c_{12} = 0.9$;
(ii) X_{P03}: $c_0 = (\ 2 \pm 10)\ \mu$as; $c_1 = (-1119 \pm 304)\ \mu$as; $c_2 = (-13296 \pm 2580)\ \mu$as; $c_{12} = 0.9$;
(iii) $Y_{IAU2000A}$: $c_0 = (33 \pm 11)\ \mu$as; $c_1 = (+2134 \pm 338)\ \mu$as; $c_2 = (+24024 \pm 2870)\ \mu$as; $c_{12} = 0.9$;
(iv) Y_{P03}: $c_0 = (33 \pm 11)\ \mu$as; $c_1 = (+1620 \pm 338)\ \mu$as; $c_2 = (+23991 \pm 2870)\ \mu$as; $c_{12} = 0.9$.

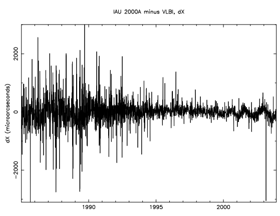

Figure 1. Fit of X(IAU 2000) to VLBI data

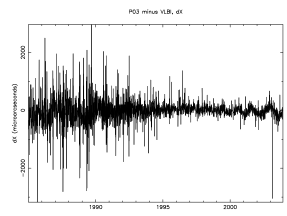

Figure 2. Fit of X(P03) to VLBI data

4. Conclusion

This paper has tried to make clear the following points:

- VLBI is potentially the most powerful technique to estimate the GCRS motion of the celestial equator (and consequently the precession of the equator) but not the ecliptic precession,

- the IAU 2000A precession-nutation is not "dynamically consistent" but gives a very good fit to VLBI,

- improvement in the precession model for the ecliptic is necessary, the resulting effect on the precession of the equator being at a level of 100 μas for one century (in the t^2 term in ψ),

- improvement in the precession model for the equator is necessary. However, the possible improvement in the model is dependent on the model for some parameters of the non-rigid Earth as the J_2 rate,

- observations covering a longer period of time are necessary in order to separate

(i) the precession rates and amplitudes of long-period nutations, (ii) the precession rates and the t^2 terms in the developments (which would give an indirect access to the motion of the ecliptic).

What is required from VLBI in the future in order for it to be a powerful tool, at the present level of accuracy, for discriminating between various precession models is the following:

- the availability of a refined International Celestial Reference Frame (ICRF) both without any global rotation and with a larger number of sources,

- the availability of a long interval of celestial pole offsets with low noise level and no systematic error (*i.e.* with the FCN corrected by a model),

- the adoption of IAU 2000 precession-nutation model in order than the celestial pole offsets can be considered as being first order quantities, concentrating on the X, Y representation that is close to the parameters to which VLBI is sensitive, and

- adoption of the CEO instead of the equinox to avoid possible risks of inconsistencies in the terrestrial to celestial transformation (enabling microarcsecond accuracy).

It should be noted that it would be necessary that, in parallel, models for the contributions to the precession of a non-rigid Earth (t term and t^2 term) be improved (resulting in an "improved" MHB model).

References

[1] Bretagnon, P. and Francou, G., 1988, "Planetary theories in rectangular and spherical variables VSOP87 solutions," *Astron. Astrophys.*, **202**, pp. 309.

[2] Bretagnon, P., Francou, G., Rocher, P., and Simon, J.-L., 1998, "SMART97: a new solution for the rotation of the rigid Earth," *Astron. Astrophys.*, **329**, pp. 329–338.

[3] Bretagnon, P., Fienga, A., Simon, J.-L., 2003, "Expressions for precession consistent with the IAU 2000A model. Considerations about the ecliptic and the Earth Orientation Parameters," *Astron. Astrophys.*, **400**, pp. 785–790.

[4] Capitaine, N., 1990, "The Celestial Pole Coordinates," *Celest. Mech. Dyn. Astr.*, **48**, pp. 127–143.

[5] Capitaine, N., 2002, "The essential contribution of VLBI to Fundamental Astronomy," in IVS 2d General Meeting Proceedings, N.R. Vandenberg and K. Bavers (eds), pp. 14–23, http://ivscc.gsfc.nasa.gov/publications/gm2002/capitaine/.

[6] Capitaine, N., Chapront, J., Lambert, S., and Wallace, P., 2003, "Expressions for the coordinates of the CIP and the CEO using the IAU 2000 precession-nutation model," *Astron. Astrophys.*, **400**, pp. 1145–1154.

[7] Capitaine, N., Wallace, P. T., and McCarthy, D. D., 2003, "Expressions for the Earth Rotation Angle and Sidereal Time consistent with the IAU 2000A precession-nutation model," *Astron. Astrophys.*, **406**, pp. 1135–1149.

[8] Capitaine, N., Wallace, P. T., and Chapront, J., 2003, "Improved expressions for precession quantities consistent with MHB2000," *Astron. Astrophys.*, **412**, pp. 567–586.

[9] Capitaine, N., Wallace, P. T., and Chapront, J., 2004, "Comparison between high precision precession models for the ecliptic and the equator," *Astron. Astrophys.*, accepted.

[10] Fukushima, T., 2003, "A new precession formula," *Astronomical Journal*, **, 126**, pp. 494–534.

[11] Guinot B., 1979, "Basic problems in the kinematics of the roation of the Earth", in Time and the Earth's Rotation, IAU Symposium N 82, McCarthy D.D, Pilkington D.H., eds, D. Reidel, pp. 7–18.

[12] IERS Conventions (2003), IERS Technical Note 31, D.D. McCarthy and G. Petit (eds), in press.

[13] Lieske, J. H., Lederle, T., Fricke, W., and Morando, B., 1977, "Expressions for the Precession Quantities Based upon the IAU (1976) System of Astronomical Constants," *Astron. Astrophys.*, **58**, pp. 1–16.

[14] Mathews P.M., Herring, T.A., Buffett B.A., 2002, "Modeling of nutation-precession: New nutation series for nonrigid Earth, and insights into the Earth's Interior," *J. Geophys. Res.*, 107, B4, 10.1029/2001JB000165.

[15] Shirai, T., Fukushima, T., 2001, "Construction of a new forced nutation theory of the nonrigid Earth," *Astronomical Journal*, **121**, pp. 3270.

[16] Standish, E.M., 1998, "JPL Planetary and Lunar Ephemerides, DE405/LE405", JPL IOM 312.F-98-048.

[17] Souchay, J., Loysel, B., Kinoshita, H., Folgeira, M., 1999, "Corrections and new developments in rigid Earth nutation theory : III. Final tables REN-2000 ," *Astron. Astrophys. Supp. Ser.*, **135**, pp. 111–131.

[18] Wallace, P., T. 2002, IERS Technical Note 29, N. Capitaine *et al.* eds, Verlag des Bundesamts für Kartographie und Geodäsie, Frankfurt am main, pp. 65–67.

[19] Williams, 1994, "Contributions to the Earth's obliquity rate, precession and nutation," *Astron. J.*, **108 (2)**, pp. 711–724.

D. E. Smylie et al.: Ring Downs of Free Core Nutations in the GSFC and USNO VLBI Nutation Series, IVS 2004 General Meeting Proceedings, p.371–380
http://ivscc.gsfc.nasa.gov/publications/gm2004/smylie

Ring Downs of Free Core Nutations in the GSFC and USNO VLBI Nutation Series

D. E. Smylie [1], *Andrew Palmer* [2]

1) *Department of Earth and Space Science and Engineering, York University*

2) *Department of Physics and Astronomy, York University*

Contact author: D. E. Smylie, e-mail: doug@core.yorku.ca

Abstract

The VLBI nutation series from GSFC and the USNO, now both in excess of 23 years in length, allow the exploration of the temporal behaviour of the retrograde (RFCN) and prograde (PFCN) free core nutations.

Our analysis implements Singular Value Decomposition to solve the least squares problem of fitting the Discrete Fourier Transform to the non-equispaced VLBI nutation observations. A novel feature of our procedure is to use the Parseval relation to determine the number of singular values of the coefficient matrix to be eliminated.

We report the observation for the first time of the prograde mode predicted by Jiang (1993). We find periods of -417 ± 5 and -413 ± 4 days for the retrograde mode and 388 ± 2 and 387 ± 5 days for the prograde mode. Spectral analyses at 500 day intervals down the two records show the RFCN in both the GSFC and USNO data to be in free ring down. The PFCN in the GFSC series appears to be in a similar free ring down. The PFCN in the USNO series does not show similar behaviour, possibly because it is at the noise level.

Free decay of the nutation modes allow the direct measurement of the viscosity at the top of the core. We find a value of 795 $Pa \cdot s$ in contrast to the commonly cited value of 0.008 $Pa \cdot s$ found by Gans (1972) by the extrapolation of laboratory measurements.

1. Introduction

Earth's outer liquid core is capable of nearly rigid-body rotations relative to the shell (mantle and crust). Although the motions are mainly confined to the core (Jiang, 1993), conservation of angular momentum produces very small nutations of the rotation axis in space. The theoretical possibility of such motions has a long history (Rochester, Jensen and Smylie, 1974), going back to the classical literature. Only with the emergence of the VLBI technique (Rogers et al., 1983), in providing a close approximation to an inertial space frame, have these motions been brought into the realm of observation (Herring, Mathews and Buffet, 2003).

The VLBI nutation observations are inherently non-equispaced, since measurements can only be made when the radio sources are visible. Working in the frequency domain, we find the Discrete Fourier Transform (DFT) of the non-equispaced record by minimizing an objective function that weights the error power between the DFT and the measured values in inverse proportion to the squares of their standard errors. The Singular Value Decomposition (SVD) method (Golub and van Loan, 1989) is used in solving the resulting large least squares system of conditional equations. An innovation in our application of the SVD technique is the use of the Parseval relation in determining the number of singular values to be eliminated.

The long VLBI nutation series, now in excess of 23 years, allows us to explore the temporal behaviour in the frequency domain of both free core nutations. We discover that they are in free ring down. This opens the possibility of an accurate measure of the viscosity just below the core-mantle boundary. Since the motion there is largely a rotational shear, simple Ekman boundary layer theory permits the decay rates to be directly related to viscosity.

2. Fourier Analysis in the Non-Equispaced Case

When the time sampling is uneven and g_j samples are at arbitrary times t_j, we make a least squares fit, g'_j, of $(2L+1)$ points to the sum

$$g'_j = \frac{1}{M}\sum_{k=-N}^{N} G_k e^{i2\pi k\Delta f t_j}, \tag{1}$$

where $N \leq L$. The $(2N+1)$ values of G_k, once calculated, give a frequency domain representation that is equispaced with sample interval $\Delta f = 1/M$.

The VLBI nutations series have accompanying standard errors σ_j. If the error series in the representation is $\epsilon_j = g_j - g'_j$, we fit to the G_k that minimize the objective function

$$I = \sum_{j=-L}^{L} \frac{\epsilon_j \epsilon_j^*}{\sigma_j^2}, \tag{2}$$

where the superscript asterisk indicates complex conjugation. The resulting conditional equations are

$$\sum_{k=-N}^{N} C_{m-k} G_k = d_m, \quad m = -N, \cdots, N, \tag{3}$$

with

$$C_m = \sum_{j=-L}^{L} \frac{1}{\sigma_j^2} e^{-i2\pi m\Delta f t_j}, \quad d_l = M \sum_{j=-L}^{L} \frac{g_j}{\sigma_j^2} e^{-i2\pi l\Delta f t_j}. \tag{4}$$

Although the coefficient matrix in the system of equations (3) is equidiagonal and Hermitean, and therefore of Toeplitz form, the Levinson algorithm is found inadequate for their solution even when implemented in double quad precision (Hida, Lee and Bailey, 2000). Instead, we employ the method of Singular Value Decomposition (SVD) considered in the next Section.

3. Singular Value Decomposition and Parseval's Theorem

The reason for the failure of the Levinson algorithm, when applied to the solution of the system (3), is that the coefficient matrix for large N is nearly singular (Lawson and Hanson, 1974). The DFT values are typically very large, and the representation (1) of the original time sequence always has isolated values greatly in error. For such large, least squares systems, there is a wide range of literature which suggests the application of Singular Value Decomposition (Press et al., 1992, Chs. 2 and 15).

In matrix notation, the system (3) is $\mathbf{C} \cdot \mathbf{G} = \mathbf{d}$. In SVD, the matrix $\mathbf{C}$ is factored into the triple product $\mathbf{C} = \mathbf{U} \cdot \mathbf{W} \cdot \mathbf{V}^{*T}$. $\mathbf{U}$ and $\mathbf{V}$ are unitary matrices and $\mathbf{W}$ is a diagonal matrix with the singular values of $\mathbf{C}$ in descending order down the diagonal. In our analysis, we represent the position of the celestial pole as the complex valued sequence g_j. The system (3) is then complex as are the unitary matrices $\mathbf{U}$ and $\mathbf{V}$. The singular values and $\mathbf{W}$ are real as a consequence of the Hermitean symmetry of $\mathbf{C}$. We have implemented algorithm 358 of Businger and Golub (Businger and Golub, 1969) for the SVD of a complex matrix in both double and quadruple precision.

Since the unitary matrices $\mathbf{U}$ and $\mathbf{V}$ have inverses which are the complex conjugates of their transposes, the factored form of $\mathbf{C}$ allows the solution to be written $\mathbf{G} = \mathbf{V} \cdot \mathbf{W}^{-1} \cdot \mathbf{U}^{*T} \cdot \mathbf{d}$.

Implementation of the SVD procedure involves the inverses of the smallest singular values in $\mathbf{W}^{-1}$ being set to zero, giving a modified diagonal matrix $\mathbf{W}'^{-1}$. This leads to an approximate DFT, $\mathbf{G}'$, such that the residual error vector in the solution is minimized in length (Press et al., 1992, pp. 53-56). $\mathbf{G}'$ is found as the product of a matrix and a vector as $\mathbf{G}' = \mathbf{V}\mathbf{W}'^{-1} \cdot \mathbf{U}^{*T}\mathbf{d}$.

The main difficulty in implementing the SVD procedure, as described in the existing literature, is choosing the number of singular values to discard. Our solution to this problem is to use the Parseval relation between the mean square in the time domain and the mean square in the frequency domain. Before any singular values are discarded, the DFT is many orders of magnitude too large. As the smallest singular values are discarded, its magnitude decreases monotonically until the Parseval relation is closely satisfied.

The sinusoids in the representation (1) are orthogonal in addition over equispaced time sample points, yielding the Parseval relation in the discrete case,

$$\frac{1}{2L+1} \sum_{j=-L}^{L} g'_j g'^*_j = (\Delta f)^2 \sum_{k=-N}^{N} G_k G^*_k. \tag{5}$$

The left hand side of this expression is just the power in the time domain signal. For stationary sequences it is $E\{g'_j g'^*_j\}$, the expected value of the mean square in the time domain. In the case of stationary sequences, the expected value of the mean square will be independent of whether or not the sampling is equispaced or non-equispaced. For stationary sequences, the Parseval relation holds for both cases.

Our procedure then is to discard the smallest singular values in W^{-1} until the Parseval ratio R given by

$$R = \frac{(\Delta f)^2 \sum_{k=-N}^{N} G_k G^*_k}{E\{g'_j g'^*_j\}} \tag{6}$$

is closest to unity.

4. Spectral Analysis of the GSFC and USNO Nutation Series

The Goddard Space Flight Center (GSFC) nutation series were extracted from the file 2003b.eops on their website (http://gemini.gsfc.nasa.gov/solutions/2003b/2003b.eops). The file contains the residuals in longitude, $\Delta\psi$, and obliquity, $\Delta\epsilon$, compared to the IAU 1980 nutation series, and their standard errors, in milliarcseconds. The series runs from Julian day $2,444,089.993750$ (August 3, 1979) to Julian day $2,452,705.270139$ (March 6, 2003) and consists of 3369 points. Tests reveal that four of the points have null values and 23 have identical time tags. The former were removed and the values of the latter were averaged with weights in inverse proportion to the squares of their standard errors. A series of 3,342 points were left for analysis.

Nutation series from the United States Naval Observatory (USNO) were extracted from the file usn2002c.eops obtained by anonymous ftp (ftp://cddisa.gsfc.nasa.gov/vlbi /ivsproducts/eops). Again residuals in longitude and obliquity compared to the IAU 1980 nutation series are provided, along with standard errors in milliarcseconds. The series runs from Julian day 2, 444, 089.993750 (August 3, 1979) to Julian day 2, 452, 719.269444 (March 20, 2003) and consists of 2,944 points. Fifteen of the points were found to have identical time tags and these were again averaged with weights in inverse proportion to the squares of their standard errors. A series of 2,929 points were left for analysis.

Before performing spectral analysis on these two series, they were first converted to series in the Cartesian coordinates of the celestial pole, $x = \Delta\psi \sin\epsilon$, where ϵ is the obliquity with sine 0.39777716, and $y = \Delta\epsilon$, with corresponding conversion of the standard errors. Linear trends and 18.6 yr (6,798.58 d), 9.3 yr (6,798.58/2 d), annual (365.2597 d) and semi-annual (365.2597/2 d) periodic terms were then removed by least squares fits. Spectral analyses were performed on the residuals of the complex valued series of positions of the celestial pole, $g_j = x_j + iy_j$.

The GSFC series covers a time span of $8,615.276d$. The total record length was taken as $8,617d$ and it was divided into four segments of length $M = 4,924d$ with 75% overlap. The USNO series covers a time span of $8,629.276d$ and was divided into four segments of length $M = 4,932d$, again with 75% overlap. Before the DFTs of the segments were calculated, they were windowed for $-M/2 < t < M/2$ with a Parzen window to suppress finite record effects.

Power spectral estimates were calculated as the average over the four segments, for each series, of the squared magnitudes of the DFTs, normalized by division with the integral of the square of the Parzen window (Smylie, Hinderer, Richter and Ducarme, 1993). They are shown plotted in Figure 1.

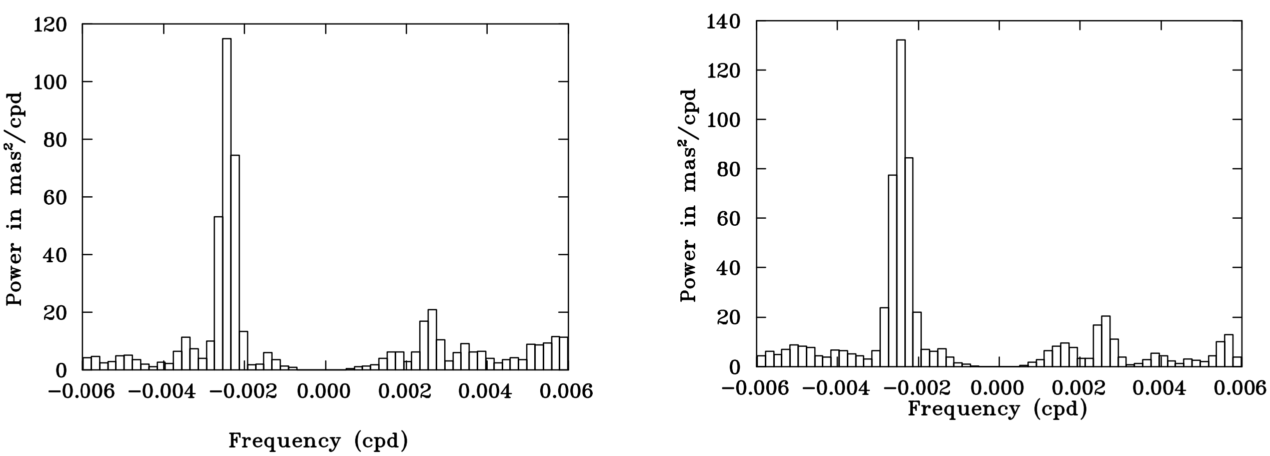

Figure 1. Average spectral estimates of the free core nutation modes. Those for Goddard Space Flight Center data are shown on the left, while those for data from the United States Naval Observatory are shown on the right.

Parameters for the Retrograde Free Core Nutation (RFCN) and the Prograde Free Core Nutation (PFCN) were recovered by fitting resonances of the form

$$\frac{A^2}{1 + 4Q^2\left(\frac{f-f_0}{f_0}\right)^2}. \tag{7}$$

Recovered parameters are listed in Table 1.

Table 1. Fitted parameters of the RFCN and PFCN resonances in the average spectral estimates of the GSFC and USNO series shown in Figure 1.

		RFCN		
	A^2 (mas^2/cpd)	f_0 $(10^{-3}cpd)$	Period(days)	Q
GSFC	122.44	-2.39773	-417.061	6.4263
USNO	135.46	-2.42368	-412.596	5.4113
		PFCN		
GSFC	22.932	2.57627	388.158	5.7932
USNO	22.547	2.58356	387.063	5.8856

The power spectral estimates for each segment were based on DFTs calculated by Singular Value Decomposition, eliminating the smallest singular values until the Parseval ratio R, defined in expression (6), is as close as possible to unity.

5. Poinsot Representation of Nutations and Wobbles

In the Earth frame, free core nutation modes have an associated nearly diurnal retrograde wobble. The relation between nutation and wobble is best understood by the Poinsot construction. In the case of the RFCN, a small body cone rolls, without slipping, once per sidereal day on the inside of a large space-fixed cone, as illustrated on the left of Figure 2. The PFCN can be described by a small body cone rolling, without slipping, once per sidereal day on the outside of a large space-fixed cone, as illustrated on the right of Figure 2.

The kinematics of the wobble-nutation modes, illustrated by the Poinsot constructions, allow the amplitudes and Q's to be related by

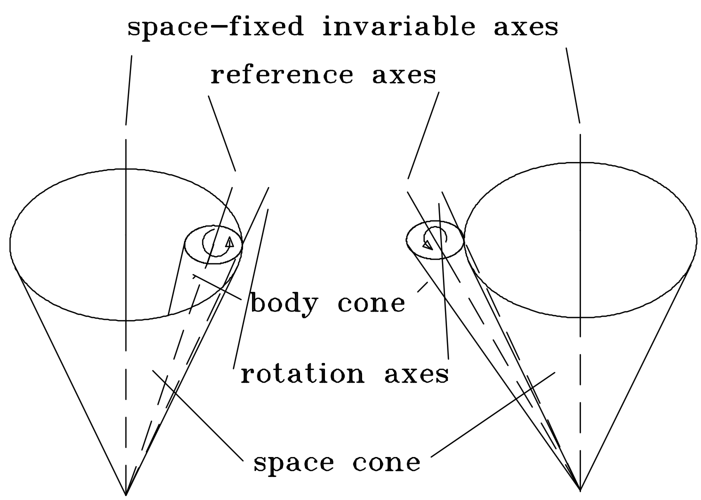

Figure 2. Poinsot constructions for the RFCN (left) and the PFCN (right).

$$a_W = \pm \frac{f_{N_0}}{f_{N_0} - 1/T_s} a_N, \tag{8}$$

and

$$Q_W = \pm \frac{f_{N_0} - 1/T_s}{f_{N_0}} Q_N, \tag{9}$$

with the positive sign referring to the RFCN and the negative sign referring to the PFCN.

The wobble and nutation frequencies are related by $f_W = f_N - 1/T_s$. The wobble period T_W and the nutation period T_N are related by

$$T_W = \frac{T_N T_s}{T_s - T_N}. \tag{10}$$

Estimates of the squares of the nutation and wobble amplitudes can be made from the peak spectral densities A_N^2 and A_W^2, returned from fits to the resonances of the form (7), by integrating between half-power points. The estimates of the squares of the amplitudes are then

$$a_N^2 = \mp \pi A_N^2 f_{N_0} / \left(2Q_N\right) \; and \; a_W^2 = -\pi A_W^2 f_{W_0} / \left(2Q_W\right). \tag{11}$$

Amplitudes, periods and Q's for the average spectral estimates shown in Figure 1, as calculated by the foregoing relations, are listed in Table 2.

Table 2. Parameters recovered for the average spectral estimates shown in Figure 1.

			RFCN			
	a_N ($\mu arcseconds$)	T_N ($days$)	a_W ($\mu arcseconds$)	T_W ($days$)	Q_N	Q_W
GSFC	267.881	-417.061	0.63902	-0.994891	6.4263	2,693.9
USNO	308.711	-412.596	0.74437	-0.994865	5.4113	2,244.2
			PFCN			
GSFC	126.566	388.158	0.32602	-0.999839	5.7932	2,249.0
USNO	124.686	387.063	0.32208	-0.999846	5.8856	2,278.5

6. Decay of the Free Core Nutation Modes and Viscosity at the Top of the Core

Spectral densities of the four individual segments entering the average spectral density shown in Figure 1 suggest the modes are in free ring down.

In order to examine the temporal behaviour more fully, we have divided the GSFC and USNO nutation series into 2,000 day segments advancing down the time axis in 500 day steps. Spectral analyses were performed on each of the 14 segments for each series by Singular Value Decomposition, using the Parseval criterion to determine the number of singular values to be eliminated. Average spectral estimates were made, based on each of four successive segments with 75% overlap. Before the analysis of each segment, the series were windowed with a Parzen window. The result was 11 spectral estimates for each series, centered at 1,750 days into the record and at 500 day increments down the time axis thereafter. Fits to the RFCN and PFCN resonances of the form (7) were used to recover amplitudes through expression (11).

In free decay, the nutation amplitude follows the exponential decay scheme

$$a_N = a_{N_0} e^{-\pi t/(Q_N T_N)}, \tag{12}$$

with a_{N_0} denoting the amplitude at time $t = 0$. On taking logarithms of both sides, if the mode is in free decay, we obtain the linear function of time, $\log a_N = ct + d$, with $c = -\pi \log e / (Q_N T_N) = -\log e/\tau$, $d = \log a_{N_0}$, $t_{1/2} = \tau \ln 2$, where τ is the e-folding time and $t_{1/2}$ is the half life of the decay. Plots of $\log a_N$ as functions of time for both nutation modes of the GSFC and USNO series are shown in Figure 3.

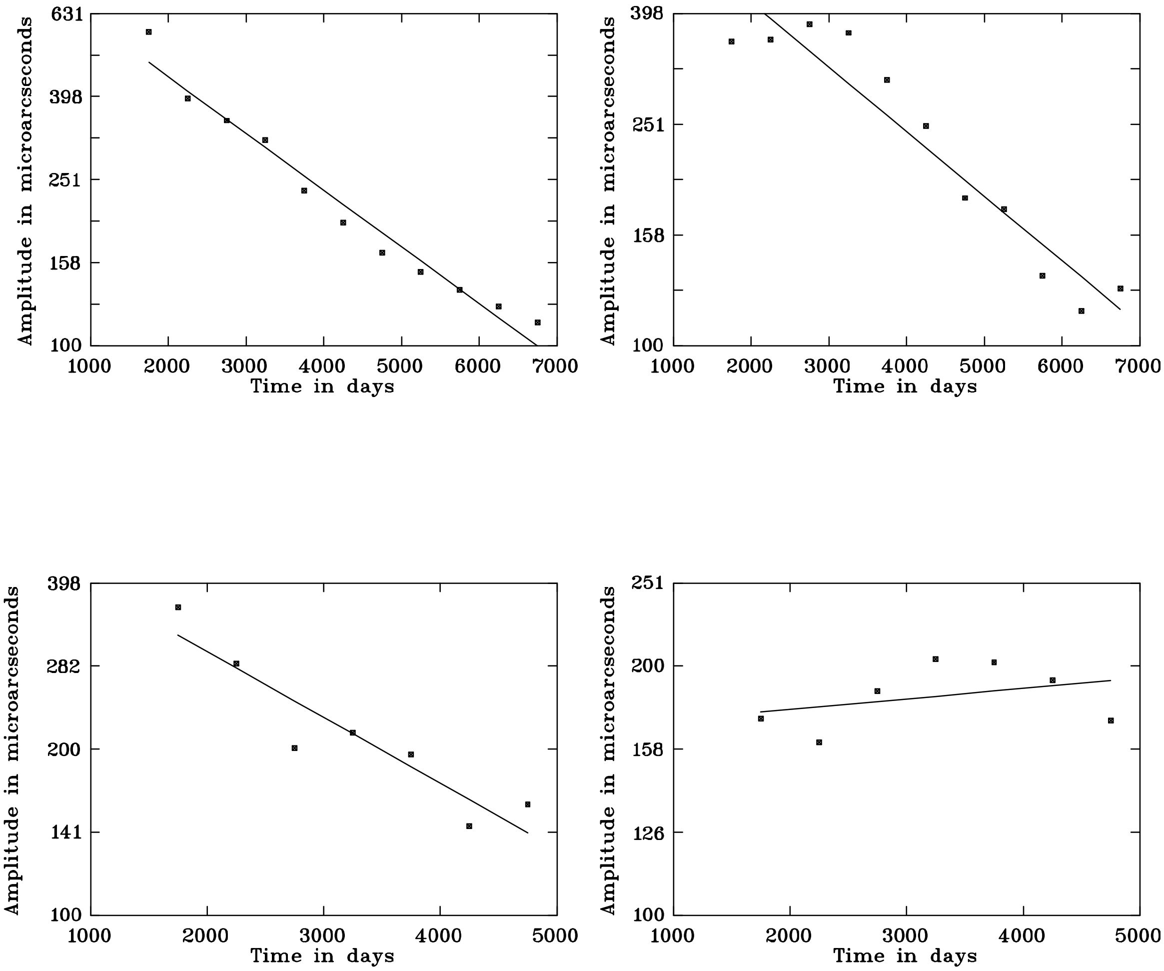

Figure 3. Logarithm of the amplitudes of the free core nutations as functions of time. The upper left plot shows the RFCN from the GSFC series while the upper right plot is that for the RFCN from the USNO series. The lower plots show the results for the prograde mode. Lower left is that for the PFCN from the GSFC series and the lower right plot is for the PFCN from the USNO series. Linear fits to the time dependencies are shown directly on the plots.

The free decay of the nutations allows direct measure of the Qs of the modes. In Table 3, we list the fitted parameters c and d and the recovered Qs, initial amplitudes a_{N_0}, half lives $t_{1/2}$, and Ekman numbers E_k, for the plots shown in Figure 3, using the periods of the average spectra given in Table 2.

The free ring downs of the nutations provide an opportunity to measure the viscosity just below the Core-Mantle boundary (CMB).

Table 3. Free decay parameters of the retrograde and prograde nutations in the spectra of the GSFC and USNO series of VLBI nutation measurements.

	c (10^{-4})	d	a_{N_0} $(\mu arcseconds)$	Q_N	Q_W	$t_{1/2}$ $(days)$	E_k (10^{-11})
			RFCN				
GSFC	-1.36446	2.9204	832.53	23.976	10,051	2206.24	10.8135
USNO	-1.16525	2.8525	712.03	28.379	11,769	2583.44	7.8869
			PFCN				
GSFC	-1.18929	2.7142	517.85	29.556	11,474	2531.22	8.2976
USNO	0.126810	2.2224	168.88	-278.0	-107,608		

Even in realistic Earth models, the free core nutations are closely rigid-body rotations of the outer fluid core with respect to the nearly stationary mantle and crust (shell) (Jiang, 1993). They are both nearly diurnal retrograde wobbles with angular frequencies close to $-\Omega$. For a nearly diurnal retrograde wobble of amplitude A, the velocity field at radius r is $-Ar\left(\hat{\theta}\sin\Omega t + \hat{\phi}\cos\theta\cos\Omega t\right)$. By comparison, the shell is in nearly uniform rotation and the adjustment of the velocity field to that of the shell takes place across an Ekman layer of thickness δ of $O\left(\sqrt{E_k}\right)$ with the Ekman number given by

$$E_k = \frac{\nu}{b^2\Omega}, \tag{13}$$

where b is the radius of the core-mantle boundary and ν is the kinematic viscosity. The leading order boundary layer equations (Moore, 1978; Smylie and McMillan, 1998) yield a boundary layer thickness

$$\delta = \sqrt{\frac{\nu}{\Omega\left(1/2 + |\cos\theta|\right)}}. \tag{14}$$

The leading order stresses are

$$\sigma_{r\theta} = \frac{\eta}{\delta}v_\theta, \quad \sigma_{r\phi} = \frac{\eta}{\delta}v_\phi, \tag{15}$$

where η is the dynamic viscosity. The rate of dissipation of energy per unit area in the motion against these stresses is

$$\frac{de}{dt} = v_\theta\sigma_{r\theta} + v_\phi\sigma_{r\phi} = A^2b^2\frac{\eta}{\delta}\left[\sin^2\Omega t + \cos^2\theta\cos^2\Omega t\right]. \tag{16}$$

With ρ_0 representing the density at the top of the core, and integrating over the CMB and over one cycle, the energy dissipated per cycle is found to be

$$\frac{2}{105}\pi^2\rho_0A^2b^4\sqrt{\frac{2\nu}{\Omega}}\left(138\sqrt{3} - 37\right). \tag{17}$$

The energy of the motion is closely

$$\frac{1}{2}I_{oc}A^2, \tag{18}$$

where $I_{oc} = 912 \times 10^{34}\ kg \cdot m^2$ is the moment of inertia of the outer core.

The quality factor Q_W is defined as 2π times the ratio of the energy E to the energy dissipated per cylce, and is then

$$Q_W = \frac{105 I_{oc}}{2\pi\rho_0 b^4 \sqrt{2\nu/\Omega}\left(138\sqrt{3}-37\right)}. \tag{19}$$

The kinematic viscosity just below the CMB can then be retrieved from the Q_W of the ring down as

$$\nu = \frac{11025 I_{oc}^2 \Omega}{8\pi^2\rho_0^2 b^8 \left(138\sqrt{3}-37\right)^2 Q_W^2}. \tag{20}$$

With $b = 3,480$km as the radius of the core-mantle boundary, using the values of Q_W in Table 3, the ring down of the RFCN from the GSFC series gives a kinematic viscosity of 0.0955 $m^2\ s^{-1}$, while the ring down of the RFCN in the USNO series gives 0.0696 $m^2\ s^{-1}$. The ring down of the PFCN in the GSFC series gives 0.0733 $m^2\ s^{-1}$. Since the density at the top of the core is close to $10^4\ kg \cdot m^{-3}$, the respective values of the dynamic viscosities are 955 $Pa \cdot s$, 696 $Pa \cdot s$ and 733 $Pa \cdot s$. These compare with the value of Gans (1972) of 8 centipoise or $8 \times 10^{-3}\ Pa \cdot s$, based on the extrapolation of laboratory data, and commonly used by dynamo theorists! Our values are closer to the value of 7 $m^2\ s^{-1}$, measured by Davis and Whaler (1997), from the spin-up of the core following the 1969 geomagnetic jerk.

7. Discussion

Two unusual circumstances have allowed us to make an important direct measurement of the viscosity at the top of the core. First, we now have available quite long VLBI nutation measurement series which allow us to explore the temporal behaviour of the free core nutations. Second, during the more than twenty-three year lengths of the records from Goddard Space Flight Center and the United States Naval Observatory, the free core nutations appear to have been in free decay.

Since, in the Earth frame, the free core nutations are closely rigid-body rotations of the outer fluid core with respect to a nearly stationary mantle at close to a retrograde diurnal period, their ring downs, in combination with simple Ekman boundary layer theory, provide direct measures of viscosity at the top of the core.

The average recovered viscosity of 795 $Pa \cdot s$ is very much larger than the value of $8 \times 10^{-3}\ Pa \cdot s$ estimated by Gans (1972), on the basis of the extrapolation of laboratory measurements, and commonly used by dynamo theorists. We are fortunate in the fact that, at these short periods, the Lorentz force and electromagnetic damping effects are completely negligible (Crossley and Smylie, 1975).

The detailed spectral analyses involved have been made possible by the addition of the Parseval criterion for the determination of the number of smallest singular values to be eliminated, in the Singular Value Decomposition technique, used to solve the conditional equations for the calculation of the Discrete Fourier Transforms of the non-equispaced series of nutation observations.

While the free core nutations have now rung down to nearly unobservable levels, at the outset of the observations in 1979, the newly observed Prograde Free Core Nutation, predicted by Jiang (1993), had an amplitude in the GSFC data as high as 62% of the dominant RFCN. Should the modes be excited again, they promise to allow further refinement of Earth property measurements at the top of the core.

8. Acknowledgments

D.E.S. is grateful for financial support from the Natural Sciences and Engineering Research Council of Canada.

References

[1] Businger, P. A. and G. H. Golub 1969. Singular Value Decomposition of a Complex Matrix,*Comm. ACM,*, **12**, 564-565.

[2] Crossley, D. J. and D. E. Smylie 1975. Electromagnetic and Viscous Damping of Core Oscillations, *Geophys.J.R. astr.Soc.,* **42**, 1011-1033.

[3] Davis, R. G. and K. A. Whaler 1997. The 1969 geomagnetic impulse and spin-up of the Earth's liquid core, *Phys. Earth Planet. Inter.,* **103**, 181-194.

[4] Gans, R. 1972. Viscosity of the Earth's core, *J. Geophys. Res.,* **77**, 360-366.

[5] Golub, G. H. and C. F. van Loan 1989. *Matrix Computations,*, 3rd ed., Johns Hopkins University Press, Baltimore, Md.

[6] Herring, T. A., P. M. Mathews and B. A. Buffett, 2002. Modeling of Nutation-Precession: Very long baseline interferometry results, *J. Geophys. Res.*, **107**, ETG4-1 to ETG4-13.

[7] Hida, Y., X. Li and D. Bailey, 2000. Quad Double Arithmetic: Algorithms, Implementation, and Application, *Technical Report LBNL-46996,* Lawrence Berkeley National Laboratory, Berkeley, CA 94720, October 2000. Available at http://www.nersc.gov/dhbailey/ mpist/mpdist.html.

[8] Jiang, Xianhua and D. E. Smylie, 1996. Variational Calculation of the Free Core Nutation Mode, *Phys. Earth Planet. Inter.,* **94**, 159-182.

[9] Jiang, Xianhua, 1993. Wobble-Nutation Modes of the Earth, Ph.D. thesis, York University, Toronto, Canada.

[10] Lawson, C. L. and R. Hanson, 1974. *Solving Least Squares Problems*, Prentice-Hall Inc., Englewood Cliffs, New Jersey.

[11] Moore, D. W., 1978. Homogeneous Fluids in Rotation. In: Roberts, P. H., Soward, A. M. (Eds.), Rotating Fluids in Geophysics, Academic Press, New York.

[12] Press, W. H., S. A. Teukolsky, W. T. Vetterling and B. P. Flannery 1992. *Numerical Recipes,*, 2nd ed., Cambridge University Press, Cambridge UK.

[13] Rochester, M. G., O. G. Jensen and D. E. Smylie, 1974. A Search for the Earth's 'Nearly Diurnal Free Wobble', *Geophys. J. R. astr. Soc.*, **38**, 349-363.

[14] Rogers, A., R. Cappallo, H. Hinteregger, J. Levine, E. Nesman, J. Webber and A. Whitney 1983. Very-Long-Baseline Radio Interferometry: the Mark III System for Geodesy, Astrometry, and Aperture Synthesis, *Science*, **219**, 51-53.

[15] Smylie, D. E. and D. G. McMillan, 1998. Viscous and Rotational Splitting of the Translational Oscillations of Earth's Solid Inner Core, *Phys. Earth Planet Inter.*, **106**, 1-18.

Véronique Dehant et al.: Investigation of Nutation beyond the IAU2000 Model, IVS 2004 General Meeting Proceedings, p.381–382
http://ivscc.gsfc.nasa.gov/publications/gm2004/dehant

Investigation of Nutation beyond the IAU2000 Model

Véronique Dehant [1], *Olivier de Viron* [1], *Martine Feissel-Vernier* [2]

[1] *Royal Observatory of Belgium*

[2] *Observatoire de Paris/SYRTE and Institut Géographique National/LAREG*

Contact author: Véronique Dehant, e-mail: Veronique.Dehant@oma.be

1. Introduction

Precession and nutations are mainly generated by the luni-solar attraction on the Earth equatorial bulge. Diurnal variations in the atmospheric and oceanic angular momenta in an Earth-fixed reference system induce additional contributions to some nutation motions.

Precession and nutations are observed through the variations of the Earth Orientation Parameters obtained using Very Long Baseline Interferometry (VLBI) data, assuming that the direction of observed quasars are fixed in space. We may consider different ways of interpretting the discrepancies between the observed nutations and the model MHB2000 ([5], model adopted by the International Astronomical Union): either the model needs to be improved, or that there are imperfections in the observed nutation series. In particular, we investigate in this study the time variable atmospheric and oceanic effects. The possible contamination of VLBI-derived nutation amplitudes by apparent changes in the directions of the extragalactic radio sources is examined in [3].

The residuals between the observed nutation using VLBI and the MHB2000 model adopted by the International Astronomical Union (IAU2000) are of the order of a few tens of microarcseconds for particular frequencies. Considering the relatively small mass of the external fluid, there are only two ways that their effects on nutation can reach the observable level: (1) at frequencies corresponding to special frequencies in the fluid dynamics such as the annual prograde nutation, corresponding to exactly one solar day in the terrestrial frame, and (2) by exciting the nutation free modes namely the Free Core Nutation (FCN) and the Free Inner Core Nutation (FICN). In the adopted model MHB2000, a constant prograde annual contribution attributed to the external geophysical fluids is adjusted. Additionally, a time variable FCN amplitude is adjusted on the observations. This partly accounts for the atmospheric and oceanic contributions.

2. Atmospheric Excitation of FCN and FICN and their VLBI Detection

For this study, we have considered a nutation series obtained from a subset of radio-sources which are selected for their stability (see [2], [4]). Wavelet analysis and moving window Fourier transform of the residuals show peaks around 500 days and 900 days. The 500-day signal can be explained by a direct atmospheric effect, as we have found that signal at the same frequency and at the same level. Conversely, there is practically no power at all in the atmospheric data at 900 days. If we believe that the 900-day peak is of geophysical origin, the power can only be explained if either the geophysical fluids excite the FICN (the theoretical period of the FICN is 1025 days [930,1140] in Mathews et al. [5]), or the atmopsheric models fail to adequatly represent the dynamics of the atmosphere at that frequency.

Assuming a random signal in the atmosphere and ocean excitation function, we investigate the level of the FICN signal that would result from that excitation, using a simple Earth model. From the angular momentum data, it is not possible to obtain a reliable evaluation of the noise level at the FICN frequency. Consequently, we have assumed that the noise level at the FICN is close to the noise level at the FCN frequency. Accounting for a ratio of the resonance strengths at the FICN and FCN frequency of 1.8 x 10^{-4}, we obtain a 0.05 μas signal at the FICN. This is far too small compared to the observed residual which is at 20 μas level.

On the other hand, a candidate FICN with an amplitude of 37 $\pm$ 10 μas, that is detected in the VLBI observations in the 1990-1995 time frame, is believed to be partly an artefact of residual source instabilities [3].

3. Conclusion

We study the residuals between the observed nutation and the adopted nutation model (MHB2000). By improving the source selection strategy, we obtain residuals more physically meaningful. But the contamination of source instability is still a question (see [3]). We observe that some part of the residuals can be explained by the atmosphere even outside the annual prograde nutation. We have also observed a large peak around 900 days, which is close to the FICN frequency as expected from the forced nutation (1025 days [930,1140]). Note that this peak is only present for a few years around 1995. The estimation of the FICN signal resulting from a random noise excitation by the ocean and the atmosphere is too small, below the μas level.

In our evaluation, we assumed that the geophysical excitation of the FICN was at the same level as the one of the FCN; it is possible, but not likely, that this excitation would be much larger. In this case, we need to have power at the FICN that is two orders of magnitude larger than at the FCN, which does not seem reasonable. So far in our investigation, an artefact from the data analysis seems the most probable explanation. We would like to invite the VLBI community to clarify the effect of the stability of the network, which might also be mapped in the VLBI residuals.

References

[1] V. Dehant, M. Feissel-Vernier, O. de Viron, C. Ma, M. Yseboot, C. Bizouard, 2002, JGRB, 108, 2275

[2] M. Feissel-Vernier, 2003, A&A, 403, 105

[3] M. Feissel-Vernier, J. Ray, Z. Altamimi, V. Dehant, O. de Viron, 2004, this volume

[4] M. Feissel-Vernier, 2004, this volume

[5] P.M. Mathews, T. A. Herring, B. Buffett, 2002, JGRB, 107, 10.1029

George A. Krasinsky: Viscosity of the Earth's Fluid Core from VLBI Data, IVS 2004 General Meeting Proceedings, p.383–387
http://ivscc.gsfc.nasa.gov/publications/gm2004/krasinsky

Viscosity of the Earth's Fluid Core from VLBI Data

George A. Krasinsky

Institute of Applied Astronomy
e-mail: kra@quasar.ipa.nw.ru

Abstract

Differential equations of the Earth's rotation are developed parameterizing dissipative perturbations with the help of the lag δ of the tides in the Earth as a whole, and the lag δ_c of those in its fluid core. The equations generalize the SOS model which is the basis of Nutation IAU 2000. Preliminary estimates of δ_c from analysis of the VLBI based obliquity rate and out-phase nutational amplitudes are presented.

1. Nutation IAU 2000 and Its Deficiencies

Nutation IAU 2000, recently adopted as an international standard, has significantly improved fitting to positions of the Celestial Pole obtained by the VLBI technique. However this theory is semi-empirical when modelling the effects of dissipation of energy in the Earth's rotation and that is why it is hard, if possible, to derive physically meaningful conclusions concerning the Earth's interior with such a theory. The dynamical model behind it is based on the work by Sasao, Okubo, and Saito, developed for the case of the Earth with the elastic mantle and the ideal fluid of its core (so called SOS model; see [4]). When applying this model to construct the new nutation theory, the dissipative effects of the Earth's rotation are usually treated in a formal way assuming that some of constants of the SOS model (for instance Love numbers involved) have imaginary parts and estimating them from the observed positions of the Celestial Pole (see, for instance, Shirai & Fukushima, 2001, [6]). Such semi-empirical approach is equivalent to incorporation of empirical terms into the differential equations of the SOS model. In fact at least five empirical terms must be incorporated to reach a good fit to observations.

The second defficiency of the SOS model (and thus of Nutation IAU 2000) is that only a part of perturbations caused by the non-rigidity of the Earth is accounted for, namely those from the tidal variations of the matrices of inertia of the mantle and the core, the rigid body approximation still being used to model the perturbing torques. In this approximation so called method of transfer function may be applied. However the omitted perturbing terms cannot be accounted for by any transfer function and thus perturbations from them are absent in Nutation IAU 2000.

2. Conventional and Revised SOS Model of the Earth's Rotation

Parameters of the SOS model are so called compliances κ, γ, β. The compliances κ, γ may be expressed in terms of the static k_2 and dynamic k_2^d Love numbers, relatively, while the compliance β is connected with the Love number k_2^c of the fluid core. The compliances (or the corresponding Love numbers) may be obtained either theoretically making use of constants of the adopted up-to-date models of the Earth's interior, or from analysis of VLBI data by fitting the rotation theory. Instead of compliances τ, γ, β we prefer to use the normalized Love numbers σ, ν, μ defined by the relations

$$\kappa = e\sigma,\ \gamma = e\frac{\nu}{\alpha},\ \beta = e\frac{\mu}{\alpha},$$

in which the constant α is the ratio of the main moment of inertia of the fluid core to that of the Earth as a whole, and e is the dynamical flattening.

If the "secular" Love number k_s is defined in the standard way by the expression

$$k_s = \frac{3Gm_E J_2}{R^3\omega^2} \approx 0.93831,$$

in which G, m_E, J_2, R, ω are the gravitational constant, the mass, the coefficient of the main zonal harmonics, the mean radius and the rotational rate of the Earth, then the parameters $\sigma,\ \nu,\ \mu$ may be presented in terms of the Love numbers k_2, k_2^d, k_2^c by the relations

$$\sigma = \frac{k_2}{k_s},\ \nu = \frac{k_2^d}{k_s},\ \mu = \frac{k_2^c}{k_s}.$$

In these notations the standard SOS equations of the Earth's rotation (see Moritz & Mueller, 1987, [4]) may be written in the form

$$\begin{aligned}
&\dot{u}(1+e\sigma) - ie\omega(1-\sigma)u + (\alpha+e\nu)(\dot{v}+i\omega v) = L + i\frac{\sigma}{\omega}\frac{\partial L}{\partial t},\\
&\dot{u} + \dot{v} + iv\omega\left(1 + e_c - \mu\frac{e}{\alpha}\right) = \frac{\nu}{\alpha}\left[L\left(1-e\right) - \frac{i}{\omega}\frac{\partial L}{\partial t}\right],
\end{aligned}$$

where the term L at the right parts is the normalized rigid body torque, $u = \omega_1 + i\omega_2, v = v_1 + iv_2$ are the complex combinations of the components of the vectors of the angular velocities $\overline{\omega} = (\omega_1, \omega_2, \omega_3)$ of the mantle, and $\overline{v} = (v_1, v_2, 0)$ of the differential rotation of the core.

The normalized rigid body torque L is given by the expression

$$L = -ip\omega\xi\zeta,$$

where p is the parameter of the lunar or solar precession

$$p = \frac{3}{2}\frac{mG}{r^3}e,$$

$\xi = \rho_1 + i\rho_2,\ \zeta = \rho_3$ are the ecliptical coordinates of the tide arousing body, and e is the dynamical flattening. (In fact the rigid body torque is the sum of the lunar and solar components: $L = L^1 + L^2$ where $L^k = -ip_k\xi^k\zeta^k$, $p = p_1 + p_2$, and p_1, p_2 are parameters of the lunar and solar precession.)

In the more rigorous formulation the SOS equations have to be replaced by the following ones

$$\begin{aligned}
&\dot{u}\left(1+\frac{2}{3}e\sigma\right) - ie\omega(1-\sigma)u + \left(\alpha + \frac{2}{3}e\nu\right)(\dot{v}+i\omega v) + iv\sum_{k=1,2}(1-3\zeta_k^2)p_k =\\
&= L + (\delta+i)\frac{\sigma}{\omega}\frac{\partial L}{\partial t} + L^d + L_c^d,\\
&\dot{u} + \dot{v} + iv\omega\left[1 + e_c - \frac{\mu e}{\alpha}\left(1+i\delta_c\right)\right] =\\
&= \frac{\nu}{\alpha}\left[L\left(1-\frac{2}{3}e\right) - \frac{i}{\omega}\frac{\partial L}{\partial t}\right] + i\delta\frac{\nu}{\alpha}\left[L(1-e) + i\left(\frac{2}{\omega}\right)\frac{\partial L}{\partial t}\right] = 0,
\end{aligned}$$

in which the normalized dissipative torque L^d consists of the lunar L_1^d and solar L_2^d components caused by the dissipation in the lunar and solar tides, and of the cross interaction torque $L_{1,2}^d$ of these tides

$$\begin{aligned}
L^d &= L_1^d + L_2^d + L_{1,2}^d,\\
L_k^d &= -4p_k\epsilon_k\sigma\delta\left[\omega\xi_k\zeta_k + i\left(\zeta_k\frac{\partial}{\partial t}\xi_k - \xi_k\frac{\partial}{\partial t}\zeta_k\right)\right] (k = 1, 2),\\
L_{1,2}^d &= 2\sigma\delta\omega(p_1\epsilon_2 + p_2\epsilon_1)(\xi_2\zeta_1 + \xi_1\zeta_2),
\end{aligned}$$

while L_c^d includes the terms due to the dissipation in the fluid core

$$L_c^d = \nu\delta_c\left[\frac{1}{2}pv(3\cos^2\theta - 2\cos\theta - 1) + ie\left(1 - \frac{\nu}{\alpha}\right)L\right],$$

θ being the mean obliquity (see Krasinsky, 2003, [3]; a minor error in L_c^d is here corrected).

These equations explicitly depend on the two dissipative parameters δ and δ_c. The parameter δ is the well-known tidal lag of the Earth as a whole that strongly affects the orbital motion of the Moon and is responsible for the evolution of the Earth-Moon system. The parameter δ_c is the phase lag of the tides caused by the differential rotation of the fluid core and as we show further, it plays important part in the Earth's rotation.

Setting the tidal lags δ, δ_c equal to zero one could expect that the standard and revised systems of the differential equations become equivalent. However there is no full equivalence: in the revised version of the equation for the variable u the factor $1 + 2e\sigma/3$ stands in place of the factor $1 + e\sigma$ in the standard SOS system. The origin of this small but not negligible discrepancy has been traced as arising due to the incomplete form of the centrifugal tidal potential commonly used to account for effects of elasticity (only the tesseral components of this potential have been taken into consideration).

3. Contribution from Viscosity of the Fluid Core to the Obliquity Rate

From the geophysical point of view it seems interesting to interpret the observed value $\dot\theta_{obs} = -24.08 \pm 0.017$ mas/cy of the obliquity rate based on VLBI data (see Shirai & Fukushima, 2001, [6]). The main part of this effect may be explained in the frame of the rigid body model (Williams, 1994, [7]). In fact it is not a secular but long periodic term broken to the time series. After Williams this rigid body obliquity rate is equal to -26.8 mas/cy which value may be compared with results of the more recent rigid body models of nutation: -26.5 in SMART97 (Bretagnon et all. 1998, [1]) and -27.2 in RDAN97 (Roosbeck & Dehant, 1998, [5]). Removing the rigid body effect the remaining discrepancy of the obliquity rate $\dot\theta_{obs}$ with observations due to dissipative effects is as follows:

$$\dot\theta_{obs} = 2.7 \div 3.1 \text{ mas/cy},$$

depending on the applied rigid body model.

From the revised version of the SOS equations one can derive the simple analytical expressions for the two components of the obliquity rate: $\dot\theta_\delta$ induced by dissipation of the Earth as a whole and $\dot\theta_{\delta_c}$ due to the dissipation caused by the differential rotation of the fluid core:

$$\begin{aligned}\dot\theta_\delta &= 2p\sigma\delta\sin\theta(\epsilon\cos\theta - 2\tilde\epsilon),\\ \dot\theta_{\delta_c} &= p\nu e\left(1-\frac{\nu}{\alpha}\right)\delta_c\sin\theta\cos\theta,\end{aligned}$$

where $\epsilon = (p_1\epsilon_1 + p_2\epsilon_2)/p = 2.04\times10^{-5}, \tilde\epsilon = (p_1n_1\epsilon_1 + p_2n_2\epsilon_2)/\omega p = 6.27\times10^{-7}$.

The component $\dot\theta_\delta$ of the obliquity rate may be reliably evaluated making use of the estimate $\delta = 0.0376$ based on LLR data, that gives the positive rates 0.675 mas/cy and 0.153 mas/cy for perturbations from the Moon and Sun, relatively, with the total value 0.928 mas/cy. Then the remaining part of the observed obliquity rate must be attributed to the effect of the fluid core:

$$\dot\theta_{\delta_c} = 1.8\div2.2 \text{ mas/cy}.$$

Applying the given above theoretical expression for $\dot\theta_{\delta_c}$ we obtain the estimate of δ_c:

$$\delta_c \approx 0.01,$$

that may be interpreted as an evidence of quite unsignificant viscosity of the fluid core.

4. Amplitudes of Out-Phase Nutations and FCN Tidal Damping

From the revised SOS equations it is easy to derive that the out-phase amplitudes of the main nutations (18.6 and half year periods) with the sufficient accuracy may be written in the form:

$$\begin{aligned}d\theta^f &= -R_f^{out}\sin\theta_0 d\phi_0^f,\\ \sin\theta d\phi^f &= R_f^{out}d\theta_0^f,\end{aligned}$$

where

$$\begin{aligned}R_f^{out} &= [-\nu\delta + \sigma_f(\alpha-\nu)\delta_c]\frac{f}{f+f_c}(1-\alpha)^{-1},\\ f_c &= \omega e_c(1-\sigma_f)(1-\alpha)^{-1}\end{aligned}$$

f^c being the frequency of Free Core Nutation (FCN), and $\sigma_f = \beta/e_c = e\mu/\alpha e_c \approx 0.239$ is its correction for tides in the fluid core.

In Table 1 the observed in-phase and out-phase amplitudes (in mas) are reproduced from the work (Shirai & Fukushima, 2001, [6]) for the two main nutations. In this table there are also given the corresponding estimates of δ_c, obtained with the help of the given above analytical expression for the coefficient R_f^{out}. Note that the amplitudes presented in the table are not really observed quantities but the theory-dependent ones because they are obtained by the mentioned above formal method estimating the imaginary parts of the coefficients of the transfer function as solve-for parameters from which the “observed” out-phase amplitudes have been derived.

Table 1. Observed main nutations and estimates of δ_c

Period	$d\phi_{in}$	$d\phi_{out}$	δ_c	$d\theta_{in}$	$d\theta_{out}$	δ_c
6798.38	17206	3.341	0.38	9205	-1.506	0.47
182.62	-1317	-1.717	0.46	579	-0.570	0.44

One can see that the four independent estimations of δ_c presented in Table 1 are in a good accordance. The rather large values of δ_c are marginally out the boundary of the physically meaningful range $\delta_c < \delta/\alpha \approx 0.35$ (obtained assuming that the dissipation takes place only in the fluid core) and are inconsistent with the small values δ_c derived above from the obliquity rate. It is noteworthy that the resulting out-phase amplitudes are small differences between the large contributions caused by the phase lags δ and δ_c. So the calculations are very sensitive to the numerical values of the parametres involved. Modelling the obliquity rate is sensitive to the ratio ν/α and probably uncertainty of the parameters is one of the reasons of this inconsistency. From the other hand in the work (Dehant & Defraigne, 1997, [2]) it is shown that the indirect action of the oceanic tides through the fluid core contributes half of the observed out-phase amplitudes of both the 18.6 year and semi-annual nutations. Thus we may suppose that the estimated δ_c is an effective parameter that includes both these effects (viscosity of the fluid core and the ocean tides). Probably in this way one could explain the inconsistency of δ_c in Table 1 with the value derived from the observed obliquity rate which is not affected by the ocean tides.

The developed theory shows that the parameter $\delta_f = \sigma_f \delta_c$ in the expression for the out-phase amplitudes has meaning of the parameter of FCN damping. For the corresponding quality factor Q_{FCN} we obtain

$$Q_{FCN} = \frac{1}{2\delta_f} \approx 20 \div 200.$$

References

[1] Bretagnon, P., Francou, G., Rocher, P, Simon, J.L. SMART97 and solution for the rotation of the rigid earth. Astron. Astroph., **329**, 329-338, 1998.

[2] Dehant, V., Defraigne, P. New transfer functions for nutations of a nonrigid Earth. J. Geophys. Res., **102**, NO B12, 1997, 27569-27687

[3] Krasinsky, G.A. Rotation of the deformable Earth with the viscous fluid core. Comminications of IAA RAS N 157, 2003. (see also ananymous FTP file *quasar.ipa.nw.ru/incoming/era/SOSMODEL.ps*).

[4] Moritz, H., Mueller I.I. Earth Rotation: Theory and Observation Unger Publ. Co., New York, 1987.

[5] Roosbeck, F., Dehant, V. RDAN97: An analytical of rigid earth nutation series using the torque approach. Celest. Mech. Dyn. Astron. **70**, 215, 1998.

[6] Shirai, T., Fukushima, T. Construction of a new forced nutation theory of the nonrigid Earth. AJ, **121**, N 1746, 2001, 3270–3283.

[7] Williams, J.G. Contribution to the Earth's obliquity rate, precession, and nutation. AJ, **108**, N 2, 1994, 711–724.

Zinovy Malkin: A New Free Core Nutation Model with Variable Amplitude and Period, IVS 2004 General Meeting Proceedings, p.388–392
http://ivscc.gsfc.nasa.gov/publications/gm2004/malk3

A New Free Core Nutation Model with Variable Amplitude and Period

Zinovy Malkin

Institute of Applied Astronomy of Russian Academy of Sciences (IAA)

e-mail: malkin@quasar.ipa.nw.ru

Abstract

Three most long and dense VLBI nutation series obtained at the Goddard Space Flight Center, Institute of Applied Astronomy, and U.S. Naval Observatory were used for investigation of the Free Core Nutation (FCN) contribution to the celestial pole offset. Some recent studies have showed that the FCN period or/and phase does not remain constant, but varies in a rather wide range of about 410–490 days (for equivalent period). To implement this result in practice, a new FCN model with variable amplitude and period (phase) is developed. Comparison of this model with observations shows better agreement than existing one. After correction of the differences between observed VLBI nutation series and the IAU2000A model, they decreased to a level about 100 microarcseconds.

1. Introduction

Free Core Nutation (FCN) of the Earth is predicted more than a century ago as a common rotational mode of a body having an ellipsoidal solid shell and fluid core. Investigation of the FCN is an important scientific task. First, the FCN parameters determined from observations provide valuable, sometimes unique, information about processes in the Earth's interior. From the practical point of view, accurate modelling of the FCN term, including prediction, is necessary to compute celestial pole offset with accuracy compatible with modern VLBI observations.

The IAU2000A model based on the MHB2000 model developed in Mathews, *et al.*, (2002) and adopted as a new IAU standard can predict a regular part of the nutation with accuracy of about 100 μas. However, the FCN contribution is much larger, up to 400 μas, which yields degradation of accuracy in modelling celestial pole offset, if FCN not accounted for. It is well known also that the FCN contribution gives the prevailing contribution to the power spectrum of the differences between observed nutation series and modern models.

The IAU2000A model, like the previous ones, is constructed as a Poisson series, and does not include free mode terms, such as the FCN, which cannot be presented as a Poisson series term with predictable parameters. For this reason, FCN parameters are to be determined from the VLBI observations.

Historically, the FCN frequency is considered as a constant fundamental value included in transfer function expression describing the relationship between the amplitudes of nutation terms for real and rigid Earth. Many authors have made an effort to estimate the FCN period and possible reasons for its excitation (see *e.g.* Mathews and Shapiro, 1995; Brzeziński and Petrov, 1998; Shirai and Fukushima, 2001a; Herring *et al.*, 2002; Malkin and Terentev, 2003a, 2003b). They found the FCN period to be in the range of 425–435 solar days, with average value about 430^d.

Recently, it was found from a wavelet analysis of VLBI nutation series that the FCN period likely varies in a range of about 410–490 days (Malkin and Terentev, 2003a, 2003b). This result is also confirmed by means of another method, Short-time Periodogram with Gabor Function, proposed by T. Shirai (Shirai *et al.*, 2004). Of course, found variability of the FCN period may be fully or partially a transformation of the variations of the FCN phase, which maybe has more geophysical meaning. However, geophysical considerations of the FCN variability lie beyond this study.

In this paper we develop a practical model for computation of the FCN contribution to the celestial pole offset taken into account variability both amplitude and period (phase) of the FCN oscillation.

2. Computation of the FCN Parameters

Three most long and dense VLBI nutation series obtained at the Goddard Space Flight Center (GSF), Institute of Applied Astronomy (IAA), and U.S. Naval Observatory (USN), each containing more than 3000 estimates of the nutation angles for the period from 1979 up to now were used for investigation of the FCN parameters.

Firstly, estimates of $d\psi$ and $d\varepsilon$ w.r.t. the IAU1976/1980 nutation model computed at the GSF and USN were transformed to the dX_c and dY_c w.r.t. IAU2000A model (IAA series already contains this data).

Then combined series was computed. Since preliminary analysis showed that the three input series are of very similar quality, no weighting was applied, however formal errors reported in the input series were scaled for uniformity. After that, input series were averaged, saving only the epochs present in all the series. Band-pass Gaussian filtering was applied to the combined series. Transfer function of the filter at the FCN frequency is 0.988.

At this step we also computed the smoothed values at equally sampled epochs with 20-day step. However, a smoothed series given at the original epochs also can be used for analysis with a similar final result (Malkin and Terentev, 2003a, 2003b).

The FCN amplitude time series was computed using the simple formula

$$A(t) = \sqrt{(dX_c(t))^2 + (dY_c(t))^2}\,, \tag{1}$$

Indeed, using such an approach we suppose that all the differences can be attributed to the FCN, and this seems to be a good approximation to reality. However, a resonance impact on the nutation terms at the frequencies close to the FCN evidently should be accounted for in future developments.

Finally, the FCN period variation was computed using a wavelet analysis technique as described in Malkin and Terentev (2003a, 2003b). For this analysis we used program WWZ developed by the American Association of Variable Star Observers.

3. Computation of the FCN Contribution

Let us consider how a model with variable amplitude and period (phase) can be used in practice. One can describe the FCN term as

$$\begin{aligned} dX_c &= A(t)\sin(\Phi(t))\,, \\ dY_c &= A(t)\cos(\Phi(t))\,. \end{aligned} \tag{2}$$

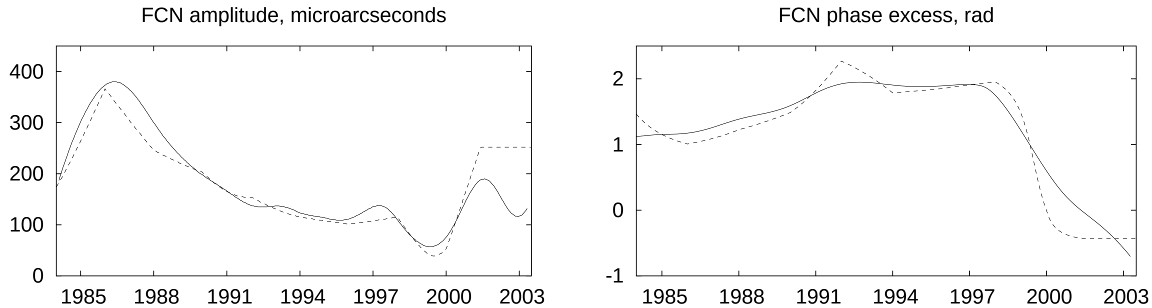

Figure 1. The FCN amplitude and phase (after removing linear trend corresponding to the constant FCN period 430.2^d) variations found in this study (solid line), and the MHB2000 model (dashed line).

Mathematically (not geophysically, indeed!), we can suppose three equivalent models for the FCN phase $\Phi(t)$

$$\Phi(t) = \begin{cases} \dfrac{2\pi}{P(t)}\, t + \Phi_0 \,, \\[2ex] \dfrac{2\pi}{P_0}\, t + \Phi(t) \,, \\[2ex] \dfrac{2\pi}{P(t)}\, t + \Phi(t) \,, \end{cases} \tag{3}$$

where P is the FCN period, and zero subscripts mean constant values. In other words, we can consider three models: with variable period and constant phase, variable phase and constant period, or variable both period and phase. Of course, this is a subject of geophysical consideration, but does not matter for an empirical FCN model using time variations of the FCN parameters found from analysis of the observed data.

In practice, one can compute $\Phi(t)$ as

$$\Phi(t) = \int\limits_{t_0}^{t} \frac{2\pi}{P(t)}\, dt + \varphi_0 \,, \tag{4}$$

where φ_0 is the parameter to be adjusted.

Variations of the FCN amplitude $P(t)$ and phase $\Phi(t)$ are shown in Figure 1 along with the corresponding FCN parameters included in the MHB2000 model which is, in fact, also a model with variable phase and amplitude, though this is not stated explicitly (we used the text of the FCN_NUT routine included in the MHB_2000 code to extract the FCN(MHB) amplitude and phase variations). One can see that both models show similar behavior of the FCN parameters, however new approach allow us to get continues, non-inflecting and predictable functions $A(t)$ and $\Phi(t)$. Comparing these two models one should keep in mind that MHB2000 model is developed only for the period till 2001.4, and after this epoch the difference between the models grows rapidly.

Figure 2 shows spectra of the differences between observed nutation series and the IAU2000A model computed for raw differences and after removing the FCN contribution. One can see that the FCN signal is completely eliminated.

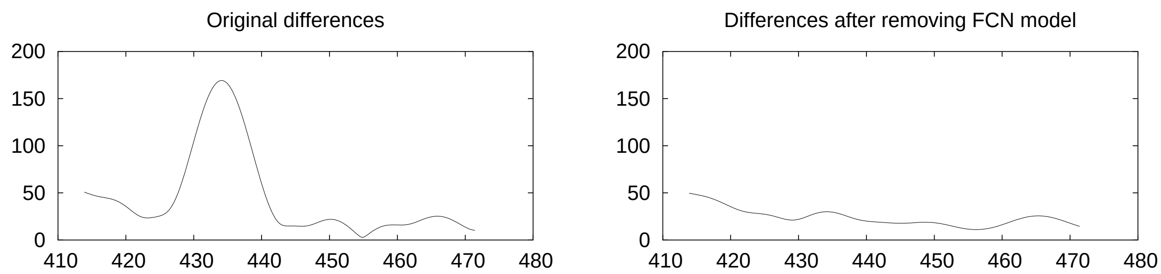

Figure 2. Spectrum of the differences between observed nutation series and the IAU2000A model, period in days, amplitude in μas.

Table 1. WRMS of differences with two FCN models, μas (No – no FCN model, MHB – MHB2000 FCN model, New – model proposed in this paper applied; NEOS – NEOS-A VLBI sessions observed in 1993–2001, R1R4 – IVS R1 and R4 VLBI sessions only observed since 2002).

Series	All sessions			NEOS			R1R4		
	FCN model			FCN model			FCN model		
	No	MHB	New	No	MHB	New	No	MHB	New
GSF	166	146	138	138	122	120	134	150	102
IAA	170	152	144	140	123	123	138	154	111
USN	161	144	136	138	122	122	136	156	107
Mean	156	136	126	131	113	112	129	146	97

However, the differences between observed nutation series and model have a noise of various origins with the rms compatible with the FCN contribution. To estimate the actual contribution of the FCN model to this noise we have computed rms of differences between the observations and the IAU2000A model after applying three different FCN models: no FCN (raw differences), extracting the MHB2000 FCN term, and extracting the FCN term according to the model described here. The results are shown in Table 1.

One can see that accounting for the FCN contribution leads to decreasing of the differences. Especially interesting is the last part of the table corresponding to the period of observations 2002–2003. Using the MHB2000 FCN model for this period leads to degradation of differences between observations and the IAU2000A model, which is natural for this model is developed only for the epochs until 2001.4.

A FCN model with variable period and phase allow us to try a new approach to FCN prediction. One can consider two possibilities. The first one is a prediction of actual FCN contribution, which is developed *e.g.* in Brzeziński and Kosek (2004). Another possibility is to predict functions $A(t)$ and $\Phi(t)$ separately, and then use predictions to construct the FCN contribution using the formulas given above.

4. Conclusions

We have developed a new FCN model with variable amplitude and period (phase) which provides a computation of a continuous FCN contribution to the celestial pole offset with good accuracy for whole interval of the VLBI observations, and convenient prediction of the FCN contribution. Using this model allows us to reduce the differences between VLBI observations and model to the level 100μas.

It is clear that the proposed model is a purely empirical one. Considerable efforts should be made to understand the physical origin of the variability of the FCN period and/or phase, and its consequences in a theory of nutation.

The proposed model is routinely used in the VLBI processing at the Institute of Applied Astronomy since September 2003.

References

[1] Brzeziński, A., and W. Kosek, (2004), Free core nutation: stochastic modelling versus predictability, in *Proc. Journées Systèmes de Réfŕence Spatio-temporels 2003, St. Petersburg, Russia, Sep 22-25, 2003*, edited by N .Capitaine, and A. Finkelstein, in press.

[2] Brzeziński, A., and S. Petrov (1999), Observational evidence of the free core nutation and its geophysical excitation, in: *Proc. Journées Systèmes de Réfŕence Spatio-temporels 1998, Paris, France, Sep 21–23, 1998*, edited by N .Capitaine, 169–174.

[3] Herring, T. A., P. M. Mathews, and B. A. Buffet, (2002), Modelling of nutation-precession: Very long baseline interferometry results, *J. Geophys. Res., 107*, doi:10.1029/2001JB000165.

[4] Malkin, Z., and D. Terentev, (2003a), Preliminary analysis of the Free Core Nutation from VLBI data, in *Proc. 16th Working Meeting on European VLBI for Geodesy and Astrometry, Leipzig, Germany, 9–10 May 2003*, 227–235.

[5] Malkin, Z., and D. Terentev, (2003b), Investigation of the Parameters of the Free Core Nutation from VLBI data, *Comm. IAA RAS, 149.*

[6] Mathews, P.M., and I. I. Shapiro (1996) Recent advances in nutation studies, in: *Proc. Journées Systèmes de Réfŕence Spatio-temporels 1995, Warsaw, Poland, Sep 18–20, 1995*, edited by N .Capitaine, 61–66.

[7] Mathews, P. M., T. A. Herring, and B. Buffett, (2002), Modeling of nutation and precession: New nutation series for nonrigid Earth and insights into the Earth's interior, *J. Geophys. Res., 107*, doi:10.1029/2001JB000390.

[8] Shirai, T., and T. Fukushima, (2001a), Construction of a New Forced Nutation Theory of the Nonrigid Earth, *Astron. J., 121*, 3270–3283.

[9] Shirai, T., and T. Fukushima, (2001b), Did Huge Earthquake Excite Free Core Nutation?, *J. Geodetic Soc. Japan, 47*, 198–203.

[10] Shirai, T., T. Fukushima, Z. Malkin (2004), Short-time Periodogram with Gabor Function and its Application to Free Core Nutation Period Analysis, *Astron. J.*, submitted.

Daniel Gambis et al.: Contribution of VLBI to Earth Orientation Monitoring: State-of-the-Art and Future Prospects,
IVS 2004 General Meeting Proceedings, p.393–393
http://ivscc.gsfc.nasa.gov/publications/gm2004/gambis

Contribution of VLBI to Earth Orientation Monitoring: State-of-the-Art and Future Prospects

Daniel Gambis, Christian Bizouard

Observatoire de Paris

Contact author: Daniel Gambis, *e-mail:* gambis@hpopa.obspm.fr

Abstract

The Earth Orientation Center of the IERS is making use of the different astro-geodetic techniques, SLR, GPS and VLBI to derive optimal combined time series of Earth Orientation Parameters (EOP). VLBI as the only inertial astro-geodetic technique is essential for UT1 and nutation offsets variabilities determination in addition to pole coordinates. In the presentation we discuss the weaknesses and the strengths of VLBI contributions for EOP time series combinations, and present the evolution and the state-of-the-art of the contribution in the IERS analyses with respect to the other techniques. A fundamental issue is the consistency of long-term EOP with respect to both terrestrial and celestial reference frames, ITRF and ICRF. We present the various methods currently applied at the IERS to check and monitor it. Future prospects are finally presented. They concern rigorous methods based on a simultaneous estimation of the terrestrial frame and EOP and which are now being implemented within the IERS.

Karen Baver et al.: Analysis of the VLBI Intensive Sessions, IVS 2004 General Meeting Proceedings, p.394–398
http://ivscc.gsfc.nasa.gov/publications/gm2004/baver

Analysis of the VLBI Intensive Sessions

Karen Baver [1], *Daniel MacMillan* [2], *Leonid Petrov* [2], *David Gordon* [1]

[1] *Raytheon ITSS/NASA Goddard Space Flight Center*
[2] *NVI, Inc./NASA Goddard Space Flight Center*
Contact author: Karen Baver, e-mail: kdb@leo.gsfc.nasa.gov

Abstract

Intensive sessions were designed to determine UT1 with minimum latency. Therefore UT1 from these sessions is the highest priority service which IVS provides to a wide community of users. We have analyzed the IVS-INT1 (KOKEE-WETTZELL) Intensives and the IVS-INT2 (TSUKUB32-WETTZELL) Intensives. Here we present results of our analysis of the performance of these two Intensive series, and we compare them to other UT1 series. We investigate the precision of the Intensive UT1 series. We also examine the dependence of session performance on the selection of observed sources, and we discuss improvement of the observing schedules.

1. Introduction

Intensive sessions were designed to determine UT1 with minimum latency. Therefore these sessions provide a high priority service to a wide community of users. UT1 from the Intensive sessions was of recent critical importance to the Mars spacecraft navigation team at JPL. IVS currently provides two series, the IVS-INT1 or NEOS series, which used the NRAO20-WETTZELL baseline until July 2000 but has subsequently used the KOKEE-WETTZELL baseline, and the IVS-INT2 series, which uses the TSUKUB32-WETTZELL baseline. The IVS-INT1 series provides most of the data–approximately four sessions weekly (currently Monday, Tuesday, Wednesday, and Friday) since January 1997; earlier sessions exist but are not currently included in the GSFC VLBI eopi product. The IVS-INT2 series began in July 2002, with two to six sessions per month except for a hiatus from mid-December of 2002 through mid-April of 2003. This series plays an important role in supplementing the IVS-INT1 series, because it provides data on a day of the week not covered by the IVS-INT1 series (Saturday).

2. Performance of the IVS-INT1 and the IVS-INT2 Series

To compare the IVS-INT1 and the IVS-INT2 series, we ran a solution for each series, using SOLVE to estimate six parameters (UT1-TAI offset, one atmospheric offset per site, and a clock offset, rate and second order term). We restricted the IVS-INT1 solution to 275 sessions between July 2002 and December 2003 to match the time frame of the 48 available IVS-INT2 sessions. All IVS-INT1 sessions used KOKEE-WETTZELL during this time, except for four sessions in October 2003 in which WESTFORD replaced KOKEE due to operational problems at KOKEE.

Figure 1 shows differences of the IVS-INT1 UT1 (left column) values and the IVS-INT2 (right column) values to UT1 from the GSFC 2004a solution for 24-hour sessions (top row) and the IERS C04 series (bottom row). Note that here time differences between each Intensive session and the nearest 24-hour session were up to 12 hours for IVS-INT1 and up to 28 hours for IVS-INT2, which accounts for the larger IVS-INT2 WRMS difference.

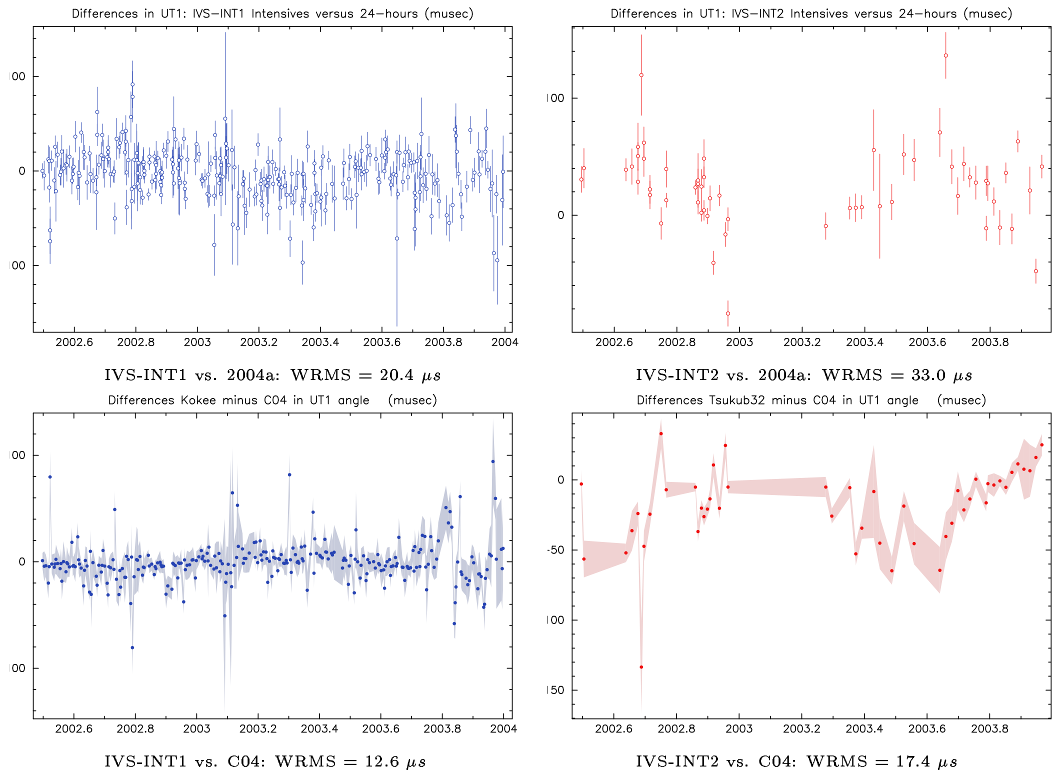

Figure 1. Differences between UT1 from the Intensives (IVS-INT1: left, IVS-INT2: right) and from the 24-hour series (GSFC 2004a quarterly solution) (top row) and from the C04 series (bottom row).

Comparisons of IVS-INT1 and IVS-INT2 in Figure 2 and Table 1 show that the formal errors and the session fits (WRMS residual delays) are better for IVS-INT2. This conclusion may change somewhat with more IVS-INT2 sessions, but at this point, the comparison shows that IVS-INT2 is performing at least as well as IVS-INT1.

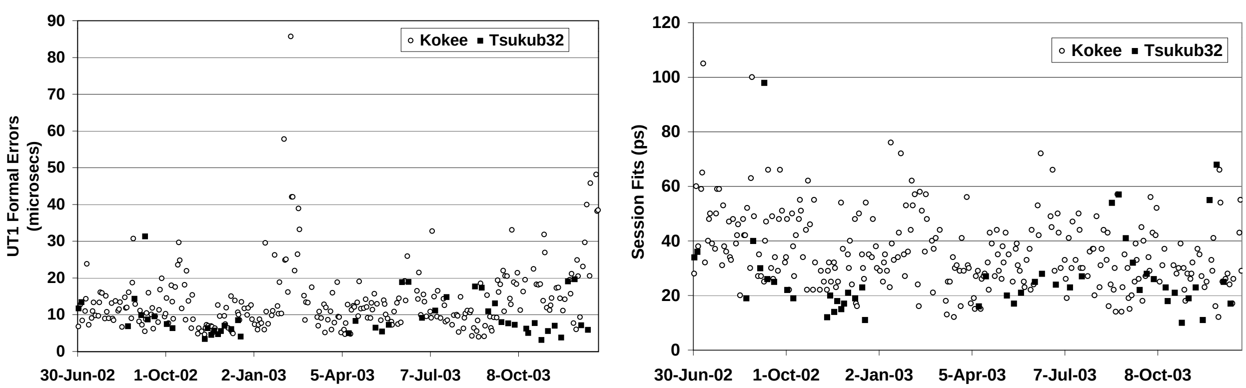

Figure 2. IVS-INT1 and IVS-INT2 UT1 formal errors (left) and session fits.

Table 1. Comparison of IVS-INT1 and IVS-INT2

UT1 Formal Error (μs)		
	IVS-INT1	IVS-INT2
average	13.94	9.45
st. dev.	9.19	5.60

Session Fit (ps)		
	IVS-INT1	IVS-INT2
average	36.11	27.02
st. dev.	13.86	16.10

3. Intensive Session Precision

We have computed the differences between UT1 from each Intensive and the UT1 from the 24-hour session that is closest in time to this Intensive. The UT1 from the 24-hour session was linearly extrapolated to the Intensive session time using the UT1 rate for the 24-hour session. For each Intensive series, the observing time differences fall within several distinct groups, where the time differences are all within 2-3 hours of each other in each group. The WRMS of the differences for each group are shown in Figure 3 as a function of the corresponding time differences. This WRMS is a measure of the precision of the Intensives. The WRMS grows due to extrapolation error. An estimate of the linear extrapolation error was computed from a spline (degree 3) interpolation of a standard GSFC daily UT1 Kalman-filtered series that was generated from 24-hour session estimates. The extrapolation error roughly follows the curve $20\mu s/day^{3/2}T^{3/2}$. The open points were obtained by subtracting this extrapolation error (in quadrature) from the observed WRMS. The observed precision is then 18-22 μs for both series for comparisons with T $<$ 24 hours.

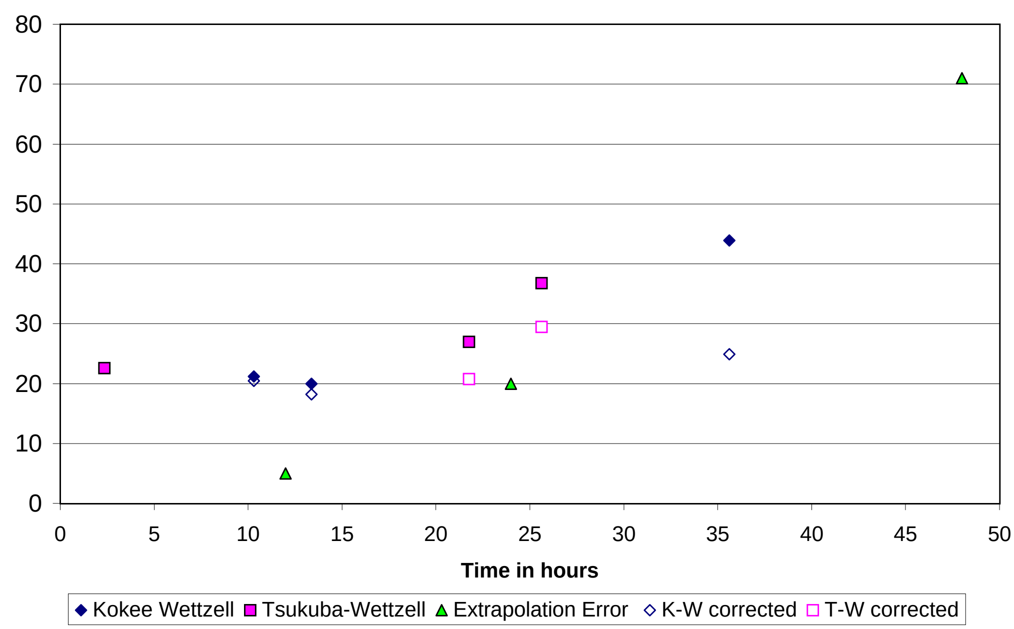

Figure 3. Original and corrected UT1 WRMS Differences in μs between Intensives and 24-hour sessions.

4. Formal Precision of the IVS-INT1 Series from 1999 through 2003

Figure 4 shows UT1 formal error measurements for the primary (IVS-INT1) series over five years (January 1999 through December 2003) except for seven outliers over 60 μs excluded to better show the scale. The time period is divided into three periods delimited by the vertical lines. The first period (January 1999 through June 2000) used the NRAO20-WETTZELL baseline. The middle and last periods (July 2000 through December 2003) both replaced NRAO20 with KOKEE (except for four October 2003 sessions in which WESTFORD replaced KOKEE due to problems at KOKEE), but different observing modes were used during these periods. The middle period (July 2000 through May 2001) used the same mode as the first period, but during the last period (June 2001 through December 2003), the data acquisition rate was doubled to 8 Mbps, and the observing time was reduced from ∼1.5 hours to ∼1 hour. Average session fits and average UT1 formal errors for the three periods are given in Table 2. The session fits were significantly better for the shorter NRAO20-WETTZELL baseline sessions. The third period UT1 formal error shows noticeable improvement over the other periods. More investigation is required to understand the effects of the changes in baseline and observing mode.

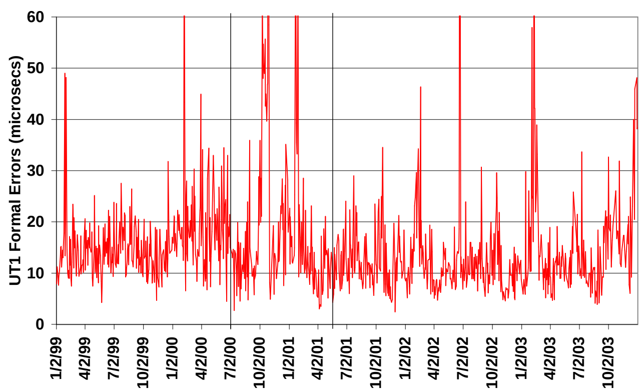

Figure 4. IVS-INT1 formal precision, 1999-2003.

Table 2. IVS-INT1 statistics, 1999-2003.

	NRAO20-WETTZELL	KOKEE-WETTZELL	
	4 Mbps/1.5 hr (1/99-6/00)	4 Mbps/1.5 hr (7/00-5/01)	8 Mbps/1 hr (6/01-12/03)
Avg. UT1 formal error (μs)	16.039	18.076	13.541
Avg. Session fit (ps)	28.215	36.612	38.690
Number of sessions	326	170	484

5. Source Selection

Source distribution is important to achieving a low UT1 formal error. Figure 5 shows the distributions of sources for $00OCT16XU and $00NOV20XU, two IVS-INT1 sessions with similar session fits (31 and 32 ps, respectively) and equal numbers of observations (15), but with very different UT1 formal errors (48.97 and 12.66 μs, respectively). The session with the smaller formal error has lower declination sources and wider sky coverage. Examination of source distribution plots for other sessions empirically shows a general connection between wider sky coverage and smaller formal errors. It is generally considered to be important to observe sources closer to the equator. However, there are sessions with small UT1 formal errors that have wide sky coverage but no observations of sources below 30 degrees in declination. More work is required to completely understand this.

Since the distribution of lower declination sources in the geodetic observing catalog is not optimal for the Intensives, we tested the suitability of potential sources by scheduling them in IVS-R4 and IVS-R1 sessions to determine their current flux densities. These sources range in declination from 11.5 to 25 degrees and were mostly drawn from the VCS1 and VCS2 VLBA calibrator survey sessions. Figure 6 shows the standard GSFC VLBI geodetic catalog sources and the candidate Intensive sources.

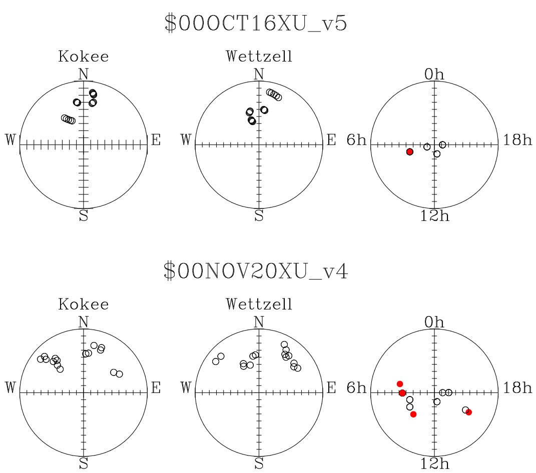

Figure 5. Effects of source distribution which resulted in bad (top) and good (bottom) UT1 formal errors (48.97 vs. 12.66 μs, respectively). The filled circles on the RA/DEC plots represent observations that were under 15 degrees of elevation at one site.

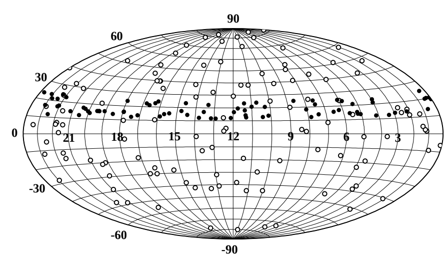

Figure 6. Existing GSFC VLBI sources (open circles) and candidate Intensive sources (solid circles).

Dorothee Fischer et al.: UT1 Intensive Series Using K4 Technology, IVS 2004 General Meeting Proceedings, p.399–402
http://ivscc.gsfc.nasa.gov/publications/gm2004/fischer

UT1 Intensive Series Using K4 Technology

Dorothee Fischer [1], *Axel Nothnagel* [1], *Richard Kilger* [2], *Shinobu Kurihara* [3], *Wolfgang Schlüter* [2], *Kazuhiro Takashima* [3]

[1] *Geodetic Institute of the University of Bonn*

[2] *Bundesamt für Kartographie und Geodäsie*

[3] *Geographical Survey Institute of Japan*

Contact author: Dorothee Fischer, e-mail: `dorothee.fischer@uni-bonn.de`

Abstract

In July 2002 the INT2 project on the Tsukuba – Wettzell baseline has been started for regular monitoring of UT1 using the K4 technology. It is a complement and independent control of the existing regular INT1 observation series on the Kokee Park – Wettzell baseline. A comparison of both independent UT1 series and a closer look at the differences will help to learn more about the error budget and the systematic effects of UT1 results from 1 - 1.5 hour observing sessions.

1. The INT2 Project

The INT2 series is a joint project of the Bundesamt für Kartographie und Geodäsie (BKG), the Geographical Survey Institute (GSI) and the Geodetic Institute of the University of Bonn (GIUB). A pilot phase with 20 almost weekly sessions was started in July 2002 [1] and since April 2003 observations have been carried out regularly on Saturdays. The INT2 observing series was established as complement and independent control of the Mark 5 Intensive sessions (INT1) using the baseline Wettzell–Tsukuba and recording with K4 technology. The correlation is done at GSI in Tsukuba and the schedules are prepared at GIUB. The time delay between observation and creation of the database on average is about 6 days.

Each session is scheduled manually and requires about 70 minutes. INT2 sessions contain 20 scans with a minimum duration of 120 seconds and a minimum SNR of 25 for X-Band and 20 for S-Band. The minimum elevation is fixed to 10°.

2. Analysis and First Results

Due to the low number of scans per session it is only possible to solve for the minimum number of five unknowns: clock offset and rate, wet zenith path delay per station and UT1-UTC as the primary objective. It is necessary to fix the celestial and terrestrial reference frame as well as the pole coordinates for the parameter estimation and, therefore, the estimated UT1-UTC parameters are directly connected with the selection of reference frames.

A first standard solution was calculated with source positions fixed to ICRF, station coordinates of ITRF2000 and pole information from usno_finals.erp. The dry part of the atmospheric path delay was modeled by the modified Saastamoinen model and the Niell dry and wet mapping functions were used for atmospheric mapping [3].

The results of both series (Fig. 1) mostly fit quite well to each other and differences are below 20 microseconds. However, at the end of 2002 as well as in November and December 2003 the

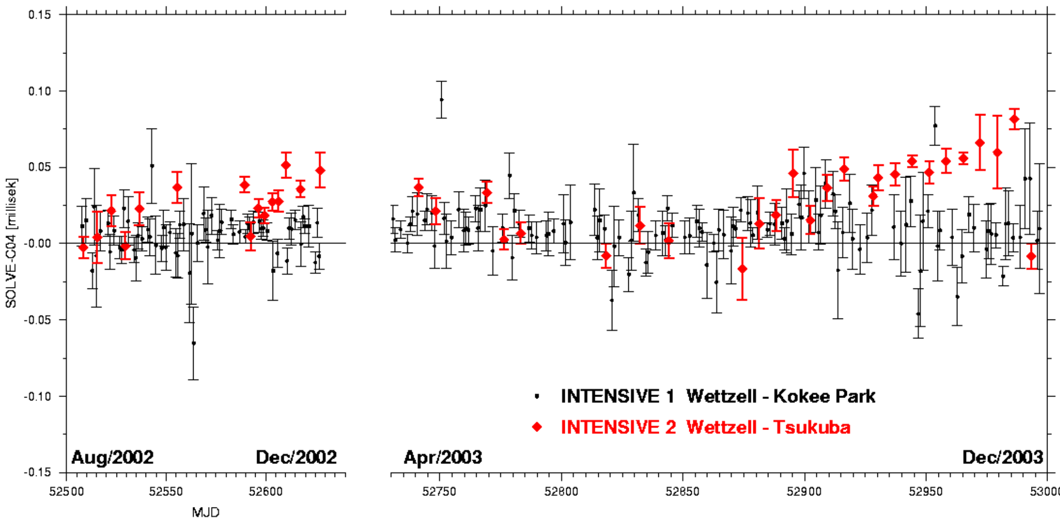

Figure 1. Results from uniform analysis of both Intensives series. A quadratic interpolation of C04 [2] is subtracted.

differences between the two series become larger and the INT2 series seems to drift off slightly.

In order to arrive at one consistent UT1 series from both Intensive observing programmes it is necessary to consider all possible differences between the two series which may influence the UT1 results in different ways. This will also lead to a better understanding of the error budget of the Intensive UT1 estimation itself and may help to find systematic effects. In the following, the most obvious differences between the two series will be discussed.

Geometry of baselines: The INT1 baseline Wettzell - Kokee Park is about 1900 km longer than Wettzell - Tsukuba and, therefore, it may be expected that INT1 is somewhat more senisitive to earth rotation than INT2. In addition, Tsukuba is approximately 14 degrees further north than Kokee Park. Owing to these differences it is not possible to use identical schedules or radio sources and individual scheduling is necessary.

Scheduling: Due to independent procedures of optimization and due to different baseline geometries the schedules of both Intensives differ in terms of source selection, sky coverage and number of scans per session. While each INT2 schedule contains 20 scans, the number of scans per INT1 session varies between 14 and 20. The schedules of INT2 are prepared manually in order to minimize the simulated formal errors of UT1-UTC and of atmospheric path delays. The simulated sigmas are computed by creating normal equation matrices from the schedules using the SOLVE software package. A comparison of the simulated formal errors on average shows better results for the INT2 sessions than for INT1 (Table 1).

Table 1. Comparison of Intensive schedules.

		INT1 Wettzell - Kokee Park	**INT2** Wettzell - Tsukuba
Number of scans per schedule in average		17.5 (14 to 20)	20
Number of successful scans per session in average		17.1	19.6
Average Formal Errors from SOLVE simulation	σ **ATM(1)** σ **ATM(2)** σ **UT1-UTC**	9.6 ps 9.0 ps 8.5 μs	4.3 ps 4.0 ps 4.5 μs

Errors of pole coordinates: Due to the necessity of fixing the pole coordinates in the least squares adjustment, errors and inconsistencies of the pole coordinates affect the UT1-UTC estimates. Simulations have shown that there is a linear dependency of the UT1-UTC estimates on the variations of the pole components.

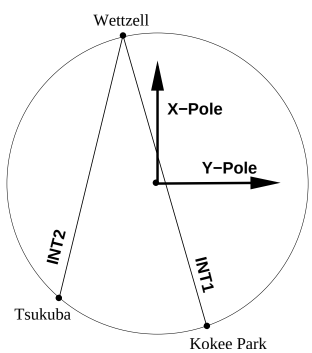

Figure 2. Geometry of Intensive baselines and direction of pole coordinates.

$\left[\frac{mas}{mas}\right]$	**INT1** Wettzell - Kokee Park	**INT2** Wettzell - Tsukuba
$\frac{d(UT1-UTC)}{dXpole}$	-0.13	0.47
$\frac{d(UT1-UTC)}{dYpole}$	-0.16	0.01

Figure 3. Linear effects of pole errors on UT1-UTC estimates from empirical study.

Fig. 2 shows the baseline geometry projected in the equatorial plane together with the directions of X and Y pole components. The results of an empirical test verify what has to be expected from the geometry (Fig. 2). Errors in the pole coordinates affect the UT1-UTC results of the two intensive sessions in a different way and with opposite sign. In particular, the X pole component has a significant effect on the INT2 UT1-UTC estimates. An error in the X pole component of 1 milliarcsec causes a change in UT1-UTC of -0.13 mas on the one baseline and +0.47 mas on the other baseline resulting in an accumulated effect of 0.6 milliarcsec which is equivalent to 40 μs.

3. Summary of Intensive Sessions in 2002 and 2003

Between July and December 2002 and between April and December 2003 a total number of 45 INT2 and 222 INT1 sessions were carried out successfully. The formal errors of the UT1-UTC estimates of INT2 are on average significantly lower than those of the INT1 sessions. The mean formal errors were 14.4 microsec for INT1 and 9.6 microsec for INT2 although. One reason for this may be the higher number of successful scans per INT2 session which are used in the analysis. On average the INT2 sessions contain about 18.7 successful scans while the INT1 sessions have only 16.5. The main reason for the smaller formal errors of the INT2 results, however, may be that the Tsukuba – Wettzell baseline provides a better geometry owing to its optimal length of 8400 km combined with careful scheduling of each individual session.

4. Outlook

Regular INT2 observations on Saturdays as they were started in April 2003 will be continued in 2004. Additional sessions on Sundays are currently being negotiated. Regular sessions on Thursdays will help to realize complete UT1 monitoring over the whole week.

The analysis of the observations will be refined taking into account thermal deformation effects of the antennas and vertical displacements due to ground water extraction.

In order to generate a uniform UT1-UTC series from both Intensives series, questions of consistency and accuracy need to be investigated further and a consistent integration into the results of 24 hour experiments is intended.

5. Acknowlegements

Part of this work is kindly supported by the German *Bundesministerium für Bildung und Forschung* under project *Geotechnologien*, 03F0336B.

References

[1] Fischer D., A. Nothnagel, R. Kilger, W. Schlüter, S. Kurihara, K. Takashima (2003), The K4 Intensive project 2002 for UT1 determination; Proceedings of the 16th Working Meeting on European VLBI for Geodesy and Astrometry, BKG, Leipzig , May 2003, 165–170

[2] IERS (2003), Data publically available under http://hpiers.obspm.fr/eoppc/eop/eopc04/eopc04.62-now

[3] Niell A.E. (1996), Global mapping functions for the atmosphere delay at radio wavelengths, J. of Geophys. Res.,Vol. 101, No. B2, 3227-3246

[4] Nothnagel A., G. Engelhardt, H. Hase, R. Kilger, S. Ogi, K. Takashima, V. Thorandt, D. Ullrich (2000): First Results of the 1999 Tsukuba - Wettzell UT1 Test Series; 2000 General Meeting Proceedings, International VLBI Service for Geodesy and Astrometry, Kötzting, Febr. 21-24, 2000, 252-256

[5] Vandenberg N.R. (1999), Sked: Interactive/Automatic Scheduling Program; Mark IV Software Documentation, NASA/ Goddard Space Flight Center, Space Geodesy Program

Rüdiger Haas et al.: Investigations of High-Frequency Earth Rotation Variations from VLBI CONT Observations, IVS 2004 General Meeting Proceedings, p.403–407
http://ivscc.gsfc.nasa.gov/publications/gm2004/haas

Investigations of High-Frequency Earth Rotation Variations from VLBI CONT Observations

Rüdiger Haas, Raymundo Del Cojo López, Juan Mata Lozano

Onsala Space Observatory, Department of Radio and Space Science, Chalmers University of Technology
Contact author: Rüdiger Haas, e-mail: haas@oso.chalmers.se

Abstract

Several theoretical models have been developed in the last decade that predict high-frequency earth rotation variations. These are induced for example by variations in the oceanic and atmospheric angular momentum. In order to investigate these geophysical phenomena, we compare observational results of polar motion and UT1 from the continuous VLBI series with these theoretical models. Also the different CONT campaigns observed in the years 1994, 1995 and 2002 are compared to each other. Different spectral analysis tools and wavelet analysis are used for the investigations.

1. Models for High-Frequency Earth Rotation Variations

High-frequency earth rotation variations are predicted by a number of theoretical models. These models are mainly based on oceanic and atmospheric dynamics and predict variations in polar motion and UT1 in the diurnal and semidiurnal frequency bands.

- Influence of oceanic tidal angular momentum:

  Oceanic tides and currents evoke oceanic tidal angular momentum, see e.g. [1]. Due to conservation of the total angular momentum of the earth-ocean system, changes in the earth's rotation are induced [2]. The oceanic tidal angular momentum can be modeled based on ocean tide models which are derived empirically from altimetric observations [3]. Earth rotation variations in the diurnal and semi-diurnal frequency bands with amplitudes of several tenths of μas are predicted.

- Influence of luni-solar gravitational tides:

  Variations in earth rotation are also induced due to the external luni-solar torques acting on the triaxial figure of the earth [4]. These torques cause small polar motion variations in the diurnal frequency band and small variations in UT1 in the semi-diurnal frequency band. All terms in these frequency bands with amplitudes larger than 0.5 μas are modeled.

- Influence of non-tidal oceanic angular momentum:

  Besides tidal influences, the oceanic angular momentum is influenced by non-tidal fluctuations in water height and currents [5]. These are partly caused by atmospheric wind and pressure variations. Diurnal variations in polar motion and UT1 with amplitudes on the order of several μas are modeled.

- Influence of atmospheric tides:

  Furthermore, thermal and tidal atmospheric tides cause variations in polar motion and UT1 [6]. These variations are in the diurnal and semi-diurnal frequency bands and have amplitudes on the order of some μas.

2. The VLBI CONT Campaigns and the Corresponding Data Analysis

In order to study the high-frequency earth rotation variations we analyzed the continuous VLBI campaigns CONT94, CONT95 and CONT02. These campaigns involved continuous VLBI observations between 7 and 14 days in dedicated multi-station VLBI networks. CONT94 was observed between January 12 and 25 in 1994, with a break of one day, CONT95 was observed between August 23 and 29 in 1995, and CONT02 was observed between October 16 and 31 in 2002. The three campaigns were analyzed using the CALC/SOLVE software [7]. Station coordinates were kept fixed to VTRF2003 [8], while radio source positions were kept fixed on ICRF [9]. Clock parameters relative to a reference clock in the network were estimated every 1 hour, atmospheric zenith wet delay parameters were estimated every 1 hour using the New Mapping Functions (NMF) [10] and horizontal delay gradients every 3 hours. Polar motion and UT1 values were estimated every 1 hour with respect to the IERS C04 series earth rotation parameters [11], and one pair of nutation corrections with respect to the IAU1980 model of nutation [12] was estimated for each 24 hour VLBI session. The resulting high-frequency earth rotation estimates with respect to the a priori values form the basis for further analysis using spectrum analysis tools.

3. Spectrum Analysis Tools

To investigate high-frequency signals in the observed time series of earth rotation parameters, spectum analysis tools can be applied. Since the CONT94 time series are not evenly sampled but have a one day gap, a usual Fourier analysis was not suitable. Instead, other spectrum analysis tools were applied that allow the analysis of unevenly sampled data, the Lomb Periodogram [13], the CLEAN algorithm [14] and Wavelet analysis [15].

- The Lomb Periodogram:

  The general expression for the normalized Lomb Periodogram is obtained from a linear least-squares estimation of the harmonic signal content. The algorithm works on a per-point basis and can be used for unevenly sampled, but not clumped data [13].

- The CLEAN algorithm:

  This algorithm uses a step-wise deconvolution of the signal to be analysed in order to avoid sampling effects on the derived spectrum. Thus, a considerable part of the noise resulting from the irregular sampling is removed [14]. The algorithm works on a per-interval basis and has a better performance than the Lomb Periodogram for unevenly sampled and highly clumped data sets.

- The Wavelet analysis:

  The Wavelet Transform allows both the detection of time varying amplitudes and frequencies, and a robust implementation for irregular sampling [15]. The Continuous Wavelet Transform (CWT) decomposes signals over a set of dilated and translated versions of a so-called mother wavelet. In geosciences the Morlet wavelet is often used which has quasi-compact support both in time and frequency domain and allows for adaptive time-frequency resolution. Furthermore, so-called cross-scalograms and the corresponding normalized coherence allow comparison of wavelet transforms of different signals [16].

4. Analysis Results

The time series of polar motion and UT1 derived from the three CONT VLBI campaigns were analyzed with the spectrum analysis tools described in Section 3. Figure 1 shows the spectra derived with the CLEAN algorithm. The three campaigns show similar spectral content with significant signal power in the diurnal and semi-diurnal frequency bands. However, the CONT95 campaign gives less resolution than the other two campaigns. The CONT02 campaign is the only campaign that reveals some signal power at a period of 8 hours for the Y-pole component.

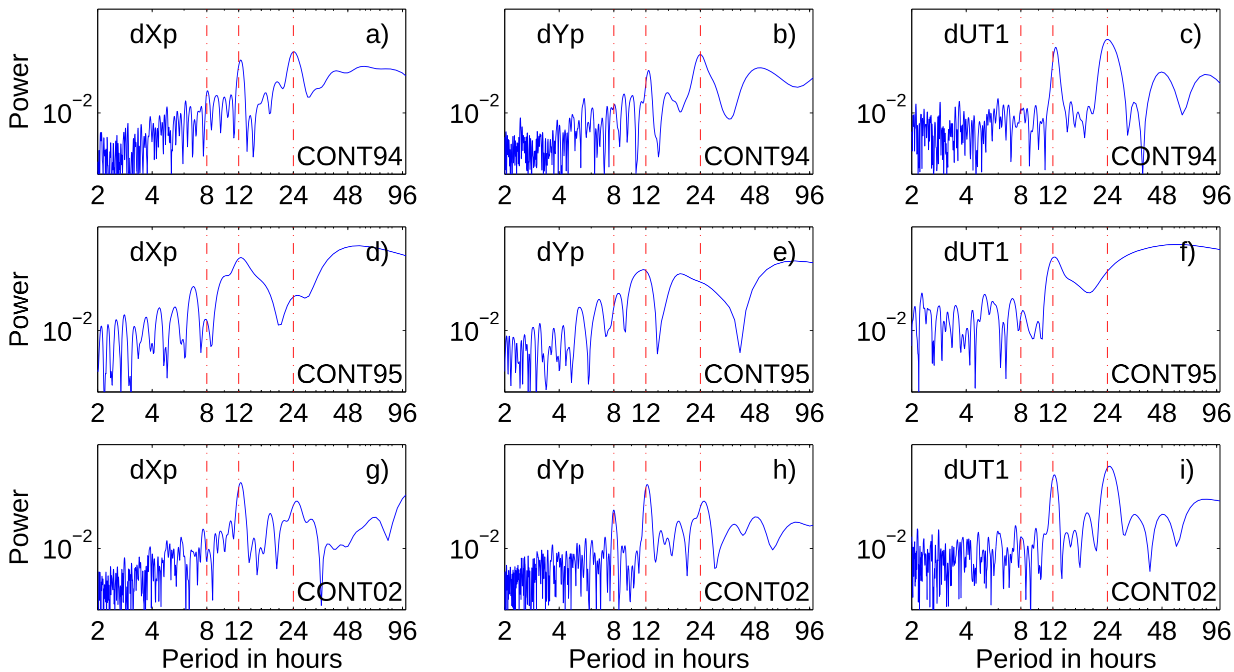

Figure 1. Spectra of polar motion and UT1 of the CONT campaigns derived with the CLEAN algorithm.

Figure 2 shows Lomb Periodograms for polar motion and UT1 during CONT02. The upper plots (a–c) show periodograms of the original CONT02 data (O.), while the lower plots (d–f) show periodograms of the original CONT02 data reduced by the theoretical model predictions (O.-M.). The horizontal lines indicate significance levels of 0.005 (dashed), 0.05 (dashed-dotted) and 0.5 (dotted). The theoretical models explain at least partly the detected signal power in the diurnal and semi-diurnal frequency bands. After removing the theoretical predictions from the observed data the diurnal and semi-diurnal signal power are reduced and the periodicity at about 8 hours for the Y-pole component becomes more clear and passes the significance level of 0.005.

Figure 3 shows Wavelet scalograms of the complex polar motion signal during CONT02 after removing the theoretical model predictions described in Section 1 from the data. The upper plots (a–b) show retrograde and prograde polar motion in the period interval 2–100 hours. Retrograde semi-diurnal, prograde semidiurnal and prograde diurnal signals are detected. The lower plots (c–d) zoom in into the period interval 5–10 hours. A retrograde signal at 8 hours is clearly visible, and there is also some prograde signal, though less clear. Polar motion variations with an 8 hour periodicity are predicted [17] based on an ocean tide model [18].

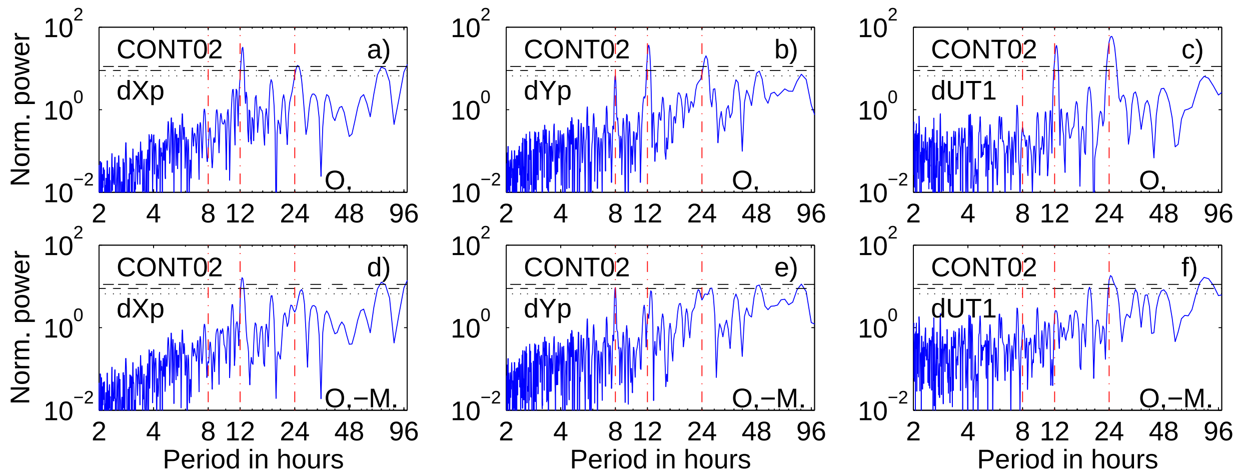

Figure 2. Lomb Periodograms of polar motion and UT1 during CONT02. See text for further explanations.

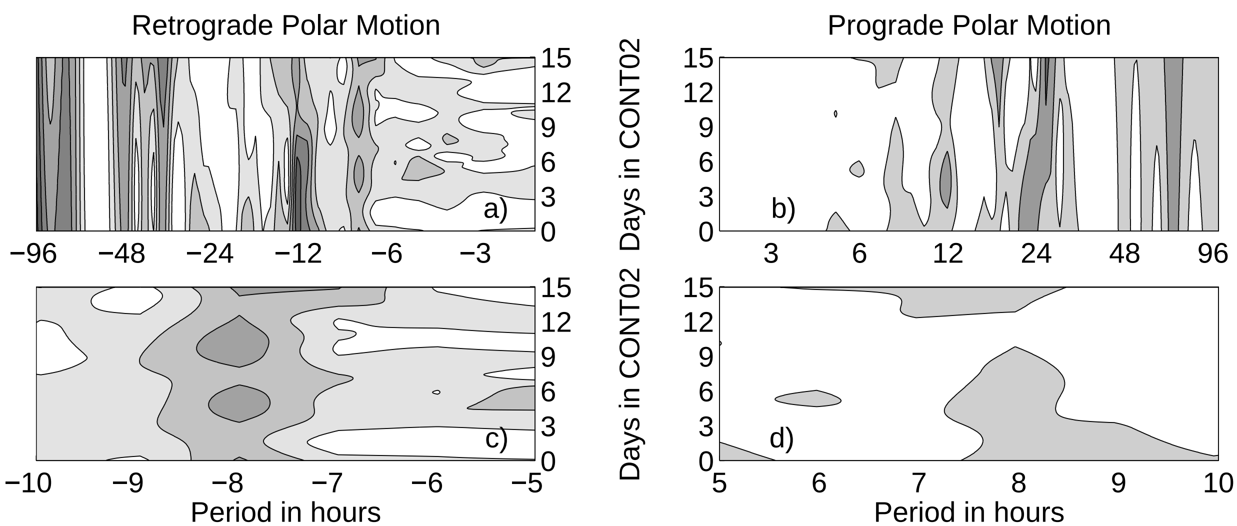

Figure 3. Wavelet scalograms of reduced polar motion during CONT02. See text for further explanations.

5. Conclusions and Outlook

The analysis of earth rotation parameters derived from the VLBI campaigns CONT94, CONT95 and CONT02 shows clearly that variations in the diurnal and semi-diurnal frequency bands exist. Different spectrum analysis tools give similar results, and the three campaigns also display similar signal content when compared to each other. However, the resolution of CONT95 is worse than for the other two campaigns, and only CONT02 shows a significant signal in polar motion with a periodicity of 8 hours. The existing theoretical models for high-frequency earth rotation variations partly explain the observed signals and signal power is reduced for these periods when the predictions are removed from the observations. Nevertheless, there is still remaining significant signal power at some periods and for some earth rotation parameters. The CONT02 campaign reveals signal power for retrograde and prograde polar motion around 8 hours period. We plan to continue the investigations concerning high-frequency earth rotation variations. Future continuous VLBI campaigns with high data quality will be very helpful for this work.

References

[1] Chao, B.F., Ray, R.D., Gipson, J.M., Egbert, G.D. and Ma, C.: Diurnal/semidiurnal polar motion excited by oceanic tidal angular momentum. *J. Geophys. Res.*, **101(B9)**, 1996.

[2] Ray, R.D., Steinberg, D.J., Chao, B.F., and Cartwright, D.E.: Diurnal and semidiurnal variations in the Earth's rotation rate induced by oceanic tides. *Science*, **264**, 830–832, 1994.

[3] Ray, R.D., Sanchez, B. V., and Cartwright, D.E.: Some extensions to the response method of tidal analysis applied to TOPEX/Poseidon. *EOS Trans. AGU*, **75(16)**, 108, 1994.

[4] Brzeziński, A. and Capitaine, N.: Lunisolar perturbations in Earth rotation due to the triaxial figure of the Earth: geophysical aspects. In: *Proc. Journees Systemes de Reference Spatio-Temporels 2001*, N. Capitaine (ed.), Paris Observatory. 2002.

[5] de Viron, O., Goose, H., Bizouard, C., and Lambert: EGS General Assembly 2002. see also `http://hpiers.obspm.fr/eop-pc/models/PM/PM_oceanic_nt_hf_tab.html`

[6] Brzeziński, A., Bizouard, C., and Petrov, S.D.: Influence of the atmosphere on earth rotation: what new can be learned from the recent atmospheric angular momentum estimates? *Surv. Geophys.*, **23(1)**, 2002.

[7] Ma, C., Sauber, J.M., Bell, L.J., Clark, T.A., Gordon, D., Himwich, W.E., and Ryan, J.W.: Measurements of horizontal motions in Alaska using very long baseline interferometry. *J. Geophys. Res.*, **95(2)**, 21991–22011, 1990.

[8] Nothnagel, A.: VTRF2003: A conventional VLBI terrestrial reference frame. In: W. Schwegmann, V. Thorandt (eds.): *Proc. of the 16th Meeting on European VLBI for Geodesy and Astrometry*, Bundesamt für Kartographie und Geodäsie, Frankfurt/Leipzig, 195–199, 2003.

[9] Ma, C., Arias, E.F., Eubanks, T.M., Fey, A.L., Gontier, A.-M., Jacobs, C.S., Sovers, O.J., Archinal, B.A., and Charlot, P.: The International Celestial Reference Frame realized by VLBI. *Astron. Astrophys.*, **116**, 516–546, 1998.

[10] Niell, A.: Global mapping functions for the atmospheric delay at radio wavelength. *J. Geophys. Res.*, **101(B2)**, 3227–3246, 1996.

[11] IERS C04 series, http://www.iers.org/iers/products/eop/combined04.html

[12] Seidelmann, P.K.: 1980 IAU Nutation: The final report of the IAU working group on nutation. *Celestial Mech.*, **27**, 79–106, 1982.

[13] Press, W.H., Teukolsky, S.A., Vetterling, W.T., and Flannery, B.P: Numerical recipes in FORTRAN. 2nd edition, Cambridge, 1992.

[14] Baisch, S., and Bokelmann, G.H.R.: Spectral analysis with incomplete time series: an example from seismology. *Computers & Geosciences*, **25**, 739–750, 1999.

[15] Foster, G.:. Wavelets for period analysis of unevenly sampled time series. *Astron. J.*, **112(4)**, 1996.

[16] Schmidt, M.: Wavelet analysis of stochastic stignals. In: *IERS Technical Note 28*, B. Kolaczek, H. Schuh, D. Gambis (eds.), 2000.

[17] Wünsch, J.: personal communication, 2001.

[18] Seiler, U., and Wünsch, J.: *Astron. Nachr.*, **316**, 419, 1995.

Jolanta Nastula et al.: High Resolution Earth Rotation Parameters Determined During the CONT02 Campaign ,
IVS 2004 General Meeting Proceedings, p.408–412
http://ivscc.gsfc.nasa.gov/publications/gm2004/nastula

High Resolution Earth Rotation Parameters Determined During the CONT02 Campaign

Jolanta Nastula [1], *Barbara Kolaczek* [1], *Robert Weber* [2], *Johannes Boehm* [2], *Harald Schuh* [2]

[1] *Space Research Centre of PAS*

[2] *Institute of Geodesy and Geophysics, Vienna University of Technology*

Contact author: Jolanta Nastula, e-mail: nastula@cbk.waw.pl

Abstract

For the two weeks of the CONT02 campaign in October 2002 the Earth rotation parameters, ERP (xpol, ypol, UT1-UTC) were determined with a resolution of one hour by VLBI and also by GPS. Analyses of these two very precise polar motion series reveal oscillations with periods of 8h, 6h and 4h-5h. Rapid oscillations of polar motion with periods of 8h and 5h-6h had already been found in the two-hourly polar motion series determined by GPS (CODE) in the period 1997.5 through 2001.0 but in that time it was unclear whether these phenomena are real or connected with the observational technique, e.g. with effects of the satellite orbits.

The detection of the 8h, 6h and 4h-5h oscillations in polar motion independently determined by two accurate space geodetic techniques is a first evidence for a real sub-semidiurnal variation of the ERP. On the other hand the oscillations might still be an artifact stemming from similar methods of data sampling or from un-recovered diurnal drifts in the time series. Oscillations with periods of 8h, 6h, 4h-5h were also detected in the time series of UT1-UTC determined by GPS and VLBI.

1. Analyses

Rapid oscillations of polar motion and UT1-UTC with subdaily periods had been detected by GPS and VLBI in former investigations (Kolaczek et al., 2000; Schmitz-Hübsch and Schuh, 2003; Weber et al., 2002) (Fig.1). The oscillation with a period of 8 hours was also detected in the series of Atmospheric Excitation Functions (Chi1, Chi2) which were available with a resolution of 3 hours (Weber et al., 2002, Fig.1).

In that time the analyzed series were not simultaneous and it was not possible to find the origin of the oscillation and to decide whether the oscillation of 8 hours comes from the GPS technique (e.g. caused by the orbit computation) or is a real oscillation of polar motion.

The CONT02 campaign observed in October 2002 by the IVS delivered dense simultaneous series of Earth rotation parameters determined by VLBI with a resolution of one hour. The GPS results were taken from the CODE Analysis Center. Spectra of polar motion and UT1-UTC computed by the Fourier Transform Band Pass Filter (Kosek, 1995) clearly show similarities. In the results of both techniques, oscillations with periods of 8h, 6h, 4h-5h are detected besides the well-known semi-diurnal oscillations (Fig.2). However, there is a discrepancy at the 8 hours oscillation which shows up as prograde wave in the VLBI spectrum of polar motion but retrograde in GPS (see Figs.2a, 5). Computed time variable spectra (FTBPF) of polar motion show some time variations of amplitudes of these rapid oscillations (Figs.3, 5). Amplitudes of these oscillations are usually higher in the case of the VLBI data while variability of amplitudes is larger in the case of the GPS data (Figs.3, 5). The amplitude of the retrograde part of the 12h oscillation in the

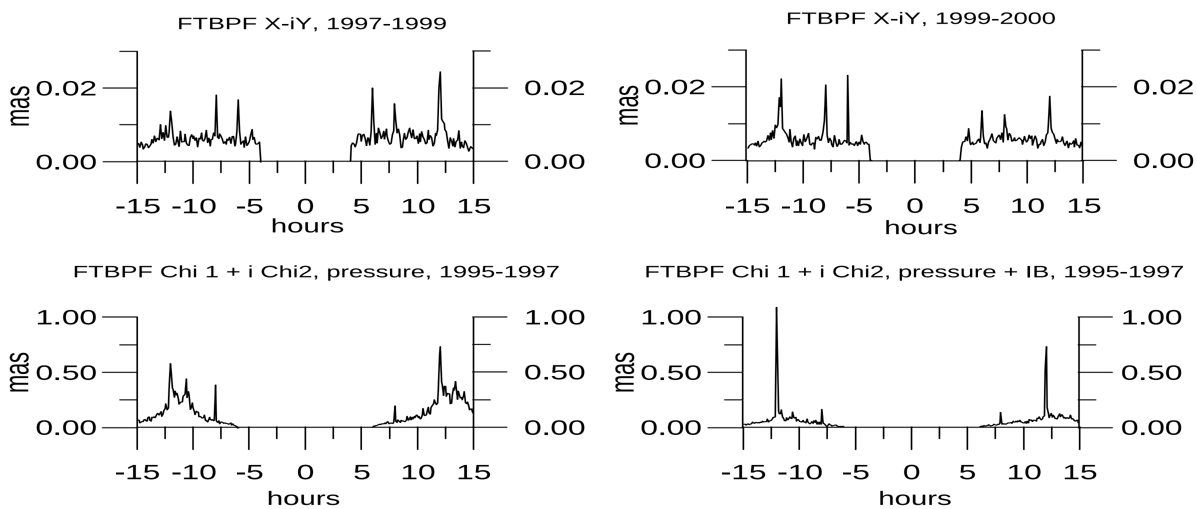

Figure 1. FTBPF spectra of short period oscillations of GPS (CODE) polar motion and atmospheric excitation functions computed with parameter $\lambda = 0.007$ [3].

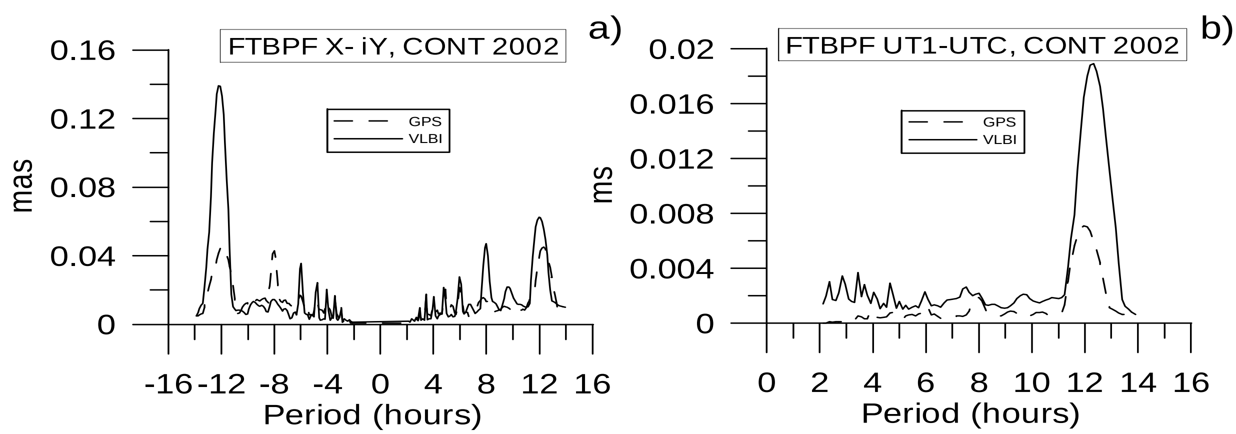

Figure 2. FTBPF spectra of short period oscillations of GPS and VLBI polar motion and UT1-UTC, respectively computed with parameter $\lambda = 0.006$.

VLBI data is two times higher than in the case of the GPS data (Figs.2a,3). The detection of rapid oscillations with periods of 8h, 6h, 4h-5h by two different techniques suggests that these are real oscillations of polar motion. Their origins need further studies.

Analyses of UT1-UTC data determined during the CONT02 campaign by VLBI and GPS detected besides the strong 12 hours oscillation additional short period variations (Figs.2b, 4, 6). Again, there are time variations of the amplitudes, especially in the case of the GPS data.

The amplitude of the 12h oscillation of UT1-UTC is much stronger in the case of the VLBI data

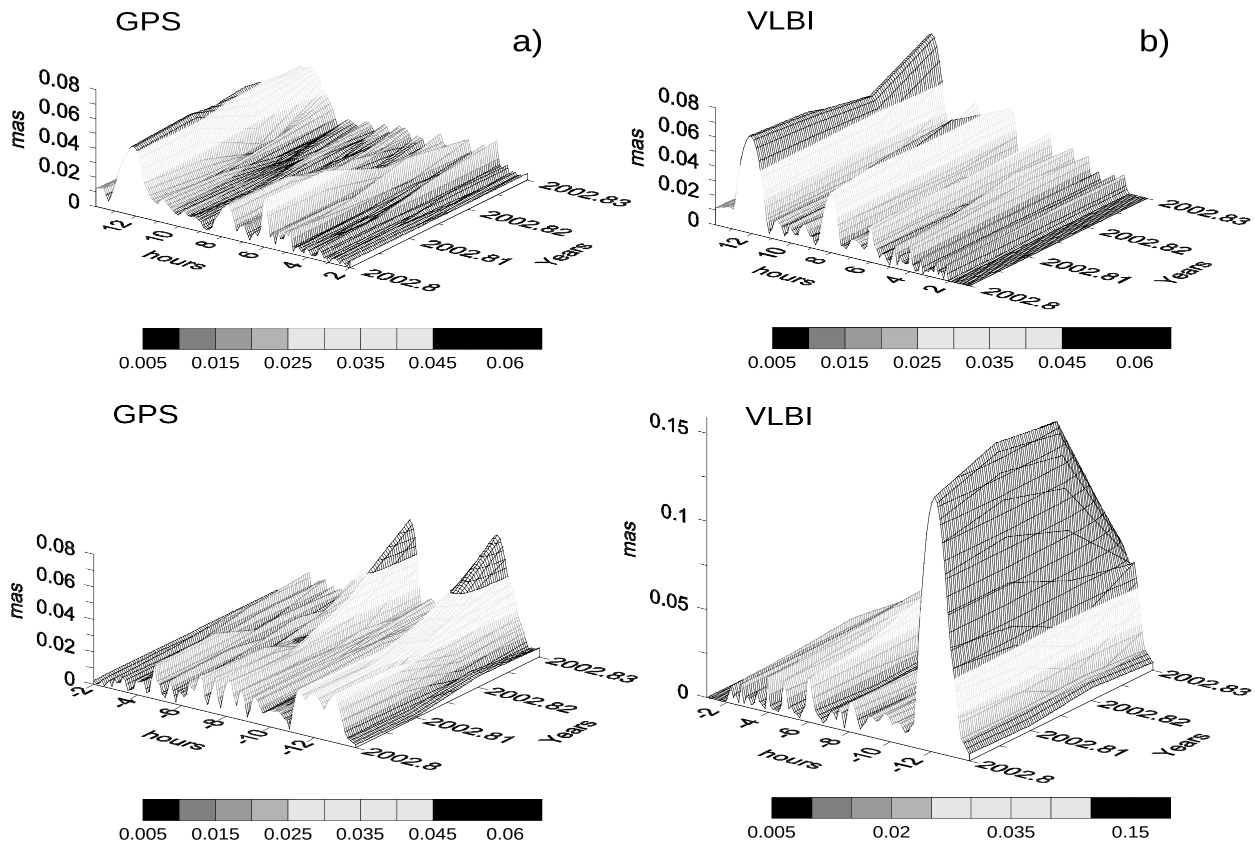

Figure 3. FTBPF spectra of short period oscillations (periods < 13 hours) of polar motion determined by GPS and VLBI respectively, computed with parameter $\lambda = 0.006$.

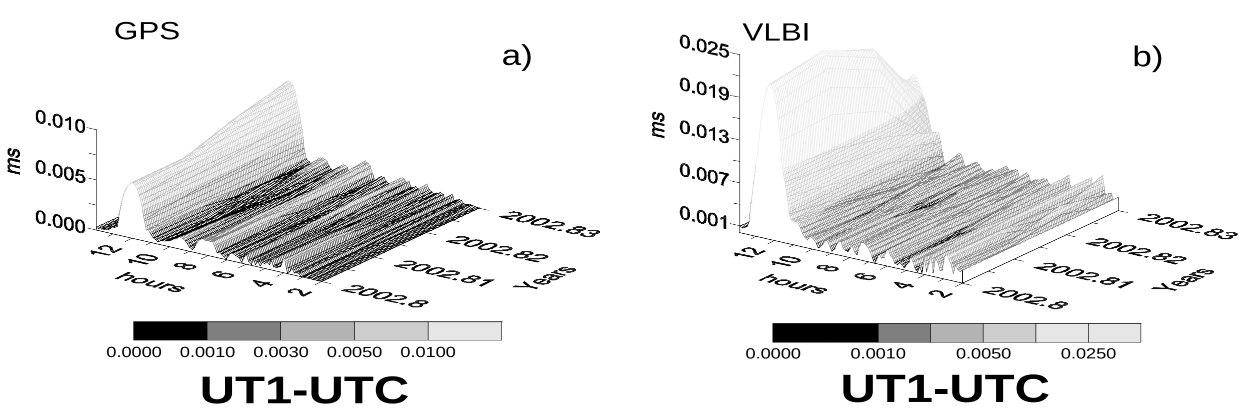

Figure 4. FTBPF time variable spectra of short period oscillations (periods < 13 hours) of UT1-UTC determined by GPS and VLBI respectively, computed with parameter $\lambda = 0.006$.

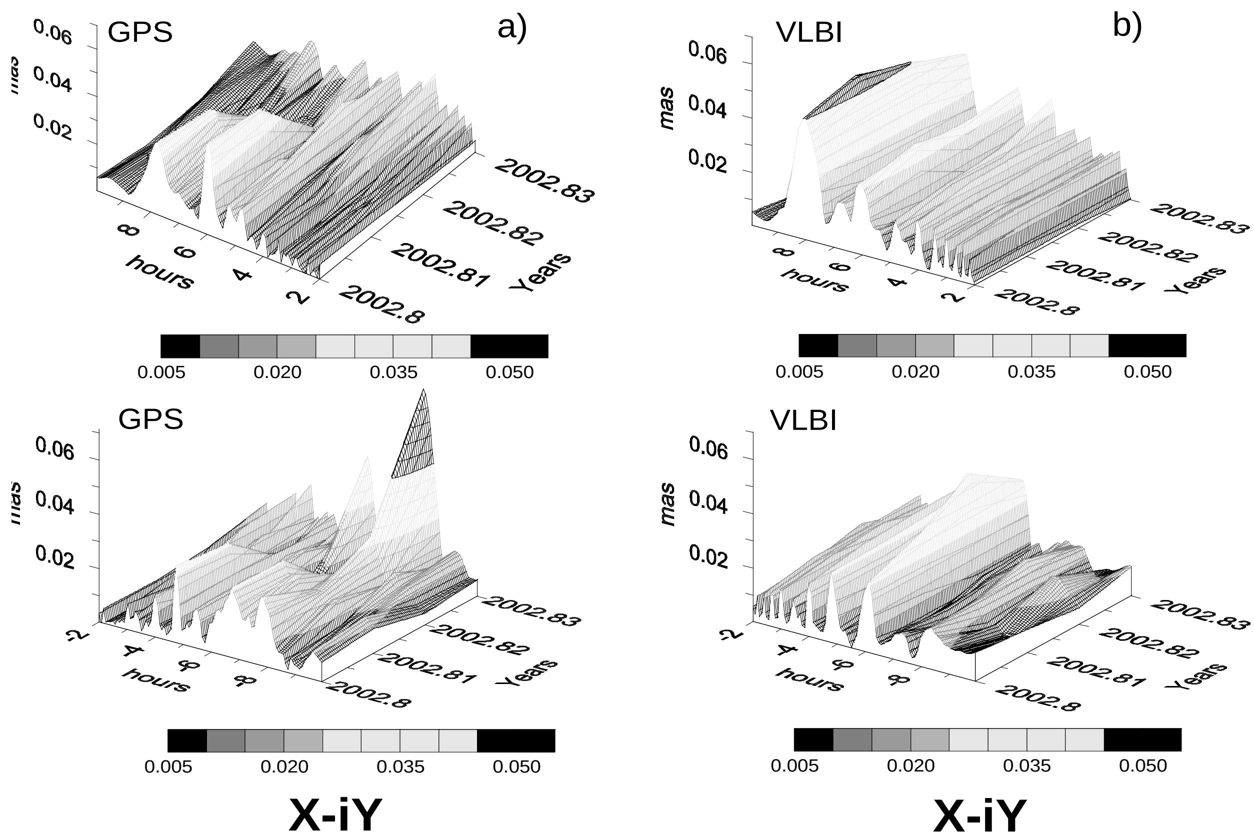

Figure 5. FTBPF time variable spectra of short period oscillations (periods $<$ 10 hours) of polar motion determined by GPS and VLBI respectively, computed with parameter $\lambda = 0.01$, which gives higher time resolution of spectra than $\lambda = 0.006$.

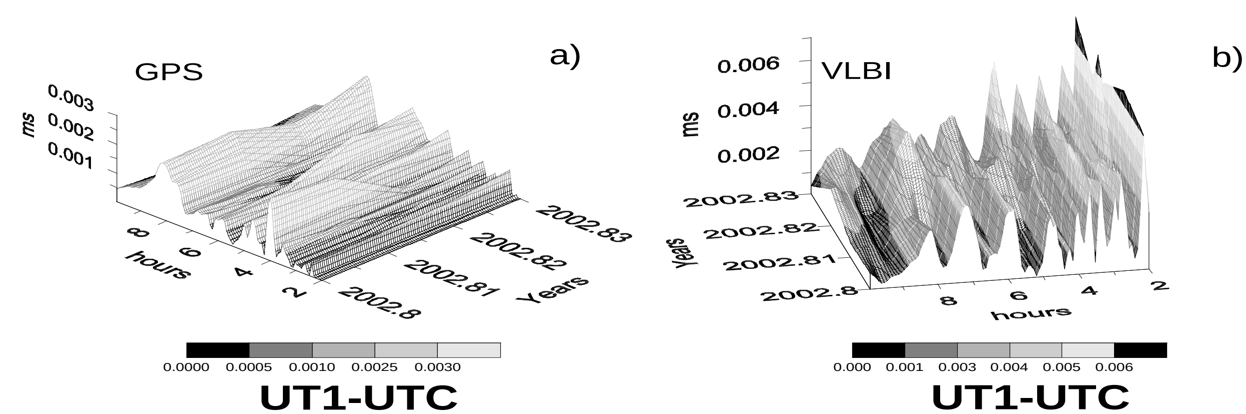

Figure 6. FTBPF time variable spectra of short period oscillations (periods $<$ 10 hours) of UT1-UTC determined by GPS and VLBI respectively, computed with parameter $\lambda = 0.01$, which gives higher time resolution of spectra than λ =0.006.

than of the GPS data. It is interesting that the VLBI results contain several strong oscillations in the spectral range between 2 and 4 hours (Fig.6).

2. Conclusions

Oscillations with periods of 8h, 6h, 4h-5h were detected by VLBI and GPS in polar motion and UT1-UTC, determined during the CONT02 campaign. It suggests that these oscillations can be real oscillations of Earth rotation parameters. Their origins need further studies.

There are temporal variations of the amplitudes of these rapid oscillations.

There is a discrepancy at the 8 hours oscillation of polar motion (prograde in VLBI and retrograde in GPS) that needs further investigations.

3. Acknowledgements

This research has been supported by the Polish Ministry of Scientific Research and Information under grant No 5 T12E 039 24 and the Science and Technology Cooperation Program between Poland and Austria under the project 24/2003/2004. We thank M. Sawicki for preparation of the graphics.

References

[1] Kolaczek, B, W. Kosek, H. Schuh, Short Period Oscillations of Earth Rotation In: Polar Motion Historical and Scientific Problems, IAU Colloquium 178. Astronomical Society of the Pacific Conference Series, Vol. 208, 533–544, 2000.

[2] Kosek, W., Time Variable Band Pass Filter Spectra of Real and Complex-Valued Polar Motion Series In: Artificial Satellites, Planetary Geodesy, 30, Warsaw, Poland, 27–43, 1995.

[3] Weber, R, J. Nastula, B. Kolaczek, D.A. Salstein, Analysis of Rapid Variations of Polar Motion Determined by GPS. In: Vistas for Geodesy in the New Millenium, eds. J. Adam, K.P. Schwarz (eds); Vol 125, 445–450, Springer-Verlag, 2002.

[4] Schmitz-Hübsch, H., H. Schuh, Seasonal and Short-Period Fluctuations of Earth Rotation Investigated by Wavelet Analysis. In: Geodesy, The Challenge of the Third Millenium; E.W. Grafarend, F.W. Krumm, V.S. Schwarze (eds), 125–134, Springer-Verlag, 2003.

Christoph Steinforth et al.: Considering a Priori Correlations in the IVS Combined EOP Series, IVS 2004 General Meeting Proceedings, p.413–417
http://ivscc.gsfc.nasa.gov/publications/gm2004/steinforth

Considering a Priori Correlations in the IVS Combined EOP Series

Christoph Steinforth, Axel Nothnagel

Geodetic Institute of the University of Bonn

Contact author: Christoph Steinforth, e-mail: steinforth@uni-bonn.de

Abstract

The current combination of EOP time series actually implies a violation of the basic rule that the same data cannot be used twice in an adjustment process. This fact is presently neglected by treating the input data of the IVS Analysis Centers as "new" or independent data. However, this deficiency can be mitigated by introducing proper correlation coefficients between the Analysis Centers. Different approaches for deriving such correlations as well as results are presented in this paper.

1. Introduction

The generation of the IVS combined EOP series actually implies a violation of the basic rule that an observation can only be used once in an adjustment process. However, due to different modelling of the observations or different data editing and outlier elimination procedures utilized by the Analysis Centers it can be assumed that the resulting EOP series can be treated as (approximately) independent data[1]. Nevertheless, it is possible to process estimates from the same set of observations in a rigorous way by using the correlations between the estimates. In the case of the IVS combined series two types of correlations have to be considered:

- correlations between EOP components ρ_{x_p,y_p}, $\rho_{x_p,dUT1}$, $\rho_{y_p,dUT1}$ and $\rho_{d\psi,d\varepsilon}$, reported by the respective Analysis Center with
$$\rho_{ij} = \frac{\sigma_{ij}}{\sigma_i \sigma_j}$$
- correlations between the Analysis Centers

Both types of correlations are necessary to form a rigorous combination. As an example eq. 1 shows the covariance matrix for two Analysis Centers and two components as it should be used in the combination.

$$\mathbf{\Sigma_{combi}} = \begin{vmatrix} \sigma_{x_1}^2 & \sigma_{12} & \sigma_{x_1 y_1} & \sigma_{x_1 y_2} \\ & \sigma_{x_2}^2 & \sigma_{x_2 y_1} & \sigma_{x_2 y_2} \\ & & \sigma_{y_1}^2 & \sigma_{12} \\ & & & \sigma_{y_2}^2 \end{vmatrix} \tag{1}$$

The covariance matrix contains three types of covariances:

σ_{12} – covariances between different Analysis Centers

$\sigma_{x_1 y_1}$ – covariances between EOP components of the same Analysis Center

$\sigma_{x_1 y_2}$ – "mixed" covariances (between Analysis Centers and EOP components)

[1] The IGS uses this approach (Kouba, pers. communication).

In this paper we develop the correlations between the Analysis Centers. For clarity reasons the correlations between the components ρ_{x_p,y_p}, $\rho_{x_p,dUT1}$, $\rho_{y_p,dUT1}$ and $\rho_{d\psi,d\varepsilon}$ and the "mixed" covariances are neglected here.

EOP series from five IVS Analysis Centers are currently being combined to form the official IVS product (two OCCAM solutions from AUS – Geoscience Australia and IAA – Institute of Applied Astronomy, St. Petersburg and three Calc/Solve solutions from BKG – Bundesamt für Kartographie und Geodäsie, GSF – Goddard Space Flight Center, and USN – U.S. Naval Observatory). Embarking on a rigorous approach we first develop a correlation matrix purely on the basis of a thought experiment taking into account the general facts of the different solutions (table 1). Small correlations are entered between Analysis Centers using different software packages, high correlations between the same software package and even a little higher between GSF and USN, using the same software and the same procedures.

Table 1. A priori correlation matrix from a thought experiment

	AUS	BKG	GSF	IAA	USN
AUS	–	0.2	0.2	0.7	0.2
BKG		–	0.7	0.2	0.7
GSF			–	0.2	0.8
IAA				–	0.2
USN					–

2. Covariances and Correlations

This section summarizes briefly the formulas for the derivation of a theoretical covariance matrix. These formulas were mainly taken from [4]. The basis is a two-dimensional random vector as a realization of a two-dimensional random variable. The two observation vectors $\mathbf{l}_1$ and $\mathbf{l}_2$ contain the EOP time series determined by two different Analysis Centers. The observations can be grouped pairwise according to the epoch of observation.

$$\mathbf{L} = \begin{vmatrix} L_1 \\ L_2 \end{vmatrix}; \quad \mathbf{l}^T = \begin{vmatrix} \mathbf{l}_1^T \\ \mathbf{l}_2^T \end{vmatrix} = \begin{vmatrix} l_{11} & l_{12} & \cdots & l_{1n} \\ l_{21} & l_{22} & \cdots & l_{2n} \end{vmatrix} = \begin{vmatrix} \begin{pmatrix} l_{11} \\ l_{12} \end{pmatrix} \begin{pmatrix} l_{21} \\ l_{22} \end{pmatrix} \cdots \begin{pmatrix} l_{n1} \\ l_{n2} \end{pmatrix} \end{vmatrix} \tag{2}$$

Eq. 3 gives the definition of the expectation values of the random variables.

$$E(\mathbf{L}) = \begin{vmatrix} E(L_1) \\ E(L_2) \end{vmatrix} = \begin{vmatrix} \lim_{n\to\infty} \frac{1}{n} \sum_{j=1}^{n} l_{1j}; & \lim_{n\to\infty} \frac{1}{n} \sum_{j=1}^{n} l_{2j} \end{vmatrix}^T = \begin{vmatrix} \mu_1 \\ \mu_2 \end{vmatrix} = \boldsymbol{\mu} \tag{3}$$

In the next step true errors can be calculated according to eq. 4.

$$\boldsymbol{\varepsilon}^T = \begin{vmatrix} \boldsymbol{\varepsilon}_1^T \\ \boldsymbol{\varepsilon}_2^T \end{vmatrix} = \begin{vmatrix} l_{11}-\mu_1 & l_{12}-\mu_1 & \cdots & l_{1n}-\mu_1 \\ l_{21}-\mu_2 & l_{22}-\mu_2 & \cdots & l_{2n}-\mu_2 \end{vmatrix} = \boldsymbol{l}^T - \boldsymbol{\mu}\boldsymbol{e}^T \tag{4}$$

The covariance matrix follows according to

$$\boldsymbol{\Sigma}_{\mathbf{ll}} = E\left\{ \begin{vmatrix} \boldsymbol{\varepsilon}_1^T \\ \boldsymbol{\varepsilon}_2^T \end{vmatrix} \begin{vmatrix} \boldsymbol{\varepsilon}_1^T & \boldsymbol{\varepsilon}_2^T \end{vmatrix} \right\} = E\left\{ \begin{vmatrix} \boldsymbol{\varepsilon}_1^T\boldsymbol{\varepsilon}_1 & \boldsymbol{\varepsilon}_1^T\boldsymbol{\varepsilon}_2 \\ \boldsymbol{\varepsilon}_2^T\boldsymbol{\varepsilon}_1 & \boldsymbol{\varepsilon}_2^T\boldsymbol{\varepsilon}_2 \end{vmatrix} \right\} = \begin{vmatrix} \sigma_{01}^2 & \sigma_{12} \\ \sigma_{21} & \sigma_{02}^2 \end{vmatrix} \tag{5}$$

with $E\left(\boldsymbol{\varepsilon}_1^T\boldsymbol{\varepsilon}_1\right)=\sigma_{01}^2$, $E\left(\boldsymbol{\varepsilon}_2^T\boldsymbol{\varepsilon}_2\right)=\sigma_{02}^2$ and $E\left(\boldsymbol{\varepsilon}_1^T\boldsymbol{\varepsilon}_2\right)=E\left(\boldsymbol{\varepsilon}_2^T\boldsymbol{\varepsilon}_1\right)=\sigma_{12}=\sigma_{21}$.
In the last step the correlation matrix can be deducted by simple matrix algebra (cf. [3])

$$\mathbf{R}=\begin{vmatrix} 1 & \rho_{12} \\ \rho_{21} & 1 \end{vmatrix} \tag{6}$$

with $\mathbf{R}=\mathbf{F}\,\boldsymbol{\Sigma}_{\mathbf{ll}}\,\mathbf{F}$ and $\mathbf{F}=diag\,(1/\sigma_{01},1/\sigma_{02})$.

3. Determination of Correlation Coefficients

The target of this investigation is to determine empirical correlation coefficients between the Analysis Centers. Two cases have to be distinguished (cf. [4]):

1. True values are unknown. In this case mean values have to be calculated in a first step. The mean values are then used to calculate a vector of corrections $\mathbf{v}$.

$$\bar{\mathbf{x}}=\begin{vmatrix} \bar{x}_1 \\ \\ \bar{x}_2 \end{vmatrix}=\frac{1}{n}\begin{vmatrix} \sum_{i=1}^{n} l_{1i} & \sum_{i=1}^{n} l_{2i} \end{vmatrix}^T;\ \mathbf{v}^T=\begin{vmatrix} \mathbf{v}_1^T \\ \mathbf{v}_2^T \end{vmatrix}=\begin{vmatrix} \bar{x}_1-l_{11} & \bar{x}_1-l_{12} & \cdots & \bar{x}_1-l_{1n} \\ \bar{x}_2-l_{21} & \bar{x}_2-l_{22} & \cdots & \bar{x}_1-l_{2n} \end{vmatrix} \tag{7}$$

   The empirical covariance matrix can be obtained according to eq. 8.

$$\bar{\boldsymbol{\Sigma}}_{\mathbf{ll}}=\frac{1}{n-1}\,\mathbf{v}^T\mathbf{v}=\frac{1}{n-1}\begin{vmatrix} \boldsymbol{v}_1^T\boldsymbol{v}_1 & \boldsymbol{v}_1^T\boldsymbol{v}_2 \\ \\ \boldsymbol{v}_2^T\boldsymbol{v}_1 & \boldsymbol{v}_2^T\boldsymbol{v}_2 \end{vmatrix}=\begin{vmatrix} s_1^2 & s_{12} \\ \\ s_{21} & s_2^2 \end{vmatrix} \tag{8}$$

2. True values $\tilde{L}_i$ or expectation values μ_i are known. In this case the empirical covariance matrix follows directly:

$$\bar{\boldsymbol{\Sigma}}_{\mathbf{ll}}=\begin{vmatrix} \frac{1}{n}\boldsymbol{\varepsilon}_1^T\boldsymbol{\varepsilon}_1 & \frac{1}{n}\boldsymbol{\varepsilon}_1^T\boldsymbol{\varepsilon}_2 \\ \\ \frac{1}{n}\boldsymbol{\varepsilon}_2^T\boldsymbol{\varepsilon}_1 & \frac{1}{n}\boldsymbol{\varepsilon}_2^T\boldsymbol{\varepsilon}_2 \end{vmatrix}=\begin{vmatrix} s_1^2 & s_{12} \\ \\ s_{21} & s_2^2 \end{vmatrix} \tag{9}$$

   In both cases the result is the empirical correlation coefficient:

$$\boxed{\rho=\tfrac{s_{12}}{s_1\,s_2}}$$

4. Significance Tests

Empirical correlation coefficients r are normally distributed:

$$r\sim N\left(\rho,\frac{1-\rho^2}{\sqrt{n-1}}\right) \tag{10}$$

for $n\longrightarrow\infty$. In case of small samples a transformation is needed (eq. 11) This transformation permits the use of the normal distribution even for small samples (e.g. [2]).

$$z=\frac{1}{2}\log\frac{1+r}{1-r},\ z\sim N\left(\zeta,\sigma_z\right)\quad\text{and}\quad\frac{z-\zeta}{\sigma_z}\sim N\left(0,1\right) \tag{11}$$

with

$$\zeta = \frac{1}{2}\log\frac{1+\rho}{1-\rho} + \frac{\rho}{2\,(n-1)} \tag{12}$$

and

$$\sigma_z = \frac{1}{\sqrt{n-3}} \tag{13}$$

In addition it is possible to give confidence regions for the calculated correlation coefficients. Another possibility to express the significance test for correlation coefficients using the t-distribution is given in [5].

5. Results

To investigate the correlation coefficients a subset of sessions common to all Analysis Centers series currently incorporated in the combination was chosen (NEOS-A, R1 and R4). The number of 634 sessions was sufficient to calculate significant correlation coefficients. As already pointed out in section 3 two cases have to be distinguished:

1. True values are unknown. This test failed because this method cannot remove the deterministic signal properly. It turned out that all correlation coefficients are 1, hence the resulting covariance matrix is singular.
2. "True" values can be simulated by using a series of higher accuracy level or an independent series ([1]). A suitable series to remove the deterministic signal from the input EOP series of the Analysis Centers is the IERS C04 series.

   Fig. 1 shows a comparison of the "thought experiment" matrix and the correlation matrix for $d\psi$ after removal of the deterministic signal from the EOP series subtracting the IERS C04 series.

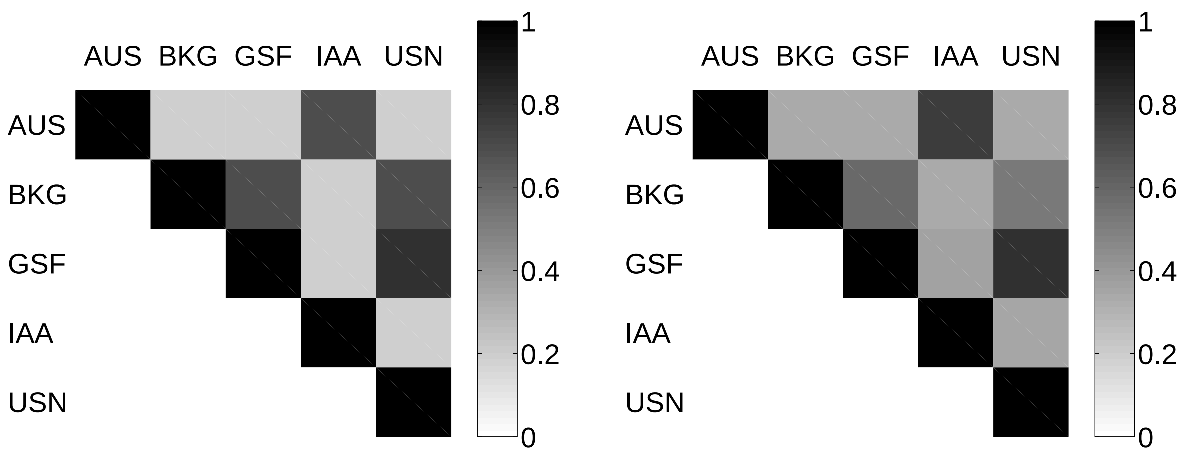

Figure 1. Correlation matrix from thought experiment (cf. tab. 1) (left) and correlation matrix for parameter $d\psi$ after removing the deterministic signals subtracting IERS C04.

To test this approach a combined series was calculated using the correlation coefficients shown on the right hand side of fig. 1. Figure 2 shows a comparison of the uncorrelated and the correlated approach for x_p. The differences are mainly within the range of ± 100 μas.

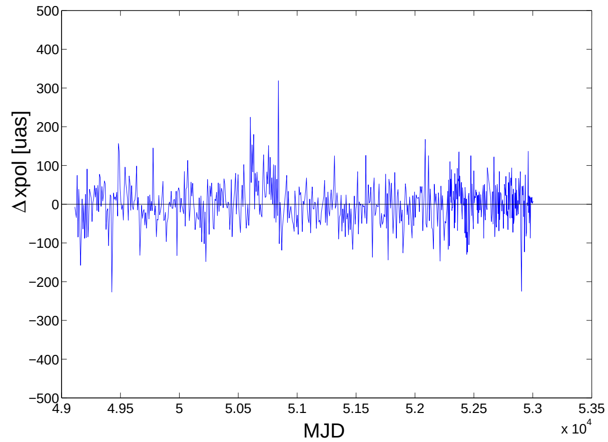

Figure 2. Differences between EOP combinations using a covariance matrix which contains covariances between the Analysis Centers and a diagonal covariance matrix respectively for parameter x_p.

6. Conclusions and Outlook

The use of correlation coefficients between Analysis Centers is another step forward to a rigorous combination of EOP time series. It has been shown that the correlation matrix computed using real data agrees surprisingly well with the one developed by purely taking into account known facts. As it had to be expected the average formal errors of the combined series increased by a factor of ~ 1.4 as compared to the combination where the results of the Analysis Centers are treated as uncorrelated. In the next step, the correlations between the individual parameters and between the Analysis Centers have to be consolidated to form a single covariance matrix containing both types of correlations. Only then the formal errors of the combined earth orientation parameters will become really meaningful.

References

[1] Großmann, W., Grundzüge der Ausgleichungsrechnung, Springer-Verlag, Berlin, 1969

[2] Höpcke, W., Fehlerlehre und Ausgleichungsrechnung, Verlag de Gruyter, Berlin, 1980

[3] Koch, K.-R., Parameter Estimation and Hypothesis Testing in Linear Models, Springer-Verlag, Berlin, 1988

[4] Niemeier, W., Ausgleichungsrechnung, Verlag de Gruyter, Berlin, 2002

[5] Wolf, H., Ausgleichungsrechnung I, Dümmler Verlag, Bonn, 1994

Manuela Krügel et al.: CONT02 Campaign - Combination of VLBI and GPS, IVS 2004 General Meeting Proceedings, p.418–422
http://ivscc.gsfc.nasa.gov/publications/gm2004/kruegel

CONT02 Campaign - Combination of VLBI and GPS

Manuela Krügel [1], *Volker Tesmer* [1], *Detlef Angermann* [1], *Daniela Thaller* [2], *Markus Rothacher* [2], *Ralf Schmid* [2]

[1] *DGFI, Deutsches Geodätisches Forschungsinstitut*

[2] *FESG, Forschungseinrichtung Satellitengeodäsie, Technical University of Munich*

Contact author: Manuela Krügel, e-mail: `kruegel@dgfi.badw.de`

Abstract

In October 2002, the International VLBI Service for Geodesy and Astronomy (IVS) arranged the VLBI campaign CONT02 which was designed to provide 15 days of continuous VLBI observations of eight participating stations. Using this data as well as the observations from a global GPS network, free daily normal equations were generated for both techniques, adapting the functional models as much as possible. The following parameters contained in these normal equations were combined: station positions (using a set of selected local ties), tropospheric parameters (zenith delays and horizontal gradients) and Earth Orientation Parameters (EOP). The paper gives an overview of the solution setup and provides first combination results for the common parameters.

1. Introduction

Combining solutions or normal equations from one technique is a method to remove outliers, to detect systematics and to reduce the "analysts-noise" and thus to achieve a better robustness of the corresponding parameters. But, in contrast to the case when solutions or normal equations of different techniques are combined, no independent information is introduced, because the contributions make use of the same observations only. If much care is taken to perform an inter-technique combination as rigorously as possible, some of the techniques' inherent strengths and weaknesses can be overcome. E.g., if VLBI and GPS data are combined, the benefit for both techniques is expected to be high because of the large number of common parameters (station coordinates, EOP and troposphere parameters). An excellent basis for studying combination aspects is the two-week VLBI campaign CONT02 which was used for this work: all eight observing VLBI sites provide a co-location with GPS, and all are of high quality.

2. Required Preparations Concerning the Data and the Software Packages

In a first step, the VLBI data was concatenated to daily files from 0 h to 0 h UTC, in contrast to the original data files starting and ending at 17 h UTC. This was done to optimise the comparability of parameters, especially those estimated in 24 h intervals.

The generation of the VLBI normal equations was performed with the OCCAM software at DGFI (Titov et al. 2001). The GPS contributions, consisting of about 150 globally distributed stations were generated with the Bernese GPS Software (Hugentobler et al. 2001) at the FESG (Forschungseinrichtung Satellitengeodäsie TU München). To be able to perform a combined solution as rigorous as possible, the functional models of the two techniques were adapted as much as possible: on the one hand, identical a priori models were used (solid earth tides, pole tide, ocean loading, tropospheric delay, a priori EOP values as well as their interpolation to the observation epoch, subdaily EOP model, nutation model). Furthermore, unknown parameters were set up identically (one set of station coordinates per day, daily nutation parameters, two-hourly pole coordinates and UT1-UTC, two-hourly tropospheric zenith delays, one daily set of tropospheric gradients). It should be emphasised that the mathematical representation of some parameters was kept simple to reach homogeneity, as e.g. for the tropospheric zenith delay, which is often parameterised in a more sophisticated way.

3. Combination and Comparison

The weighting of the normal equations of both techniques was done empirically: In a first approximation, the matrices were scaled to the same variance level, using the mean standard deviations for the station coordinates. In a second step, the "real accuracies" were considered, generating weight factors using the RMS values of residual positions after a Helmert transformation of each techniques' two-weekly combined solution w.r.t. ITRF2000.

3.1. Coordinates

If station coordinates of different techniques are to be combined, it is necessary to include inter-station vectors (local ties) between the corresponding reference points (e.g. ftp://lareg.ensg.ign.fr/pub/itrf/itrf2000/tiesnx/*.SNX). The approach to select or exclude given local tie information is like the weighting procedure: preliminary and of empirical nature. Several criteria for selecting suitable local ties were applied: to detect gross outliers in a first step, the given local tie information was compared to differences between coordinates of co-located instruments, determined from technique-specific solutions. The second step was to consider how much each single local tie affects the other inter-station vectors on the one hand and the estimated EOP values on the other. Finally, seven local ties were assessed to be useful, i.e. only the local tie for Kokee Park was excluded.

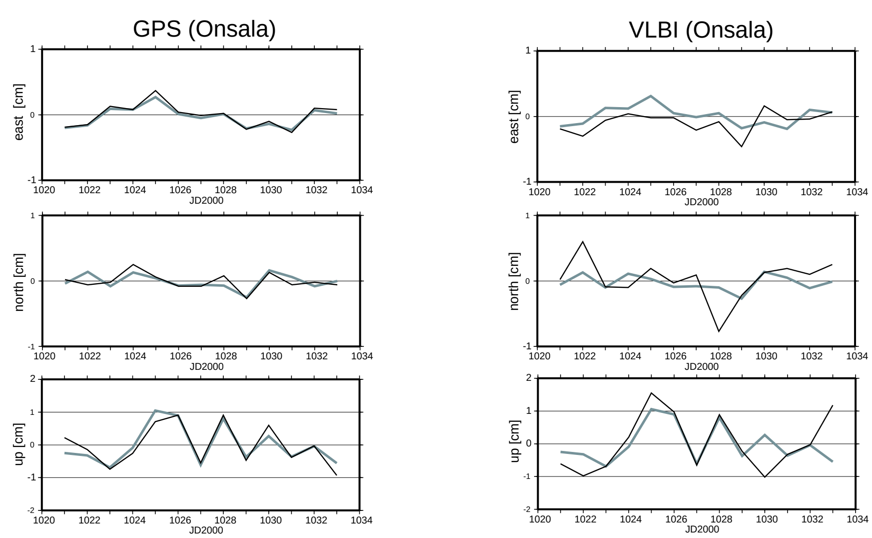

Figure 1. Time series of station coordinates for Onsala, before (black) and after (grey) combination.

Figure 1 shows the time series for the station coordinates of the VLBI and the GPS station in Onsala before and after the combination. Comparing the time series of the height components before the combination (black lines), we can recognise a similar characteristic, especially during the days 1021-1029. That suggests that both techniques are affected by the same physical effect in this time period. Comparing the time series before and after the combination, the combination leads to a smoothing effect for both stations. For the selected example the effect is stronger for the VLBI station, but this is not the case for all co-locations as we can see in Figure 2, which shows the repeatabilities of all stations.

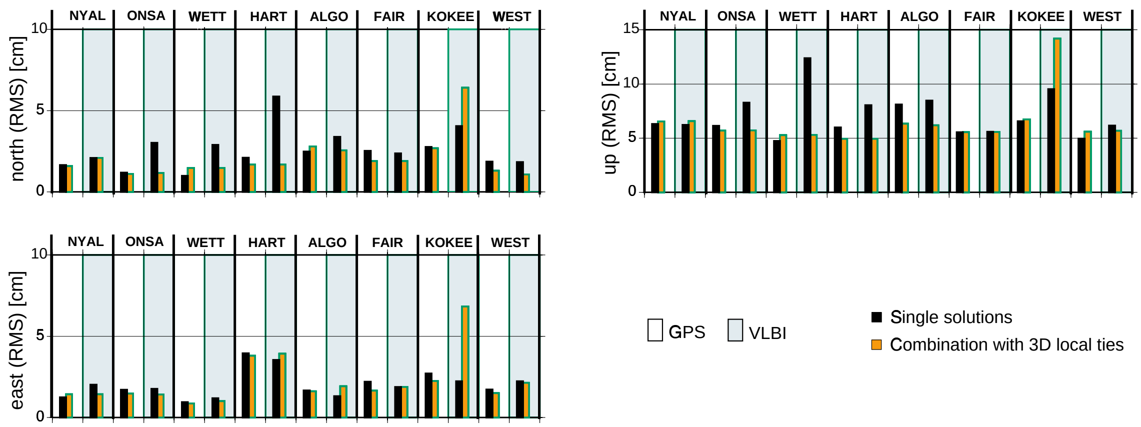

Figure 2. Repeatabilities of station coordinates, before and after the combination.

For most of the stations, the repeatabilities in the north and east component improve as a consequence of the combination. An exception is the VLBI station in Kokee Park, for which the corresponding local tie information was not used. For this station, the degradation of the repeatabilities suggests a problem in one of the space techniques (either in the data or in the solution) or in the local ties for the other stations. Alike for the horizontal components, the height components' repeatabilities improve for both techniques at most of the stations. Exceptions are the sites Ny Alesund, the GPS stations Wettzell and Westford and, again, Kokee Park. One reason for the generally slightly larger repeatabilities of the VLBI stations w.r.t. GPS might be the poorer network configuration. It should be mentioned, however, that the computed repeatabilities (RMS, root mean square) do not account for the formal errors of the estimated parameters.

3.2. Troposphere

The estimation of the tropospheric zenith delays was performed for GPS and VLBI in the same way. Therefore the zenith delay is divided into two parts, a dry part, modelled a priori using the Saastamoinen model as it is implemented in the Bernese GPS software (Hugentobler et al. 2001) and an estimated wet part. Both are mapped using the Niell mapping functions. For the VLBI stations we used the same dry delay as for the co-located GPS stations as a priori. Thus the estimated delays for the VLBI stations must differ by a small fraction from the ones estimated with GPS, caused by the height differences w.r.t. the GPS stations. Figure 3 shows the zenith delay time series for the GPS and the VLBI station in Algonquin Park. This is the co-location site with the largest height difference of about 23 m between the GPS and the VLBI reference points. We recognise a very good agreement for the time dependent characteristics of the two time series. The mean offset of 5.9 mm is mainly caused by the height difference.

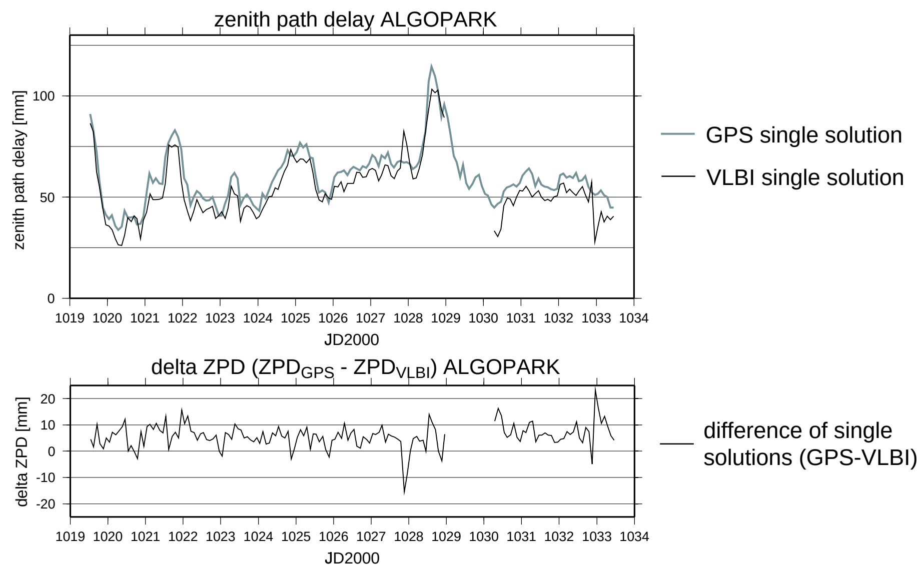

Figure 3. Tropospheric zenith delays for Algonquin Park.

If the zenith delays should be combined, this offset has to be considered, e.g. as a tropospheric tie. We used the Saastamoinen model and a standard atmosphere to derive theoretical zenith delay differences. Table 1 displays these theoretical offsets and the mean differences derived from technique specific solutions. For some stations the agreement between the theoretical and estimated value is very good (Algonquin Park, Wettzell, Westford). But there are also co-locations with differences in the order of 3-5 mm (Kokee Park, Ny Alesund, Fairbanks and Onsala). It is also remarkable that for some stations (the European stations as well as Hartebeesthoek and Fairbanks) the estimated zenith path delay for GPS is smaller than for VLBI although the reference point for GPS has a lower ellipsoidal height than that for VLBI. The reason is still unknown and further investigations are necessary.

Table 1. Theoretical offsets and mean differences between the single technique solutions.

	Δ height (VLBI-GPS) [m]	Δ ZPD (theory) (GPS-VLBI) [mm]	ΔZPD (estima.) (GPS-VLBI) [mm]	Δ ZPD (theory) - ΔZPD (estima.) [mm]
Ny Alesund	3.1	1.1	-2.8	3.9
Onsala	13.7	4.3	-0.7	5.0
Wettzell	3.1	0.8	-1.1	1.9
Hartebeesthoek	1.5	0.3	-1.4	1.7
Algonquin Park	23.1	6.2	5.9	0.3
Fairbanks	13.1	3.5	-0.8	4.3
Kokee Park	9.2	2.3	5.4	-3.1
Westford	1.7	0.5	1.6	-1.1

We combined the tropospheric zenith delay estimates of both techniques, including tropospheric ties with an a priori sigma of 0.1 mm. It was expected that this combination would stabilise the height determination. Unfortunately, first combination results show increased position repeatabilities (about 0.5-1 mm) for most stations. This indicates that there are problems regarding the combination of tropospheric parameters, and further investigations must be performed.

A comparison of tropospheric gradient estimates obtained from VLBI and GPS shows an excellent agreement for most of the stations. As an example, the pair of daily estimated gradients at the site Ny Alesund is presented in Figure 4. We combined the gradients of both techniques by introducing constraints with an a priori sigma of 0.1 mm. The effect on the estimated parameters was very small, suggesting that possibly stronger constraints should be applied, which need to be studied in more detail.

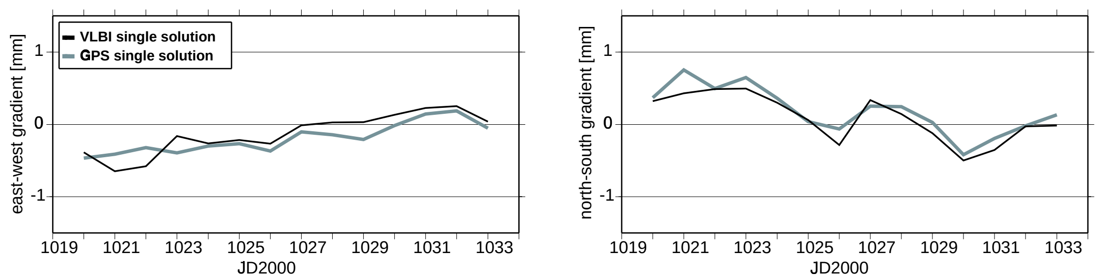

Figure 4. Tropospheric gradients for Ny Alesund.

4. Conclusions, Remaining Questions and Motivation for the Future

The CONT02 campaign is an excellent basis to study combination issues in detail. In a first step we compared the parameters resulting from single GPS and VLBI solutions. Because of the good agreement, we assumed that a combination of common parameters is unproblematic and we expected to see a stabilising effect for the solutions, especially for the combined parameters. As a matter of fact, combining the coordinates, the time series for most of the stations, both VLBI and GPS, were smoothed. If tropospheric zenith delays are combined, we recognise unfortunately a small worsening of the repeatabilities of station positions.

The combination of the EOP, which is not shown here, implies that further studies are necessary to understand the reasons for offsets between the GPS and VLBI derived parameters and to investigate the effect of local ties on the estimated EOP (see also Thaller et al. 2003). Additionally, it is planned to introduce SLR to our combination, because this technique is most capable for defining the origin of a terrestrial reference frame.

Acknowledgements. This research was supported by the program Geotechnologien of BMBF and DF, Grant 03F0336C. The publication number is: 49.

References

[1] Angermann, D., H. Drewes, M. Gerstl, R. Kelm, M. Krügel, B. Meisel: ITRF Combination - Status and recommendations for the future. submitted to IAG Proceedings, IUGG 2003 (in press)

[2] Thaller, D., R. Schmid, M. Rothacher, V. Tesmer, D. Angermann: Towards a rigorous combination of VLBI and GPS using the CONT02 campaign. submitted to IAG Proceedings, IUGG 2003 (in press)

[3] Titov O., V. Tesmer, J. Böhm: OCCAM 5.0 users guide, AUSLIG Technical Report 7, AUSLIG, Canberra, Australia 2001

[4] Hugentobler, U., S. Schaer, P. Fridez (eds.): Bernese GPS Software Version 4.2, Astronomical Institute, University of Berne, Switzerland, 2001

Markus Vennebusch: First Results of SINEX Combinations, IVS 2004 General Meeting Proceedings, p.423–426
http://ivscc.gsfc.nasa.gov/publications/gm2004/vennebusch

First Results of SINEX Combinations

Markus Vennebusch

Geodetic Institute of the University of Bonn
e-mail: vennebusch@uni-bonn.de

Abstract

Up to now combinations of VLBI sessions have been performed on the level of results, i.e. different analysis centers generate series of earth orientation parameters and compute terrestrial reference frames. These series are collected and combined by computing weighted means. This kind of combination is done routinely and the results are official IVS products. A new approach uses datum-free normal equation matrices of VLBI sessions which are provided as SINEX files. Using this kind of strategy a common reference frame is introduced. The lack of a common reference frame has been the likely reason for offsets in current EOP series. Within this paper first results of EOP combinations will be presented.

1. Purpose of SINEX Combination

A new approach of combining all the advantages of the different geodetic space techniques is the IERS Combination Pilot Project. In order to provide a unique VLBI solution to this combination project the Bonn VLBI group is developing ways to combine different solutions of VLBI sessions computed by different Analysis Centers.

2. Current Method of Combining VLBI Sessions

Combination of VLBI sessions can be performed by at least two different methods. On the one hand sessions can be combined on the level of results i.e. analysis centers create time series and send them to a combination center where the different solutions are combined by computing weighted means. On the other hand different VLBI sessions can be combined at an earlier step of analysis i.e. on the level of normal equation matrices.

Advantages of the first approach are the capability of an easy outlier detection and error estimation. This is a widely accepted and established approach which the official combined EOP time series provided by the IVS is based on. However, using this way of combination offsets of up to 300 microarcseconds for the pole coordinates and 7 microseconds for dUT1 were detected (Steinforth, personal communication). It is assumed that a possible cause of these offsets may be seen in the underlying TRFs.

3. New Approach of Combining VLBI Sessions

A new approach of combining VLBI solutions is based on the principle of addition of normal equation matrices and thus begins in an earlier step of analysis. This approach is also known as "Adjustment of groups of observations" (see Strang, Borre, 1997, Mikhail 1976) and reads as follows:

$$\sum_{i=1}^{n}(A_i'P_iA_i)\hat{x} = \sum_{i=1}^{n}A_i'P_iy_i \quad (n = \text{nr. of ACs})$$

with
- A_i Jacobian matrix of solution of the ith analysis center
- P_i matrix of weights of solution of the ith analysis center
- y_i vectors of observations of solution of the ith analysis center
- $\hat{x}$ common vector of unknowns

An advantage of this approach is that all relations/correlations between parameters are correctly considered. Since this approach can only be used when all data is based on the same apriori values a transformation of the individual normal equation matrices to common apriori values must be performed. This approach can be used to analyse the aforementioned offsets in the EOP time series. The advantages of this method are costly in a way that much more data (i.e. entire normal equation matrices, right hand sides of normal equation matrices, weighted square sum of observations, number of observations etc.) is needed and the actual process of combination is quite sophisticated.

In order to be able to perform this alternative way of combination various data of single sessions have to be provided. As an appropriate data format the IERS recommends SINEX V 2.0 (=Solution Independent Exchange format). These standardised files contain information about the type of session, about apriori values, the (decomposed) normal equation matrix and its right hand side, information about constraints and further statistical information.

So far only the CALC/SOLVE software is able to create SINEX files which contain decomposed normal matrices (see Ma, Petrov 2003).

4. Datum Free (Singular) Normal Equation Matrices

The process of combination is divided into the addition of normal equation matrices and the definition of the geodetic datum: in the first step so-called datum free or singular normal equation matrices are added. These matrices are created by estimating coordinate components of all participating stations, all earth orientation parameters and their rates as well as nutation parameters. Since datum free normal equation matrices are singular they can not be inverted and therefore no solution can be computed without defining a geodetic datum.

The geodetic datum can be defined by imposing constraints which is analogous to adding a "constraint matrix" or it can be defined by simply eliminating a specific number of unknowns.

5. Software

The new approach of SINEX combination is performed by using two different kinds of softwares. On the one hand there is an already established composition of scripts for adding normal equations, eliminating unknowns, inverting matrices and other tasks concerning the combination on the basis of normal equation matrices. This software package is called DOGS-CS (abbreviation for DGFI Orbit- und Geodätische Parameterbestimmungs-Software - Combination & Solution) which has been developed by the German Geodetic Research Institute (DGFI), Munich (see e.g. IERS Annual Report 2002).

On the other hand a second software called combine_sinex is used which consists of different FORTRAN programs and PERL scripts in order to control DOGS-CS. The module combine_sinex performs quality checks of the (singular) normal equation matrices like verification of rank deficiency and apriori values and transforms all input normal equation matrices to equal epochs.

6. Results

At present only those Analysis Centers which use CALC/SOLVE can create SINEX V 2.0 files regularly, so data from only three analysis centers (BKG, GSFC and USNO) can be used for the new combination approach. So far GSFC and BKG have already produced SINEX files of previous sessions and are creating them regularly. Several selected SINEX files from USNO were used for test purposes so that soon USNO will also create this type of files regularly.

So far combine_sinex only combines different solutions of equal sessions. As it can be seen in the left part of figure 1 a reasonable result can be obtained by fixing all coordinate components. Then differences between the estimated parameters are normally below 0.1 mas for the pole coordinates and below 2 microsec for dUT1. The standard deviation of the combined pole coordinates of single sessions is usually less than 0.1 mas and about 2.0 microsec for dUT1. These results are quite similar to the results of the routine analyses.

On the right hand side of figure 1 the impact of fixing different numbers of station coordinate components can be seen. There, only a minimum number of station components has been fixed which results in much larger standard deviations of the single solutions. In these cases the combination process obviously fails.

Both results have been obtained by transforming each solution to apriori values of the BKG solution and by transforming them to equal epochs.

7. Outlook

- For a regular combination of VLBI sessions in future a regular generation of SINEX files by all IVS Analysis Centers is required. Therefore not only the CALC/SOLVE software should be able to create SINEX files.
- General investigations of all VLBI sessions can be performed when all Analysis Centers have processed their databases again for the creation of SINEX files for all sessions since 1980.
- In order to provide a unique VLBI solution to the IERS Combination Pilot Project the combined solution has to be provided again as a SINEX file. Therefore the output of the combined solution in SINEX format has to be accomplished.
- Since this approach neglects correlations between solutions of different Analysis Centers (of essentially the same data) the standard deviations of the results might be too optimistic.

References

[1] Ma, Petrov, SINEX File Implementation in the VLBI Calc/Solve Analysis System, IERS Technical Note No. 30, 2003

[2] Mikhail, Observations and Least Squares, IEP-A Dun-Donnelley Publisher, 1976

[3] Strang, Borre, Linear Algebra, Geodesy and GPS, Wellesley-Cambridge Press, 1997

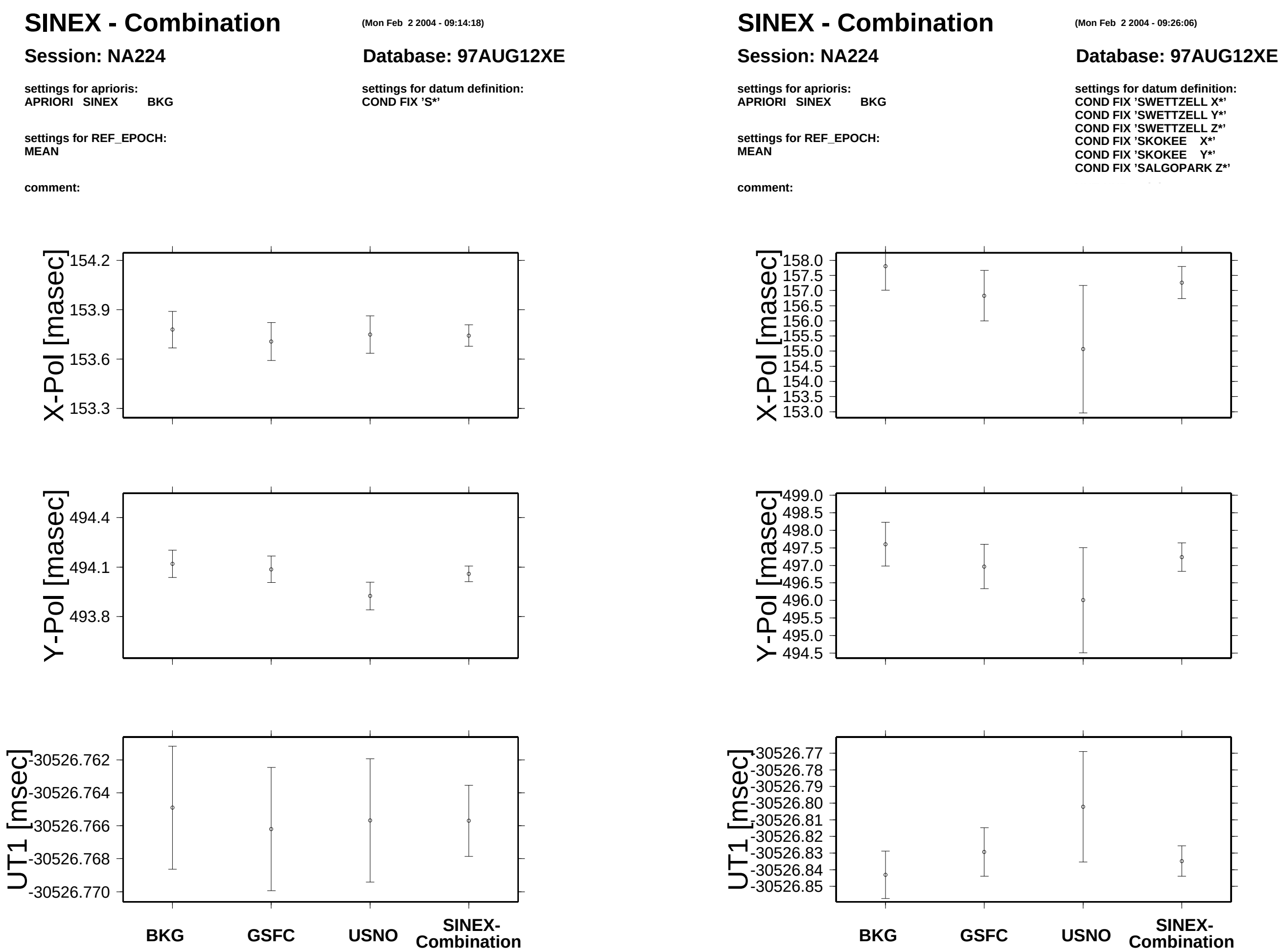

Figure 1. Example for combine_sinex results.

Mamoru Sekido et al.: Evaluation of Global Ionosphere TEC by Comparison with VLBI Data, IVS 2004 General Meeting Proceedings, p.427–436
http://ivscc.gsfc.nasa.gov/publications/gm2004/sekido2

Evaluation of Global Ionosphere TEC by Comparison with VLBI Data

Mamoru Sekido [1], *Tetsuro Kondo* [1], *Eiji Kawai* [1], *Michito Imae* [2]

[1] *Kashima Space Resaerch Center/CRL*

[2] *Applied Research and Standards Division/CRL*

Contact author: Mamoru Sekido, e-mail: `sekido@crl.go.jp`

Abstract

Global Ionosphere map (GIM) produced from world IGS network observation by the CODE was compared with dual frequency geodetic VLBI observation data for evaluation of the accuracy of GIM/CODE. Error spectrum of the GIM/CODE was estimated from the comparison statistically. The GIM/CODE seems to have error of about 3 TECU in low spatial frequency coefficient of the spherical harmonics (SH) expression. About 5 milli-TECU of precision is required to ionosphere TEC map to achieve 1 picosecond precision at observation frequency 8.3 GHz. Estimating from the error spectrum of the GIM/CODE, the GIM will need spherical harmonics up to degrees of about 100 to get such precision. Low correlation was found on TEC rate between GIM/CODE and VLBI data. It should be due to lack of high frequency components in both temporal and spatial scales in the expression of current GIM/CODE. Small (100 km) scale ionospheric disturbances traveling with speed of around 300 km/h are known. The scale of such small structure correspond to SH component in 100 degrees and it can contribute to TEC rate 1 milli-TECU/sec. Thus, 100 degrees of SH expression of ionosphere map every a few tens of minutes might be necessary for practical use of GIM for ionospheric delay and delay rate correction in VLBI observation in the same level with current dual band observations. A pilot project to make precise regional ionospheric map with dense Japanese GPS network (GEONET) is going on. It is interesting to see how accurate TEC map can be produced from dense GPS observations.

1. Introduction

Ionospheric plasma of the earth is a cause of disturbance in space measurement technique using microwave signal such as GPS, VLBI, and spacecraft navigation. Precise ionospheric map is quite useful for those radiometric space measurement systems. Global Positioning System (GPS) technology has been developed dramatically in this decade, and GPS observation sites are distributed all over the world. Now they can be a tool not only for geodesy but also for monitoring the earth environment such as the earth troposphere and ionosphere [1][2]. When a microwave travels in the ionosphere, the signal is delayed by ionospheric plasma in proportional to the total number of free electrons content (TEC) in the ray path. Then dual-frequency GPS receivers are good sensors for ionosphere monitoring [3][4][5][6]. GPS-based TEC measurement has potential to contribute microwave measurement system such as single frequency GPS receiver, VLBI astrometry, and spacecraft navigation. To make clear how much accuracy the global ionospheric map produced from GPS observations has, we compared GPS-based global ionosphere map and VLBI data. Since detailed description on the comparison is in another paper [7], we will review the main part of the comparison and introduce a pilot project to make precise regional ionosphere map over the Japanese Islands from dense GPS network (GEONET).

2. Basic Idea of GPS-Based Ionospheric TEC Evaluation

2.1. Global Ionosphere Model of the CODE

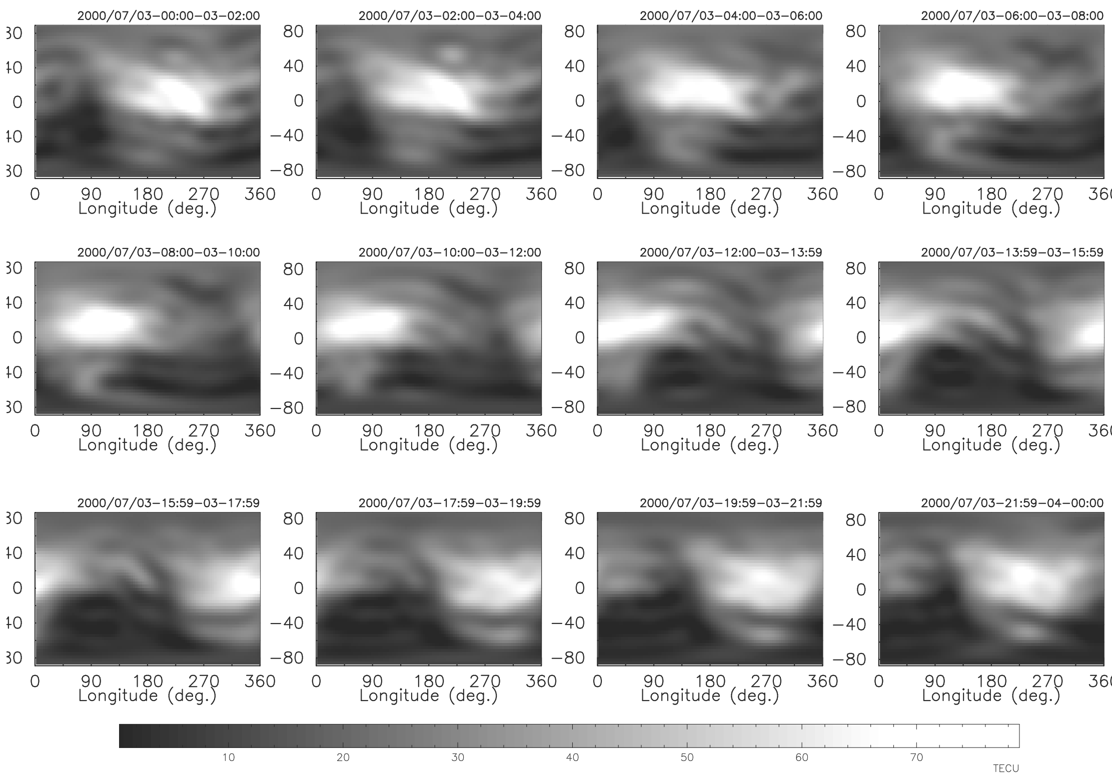

Figure 1. Global ionosphere map on 3rd of July 2000 provided by CODE.

The CODE at Bern University is one of the IGS analysis centers. This institute determines precise GPS orbit by using IGS network observation data and provides the orbit information for world wide GPS users. The CODE has been also routinely generating global ionosphere maps (GIM) on daily basis since 1 January 1996 [9][6] by using more than 130 IGS station's data. Some other IGS analysis centers are generating GIM from GPS data, although we used GIM/CODE for evaluation since it is superior to others at some points. The GIM/CODE is modeled with 256 coefficients of SH expansion up to 15 degrees and 15 orders[1]. Thirteen GIMs and their errors in 2 hour intervals (13 maps per day) are included in a GIM/CODE data. The GIM/CODE is regarded as one of the most precise TEC maps generated from GPS observations. The GIM/CODE data is provided in Bernese ION file format and IONOEX format [8], and it is available since 1995 without any interruption. Additionally, the data and related subroutines are accessible through the Internet[2] any time.

Solar-geomagnetic reference frame or Solar-geographic reference frame is used to express the GIM/CODE. Figure 1 displays an example of TEC map and its error of GIM/CODE data on 5th

[1] GIM data in 2000, which was used for this comparison, was expressed with 149 coefficients of 12 degree 8 order of SH.

[2] http://www.cx.unibe.ch/aiub/ionosphere/

Table 1. VLBI Experiments used for TEC comparison

Date	Experiment name	Station name
2000/4/7-18	6 KSP sessions	Kashima11, Koganei
2000/7/5-6	NEOS-A375	Algonquin, Fortleza, Kokee, Wettzell, Gilcreek
20007/10-11	CORE-1001	Algonquin, Gilcreek, Hartrao, Hobart, Matera, Tsukuba
2000/7/11-12	NEOS-A376	Algonquin, Fortleza, Kokee, Nyales, Wettzell,
2000/7/12-13	CORE-3001	Gilcreek, Kokee, Onsala, Westford, Wettzell
2000/7/18-19	NEOS-A377	Algonquin, Fortleza, Kokee, Wettzell, Gilcreek,
2000/7/25-26	NEOS-A378	Algonquin, Fortleza, Kokee, Nyales, Wettzell

July 2000. It is expressed in geographical coordinates, hence it is seen that the TEC structure is meandering along geomagnetic equator.

2.2. Comparison of VLBI-Based TEC and GIM

The GPS technique can measure the TEC along the ray path from GPS satellite to an observation station, whereas VLBI measure the difference of TEC in the ray path to the radio source between two stations. Then TEC measured by VLBI and that by GPS were compared with the following procedures. (i) The coordinates of ionospheric point, which is the intersection between ionospheric layer and line of sight from VLBI station to the observed radio source at VLBI observation epoch, is calculated. Then vertical TEC value at that location is computed from GIM/CODE maps. (ii) Slant TEC is computed from the vertical TEC by taking into account a ionosphere mapping function, then difference of the slant TECs between two stations is taken as $VTEC_{\rm y} \cdot Fm(El_{\rm y}) - VTEC_{\rm x} \cdot Fm(El_{\rm x})$, where $VTEC_{\rm i}$ is ionospheric TEC in zenith direction. GIM/CODE has been using isotropic spherical single layer mapping function as

$$Fm(El) = \frac{1}{\cos\{\sin^{-1}[\frac{R}{R+H}\cos(El)]\}}, \tag{1}$$

where R is earth radius, and ionosphere height from earth surface is assumed to be constant H=450 km. (iv) Finally the derived GPS-based TEC is compared with VLBI-based TEC.

Precision of VLBI-based TEC measurement is simply determined by group delay measurement precision and its error is evaluated by signal to noise ratio (SNR). By supposing that error of VLBI-based TEC measurements is known, then error of GPS-based TEC map can be evaluated statistically. Even the comparison of TEC map with VLBI data is relative difference of slant TEC at two points of earth ionosphere, that has sensitivity to vertical absolute TEC through mapping function. Thus as far as the error of the TEC map follows appropriate mapping function, the error in slant TEC can be projected upon the vertical absolute TEC value. This is basic idea of evaluating TEC map accuracy by comparison with VLBI data.

Each quantities for comparison from GPS and VLBI are modeled as follows:

$$\mathrm{d}TEC_{\rm GIM} = (VTEC_{\rm y} + \epsilon_{\rm GIM,y}) \cdot Fm(El_{\rm y}) - (VTEC_{\rm x} + \epsilon_{\rm GIM,x}) \cdot Fm(El_{\rm x}) \tag{2}$$

$$\mathrm{d}TEC_{\rm VLBI} = STEC_{\rm y} - STEC_{\rm x} + \epsilon_{\rm VLBI}, \tag{3}$$

and supposing $< \epsilon^2_{\rm VLBI} >$ is known from VLBI data, $\epsilon_{\rm GIM}$ is evaluated statistically.

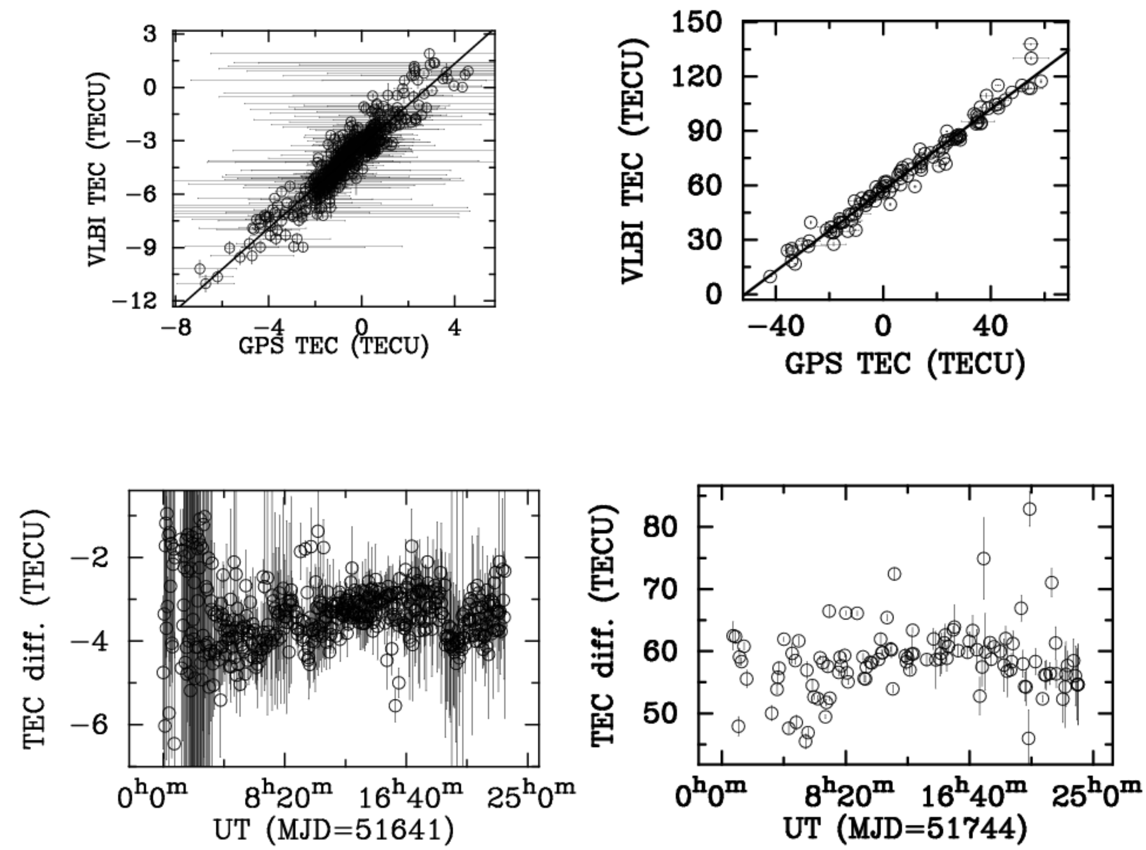

Figure 2. Correlation (upper panels) and difference (lower panels) between GIM/CODE and VLBI data. (Left): Kashima-Koganei (109km) baseline on 7 April 2000. The correlation coefficient, proportional coefficient, and offset were respectively 0.93, 1.01, and -3.4 TECU. Root-mean-square (RMS) difference was 0.77 TECU. (Right): Algonquin-Wettzell (6000km) baseline on 18 June 2000. The correlation coefficient, proportional coefficient, and offset were respectively 0.99, 1.13, and 57.6 TECU. The RMS of the difference was 5.4 TECU. The offsets comes from S/X VLBI receiver offset (see section 5).

3. Comparison of TEC

3.1. Statistical Comparison between VLBI and GPS-Based TEC Map

Six KSP (Kashima11-Koganei) VLBI experiments (2683 scans) and six intercontinental VLBI experiments (total 6855 scans of 37 baselines) are used for the comparison (Table 1). Correlation and difference between VLBI-based TEC and that computed from GIM/CODE are plotted in Figure 2 as an example.

To evaluate GIM error correctly we need to remove the factor of mapping funtion and to survey the characteristic of baseline dependency. For this purpose, we divided the whole data set into several subsets by elevation angles and baseline lengthes. Then mean square of TEC differene between VLBI and GIM are computed for each subset. Mathematical expression of this procedure might be derived from equation (2), (3) as follows (see appendix A of [7]):

$$< \Delta TEC^2 > \cong \sigma^2_{\rm GIM} < Fm^2(El_{\rm x}) + Fm^2(El_{\rm y}) > + \sigma^2_{\rm VLBI}, \tag{4}$$

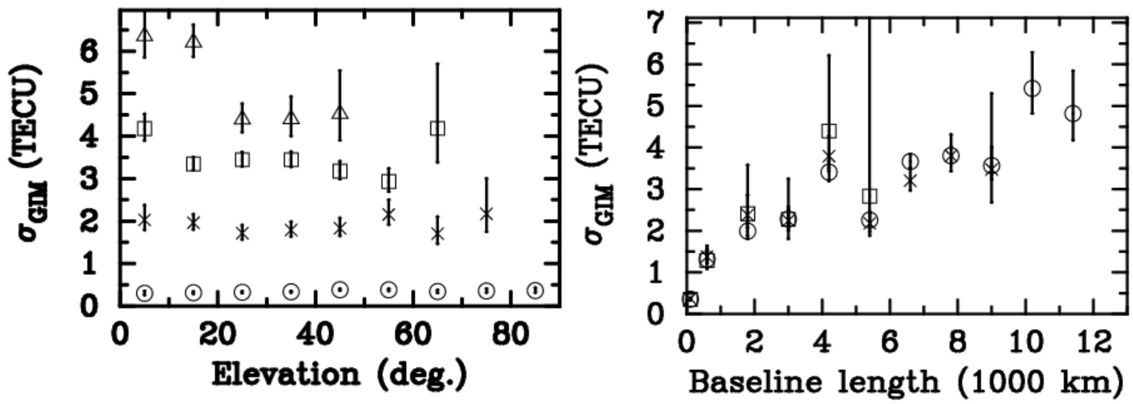

Figure 3. Estimated GIM/CODE TEC error is plotted with respect to elevation angle (left panel). TEC difference (GPS - VLBI) data set was divided into data subset by 10 degree intervals of lower elevation angle of the VLBI station pair. The data subsets were again divided into 4 groups by the baseline length, ◯: 0 – 500 km (KSP), ×: 500 – 4000 km, open box: 400 – 8000 km, and △: longer than 8000 km. The GIM/CODE error was computed by using equation (5). Estimated GIM/CODE errors are plotted with respect to baseline length in right panel. The data was divided into subsets by 1200 km interval of baseline length except for the KSP data (109 km). Elevation cut-off test was also performed at elevation limit 20 (◯), 40 (×), and 60 (open box) degrees. The error bars in the plots indicate 95% confidence interval.

where $\Delta TEC = \mathrm{d}TEC_{\mathrm{GIM}} - \mathrm{d}TEC_{\mathrm{VLBI}}$. Since σ^2_{VLBI} is supposed to be known, error of GIM is evaluated by

$$\sigma_{\mathrm{GIM}} = \sqrt{\frac{< (\Delta TEC)^2 > - < \sigma^2_{\mathrm{VLBI}} >}{< Fm^2(El_x) + Fm^2(El_y) >}}. \tag{5}$$

for each data subset and plotted in Figure 3. The flat elevation dependency of the left panel indicates the mapping function and the statistical treatment are appropriate. The baseline dependency is plotted with data sets of elevation cutoff test (20, 40, and 60 degrees). Since plots of elevation cutoff test almost coincide regardless different elevation cutoff angles, it indicates that factor of mapping function is appropriately calibrated and GIM error is projected to vertical one correctly. Interpreting the baseline dependency of σ^2_{GIM} as structure function of GIM error $R(l) =< (er(x) - er(x+l))^2 >$, power spectrum of GIM error can be computed from it. Figure 4 (left) shows the σ_{GIM} dependency on geocentric angle. Since structure function is monotonically increasing function, two sorts of lines are drawn as test models of the structure function. Autocorrelation function of GIM error computed from the test models are superimposed in right lower corner of the figure. Two error spectrum models of GIM, which is estimated from the structure function, are displayed in the right panel. Mean-square of SH coefficients and errors of each coefficient attached with the GIM/CODE data are also plotted in the same figure. Two conclusions on precision of GIM/CODE are inferred from this figure. The GIM/CODE seems to have error around 3 TECU in lower spectrum of SH expression. Ionospheric delay of 1 picosecond corresponds to 0.05 TECU at radio frequency 8.3 GHz. Therefore to use GIM/CODE for ionospheric delay correction in the same precision with current geodetic VLBI, about one hundred of order of SH expansion will be necessary.

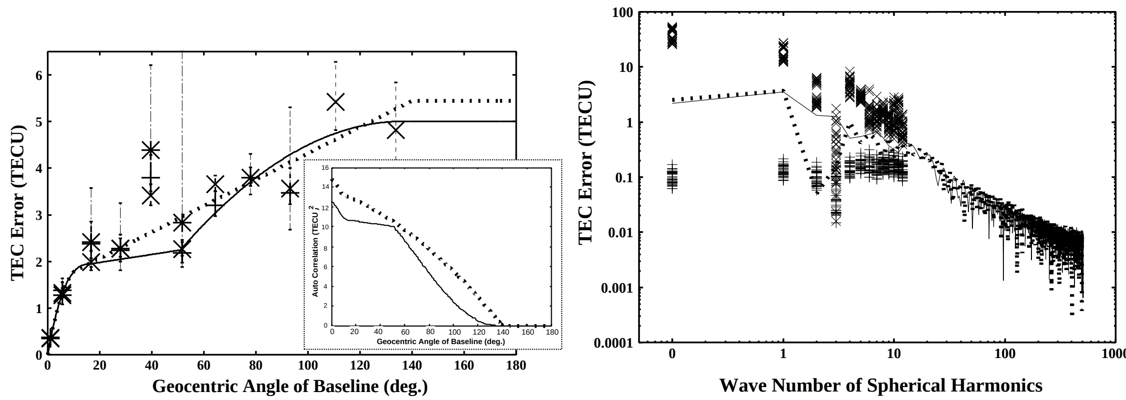

Figure 4. (Left):Square-root of structure function of TEC error. Three kinds of marks correspond to data of elevation cut-off test (20, 40, and 60 degrees). Solid and broken lines are two kinds of models of structure function composed of three truncated functions. Small screen at right corner shows auto-correlation functions derived from two models of structure functions. (Right):TEC error spectrum of GIM/CODE model. Solid line and broken line correspond to the structure function models in left panel. Mark "×" indicates root-sum-square of SH components of GIM/CODE. and "+" indicates root-sum-square of errors attached with GIM/CODE data. Larger index between degree and order of SH index set was used as wave number and the root-sum-square was taken for the same wave number. Horizontal coordinate 0 is indicated at coordinate of 0.1 to express DC component of the error spectrum.

4. Comparison of TEC Rate

TEC rates between VLBI measurements and counterpart computed from GIM/CODE data also were compared. VLBI-based TEC rate consists of the temporal variation of TEC and spatial change of the line of sight due to tracking of radio source. We computed TECs in line of sight to radio source at desired epoch and at other 4 epochs with 10 minute intervals before and after the desired epoch. Then TEC rate was derived by numerical derivation by using the 5 points of TEC data.

The TEC rates comparison was performed from short baseline (KSP) to intercontinental baseline (IVS data listed in Table 1). Unfortunately correlation between VLBI-based TEC rate and TEC rate computed from GIM/CODE was almost close to zero for short (109 km) baselines. Some correlation around 0.6 – 0.8 were found on longer baselines, although it was far from the accuracy for phase delay rate correction. Figure 5 shows an example of TEC rate comparison result of Algonquin - Wettzell baseline on 18th July 2000. RMS difference of TEC rate between the GIM/CODE and VLBI is several milli-TECU per second, which is one order larger than the accuracy of TEC rate needed for delay rate correction in VLBI observation at radio frequency 8.3 GHz. The reason for the poor coincidence of TEC rate is understood by following two reasons. (i) The GIM/CODE data has time resolution of 2 hours. Thus shorter time scale TEC variation is not included in the data. (ii) The GIM/CODE data compared here are expressed with up to 12 degrees 8 orders of SH components. Then ionospheric TEC structure smaller than a minimum spatial scale (2500 km x 1700 km) is not contained in the data. The lack of higher frequency component in both time and spatial domain in GIM/CODE will be the main cause of low precision of TEC rate derived from GIM/CODE.

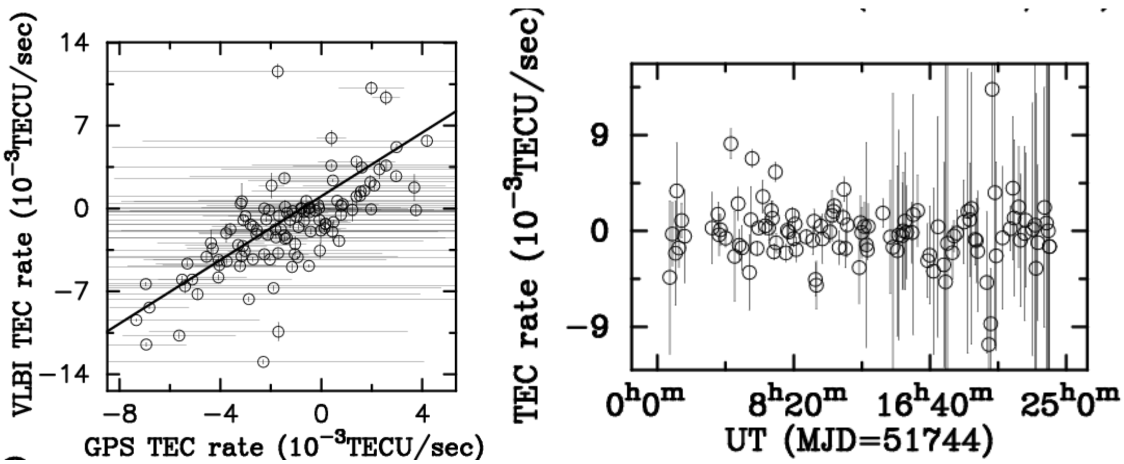

Figure 5. Comparison of TEC rate between GIM/CODE and VLBI data on 18 July 2000 on Algonquin - Wettzell baseline. The TEC rate of GIM/CODE were computed by numerical derivation. Left panel shows scatter plot of TEC rate measured by VLBI and counterpart computed from GIM/CODE. Right panel is residual plot of the TEC rate difference between GIM/CODE model and VLBI data. Correlation was 0.7 and the RMS residual was 2.9×10^{-3}.

5. S/X VLBI Receiver Offset

From comparison between GPS-based TEC measurements and VLBI data, difference of signal transmission delay between X-band and S-band of VLBI receiver system is derived as a by-product. Since most of the offsets (difference of 0 point between VLBI and GPS in Figure 2) derived from these comparisons were almost constants for each baseline regardless of difference of experiments, it is sure that these offsets originate from each VLBI station. This S/X VLBI receiver offset does not come only from hardware but also it can be introduced by manual operation of phase calibration (PCAL) data. Actually, the offsets on Kokee station related baselines in CORE-3001 were inconsistent with ones of other experiments. It is known that manual pcal phase was used for Kokee station, and that operation of PCAL data on Kokee related baseline might cause the shift of the offset in CORE-3001 experiment. Table 2 shows the S/X VLBI receiver offset at each station computed by least square method under the constraint that total sum of the offset equals to zero. The constraint was used because we have no a priori knowledge of absolute value of the offset at any station. Then relative values in the table have meaning but the absolute values may not.

This (hardware) delay offset between S and X band VLBI receivers has not been made aware in normal geodetic VLBI observation, because it is normally absorbed in station clock offset in the analysis. These have already been pointed out by T. Herring [10]. But these offsets were not actually measured due to lack of independent measurements of ionospheric TEC to distinguish the VLBI receiver offsets from the ionospheric dispersive delay. Attention may have to be paid to these offsets when precise calibration of station delay is needed such as VLBI experiment for precise time transfer or VLBI observation with phase delay.

Station	offset (n sec)	Error (n sec)
Algonquin	-0.43	0.4
Fortleza	-5.3	0.4
Gilcreek	0.13	0.4
Hobart	1.2	0.6
Hartrao	-16.5	0.6
Kokee	-18.4	0.4
Wettzell	13.6	0.4
Westford	0.5	1
Tsukuba	5.6	0.6
Nyales	-0.4	0.6
Onsala	14.4	0.8
Matera	5.5	0.5

Table 2. VLBI receiver offset derived from comparison between VLBI-based TEC and GPS-based TEC. Each station's offsets were derived with assuming that sum of all stations offsets equals to 0. Error is formal error of least square solution. To make reduced-χ^2 equal to unity, square of extra 1.2 nanoseconds of error was added to square of each error.

6. Small Scale Structure of Ionosphere

Geographical Survey Institute (GSI) of Japan is operating about 1000 GPS receivers placed on the Japanese Islands. That system is named GEONET [11], since it is thought to be not only a sensor for crustal deformation but also a sensor for earth environment including atmosphere and ionosphere. Saito et al. [12] demonstrated the presence of small scale traveling ionosphere turbulence (TID), which has 100 km scale with about 1 TECU amplitude (Figure 6). One hundred km scale on the earth surface correspond to SH component at 100 degrees, and it corresponds to the conclusion derived from comparison with VLBI data in Section 3.1. The traveling speed of the TID is around 300 km/hour, thus TID with 1 TECU of amplitude can cause 1 milli-TECU/sec, which is in the same order with the residual of TEC rate comparison (Figure 5) in Section 4. Thus this sort of TID needs to be included in ionosphere TEC map model from both delay and delay rate viewpoints. Ping et al. [13] has made a regional ionosphere map (RIM) expressed by 60 degrees and orders of SH expansion every 10 minutes interval from joint use of GEONET data and GIM/CODE. Currently we are collaborating for accuracy evaluation of the RIM.

7. Conclusions

Accuracy of GIM/CODE was evaluated by comparison with VLBI data on various baselines. Error spectrum of the GIM/CODE was derived from the statistical comparison. The GIM/CODE seems to have about 3 TECU of error at low degree of SH components. To apply ionospheric delay correction to VLBI data (X-band) with the GIM/CODE at accuracy of 1 picosecond, accuracy of 50 milli-TECU is necessary. Estimating from the obtained error spectrum of GIM/CODE, about 100 degree of SH expansion will be necessary to achieve that accuracy. TEC rate was compared with VLBI data, too. However, the difference was one order larger than required accuracy. The poor coincidence should be caused from lack of high frequency components in the data in both temporal and spatial scale.

Presence of small (100 km) scale ionospheric disturbances with 1 TECU magnitude are known and they travel about 300 km per hour. This order of spatial scale also corresponds to SH component at about 100 degrees. This sort of TID needs to be included in ionospheric TEC model for practical use in VLBI ionospheric delay and delay rate correction. Ping et al. [13] has made high

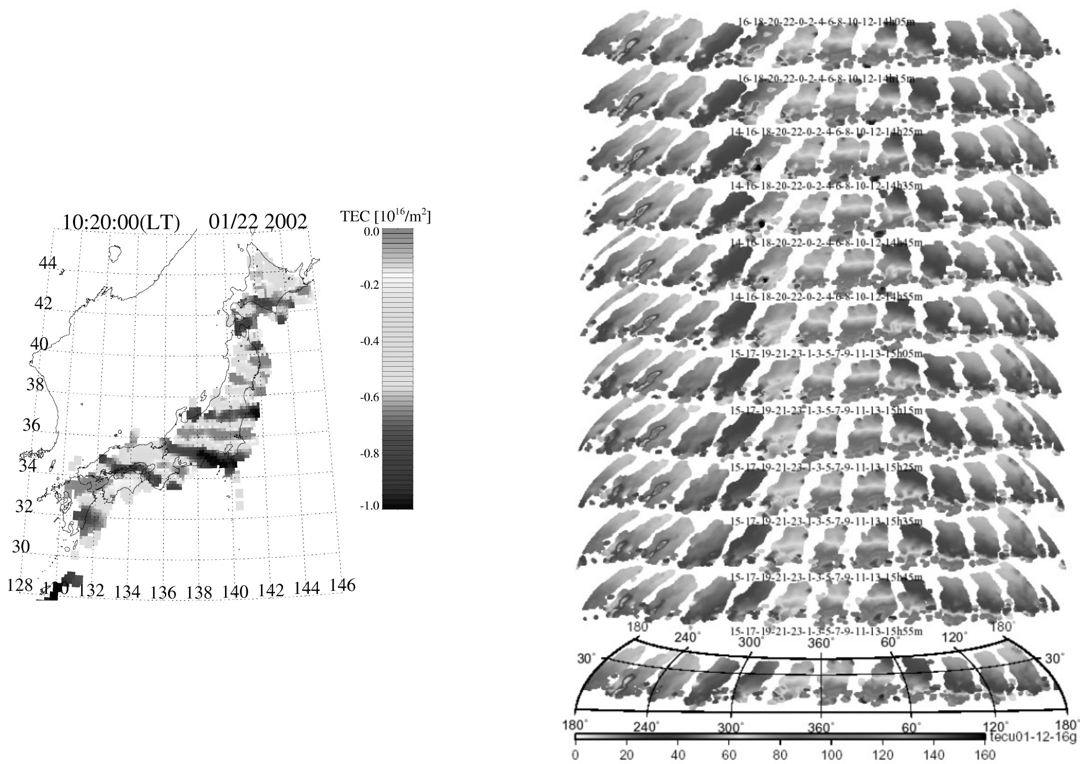

Figure 6. Traveling ionospheric disturbance (TID) detected with GEONET by Saito et al.[12] (left) and Regional Ionosphere map (RIM) made from joint use of GIM/CODE and GEONET data by Ping et al.[13](right). The RIM is expressed by 60 degree of SH expansion at every 10 minutes interval.

resolution regional ionospheric model over the Japanese Islands from joint use of GEONET data and GIM/CODE. The RIM is expressed with SH expansion of 60 degrees and orders, and its time interval is 10 minutes. Evaluation and improvement of the RIM by comparison with VLBI and with satellite data (Topex/Poseidon) is going on. This project is interesting to see how accurate an ionospheric map can be derived from dense GPS network.

As a by-product of the comparison between VLBI and GPS-based GIM, S/X VLBI receiver biases are detected. This bias was pointed out by T. Herring [10], however it was not obvious because it is easily absorbed in clock parameters in VLBI analysis.

This comparison was made with data in 2000, when the GIM/CODE was expressed with 12 degrees and 8 order of SH expansion. Now the model of GIM/CODE is updated to 15 degrees and 15 order of SH expansion. Thus the precision of the map might be somewhat improved than these results, although basic sense of the conclusion in this paper may not be changed.

Acknowledgments Authors thanks Stefan Schaer at Bern University for providing GIM data and related subroutines. This research has made use of international geodetic VLBI data provided by the International VLBI Service for Geodesy and Astrometry.

References

[1] Beutler, G., EXECUTIVE SUMMARY, *IGS Analysis Center Workshop,* 9-18,1998.

[2] Feltens J., and S. Schaer, IGS PRODUCTS FOR THE IONOSPHERE, *IGS Analysis Center Workshop*, 225-232,1998.

[3] Lanyi G. E., and T. Roth, A comparison of mapped and measured total ionospheric electron content using global positioning system and beacon satellite observations, *Radio Sci., 23,* 483-492. 1988.

[4] Wilson B. D., J. A. Mannucci, and D. C. Edwards, Subdaily northern hemisphere ionospheric maps using an extensive network of GPS receivers, *Radio Sci., 30,* 639-648, 1995.

[5] Ho C. M., Wilson B. D., J. A. Mannucci, J. U. Lindqwister, N. D. Yuan, A comparative study of ionospheric total electron content measurements using global ionospheric map of GPS, TOPEX radar, and the Bent model, *Radio Sci., 32,* 1499-1512, 1997.

[6] Schaer S., Mapping and Predicting the Earth's Ionosphere Using the Global Positioning System, *Ph.D. thesis at Bern University,* 1999.

[7] Sekido M., T. Kondo, E. Kawai, & M. Imae, Evaluation of GPS-based ionospheric TEC map by comparing with VLBI data, *Radio Science, 38*, 1069-1090, 2003.

[8] Schaer S., W. Gurtner, and J. Feltens, IONEX: The ionosphere Map EXchange Format Version 1, *Proc. of IGS Analysis Center Workshop, ESA/ESOC Darmstadt in Germany, February 9-11 1998,* 233-247, 1998.

[9] Schaer S., G. Beutler, and M. Rothacher, MAPPING AND PREDICTING THE IONOSPHERE, *Proc. IGS Analysis Center Workshop 1998, ESA/ESOC Darmstadt in Germany, February 9-11 1998,* 307-318, 1998.

[10] Herring T. A., The precision and accuracy of intercontinental distance determinations using radio interferometry, *Ph.D. thesis at the Massachusetts Institute of Technology*, section 4.1.1, 1983.

[11] Miyazaki S., T. Saito, M. Sasaki, Y. Hatanaka, and Y. Iimura, Expansion of GSI's Nationwide GPS Array, *Bull. Geogr. Surv. Inst., 43.* 23-34, 1997.

[12] Saito A., S. Fukao, and S. Miyazaki, High resolution mapping of TEC perturbations with the GSI GPS network over Japan, *Geophys. Res. Lett., 25,* 3079-3082, 1998.

[13] Ping J., Y. Kono, K. Matsumoto, Y. Otsuka, A. Saito, C. Shum, K. Heki, and N. Kawano, *Earth Planets Space, 54*, e13-e16, 2002.

Thomas Hobiger et al.: How VLBI Contributes to Ionospheric Research, IVS 2004 General Meeting Proceedings, p.437–441
http://ivscc.gsfc.nasa.gov/publications/gm2004/hobiger3

How VLBI Contributes to Ionospheric Research

Thomas Hobiger, Harald Schuh

Institute of Geodesy and Geophysics, University of Technology, Vienna

Contact author: Thomas Hobiger, e-mail: thobiger@mars.hg.tuwien.ac.at

Abstract

Geodetic VLBI observations are carried out at two distinct frequencies in order to determine ionospheric delay corrections. Each ionospheric delay corresponds to the total electron content (TEC) along the ray path through the ionosphere. Because VLBI is a differential technique the observed ionospheric delays represent the differences of the behaviour of the propagation media above each two stations. Additionally, there is a constant instrumental delay offset per baseline that contributes to the observed ionospheric delay. This instrumental offset is independent of azimuth and elevation in which the antennas point which allows us to separate it from the variable ionospheric parameters for each station which can be represented by different functional approaches. If horizontal gradients in the ionosphere above the stations are neglected we are able to separate the instrumental offsets from the ionospheric parameters by a least-squares fit. A weakness of this approach is the assumption that the TEC values are assigned to the station coordinates but not to the geographical coordinates of the intersection point of the ray path and the infinitely thin ionospheric layer. Nevertheless, the results agree well with results of other techniques like GPS on short and long time scales.

1. Estimation of Ionospheric Parameters

Each dual-frequency VLBI observation provides the baseline dependent ionospheric delay ($\tau_{measured}$) in the form of equation (1).

$$\tau_{measured}(t) = \tau_{ion,1}(t) - \tau_{ion,2}(t) + \tau_{offset,1} - \tau_{offset,2} \tag{1}$$

The ionospheric delay at X-band measured at station i can be described by equation (2) with an appropriate mapping function $M_f(\varepsilon_i)$ depending on the elevation angle ε_i (e.g., Schaer, 1999, [1], Hobiger and Schuh, 2004, [2]).

$$\tau_{ion,i}(t) = \frac{1.34 \cdot 10^{-7}}{f_x^2} \cdot M_f(\varepsilon_i) \cdot VTEC_i(t) \tag{2}$$

If the Vertical Total Electron Content (VTEC) above a single station shall be estimated the problem occurs that each measurement contains 4 unknowns. Thus, some assumptions and simplifactions have to be made and an estimation method has to be used that takes the physical behaviour of the ionosphere into account (TEC values cannot be negative).

1. As indicated in equation (1), instrumental offsets caused by the receiving system (e.g., Ray, 1991, [3]) are supposed to be constant within a 24h VLBI session. In GPS there is a similar problem called differential code biases, DCBs [1], when solving for absolute ionospheric parameters. In VLBI the same assumption as in GPS is applied by postulating that the sum of all station-dependent offsets equals to zero.

$$\sum_{i=1}^{N_{stat}} \tau_{offset,i} = 0 \tag{3}$$

2. However, measurements are made at different elevation angles and azimuths and the observed VTEC value has to be assigned to the intersection point of the ray path with the ionospheric shell which is not vertically located above the station. By negelecting horizontal gradients within an area around each station it can be concluded that the values at the intersection points correspond to the values in zenith direction above the antenna.

3. Under the previous assumption the VTEC values for each station can be modeled by means of least-squares. Different elevation angles for each station will enable the separation of the station-dependent parameters.

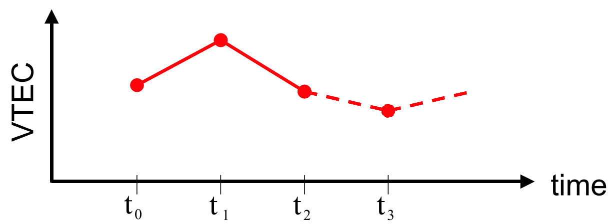

Figure 1. Piece-wise linear function as a representation of vertical total electron content.

4. The ionospheric parameters are modeled in the form of piece-wise linear functions (figure 1, equation 4) with only positive VTEC values allowed (solution within positive half-space).

$$VTEC_{PLF}(t) = offset + rate_1(t_1 - t_0) + rate_2(t_2 - t_1) + \ldots + rate_n(t_n - t) \tag{4}$$

$$\begin{array}{lcl} (offset_0 + \Delta offset) & \geq & 0 \\ (offset_0 + \Delta offset) + (rate_{1,0} + \Delta rate_1)(t_1 - t_0) & \geq & 0 \\ (offset_0 + \Delta offset) + (rate_{1,0} + \Delta rate_1)(t_1 - t_0) + (rate_{2,0} + \Delta rate_2)(t_2 - t_1) & \geq & 0 \\ \vdots & \vdots & \vdots \end{array} \tag{5}$$

Applying the non-negative constraint to all points at the interval boundaries yields equation (5). Parameters indicated with $_0$ stand for the initial guess and a Δ symbolizes the improvement from any adjustment process. If all conditions are summed up using matrix notation equation 6 is obtained.

$$\underbrace{\begin{pmatrix} 1 & 0 & 0 & 0 & \cdots \\ 1 & t_1 - t_0 & 0 & 0 & \cdots \\ 1 & t_1 - t_0 & t_2 - t_1 & 0 & \cdots \\ \vdots & \vdots & \vdots & \vdots & \ddots \end{pmatrix}}_{\mathbf{B}} \mathbf{X_0} + \underbrace{\begin{pmatrix} 1 & 0 & 0 & 0 & \cdots \\ 1 & t_1 - t_0 & 0 & 0 & \cdots \\ 1 & t_1 - t_0 & t_2 - t_1 & 0 & \cdots \\ \vdots & \vdots & \vdots & \vdots & \ddots \end{pmatrix}}_{\mathbf{B}} \mathbf{\Delta X} \geq 0 \tag{6}$$

Re-aranging equation (6) yields

$$\mathbf{B} \cdot \mathbf{\Delta X} \geq -\mathbf{B} \cdot \mathbf{X_0} \quad \Rightarrow \quad \mathbf{B} \cdot \mathbf{\Delta X} \geq \mathbf{C} \tag{7}$$

Incorporation of equation (7) into the adjustment process (least-squares method, Gauss-Markov model) leads to

$$\begin{array}{ccc} \mathbf{\Delta X} = \left(\mathbf{A^T W A}\right)^{-1} \mathbf{A^T W \Delta Y} & & \mathbf{B} \cdot \mathbf{\Delta X} \geq \mathbf{C} \\ \downarrow & & \downarrow \\ \rightarrow & \text{“}reflective\ Newton\ method\text{”} & \leftarrow \end{array} \qquad (8)$$

As pointed out by equation (8) the usage of a reflective Newton method allows us to combine the classical least-squares approach with non-negative conditions.

5. Normally piece-wise linear functions are modelled with constant interval lengths (figure 2). For periods with no data additional constraints are needed to stabilize the solution. To

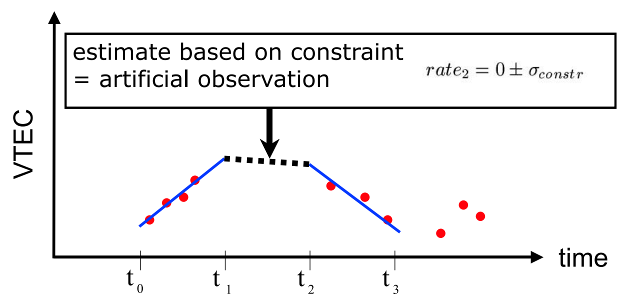

Figure 2. Piece-wise linear function - constant interval lengths.

avoid the introduction of constraints an adaptive piece-wise linear function was devoloped that shifts the interval boundaries that every interval contains the same (given) number of observations (figure 3).

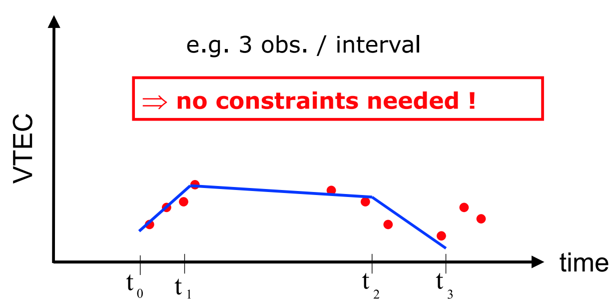

Figure 3. Piece-wise linear function - adaptive interval lengths with 3 observations per interval.

2. Results

2.1. VTEC on Short Time Scales

Results on daily or weekly time scales can be found in this volume (Hobiger and Schuh, 2004, [2] or Hobiger et al., 2004, [4]).

2.2. VTEC on Long Time Scales

A two year period of NEOS-A sessions covering the years 2000 and 2001 was used to demonstrate the capability of VLBI to monitor long-term trends or signals in the ionosphere. As an example for station Fortaleza, Brazil, VTEC values were determined for sunrise (local time 6 am), noon (local time 12 am) and sunset (local time 6 pm) for each session during the relevant period. The results are shown in figure 4 (red, thick line - VLBI; blue, thin dashed line - CODE/GPS, [5]). The agreement between both techniques is very high and especially local noon values differ very little. As for many VLBI stations almost two complete solar cyles ($\sim$ 22 years) are covered by dual-frequency observations it will be possible to provide input for long-term ionospheric studies.

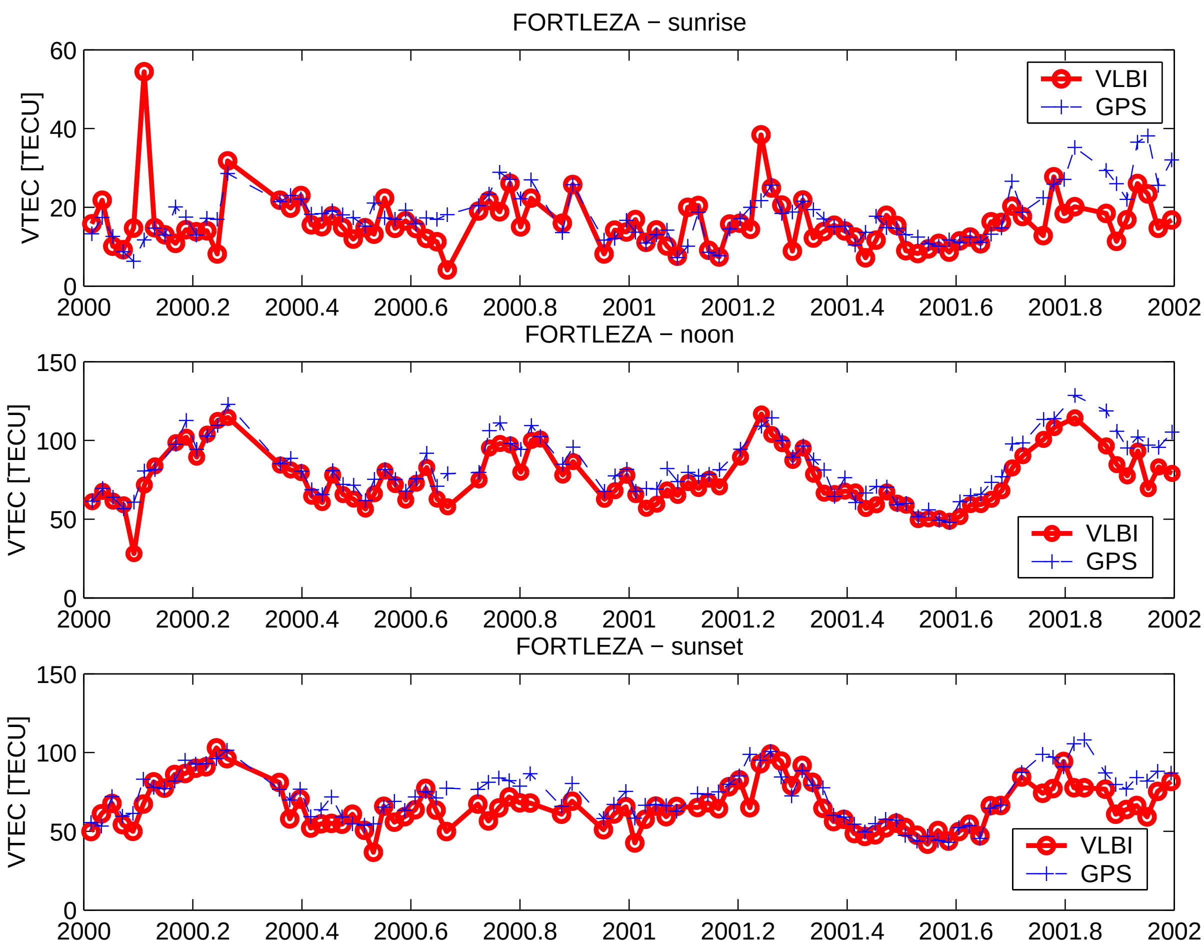

Figure 4. VTEC for station Fortaleza, NEOS-A sessions of the years 2000 and 2001, results from VLBI (red, thick line) and GPS (blue, thin dashed line) for sunrise, noon, sunset.

3. Conclusions and Outlook

VLBI is able to provide absolute ionospheric parameters above globally distributed stations. Our first results agree well with values derived by GPS and it is possible to study the behaviour of the ionosphere on long- and short-term time scales. Therefore, VLBI can be used as a source for global ionospheric models.

4. Acknowledgements

Research project P16136-N06 “Investigation of the ionosphere by geodetic VLBI” is funded by the Austrian Science Fund (FWF).

References

[1] Schaer, S., Mapping and Predicting the Earths Ionosphere Using the Global Positioning System, Inaugural Dissertation der Philosophisch-naturwissenschaftlichen Fakultaet der Universitaet Bern, Bern, 1999

[2] Hobiger, T., H. Schuh, Modeling Vertical Total Electron Content from VLBI Observations, this volume, 2004

[3] Ray, J.R, B.E. Corey, Current Precision of VLBI Multi-Band Delay Observables, Proceedings AGU Chapman Conference on Geodetic VLBI: Monitoring Global Change, Washington D.C., 22-26 April, 1991

[4] Hobiger, T., S. Todorova, H. Schuh, Ionospheric Parameters Obtained by Different Space Geodetic Techniques During CONT02, this volume, 2004

[5] `http://igscb.jpl.nasa.gov/components/dcnav/cddis_products_ionex.html`

Thomas Hobiger et al.: Ionospheric Parameters Obtained by Different Space Geodetic Techniques during CONT02, IVS 2004 General Meeting Proceedings, p.442–446
http://ivscc.gsfc.nasa.gov/publications/gm2004/hobiger1

Ionospheric Parameters Obtained by Different Space Geodetic Techniques during CONT02

Thomas Hobiger, Sonya Todorova, Harald Schuh

Institute of Geodesy and Geophysics, University of Technology, Vienna
Contact author: Thomas Hobiger, e-mail: thobiger@mars.hg.tuwien.ac.at

Abstract

The goal of the CONT02 campaign in October 2002 was the acquisition of the best possible VLBI data to demonstrate the high accuracy of which VLBI is capable. The campaign provides the chance to study the ionosphere continously over a period of more than two weeks by means of VLBI. Vertical total electron content (VTEC) values above the contributing stations were determined. By comparison with results from other techniques, like GPS or satellite altimetry, systematic differences could be detected of which the reasons are still unclear. Anyway, the histograms of the differences show that generally the agreement is very good between the parameters derived by VLBI and the results from other space geodetic techniques. This is also confirmed by Fourier and wavelet analyses which reveal variations with the same periods (diurnal, semi-diurnal and quarter-diurnal) in GPS and VLBI time series.

1. Techniques Used

- VLBI: For the computation of the ionospheric parameters (vertical total electron content - VTEC) the whole 15 days of observations were analyzed. Three continuous days of observations were taken to estimate robust values for the central day. For the first and last day of the data set, i.e. Oct. 16th 2002 and Oct. 30th 2002, two consecutive days were used, only. The vertical total electron content above each station was modeled with a modified piece-wise linear function (PLF) approach [1]. Instead of the classical PLF with constant interval length adaptive interval lengths were chosen. Implementation was done by a reflective Newton method to avoid negative values which are impossible due to the physical nature of wave propagation.
- GPS: Global ionospheric maps provided by the Center for Orbit Determination in Europe (CODE), an analysis center within the International GPS Service (IGS) [2], were used to interpolate VTEC values for the contributing CONT02 stations. The data are given in gridded form and represent the ionosphere as an infinite thin layer at a height of 450 km. As an official IGS ionosphere product is not available for the period covered by CONT02, the CODE solution was chosen, which turned out to be one of the best VTEC estimations within the IGS.
- TOPEX/Poseidon: Data was kindly provided by ADS Central, GeoForschungsZentrum Potsdam (GFZ) [3]. We used only data within $\pm$ 5 degrees in latitude and longitude of Kokee Park on Hawaii, which is the only station that is completely surrounded by the sea. The sub-satellite tracks for all observations during CONT02 are plotted in figure 1.

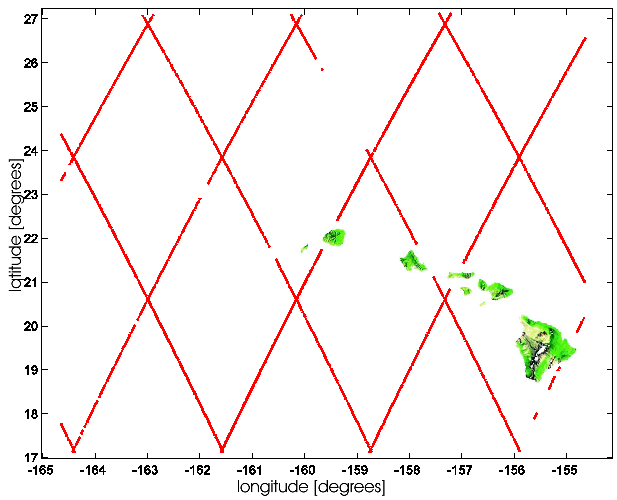

Figure 1. TOPEX/Poseidon footprints during CONT02.

2. Results

In figures 2 and 3 the VLBI solutions (blue-solid line) for station Hartebeesthoek and Westford are plotted together with the corresponding GPS results (red-dashed line).

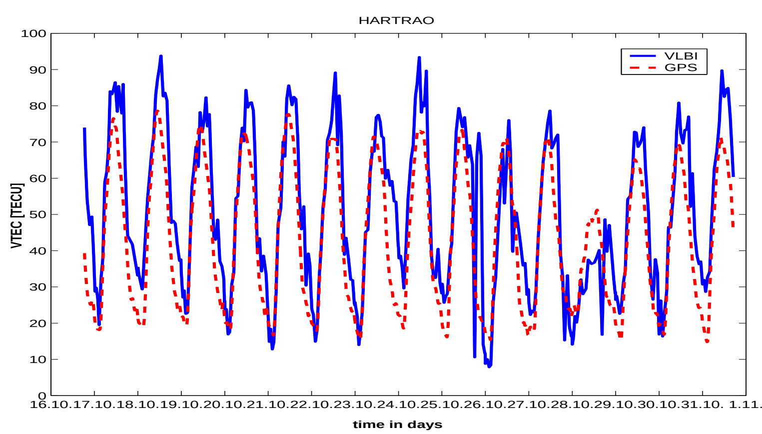

Figure 2. VTEC values for station HARTRAO derived by VLBI (solid line) and GPS (dashed line).

Histograms of the differences for both stations are given in figure 4. The standard deviation between both techniques is about 10 TEC units (TECU), what is quite satisfying. On the other hand, an outlier in the VLBI solution at station Westford at the end of Oct. 25th, 2002 can be detected clearly. Such an effect may be due to the method applied that forces the solution to be strictly positive. The left plot of figure 5 summarizes the results from all eight contributing stations. The values derived by GPS are plotted against the corresponding values from VLBI. The correlation is high (~ 0.87) and a systematic offset (VLBI minus GPS) of about -3 TECU can be detected. The differences, which are plotted in a histogram (centre, figure 5) are not normally

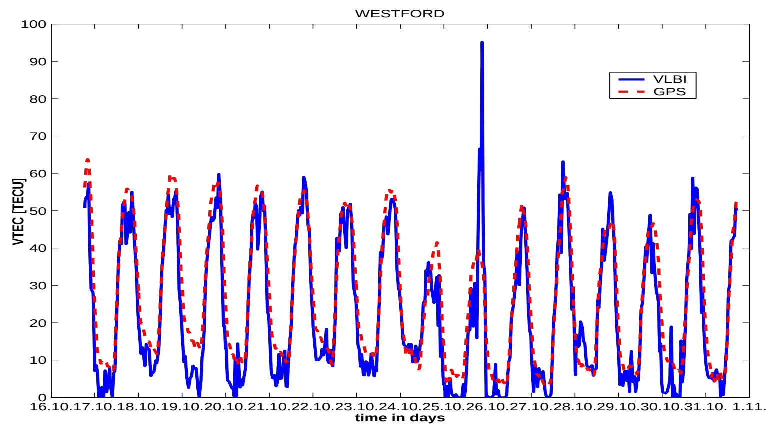

Figure 3. VTEC values for station WESTFORD derived by VLBI (solid line) and GPS (dashed line).

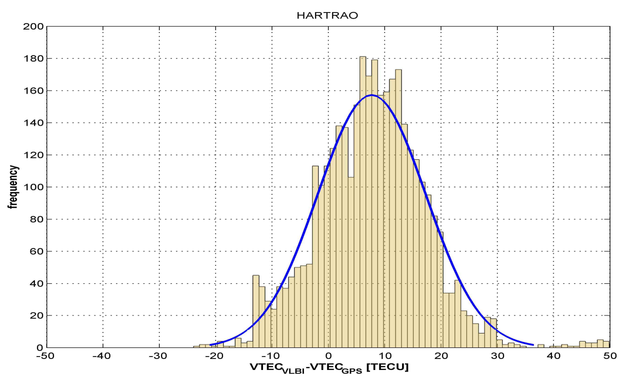

VTEC differences for station HARTRAO

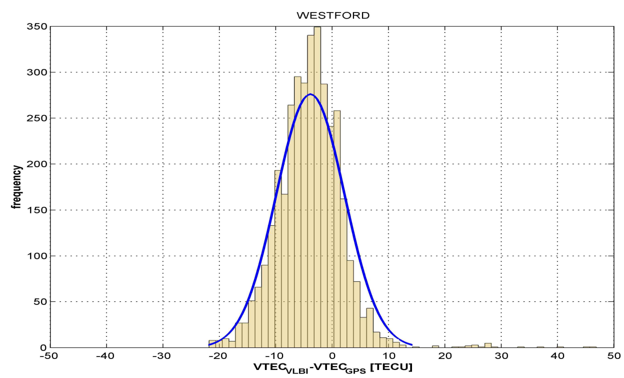

VTEC differences for station WESTFORD

Figure 4. Histograms of the VTEC differences between VLBI and GPS (VLBI-GPS)

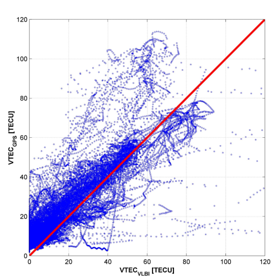

VTEC VLBI vs. GPS

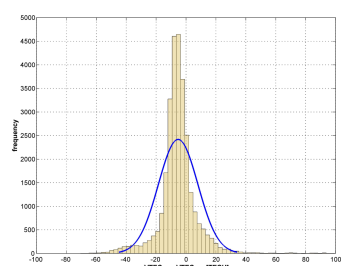

VTEC differences between VLBI and GPS, all CONT02 stations (VLBI-GPS)

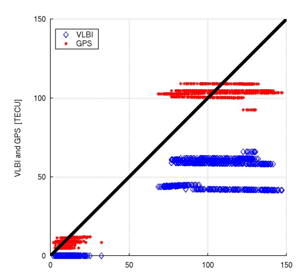

VTEC T/P vs. VLBI (blue,diamonds) and GPS(red, stars)

Figure 5. Comparison to results from GPS and TOPEX/Poseidon.

distributed and show a positive asymmetry. The standard deviation of the differences is about 11 TECU. Comparisons with the results of TOPEX/Poseidon for station Kokee Park are plotted in the right graph of figure 5. Although the differences between VLBI and TOPEX/Poseidon are bigger than the differences between GPS and TOPEX/Poseidon both results agree within an error range that is due to the assumption that all VTEC values within a range of ± 5 degrees in latitude and longitude can be assigned to station Kokee Park, which is located in a region of high ionospheric activity.

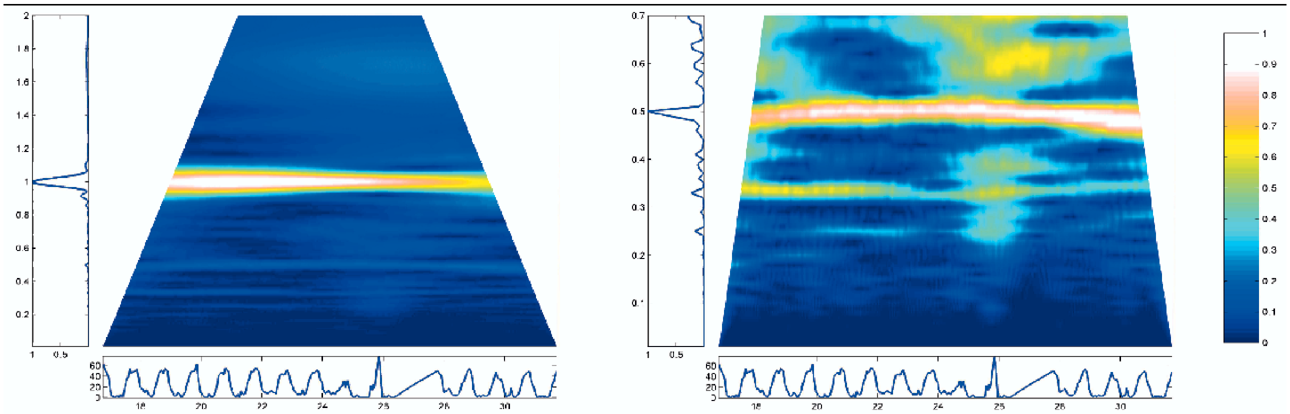

Figure 6. Daily and subdaily periods for station ALGOPARK, VLBI solution, Fourier and wavelet transformation (normalized to maximum amplitude); periods in days.

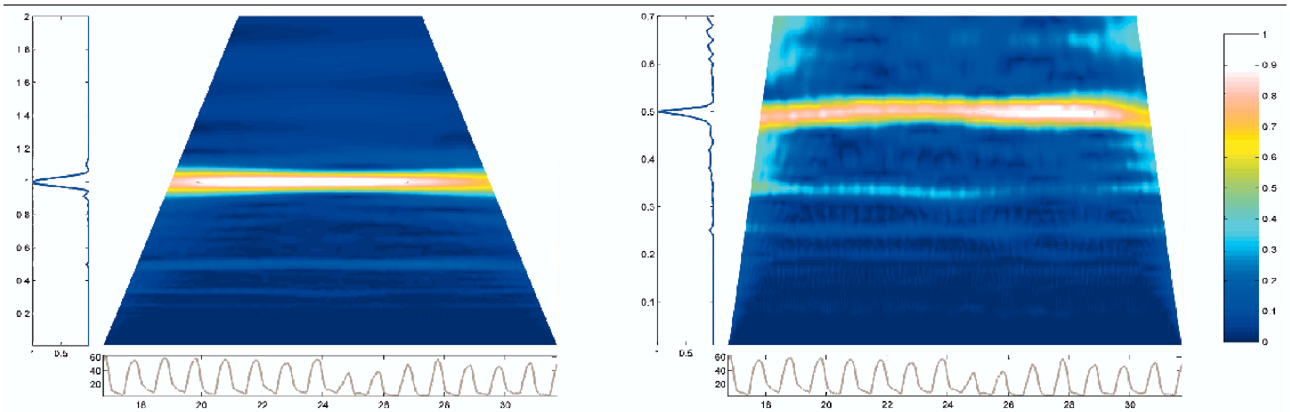

Figure 7. Daily and subdaily periods for station ALGOPARK, GPS solution, Fourier and wavelet transformation (normalized to maximum amplitude); periods in days.

To get an idea about the spectral content of the solutions derived by VLBI and GPS the results for station Algonquin Park were subject to Fourier and wavelet transformations. As on Oct. 27th, 2002 this station did not observe within CONT02 the adaptive PLF approach produces a linear trend for this time span (figure 6, lower graph), which does not influence the results of the frequency analysis because only periods shorter than two days were investigated here. A big diurnal variation can be seen in the Fourier spectrum of the VLBI results (left plot of figure 6), of the GPS data (7), and in the wavelet scalograms (left plots, figures 6 and 7). Both techniques show a decreasing diurnal amplitude during the 15 days covered by CONT02. If we concentrate on the periods shorter than 0.7 days we are able to recover a semi-, ter- and quarter-diurnal signal in the results from both techniques (right plots, figures 6 and 7).

3. Conclusions

CONT02 offers the opportunity to study the ionosphere by means of VLBI during more than two weeks of continuous measurements. Ionospheric parameters derived by VLBI and GPS show similar trends and differ within a few TECU, only. The main periods of the ionosphere (diurnal, semi-, ter- and quarter-diurnal) are found in the Fourier spectrum and the wavelet scalograms of both techniques agree well.

4. Acknowledgements

Research project P16136-N06 “Investigation of the ionosphere by geodetic VLBI” is funded by the Austrian Science Fund (FWF).

References

[1] Hobiger T., Boehm J., Schuh H., VLBIONOS - Probing the ionosphere by means of very long baseline interferometry, Oesterreichische Zeitschrift fuer Vermessung & Geoinformation (VGI), 1/2003, ed. by H. Schuh, F. Brunner, and H. Kahmen, pp. 29 - 39, 2003.

[2] Schaer, S., Mapping and Predicting the Earths Ionosphere Using the Global Positioning System, Inaugural Dissertation der Philosophisch-naturwissenschaftlichen Fakultaet der Universitaet Bern, Bern, 1999.

[3] ADS Central, GeoForschungsZentrum Potsdam (GFZ), `http://op.gfz-potsdam.de/`

Sten Bergstrand et al.: Comparison of Ionospheric Activity Derived from GPS and Different VLBI Networks, IVS 2004 General Meeting Proceedings, p.447–451
http://ivscc.gsfc.nasa.gov/publications/gm2004/bergstrand

Comparison of Ionospheric Activity Derived from GPS and Different VLBI Networks

Sten Bergstrand, Rüdiger Haas

Onsala Space Observatory, Department of Radio and Space Science, Chalmers University of Technology
Contact author: Sten Bergstrand, e-mail: sten@oso.chalmers.se

Abstract

GPS is currently the space geodetic technique most widely used for ionospheric studies, and provides broad coverage with high spatial and temporal resolution. Due to the nature of the dual frequency observations, VLBI is also capable of sensing the total electron content (TEC) of the ionosphere. We compare the ionospheric activity derived from different VLBI networks with the global GPS results from the Center of Orbit Determination in Europe and find that the difference between the techniques is on the order of 10 TEC units.

1. Introduction

The ionosphere is the region surrounding Earth that consists of particles charged by radiation processes, e.g. the ultraviolet radiation from the Sun. The resulting ions are subject to an electrodynamic drift over the magnetic equator, and their subsequent distribution along magnetic field lines results in an equatorial anomaly that is characterized by two crests around 30° geomagnetic latitude and a trough in between. Due to the strong dependency on solar activity, the ionosphere exhibits significant increase during local daytime.

Generally, an electromagnetic wave propagating through a medium is governed by the refractive index, n, of the medium. For the radio frequencies used by space geodetic techniques like VLBI and GPS, the ionosphere acts as a dispersive medium. With dispersiveness it is understood that the refractive index is frequency dependent, a frequency dependence that also can be utilized to study the ionosphere. The phase refractive index, n_{ph}, of a dispersive medium can be approximated with the series

$$n_{ph} = 1 + \frac{c_2}{f^2} + \frac{c_3}{f^3} + \frac{c_4}{f^4} + ...$$

where c_2, c_3 and c_4 are coefficients that depend on the electron density, N_e, along the signal path and not on the frequency. Higher order expansions are usually cut off and with an estimate of $c_2 = -40.3N_e$ [Hz^2], the phase refractive index becomes

$$n_{ph} = 1 - \frac{40.3}{f^2}$$

The propagating signals are affected by the total electron content (TEC) during their way through the ionosphere. TEC is the integral of the electron densities along the signal path, s,

$$\text{TEC} = \int N_e ds$$

and using the above, the ionospheric phase refraction Δ_{ph}^{Iono} results:

$$\Delta_{ph}^{Iono} = -\frac{40.3}{f^2}\mathrm{TEC}$$

Usually, TEC is measured in TEC units (TECU) corresponding to 10^{16} electrons. Although the ionosphere ranges from roughly 75 km to 1000 km height, a thin shell approximation is sufficient for most applications. More thorough derivations and descriptions than the above can be found in e.g. [1]. Utilizing the dual-frequency observations that are used in both VLBI and GPS, information about the TEC in the ionosphere can be derived [2], [3].

Comparison of differential TEC values derived from global GPS-based TEC maps and VLBI observations show a high degree of agreement between the two techniques [4]. Correlation on the level of 0.6–0.9 was achieved on short and intercontinental baselines.

In another comparison between VLBI and GPS [5], it was shown that the two techniques can yield similar TEC values at a VLBI site. Although using the same fundamental equations, the TEC solutions at each site were determined in different ways for the two techniques. For VLBI, the solutions were obtained from one point (the station) and mapped to the zenith, whereas for GPS, the solutions were based on a global spherical harmonics expansion of several sites.

In this study, we use the full set of ionospheric data obtained by VLBI at all observing sites for an experiment and compare these to a global set of GPS TEC observations. The comparison is then made for the region of a global spherical harmonics expansion confined by the outer limits of the VLBI observations.

2. Ionospheric Information Derived from VLBI

Differential ionospheric VLBI delays were used to estimate coefficients of the spherical harmonic expansion of the global field of vertical TEC. A simple single-shell model for the ionosphere with an ionospheric height of 450 km was applied. The point where the signal propagates through the infinitesimally thin modelled ionospheric shell is termed the ionospheric pierce point (IPP). Figures 1a shows an example of the IPPs for the T2002 experiment, observed February 12, 2002. The geographic longitudes λ_{pp} of the IPPs were then rotated to a sun-fixed longitude $\lambda_{\odot}$. With $\lambda_{pp} = 0°$ at 12 UT in the rotating earth-fixed frame corresponding to $\lambda_{\odot} = 0°$ in the sun-fixed frame, the generalized

$$\lambda_{\odot} = \lambda_{pp} + \mathrm{T} \cdot \omega_e \pm \pi$$

appears, where T is time (UT) and ω_e is the angular velocity of the earth. By rotating the earth-fixed observations of the experiment, an essential 360° longitudinal spread was obtained, Figure 1b. The importance of the VLBI network geometry for the spatial distribution of the IPPs and thus the sampling of the ionosphere is obvious.

Weak constraints were used to stabilize the least-squares estimation process to determine the coefficients of the spherical harmonic approach to degree and order 6. The estimated coefficients were used to create global VLBI TEC maps.

3. Ionospheric Information Derived from GPS

The international GPS service (IGS) homepage currently features daily ionospheric global solutions from five different analysis centers world-wide [6]. For our comparisons, we chose the

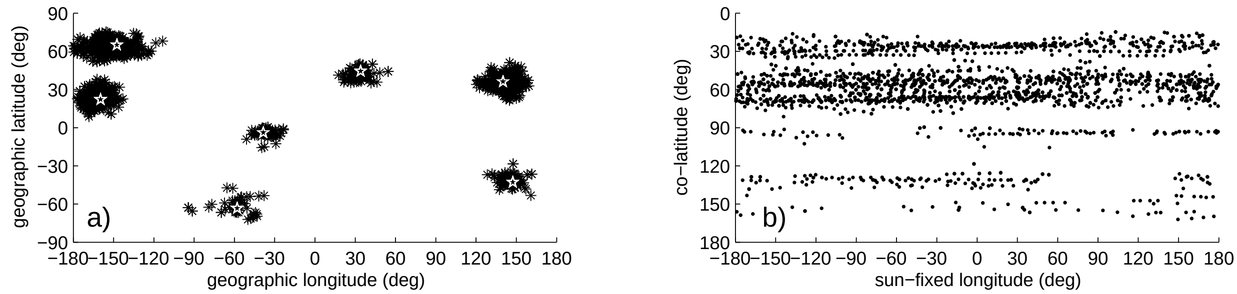

Figure 1. VLBI ionospheric pierce points during T2.002 in a) earth-fixed and b) sun-fixed reference frame. The VLBI stations are indicated by white pentagrams in a).

solutions by the Center of Orbit Determination in Europe (CODE) at the University of Berne [7]. CODE uses observations from around 150 sites to obtain bi-hourly solutions of the total vertical electron content and each 24-hour period is represented by thirteen[1] maps with a resolution of 2.5° in latitude and 5° in longitude. The IONEX maps generated at CODE are obtained using a modified single-layer model mapping function and are based on a spherical harmonics expansion of the observations up to degree and order 15. The maps correspond to the results for the middle day of a 3-day combination analysis in order to provide a set with consistent accuracy throughout. Further information on IONEX files and how they are generated is available at the CODE homepage. We used the bi-hourly IONEX data to create maps of the average TEC content during 24 hours, corresponding to the simultaneously observed VLBI experiments, see Figure 2.

4. Comparison of GPS and VLBI Results

To make the comparison between GPS and VLBI data feasible, we chose the following approach. The geographic coordinates (ϕ_{dp}, λ_{dp}) of the ionospheric pierce points (VLBI) and IONEX grid nodes (GPS), henceforth referred to as data points, were rotated into solar-geomagnetic coordinates in two steps. Following [8], the geomagnetic latitudes ϕ_m of the data points were calculated using

$$\sin\phi_m = \sin\phi_{dp}\sin\phi_p + \cos\phi_{dp}\cos\phi_p\cos(\lambda_{dp} - \lambda_p)$$

approximating the Boreal pole at $\phi_p = 78.7°$N and $\lambda_p = 290.1°$E. The IONEX data and the VLBI observations were rotated to a sun-fixed longitude as described in the previous section. GPS data were averaged over the 24-hour period before being compared to the VLBI maps, in order to make the data sets represent equal periods in time. The data points thus observed at non-uniformly spaced solar-geomagnetic coordinates were then projected onto a uniform grid (2.5°lat×5°lon) of solar-geomagnetic coordinates in order to make the comparison efficient. To avoid extrapolation of the observed data, the comparison has been confined to a region bound by the geomagnetic northern- and southernmost IPPs.

Figure 2 shows GPS and VLBI derived TEC maps for the dates of eight VLBI experiments in 2002 with different network geometries. To derive some statistics of VLBI and GPS differences, we followed the scheme described above also for the CONT02 campaign, which observed continuously for two weeks in October 2002. Figure 3 shows the differences for all experiments during

[1]Until 2002 day 306, twelve maps corresponding to UT 1,3,...,23 were generated (valid for this study).

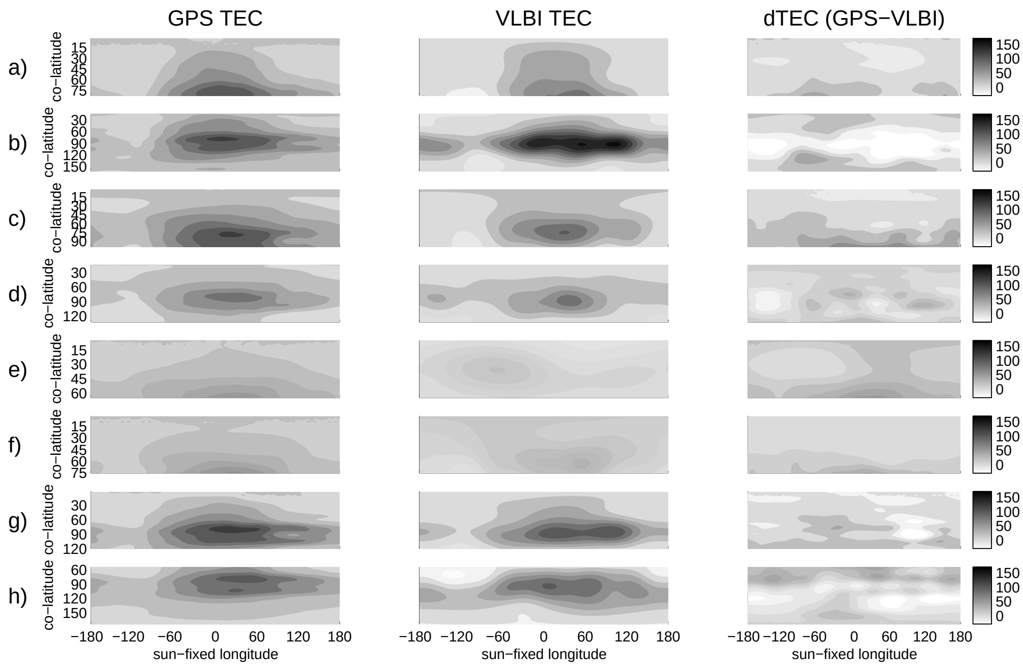

Figure 2. Solar-magnetic TEC maps from GPS and VLBI together with the difference between the two techniques for: a) RDV31, b) T2002, c) R4015, d) R1020, e) EURO64, f) R&D-7, g) CONT02.02 h) OHIG20. All values are given in TECU.

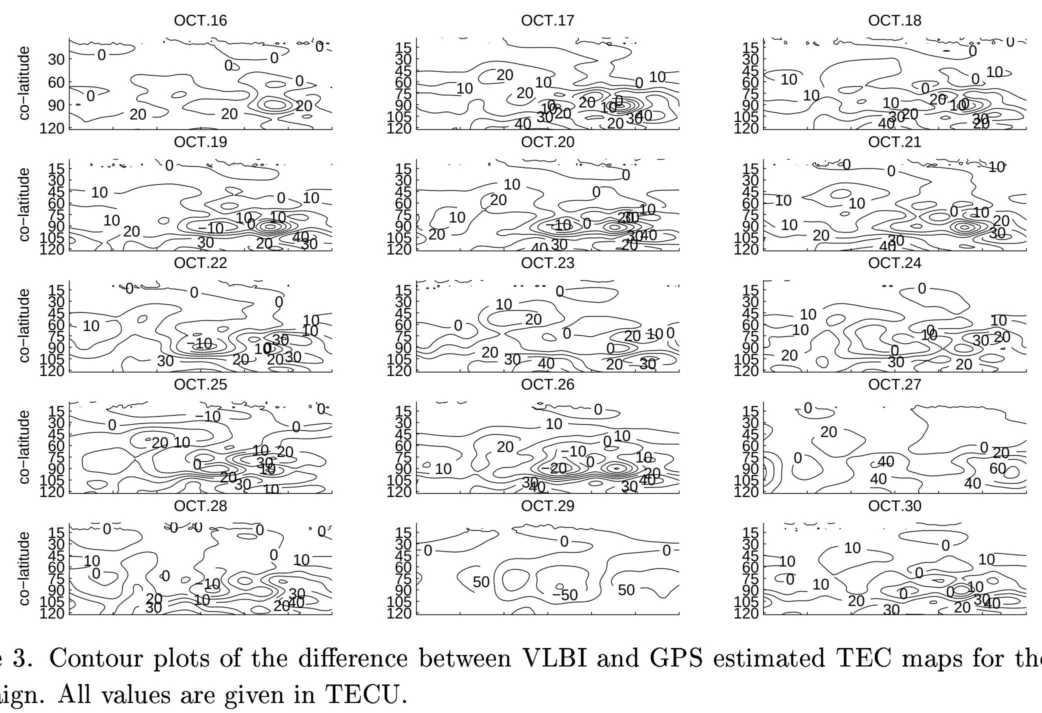

Figure 3. Contour plots of the difference between VLBI and GPS estimated TEC maps for the CONT02 campaign. All values are given in TECU.

the CONT02 campaign. Mean TEC differences and their standard deviations for the CONT02 campaign are given in Table 1.

Table 1. Mean TEC differences in TECU between GPS and VLBI for CONT02.

Day	dTEC(GPS-VLBI)			Day	dTEC(GPS-VLBI)			Day	dTEC(GPS-VLBI)		
Oct16	9.904	$\pm$	13.310	Oct21	8.344	$\pm$	11.110	Oct26	9.658	$\pm$	13.043
Oct17	12.541	$\pm$	11.748	Oct22	9.856	$\pm$	11.793	Oct27	15.335	$\pm$	19.893
Oct18	11.531	$\pm$	10.882	Oct23	10.377	$\pm$	11.268	Oct28	7.798	$\pm$	11.713
Oct19	9.307	$\pm$	11.185	Oct24	11.052	$\pm$	10.162	Oct29	8.368	$\pm$	33.395
Oct20	11.000	$\pm$	12.156	Oct25	8.151	$\pm$	12.778	Oct30	10.165	$\pm$	9.706

5. Conclusions and Outlook

Both GPS and VLBI allow derivation of the total electron content in the ionosphere. An important restriction for ionospheric studies with VLBI is the sparse spatial sampling of the ionosphere provided by current VLBI networks. The analyzed examples show similarities, but also significant discrepancies between the two techniques. The agreement of TEC maps derived from the two techniques is of the order 10 TECU. Current VLBI networks with 8–20 participating stations do not allow as highly and well distributed samplings of the ionosphere as GPS does. It also appears that regional observations (e.g. EURO experiments) are less suitable for this type of analysis. Derivation of accurate global TEC maps with high resolution from VLBI data is thus a challenging task and requires further investigations. The combined use of the two complementary techniques for ionospheric studies might be a meaningful approach.

References

[1] Hofmann-Wellenhof, B., Lichtenegger, H., and Collins J.: GPS Theory and Practice, 5th revised edition, Springer Verlag, 2001.

[2] Kondo, T.: Application of VLBI data to measurements of ionospheric total electron content. *Journal of the Communications Research Laboratory*, **38(3)**, 613-622, 1991.

[3] Schaer, S.: Mapping and Predicting the Earths Ionosphere Using the Global Positioning System, Dissertation, Universität Bern, 1999.

[4] Sekido, M., Kondo, T., and Kawai, E.: Evaluation of GPS-based ionospheric TEC map by comparing with VLBI data. *Radio Science*, **38(4)**, doi:10.1029/2000RS002620, 2003.

[5] Hobiger, T., Boehm, J., and Schuh, H.: VLBIONOS - Probing the Ionosphere by Means of Very Long Baseline Interferometry. *Österr. Zeitschrift für Vermessung & Geoinformation*, **91(1)**, 29–37, 2003.

[6] IGS: International GPS Service (IGS) homepage http://igscb.jpl.nasa.gov

[7] Center for Orbit Determination in Europe (CODE), Universität Bern, webpage: http://www.aiub.unibe.ch/ionosphere.html

[8] Biel, H.A. von: The geomagnetic time and position of a terrestrial station. *Journal of Atmospheric and Terrestrial Physics*, **52(9)**, 687–694, 1990.

Gabor Lanyi et al.: Limitations to Dual Frequency Ionosphere Corrections for Frequency Switched K-Q-Band Observations with the VLBA, IVS 2004 General Meeting Proceedings, p.452–455
http://ivscc.gsfc.nasa.gov/publications/gm2004/lanyi

Limitations to Dual Frequency Ionosphere Corrections for Frequency Switched K-Q-Band Observations with the VLBA

Gabor Lanyi [1], *David Gordon* [2], *Ojars J. Sovers* [3]

1) *Jet Propulsion Laboratory, Caltech*
2) *Raytheon ITSS/NASA Goddard Space Flight Center*
3) *RSA Systems/Jet Propulsion Laboratory*

Contact author: Gabor Lanyi, e-mail: gelanyi@jpl.nasa.gov

Abstract

A series of VLBA experiments were carried out at K and Q bands for astrometry and imaging within the KQ VLBI Survey Collaboration. The paired K and Q observations of each source are separated by approximately 3 minutes of time. We investigate the delay effect of the ionosphere between K and Q bands involving the interscan separation. This differential delay effect is intermixed with the differential fluctuation effect of the troposphere.

1. Dual-Band Ionospheric Delay Reduction

In dual-band VLBI observations the delay effect of the ionosphere is greatly reduced by forming the ionospheric-delay free combination of the dual delay observables:

$$\tau = a\tau_1 + b\tau_2. \tag{1}$$

The two coefficients

$$a = \nu_1^2/(\nu_1^2 - \nu_2^2), \tag{2}$$
$$b = \nu_2^2/(\nu_2^2 - \nu_1^2) \tag{3}$$

sum to 1, therefore the nondispersive component of the delay remains unaltered. Of course, this treatment assumes that the two observations made at two frequencies are simultaneous. At the Very Long Baseline Array (VLBA), currently only S- and X-band observations can be simultaneously performed. The measurements described in this report (e.g. [1]), involve K (24 Ghz) and Q (43 GHz) band frequencies, therefore a frequency switching is performed in the middle of each source observation. Therefore, we must include appropriate corrections to Eq. 1, which are

$$\tau \rightarrow \tau - b\Delta M - b\Delta K/\nu_2^2, \tag{4}$$

where $\Delta M = M_2 - M_1$ is the nonionospheric model-contribution difference, and ΔK is inospheric-content coefficient difference corresponding to the relation $\tau_{ion} = K/\nu^2$. The differential quantities ΔM and ΔK are not measured; they must be estimated. While we do not a have a solid estimate, S-X band VLBI studies indicate that the average K-band ionospheric delay effect at the VLBA is perhaps 25 ps. The delay effect is distributed among the post-fit observables and residuals. The question is whether such a magnitude of delay effect is reducible by dual-band observations.

2. Tropospheric Fluctuation

The temporal separation between the K- and Q-band observations is nearly 200 seconds. Besides the columnar ionospheric content change between these observations the tropospheric delay also changes. The quasi-static part of this effect can be nearly eliminated by estimating the zenith tropospheric delay. However, the fluctuation effect remains undetermined.

We may estimate the change in average tropospheric fluctuation delay during the scan separation period from the mean tropospheric delay rate. The delay rate is dominated by the water vapor fluctuation [2]. It is found that in the VLBA K-Q experiments the root-mean-square (rms) of the tropospheric delay-rate is 0.08 ps/s. Therefore, a rough estimate of the fluctuation change over 200 s is $0.08 \times 200 = 16$ ps. This value is not an insignificant part of the ionospheric delay to be calibrated. However, as shown in the next section, the system noise is the dominant factor which makes it impossible to perform ionospheric calibration.

3. Results and Conclusion

We have evaluated the distribution of the rms system noise, as calculated by the fringe fitting; the results are displayed in Figures 1 and 2. The distribution is normalized to its theoretical form that should be a χ distribution if the underlying random noise is Gaussian. Note that the ratio of the rms noise at Q- and K-band is about 2. Beside the large rms value, the Q-band distribution also exhibits a non-Gaussian tail.

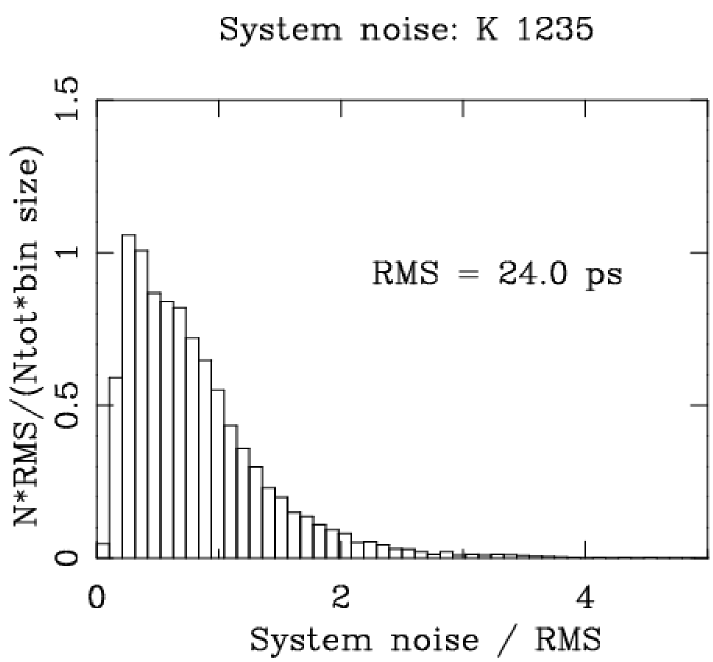

Figure 1. Normalized K-band noise distribution.

The distribution of post-fit residuals of observation, Figs. 3 and 4, exhibit a similar trend. These distribution are also normalized. The K-band residual distribution has a small non-Gaussian component, while the calibrated residual distribution deviates substantially from a Gaussian dis-

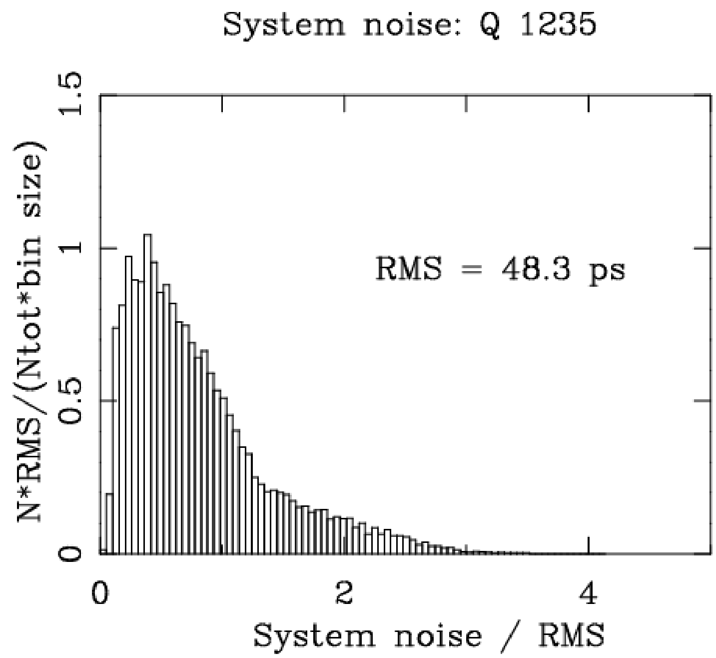

Figure 2. Normalized Q-band noise distribution.

tribution. The calibrated residual distribution is essentially dominated by the Q-band residual distribution with an rms of $\approx$ 45 ps. The non-Gaussian phenomenon is still under investigation. What is certain is that the rms value of Q-band noise and the corresponding post-fit residuals inhibit estimation of the ionospheric delay not only for switched, but for simultaneous K- and Q-band observation as well. Simultaneous X-K band observations may be a possibility for K-band ionospheric calibration. A 24-h (S/X)-K-(S/X) triple-scan observation sequence was carried out to investigate the ionospheric calibration effect.

4. Acknowledgments

The research in this report was performed under a contract between the California Institute of Technology and NASA.

References

[1] Jacobs, C.S, P. Charlot, D. Gordon, G.E. Lanyi, C. Ma, C.J. Naudet, O.J. Sovers, L.D. Zhang, and the KQ VLBI Survey Collaboration, “Extending the ICRF to higher radio frequencies: 24 & 43 GHz,” IAU General Assembly XXV, Sydney Australia, 13-26 July 2003.

[2] Treuhaft, R. N., and G. E. Lanyi, 1987, Radio Science **22**, 251.

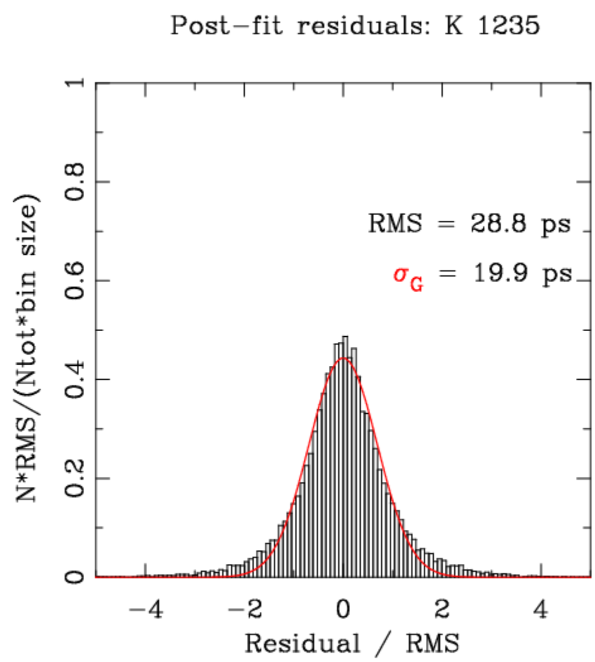

Figure 3. K-band residual distribution, normalized.

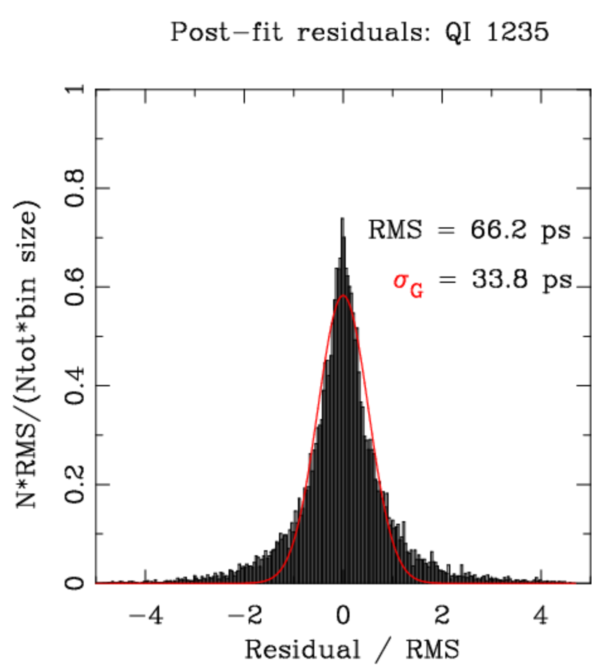

Figure 4. Calibrated residual distribution, normalized.

Monia Negusini et al.: Tropospheric Parameters Estimated by Geodetic VLBI Data IVS, IVS 2004 General Meeting Proceedings, p.456–460
http://ivscc.gsfc.nasa.gov/publications/gm2004/negusini

Tropospheric Parameters Estimated by Geodetic VLBI Data IVS

Monia Negusini, Paolo Tomasi

Istituto di Radioastronomia
Contact author: Monia Negusini, e-mail: negusini@ira.cnr.it

Abstract

The Institute of Radioastronomy (IRA) joined since the beginning the IVS TROP project providing regular submission of tropospheric parameters (wet and total zenith delays, horizontal gradients) for all IVS-R1 and IVS-R4 sessions since January 1st, 2002. In order to determine reliable time series of tropospheric parameters, we analyzed all the 2000-2003 databases available on the IVS data centers. Some of the tropospheric results are presented here. We have also compared the VLBI tropospheric estimates and the GPS-derived troposphere provided by IGS (International GPS Service), for the co-located sites. Post-processing analysis has been carried out on the time series and trends and seasonal signals are highlighted. Constant biases are found between the zenith delays derived by VLBI and GPS, although the same effects should affect both techniques.

1. Introduction

The Institute of Radioastronomy (IRA) joined the IVS TROP project on Tropospheric Parameters since the beginning, submitting the estimates of tropospheric parameters (wet and total zenith delays, horizontal gradients) for all IVS-R1 and IVS-R4 sessions since January 1st, 2002, on a regular basis. Our institute had a large experience of analyzing VLBI data for studying the effect of the tropospheric delay on the results [1], and participating in the project was a natural broadening of our activity. Our analysis center submits the requested parameters to IVS as a Sinex file. For the VLBI data analysis a 5 degree elevation cut-off angle and Niell mapping functions were used. The solution has been computed into ITRF2000 without fixing the stations coordinates, using a no-net-translation constraint. One total and one wet zenith delay parameter per hour for all the stations involved in the experiment and only one value for both east and north gradient per station per session were computed. The data submitted by the different ACs are combined at the IVS Tropospheric Combination Center at IGG in Vienna in order to obtain IVS combined products, i.e. stable and robust tropospheric parameters with 1 hour resolution and high accuracy [2].

2. VLBI Data Analysis of All 2000-2003 Databases

Space geodesy techniques are proving to be a powerful tool for studying climate change and global warming. An important parameter to monitor is the behavior of the troposphere and VLBI can be very useful, computing long time series of tropospheric parameters. To achieve this goal, we analyzed all the other 2000-2003 databases available on the IVS Data Centers, using a setup identical to the one described above. As a product of this analysis we obtained tropospheric parameters for each station and for every experiment available in our catalogue and the relevant time series. In Figures 1 and 2 the total and wet zenith path delay time series for some of the stations involved into VLBI geodetic experiments are shown. For Wettzell we have quite a continuous time series unlike other stations, such as Medicina or Onsala, where very sparse data are present. It should be noted that all the stations present a strong seasonal signal and a large correlation of this signal between total and wet zenith path delay.

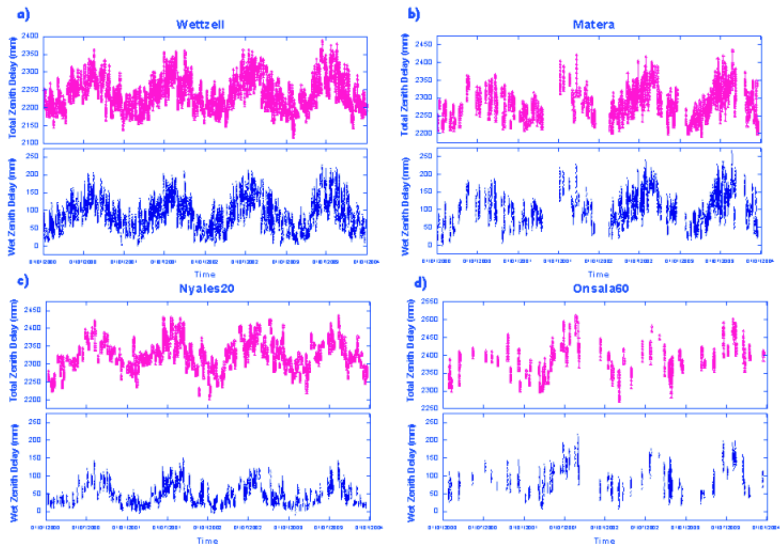

Figure 1. Total (up) and Wet (down) zenith delay time series for: a) Wettzell, b) Matera, c) Nyales20, and d) Onsala60.

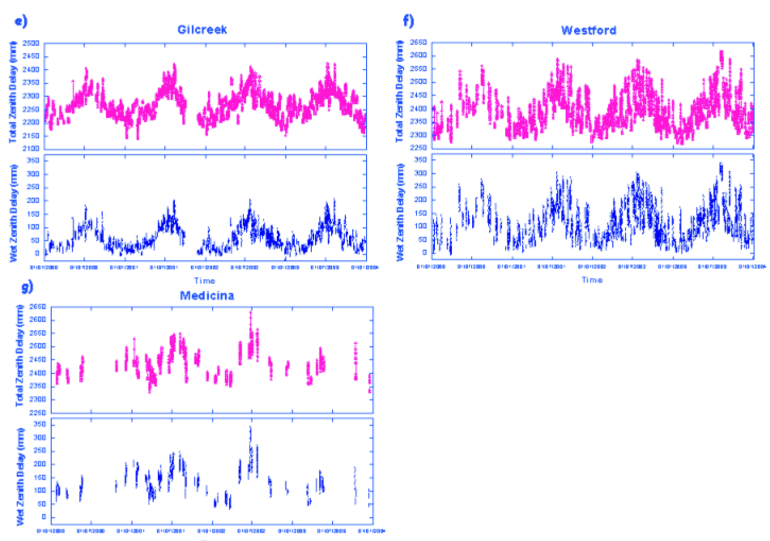

Figure 2. Total (up) and Wet (down) zenith delay time series for: e) Gilcreek, f) Westford and g) Medicina.

3. Post-Processing of the Time Series

The time series of zenith path delay for the stations present in this analysis is an interesting set of data that can be compared with the results coming from independent techniques, like GPS. For that we decided to carry out a comparison between the VLBI tropospheric estimates and the GPS-derived troposphere for co-located sites. We used GPS data available on the web site of the CODE Analysis Center and in particular the COE EUREF daily solutions, where the troposphere parameters have 1-hour resolution and, thus, they are directly comparable with the parameters computed by our VLBI data analysis. For stations not included in EUREF analysis we used the COD solutions, where every 2-hour parameters were estimated. Post-processing analysis have been carried out on both VLBI and GPS time series, spectral analysis was performed. The estimated periods are almost identical for both techniques, differences are at the level of few days.

As an example we plotted in Figure 3 Wettzell time series, both VLBI and GPS, and the seasonal signals highighted by spectral analysis. We were able to compute amplitudes and phases by means of a best-fit wave. VLBI and GPS seasonal signals have quite the same amplitudes and phases. For VLBI we found a period of 365 ± 5 days and for GPS 356 ± 3 days. For the amplitude we found 45.5 ± 0.9 mm for VLBI and 45.5 ± 0.5 mm for GPS.

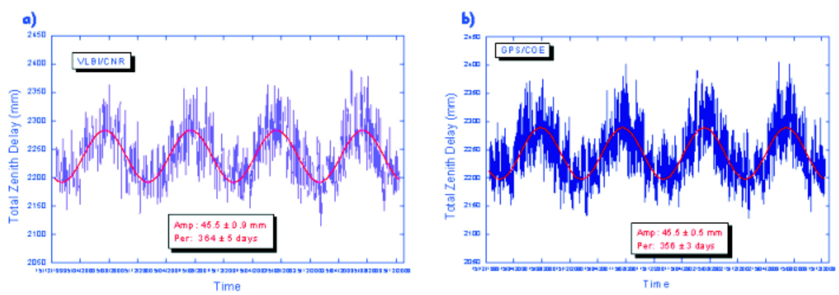

Figure 3. VLBI (a) and GPS (b) time series and best-fit annual waves for Wettzell.

Since signals present in both VLBI and GPS data were comparable, we computed the differences between the two time series and we obtained the relevant residuals. A positive bias is always present and in some cases a positive trend, too, that is to be investigated in order to understand its physical meaning. In fact, both techniques are supposed to be affected by the same effects, so it is not clear what can cause this different behavior found in the residual. One known effect, that has to be taken into account, is the difference in height of the reference points of the different instruments. Thus, for a precise comparison, we have to take into account these differences in height, convert them into differences of tropospheric zenith delay and correct the residuals time series. That is quite easy for the dry component, but not for the wet component. In fact, for the first component we can assume that the delay is a fraction, proportional to the difference in height, of all the dry delay, but that assumption is not true for the wet path delay. Table 1 shows the results for the 7 co-located sites. The first four rows represent the stations for which 1-hour tropospheric parameters from GPS are available, while for the last three we used 2-hour GPS data. After applying the height correction the positive biases are still present. We have to investigate possible causes of remaining bias: different analysis strategies between the two techniques, the different cut-off angles applied that can cause differences when station heights are estimated and, consequently, differences in the signal path through the troposphere. At this step of the work, no conclusion can be drawn.

Table 1. Biases between VLBI and GPS tropospheric zenith delay before and after height corrections

VLBI	GPS	Height diff.(m)	Bias(mm)	Bias(mm) b. corr.	Bias(mm) a. corr.
Wettzell	WTZR	3.1	1.0	4.7 ± 0.1	3.7 ± 0.1
Nyales20	NYA1	3.1	1.1	5.1 ± 0.1	4.0 ± 0.1
Matera	MATE	7.7	2.5	7.8 ± 0.1	5.3 ± 0.1
Onsala	ONSA	13.7	5.1	6.3 ± 0.2	1.2 ± 0.2
Gilcreek	FAIR	13.1	4.4	7.5 ± 0.1	3.1 ± 0.1
Westford	WES2	1.8	0.6	12.3 ± 0.2	11.7 ± 0.2
Medicina	MEDI	17.1	6.3	8.6 ± 0.4	2.3 ± 0.4

4. Long-Term Time Series

Very long-term time series of tropospheric parameters, particularly of wet zenith delay representing the content of water vapor in the atmosphere and one of the greenhouses gases, are useful for meteorological and climatologic studies. Therefore, we decided to analyze all the databases included in our AC catalogue, considering the fact that the time series can go back for about 15 years, including, for the most part, experiments that contain at least three European stations. We re-analyzed all these databases in order to obtain a homogenous set of tropospheric parameters. In Figure 4a there are the results for the wet zenith delay at the station of Wettzell since 1987 till 2003 and the estimated linear trend. We obtained a negative value, -0.5 ± 0.1 mm/yr, but the series is very uneven and with a strong annual signal. We performed a spectral analysis and fitted the wet delay time series with the annual wave and we subtracted the best-fit wave from the data. On the residual series we computed the linear trend and we obtained a slightly positive value, 0.1 ± 0.1 mm/yr, (Figure 4b) different from our previous determination [3]. In any case, the weight of the last dense four years of data certainly influences the determination of the true value. We performed the same analysis also for Medicina. In this case, a positive trend is also present and its original value is 2.7 ± 0.3 mm/yr; it becomes 1.5 ± 0.2 mm/yr for the residual wet component.

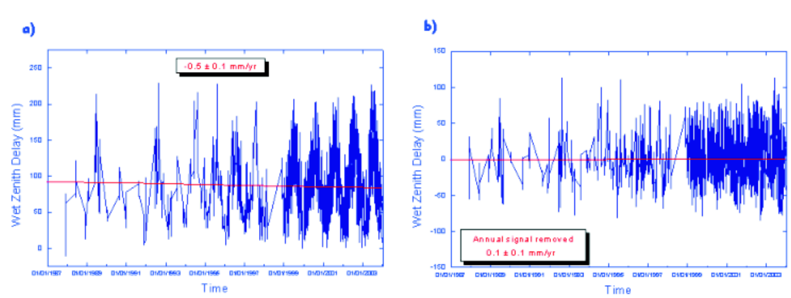

Figure 4. Wet zenith delay time series for Wettzell.

5. Conclusion and Outlook

We analyzed all 2000-2003 databases present in the IVS data centers and, as an output, we obtained time series of tropospheric zenith delays for the stations involved in geodetic VLBI experiments. We performed spectral analysis on these series and we highlighted strong annual signals mainly due to the wet component. We compared VLBI data with GPS-derived tropospheric estimates. We found out common features and differences between the two techniques, even if they are supposed to be affected by the same effects. In particular the biases between the two techniques are confirmed and do not disappear even taking into account the height differences. The long-term time series of tropospheric delays, confirm a positive linear trend, after the subtraction of the seasonal signal, for Wettzell and Medicina. However, it should be pointed out that the period is probably too short to draw a final conclusion on a modification of the trend in global warming. For the future we will continue the participation of our AC in the TROP project, submitting regularly tropospheric parameters for IVS-R1 and IVS-R4 sessions. We also agreed to submit our long-term series of tropospheric parameters. We are working in order to complete our VLBI data catalogue and, at the moment, we are able to provide the project with our available data, only. But very soon we will complete the analysis also for the data bases not present, at the moment, in our catalog. We will continue our test on comparing VLBI and GPS data and we will work on using VLBI wet zenith delay into routinely VLBI data analysis in order to improve the repeatability of station baselines.

References

[1] Rioja, M.J., Tomasi, P., "External tropospheric calibration for VLBI observations" in *Proceedings of the* 15^{th} *Working Meeting on European VLBI for Geodesy and Astrometry*, 149–153, 2001.

[2] Schuh, H., Boehm J., "Status Report of the IVS Pilot Project - Tropospheric Parameters", in *International VLBI Service for Geodesy And Astrometry 2002 Annual Report*, edited by N. R. Vandenberg and K. D. Baver, NASA/TP-2003-211619, 13-21, 2002.

[3] Negusini, M., Tomasi P., "Tropospheric Parameters From Geodetic VLBI Data Analysis", in: *Proceedings of the* 16^{th} *Working Meeting on European VLBI for Geodesy and Astrometry*, 181-194, 2003.

Harald Schuh et al.: IVS Tropospheric Parameters - Comparison with DORIS and GPS for CONT02, IVS 2004 General Meeting Proceedings, p.461–465
http://ivscc.gsfc.nasa.gov/publications/gm2004/schuh2

IVS Tropospheric Parameters - Comparison with DORIS and GPS for CONT02

Harald Schuh [1], Kristyna Snajdrova [1], Johannes Boehm [1], Pascal Willis [2], Gerald Engelhardt [3], Roberto Lanotte [4], Paolo Tomasi [5], Monia Negusini [5], Daniel MacMillan [6], Iraida Vereshchagina [7], Vadim Gubanov [7], Rüdiger Haas [8]

1) *IGG, Vienna University of Technology*
2) *Jet Propulsion Laboratory, California Institute of Technology*
3) *Federal Agency for Cartography and Geodesy*
4) *Centro di Geodesia Spaziale*
5) *Istituto di Radioastronomia*
6) *NASA Goddard Space Flight Center*
7) *Institute of Applied Astronomy*
8) *Onsala Space Observatory, Chalmers University of Technology*

Contact author: Harald Schuh, *e-mail:* `harald.schuh@tuwien.ac.at`

Abstract

In April 2002 the IVS (International VLBI Service for Geodesy and Astrometry) set up the Pilot Project - Tropospheric Parameters, and the Institute of Geodesy and Geophysics (IGG), Vienna, was put in charge of coordinating the project. Seven IVS Analysis Centers have joined the project and regularly submitted their estimates of tropospheric parameters (wet and total zenith delays, horizontal gradients) for all IVS-R1 and IVS-R4 sessions since January 1st, 2002. The individual submissions are combined by a two-step procedure to obtain stable, robust and highly accurate tropospheric parameter time series with one hour resolution (internal accuracy: 2-4 mm). Starting with July 2003, the combined tropospheric estimates became operational IVS products.

In the second half of October 2002 the VLBI campaign CONT02 was observed with 8 stations participating around the globe. At four of them (Gilmore Creek, U.S.A.; Hartebeesthoek, South Africa; Kokee Park, U.S.A.; Ny-Ålesund, Norway) also total zenith delays from DORIS (Doppler Orbitography and Radiopositioning Integrated by Satellite) are available and these estimates are compared with those from the IGS (International GPS Service) and the IVS. The distance from the DORIS beacons to the co-located GPS and VLBI stations is around 2 km or less for the four sites mentioned above.

1. Comparison

Fig. 1 shows the total zenith delays derived from VLBI (see Schuh and Boehm, 2003, [1]), GPS and DORIS at the station Hartebeesthoek (South Africa) during CONT02. Fig. 2 then focuses on a detail of Fig. 1 to illustrate the different variations of the time series. Similarily, Figures 3 and 4 show the total zenith delays and a detail for the station Ny-Ålesund in Norway. The total delays for Gilmore Creek (Alaska, U.S.A.) and Kokee Park (Hawaii, U.S.A.) are plotted in Fig. 5 and Fig. 6. The figures show that the variation of the time series is larger for DORIS than for GPS and VLBI, which might be due to looser constraints in the DORIS analysis.

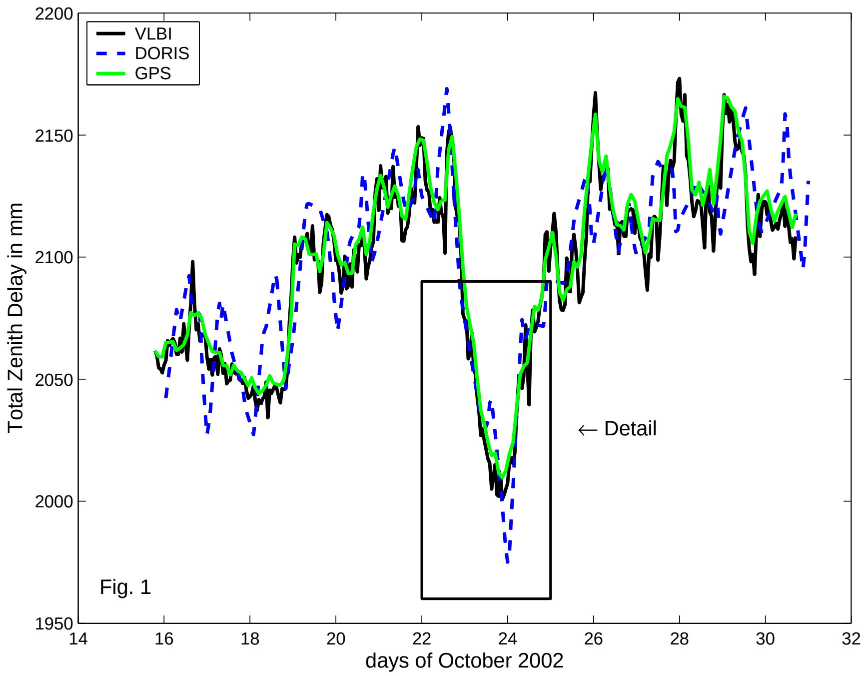

Figure 1. Total zenith delays at Hartebeesthoek during CONT02.

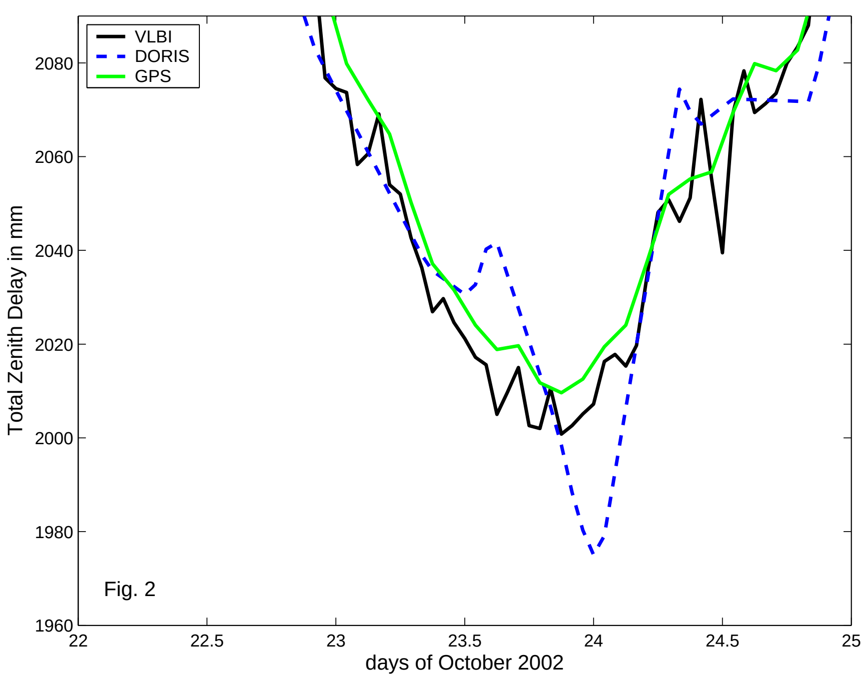

Figure 2. Total zenith delays at Hartebeesthoek, (48h detail).

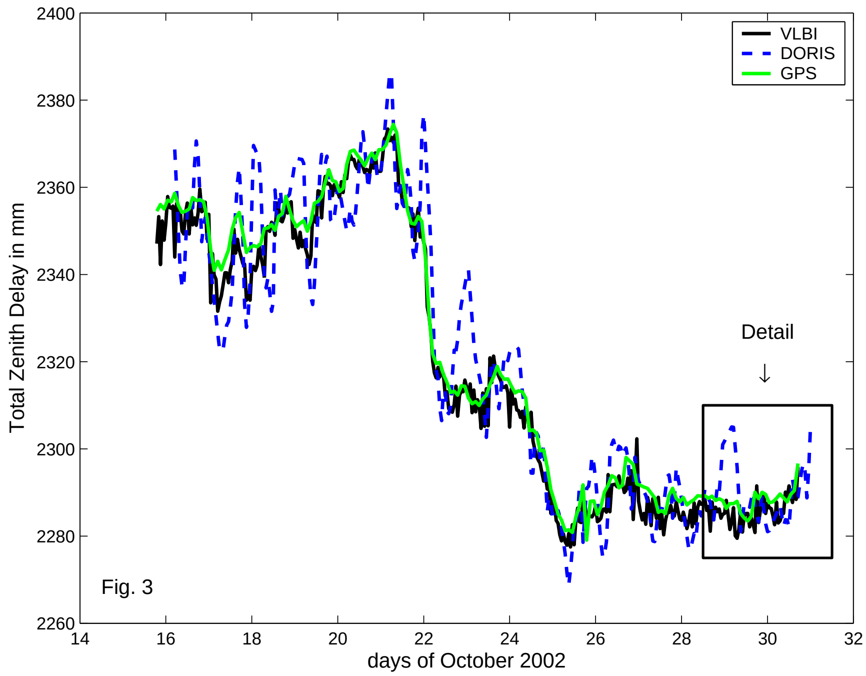

Figure 3. Total zenith delays at Ny-Ålesund during CONT02.

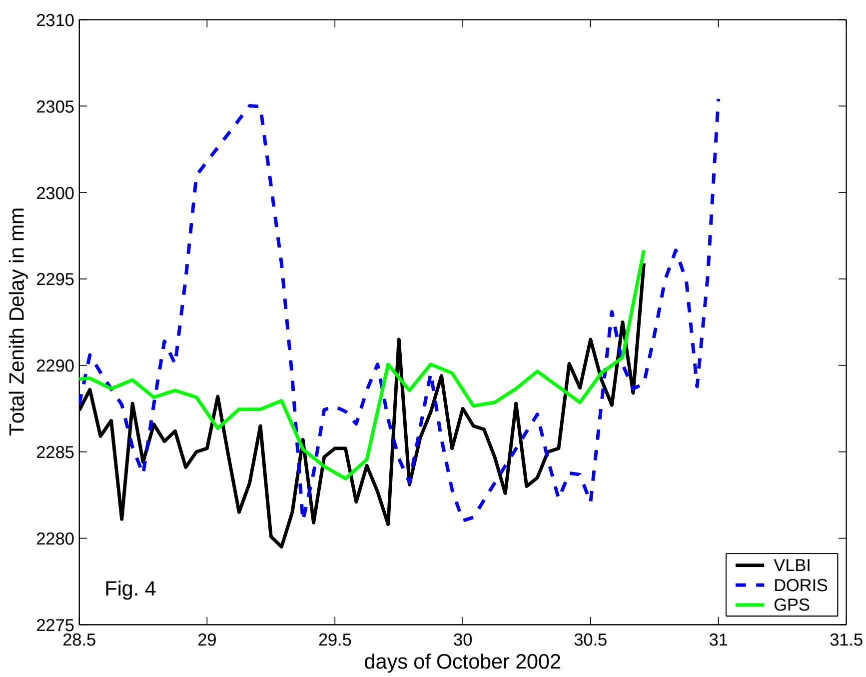

Figure 4. Total zenith delays at Ny-Ålesund, (48h detail).

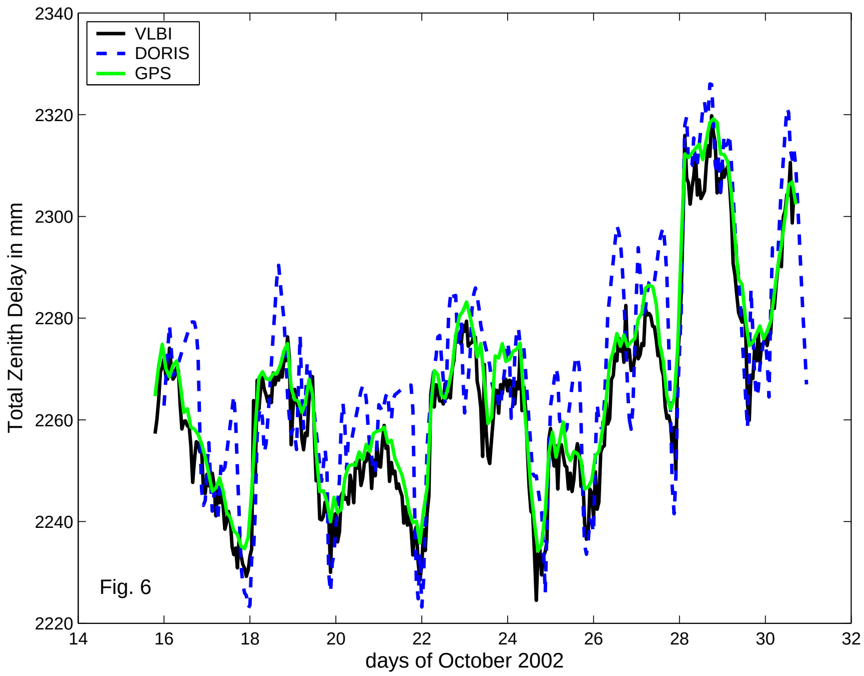

Figure 5. Total zenith delays at Gilmore Creek during CONT02.

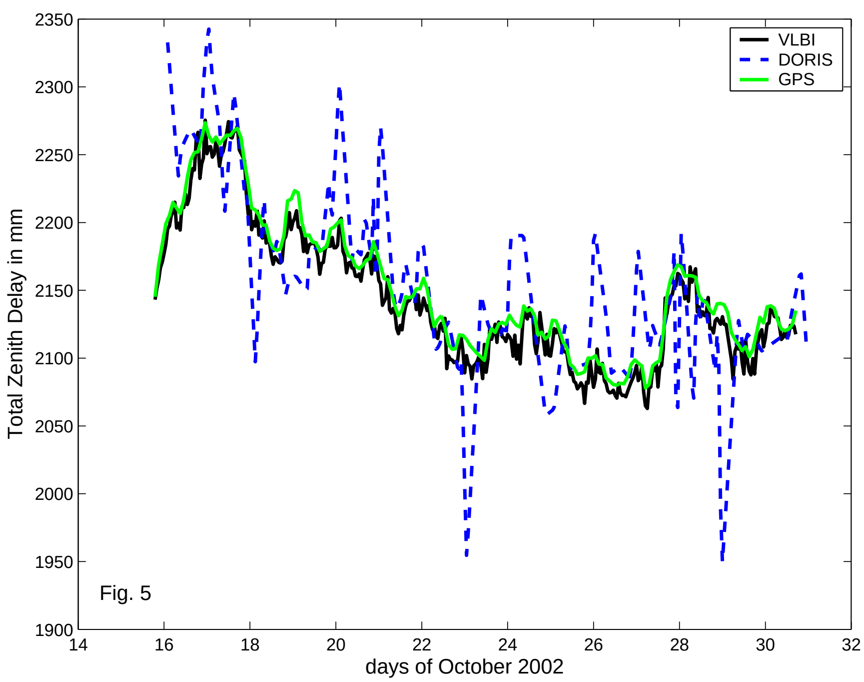

Figure 6. Total zenith delays at Kokee Park during CONT02.

Table 1. Offsets and standard deviations (in mm) for the sites Gilcreek, Hartebeesthoek, Kokee Park, and Ny-Ålesund between VLBI, GPS, and DORIS total zenith delays for CONT02. Before the data were compared, height corrections were applied (10 m height difference corresponds to ~3 mm in total zenith delay). No outlier elimination was carried out for this comparison. The offsets between the time series do not close to zero because of interpolation and rounding errors.

	DORIS - VLBI	DORIS - GPS	GPS - VLBI
Gilmore Creek	6.9 ± 10.6	3.1 ± 10.2	3.9 ± 3.5
Hartebeesthoek	2.6 ± 20.1	-1.6 ± 18.9	4.2 ± 6.3
Kokee Park	9.7 ± 45.1	0.3 ± 44.8	8.9 ± 7.2
Ny-Ålesund	2.5 ± 9.7	-0.1 ± 9.8	2.6 ± 3.5

Tab. 1 summarizes the offsets and the standard deviations of the differences between the time series after removing the offsets between VLBI, GPS, and DORIS. The big standard deviations between DORIS and the other techniques at Kokee Park might result from DORIS as non-continuous tool using loose constraints for the total zenith delays in the estimation.

2. Conclusions

- There are positive biases of ~5 mm between the total zenith delays from GPS and VLBI although height corrections are applied. The biases between DORIS and GPS are close to zero.
- VLBI and GPS agree better (~5 mm) than VLBI or GPS with DORIS.
- There are some outliers in the DORIS data, which might be due to the fact that DORIS is a non-continuous tool for a specific ground station (compare Fig. 6: rapid variations with few DORIS passes).

3. Acknowledgements

The realization of the DORIS tropospheric estimation was carried out at the Jet Propulsion Laboratory, California Institute of Technology, under a contract with the National Aeronautics and Space Administration.

References

[1] H. Schuh and J. Boehm, Status Report of the IVS Pilot Project - Tropospheric Parameters, in International VLBI Service for Geodesy and Astrometry 2002 Annual Report, edited by N. R. Vandenberg and K. D. Baver, NASA/TP-2003-211619, 13-21, 2003.

Elena Skurikhina: Long Time Wet Tropospheric Delay Series for Some Stations, IVS 2004 General Meeting Proceedings, p.466–470
http://ivscc.gsfc.nasa.gov/publications/gm2004/skurik

Long Time Wet Tropospheric Delay Series for Some Stations

Elena Skurikhina

Institute of Applied Astronomy of Russian Academy of Sciences (IAA)
e-mail: sea@quasar.ipa.nw.ru

Abstract

Long time WTD series for selected stations were obtained from all 24 h series VLBI data processing with OCCAM package using Kalman filter technique for estimation of stochastic parameters (clock offset and WTD). One WTD value for each 24 h session is computed. Long time WTD behavior can be described as combination of seasonal part and linear trend. Parameters of linear trend (bias, rate) and seasonal harmonic (amplitude, phase) for 20 VLBI stations with long observational history are presented. The comparison with mean diurnal values of meteodata is made.

We analysed the time series of WTD (Wet Tropospheric Delay) for some stations with sufficiently long observation history. WTD values were calculated with OCCAM software as one value per session and relate to the last observation at the session. They are modeled as random walk stochastic process and estimated using Kalman filter technique. We used VTRF2003 to fix terrestrial reference system. Numeric atmospheric loading model based on the station displacement time series computed at GSFC is applied. The mapping functions by Niell (1996) were used.

The long time WTD series for some stations was calculated from data processing of all 24-hour sessions.

The preliminary analysis of meteo data was made (to select stations with sufficient number of observations to study seasonal effects). Average daily values of meteo data (temperature (T), pressure (P), humidity (H)) was extracted from VLBI data statistic [8] (unreliable data was refused). The average daily values of temperature can be presented as combination of linear trend and seasonal part (see Fig-1, Fig-2). The values on linear trend coefficients (bias for the middle of time interval and trend), amplitude (A_1) and phase of annual term, wrms from this model and also average values (bias) for pressure and humidity are presented in the table 1. Values of biases and annual amplitudes for time series of average daily temperature are correlated with latitude of station (correlation coefficient is about 0.6).

We can regard the long time WTD series as combination of linear trend and annual term, too (see Fig-1, Fig-2). The quantities of linear trend coefficients (bias and rate), amplitude (A) and phase of annual term and wrms from this model are presented in the table 1. The string NRAO corresponds both NRAO20 and NRAO85 3 stations. The values of trends are not in a good agreement with [1, 4, 5], but rather closely to the values for Wettzell. (For Wettzell station the values of linear trend [4] obtained for the period since 1984 from 6-hour values by unweighted least-squeares fit was estimated to 0.83 mm/year. The time series was obtained from all geodetic sessions analysis with OCCAM package v.5.1 [7] using Gauss-Markov model for the least-squeares adjustment. WZD was estimated as 1-h piecewise linear function. ITRF2000 was used to fix TRS, Niell mapping functions (1996) and the elevation angle cutoff 8° were upplied. The mean seasonal values have trend of 0.73 mm/year. Analysis of [5] for WZD time series was obtained for the period since 1987 till 2002 with CALC/SOLV, into ITRF2000 without fixing the stations coordinates, using no-net-translation constraint and 5° elevation cutoff and the Niell mapping functions. WZD

Table 1. Average daily values of meteoparameters for VLBI stations.

Station	T, bias, °C	T, rate, °C/year	T, A_1 °C	T, Phase, deg	T, wrms,°C	P, Pa	H, %
WETTZELL	8.4 ±0.1	0.1 ±0.0	9.4 ±0.2	255 ±1	4	945.5	75
GILCREEK	1.3 ±0.1	-0.0 ±0.0	13.6 ±0.2	262 ±1	5	973.0	55
KOKEE	16.1 ±0.1	-0.4 ±0.1	2.4 ±0.1	218 ±3	2	890.1	89
WESTFORD	9.9 ±0.2	0.0 ±0.0	11.8 ±0.2	249 ±1	4	1004.4	61
RICHMOND	21.9 ±0.5	-0.4 ±0.1	4.0 ±0.2	235 ±3	4	1017.1	69
FORTLEZA	29.0 ±0.1	-0.0 ±0.0	1.0 ±0.1	93 ±3	1	1009.4	64
HARTRAO	18.0 ±0.1	0.1 ±0.0	5.8 ±0.2	91 ±2	3	869.3	55
MOJAVE12	20.6 ±0.5	0.5 ±0.1	11.1 ±0.2	253 ±1	4	910.5	23
HRAS 085	16.9 ±0.7	0.3 ±0.1	7.8 ±0.2	255 ±2	4	836.9	45
ALGOPARK	5.5 ±0.2	0.1 ±0.1	13.5 ±0.3	252 ±1	5	986.2	73
NRAO85 3	9.2 ±0.5	-0.1 ±0.1	10.6 ±0.3	252 ±2	4	925.6	72
NRAO20	9.6 ±0.3	0.6 ±0.2	10.4 ±0.4	254 ±2	4	923.1	69
MATERA	15.0 ±0.2	0.1 ±0.0	9.9 ±0.2	247 ±1	4	959.6	67
KAUAI	16.0 ±0.2	-0.1 ±0.0	2.5 ±0.1	223 ±3	2	888.0	79
ONSALA60	9.9 ±0.2	0.1 ±0.0	8.3 ±0.2	249 ±1	3	1010.8	75
NYALES20	-2.4 ±0.2	-0.0 ±0.1	6.2 ±0.2	244 ±2	3	1006.9	70
HOBART26	12.0 ±0.2	-0.3 ±0.1	3.6 ±0.3	82 ±4	3	1011.4	66
KASHIMA	15.0 ±0.4	0.1 ±0.1	8.6 ±0.4	239 ±3	4	1011.1	76
MEDICINA	13.3 ±0.3	-0.1 ±0.1	10.9 ±0.4	260 ±2	4	1013.4	64

was computed with one hour resolution. The linear trend calculated for this series is -0.23 ± 0.11 mm/year. The linear trend after removing annual wave is 0.60 ± 0.08 mm/year. For Medicina station linear trend for WZD time series is 3.3 ± 0.3 mm/year.)

Possible reason of this discrepancy is in different values used for analysis. Values of biases (for the middle of time interval) and annual amplitudes seems in rather good agreement with the average data for stations Wettzell, Westford, Gilcreek, Nyales20, Onsala60, Medicina and Matera [1, 4, 5]. Values of biases for time series of average daily temperature and time series of WZD have a high correlation degree (0.75).

References

[1] *Boehm, J., Schuh, H., Tesmer, V., Scmitz-Huebsch, H.* Determination of Tropospcheric Parameters by VLBI as Contribution to Climatologial Studies. Vermessung & Geoinformation, VGI, 1/2003, 21–28.

[2] *Schuh, H., Boehm, J.* Status Report of the IVS Tropospheric Pilot Project – Tropospheric Parameters in International VLBI Service for Geodesy and Asrtometry. 2002 Annual Report, ed. Vandenberg, N., Baver, K., NASA/TP–2003–211619, 13–21.

[3] *Schuh, H., Boehm, J.* Determination of Tropospheric Parameters Within the new IVS Pilot Project. In: Proceedings of 16th Working Meeting on European VLBI for Geodesy and Asrtometry, Leipzig, Germany, 2003, 257–264.

Table 2. WZD time series parameters.

Station	Obs. Number	T_{beg} - T_{end}	Bias, mm	Trend, mm/year	A, mm	Phase, Deg	wrms, mm
WETTZELL	1078	1984.1 - 2004.0	83.1±1.2	0.4±0.2	37.1±1.5	243 ±3	16
GILCREEK	818	1984.5 - 2003.9	53.9±1.2	0.0±0.2	50.4±1.6	328 ±2	12
KOKEE	881	1993.4 - 2004.0	91.8±1.3	0.4±0.4	20.6±1.9	95 ±5	9
KAUAI	346	1985.6 - 1994.2	108.3±3.2	-2.2±1.4	20.7±4.0	120 ±11	25
WESTFORD	830	1981.4 - 2003.9	102.3±2.4	1.4±0.4	67.0±3.4	123 ±3	18
RICHMOND	553	1984.0 - 1992.6	211.3±2.5	2.1±1.0	65.4±3.5	350 ±3	32
FORTLEZA	645	1993.3 - 2004.0	255.3±1.7	0.3±0.5	62.4±2.4	225 ±3	11
HRAS 085	505	1980.6 - 1990.8	95.6±2.5	-1.0±1.2	50.3±3.4	124 ±4	29
HARTRAO	466	1986.0 - 2003.9	88.1±2.4	3.6±0.5	57.4±3.3	76 ±3	24
MOJAVE12	351	1989.1 - 1992.7	64.0±2.0	9.7±2.1	28.1±2.7	203 ±6	18
ALGOPARK	250	1999.0 - 2004.0	88.5±3.0	-3.4±2.1	68.2±2.1	61 ±4	23
NRAO	541	1989.4 - 2000.5	90.1±2.3	-1.7±0.8	60.8±2.9	230 ±3	11
MATERA	398	1990.8 - 2004.0	98.6±1.7	1.1±0.4	47.5±2.4	6 ±3	20
ONSALA60	354	1980.6 - 2003.8	87.4±2.2	-1.1±0.3	38.6±3.0	315 ±5	12
NYALES20	364	1994.8 - 2004.0	42.0±1.1	1.6±0.4	30.2±1.5	4 ±3	22
HOBART26	256	1989.9 - 2003.9	89.0±3.0	-0.4±0.8	25.9±4.1	15 ±10	27
KASHIMA	198	1984.6 - 2002.4	133.1±6.7	-1.9±1.2	74.2±9.3	49 ±9	38
MEDICINA	152	1987.3 - 2003.8	119.7±3.6	0.3±0.7	54.1±5.4	99 ±5	17
FD-VLBA	98	1992.0 - 2003.5	84.7±4.2	-0.2±1.2	80.8±5.5	262 ±6	38
TSUKUB32	92	1998.5 - 2003.8	172.9 ±6.4	-12.7±4.8	90.9±8.8	315 ±6	31
SANTIA12	87	1991.9 - 1996.9	65.1±6.7	-3.1±2.1	22.8±4.5	55 ±12	30
LA-VLBA	100	1991.4 - 2003.5	73.0±5.2	0.7±1.4	64.1±5.6	37 ±5	13
SC-VLBA	84	1993.5 - 2003.5	215.7±5.3	-0.7±1.8	28.6±6.8	262 ±16	47

[4] *Schuh, H., Boehm, J., Tesmer, V., Schmitz-Huebsch, H.* Tropospheric Zenith Delays by VLBI as Contribution to Climatologial Studies. In: Proceedings of 16th Working Meeting on European VLBI for Geodesy and Asrtometry, Leipzig, Germany, 2003, 237–246.

[5] *Negusini, M., Tomasi, P.* Tropospheric Parameters from Geodetic VLBI Data Analysis. In: Proceedings of 16th Working Meeting on European VLBI for Geodesy and Asrtometry, Leipzig, Germany, 2003, 189–202.

[6] *Malkin, Z., Skurikhina, E., Sokolskaya, M., Krasinsky, G., Gubanov, V., Surkis, I., Kozlova, I., Rusinov, Yu.* IAA VLBI Analysis Center Report for 2000. In: 2000 IVS Annual Report, 2001, 232–235.

[7] *Titov, O., Tesmer, V., Boem, Y.* OCCAM 5.1 User's Guide. AGU, 2002.

[8] `http://www.ipa.nw.ru/PAGE/DEPFUND/GEO/\-ac_vlbi/index.htm/sessstat.dat`

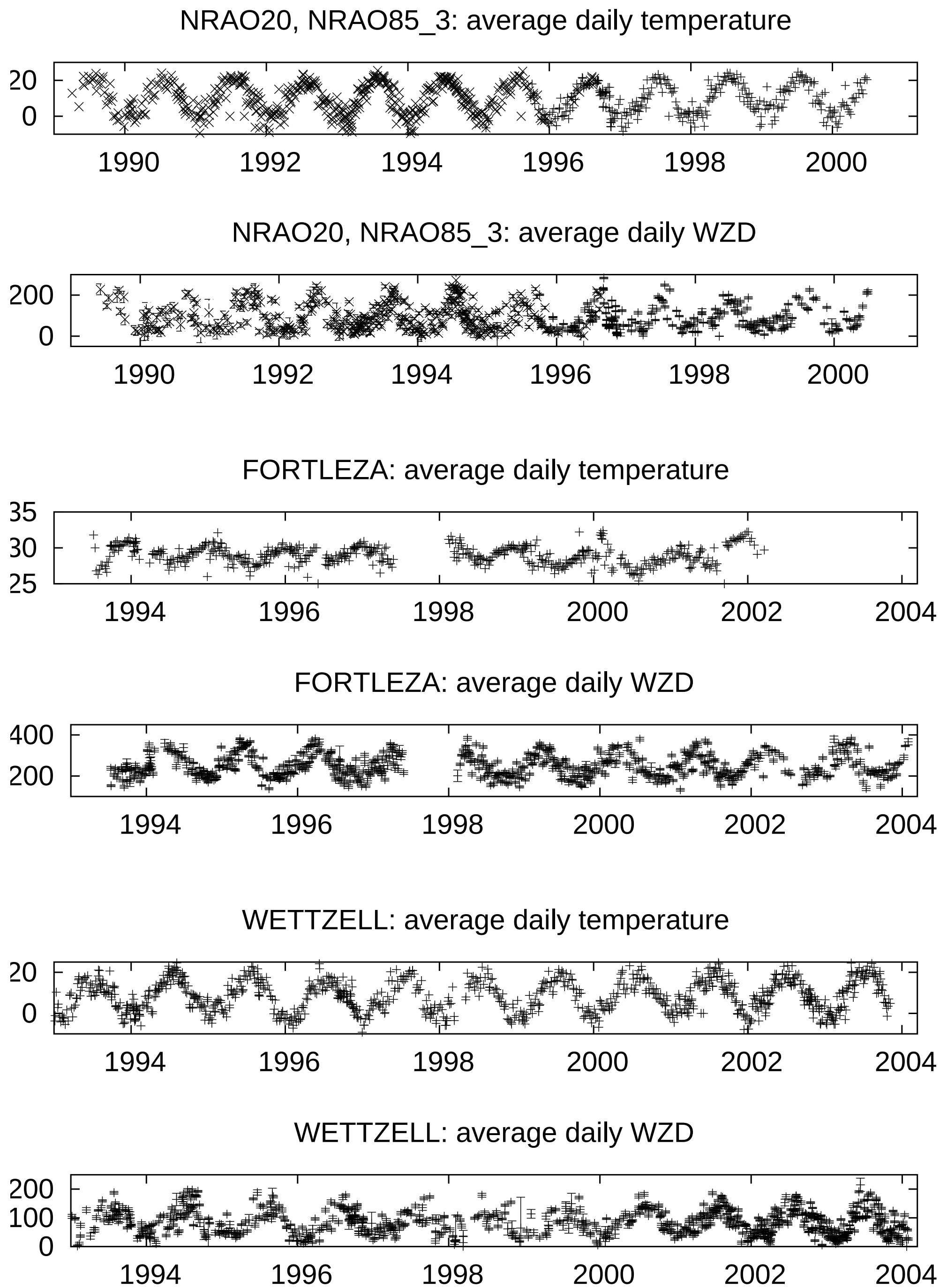

Figure 1. WZD and daily average temperature.

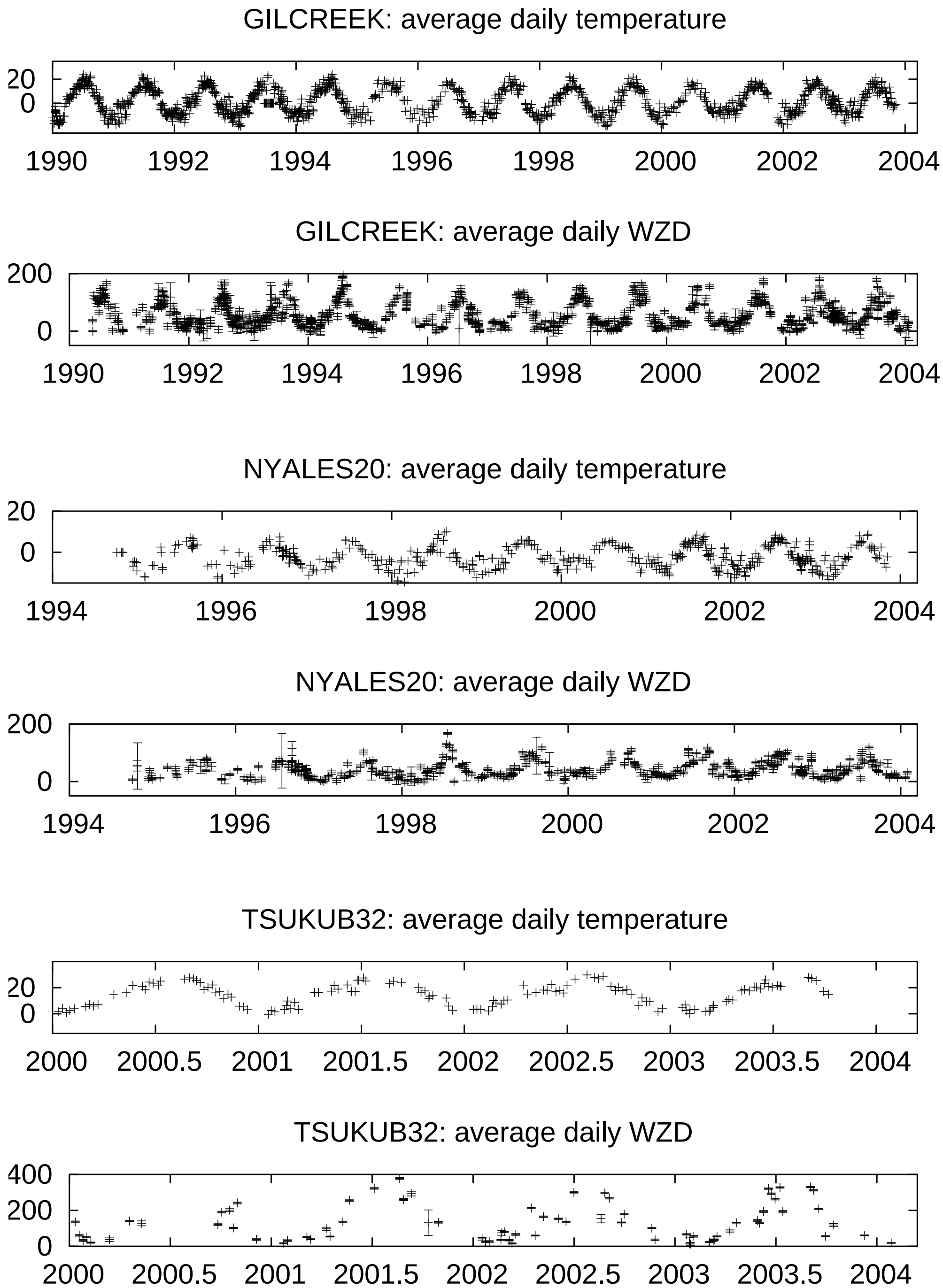

Figure 2. WZD and daily average temperature.

Bisser Stoyanov et al.: Calculating Mapping Functions from the HIRLAM Numerical Weather Prediction Model,
IVS 2004 General Meeting Proceedings, p.471–475
http://ivscc.gsfc.nasa.gov/publications/gm2004/stoyanov

Calculating Mapping Functions from the HIRLAM Numerical Weather Prediction Model

Bisser Stoyanov, Rüdiger Haas, Lubomir Gradinarsky

Onsala Space Observatory, Department of Radio and Space Science, Chalmers University of Technology
Contact author: Rüdiger Haas, *e-mail:* `haas@oso.chalmers.se`

Abstract

Modelling of the tropospheric effects caused by neutral atmosphere in space geodetic techniques like VLBI and GPS requires the use of mapping functions. Several different mapping functions are presently in use, some of them based on numerical weather models. We used the HIRLAM 3D-VAR numerical weather prediction model for a direct calculation of mapping functions via raytracing. The advantages of this approach are the high spatial resolution (0.2° x 0.2°) of this model as well as its capability to provide data every 3 hours in a prediction mode. Mapping functions were fit down to a 3.0° elevation angle for the VLBI sites Onsala (Sweden) and Wettzell (Germany). These new HIRLAM based mapping functions (HBMF) were tested on VLBI measurements acquired in the year 2000.

1. Mapping Functions

On their way through the earth's atmosphere, the electromagnetic signals used by space geodetic techniques like VLBI and GPS experience propagation delays. The propagation delays relate to the refractivity of the medium which for the so-called neutral part of the atmosphere is influenced by temperature, pressure and humidity. To model these delays, usually so-called mapping functions are used to relate the slant delay at an elevation angle ϵ to a zenith delay value. Usually the total slant delay is separated into a so-called hydrostatic (h) and a wet part (w):

$$\Delta L(\epsilon) \quad = \quad \Delta L_w^z \times m_w(\epsilon) + \Delta L_h^z \times m_h(\epsilon) \tag{1}$$

The left hand side of Equation 1 gives the total slant delay, the zenith wet delay is depicted with superscript z and subscript w, the zenith hydrostatic delay is depicted with superscript z and subscript h, and the corresponding mapping functions m as a function of elevation ϵ are shown with subscripts w and h, respectively.

Today widely used mapping functions are based either on surface meterological data [1], on climatology, e.g. [2], or to some extend on numerical weather models, e.g. [3], [4]. A continued fraction form is often used as mapping function:

$$m(\epsilon) \quad = \quad \frac{1 + \frac{a}{1+\frac{b}{1+c}}}{\sin\epsilon + \frac{a}{\sin\epsilon + \frac{b}{\sin\epsilon + c}}} \tag{2}$$

2. Numerical Weather Prediction Models

The physical laws of motion and conservation of energy, e.g. Newton's Second Law of Motion and the First Law of Thermodynamics, govern the evolution of the atmosphere. These laws can be converted into a series of mathematical equations that make up the basics of what is called numerical weather prediction. In 1904, Vilhelm Bjerknes suggested that numerical weather prediction was possible [5]. He proposed that weather prediction could be seen as an initial value problem in mathematics. In NWP, future values of meteorological variables are obtained by finding their initial values and then adding the physical forcing that acts on the variables over the time period of the forecast.

3. The HIRLAM 3D-VAR Numerical Weather Prediction Model

The HIgh Resolution Limited Area Model (HIRLAM) was established in order to provide the best available operational short-range forecasting system for the HIRLAM member institutes. These are the National Meteorological Services in Denmark, Finland, Iceland, Ireland, Netherlands, Norway, Spain and Sweden. Meteo-France has a research cooperation agreement with HIRLAM. The HIRLAM system is a complete NWP system including data assimilation with analysis of conventional and non-conventional observations and a limited area forecasting model with a comprehensive set of physical parameterisation [6]. The boundary conditions are adopted from the ECMWF (European Centre for Medium-Range Weather Forecasts) analysis. The HIRLAM forecast model is a limited area model with a boundary relaxation scheme. Figure 1 shows an example of a HIRLAM area and Table 1 gives some characteristics of the ECMWF and HIRLAM numerical weather models.

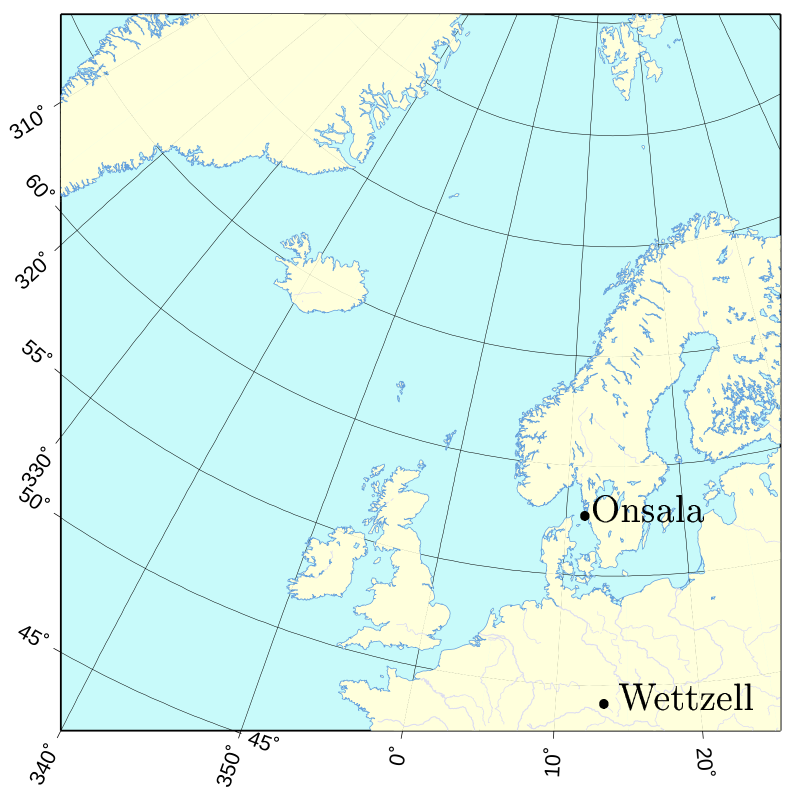

Figure 1. An example of a HIRLAM model area. Shown are the locations of Onsala and Wettzell.

Table 1. Some characteristics of numerical weather models.

	ECMWF	HIRLAM
Spatial resolution	$2.5^o \times 2.5^o$	$0.2^o \times 0.2^o$
Number of pressure levels	15	31
Temporal resolution in post processing mode	6 hours	6 hours
Temporal resolution in prediction mode	6 hours	3 hours

4. HIRLAM Based Mapping Functions

The HIRLAM based mapping functions were calculated via ray-tracing through HIRLAM model fields. For each location (λ, β) and time epoch the values for pressure (P), temperature (T in Kelvin), specific humidity (sH) were extracted from the model in the form of 31 vertical levels. In order to be used with the Raytrace software [7] the equivalent values for height (h), pressure (P), temperature (t in Celsius) and relative humidity (rH) were computed. The hydrostatic and wet mapping functions were then determined by raytracing at 25 different elevation angles and estimating the coefficients a, b, c in Equation 2 from a least-squares analysis. The raytracing was performed for elevations 3^o–25^o in steps of 2^o, and elevations 25^o–90^o in steps of 5^o. This was done for the stations Onsala and Wettzell for 30 VLBI experiments between June and November 2000. Wettzell was included in all 30 experiments, while Onsala was only included in 4 of them.

The HIRLAM Based Mapping Functions (HBMF) were compared to the New Mapping Functions (NMF) [2] and the fast version of the Vienna Mapping Functions (VMF) [4] for identical time epochs and elevation angles for Onsala and Wettzell. Figure 2 shows the differences between HBMF and NMF (dashed, red lines), and HBMF and VMF (blue, solid lines) for 5^o elevation. The differences are larger for the wet mapping functions than for the dry mapping functions. In general the agreement is better between HBMF and VMF than between HBMF and NMF. However, there also appear to be systematic differences between the ECMWF and HIRLAM models.

5. Application of HBMF in VLBI Data Analysis

We applied the HBMF in the VLBI data analysis of 30 VLBI experiments including Onsala and/or Wettzell between early June and end of October 2000. For this purpose the VLBI analysis software SOLVE was modified to incorporate the new mapping functions. We performed three different analysis strategies: a) NMF for all sites, b) VMF for Onsala and Wettzell but NMF for all other sites, and c) HBMF for Onsala and Wettzell but NMF for all other sites. Figure 3 shows baseline length repeatability in terms of weighted root mean-square (wrms) as a function of baseline length for all baselines connecting to Onsala and/or Wettzell. For all but one baseline the repeatability improved when either VMF or HBMF were used instead of NMF. For 5 out of 8 baselines the reapeatability impoved when HBMF were used instead of VMF. The average improvement in wrms was 5% when HBMF were used instead of NMF, and 3% when HBMF were used instead of VMF. The baseline with the largest improvement in terms of wrms is the baseline Onsala-Wettzell (920 km), with an improvement of 11% and 9% when HBMF were used instead of NMF or VMF, respectively.

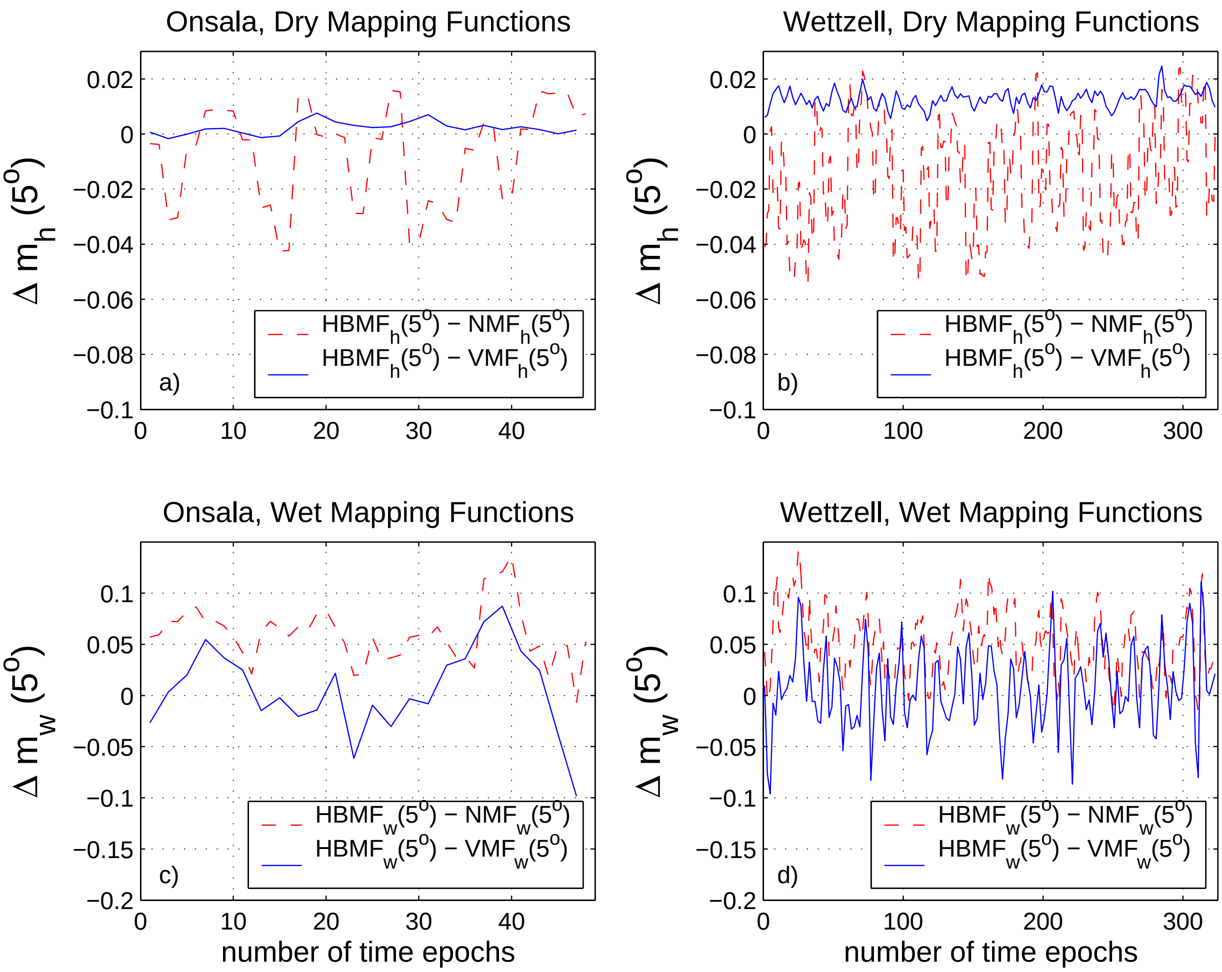

Figure 2. Comparison of HBMF with NMF (dashed, red lines) and HBMF with VMF (blue, solid lines) for identical time epochs and 5° elevation for Onsala and Wettzell. Differences of the hydrostatic mapping functions are shown in the two upper plots, differences of the wet mapping functions in the two lower plots. The x-axes depict the number of time epochs for which the differenes were calculated, while the y-axes depict unitless differences. The total number of displayed differences HBMF-NMF and HBMF-VMF are 48/24 for Onsala and 324/162 for Wettzell.

6. Conclusions and Outlook

New HIRAM based mapping functions (HBMF) were derived and successfully tested in VLBI data analyses. Six months of VLBI experiments in the year 2000 that included the VLBI sites Onsala and/or Wettzell were analysed with these new mapping functions. Comparison to analyses with the New Mapping Functions (NMF) and the fast version of the Vienna Mapping Functions (VMF) show, that the HBMF perform better than the other two approaches. The average improvement in terms of baseline repeatability is on the level of 5% with respect to NMF and on the level of 3% with respect to VMF. Although so far only six months of VLBI data from two

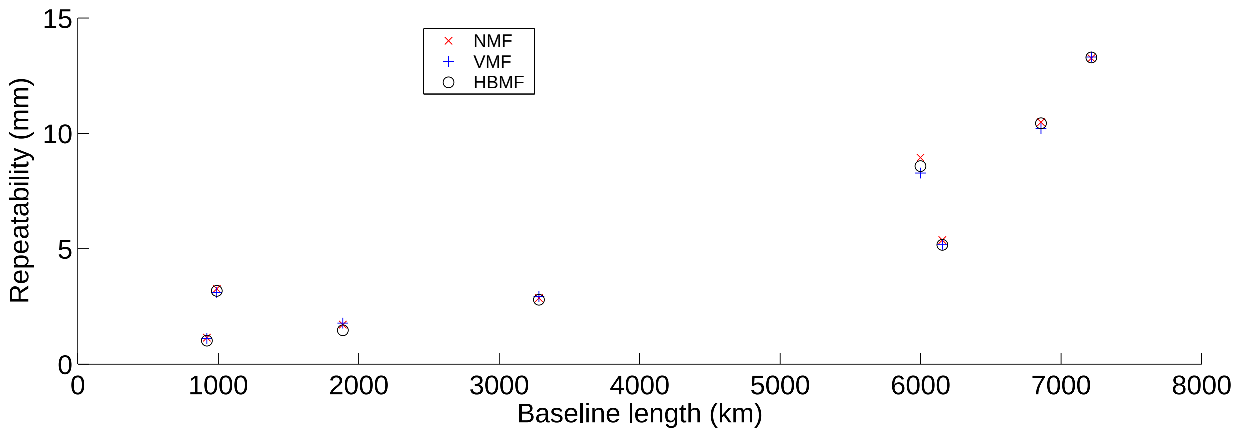

Figure 3. Baseline length repeatability for all baselines that connect to the stations Onsala and/or Wettzell between June 6 and October 24, 2000. Weighted root-mean-square (wrms) values are plotted against baseline length. For all but one baseline the repeatability impoved when either VMF or HBMF were used instead of NMF. For 5 out of 8 baselines the repeatability improved when HBMF were used instead of VMF.

European sites have been analysed with HBMF, these preliminary results indicate the potential to base new mapping functions on high temporal and spatial resolution numerical weather prediction models, such as HIRLAM.

References

[1] Herring, T.A.: Modelling atmospheric delay in the analysis of space geodetic data. In: *Proceedings of Symposium on Refraction of Transatmospheric Signals in Geodesy*, J.C. de Munck and T.A.Th. Spoelstra (eds.), Netherlands Geodetic Commission, Publications on Geodesy, No. 36, New Series, 157–164, 1992.

[2] Niell, A.E.: Global mapping functions for the atmosphere dalay at radio frequences. *Journal of Geophysical Research*, **101(B2)**, 3227–3246, 1996.

[3] Niell, A.E.: Preliminary evaluation of atmospheric mapping functions based on numerical weather models. *Physics and Chemistry of the Earth*, **26**, 475–480, 2001.

[4] Böhm, J., and Schuh, H.: Vienna mapping functions in VLBI analysis. *Geophysical Research Letters*, **31**, L01603, doi:10.1029/2003GL018984, 2004.

[5] Bjerknes, V.: Das Problem der Wettervorhersage betrachtet vom Standpunkt Mechanik und Physik. (The problem of weather forecasting as a problem in mechanics and physics.) *Meteorologische Zeitschrift*, **21**, 1–7, 1904.

[6] Källén, E.: HIRLAM Documentation Manual. System 2.5. Technical report, SMHI, Norrköping, Sweden, 1996.

[7] Davis, J.L., Herring, T.A.H, and Niell, A.E.: The Davis/Herring/Niell raytrace program, 1987-1989.

Daniel MacMillan et al.: Mass Loading Effects on Crustal Displacements Measured by VLBI, IVS 2004 General Meeting Proceedings, p.476–480
http://ivscc.gsfc.nasa.gov/publications/gm2004/macmillan1

Mass Loading Effects on Crustal Displacements Measured by VLBI

Daniel MacMillan [1], *Jean-Paul Boy* [2]

[1] *NVI, Inc./NASA Goddard Space Flight Center*
[2] *Institut de Physique du Globle de Strasbourg*
Contact author: Daniel MacMillan, e-mail: dsm@leo.gsfc.nasa.gov

Abstract

The geodetic precision of VLBI (very long baseline interferometry) has improved to the level that baseline lengths can be measured with a wrms precision of 1 ppb and site positions with precision of 8-14 mm in the vertical and 2-3 mm in the horizontal components. Observed VLBI site position variations contain significant contributions at seasonal (annual and semiannual) frequencies. Here, we will concentrate on the site vertical annual amplitudes that mostly range from 2-6 mm. We determine the extent to which annual site variations can be explained by mass loading signals. Specifically, we examine the contributions from atmosphere pressure loading, hydrologic loading, and nontidal ocean loading. We have also examined the effect of two modeling errors specific to the VLBI measurements: tropospheric delay mismodeling (hydrostatic mapping function) and antenna thermal deformation.

1. Loading Models

We have computed the site displacements due to each contribution to mass loading using the Green's function approach [Farrell, 1972]. For atmospheric pressure loading, the NCEP Reanalysis numerical weather model gridded data was used. A complete description of the procedure used and the validation of the model using VLBI observations is given in Petrov and Boy [2003]. Hydrologic loading was computed using a model of large-scale continental water and energy balances developed by Milly and Shmakin [2002]. The sum of model storage outputs of soil water, groundwater, and snow yields the monthly continental water storage. Nontidal ocean loading was computed using ocean bottom pressure fields from the ECCO (Estimating the Circulation and Climate of the Ocean ocean) model. The annual amplitude and phase for hydrology loading is shown in Figure 1. The maximum amplitude over the continents is 4 mm, but the average amplitude for VLBI sites is about 2 mm. The phase (where the signal is maximum) over most of the northern hemisphere is around 180 days (summer months).

2. Solution Description

Group delay data were analyzed from more than 3500 experiment sessions carried out from 1984 through 2003 amounting to over 4 million observations. For this work, we have concentrated on observations from 36 VLBI stations that have observed the most frequently. In our standard terrestrial reference frame (TRF) solutions, we estimate the site positions, velocities, and radio source positions as global parameters. The VLBI program SOLVE and most of the theoretical models that are generally applied are described in Ma et al. [1990]. The VLBI delay observable is invariant to several transformations of the estimated variables. To remove the corresponding

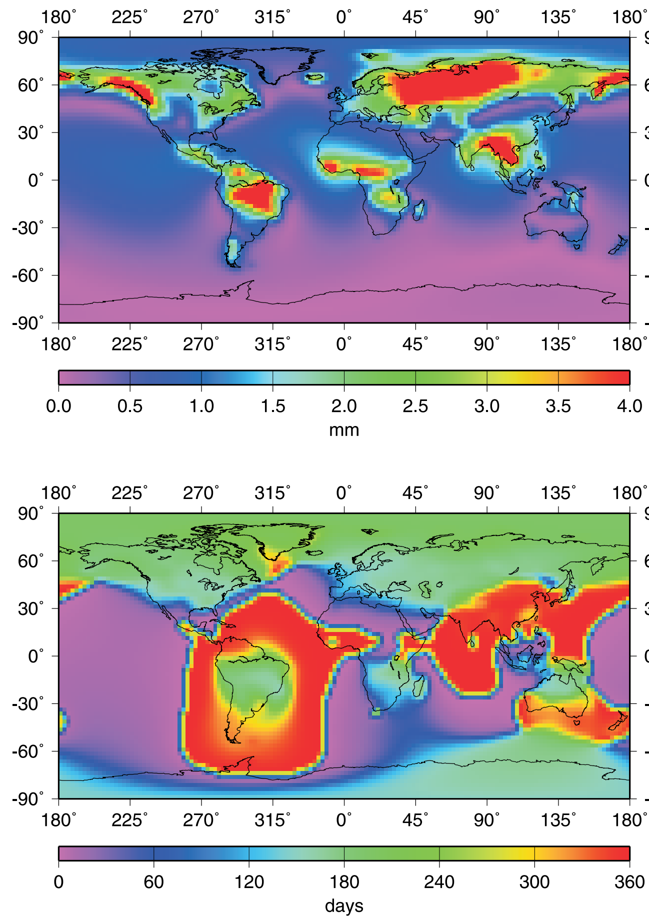

Figure 1. Annual amplitude (top) and phase (bottom) of the vertical displacement due to loading computed using the hydrology model of Milly and Shmakin [2003].

degeneracies, no net translation (NNT) and no net rotation (NNR) conditions are applied to align the TRF with the ITRF2000 and celestial reference frame with the ICRF positions. For the analysis of seasonal variation, we estimated the cosine and sine components of site displacement at annual and semiannual frequencies as additional global parameters for the 36 sites. To remove translational and rotational degeneracies, additional NNR and NNT constraints were applied. The phase of the variations of the expected seasonal vertical signals (mass loading, antenna thermal deformation) for Northern Hemisphere sites will generally be opposite the phases for Southern Hemisphere sites. In order not to constrain the estimated vertical seasonal variation and avoid biasing results due to predominance of Northern Hemisphere sites, the NNT condition constrained the sum of only the horizontal components of site amplitude adjustments to zero.

3. Results

We have run several solutions in which different combinations of models have been appplied. In Figures 2 and 3, the annual vertical amplitudes are shown for the most frequently observing VLBI

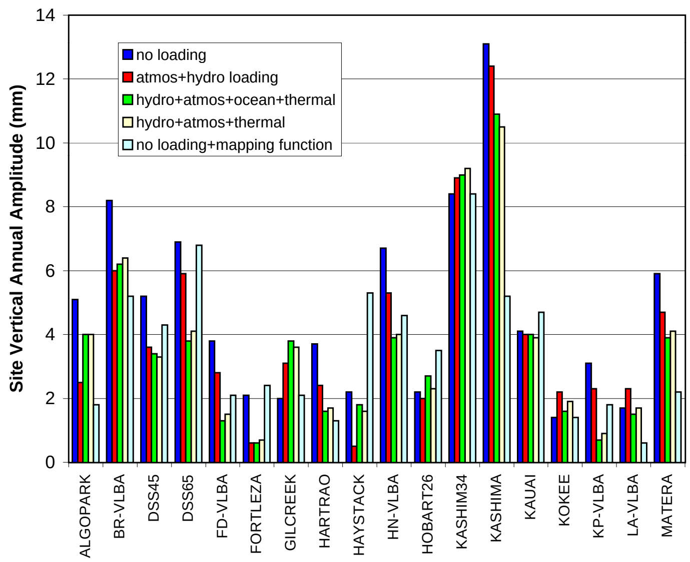

Figure 2. Observed site annual vertical amplitudes and effect of applying different models.

sites. The observed amplitudes are mostly in the range 2-8 mm. After applying hydrology loading, 70% of the amplitudes are reduced by up to 3 mm. Since the nontidal ocean loading amplitude is at most 1 mm (coastal sites), its contribution to the observed amplitudes is very small.

Phasor plots of the observed site amplitudes and the different model contributions are shown in Figure 4 for Medicina and Fairbanks. The sum of the model contributions lies within the 2-sigma error ellipse of the observed annual variation at Medicina. For Fairbanks, we do not see this agreement, but it can be seen that if the contribution from snow loading is not included, that the agreement is better. Snow modeling is known to be poor at higher latitudes mainly due to lack of sufficient data.

We have made comparisons of site vertical amplitudes from colocated VLBI and GPS antennas using GPS amplitudes from Dong et al. [2002]. Figure 5 shows that there is good agreement for a few sites, but the overall agreement is not very good. The amplitudes are within 1 mm for only 4 sites and within 2 mm for 13 sites.

4. Other Seasonal Errors

The reference points on VLBI antennas range from 5-25 meters above the ground. An antenna structure will expand and contract in response to temperature variations. For an expansion coefficient of 1.2 x 10^{-5} K^{-1} for steel, an annual variation of 40 C (Fairbanks, Alaska) and a reference height of 15 meters, the annual variation in height will be about 4 mm. To model this variation in our analysis, we applied a simple expansion model for each antenna using the height of the reference point and the expansion coefficient (either for steel, aluminum, or concrete depending on the antenna). For each 24-hour session, the average measured temperature was used since we were only interested in seasonal variations and were not trying to model the diurnal variation of antenna height. For many sites, the estimated annual vertical amplitude is reduced when this model is applied. See Figures 2 and 3 and the example of Medicina in Figure 4. This can be seen

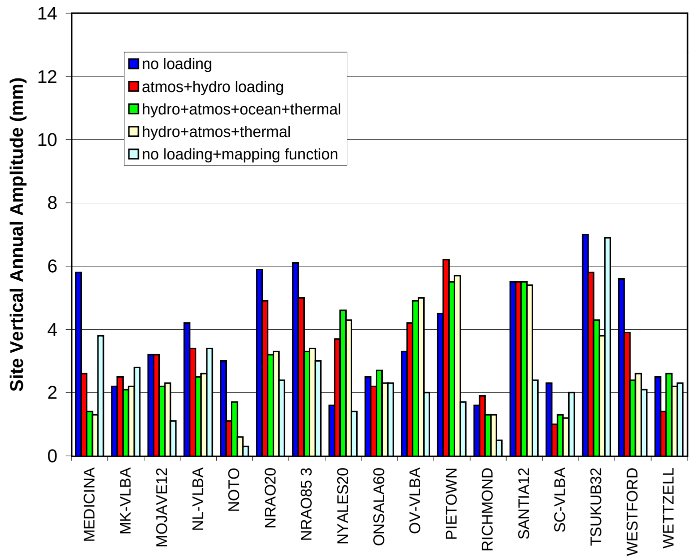

Figure 3. Observed site annual vertical amplitudes and effect of applying different models.

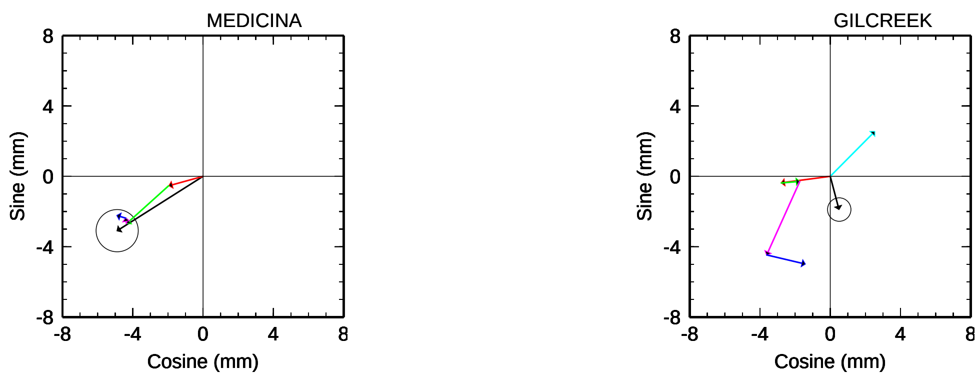

Figure 4. Annual site vertical amplitudes observed at Medicina and Gilcreek (black with 2-sigma error ellipse). For comparison the model contributions to the observed amplitude are summed head to tail starting at the origin: antenna thermal deformation, soil moisture loading, snow loading,and pressure loading.

by comparing the second and fourth bars for each site in Figures 2 and 3.

Our current modeling of tropospheric delay uses the NMF [Niell, 1996] hydrostatic and wet mapping functions. The NMF hydrostatic mapping function has annual amplitudes that depend on latitude. The NMF annual variation reproduces the radiosonde raytrace annual variation reasonably well, but there are errors in amplitude and phase at some sites. To investigate this, we estimated site dependent mapping function parameters (offsets and annual amplitudes of the mapping function coefficients) from the VLBI data. Figures 2 and 3 show that the annual site vertical amplitudes are significantly reduced when these estimated mapping function parameters are applied as a model. This is indicated by the difference between the first and last bars for each site in these figures. More work is required to verify that the estimated mapping functions are reasonable; specifically they will be compared with mapping functions derived from numerical weather model

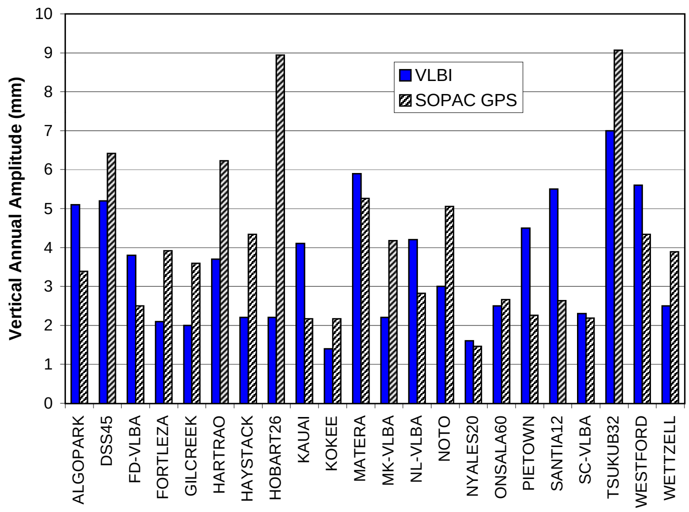

Figure 5. Comparison of annual vertical amplitudes from colocated VLBI and GPS sites.

data (for example, the IMF mapping function derived by A. Niell).

5. Discussion

We find that the annual amplitudes of VLBI vertical displacement are mostly 2-8 mm. The phase of southern hemisphere site variation is generally opposite that for northern hemisphere sites. When hydrology loading models are applied, annual amplitudes are reduced for 70% of the most frequently observing VLBI sites. For most baselines, length repeatabilities are improved. The sum of the annual contributions from mass loading and antenna thermal deformation account for a significant portion of the observed VLBI annual signal at many sites.

References

[1] Dong, D., P. Fang, Y. Bock, M. K. Cheng, and S. Miyazaki, Anatomy of apparent seasonal variations from GPS-derived site position time series, J. of Geophys. Res., 107, B4, 10.1029/2001JB000573,2002.

[2] Farrell, W. E., Deformation of the Earth by surface loads, Rev. Geophys. Space Phys., 10, 761-797, 1972.

[3] Ma, C., J. M. Sauber, L. J. Bell, T. A. Clark, D. Gordon, W. E. Himwich, and J. W. Ryan, Measurement of horizontal motions in Alaska using very long baseline interferometry, J. Geophys. Res, 95(B13), 21991-22011, 1990.

[4] Milly, P. C. D. and A. B. Shmakin, Global modeling of land water and energy balances. Part I: The land dynamics (LaD) model, J. Hydrometeorology, 3, 283-299, 2002.

[5] Niell, A. E., Global mapping functions for the atmospheric delay at radio wavelengths, J. Geophys. Res, 101(B2), 3227-3246, 1996.

[6] Petrov, L. and J. -P. Boy, Study of the atmospheric pressure loading signal in VLBI observations, J. Geophys. Res, 2004 (in press).

Zhigen Yang et al.: Relative Deformations between Co-located VLBI Stations and Comparisons with VTRF2003,
IVS 2004 General Meeting Proceedings, p.481–485
http://ivscc.gsfc.nasa.gov/publications/gm2004/Yang1

Relative Deformations between Co-located VLBI Stations and Comparisons with VTRF2003

Zhigen Yang [1], *Mario Bérubé* [2], *Anthony Searle* [2]

[1] *Shanghai Astronomical Observatory (SHAO), Chinese Academy of Sciences (CAS)*
[2] *Geodetic Survey Division (GSD), Natural Resources Canada (NRCan)*

Contact author: Zhigen Yang, *e-mail:* `yangz@center.shao.ac.cn`

Abstract

This study discusses results of the relative deformations between nearby stations at 6 co-located VLBI sites based on the 3-D velocity solutions in ITRF2000 as references and using the NNR- NUVEL-1A model to calculate the modelled horizontal motions. Some international VLBI stations, which, in this method, have large difference for vertical deformations relative to previous solutions, are also discussed. Comparisons of the results with those of the ITRFs, VTRF2003 are addressed. The technique determines improved deformations at a regional or local spatial scale, isolating the "inconsistencies" from the ITRF solutions.

1. Introduction

Our knowledge of the regional/local crustal deformation is not perfect. As an example, In 1996, different values of vertical deformation rate (VDR) and horizontal deformation rate (HDR) of KASHIMA and KASHIM34 VLBI stations at the KASHIMA VLBI site in Japan, were published [1]. In the ITRF96, ITRF97 and ITRF2000 solutions the same 3-D velocity values for these two stations were published [2]. Similar examples include NRAO85-3, NRAO20 and NRAO140 stations at GREENBANK, Westford and Haystack stations at Westford Massachusetts, HRAS 085 and FD-VLBA stations at Fort Davis, and KAUAI and KOKEE stations in Hawaii, where the same 3-D station velocity values are used for each site.

At present, the estimated average uncertainty for VLBI baseline rates in glb2001 is ± 1.62 mm/yr. The recent global baseline rate solution in glb2003 [3] is about ± 1.45 for average uncertainty. Therefore, the further analysis of the relative deformation between two closely spaced VLBI stations separated by a few hundred to few thousand meters has been possible. Some international VLBI stations, which in this approach have large difference in vertical deformation relative to previous solutions, are also addressed. The results in VTRF2003 [4] were used as available comparisons.

2. Methodology

Let B_{ki} be the determined baseline length from target station k to a international VLBI station i , $\dot{B}_{ki}$ is its changing rate, the observation equation can be written as:

$$B_{ki} \cdot \dot{B}_{ki} = (\vec{R}_i - \vec{R}_k) \cdot \vec{\Omega}_{ki} \tag{1}$$

where $\vec{R}_k$ and $\vec{R}_i$ are the position vectors of k and i, respectively, $\vec{\Omega}_{ki}$ is the relative changing rates between $\dot{\vec{R}}_k$ and $\dot{\vec{R}}_i$, in which the $\dot{\vec{R}}_i$ is the velocity vector of $\vec{R}_i$, which is taken from ITRF reference frame, while $\dot{\vec{R}}_k$ is the velocity vector of target station, which is regarded as unknown quantities to be estimated by the weighted least squares algorithm under constraints of the $\dot{B}_{ki}$. In our problem, the effects of uncertainties of the $\dot{\vec{R}}_i$ to the estimation of $\dot{\vec{R}}_k$ can be considered as random errors in a certain degree. The deformation rates $\vec{V}_{def}$ of target station then follow from

$$\vec{V}_{def} = \dot{\vec{R}}_k - \omega_{mod} \times \vec{R}_k, \tag{2}$$

where ω_{mod} is the Eulerian vector of plate which the target station is located in. Thus, the deformation vector of target station $\vec{V}_{def}$ can be precisely estimated. In the estimation above, due to the determination of the relative distance between two points on the surface of the Earth along the direction of baseline is theoretically independent of the adopted terrestrial reference frame (TRF) [5], and the uncertainties of $\dot{\vec{R}}_i$ in ITRF reference frame can be considered as random errors, thus, under the constraints of $\dot{B}_{ki}$, the estimation of the $\dot{\vec{R}}_k$ and $\vec{V}_{def}$ of target station can be relatively accurately estimated. In our estimation above, the weight W_p is expressed as:

$$W_p = \frac{1}{\sigma_i^2} + \frac{1}{\sigma_{ki}^2} \tag{3}$$

where σ_i and σ_{ki} are the uncertainties of the $\dot{\vec{R}}_i$ and the $\dot{B}_{ki}$, respectively.

3. Data

VDR and HDR of co-located stations can be estimated by using all baseline rates to each station (BR 1) and by using only baselines with stations common to the co-located stations (BR 2). For this work, all baseline rates came from the glb2001 solution. For comparison, VDR and HDR were determined from the VTRF2003 solution (BR 3).

The VDR and HDR of the KOKEE and KAUAI stations, which are located on the Pacific plate, were analysed using the rates of baseline length change from KOKEE to 31 global VLBI stations, and from KAUAI to 16 international VLBI stations. The velocity vectors of the global VLBI stations were referenced to ITRF2000, and Eulerian vectors of NNR-NUVEL-1A plate model, which was used to calculate the modelled horizontal motions of these two stations. The baseline rates of the KOKEE and KAUAI station relative to 13 common international VLBI stations were used for addressing the relative deformation between these two stations.

The baseline rates between KASHIMA and 27 global VLBI stations and between KASHIM34 and 12 global stations were used as input parameters to determine the 3-D deformation and the relative deformation between these two stations. The baseline rates of the KASHIMA and KASHIM34 stations relative to 9 common global VLBI stations were processed to validate the VDR difference above. The 3-D deformation rates of the NRAO85-3, NRAO20 and NRAO140 VLBI stations at the GREENBANK site were accordingly addressed for obtaining the relative deformation rates between NRAO20 and NRAO85-3, and between NRAO140 and NRAO85-3. The baseline rates of the NRAO85-3 and NRAO20 stations relative to 9 common international VLBI stations were also processed for validating the relative deformation rates between NRAO20 and NRAO85-3.

Finally, the relative deformations between Westford and Haystack station at Westford VLBI site, and between HRAS 085 and FD-VLBA station at Fort Davis VLBI site, were addressed using the similarly method mentioned above.

4. Results

The VDRs and HDRs of stations in 6 co-located VLBI sites were estimated, and the relative deformation rates between co-located stations are given in Table 1. The velocity vectors of the global VLBI stations were referenced to ITRF2000. In additional, the VDRs and HDRs of about 50 international VLBI stations were re-estimated using our method above. The majority of stations showed no significant deviation from published TRF values. Eight stations which show visible vertical deformation differences relative to global solutions, are given in Table 2.

Table 1. The relative local/regional crustal VDRs and HDRs between co-located VLBI stations.

Co-located station	BR	Rel. Ver. def. rate (mm/yr)	Rel. Hor. def. rate E(mm/yr)	Rel. Hor. def. rate N(mm/yr)
KAUAI-KOKEE	1	1.01±0.90	-1.96±0.66	1.56±1.15
	2	3.15±0.97	-4.25±0.62	2.48±1.20
	3	-0.18±0.49	-1.82±0.43	1.05±0.50
KASHIM34-KASHIMA	1	-3.74±1.33	-0.10±1.08	0.57±1.47
	2	-3.94±1.64	-0.14±1.34	1.35±1.78
	3	-2.17±0.52	0.10±0.50	2.44±0.54
NRAO20-NRAO85 3	1	3.10±0.87	-0.28±0.59	0.24±0.93
	2	3.92±0.62	-0.34±0.46	0.60±0.67
	3	3.06±0.45	0.68±0.42	0.89±0.47
NRAO140-NRAO85 3	1	3.54±1.27	-1.78±0.63	1.02±1.36
	3	-0.30±0.52	0.67±0.42	-0.24±0.54
FD-VLBA-HRAS 085	1	-2.70±1.46	-0.68±0.46	-2.76±1.67
	3	4.04±0.64	-0.24±0.44	0.63±0.60
HAYSTACK-WESTFORD	1	1.64±1.48	-0.14±0.84	0.13±1.50
	3	2.14±0.57	0.79±0.45	0.21±0.57

5. Concluding Remarks and Discussion

1. The VDR and HDR of stations at 6 co-located VLBI sites are directly estimated using the observed baseline rates as input parameters. The determination of the relative distance between two points on the surface of the Earth is theoretically independent on the adopted TRF, the uncertainties of the velocities of the international VLBI stations in ITRF2000 can be considered as random errors in the weighted least squares estimator, and the definition of the adopted TRF in this estimation is clear. Therefore, the obtained results in Table 1 and 2 are probably reliable.

2. To validate the results above, the baseline rates of KOKEE and KAUAI stations relative to 13 common global VLBI stations, KASHIMA and KASHIM34 stations relative to 9 common VLBI stations, and NRAO85 3 and NRAO20 stations relative to 9 common VLBI stations are respectively processed using the same method. In Table 1, the relative VDR value between Kashima and Kashima34 stations is about 4 mm/yr, which is approximately the same as the 5.10±1.12 mm/yr obtained by Yang et al.(2002) based on ITRF97 reference frame. This shows that the VDRs of

these two stations in Japan probably indeed differ with each other, while their HDRs are basically the same. Additional, the local/regional VDRs and HDRs between KOKEE and KAUAI stations are also probably different from each other. The relative VDR values between NRAO20 and NRAO85 3, and between Haystack and Westford are basically the same as those of VTRF2003, respectively. The VDR of HRAS 085 station needs to be further discussed.

3. As the separation between the stations in each co-located VLBI site is only about few hundred to few thousand meters apart, we re-estimated their local/regional deformation rates by combining their respective rates for each site based on ITRF2000 reference frame and NNR-NUVEL-1A plate model. It is found that the common deformation rate of stations in each co-located VLBI site is basically same as those of ITRF2000 solution.

4. We estimated the VDRs and HDRs of about 50 global VLBI stations by using the same method. The deformation rates of 8 stations (see Table 2), especially their vertical deformation components, show visible differences compared to previous solutions. The estimated deformation rates by using the observed baseline rates from glb2003 (see BR(2) results) basically validated the estimated results by using the baseline rates from glb2001 (see BR(1) results). Most of the estimated HDRs show approximately coherent results with those of ITRFs and/or VTRF2003 solution. The outlier stations suggest that this method can be used to monitor the results of TRF solutions derived from VLBI observations. It would be necessary for ITRF to separately give out the velocity vectors of stations in co-located VLBI site so as to perform studies of station's 3-D deformation rates.

On a research leave at GSD, NRCan from SHAO, CAS. Supported by key research project of National Astronomical Obs., CAS and GSD, NRCan.

References

[1] 1996 IERS ANNUAL REPORT, Observatoire de Paris, 1997.

[2] Boucher C.,Altamimi Z., Sillard P., and Martine Feissel-Vernier, The ITRF2000 reference frame, IERS technical Note No.31, Observatoire de Paris, 2001.

[3] Ma C., D. MacMillan, L. Petrov, D. Gordon, K. Baver, glb2003cn, NASA Goddard Space Flight Center, http://lupus.gsfc.nasa.gov/global/glb.html/, August 2003.

[4] Nothnagel A., VTRF2003: A Conventional VLBI Terrestrial Reference Frame, http://miro.geod.uni-bonn.de/vlbi/IVS-AC/vtrf2003/vtrf2003, 2003.

[5] Ma C., M. Sauber, L.J.Bell, T.A. Clark, D.Gordon, W.E. Himwich, and J.W. Ryan, measurement of Horizontal Motion in Alaska using Very Long Baseline Interferometry, J.Geophys.Res., 95(B13): 21991-22011, 1990.

Table 2. Crustal deformation rates of eight global VLBI stations and its comparisons with ITRF solutions

VLBI station	TRF	VDR(mm/yr)	HDR(mm/yr)	AZ(deg)	Plate
SC-VLBA	ITRF97	3.37±0.90	6.50±0.63	91.9±2.0	CARB
	ITRF2000	1.10±0.54	7.33±0.42	73.5±3.3	
	BR(1)	5.89±0.78	6.94±0.54	71.3±5.3	
	BR(2)	-2.62±0.69	8.25±0.43	77.3±4.1	
	VTRF2003	-1.73±0.38	7.09±0.32	75.9±2.5	
San Fran.	ITRF97	-8.41±5.07	17.83±4.95	159.1±3.5	PCFC
(PRESIDIO)	ITRF2000	-7.27±6.46	16.02±6.30	159.6±20.0	
	BR(1)	4.11±3.66	14.83±3.52	151.9±11.5	
	BR(2)	-2.94±13.89	15.82±13.61	157.2±41.4	
	VTRF2003	-7.87±5.78	15.91±5.65	159.8±17.9	
YUMA	ITRF97	16.32±6.99	1.01±5.85	212.4±296.3	NOAM
	ITRF2000	15.58±7.76	1.37±6.78	339.9±228.5	
	BR(1)	23.26±7.94	2.56±7.50	12.1±112.8	
	BR(2)	24.25±7.74	2.51±7.31	13.3±112.5	
	VTRF2003	10.88±7.24	1.12±5.10	291.5±321.4	
URUMQI	ITRF97	-0.24±2.65	13.01±2.63	22.2±11.1	EURA
	ITRF2000	-5.28±2.11	11.30±1.63	26.8±6.3	
	BR(1)	-11.13±4.02	8.45±4.04	16.0±14.2	
	BR(2)	-10.62±5.91	8.16±5.95	17.8±25.6	
	VTRF2003	-4.64±0.80	14.21±0.73	31.6±2.4	
OHIGGINS	ITRF97	13.19±1.52	1.61±1.07	241.0±41.1	ANTA
	ITRF2000	9.35±0.94	1.97±0.53	276.3±19.5	
	BR(1)	2.06±0.46	4.17±0.41	189.2±5.9	
	BR(2)	1.58±0.81	3.06±0.77	225.4±14.5	
	VTRF2003	4.51±0.94	2.10±0.64	231.3±17.9	
EFLSBERG	ITRF97	-1.36±0.73	0.50±0.68	190.5±47.8	EURA
	ITRF2000	-2.10±0.66	0.51±0.37	59.1±62.5	
	BR(1)	4.59±1.42	0.91±0.35	94.0±85.3	
	BR(2)	1.88±0.98	0.51±0.65	131.6±81.0	
	VTRF2003	-1.32±0.50	0.45±0.48	24.7±44.2	
CRIMEA	ITRF97	-0.53±0.78	3.28±0.78	339.9±12.9	EURA
	ITRF2000	0.70±1.06	4.54±1.07	359.1±2.6	
	BR(1)	3.72±0.79	2.32±0.97	19.3±14.9	
	BR(2)	2.97±0.78	2.06±0.85	36.6±20.4	
	VTRF2003	2.01±0.49	5.36±0.49	3.1±4.6	
KWAJAL26	ITRF97	-6.17±6.01	5.64±2.83	220.8±28.0	PCFC
	ITRF2000	1.35±8.41	6.45±3.12	254.0±31.9	
	BR(1)	-12.65±0.19	11.23±0.12	225.5±0.8	
	BR(2)	-12.37±1.36	11.35±0.79	229.2±4.5	
	VTRF2003	1.23±7.84	8.59±2.94	261.6±23.3	

Axel Nothnagel: First Results of the IVS Pilot Project “Time Series of Baseline Lengths”, IVS 2004 General Meeting Proceedings, p.486–490
http://ivscc.gsfc.nasa.gov/publications/gm2004/nothnagel1

First Results of the IVS Pilot Project “Time Series of Baseline Lengths”

Axel Nothnagel

Geodetic Institute, University of Bonn
e-mail: nothnagel@uni-bonn.de

Abstract

Although earth orientation parameters have played a dominant role in recent years' VLBI activities, baseline length results have kept their importance from the very early days of geodetic VLBI. For various purposes the IVS has established a Pilot Project “Time series of baseline lengths” which is preparing procedures for making baseline length results fully qualified IVS products. In this paper, we describe the current stage of the development, first level analysis procedures and initial results.

1. Introduction and Motivation

Baseline lengths have been among the first types of VLBI results in the history of geodetic VLBI, e.g. [3] . Although earth orientation parameters (EOP) have been in the focus of analysts in recent years, baseline lengths have not lost their importance. In order to exploit the properties of baseline length results for the benefit of users but also for diagnosis purposes an IVS Pilot Project “Time series of baseline lenghts” has been established.

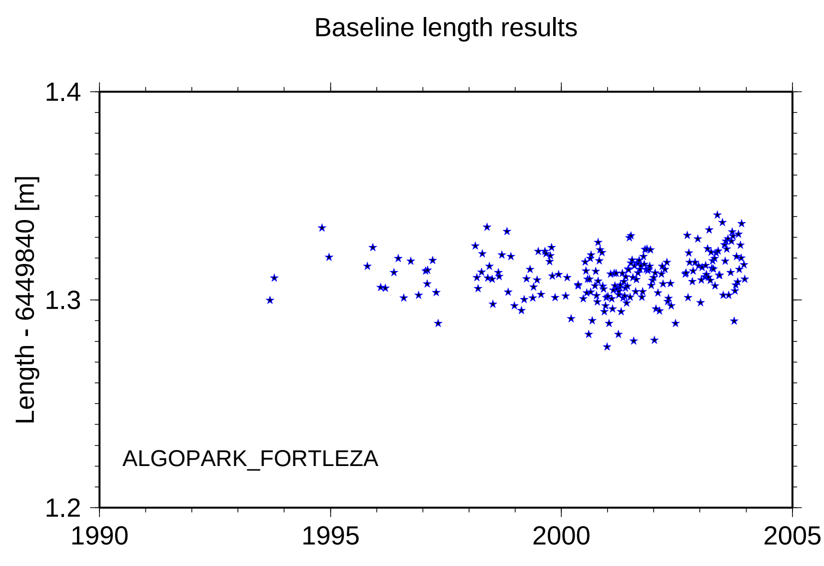

Figure 1. Baseline length results of a solution of a single IVS Analysis Center.

For the users baseline length time series as well as baseline lengths at epoch plus their time derivatives will have various applications. In the context of a global polyhedron, baseline length results are a much better indicator of scale and possibly scale evolution effects than station coordinates because the radial component is, off course, dependent on the station height.

Linking the VLBI results with and comparing them to those of other space geodetic techniques like GPS, DORIS and SLR are other applications where baseline length results can be used. Here also the pre-combination comparison of individual input series will be a main application.

Conceptually, VLBI baseline length results are invariant to translational and rotational changes in the reference frames. For this reason they are the ideal quantity for a detailed intercomparison of results generated by different analysis software packages. In addition, different analysis centers use different analysis strategies and models, e.g. for geophysical effects and most importantly for atmospheric refraction. Differences in the baseline length results can, therefore, be used for detailed analyses of possible deficiencies in models but also in analysis strategies. This is of particular importance to analysts who like to check the quality of their results and just submit time series for the purpose of comparison.

Finally, baseline length results will be well suited for an instant quality and plausibility check including warning mechanisms at primary level data analysis steps. For all these reasons, combination and comparison of baseline length results forms the ideal basis, independent of any reference frame issues.

2. Organisational Aspects

In preparation for making time series of baseline lengths an official IVS product, an IVS Pilot Project had to be set up requiring a few formal steps.

April 2003	Proposal to IVS Directing Board
July 2003	Acceptance by IVS Directing Board
August 2003	Call for Proposals to IVS Analysis Centers
October 15, 2003	Deadline for initial proposals

In the first round the following IVS Analysis Centers proposed to submit their baseline length results on a routine basis by 6 weeks after correlation of the respective session:

Agencia Spatiale Italiana, Matera (ASI)
Bundesamt für Kartographie und Geodäsie, Leipzig (BKG)
Deutsches Geodätisches Forschungsinstitut, München (DGFI)
Institute for Applied Astronomy, St. Petersburg (IAA)
Institut für Geodäsie und Geophysik, Wien (IGG)
NASA Goddard Space Flight Center, Greenbelt MD (GSFC)

For the submission of the results it was decided that the IVS Analysis Centers estimate station coordinates on a session by session basis from which baseline lengths with full covariance matrix can be inferred. Since the SINEX data format Version 2.0 (see http://alpha.fesg.tu-muenchen.de/iers) is now fully established for exchanges of space geodetic results it can be used without any further modifications.

The SINEX files which are submitted by the Analysis Centers only for the Pilot Project are being kept at separate directories of the IVS Data Centers. Currently, IVS Analysis Centers using the Calc/Solve analysis software package routinely generate SINEX files for the submission of their EOP results. In theses SINEX files station coordinate results are already embedded and no separate submission for the Pilot Project is required. For this reason also the SINEX files of the US Naval Observatory at Washington D.C. (USNO) can be used for the Pilot Project straight away.

In order to support the Pilot Project, an IVS Pilot Project Group was set up in the framework of the charter of the project. This group will discuss future steps and will guide the project from the pilot to the operational phase. Each Analysis Center has one delegate in the Pilot Project Group but any other person interested in the topic is welcome to join. The director of the IVS Coordinating Center is an ex-officio member of the Project Group.

3. Analysis Procedures

At present, initial baseline lengths and formal errors are computed from the station coordinates in the SINEX files of a single Analysis Center and are stored in a separate file for each baseline in a separate directory for each Analysis Center. Stations are identified by their DOMES number [1] and are subsequently converted into IVS names using the IVS conversion table (see http://gemini.gsfc.nasa.gov/solve_save/antenna.dat). For the coordinates themselves an initial outlier rejection filter is introduced identifying estimated station positions which differ by more than 0.5 m from the ITRF2000 position of date. Through this mechanism blunders in the generation of the files and very obvious outliers are eliminated at a very early stage.

Linear regressions by baseline and Analysis Center then offer a first impression of the quality of the submissions, providing an extra level of possible low pass filtering through weighted RMS (WRMS) criteria and outlier identification. In this step possible episodic motions of stations have to be taken into account in order to permit a correct piece-wise linear modeling of the baseline behaviour. Differences in baseline length of epoch (currently Jan. 1, 2000), baseline rate as well as WRMS give already a very good insight in the general agreement of the contributing Analysis Centers.

The combination of baseline lengths itself is currently being carried out on the basis of weighted averaging using the formal errors of the input series. Due to the fact that not all Analysis Centers have processed all sessions, combined baseline length results may have been computed using between one and all Analysis Centers. The implications of this deficit still have to be investigated.

In the current realization of the software, linear regressions of the combined time series and their statistical parameters are computed and can be compared with the ones of the individual input series. The residuals of the combined series as well as the residuals of the input series relative to the linear regression will give good insight into the advantages and disadvantages of the combination and various ways of combination. One of the most interesting parameters will be the scale between different analysis packages and Analysis Centers with its rate and possibly further signatures.

4. First Results

Owing to timing constraints, detailed investigations in the results and in the residuals have not been accomplished yet. However, the results of just a single baseline should be displayed as a first example here. Fig. 2 depicts the residuals of the input time series of three IVS Analysis Centers (BKG, GSFC, IAA) with respect to a combined time series. It can easily be seen that there are significant systematic offsets between the three series. In addition, the noise level gives some impression of the input series. Since the weighting scheme is not yet developed properly this initial result has to be considered as very preliminary. Nevertheless, this residual plot is a good indication of the potential of baseline length time series for various types of investigations.

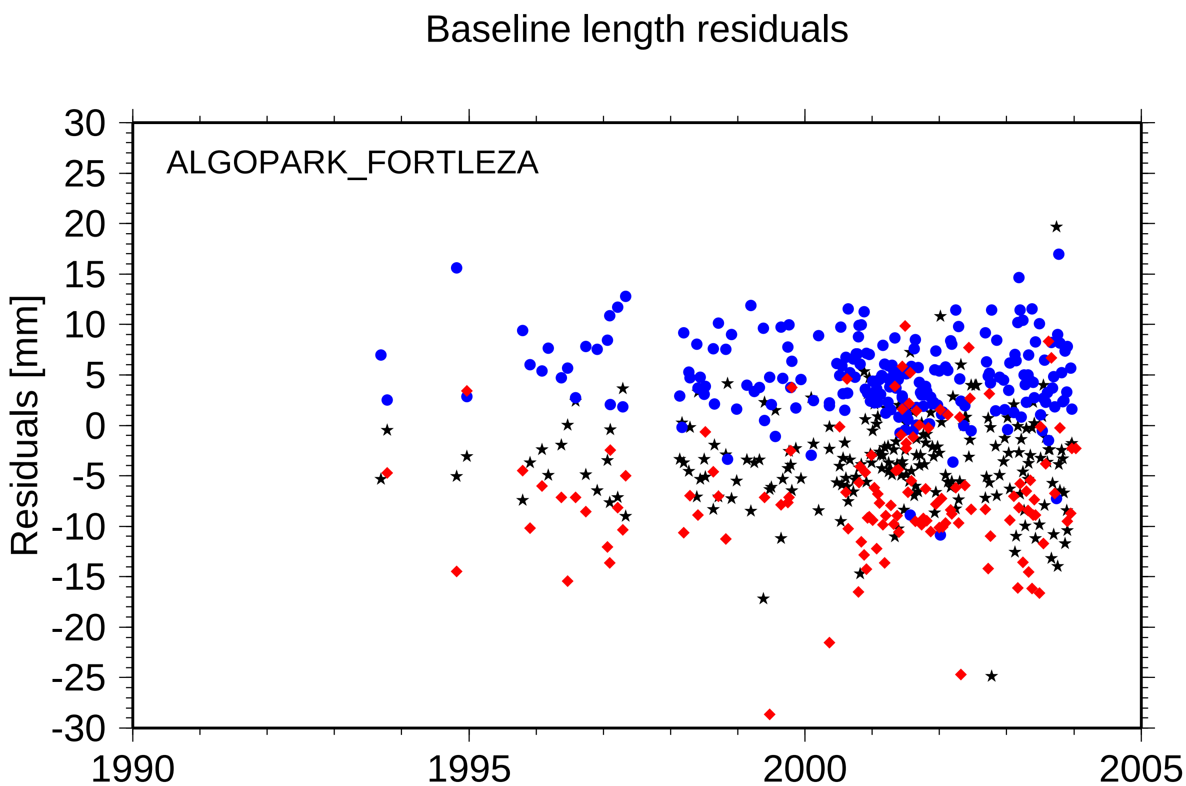

Figure 2. Baseline length residuals after combination. *asterisk* = BKG, *circle* = GSFC, *square* = IAA

5. Outlook

As a next step, correlations between Analysis Centers having processed the same VLBI observing session will be introduced shortly. Initial values for the correlation coefficients between Analysis Centers will be taken from [2] before correlation coefficients will be computed from the baseline length results themselves.

The combination process and its post-fit residuals will help to establish a correct relationship between the formal errors of the input series and will lead to scaling factors between them. After re-scaling the formal errors of the input series the combination will be done iteratively to end up with more realistic weights.

Using local tie information between the VLBI telescopes and other space techniques like GPS, SLR and DORIS will permit a detailed study of scaling differences and possible correlations between the time series at various time scales.

As soon as all basic computation mechanisms have been established a web page will be set up which will permit a button-based selection of baseline results together with ftp retrieval of raw data and residuals.

References

[1] Boucher C., Z. Altamimi, P. Sillard (1999): The 1997 International Terrestrial Reference Frame (ITRF97); IERS Technical Note 27, Observatoire de Paris

[2] Steinforth C., A. Nothnagel (2004); Considering a priori Correlations in the IVS combined EOP Series; Proceedings of the 3rd IVS General Meeting, Ottawa, Canada, Feb 9 - 11, 2004; this volume

[3] Hinteregger, H.F., I.I. Shapiro, D.S. Robertson, C.A. Knight, R.A. Ergas, A.R. Whitney, A.E.E. Rogers, J.M. Moran, T.A. Clark, B.F. Burke (1972): Precision Geodesy via Radio Interferometry; Science, Vol. 178, 396 - 398

Daniel MacMillan et al.: Postseismic Transient after the 2002 Denali Fault Earthquake from VLBI Measurements at Fairbanks, IVS 2004 General Meeting Proceedings, p.491–495
http://ivscc.gsfc.nasa.gov/publications/gm2004/macmillan2

Postseismic Transient after the 2002 Denali Fault Earthquake from VLBI Measurements at Fairbanks

Daniel MacMillan [1], *Steven Cohen* [2]

[1] *NVI, Inc./NASA Goddard Space Flight Center*
[2] *NASA Goddard Space Flight Center*
Contact author: Daniel MacMillan, e-mail: dsm@leo.gsfc.nasa.gov

Abstract

The VLBI antenna (GILCREEK) at Fairbanks, Alaska observes in networks routinely twice a week with operational networks and on additional days with other networks on a more uneven basis. The Fairbanks antenna position is about 150 km north of the Denali fault and from the earthquake epicenter. We examine the transient behavior of the estimated VLBI position during the year following the earthquake to determine how the rate of change of postseismic deformation has changed. This is compared with what is seen in the GPS site position series.

1. Solution Description and Observed Motion at Fairbanks

To investigate the behavior of the position of GILCREEK after the Denali earthquake in November 2002, we modified our standard solution to estimate the GILCREEK position for each epoch (VLBI 24-hour experiment). In a standard terrestrial reference frame solution, we estimate site positions and velocities as global parameters. Ma et al. [1990] gives a description of the VLBI SOLVE analysis program and most of the theoretical models that are generally applied. To remove degeneracies corresponding to invariances of the VLBI group delay observable, no net translation and no net rotation conditions are imposed on station positions and velocities in order to align the terrestrial reference frame with ITRF2000. The standard solution models site episodic motion as a simple offset with the same velocity before and after the episodic event.

After several months of observing after the Denali earthquake, it became apparent that the rate of change of the position of Fairbanks in the horizontal directions after the earthquake was significantly different from the rate before the earthquake. We now have a little more than a year of data since Denali and find that the rates have still not returned to their pre-earthquake values.

In Figures 1, 2, and 3 are shown a recent solution for the local site coordinate series at GILCREEK. The last VLBI data point before the Denali fault earthquake (Nov. 3, 2002) was measured on Oct. 31, 2002 and the first point afterwards was on Nov. 4, 2002. For each series, the offset, rate, and annual terms were estimated using only data prior to the earthquake and then removed from the entire series.

In the plots of horizontal motion in Figures 2-3, we show a fit to the postseismic data using a transient decay model,

$$X(t) = X_0 + X_1[1 - exp(-(t - t_0)/\tau_c)]$$

where t_0 is the epoch of the earthquake. The fits gave characteristic decay times, τ_c, of 1.18 years for the North and 0.32 years for the East. The postseismic amplitudes, X_1, assuming this model were -29 mm in the North and 10 mm in the East. Coseismic offsets, X_0, were -56 mm and 23

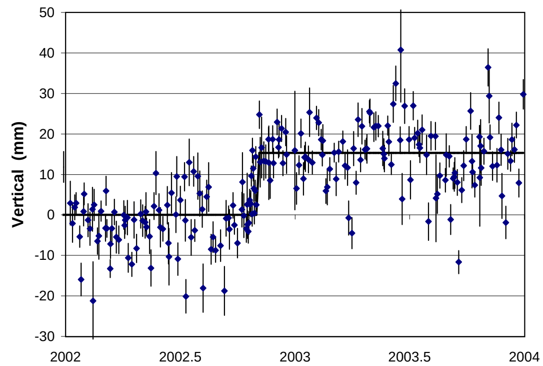

Figure 1. VLBI Fairbanks vertical position time series. Offsets, linear rates, and annual terms were estimated from data before the earthquake and then removed from the series. The episodic site adjustment is shown with a solid line.

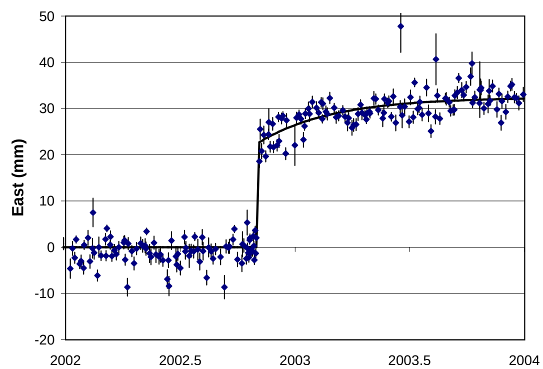

Figure 2. VLBI Fairbanks east position time series. Offsets, linear rates, and annual terms were estimated from data before the earthquake and then removed from the series. The transient decay model fit to the data after the earthquake is indicated by the solid line.

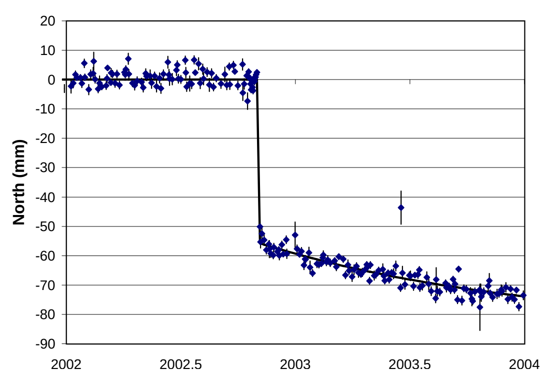

Figure 3. VLBI Fairbanks north position time series and the corresponding transient decay model (solid line)

mm for North and East respectively. The average rates of change over the year following the earthquake are about -16 mm/yr in the North and about 8 mm/yr in the East. It is possible that some of the deviations from the model are systematic and indicate that a more complicated model is needed but this will require further investigation.

2. GPS Comparisons

We have compared the postseismic trends from VLBI and GPS measurements. Here we show the operational JPL series from the web site maintained by Mike Heflin [Heflin, 2004]. To compare the GPS and VLBI series, offsets, rates, and annual terms were estimated from data before the earthquake and removed from each entire series. The observed precision (wrms residual motion) of the GPS series (4.9 mm for East and 4.1 mm for North) is not as good as for VLBI (3.0 mm for East and 3.1 mm for North). Looking at Figure 4 there is reasonably good agreement between the trends of the two series after the earthquake although there appear to be some possible systematic differences in the first several months of the East motion series.

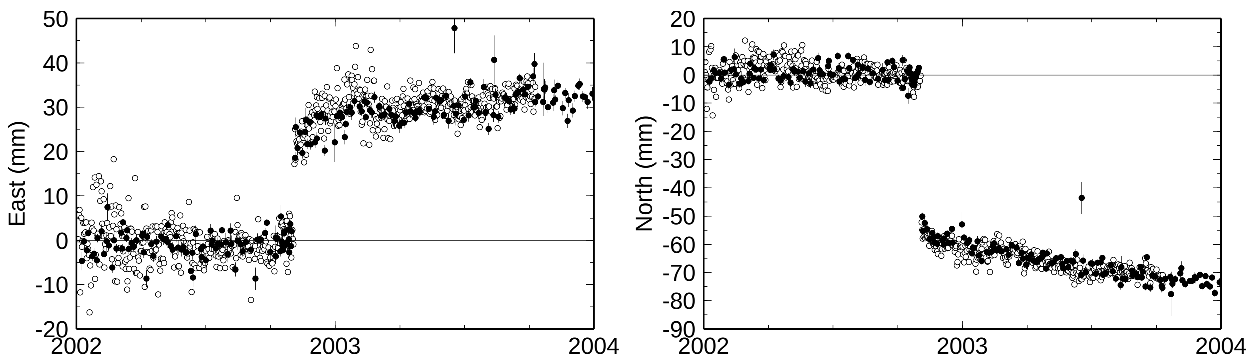

Figure 4. Comparison of VLBI (black circles with error bars) and GPS (open black circles) motion at Fairbanks. Error bars for GPS (not shown) are 3-4 mm. The GPS series is from JPL [Heflin, 2004].

3. EOP Errors from Fairbanks Motion

If the postseismic behavior of Fairbanks is not modeled in a VLBI terrestrial reference frame solution, EOP estimates will exhibit systematic errors. We show the effect in Figures 5- 7 of not modeling the post-seismic behavior at Fairbanks for the R1 sessions. The figures show the difference between a solution where there was no Fairbanks model and one where the above transient model was applied. For polar motion, we can make comparisons with GPS IGS series to evaluate the model. For the period of time after the earthquake, modeling reduced the WRMS X-pole difference from 130 μas to 115 μas and the WRMS Y-pole difference from 127 μas to 113 μas.

4. Discussion

The frequent measurement of geodetic site positions allows one to investigate geophysical effects on time scales of weeks to months to years. At GPS sites that are closer to the Denali fault the postseismic change is similar but much larger than for Fairbanks and the exponential decay trend is more clear. At Fairbanks, it will probably take a year or two to discern the true postseismic trend.

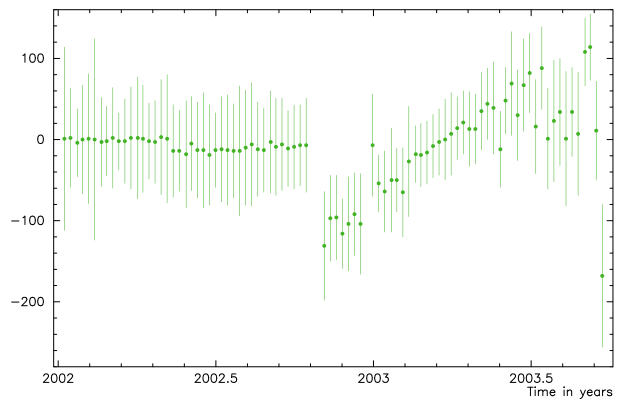

Figure 5. Effect on x-pole estimates (μas) from the R1 series of experiments when the transient behavior at Fairbanks is not modeled. The model used is the one shown in Figures 2-3.

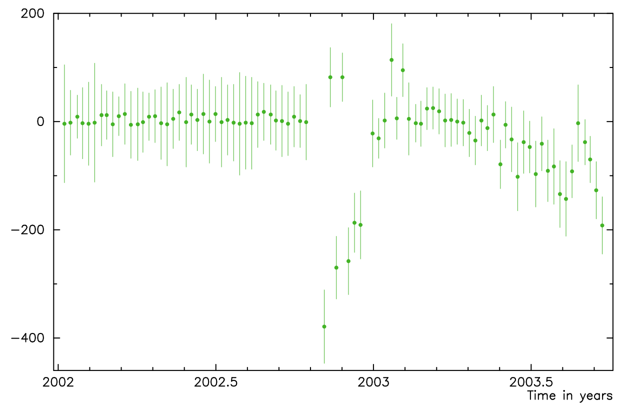

Figure 6. Same as Figure 5 except here the effect on y-pole (μas) is shown.

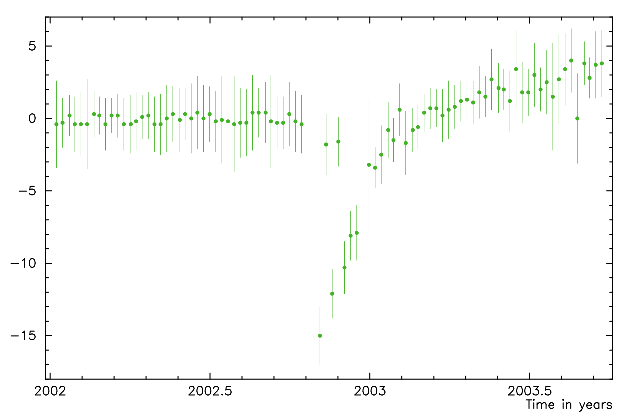

Figure 7. Same as for Figure 5 except here the effect on UT1 (μs) is shown.

At this point, eastward motion at Fairbanks appears to have nearly returned to the long-term pre-earthquake rate. Immediately after the earthquake, it was 31.2 mm/yr relative to the long-term rate (-9.1 mm/yr). Relative to the long-term rate (-22.4 mm/yr) before the earthquake, the current northward motion is about -9 mm/yr compared to the initial relative rate of -24.5 mm/yr. The rate of change at Fairbanks appears to begin immediately after the earthquake suggesting that the postseismic deformation is controlled by the coseismic stress change. We have no evidence to suggest a diffusing signal that first arrives at the observing site with a time offset delay from the earthquake occurrence.

References

[1] Heflin, M. B., GPS time series, http://sideshow.jpl.nasa.gov/mbh/series.html/, 2004.

[2] Ma, C., J.M. Sauber, L.J. Bell, T.A. Clark, D. Gordon, W.E. Himwich, and J. W. Ryan, Measurement of horizontal motions in Alaska using very long baseline interferometry, J. Geophys. Res., 95(B13), 21991-22001, 1990.

Oleg Titov et al.: Post-Seismic Motion of Gilcreek Geodetic Sites Following the November, 2002 Denali Earthquake,
IVS 2004 General Meeting Proceedings, p.496–500
http://ivscc.gsfc.nasa.gov/publications/gm2004/titov2

Post-Seismic Motion of Gilcreek Geodetic Sites Following the November, 2002 Denali Earthquake

Oleg Titov [1], *Paul Tregoning* [2]

[1] *Geoscience Australia*

[2] *Research School of Earth Sciences, The Australian National University*

Contact author: Oleg Titov, *e-mail:* olegtitov@ga.gov.au

Abstract

We have detected post-seismic motion of the Gilcreek observatory in Fairbanks, Alaska after the 2002 Denali earthquake from an analysis of VLBI and GPS data recorded at the site in the 12-month period following the event. The motion is non-linear, indicating that either a relaxation process or afterslip on the fault is occuring. The co-seismic estimate of displacement from VLBI measurements agrees well with those from GPS analysis in all components.

1. Introduction

The $M_w = 7.9$ earthquake that occurred on the Alaska Peninsula on 3 November 2002 was the largest of the year. The epicenter was located approximately 135 km south of Fairbanks on the Denali Fault that stretches over 700 km, dividing Alaska into two parts. The earthquake caused numerous landslides with measured surface offsets of up to a few meters. The co-seismic displacement field of the earthquake has been modelled from displacement of GPS [2]. The northern part of the Denali Fault moved to the east and vertically up. The Gilcreek observatory [9] located near the event epicenter produced valuable information about the displacement.

2. VLBI Data Analysis

VLBI has been used to estimate the deformation caused by two earthquakes in Alaska during 1987-1988 [8] and also the dynamic crystal deformation associated with Miyake-jima volcano in Japan (VLBI site Tateyama) in the framework of the Keystone Project [6]. However, post-seismic deformation following a major earthquake as observed by VLBI has not been reported previously.

We have analysed 92 24-hour VLBI sessions that included Gilcreek from 4 November 2002 to 1 December 2003. The analysis of the data has been performed using the OCCAM software [10]. The Geoscience Australia solution for source positions (aus2002) has been used to define the Celestial Reference Frame and the a priori VLBI site coordinates. Observations of each daily session were processed separately to estimate all site coordinates, nutation offsets, EOPs, clock offsets and rates as well as tropospheric delays and horizontal tropospheric gradients. We performed a 6-parameter Helmert transformation of the daily estimates of the coordinates of all VLBI sites (except Gilcreek) onto their ITRF2000 values in order to define the terrestrial reference frame.

3. GPS Data Analysis

We analysed data from the GPS receiver at Gilcreek (FAIR) spanning the same time period as the VLBI data. The GPS phase data were processed using the GAMIT/GLOBK software [5], [3] in a global solution of 80-90 stations. We divided the globe into four regional subnetworks, with 3-4 overlapping sites in more than one subnetwork, and estimated site coordinates, GPS satellite orbits, EOP, tropospheric delay parameters (13/day) and horizontal troposphere gradients (3/day). All parameters are treated deterministically, with the tropospheric delay parameters modelled as piecewise linear function.

The four subnetworks/day were then linked to produce a single, free-network solution for the site coordinates and a single, coherent estimate of the satellite orbits. The resulting, global polyhedron is the same as that which can be produced by the simultaneous processing of the observations from all sites but takes considerably less computational time to produce. We then aligned the free network to the International Terrestrial Reference Frame by computing a 7-parameter Helmert transformation on the coordinates of 50 sites to their ITRF2000 values [1] to generate daily site coordinates. The time series of VLBI and GPS results are shown in Figure 1,2.

4. Discussion

Our linear velocity estimates for Gilcreek and FAIR prior to the earthquake are not significantly different from, for example, [7] (VLBI) and [1] (GPS), indicating that our analyses are of high accuracy. Furthermore, the co-seismic offsets estimated from the GPS analysis are in close agreement with those of [4] (Table 1).

Table 1. The estimated co-seismic displacement at Gilcreek from VLBI and GPS

Component	**this paper, VLBI (mm)**	**this paper GPS, (mm)**	**[4] GPS, (mm)**
radial	20 +/- 11	16 +/- 3	23.3 +/- 10.1
latitude	-53 +/- 8	-56 +/- 1	-51.6 +/- 6.3
longitude	26 +/- 7	21 +/- 1	24.8 +/- 5.7

Post-seismic deformation for several large earthquakes has been characterized as being caused by viscoelastic relaxation or due to afterslip on ruptured faults. Several authors have derived numerical expressions to model such non-linear motion as logarithmic, exponential or even transient function. Such analyses are performed typically on networks of sites geographically spread around the ruptured fault that have observed the post-seismic relaxations patterns. With only one VLBI site affected by the post-seismic motion, there is insufficient data to differentiate between possible causes of the post-seismic motion. We chose to represent the motion using an exponential function

$$X(t) = A + B\exp(-\frac{t - t_{Eq}}{\tau})$$

where t - the current epoch, t_{Eq} - the epoch of the earthquake. We used independent estimates of the decay constants $\tau = 0.25$ year (obtained from GPS the data using least squares method for non-linear models) to estimate the amplitude B (Table 2).

The Cartesian coordinates of Gilcreek are used routinely in VLBI for station position modeling. We proposed the following empirical model for the Gilcreek VLBI site coordinates.

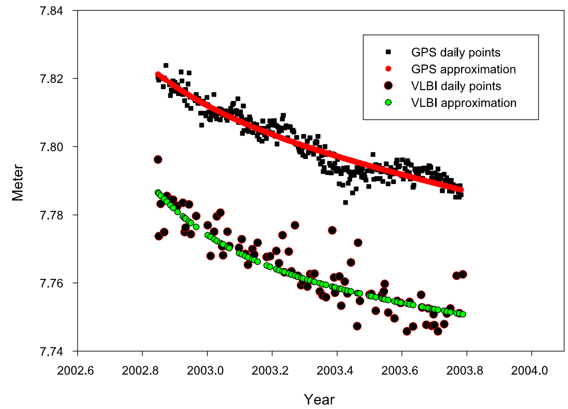

Figure 1. Evolution of the North component from GPS and VLBI.

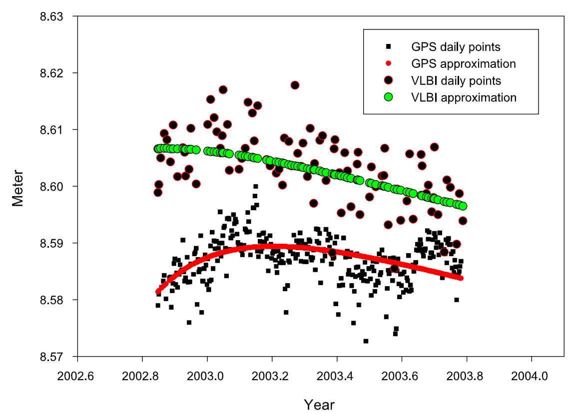

Figure 2. Evolution of the East component from GPS and VLBI.

Table 2. The estimates for amplitude of decay from VLBI for the horizontal components

Component	**B (meter)**	**τ(years)**
latitude	0.028	0.25
longitude	-0.003	0.25

$$X(t) = A_0 + A_1(t - t_0) + B_0 + B_1 \exp(-\frac{t - t_{Eq}}{\tau})$$

Here $t_0 = 1997.0$ (the reference epoch), $t_{Eq} = 2002.838$ (the epoch of the earthquake). The first and second terms describe the linear tectonic motion model in accordance with the ITRF2000, whereas B_0 introduces the co-seismic offset and B_1 the post-seismic deformation (Table 3). Figure

3-5 show how the model fits to the VLBI observations in Cartesian components. While the non-linear model is not convincing in the Y and Z components, it clearly fits the data better than a linear model in the North and East components (see Figure 1,2).

Table 3. The parameters of the expanded model for Gilcreek post-seismic motion in Cartesian coordinates

Component	A_0 (m)	A_1 (m/year)	B_0 (m)	B_1 (m)	τ (years)
X	-2281547.309	-0.0222	-0.036	0.0080	0.25
Y	-1453645.080	-0.0036	-0.058	0.0076	0.25
Z	5756993.162	-0.0092	-0.037	0.0143	0.25

References

[1] Altamimi, Z., P. Sillard and C. Boucher, ITRF2000: A new release of the International Terrestrial Reference Frame for earth science applications, J. Geoph. Res. 107, 10.1029/2001JB000561, 2002.

[2] Eberhart-Phillips, D., et al., The 2002 Denali Fault Earthquake, Alaska: A Large Magnitude, Slip-Partitioned Event, Science, 300, 1113–1118, 2003.

[3] Herring, T. A., GLOBK global Kalman filter VLBI and GPS analysis program, version 10.0, Massachusetts Institute of Technology, Cambridge, MA, 2002.

[4] Hreinsdottir, S., et al., Coseismic slip distribution of the 2002 $M_w = 7.9$ Denali fault earthquake, Alaska, determined from GPS measurements, Geophys. Res, Lett., 30(13), 10.1029/2003GL017447, 2003.

[5] King, R. W, Y. Bock, Documentation for the GAMIT GPS analysis software, release 10.0, Massachusetts Institute of Technology, Cambridge, MA, 2002.

[6] Koyama, Y., Expected Contributions of the K-4 and its Next-Generation Systems, In: Proc. of the IVS General Meeting 2002, N. R. Vandenberg and K. D. Baver (eds.), 55–59, 2002.

[7] Nothnagel, A., VTRF2003: A conventional VLBI terrestrial reference frame; In: Proc. of the 16th Working Meeting on European VLBI for Geodesy and Astrometry, W. Schwegmann and V. Thorandt (eds.), Leipzig, 195–205, 2003.

[8] Ryan, J. W, C. Ma, J. Boehm. In: NASA-GSFC's Geodetic VLBI Program: a Twenty-year Retrospective, Phys. Chem. Earth, 23, 9-10, 1041–1052, 1998.

[9] Strand, R., Gilmore Creek Geophysical Observatory, In: International VLBI Service for Geodesy and Astrometry 2002 Annual Report, NASA/TP–2003-211619, N. R. Vandenberg and K. D. Baver (eds.), 91–94, 2003.

[10] Titov, O., V. Tesmer, J. Boehm. OCCAM 5.0: User's Guide, In: AUSLIG Technical Notes, 7, 2001.

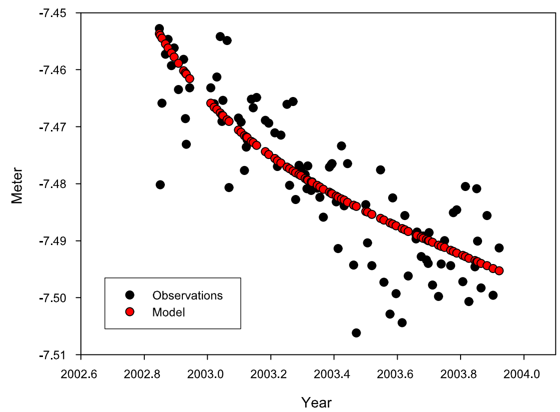

Figure 3. Evolution of the X components from the VLBI data.

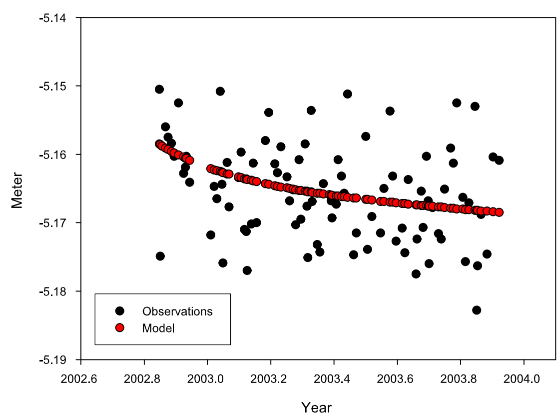

Figure 4. Evolution of the Y components from the VLBI data.

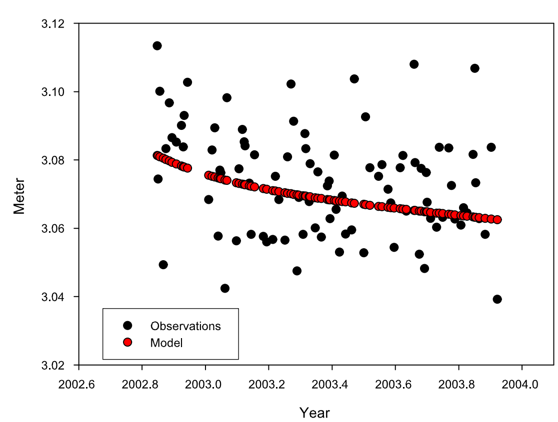

Figure 5. Evolution of the Z components from the VLBI data.

Leonid Petrov: Preliminary Results of the IVS Gravity Experiment Grav01, IVS 2004 General Meeting Proceedings, p.501–505
http://ivscc.gsfc.nasa.gov/publications/gm2004/petrov1

Preliminary Results of the IVS Gravity Experiment Grav01

Leonid Petrov

NVI, Inc/NASA GSFC

e-mail: Leonid.Petrov@lpetrov.net

Abstract

Three IVS research and development experiments were observed in order to detect terms proportional to v^3/c^3 in gravitational delay caused by Jupiter when it passed within $3'.7$ from the quasar 0839+187. Preliminary results of group delay analysis are presented. The estimate of parameter γ for gravitation delay in the Jovian gravitational field 1.2 ± 0.1 was determined.

1. Introduction

General relativity is not derived as a generalization of experimental facts, but based on a hypothesis that equations should be simple and beautiful. From one side it can be considered as a great merit of the theory which permitted to call it the most beautiful theory ever developed. Continuation of this merit is the fact that predictions of general relativity do not logically follow from experiments. Therefore, each time when the accuracy of the experiment is sufficient in order to try to determine the new effect predicted by the theory or a new term in a known effect, we have to check whether the theory agrees with the experiment, i.e. whether the simple and beautiful equations describe reality adequately.

2. Rational

On the class of metric theories of gravitation the expansion of the metric tensor over 1/c can be written [10] as

$$\begin{aligned} g_{00} &= -1 + 2\frac{U}{c^2} && + O(1/c^4) \\ g_{0i} &= -2\left(1+\gamma+\frac{\alpha_1}{4}\right)\frac{V}{c^3} && + O(1/c^5) \\ g_{ij} &= \delta_{ij}\left(1+2\gamma\frac{U}{c^2}\right) && + O(1/c^4) \end{aligned} \tag{1}$$

where U and V are retarded potentials, α_1 and γ are parameters which are 0 and 1 respectively in general relativity, but may have different values in alternative metric theories of gravitation; δ_{ij} is the Kroneker symbol. Then, the gravitation VLBI delay is:

$$\tau_{gr} = (1+\gamma)\sum_a \frac{f m_a}{c^3}\left(1+\frac{1+\zeta}{c}\vec{\mathbf{v}}_a\vec{\mathbf{s}}\right)\ln\frac{|\vec{\mathbf{x}}_1-\vec{\mathbf{x}}_a| + (\vec{\mathbf{x}}_1-\vec{\mathbf{x}}_a)\vec{\mathbf{s}} - \frac{1}{c}\vec{\mathbf{s}}\times(\vec{\mathbf{v}}_a\times\vec{\mathbf{s}}))}{|\vec{\mathbf{x}}_2-\vec{\mathbf{x}}_a| + (\vec{\mathbf{x}}_2-\vec{\mathbf{x}}_a)\vec{\mathbf{s}} - \frac{1}{c}\vec{\mathbf{s}}\times(\vec{\mathbf{v}}_a\times\vec{\mathbf{s}}))} \tag{2}$$

where $\zeta = \dfrac{\alpha_1}{2+2\gamma}$, f — the universal gravity constant, m_a is a mass of the gravitating body, $\vec{v}_a$ — velocity of the a th body, $\vec{s}$ — source vector in the barycentric reference system, $\vec{x}_i$ — vector of the i th station in the geocentric reference system. Summing is done over all major planets, Sun and Moon. Detailed derivation of this expression for the case of general relativity can be found in [3] and for general case in [10].

The second term in the brackets before logarithm and the third term in the numerator and denominator of the logarithm are proportional to v^3/c^3 and very small, except for the cases when the source is close to the gravitating body. It can be easily shown that the contribution of these terms to VLBI time delay is reciprocal to the third degree of the angular distance from a source to a gravitating body [4].

The part of the expression for VLBI time delay without terms of third order has been extensively tested. Analysis of the whole set of VLBI observations from 1979 to 2004 performed by the author gives $\gamma = 1.0004 \pm 0.0002$ when only the Sun is taken into account in the expression 2. Here 0.0002 is the unscaled formal uncertainty.

Contribution of the terms proportional to v^3/c^3 has never been before detected experimentally. The interest to these terms arose recently as S. Kopeikin pointed out in a short paper [4] that "c" in the third term of the numerator and denominator of the logarithm corresponds to the speed of propagation of gravity. General relativity postulates that the speed of propagation of gravity is equal to the speed of propagation of light, but that statement has not been checked experimentally [9], [7]. This interpretation caused a fierce criticism by [1], [10] and [8] who presented arguments that that "c" is the speed of light, not gravity. Kopeikin analyzes arguments of his opponents in details and defends his position in lengthy papers [5], [6]. Anyway, regardless of theoretical interpretation of these terms, it is tempting to detect its contribution to VLBI path delay.

3. Event of 2002.09.08

A cursory analysis shows that the best circumstances of observation of the terms in gravitational delay proportional to v^3/c^3 are when Jupiter or Saturn passes very close to a bright compact quasar. A. Kudryavtcev (personal communication, 2001) has found that on 2002.09.08 15h 56m 08.9s TAI Jupiter would pass within $3'.7$ of the quasar 0839+187 (fig. 2). There are two other quasars which were previously observed in geodetic experiments near 0839+187: 0836+182 and OJ287.

0839+187	flux 0.33Jy	min distance	$3'.7$
0836+182	flux 0.17Jy	min distance	$49'$
OJ287	flux 2.0Jy	min distance	$3°15'$

Simulation showed (figure 1) that the contribution of terms proportional to v^3/c^3 during that event can reach 7 psec when observed with the IVS network. Although the precision of group delays is not sufficient in order to measure such an effect, the accuracy of differential phase determination should be sufficient for detection of this contribution provided the fringe phases can be successfully connected.

Figure 1. Predicted contribution to fringe phase due to v^3/c^3 terms in phase turns

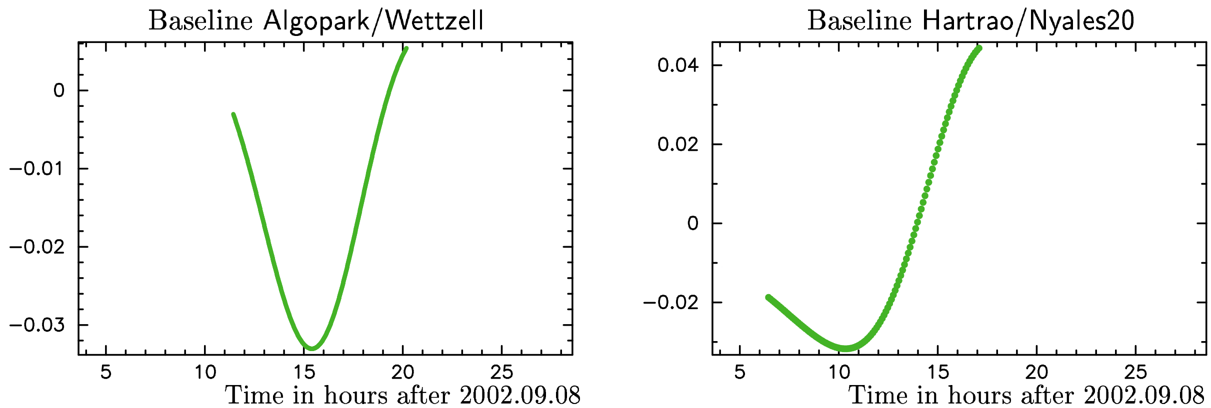

4. Design of the Experiment

Three sources, 0839+187, 0836+182 and OJ287, were observed at Algopark, Gilcreek, Hartrao, Kokee, Medicina, Nyales20, Westford, Wettzell with 256 Msamples/sec bits rate at X/S bands. Experiment start time: 2002.09.08 06 UT. Duration: 24 hours. Every two hours 3–4 troposphere calibrators were observed during the experiment.

The purpose of the experiment was 1) to get group delays at X/S bands; 2) to get differential phases.

Scan length was taken long enough in order to get the signal to noise ratio at least 20 at the baselines with weak antennas. In order to fit one tape pass, two observing sequences were used intermittently.

0836+182 — 0839+187 (840^s—250^s)

OJ287 — 0839+187 — OJ287 — 0839+187 — OJ287 — 0839+187 — OJ287 — 0839+187
(125^s—240^s—115^s—240^s—115^s—240^s—115^s—240^s)

The target sources were observed at all stations when they were 10 degrees above the horizon.

Using similar schedule two other experiments were performed: on 2002.03.20 and 2002.08.28. The purpose of these experiments was to determine the noise level when Jupiter was far away from 0839+187.

Quite independently, an analogous experiment was performed at the network which included 10 VLBA stations and Effelsberg by E. Fomalont and S. Kopeikin [2].

5. Analysis of Group Delays

The experiment was designed for getting precise group delays along with phase delays. Two solutions were performed.

In solution G1 gravitational time delay due to Jupiter was not modeled. Parameter γ was considered as dependent on the gravitating body. Three VLBI sessions, 02MAR20XA, 02AUG28XA and 02SEP08XA were used for adjustment of the Jovian $\gamma_{\rm J}$, as well as position of 0839+187, daily nutation offsets, clock function and troposphere path delay using least squares. The additive baseline-dependent noise was added to the weights in oder to keep the ratio of χ^2 to its mathematical expectation close to unity. Result of processing these three experiments: $\gamma_{\rm J} = 1.2 \pm 0.1$.

Figure 2. Event of 2002.09.08

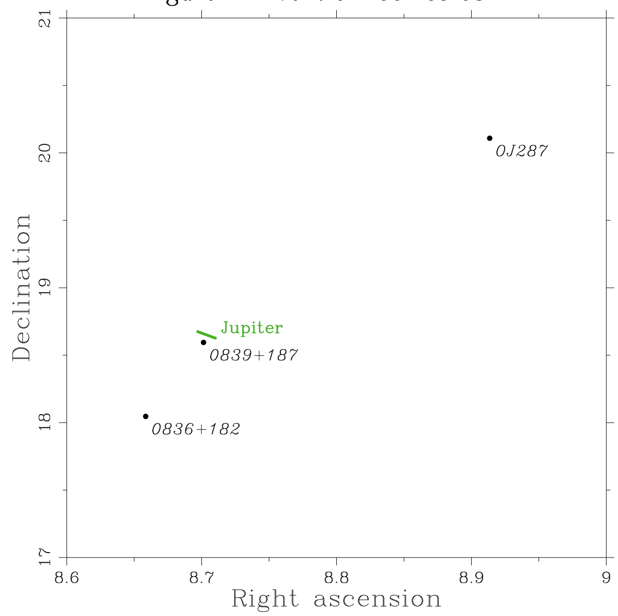

Reported uncertainty is the unscaled 1-σ uncertainty. According to metric theories of gravitation, parameter γ does not depend on the gravitating body. The experiment has confirmed it.

In solution G2 terms proportional to v^3/c^3 were excluded from the expression for gravitational delay 2. The difference, denoted as ξ, is given by

$$\xi_3 = 2\frac{f m_{\rm J}}{c^3}\left[\left(1+\frac{\vec{\mathbf{v}}_{\rm J}\vec{\mathbf{s}}}{c}\right)\ln\frac{|\vec{\mathbf{x}}_1-\vec{\mathbf{x}}_{\rm J}|+(\vec{\mathbf{x}}_1-\vec{\mathbf{x}}_{\rm J})\vec{\mathbf{s}}-\frac{1}{c}\vec{\mathbf{s}}\times(\vec{\mathbf{v}}_{\rm J}\times\vec{\mathbf{s}})}{|\vec{\mathbf{x}}_2-\vec{\mathbf{x}}_{\rm J}|+(\vec{\mathbf{x}}_2-\vec{\mathbf{x}}_{\rm J})\vec{\mathbf{s}}-\frac{1}{c}\vec{\mathbf{s}}\times(\vec{\mathbf{v}}_{\rm J}\times\vec{\mathbf{s}})}-\ln\frac{|\vec{\mathbf{x}}_1-\vec{\mathbf{x}}_{\rm J}|+(\vec{\mathbf{x}}_1-\vec{\mathbf{x}}_{\rm J})\vec{\mathbf{s}}}{|\vec{\mathbf{x}}_2-\vec{\mathbf{x}}_{\rm J}|+(\vec{\mathbf{x}}_2-\vec{\mathbf{x}}_{\rm J})\vec{\mathbf{s}}}\right] \quad (3)$$

assuming $\gamma = 1$ as it follows from solution G1. The factor $A_3\xi_3$ was included in the estimation model and the unknown parameter of A_3 of the admittance of ξ_3 into time delay was estimated. In the case if expression 2 is precise, $\gamma = 1$, $\alpha_1 = 0$, the observational noise is uncorrelated with ξ, the estimate of A_3 should be close to unity. Result of analysis of 02SEP08XA session is $A_3 = 0.9 \pm 1.2$. This confirms prediction that the group delays are not precise enough in order to confirm or refute the presence of the v^3/c^3 terms in expression 2.

6. Analysis of Phase Delays

This work is in progress.

7. Acknowledgment

The author thanks S. Kopeikin, E. Fomalont, H. Schuh, B. Corey for useful discussion, N. Vandenberg for help in scheduling and the staff of observing stations who worked on Sunday, 2002.09.08, in order to make this experiment possible.

References

[1] Asada, H., The light cone effect on the Shapiro time delay, *Astrophys. J.*, vol. 574, pp. L69–L70, 2002.

[2] Fomalont, E.B. and S.M. Kopeikin, The measurement of the light deflection from Jupiter: experimental results, *Astrophys. J.*, vol. 598(1). pp. 704–711, 2003.

[3] Kopeikin, S. and G. Schaefer, Lorentz covariant theory of light propagation in gravitational fields of arbitrary-moving bodies, *Phys. Rev. D*, vol. 60, p. 124002, 1999.

[4] Kopeikin, S., Testing the relativistic effect of the propagation of gravity by very long baseline interferometry, *Astrophys. J.*, vol. 556, pp. L1–L5, 2001.

[5] Kopeikin, S. and E. Fomalont, Aberration and the speed of gravity in the Jovian deflection experiment, *submitted*, `http://arxiv.org/abs/astro-ph/0311063`, 2004.

[6] Kopeikin, S. Speed of Gravity in General Relativity and Theoretical Interpretation of the Jovian Deflection Experiment, *submitted*, `http://arxiv.org/abs/gr-qc/0310059`, 2004.

[7] Marsh, G.E. and C. Nissim-Sabat, Comment on “The speed of gravity”, *Phys. Let. A*, vol. 262, pp. 257–260, 1999.

[8] Samuel, S., On the speed of gravity and the v/c corrections to the Shapiro time delay, *Phys. Rev. Let.*, vol. 90(23), id. 231101, 2003.

[9] Van Flandern, T., The speed of gravity – what the experiments say, *Phys. Let. A*, vol. 250, pp. 1–11, 1998.

[10] Will, C., Propagation speed of gravity and the relativistic time delay, *Astrophys. J.*, vol. 590, pp. 683–690, `http://arxiv.org/abs/astro-ph/0301145`, 2003.

Page intentionally left blank

Splinter Meeting Report

Page intentionally left blank

Axel Nothnagel: Summary of the Fifth IVS Analysis Workshop, IVS 2004 General Meeting Proceedings, p.509–513
http://ivscc.gsfc.nasa.gov/publications/gm2004/nothnagel2

Summary of the Fifth IVS Analysis Workshop

Axel Nothnagel

Geodetic Institute, University of Bonn
e-mail: nothnagel@uni-bonn.de

Abstract

On February 12, 2004, the Fifth IVS Analysis Workshop was held at the Lord Elgin Hotel at Ottawa, Canada. The one-day meeting was attended by almost 60 participants. Here, a short summary of the discussion topics and the most important results are given.

On invitation of the National Resources Canada's Geodetic Survey Division the Fifth IVS Analysis Workshop was held in conjunction with the Third IVS General Meeting at the Lord Elgin Hotel at Ottawa, Canada, on February 12, 2004. Almost 60 participants attended the meeting which was, more than ever, driven by many fruitful discussions. The program of the meeting contained a number of important parts of routine and scientific data analysis with many more aspects being raised during the discussions. This summary can, however, reflect only the general headlines of the workshop.

1. Implementation of IAU2000 Resolutions

Nicole Capitaine presented the latest developments with respect to the IAU2000 Resolutions and its effects on earth orientation parameters (EOP). The new paradigm will make the transformations easier to understand and will be a necessary innovation for improvements in UT1 determinations.

It became clear that a change to the new paradigm of the celestial pole modeling will also have an effect on the current UT1 time series itself. Currently, nutation offsets relative to IAU1980 are just transformed into celestial pole offsets relative to the IAU2000 model. However, until VLBI analysis software packages treat the parameter estimation completely consistent with the IAU2000 resolutions, also UT1 has to be transformed accordingly. In order to keep the set of EOP consistent a transformation of the estimated UT1 values has to be applied taking into account the differences in the old and the new formulation of the Equation of the Equinoxes. This difference is unofficially called the Equation of the Origins.

Currently, geodetic VLBI data analysis software packages are being modified to include the paradigm of the IAU2000 Resolutions. For the Calc/Solve software Calc 10.0 will be released in about three months, for OCCAM the modifications are also underway. GLORIA and Steelbreeze are operational in this mode already for some time while MODEST will need some more time to be converted.

2. IVS Tropospheric Parameters and Tropospheric Mapping Functions

For some time now the Institute for Geodesy and Geophysics of the Technical University of Vienna (IGG) has been computing and disseminating the official IVS tropospheric parameters. So far the series had been restricted to include only the IVS-R1 and IVS-R4 sessions. IGG is now preparing the extension of its routine processing to all IVS observing sessions. A call for proposals has been issued for IVS Analysis Centers to respond to by May 31, 2004.

Another issue related to the troposphere is the fact that met sensors have failed occasionally at some sites and surface met data has, therefore, not been available in the respective databases. These gaps in the data should be filled as soon as possible. Johannes Böhm has volunteered to extract this data from the ECWMF files if somebody will provide the epochs and the stations where the surface met data is missing. In addition, a volunteer is also needed to enter the met data in the databases.

It was noted that modeling the troposphere of Mauna Kea (VLBA) which is about 4000 m above sea level is particularly troublesome and the continuous fraction form of current mapping functions seems to fail. It was suspected that this is caused purely by the hydrostatic component since water vapor should be at a minimum at this altitude.

3. IVS EOP Combinations

The current status of the two IVS combined series was presented. The "rapid" series started on January 1st, 1999, and, by now, contains 357 data points (NEOS-A and IVS-R1/-R4 resp.). This series is updated on a weekly basis. The second series is the so-called quarterly solution which contains all sessions suitable for EOP determination (3080 data points). A comparison to IERS C04 shows that the precision of the rapid series is around 100 μas for each component (3mm on the earth's surface). One of the major problems which still has to be solved is the treatment of two sessions on the same day (e.g. NEOS-A and CORE-A or IRIS and western (eastern, central) Pacific networks).

Some additions to the paper presented at the 3rd IVS General Meeting [4] were presented. Two additional series (St. Petersburg University (SPU), Main Astronomical Observatory, Kiev (MAO)) have been incorporated in the investigations of the correlations between IVS Analysis Centers. It has been shown that the MAO EOP solution provides a high degree of independence from other EOP series mainly due to the fact it had been generated with the Steelbreeze software (S. Bolotin). For this reason, the solution submitted by MAO should routinely be used in the combination.

Daniel Gambis of the IERS Product Center for EOP stated that the IVS combined EOP series will only be included in the routine IERS combination if it also includes the IVS Intensive Series and if the data points are provided in a more timely manner.

4. Consistency of CRF, EOP and TRF

An extensive discussion centered around the issue of a consistent solution of the celestial reference frame (CRF), earth orientation parameters (EOP) and the terrestrial reference frame (TRF). The background is that the ICRF and its extensions were generated with a special setup which is optimized for the determination of radio source positions only.

Recently, several solutions have been generated estimating CRF, EOP and TRF in a consistent way. A critical point here is the correct modeling of non-linear station behaviour and of apparent proper motions of some of the radio sources. In order to validate these "complete" solutions a concerted effort has to be started to analyse the resulting radio source catalogues and compare them to the ICRF.

For phase referencing applications consistency between CRF, EOP and TRF is an essential issue. Craig Walker of the VLBA expressed the general wish of the astronomy community that IVS produces reference frames and links them with consistent EOP. Regular updates with daily EOP values would be of great help since the current unequally spaced series are not suitable for their routine operation.

Since there are currently three independent entities, the ICRF, the ITRF2000 and the IERS EOP series, it is a political question of what to change in order to arrive at a consistent set of geometric relationships.

5. Free Core Nutation

A proposal was brought forward by Zinovy Malkin to make Free Core Nutation (FCN) parameters products of the IVS since geodetic VLBI is the only technique to observe this phenomenon. The quality of current time series of nutation offsets seems to a good basis to start such a product, even more so because the MHB2000 Nutation Model includes this contribution only on an empirical basis. Since it is based on observations until 2000 it is degrading rapidly since then. There was a strong vote for this proposal and it was decided that an Analysis Working Group will be established to discuss the procedures.

6. Height Corrections

The height positions of VLBI antenna reference points are known to be affected by several phenomena. With ever increasing observing and analysis accuracy these effects have to be taken into account rigorously.

- Atmosphere Models
  The use of a simple annual model for the hydrostatic mapping function, as given by NMF for example, still leaves significant height error at annual and semi-annual periods, in addition to the shorter term noise associated with weather systems. The annual amplitude can be up to 8 mm (for 5 degree minimum elevation), as judged by comparison with the IMF mapping function, which is based on numerical weather model analysis. The semi-annual amplitude is about half of the annual amplitude. With the increased interest in assessing seasonal effects, for example to determine the signal that might be due to hydrological loading, it is imperative that the most accurate atmosphere models be used, including both the mapping functions and pressure loading corrections. Two mapping functions are available that are based on a Numerical Weather Model, IMF [3] and VMF [1]. IMF offers the advantage that an apriori hydrostatic gradient may be removed, leaving primarily an estimate of the gradient attributed to water vapor, while VMF is about a factor of two more accurate in the azimuthally symmetric hydrostatic mapping function. Since the height errors due to both IMF and VMF are considerably smaller than the sum of other error sources, the improvement in the repeatability of VLBI baseline lengths, compared to using NMF is similar but very significant [1].
- Antenna Thermal Deformatiion
  A database of antenna dimensions for modeling thermal deformation effects is available at the IVS Analysis Coordinator's web page (http://giub.geod.uni-bonn.de/vlbi/IVS-AC). So far

the respective parameters of a few telescopes are still missing and the Analysis Coordinator asks for input by anyone who can provide this information.

In addition, Onsala has an invar rod and Wettzell an invar wire to routinely measure the height variations continuously. The equipment and results were presented as very good examples of how to establish such devices at other telecopes as well. However, wheel and track antennas may need different setups since they do not have easily accessible mount points.

Although the measurements at Onsala and Wettzell have been carried out already for a long time no standardized method of including this data in the VLBI data analysis has been developed yet.

- Local Hydrology
  A talk given by Shigeru Matsuzaka at the General Meeting about height changes at Tsukuba emphasized the importance of monitoring local hydrology in the form of ground water table heights.
- Gravitational Loading
  Since gravitational loading is a phenomenom which also effects the results of other techniques like SLR and GPS and since the IERS has a separate Special Bureau for Loading it became clear that IVS should not proceed with developing its own approach. The decision on a reference pressure value (or values) for atmospheric loading, as an example, was, thus, postponed and the IERS will be asked for advice.

All these effects should be tabulated in some form or other for easy integration in the VLBI analysis chains. In order to prepare the respective procedures and file formats, a small Analysis Working Group will be established.

7. IERS Combination Pilot Project

The Analysis Coordinator outlined the call for proposals of the IERS Combination Pilot Project which was issued by the IERS Analysis Coordinator and the IERS Working Group on Combination. The Pilot Project aims at generating EOP which are consistent with the ITRF and the ICRF using datum-free SINEX files as input. The services, IVS, IGS, ILRS and IDS, are called to contribute "weekly" SINEX files which have been combined from input files of technique analysis centers. In this context "weekly" is one file per week from the satellite techniques and one file per session from IVS. From the SINEX files generated for each technique, IERS Combination Centers are planned to generate inter-technique combinations. The main products of the Pilot Project are time series of EOP, time series of station coordinates and possibly, at a later stage, also time series of source positions.

8. Assorted Analysis Topics

Leonid Petrov prepared a list of currently unsolved problems in geodetic and astrometric VLBI data analysis. A few very important ones are listed here:

- **Expansion analysis to the level of phases and amplitudes** per channel, per accumulation period (AP), down from the level of normal points. Most important advantages:

taking into account ionosphere contribution to delay at the AP-by-AP basis; solving G-code problems, computation of realistic errors of the estimates of group delays.

- **Automation of analysis** of log-files, including extraction of system temperature, post-correlator output and operational data analysis.
- Development of the technology of analysis of **observations of other types** than 24 hour sessions of R4-type and 1.5 hour Intensive-type sessions: differential VLBI, astrometry of weak objects, space navigation, etc.
- Modeling of **source structure delay**.
- Investigation of **errors caused by polarization leakage** and developments of methods for their calibration.
- Application of a model of **spurious signals in phase calibration** for routine data analysis.

9. Miscellaneous

- Oleg Titov presented his investigations in degree-1 load moment deformation.
- Anne-Marie Gontier reported on progress of developing code for the implementation of the PIVEX format (Platform Independent VLBI Exchange Format, [2]).
- A location for the next IVS Analysis Workshop early in 2005 has not been fixed yet and suggestions are still very welcome.

10. Acknowledgements

The IVS Analysis Coordinator is very grateful to the National Resources Canada's Geodetic Survey Division for hosting this meeting. Special thanks is given to Anthony Searle who took very good care of all organisational aspects on site.

References

[1] Boehm J., H. Schuh (2004): Vienna Mapping Functions in VLBI Analyses, Geophys. Res. Letters, 31, L01603, doi:10.1029/2003GL018984

[2] Nothnagel A. (2002): Summary of the Third IVS Analysis Workshop; Proceedings of the 2nd IVS General Meeting, Tsukuba, Japan; N.R. Nandenberg and K.D. Baver (eds.) NASA/CP-2002-210002, 394 - 397

[3] Niell, A.E. (2000): Improved atmospheric mapping functions for VLBI and GPS, Earth, Planets, and Space, 52, 699-702

[4] Steinforth C., A. Nothnagel (2004): Considering apriori Correlations in the IVA combined EOP Series; Proceedings of the 3rd IVS General Meeting, Ottawa, Canada, Feb 9 - 11, 2004; this volume

Page intentionally left blank

Registered Participants

Name	Institution	Country	E-mail
Andersen, Per Helge	Forsvarets forskningsinstitutt, FFI	Norway	per-helge.andersen@ffi.no
Barache, Christophe	Paris Observatory - SYRTE	France	celeste@hpopa.obspm.fr
Beck, Norman	Natural Resources Canada-NRCan	Canada	beck@nrcan.gc.ca
Bertarini, Alessandra	Geodetic Institute - Bonn University	Germany	abertari@mpifr-bonn.mpg.de
Bérubé, Mario	Natural Resources Canada	Canada	marberub@nrcan.gc.ca
Boboltz, Dave	U.S. Naval Observatory	USA	dboboltz@usno.navy.mil
Böhm, Johannes	University of Technology, Vienna	Austria	johannes.boehm@tuwien.ac.at
Brazeau, Sylvain	Geodetic Survey of Canada	Canada	brazeau@nrcan.gc.ca
Bujold, Marc	Ressources Naturelles du Canada	Canada	MBujold@NRCan.gc.ca
Campbell, Bob	Joint Institute for VLBI in Europe	the Netherlands	campbell@jive.nl
Capitaine, Nicole	Observatoire de Paris	France	capitain@syrte.obspm.fr
Chao, Ben	NASA Goddard Space Flight Center	USA	benjamin.f.chao@nasa.gov
Charlot, Patrick	Observatoire de Bordeaux	France	charlot@obs.u-bordeaux1.fr
Combrinck, Ludwig	HartRAO	South Africa	ludwig@hartrao.ac.za
Corey, Brian	MIT Haystack Observatory	U.S.A.	bcorey@haystack.mit.edu
Cox, Clyde	NASA Kokee Park / Honeywell	USA	clyde.cox@honeywell-tsi.com
Diegel, Irvin	Honeywell Technical Solutions, Inc.	USA	irv.diegel@honeywell-tsi.com
Drewes, Hermann	DGFI	Germany	drewes@dgfi.badw.de
Duval, Jean-Robert	Natural Resources Canada	Canada	rduval@nrcan.gc.ca
Ells, John	Canadian Hydrographic Service	Canada	ellsj@dfo-mpo.gc.ca
Engelhardt, Gerald	Bundesamt für Kartographie und Geodäsie (BKG)	Germany	gerald.engelhardt@bkg.bund.de
Engen, Bjorn	Norwegian Mapping Authority	Norway	bjorn.engen@statkart.no
Farley, Stephen	Natural Resources Canada	Canada	farley@geod.nrcan.gc.ca
Feissel-Vernier, Martine	Observatoire de Paris	France	feissel@ensg.ign.fr
Ferland, Remi	Natural Resources Canada	Canada	RFerland@NRCan.gc.ca
Fey, Alan	U.S. Naval Observatory	USA	afey@usno.navy.mil

Name	Institution	Country	E-mail
Fischer, Dorothee	Geodetic Institute of the University of Bonn	Germany	dorothee.fischer@uni-bonn.de
Gambis, Daniel	Observatoire de Paris	France	daniel.gambis@obspm.fr
Gipson, John	NVI/GSFC	USA	jmg@leo.gsfc.nasa.gov
Gontier, Anne-Marie	Paris Observatory - SYRTE	France	Anne-Marie.Gontier@obspm.fr
Gonzalez, Raymond	NVI, Inc. GSFC/NASA	USA	rgonzale@gemini.gsfc.nasa.gov
Gordon, David	Raytheon/Goddard Space Flight Center	USA	dgg@leo.gsfc.nasa.gov
Haas, Rüdiger	Onsala Space Observatory, Chalmers University of Technology	Sweden	haas@oso.chalmers.se
Hall, David	U.S. Naval Observatory	USA	dmh@usno.navy.mil
Han, Seog-Tae	Korea Astronomy Observatory	Korea	sthan@trao.re.kr
Hanssen, Rune	Norwegian Mapping Authority	Norway	rune.hanssen@statkart.no
Hase, Hayo	BKG - TIGO	Chile	hayo.hase@bkg.bund.de
Himwich, Ed	NASA GSFC/NVI	USA	weh@ivscc.gsfc.nasa.gov
Hinteregger, Hans	MIT Haystack Observatory	USA	hhinteregger@haystack.mit.edu
Hobiger, Thomas	University of Technology, Vienna	Austria	thobiger@mars.hg.tuwien.ac.at
Horiai, Koji	National Astronomical Observatory	Japan	horiai@miz.nao.ac.jp
Jacobs, Christopher	JPL	U.S.A.	Chris.Jacobs@jpl.nasa.gov
Johnson, Heidi	MIT Haystack Observatory	USA	hjohnson@haystack.mit.edu
Kingham, Kerry	U.S. Naval Observatory	USA	kak@cygx3.usno.navy.mil
Klatt, Calvin	Natural Resources Canada	Canada	cklatt@nrcan.gc.ca
Kodak, Charles	NASA Goddard / Honeywell	USA	charles.kodak@honeywell-tsi.com
Kondo, Tetsuro	Kashima Space Research Center/CRL	Japan	kondo@crl.go.jp
Kono, Yusuke	National Astronomical Observatory of Japan	Japan	kono.yusuke@nao.ac.jp
Kouba, Jan	Geodetic Survey Div., NRCan (retired)	Canada	kouba@geod.nrcan.gc.ca
Koyama, Yasuhiro	Kashima Space Research Center, CRL	Japan	koyama@crl.go.jp
Krasinsky, George	Institute of Applied Astronomy	Russia	kra@quasar.ipa.nw.ru
Kutterer, Hansjoerg	DGFI, Munich	Germany	kutterer@dgfi.badw.de
LaBrecque, John	NASA HQ	USA	John.LaBrecque@nasa.gov

Name	Institution	Country	E-mail
Laframboise, Robert	Natural Resources Canada	Canada	roblafra@nrcan.gc.ca
Lafrance, Jacques	Natural Resources Canada	Canada	lafrance@geod.nrcan.gc.ca
Lanotte, Roberto	Telespazio - CGS Matera	Italy	lanotte@asi.it
Lanyi, Gabor	Jet Propulsion Laboratory	USA	gabor.lanyi@jpl.nasa.gov
Lapsley, David	MIT Haystack Observatory	USA	dlapsley@haystack.mit.edu
Li, Jinling	Shanghai Astronomical Observatory	P. R. China	jll@shao.ac.cn
Lowe, Stephen	JPL	USA	steve.lowe@jpl.nasa.gov
Ma, Chopo	NASA Goddard Space Flight Center	USA	cma@virgo.gsfc.nasa.gov
MacMillan, Daniel	NVI, Inc./NASA GSFC	USA	dsm@leo.gsfc.nasa.gov
Malkin, Zinovy	Institute of Applied Astronomy	Russia	malkin@quasar.ipa.nw.ru
Manabe, Seiji	National Astronomical Observatory	Japan	manabe@miz.nao.ac.jp
Mantovani, Franco	Istituto di Radioastronomia, Bologna	Italy	fmantovani@ira.cnr.it
Matsuzaka, Shigeru	Geographical Survey Institute	Japan	shigeru@gsi.go.jp
Minh, Young Chol	Korea Astronomy Observatory	Korea	minh@trao.re.kr
Molotov, Igor	Central (Pulkovo) Astronomical Observatory	Russia	molotov@kiam1.rssi.ru
Müskens, Arno	Geodetic Institute - Bonn University	Germany	mueskens@mpifr-bonn.mpg.de
Negusini, Monia	Istituto di Radioastronomia, Bologna	Italy	negusini@ira.cnr.it
Niell, Arthur	MIT Haystack Observatory	USA	aniell@haystack.mit.edu
Nothnagel, Axel	Geodetic Institute of the University of Bonn	Germany	nothnagel@uni-bonn.de
Palmer, Andrew	York University, Toronto	Canada	palmer@core.yorku.ca
Parsley, Stephen	Joint Institute for VLBI in Europe	The Netherlands	parsley@jive.nl
Petrachenko, Bill	Natural Resources Canada (NRCan)	Canada	Bill.Petrachenko@nrc-cnrc.gc.ca
Petrov, Leonid	NVI, Inc./NASA GSFC	USA	Leonid.Petrov@lpetrov.net
Phillips, Robert	MIT Haystack Observatory	USA	rbp@haystack.mit.edu
Qian, Zhihan	Shanghai Astronomical Observatory, CAS	P.R. China	qzh@center.shao.ac.cn
Redmond, Jay	Honeywell Technology Solutions, Inc.	USA	jay.redmond@honeywell-tsi.com

Name	Institution	Country	E-mail
Rekkedal, Svein	Norwegian Mapping Authority (Statenskartverk)	Norway	svein.rekkedal@statkart.no
Rioja Capellan, Maria J.	Observatorio Astronomico Nacional (OAN)	Spain	rioja@hotaka.mtk.nao.ac.jp
Ritakari, Jouko	Metshovi Radio Observatory	Finland	Jouko.Ritakari@hut.fi
Roh, Duk-Gyoo	Korea Astronomy Observatory	Korea	dgroh@trao.re.kr
Romney, Jon	National Radio Astronomy Observatory	USA	jromney@aoc.nrao.edu
Santos, Marcelo	University of New Brunswick	Canada	msantos@unb.ca
Schlüter, Wolfgang	BKG	Germany	wolfgang.schlueter@bkg.bund.de
Schuh, Harald	Institute of Geodesy and Geophysics, Vienna University of Technology	Austria	harald.schuh@tuwien.ac.at
Schupler, Bruce	Honeywell	USA	bruce.schupler@honeywell-tsi.com
Searle, Anthony	Natural Resources Canada	Canada	asearle@nrcan.gc.ca
Sekido, Mamoru	Communications Research Laboratory, Kashima Space Research Center	Japan	sekido@crl.go.jp
Smylie, Doug	York University	Canada	doug@core.yorku.ca
Smythe, Dan	MIT Haystack Observatory	USA	dsmythe@haystack.mit.edu
Souchay, Jean	Observatoire de Paris	France	Jean.Souchay@obspm.fr
Sovers, Ojars	RSA Systems/JPL	USA	ojars@rsasys.com
Steinforth, Christoph	Geodetic Institute University Bonn	Germany	steinforth@uni-bonn.de
Takeuchi, Hiroshi	Kashima Space Research Center/CRL	Japan	ht@crl.go.jp
Tesmer, Volker	DGFI	Germany	tesmer@dgfi.badw.de
Titov, Alexander	Business Bureaus International, Inc.	USA	aragrp@aol.com
Titov, Oleg	Geoscience Australia	Australia	oleg.titov@ga.gov.au
Tuccari, Gino	Radioastronomy Institute of the Italian Research National Council	Italy	g.tuccari@ira.cnr.it
Vandenberg, Nancy	NVI, Inc./GSFC	USA	nrv@gemini.gsfc.nasa.gov
Vennebusch, Markus	Geodetic Institute University Bonn	Germany	Vennebusch@uni-bonn.de
Walker, R. Craig	National Radio Astronomy Observatory	USA	cwalker@nrao.edu
Wallace, Patrick	Rutherford Appleton Laboratory	UK	ptw@star.rl.ac.uk
Whitney, Alan	MIT Haystack Observatory	USA	awhitney@haystack.mit.edu
Wildes, William	NASA GSFC	USA	William.T.Wildes@nasa.gov

Name	Institution	Country	E-mail
Wooden, William	U.S. Naval Observatory	USA	whw@usno.navy.mil
Yang, Zhigen	Shanghai Astronomical Observatory, CAS	China	yangz@center.shao.ac.cn
Zheng, Weimin	Shanghai Astronomical Observatory, Chinese Academy of Sciences	P. R. China	zhwm@center.shao.ac.cn

Page intentionally left blank

Third IVS General Meeting
Ottawa, Canada

PROGRAM

Monday, February 9, 2004

Session 1. VLBI: Today's Results and Tomorrow's Vision
Chair: Wayne Cannon

9:00 **Welcome by host Natural Resources Canada**

9:15 **1-01 Welcome by IVS Chair and Chair's Report**
Wolfgang Schlüter, Bundesamt für Kartographie und Geodäsie (BKG)

9:30 **1-02 Coordinating Center Report**
Nancy Vandenberg, NVI, Inc./GSFC

9:45 **1-03 The ICRF: 2010 and Beyond** *(invited)*
Patrick Charlot, Observatoire de Bordeaux

10:15 **1-04 VLBI and the Earth's Rotation: Geophysical and Geodetic Challenges** *(invited)*
Martine Feissel-Vernier (1), Jim Ray (2), Veronique Dehant (3), Olivier de Viron (3), (1) Paris Observatory and IGN, (2) Bureau International des Poids et Mesures, (3) Observatoire Royal de Belgique

10:45 **Break**

Session 1. VLBI: Today's Results and Tomorrow's Vision (cont.)
Chair: Wolfgang Schlüter

11:15 **1-05 IGGOS – Its Mission, Scientific Rationale, and First Steps and Ideas for Its Design and Development** *(invited)*
Christoph Reigber, GeoForschungsZentrum Potsdam (GFZ), Hermann Drewes, DGFI

11:45 **1-06 Earth Rotation Dynamics: Review and Prospects** *(invited)*
Benjamin Chao, NASA/GSFC

12:15 **Lunch**

Session 2. VLBI2010
Chair: Alan Whitney

13:45 2-01 The International Global Network of Geodetic Fiducial Stations *(invited)*
John LaBrecque, NASA

14:15 2-02 VLBI2010: Networks and Observing Strategies
Bill Petrachenko (1), Brian Corey (2), Ed Himwich (3), Chopo Ma (4), Zinovy Malkin (5), Arthur Niell (2), David Shaffer (6), Nancy Vandenberg (3), (1) Natural Resources Canada, (2) MIT Haystack Observatory, (3) NVI, Inc./GSFC, (4) NASA/GSFC, (5) Institute of Applied Astronomy, (6) Radiometrics, Inc.

14:30 2-03 Preliminary Results of VLBI2010 Subgroup "RF/IF, Frequency and Time"
Hayo Hase (1), Brian Corey (2), Yasuhiro Koyama (3), Dave Shaffer (4), Bill Petrachenko (5), Wolfgang Schlüter (1), (1) BKG, (2) MIT Haystack Observatory, (3) Communications Research Laboratory, (4) Radiometrics Inc., (5) Natural Resources Canada

14:45 2-04 Standard Observing Bands: Is Now the Time To Replace S/X with X/Ka?
Chris Jacobs, Gabor Lanyi, and Charles Naudet, Jet Propulsion Laboratory

15:00 2-05 VLBI at Some Higher Frequencies, an Overview
Chopo Ma (1), David Gordon (2), Chris Jacobs (3), Gabor Lanyi (3), Charles Naudet, (3), Alan Fey (4), David Boboltz (4), Ed Fomalont (5), Patrick Charlot (6), Ojars Sovers (7), (1) NASA/GSFC, (2) Raytheon/GSFC, (3) Jet Propulsion Laboratory, (4) U.S. Naval Observatory, (5) National Radio Astronomy Observatory, (6) Bordeaux Observatory, (7) Remote Sensing Analysis Systems

15:15 2-06 Backend Systems -- Perspectives in 2010
Gino Tuccari (1), Alan Whitney (2), Hans Hinteregger (2), Yasuhiro Koyama (3), Tetsuro Kondo (3), (1) IRA CNR, (2) MIT Haystack Observatory, (3) Communications Research Laboratory

15:30 Break

Session 2. VLBI2010 (cont.)
Chair: Arthur Niell

16:00 2-07 Data-Acquisition and Transport – Look Forward to 2010 and Beyond
Alan Whitney (1), Hans Hinteregger (1), Tetsuro Kondo (2), Yasuhiro Koyama (2), (1) MIT Haystack Observatory, (2) Communications Research Laboratory

16:15 2-08 Correlators in 2010 and Beyond
Yasuhiro Koyama (1), Tetsuro Kondo (1), Bill Petrachenko (2), Hans Hinteregger (3), and Alan Whitney (3), (1) Kashima Space Research Center, CRL (2) Natural Resources Canada, (3) MIT Haystack Observatory

16:30 2-09 Subgroup "Data Analysis" of Working Group 3 VLBI2010
Harald Schuh, Vienna University of Technology

16:45 2-10 VLBI Data Longevity Beyond 2010
Chopo Ma, NASA/GSFC

17:00 2-11 Future Directions on the VLBA
R. Craig Walker, National Radio Astronomy Observatory

17:15 2-12 Impact of Interstellar Scintillation on Astrometric VLBI
David Jauncey (1), Jim Lovell (1), Roopesh Ojha (1), Alan Fey (2), Yasuhiro Koyama (3), Hayley Bignall (4), Lucyna Kedziora-Chudczer (5), Jean-Pierre Macquart, (6), Barney Rickett (7), Tasso Tzioumis, (1) Australia Telescope National facility, CSIRO, Australia, (2) USNO, (3) CRL Kashima

17:30 Sessions 1 and 2 Poster Overview
Arthur Niell, MIT Haystack Observatory

17:45 Poster Sessions and Refreshments

Tuesday, February 10, 2004

Session 3. Network Stations, Operation Centers, Correlators
Chair: Hayo Hase

8:30 3-01 Correlator Experiences with Mark 5 in Operation *(invited)*
Arno Mueskens (1), Walter Alef (2), David Graham (2), Geodetic Institute of the University of Bonn, (2) Max-Planck Institut for Radioastronomie

9:00 3-02 Recent Results from the EVN Mk4 Data Processor at JIVE
Bob Campbell, Joint Institute for VLBI in Europe

9:15 3-03 Washington Correlator Update
Kerry Kingham, U.S. Naval Observatory

9:30 3-04 Overview of Geodetic Experiments at the Bonn Correlator
Alessandra Bertarini, Arno Mueskens, Alexandra Hoefer, Geodetic Institute of the University of Bonn

9:45 3-05 Network Coordinator's Report
Ed Himwich, NVI, Inc./GSFC

10:00 Break

Session 3. Network Stations, Operation Centers, Correlators (cont.)
Chair: Kerry Kingham

10:30 3-06 Present Status and Future Plan on the Chinese VLBI Network
Zhihan Qian, Shuhua Ye, Xiaoyu Hong, Xiuzhong Zhang, Jin Zhang and Xizhen Zhang, Shanghai Astronomical Observatory, CAS

10:45 3-07 VLBI-GPS Collocation Results in Japan
Shigeru Matsuzaka, Y. Masaki, Hiromichi Tsuji, Kazuhiro Takashima, T. Tsutsumi, M. Ishimoto, M. Machida, H. Wada, Shinobu Kurihara, Geographical Survey Institute, Japan

11:00 3-08 Status and Plan of Geodetic and Astrometric Observations with VERA
Seiji Manabe, Yoshiaki Tamura, Takaaki Jike, Koji Horiai and VERA team, National Astronomical Observatory of Japan

11:15 Session 3 Poster Overview
Kerry Kingham, U. S. Naval Observatory

11:30 Lunch

Session 4. New Technology Developments in VLBI
Chair: Shigeru Matsuzaka

13:00 4-01 The Mark 5B VLBI Data System
Alan Whitney, Will Aldrich, John Ball, Brian Fanous, Dan Smythe, MIT Haystack Observatory

13:15 4-02 Gbit/s VLBI and eVLBI with Off-the-Shelf Components
Jouko Ritakari, Ari Mujunen, Metsähovi Radio Observatory

13:30 4-03 Current Status of Software Correlators Developed at Kashima Space Research Center
Tetsuro Kondo, Moritaka Kimura, Yasuhiro Koyama, Hiro Osaki, Kashima Space Research Center/CRL

13:45 4-04 SOFTC: An Operational Software Correlator
Stephen Lowe, Jet Propulsion Laboratory

14:00 4-05 eVLBI Developments in Europe

Stephen Parsley, Zsolt Paragi, Sergei Pogrebenco, Cormac Reynolds, Arpad Szomoru, Joint Institute for VLBI in Europe (JIVE)

14:15 4-06 E-VLBI Progress of the Chinese VLBI Network
Zheng Weimin, Zhang Xiuzhong, Shu Fengchun, Shanghai Astronomical Observatory, Chinese Academy of Sciences

14:30 Break

Session 4. New Technology Developments in VLBI (cont.)
Chair: Alan Whitney

15:00 4-07 Transporting VLBI Data Across Long Fat Networks: A Practical Approach
David Lapsley, MIT Haystack Observatory

15:15 4-08 Geodetic VLBI Experiments with the K5 System
Yasuhiro Koyama (1), Tetsuro Kondo (1), Hiro Osaki (1), Masaki Hirabaru (1), Kazuhiro Takashima (2), Kazuo Sorai (3), Hiroshi Takaba (4), Kenta Fujisawa (5), David Lapsley (6), Kevin Dudevoir (6), Alan Whitney (6), (1) Communications Research Laboratory, (2) Geographical Survey Institute of Japan (GSI), (3) Hokkaido U., (4) Gifu U., (5) Yamaguchi U., (6) MIT Haystack Observatory

15:30 4-09 Millimeter Wave Multi-Channel Receivers System for VLBI
Seog-Tae Han, Korea Astronomy Observatory

15:45 4-10 DBBC - A Wide Band Digital Base Band Converter
Gino Tuccari, IRA CNR

16:00 4-11 Toward Standard Wideband Digital Backends for Next-Generation Radio Astronomy: ATNF, LOFAR, (e)-VLBI, ATA, SKA
Hans Hinteregger, MIT Haystack Observatory

16:15 4-12 VLBI Observation for Spacecraft Navigation (NOZOMI) – Data Processing and Analysis Status Report
Mamoru Sekido (1), Ryuichi Ichikawa (1), Hiro Osaki (1), Tetsuro Kondo (1), Yasuhiro Koyama (1), Makoto Yoshikawa (2), Takafumi Ohnishi (3),Wayne Cannon (4), Alexander Novikov (4), Mario Berube (5), (1) Kashima Space Research Center, CRL, (2) ISAS/JAXA, (3) Fujitsu Co. Ltd, (4) SGL/CRESTech, (5) Natural Resources Canada

16:30 Session 4 Poster Overview
Alan Whitney, MIT Haystack Observatory

16:45 Session 5 Poster Overview
Volker Tesmer, DGFI

17:00 Session 6 Poster Overview
Rüdiger Haas, Onsala Space Observatory

18:00 Banquet

Wednesday, February 11, 2004

Session 5. Analysis Strategies and Software
Chair: Calvin Klatt

8:30 5-01 MODEST: A Tool for Geodesy and Astrometry
Ojars Sovers (1), Chris Jacobs (2), Gabor Lanyi (2), (1) Remote Sensing Analysis Systems, (2) Jet Propulsion Laboratory/NASA

8:45 5-02 OCCAM v.6.0 Software for VLBI Data Analysis
Oleg Titov (1), Volker Tesmer (2), Johannes Boehm (3), (1) Geoscience Australia, (2) DGFI, (3) Vienna University of Technology

9:00 5-03 Past, Present and Future of Sked
John Gipson, NVI, Inc/GSFC

9:15 5-04 Residual Plotting and Ambiguity Resolution in Calc/Solve
Volkmar Thorandt, Gerald Engelhardt, Bundesamt für Kartographie und Geodäsie (BKG)

Session 5. Analysis Strategies and Software (cont.)
Chair: Harald Schuh

9:30 5-05 An Advanced Stochastic Model for VLBI Observations and its Application to VLBI Data Analysis
Volker Tesmer, Hansjoerg Kutterer, DGFI

9:45 5-06 Vienna Mapping Functions in VLBI Analyses
Johannes Boehm, Harald Schuh, Vienna University of Technology

10:00 5-07 Reliability Measures for Geodetic VLBI Products
Hansjoerg Kutterer, DGFI

10:15 5-08 Activities of the IVS Analysis Center at BKG in 2003
Gerald Engelhardt, Volkmar Thorandt, Dieter Ullrich, Bundesamt für Kartographie und Geodäsie (BKG)

10:30 Break

Session 6. Results and Geodetic/Geophysical/Astrometric Interpretation
Chair: Rüdiger Haas

11:00 6-01 Refinement of the ICRF
Chopo Ma, NASA Goddard Space Flight Center

11:15 6-02 Status of the International Celestial Reference Frame
Alan Fey, U.S. Naval Observatory

11:30 6-03 VLBA Impact on Geodesy and Astrometry
David Gordon, Raytheon/Goddard Space Flight Center

11:45 6-04 The VLBI Contribution to Precession (Present and Future)
Nicole Capitaine (1), Patrick Wallace (2), (1) Observatoire de Paris/SYRTE, France, (2) HM Nautical Almanac Office, Rutherford Appleton Laboratory, UK,

12:00 Lunch

13:30 6-05 Ring Downs of Free Core Nutations in the GSFC and USNO VLBI Nutation Series *(Invited)*
Douglas Smylie, Andrew Palmer, York University

14:00 6-06 Viscosity of the Earth's Fluid Core from VLBI Data
George Krasinsky, Institute of Applied Astronomy, RAS

14:15 6-07 Contribution of VLBI to Earth Orientation Monitoring: State-of-the-Art and Future Prospects
Daniel Gambis, Christian Bizouard Observatoire de Paris

14:30 6-08 UT1 Intensive Series Using K4 Technology
Dorothee Fischer (1), Richard Kilger (2), Shinobu Kurihara (3), Axel Nothnagel (1), Wolfgang Schlüter (2), Kazuhiro Takashima (3), (1) Geodetic Insitute of the University of Bonn, (2) Bundesamt für Kartographie und Geodäsie, (3) Geographical Survey Institute of Japan

14:45 6-09 Considering a priori Correlations in the IVS Combined EOP Series
Christoph Steinforth, Axel Nothnagel, Geodetic Institute of the University Bonn

15:00 6-10 CONT02 campaign - Combination of VLBI with GPS
Volker Tesmer (1), Manuela Kruegel (1), Detlef Angermann (1), Daniela Thaller (2), Markus Rothacher (2), Ralf Schmid (2), (1) DGFI, (2) Technische Universitaet Muenchen

15:15 6-11 First Results of SINEX Combinations
Markus Vennebusch, Geodetic Institute of the University Bonn

15:30 Break

Session 6. Results and Geodetic/Geophysical/Astrometric Interpretation (cont.)
Chair: Zinovy Malkin

16:00 6-12 Evaluation of Global Ionosphere TEC Map by Comparison with VLBI Data *(invited)*
Mamoru Sekido, Tetsuro Kondo, Eiji Kawai, and Michito Imae, Communications Research Laboratory

16:30 6-13 How VLBI Contributes to Ionospheric Research
Thomas Hobiger, Harald Schuh, Vienna University of Technology

16:45 6-14 Limitations to Dual Frequency Ionospheric Corrections for Frequency Switched K-Q Observations with the VLBA
Gabor Lanyi (1), David Gordon (2), Ojars Sovers (3), (1) Jet Propulsion Laboratory, (2) Raytheon/GSFC, (3) Remote Sensing Analysis Systems

17:00 6-15 Tropospheric Parameters Estimated by Geodetic VLBI Data
Monia Negusini, Paolo Tomasi, Istituto di Radioastronomia, Bologna, Italy

17:15 6-16 Mass Loading Effects on Crustal Displacements Measured by VLBI
Daniel MacMillan, NVI, Inc./GSFC

17:30 6-17 First Results of the IVS Pilot Project "Time Series of Baseline Lengths"
Axel Nothnagel, Geodetic Institute of the University of Bonn

17:45 6-18 Preliminary Results of the IVS Gravity Experiment grav01
Leonid Petrov, NVI, Inc./GSFC

Posters

Session 1P. VLBI: Today's Results and Tomorrow's Vision

1-01P 5,000,000 Delays – Some Statistics
Zinovy Malkin, Institute of Applied Astronomy RAS

Session 2P. VLBI2010

2-01P Worlds of 1996, 2003, and 2010
Ari Mujunen, Jouko Ritakari, Metsähovi Radio Observatory

2-02P Vienna Students Project (VSP) – A VLBI Experiment by Students
Wolfgang Winkler, et al., University of Technology, Vienna

Session 3P. Network Stations, Operation Centers, Correlators

3-01P Present Status of the Korean VLBI Network Construction
Young Chol Minh, Korea Astronomy Observatory

3-02P Projects at TIGO
H. Hase (1), S. Sobarzo (2), C. Jara (2), R. Aedo (3), G. Remedi (3), M. Moreno (2), M. Sanchez (2), G. Hermosilla (2), (1) BKG, (2) UdeC, (3) UBioBio

3-03P New Technologies for the Real 3D Reference Point Determination
Maria Hennes, Cornelia Eschelbach, Geodetic Institute, University of Karlsruhe

3-04P VLBI Status of the Bear Lakes Radio Astronomy Station
Igor Molotov (1), Yurii Gorshenkov (2), Alexander Stepanov (1), Boris Lipatov (3), Gino Tuccari (4), Valery Saurin (2), Alexis Zinoviev (1), (1) Central Pulkovo Astronomical Observatory, (2) Power Engineering Institute, (3) Radio Physical Research institute, (4) Istituto di Radioastronomia CNR

3-05P Some Results of the First Year of Participation of the Svetloe Observatory in IVS Observing Programs
Andrey Finkelstein, Valery Gratchev, Alexander Ipatov, Zinovy Malkin, Ismail Rahimov, Elena Skurikhina, Sergey Smolentsev, Institute of Applied Astronomy RAS

3-06P Radio Astronomy Observatories in Svetloe, Zelenchukskaya and Badary of VLBI Network QUASAR
Andrey Finkelstein, Alexander Ipatov, Sergey Smolentsev, Institute of Applied Astronomy, Russian Academy of Sciences

3-07P The New 40-m Radiotelescope of the Spanish National Geographical Institute (IGN) at Yebes

Maria Rioja, Observatorio Astronomico Nacional (OAN), Spain

Session 4P. New Technology Developments in VLBI

4-01P FS Developments

Ed Himwich (1), Ray Gonzalez (1), Jonathan Quick (2), John Gipson (1), (1) NVI, Inc./GSFC, (2) Hartebeesthoek Radio Astronomy Observatory

4-02P The Data Acquisition System Developed for Quasar Network

Alexander Ipatov, Nikolay Koltsov, Leonid Fedotov, Institute of Applied Astronomy, Russian Academy of Sciences

4-03P Data Acquisition System of Korean VLBI Network

Duk-Gyoo Roh, Korea Astronomy Observatory

4-04P New Correlator PARSEC

Valery Gratchev, Institute of Applied Astronomy, RAS

4-05P VLBI@home – VLBI Correlator by GRID Computing System

Takeuchi Hiroshi, Kondo Tetsuro, Koyama Yasuhiro, and Nakajima Junichi, Kashima Space Research Center/CRL

4-06P A Near Real Time e-Radar/VLBI Network

Gino Tuccari (1), Igor Molotov (2), S. Buttaccio (1), G. Nicotra (1), B. Lipatov (3), Alexis Zinoviev (2), Y. Gorshenkov (4), L. Xiang (5), Xiaoyu Hong (6), Alexnder Volvach (7), (1) Istituto di Radioastronomia CNR, (2) Central Pulkova Astronomical Observatory, (3) Radio Physical Research Institute, (4) Power Engineering Institute, (5) Urumqi Astronomical Observatory, (6) Shanghai Astronomical Observatory, (7) Crimean Astrophysical Observatory

4-07P An Evaluation of VLBI Observations for Deep Space Tracking of Interplanetary Spacecraft

Ryuichi Ichikawa (1), Mamoru Sekido (1), Hiro Osaki (1), Yasuhiro Koyama (1), Tetsuro Kondo (1), T. Ohnishi (1), M. Yoshikawa (1), Wayne Cannon (2), Alexander Novikov (2), Mario Berube (3), (1) Kashima Space Research Center/CRL, (2) SGL/CRESTech, (3) Natural Resources Canada

Session 5P. Analysis Strategies and Software

5-01P VLBI Analysis at Bordeaux Observatory

P. Charlot, A. Bellanger, A.Baudry, Observatoire de Bordeaux

5-02P Calc: The Next Upgrade
David Gordon, Raytheon/GSFC

5-03P Project: Global Analysis of 1979-2004 VLBI Data
Vadim Gubanov, Institute of Applied Astronomy, RAS

5-04P VLBI Analysis at the United States Naval Observatory
David Hall, David Boboltz, Alan Fey, Kerry Kingham, U.S. Naval Observatory

5-05P Modeling Vertical Total Electron Content from VLBI Observations
Thomas Hobiger, Harald Schuh, Vienna University of Technology

5-06P Towards an IVS Analysis Conventions
Zinovy Malkin, Institute of Applied Astronomy RAS, St. Petersburg, Russia

5-07P Solve: Past, Present and Future
Leonid Petrov (1), Chopo Ma (2), James Ryan (3), John Gipson (1), Karen Baver (4), Volkmar Thorandt (5), Gerald Engelhardt (5), (1) NVI, Inc./GSFC, (2) NASA/GSFC, (3) NASA/GSFC Retired, (4) Raytheon/GSFC, (5) BKG

5-08P An Embedded Expert System for the Automation of the VLBI Data Analysis: Concept, Implementation and Results
Wolfgang Schwegmann, Bundesamt für Kartographie und Geodäsie

5-09P Towards an Operational Automatic VLBI Data Analysis Tool for INTENSIVE Sessions
Wolfgang Schwegmann, Volkmar Thorandt, Gerald Engelhardt, Bundesamt für Kartographie und Geodäsie

5-10P Simultaneous Estimation of a TRF, the EOP and a CRF from VLBI Observations - First DGFI Results using OCCAM
Volker Tesmer, Hansjoerg Kutterer, Hermann Drewes, DGFI

Session 6P. Results and Geodetic/Geophysical/Astrometric Interpretation

6-01P Stability of the VLBI-Derived Celestial Reference Frame
Martine Feissel-Vernier, Observatoire de Paris and IGN

6-02P Southern Hemisphere Astrometry
Alan Fey (1), Roopesh Ojha (2), et al., (1) U.S. Naval Observatory, (2) Australia Telescope National Facility

6-03P Extending the ICRF to Higher Radio Frequencies – Imaging and Source Structure
David Boboltz (1), Alan Fey (1), Patrick Charlot (2), Ed Fomalont (3), Gabor Lanyi (4), L.D. Zhang (4) and the K-Q VLBI Survey Collaboration, (1) U.S. Naval Observatory, (2) Bordeaux Observatory, (3) National Radio Astronomy Observatory, (4) Jet Propulsion Laboratory

6-04P Investigation of Nutation Beyond the IAU2000 Model
Véronique Dehant (1), Olivier De Viron (1), Martine Feissel-Vernier (2), (1) Royal Observatory of Belgium, (2) Paris Observatory and IGN

6-05P A New FCN Model with Variable Period and Amplitude
Zinovy Malkin (1), Toshimichi Shirai (2), (1) Institute of Applied Astronomy RAS, (2) Goldman Sachs (Japan) Ltd.

6-06P Analysis of the VLBI Intensive Sessions
Karen Baver (1), Dan MacMillan (2), Leonid Petrov (2), David Gordon (1), (1) Raytheon/GSFC, (2), NVI, Inc./GSFC

6-07P Investigations of High-Frequency Earth Rotation Variations from VLBI CONT Observations
Raymundo Del Cojo Lopez, Juan Mata Lozano, Rüdiger Haas, Onsala Space Observatory

6-08P High Resolution Earth Rotation Parameters Determined During the CONT02 Campaign
Jolanta Nastula (1), Barbara Kolaczek (1), Robert Weber (2), Johannes Boehm (2), Harald Schuh (2), (1) Space Research Center PAS, Warsaw Poland, (2) Vienna University of Technology

6-09P Ionospheric Parameters Obtained by Different Space Geodetic Techniques During CONT02
Thomas Hobiger, Sonya Todorova, Harald Schuh, Vienna University of Technology

6-10P Comparison of Ionospheric Activity Derived from GPS and Different VLBI Networks
Sten Bergstrand, Rüdiger Haas, Onsala Space Observatory

6-11P IVS Tropospheric Parameters
Harald Schuh, et al., Vienna University of Technology

6-12P Long Time ZTD Series for Some Stations
Elena Skurikhina, Institute of Applied Astronomy

6-13P Calculating Mapping Functions from the HIRLAM Numerical Weather Prediction Model
Bisser Stoyanov, Rüdiger Haas, Lubomir Gradinarsky, Onsala Space Observatory, Chalmers University of Technology

6-14P Relative Deformations Between Collocated VLBI Stations and Comparisons with VTRF2003

Zhigen Yang, (1), Mario Berube (2), Anthony Searle (2), (1) Shanghai Astronomical Observatory, Chinese Academy, (2) Geodetic Survey Division, Natural Resources Canada

6-15P Postseismic Transient After the 2002 Denali Fault Earthquake from VLBI Measurements at Fairbanks

Daniel MacMillan, NVI, Inc./GSFC

6-16P Post-Seismic Motion of Gilcreek Geodetic Sites Following the November, 2002 Denali Earthquake

Oleg Titov (1), Paul Tregoning (2), (1) Geoscience Australia, (2) Research School of Earth Sciences, ANU

Page intentionally left blank

Index of Authors

(First authors are designated by (1) at the end of the title.)

Aedo, Roberto: p. 143, **Projects at TIGO**

Alef, Walter: p. 115, **Operational Experience with the Mark 5 Recording System at the Bonn and USNO Correlator**

Altamimi, Zuheir: p. 22, **VLBI and Earth Rotation: Geophysical and Geodetic Challenges**

Angermann, Detlef: p. 418, **CONT02 Campaign - Combination of VLBI and GPS**

Baver, Karen: p. 394, **Analysis of the VLBI Intensive Sessions** (1)

Bergstrand, Sten: p. 447, **Comparison of Ionospheric Activity Derived from GPS and Different VLBI Networks** (1)

Bertarini, Alessandra: p. 120, **Overview of Geodetic Experiments at the Bonn Correlator** (1)

Bérubé, Mario: p. 253, **An Evaluation of VLBI Observations for the Deep Space Tracking of the Interplanetary Spacecrafts**

Bérubé, Mario: p. 258, **VLBI Observation for Spacecraft Navigation (NOZOMI) - Data Processing and Analysis Status Report**

Bérubé, Mario: p. 481, **Relative Deformations between Co-located VLBI Stations and Comparisons with VTRF2003**

Bignall, Hayley E.: p. 109, **The Impact of Interstellar Scintillation on Astrometric VLBI**

Bizouard, Christian: p. 393, **Contribution of VLBI to Earth Orientation Monitoring: State-of-the-Art and Future Prospects**

Boboltz, David A.: p. 329, **VLBI Analysis at the U.S. Naval Observatory**

Boboltz, David A.: p. 361, **Extending the ICRF to Higher Radio Frequencies – Imaging and Source Structure** (1)

Bogensberger, Boris: p. 105, **VIEPROJ1 - A Students' VLBI Project**

Böhm, Johannes: p. 105, **VIEPROJ1 - A Students' VLBI Project**

Böhm, Johannes: p. 267, **OCCAM v.6.0 Software for VLBI Data Analysis**

Böhm, Johannes: p. 277, **Vienna Mapping Functions in VLBI Analyses** (1)

Böhm, Johannes: p. 408, **High Resolution Earth Rotation Parameters Determined During the CONT02 Campaign**

Böhm, Johannes: p. 461, **IVS Tropospheric Parameters - Comparison with DORIS and GPS for CONT02**

Boy, Jean-Paul: p. 476, **Mass Loading Effects on Crustal Displacements Measured by VLBI**

Buttaccio, Salvatore: p. 225, **A Near Real Time e-Radar/VLBI Network**

Campbell, Robert M.: p. 123, **Recent Results from the EVN Mark IV Data Processor at JIVE** (1)

Cannon, Wayne: p. 253, **An Evaluation of VLBI Observations for the Deep Space Tracking of the Interplanetary Spacecrafts**

Cannon, Wayne: p. 258, **VLBI Observation for Spacecraft Navigation (NOZOMI) - Data Processing and Analysis Status Report**

Capitaine, Nicole: p. 366, **The VLBI Contribution to Precession (Present and Future)** (1)

Chao, Benjamin F.: p. 38, **Earth Rotational Variations Excited by Geophysical Fluids** (1)

Charlot, Patrick: p. 12, **The ICRF: 2010 and Beyond** (1)

Charlot, Patrick: p. 75, **Extending the ICRF to Higher Radio Frequencies: 24 and 43 GHz Astrometry**

Charlot, Patrick: p. 361, **Extending the ICRF to Higher Radio Frequencies – Imaging and Source Structure**

Choi, Han-Kyu: p. 248, **A Design of Data Acquisition System for Korean VLBI Network**

Chung, Hyun-Soo: p. 248, **A Design of Data Acquisition System for Korean VLBI Network**

Cifuentes, Oscar: p. 143, **Projects at TIGO**

Cohen, Steven: p. 491, **Postseismic Transient after the 2002 Denali Fault Earthquake from VLBI Measurements at Fairbanks**
Corey, Brian: p. 60, **VLBI2010: Networks and Observing Strategies**
Corey, Brian: p. 65, **Preliminary Results of the VLBI2010 Subgroup "RF/IF, Frequency and Time"**
Dehant, Véronique: p. 22, **VLBI and Earth Rotation: Geophysical and Geodetic Challenges**
Dehant, Véronique: p. 381, **Investigation of Nutation beyond the IAU2000 Model** (1)
Dementiev, Alexander: p. 166, **VLBI Status of the Bear Lakes Radio Astronomy Station**
Dementiev, Alexander: p. 225, **A Near Real Time e-Radar/VLBI Network**
de Viron, Olivier: p. 22, **VLBI and Earth Rotation: Geophysical and Geodetic Challenges**
de Viron, Olivier: p. 381, **Investigation of Nutation beyond the IAU2000 Model**
Drewes, Hermann: p. 32, **The IAG Project "Integrated Global Geodetic Observing System (IGGOS)" – Setup of the Initial Phase** (1)
Drewes, Hermann: p. 311, **Simultaneous Estimation of a TRF, the EOP and a CRF**
Dudevoir, Kevin: p. 220, **Geodetic VLBI Experiments with the K5 System**
Ellingsen, Simon P.: p. 356, **VLBI Astrometry of 22 Southern Hemisphere Radio Sources**
Engelhardt, Gerald: p. 282, **Residual Plotting and Ambiguity Resolution (REPA)**
Engelhardt, Gerald: p. 292, **Towards an Operational Automatic VLBI Data Analysis Tool for INTENSIVE Sessions**
Engelhardt, Gerald: p. 324, **Activities of the IVS Analysis Center at BKG in 2003** (1)
Engelhardt, Gerald: p. 461, **IVS Tropospheric Parameters - Comparison with DORIS and GPS for CONT02**
Eschelbach, Cornelia: p. 146, **New Technologies for the Real 3D Reference Point Determination**
Fedotov, Leonid: p. 243, **The Data Acquisition System Developed for Quasar Network**
Feissel-Vernier, Martine: p. 22, **VLBI and Earth Rotation: Geophysical and Geodetic Challenges** (1)
Feissel-Vernier, Martine: p. 346, **Stability of the VLBI-Derived Celestial Reference Frame** (1)
Feissel-Vernier, Martine: p. 381, **Investigation of Nutation beyond the IAU2000 Model**
Fengchun, Shu: p. 210, **e-VLBI Progress of the Chinese VLBI Network**
Fey, Alan L.: p. 109, **The Impact of Interstellar Scintillation on Astrometric VLBI**
Fey, Alan L.: p. 329, **VLBI Analysis at the U.S. Naval Observatory**
Fey, Alan L.: p. 341, **Status of the International Celestial Reference Frame** (1)
Fey, Alan L.: p. 356, **VLBI Astrometry of 22 Southern Hemisphere Radio Sources** (1)
Fey, Alan L.: p. 361, **Extending the ICRF to Higher Radio Frequencies – Imaging and Source Structure**
Finkelstein, Andrey: p. 128, **Some Results of the First Year of Participation of the Svetloe Observatory in IVS Observing Programs** (1)
Finkelstein, Andrey: p. 161, **Radio Astronomy Observatories Svetloe, Zelenchukskaya and Badary of VLBI Network QUASAR** (1)
Fischer, Dorothee: p. 399, **UT1 Intensive Series Using K4 Technology** (1)
Fomalont, Ed B.: p. 75, **Extending the ICRF to Higher Radio Frequencies: 24 and 43 GHz Astrometry**
Fomalont, Edward B.: p. 361, **Extending the ICRF to Higher Radio Frequencies – Imaging and Source Structure**
Fujisawa, Kenta: p. 220, **Geodetic VLBI Experiments with the K5 System**
Gambis, Daniel: p. 393, **Contribution of VLBI to Earth Orientation Monitoring: State-of-the-Art and Future Prospects** (1)
Gordon, David: p. 75, **Extending the ICRF to Higher Radio Frequencies: 24 and 43 GHz Astrometry**
Gordon, David: p. 265, **CALC: The Next Upgrade** (1)
Gordon, David: p. 351, **VLBA Impact on Geodesy and Astrometry** (1)

Gordon, David: p. 394, **Analysis of the VLBI Intensive Sessions**
Gordon, David: p. 452, **Limitations to Dual Frequency Ionosphere Corrections for Frequency Switched K-Q-Band Observations with the VLBA**
Gorshenkov, Yuri: p. 166, **VLBI Status of the Bear Lakes Radio Astronomy Station**
Gorshenkov, Yuri: p. 225, **A Near Real Time e-Radar/VLBI Network**
Gradinarsky, Lubomir: p. 471, **Calculating Mapping Functions from the HIRLAM Numerical Weather Prediction Model**
Graham, David: p. 115, **Operational Experience with the Mark 5 Recording System at the Bonn and USNO Correlator**
Gratchev, Valery: p. 128, **Some Results of the First Year of Participation of the Svetloe Observatory in IVS Observing Programs**
Gratchev, Valery: p. 195, **New Correlator PARSEC** (1)
Gubanov, V.S.: p. 315, **Project: Global Analysis of 1979-2004 VLBI Data** (1)
Gubanov, Vadim: p. 461, **IVS Tropospheric Parameters - Comparison with DORIS and GPS for CONT02**
Haas, Rüdiger: p. 403, **Investigations of High-Frequency Earth Rotation Variations from VLBI CONT Observations** (1)
Haas, Rüdiger: p. 447, **Comparison of Ionospheric Activity Derived from GPS and Different VLBI Networks**
Haas, Rüdiger: p. 461, **IVS Tropospheric Parameters - Comparison with DORIS and GPS for CONT02**
Haas, Rüdiger: p. 471, **Calculating Mapping Functions from the HIRLAM Numerical Weather Prediction Model**
Hall, David M.: p. 329, **VLBI Analysis at the U.S. Naval Observatory** (1)
Han, Seog-Tae: p. 156, **Present Status of the KVN Construction Project**
Han, Seog-Tae: p. 229, **The Multi-Channel Millimeter Wave Receiver for VLBI** (1)
Hase, Hayo: p. 65, **Preliminary Results of the VLBI2010 Subgroup "RF/IF, Frequency and Time"** (1)
Hase, Hayo: p. 143, **Projects at TIGO** (1)
Hennes, Maria: p. 146, **New Technologies for the Real 3D Reference Point Determination** (1)
Hermosilla, Gonzalo: p. 143, **Projects at TIGO**
Himwich, Ed: p. 60, **VLBI2010: Networks and Observing Strategies**
Hinteregger, Hans: p. 80, **Backend Systems – Perspectives in 2010**
Hinteregger, Hans F.: p. 85, **Data Acquisition and Transport - Looking 2010 and Beyond**
Hinteregger, Hans: p. 90, **Correlators in 2010 and Beyond**
Hinteregger, Hans: p. 238, **Low-Cost Wideband Digital Back-Ends for LOFAR⇒e-VLBI⇒SKA** (1)
Hirabaru, Masaki: p. 220, **Geodetic VLBI Experiments with the K5 System**
Hobiger, Thomas: p. 105, **VIEPROJ1 - A Students' VLBI Project**
Hobiger, Thomas: p. 306, **Modelling Vertical Total Electron Content from VLBI Observations** (1)
Hobiger, Thomas: p. 437, **How VLBI Contributes to Ionospheric Research** (1)
Hobiger, Thomas: p. 442, **Ionospheric Parameters Obtained by Different Space Geodetic Techniques during CONT02** (1)
Höfer, Alexandra: p. 120, **Overview of Geodetic Experiments at the Bonn Correlator**
Hong, Xiaou: p. 225, **A Near Real Time e-Radar/VLBI Network**
Hong, Xiaoyu: p. 133, **Present Status and Future Plan on the Chinese VLBI Network**
Horiai, Koji: p. 151, **Status and Plan of Geodetic and Astrometric Observations with VERA**
Ichikawa, Ryuichi: p. 253, **An Evaluation of VLBI Observations for the Deep Space Tracking of the Interplanetary Spacecrafts** (1)
Ichikawa, Ryuichi: p. 258, **VLBI Observation for Spacecraft Navigation (NOZOMI) - Data Pro-**

cessing and Analysis Status Report
Imae, Michito: p. 427, **Evaluation of Global Ionosphere TEC by Comparison with VLBI Data**
Ipatov, Alexander: p. 128, **Some Results of the First Year of Participation of the Svetloe Observatory in IVS Observing Programs**
Ipatov, Alexander: p. 161, **Radio Astronomy Observatories Svetloe, Zelenchukskaya and Badary of VLBI Network QUASAR**
Ipatov, Alexander: p. 243, **The Data Acquisition System Developed for Quasar Network** (1)
Ishimoto, Yoshimasa: p. 138, **VLBI-GPS Co-location Results in Japan**
Jacobs, C.S.: p. 70, **Standard Observing Bands: Is Now the Time to Replace S/X with X/Ka?** (1)
Jacobs, Christopher S.: p. 75, **Extending the ICRF to Higher Radio Frequencies: 24 and 43 GHz Astrometry** (1)
Jacobs, Christopher S.: p. 272, **MODEST: a Tool for Geodesy and Astrometry**
Jara, Cristobal: p. 143, **Projects at TIGO**
Jauncey, David L.: p. 109, **The Impact of Interstellar Scintillation on Astrometric VLBI** (1)
Jauncey, David L.: p. 356, **VLBI Astrometry of 22 Southern Hemisphere Radio Sources**
Je, Do-Heung: p. 229, **The Multi-Channel Millimeter Wave Receiver for VLBI**
Jike, Takkaki: p. 151, **Status and Plan of Geodetic and Astrometric Observations with VERA**
Johnston, Kenneth J.: p. 356, **VLBI Astrometry of 22 Southern Hemisphere Radio Sources**
Karel, Wilfried: p. 105, **VIEPROJ1 - A Students' VLBI Project**
Kawai, Eiji: p. 427, **Evaluation of Global Ionosphere TEC by Comparison with VLBI Data**
Kedziora-Chudczer, Lucyna: p. 109, **The Impact of Interstellar Scintillation on Astrometric VLBI**
Kilger, Richard: p. 399, **UT1 Intensive Series Using K4 Technology**
Kim, Hyun-Goo: p. 156, **Present Status of the KVN Construction Project**
Kim, Kwang-Dong: p. 229, **The Multi-Channel Millimeter Wave Receiver for VLBI**
Kim, Kwang-Dong: p. 248, **A Design of Data Acquisition System for Korean VLBI Network**
Kimura, Moritaka: p. 186, **Current Status of Software Correlators Developed at Kashima Space Research Center**
Kingham, Kerry: p. 115, **Operational Experience with the Mark 5 Recording System at the Bonn and USNO Correlator**
Kingham, Kerry A.: p. 329, **VLBI Analysis at the U.S. Naval Observatory**
Kistenich, Michael: p. 105, **VIEPROJ1 - A Students' VLBI Project**
Kolaczek, Barbara: p. 408, **High Resolution Earth Rotation Parameters Determined During the CONT02 Campaign**
Koltsov, Nikolay: p. 243, **The Data Acquisition System Developed for Quasar Network**
Kondo, Tetsuro: p. 80, **Backend Systems – Perspectives in 2010**
Kondo, Tetsuro: p. 85, **Data Acquisition and Transport - Looking 2010 and Beyond**
Kondo, Tetsuro: p. 90, **Correlators in 2010 and Beyond**
Kondo, Tetsuro: p. 186, **Current Status of Software Correlators Developed at Kashima Space Research Center** (1)
Kondo, Tetsuro: p. 200, **VLBI@home – VLBI Correlator by GRID Computing System**
Kondo, Tetsuro: p. 220, **Geodetic VLBI Experiments with the K5 System**
Kondo, Tetsuro: p. 253, **An Evaluation of VLBI Observations for the Deep Space Tracking of the Interplanetary Spacecrafts**
Kondo, Tetsuro: p. 258, **VLBI Observation for Spacecraft Navigation (NOZOMI) - Data Processing and Analysis Status Report**
Kondo, Tetsuro: p. 427, **Evaluation of Global Ionosphere TEC by Comparison with VLBI Data**
Konovalenko, Alexander: p. 225, **A Near Real Time e-Radar/VLBI Network**
Kovalev, Yuri Y.: p. 170, **Single Dish Flux Density Monitoring of Geodetic VLBI Sources**
Koyama, Yasuhiro: p. 65, **Preliminary Results of the VLBI2010 Subgroup "RF/IF, Frequency and Time"**

Koyama, Yasuhiro: p. 80, **Backend Systems – Perspectives in 2010**
Koyama, Yashuhiro: p. 85, **Data Acquisition and Transport - Looking 2010 and Beyond**
Koyama, Yasuhiro: p. 90, **Correlators in 2010 and Beyond** (1)
Koyama, Yasuhiro: p. 109, **The Impact of Interstellar Scintillation on Astrometric VLBI**
Koyama, Yasuhiro: p. 186, **Current Status of Software Correlators Developed at Kashima Space Research Center**
Koyama, Yasuhiro: p. 200, **VLBI@home – VLBI Correlator by GRID Computing System**
Koyama, Yasuhiro: p. 220, **Geodetic VLBI Experiments with the K5 System** (1)
Koyama, Yasuhiro: p. 253, **An Evaluation of VLBI Observations for the Deep Space Tracking of the Interplanetary Spacecrafts**
Koyama, Yasuhiro: p. 258, **VLBI Observation for Spacecraft Navigation (NOZOMI) - Data Processing and Analysis Status Report**
Koyama, Yasuhiro: p. 356, **VLBI Astrometry of 22 Southern Hemisphere Radio Sources**
KQ VLBI Survey Collaboration: p. 75, **Extending the ICRF to Higher Radio Frequencies: 24 and 43 GHz Astrometry**
KQ VLBI Survey Collaboration: p. 361, **Extending the ICRF to Higher Radio Frequencies – Imaging and Source Structure**
Krasinsky, George A.: p. 383, **Viscosity of the Earth's Fluid Core from VLBI Data** (1)
Krügel, Manuela: p. 418, **CONT02 Campaign - Combination of VLBI and GPS** (1)
Kurdubov, S.L.: p. 315, **Project: Global Analysis of 1979-2004 VLBI Data**
Kurihara, Shinobu: p. 138, **VLBI-GPS Co-location Results in Japan**
Kurihara, Shinobu: p. 399, **UT1 Intensive Series Using K4 Technology**
Kutterer, Hansjörg: p. 296, **An Advanced Stochastic Model for VLBI Observations and its Application to VLBI Data Analysis**
Kutterer, Hansjörg: p. 301, **Reliability Measures for Geodetic VLBI Products** (1)
Kutterer, Hansjörg: p. 311, **Simultaneous Estimation of a TRF, the EOP and a CRF**
LaBrecque, John: p. 55, **The International Global Network of Geodetic Fiducial Stations** (1)
Lanotte, Roberto: p. 461, **IVS Tropospheric Parameters - Comparison with DORIS and GPS for CONT02**
Lanyi, G.E.: p. 70, **Standard Observing Bands: Is Now the Time to Replace S/X with X/Ka?**
Lanyi, Gabor E.: p. 75, **Extending the ICRF to Higher Radio Frequencies: 24 and 43 GHz Astrometry**
Lanyi, Gabor E.: p. 272, **MODEST: a Tool for Geodesy and Astrometry**
Lanyi, Gabor E.: p. 361, **Extending the ICRF to Higher Radio Frequencies – Imaging and Source Structure**
Lanyi, Gabor: p. 452, **Limitations to Dual Frequency Ionosphere Corrections for Frequency Switched K-Q-Band Observations with the VLBA** (1)
Lapsley, David: p. 215, **A Practical Approach to e-VLBI over Long Fast Networks** (1)
Lapsley, David: p. 220, **Geodetic VLBI Experiments with the K5 System**
Lee, Chang-Hoon: p. 229, **The Multi-Channel Millimeter Wave Receiver for VLBI**
Liu, Xiang: p. 225, **A Near Real Time e-Radar/VLBI Network**
López, Raymundo Del Cojo: p. 403, **Investigations of High-Frequency Earth Rotation Variations from VLBI CONT Observations**
Lovell, James E. J.: p. 109, **The Impact of Interstellar Scintillation on Astrometric VLBI**
Lovell, James E. J.: p. 356, **VLBI Astrometry of 22 Southern Hemisphere Radio Sources**
Lowe, Stephen T.: p. 191, **Softc: an Operational Software Correlator** (1)
Lozano, Juan Mata: p. 403, **Investigations of High-Frequency Earth Rotation Variations from VLBI CONT Observations**
Ma, Chopo: p. 60, **VLBI2010: Networks and Observing Strategies**
Ma, Chopo: p. 75, **Extending the ICRF to Higher Radio Frequencies: 24 and 43 GHz Astrometry**

Ma, Chopo: p. 97, **Data Longevity Beyond 2010** (1)
Ma, Chopo: p. 337, **Refinement of the ICRF** (1)
Machida, Morito: p. 138, **VLBI-GPS Co-location Results in Japan**
MacMillan, Daniel: p. 394, **Analysis of the VLBI Intensive Sessions**
MacMillan, Daniel: p. 461, **IVS Tropospheric Parameters - Comparison with DORIS and GPS for CONT02**
MacMillan, Daniel: p. 476, **Mass Loading Effects on Crustal Displacements Measured by VLBI** (1)
MacMillan, Daniel: p. 491, **Postseismic Transient after the 2002 Denali Fault Earthquake from VLBI Measurements at Fairbanks** (1)
Macquart, Jean-Pierre: p. 109, **The Impact of Interstellar Scintillation on Astrometric VLBI**
Malkin, Zinovy: p. 47, **5,000,000 Delays—Some Statistics** (1)
Malkin, Zinovy: p. 60, **VLBI2010: Networks and Observing Strategies**
Malkin, Zinovy: p. 128, **Some Results of the First Year of Participation of the Svetloe Observatory in IVS Observing Programs**
Malkin, Zinovy: p. 320, **Towards IVS Analysis Conventions** (1)
Malkin, Zinovy: p. 388, **A New Free Core Nutation Model with Variable Amplitude and Period** (1)
Manabe, Seiji: p. 151, **Status and Plan of Geodetic and Astrometric Observations with VERA** (1)
Masaki, Yoshimitsu: p. 138, **VLBI-GPS Co-location Results in Japan**
Matsuzaka, Shigeru: p. 138, **VLBI-GPS Co-location Results in Japan** (1)
McCulloch, Peter M.: p. 356, **VLBI Astrometry of 22 Southern Hemisphere Radio Sources**
Minh, Young Chol: p. 156, **Present Status of the KVN Construction Project** (1)
Molotov, Igor: p. 166, **VLBI Status of the Bear Lakes Radio Astronomy Station** (1)
Molotov, Igor: p. 225, **A Near Real Time e-Radar/VLBI Network**
Moreno, Marcos: p. 143, **Projects at TIGO**
Mujunen, Ari: p. 56, **VLBI2010: Commercial-off-the-Shelf Techonology Perspectives in 1996, 2003, and 2010** (1)
Mujunen, Ari: p. 182, **Gbit/s VLBI and eVLBI with Off-The-Shelf Components**
Müskens, Arno: p. 115, **Operational Experience with the Mark 5 Recording System at the Bonn and USNO Correlator** (1)
Müskens, Arno: p. 120, **Overview of Geodetic Experiments at the Bonn Correlator**
Nakajima, Junichi: p. 200, **VLBI@home – VLBI Correlator by GRID Computing System**
Nastula, Jolanta: p. 408, **High Resolution Earth Rotation Parameters Determined During the CONT02 Campaign** (1)
Naudet, C.J.: p. 70, **Standard Observing Bands: Is Now the Time to Replace S/X with X/Ka?**
Naudet, Charles J.: p. 75, **Extending the ICRF to Higher Radio Frequencies: 24 and 43 GHz Astrometry**
Negusini, Monia: p. 456, **Tropospheric Parameters Estimated by Geodetic VLBI Data IVS** (1)
Negusini, Monia: p. 461, **IVS Tropospheric Parameters - Comparison with DORIS and GPS for CONT02**
Nicolson, George D.: p. 356, **VLBI Astrometry of 22 Southern Hemisphere Radio Sources**
Nicotra, Gaetano: p. 225, **A Near Real Time e-Radar/VLBI Network**
Niell, Arthur: p. 60, **VLBI2010: Networks and Observing Strategies**
Nothnagel, Axel: p. 399, **UT1 Intensive Series Using K4 Technology**
Nothnagel, Axel: p. 413, **Considering a Priori Correlations in the IVS Combined EOP Series**
Nothnagel, Axel: p. 486, **First Results of the IVS Pilot Project "Time Series of Baseline Lengths"** (1)
Nothnagel, Axel: p. 509, **Summary of the Fifth IVS Analysis Workshop** (1)
Novikov, Alexander: p. 253, **An Evaluation of VLBI Observations for the Deep Space Tracking**

of the Interplanetary Spacecrafts
Novikov, Alexander: p. 258, **VLBI Observation for Spacecraft Navigation (NOZOMI) - Data Processing and Analysis Status Report**
NOZOMI DVLBI Group: p. 253, **An Evaluation of VLBI Observations for the Deep Space Tracking of the Interplanetary Spacecrafts**
NOZOMI VLBI Group: p. 258, **VLBI Observation for Spacecraft Navigation (NOZOMI) - Data Processing and Analysis Status Report**
Oh, Se-Jin: p. 229, **The Multi-Channel Millimeter Wave Receiver for VLBI**
Oh, Se-Jin: p. 248, **A Design of Data Acquisition System for Korean VLBI Network**
Ohnishi, Takafumi: p. 253, **An Evaluation of VLBI Observations for the Deep Space Tracking of the Interplanetary Spacecrafts**
Ohnishi, Takafumi: p. 258, **VLBI Observation for Spacecraft Navigation (NOZOMI) - Data Processing and Analysis Status Report**
Ohsaki, Hiroo: p. 253, **An Evaluation of VLBI Observations for the Deep Space Tracking of the Interplanetary Spacecrafts**
Ojha, Roopesh: p. 109, **The Impact of Interstellar Scintillation on Astrometric VLBI**
Ojha, Roopesh: p. 356, **VLBI Astrometry of 22 Southern Hemisphere Radio Sources**
Osaki, Hiro: p. 186, **Current Status of Software Correlators Developed at Kashima Space Research Center**
Osaki, Hiro: p. 220, **Geodetic VLBI Experiments with the K5 System**
Osaki, Hiro: p. 258, **VLBI Observation for Spacecraft Navigation (NOZOMI) - Data Processing and Analysis Status Report**
Pacher, Gerold: p. 105, **VIEPROJ1 - A Students' VLBI Project**
Palmer, Andrew: p. 371, **Ring Downs of Free Core Nutations in the GSFC and USNO VLBI Nutation Series**
Pany, Andrea: p. 105, **VIEPROJ1 - A Students' VLBI Project**
Parsley, Stephen: p. 205, **eVLBI Research in the European VLBI Network** (1)
Petrachenko, Bill: p. 60, **VLBI2010: Networks and Observing Strategies** (1)
Petrachenko, Bill: p. 65, **Preliminary Results of the VLBI2010 Subgroup "RF/IF, Frequency and Time"**
Petrachenko, William T.: p. 90, **Correlators in 2010 and Beyond**
Petrov, Leonid: p. 394, **Analysis of the VLBI Intensive Sessions**
Petrov, Leonid: p. 501, **Preliminary Results of the IVS Gravity Experiment Grav01** (1)
Qian, Zhihan: p. 133, **Present Status and Future Plan on the Chinese VLBI Network** (1)
Quick, Jonathan F. H.: p. 356, **VLBI Astrometry of 22 Southern Hemisphere Radio Sources**
Rahimov, Ismail: p. 128, **Some Results of the First Year of Participation of the Svetloe Observatory in IVS Observing Programs**
Ray, Jim: p. 22, **VLBI and Earth Rotation: Geophysical and Geodetic Challenges**
Reigber, Christoph: p. 32, **The IAG Project "Integrated Global Geodetic Observing System (IGGOS)" – Setup of the Initial Phase**
Remedi, Gonzalo: p. 143, **Projects at TIGO**
Reynolds, John E.: p. 356, **VLBI Astrometry of 22 Southern Hemisphere Radio Sources**
Rickett, Barney J.: p. 109, **The Impact of Interstellar Scintillation on Astrometric VLBI**
Ritakari, Jouko: p. 56, **VLBI2010: Commercial-off-the-Shelf Techonology Perspectives in 1996, 2003, and 2010**
Ritakari, Jouko: p. 182, **Gbit/s VLBI and eVLBI with Off-The-Shelf Components** (1)
Roh, Duk-Gyoo: p. 156, **Present Status of the KVN Construction Project**
Roh, Duk-Gyoo: p. 229, **The Multi-Channel Millimeter Wave Receiver for VLBI**
Roh, Duk-Gyoo: p. 248, **A Design of Data Acquisition System for Korean VLBI Network** (1)
Roncat, Andreas: p. 105, **VIEPROJ1 - A Students' VLBI Project**
Rothacher, Markus: p. 418, **CONT02 Campaign - Combination of VLBI and GPS**

Rusinov, Yu.L.: p. 315, **Project: Global Analysis of 1979-2004 VLBI Data**
Saurin, Valerii: p. 166, **VLBI Status of the Bear Lakes Radio Astronomy Station**
Schlüter, Wolfgang: p. 7, **Chair's Report at the Third IVS General Meeting** (1)
Schlüter, Wolfgang: p. 65, **Preliminary Results of the VLBI2010 Subgroup "RF/IF, Frequency and Time"**
Schlüter, Wolfgang: p. 399, **UT1 Intensive Series Using K4 Technology**
Schmid, Ralf: p. 418, **CONT02 Campaign - Combination of VLBI and GPS**
Schuh, Harald: p. 95, **Report of the Subgroup "Data Analysis" of Working Group 3 VLBI2010 (Outline)** (1)
Schuh, Harald: p. 105, **VIEPROJ1 - A Students' VLBI Project**
Schuh, Harald: p. 277, **Vienna Mapping Functions in VLBI Analyses**
Schuh, Harald: p. 306, **Modelling Vertical Total Electron Content from VLBI Observations**
Schuh, Harald: p. 408, **High Resolution Earth Rotation Parameters Determined During the CONT02 Campaign**
Schuh, Harald: p. 437, **How VLBI Contributes to Ionospheric Research**
Schuh, Harald: p. 442, **Ionospheric Parameters Obtained by Different Space Geodetic Techniques during CONT02**
Schuh, Harald: p. 461, **IVS Tropospheric Parameters - Comparison with DORIS and GPS for CONT02** (1)
Schwegmann, Wolfgang: p. 287, **An Embedded Expert System for the Automation of VLBI Data Analysis: Concept, Implementation and Results** (1)
Schwegmann, Wolfgang: p. 292, **Towards an Operational Automatic VLBI Data Analysis Tool for INTENSIVE Sessions** (1)
Searle, Anthony: p. 481, **Relative Deformations between Co-located VLBI Stations and Comparisons with VTRF2003**
Sekido, Mamoru: p. 253, **An Evaluation of VLBI Observations for the Deep Space Tracking of the Interplanetary Spacecrafts**
Sekido, Mamoru: p. 258, **VLBI Observation for Spacecraft Navigation (NOZOMI) - Data Processing and Analysis Status Report** (1)
Sekido, Mamoru: p. 427, **Evaluation of Global Ionosphere TEC by Comparison with VLBI Data** (1)
Shabun, C.Y.: p. 315, **Project: Global Analysis of 1979-2004 VLBI Data**
Shaffer, David: p. 60, **VLBI2010: Networks and Observing Strategies**
Shaffer, David: p. 65, **Preliminary Results of the VLBI2010 Subgroup "RF/IF, Frequency and Time"**
Skurikhina, Elena: p. 128, **Some Results of the First Year of Participation of the Svetloe Observatory in IVS Observing Programs**
Skurikhina, Elena: p. 466, **Long Time Wet Tropospheric Delay Series for Some Stations** (1)
Smolentsev, Sergey: p. 128, **Some Results of the First Year of Participation of the Svetloe Observatory in IVS Observing Programs**
Smolentsev, Sergey: p. 161, **Radio Astronomy Observatories Svetloe, Zelenchukskaya and Badary of VLBI Network QUASAR**
Smylie, D. E.: p. 371, **Ring Downs of Free Core Nutations in the GSFC and USNO VLBI Nutation Series** (1)
Snajdrova, Kristyna: p. 461, **IVS Tropospheric Parameters - Comparison with DORIS and GPS for CONT02**
Sobarzo, Sergio: p. 143, **Projects at TIGO**
Song, Min-Gyu: p. 229, **The Multi-Channel Millimeter Wave Receiver for VLBI**
Sorai, Kazuo: p. 220, **Geodetic VLBI Experiments with the K5 System**
Sovers, Ojars J.: p. 75, **Extending the ICRF to Higher Radio Frequencies: 24 and 43 GHz Astrometry**

Sovers, Ojars J.: p. 272, **MODEST: a Tool for Geodesy and Astrometry** (1)
Sovers, Ojars J.: p. 452, **Limitations to Dual Frequency Ionosphere Corrections for Frequency Switched K-Q-Band Observations with the VLBA**
Steinforth, Christoph: p. 413, **Considering a Priori Correlations in the IVS Combined EOP Series** (1)
Stepanov, Alexander: p. 166, **VLBI Status of the Bear Lakes Radio Astronomy Station**
Stoyanov, Bisser: p. 471, **Calculating Mapping Functions from the HIRLAM Numerical Weather Prediction Model** (1)
Summer, Gerhard: p. 105, **VIEPROJ1 - A Students' VLBI Project**
Surkis, I.F.: p. 315, **Project: Global Analysis of 1979-2004 VLBI Data**
Takaba, Hiroshi: p. 220, **Geodetic VLBI Experiments with the K5 System**
Takashima, Kazuhiro: p. 138, **VLBI-GPS Co-location Results in Japan**
Takashima, Kazuhiro: p. 220, **Geodetic VLBI Experiments with the K5 System**
Takashima, Kazuhiro: p. 399, **UT1 Intensive Series Using K4 Technology**
Takeuchi, Hiroshi: p. 200, **VLBI@home – VLBI Correlator by GRID Computing System** (1)
Tamura, Yoshiaki: p. 151, **Status and Plan of Geodetic and Astrometric Observations with VERA**
Tesmer, Volker: p. 267, **OCCAM v.6.0 Software for VLBI Data Analysis**
Tesmer, Volker: p. 296, **An Advanced Stochastic Model for VLBI Observations and its Application to VLBI Data Analysis** (1)
Tesmer, Volker: p. 311, **Simultaneous Estimation of a TRF, the EOP and a CRF** (1)
Tesmer, Volker: p. 418, **CONT02 Campaign - Combination of VLBI and GPS**
Thaller, Daniela: p. 418, **CONT02 Campaign - Combination of VLBI and GPS**
Thorandt, Volkmar: p. 282, **Residual Plotting and Ambiguity Resolution (REPA)** (1)
Thorandt, Volkmar: p. 292, **Towards an Operational Automatic VLBI Data Analysis Tool for INTENSIVE Sessions**
Thorandt, Volkmar: p. 324, **Activities of the IVS Analysis Center at BKG in 2003**
Till, Susan M.: p. 3, **Welcome Address of Natural Resources Canada** (1)
Titov, Oleg: p. 109, **The Impact of Interstellar Scintillation on Astrometric VLBI**
Titov, Oleg: p. 267, **OCCAM v.6.0 Software for VLBI Data Analysis** (1)
Titov, Oleg: p. 496, **Post-Seismic Motion of Gilcreek Geodetic Sites Following the November, 2002 Denali Earthquake** (1)
Todorova, Sonya: p. 442, **Ionospheric Parameters Obtained by Different Space Geodetic Techniques during CONT02**
Tomasi, Paolo: p. 456, **Tropospheric Parameters Estimated by Geodetic VLBI Data IVS**
Tomasi, Paolo: p. 461, **IVS Tropospheric Parameters - Comparison with DORIS and GPS for CONT02**
Tregoning, Paul: p. 496, **Post-Seismic Motion of Gilcreek Geodetic Sites Following the November, 2002 Denali Earthquake**
Tsuji, Hiromichi: p. 138, **VLBI-GPS Co-location Results in Japan**
Tsutsumi, Takashi: p. 138, **VLBI-GPS Co-location Results in Japan**
Tuccari, Gino: p. 80, **Backend Systems – Perspectives in 2010** (1)
Tuccari, Gino: p. 166, **VLBI Status of the Bear Lakes Radio Astronomy Station**
Tuccari, Gino: p. 225, **A Near Real Time e-Radar/VLBI Network** (1)
Tuccari, Gino: p. 234, **DBBC - a Wide Band Digital Base Band Converter** (1)
Tzioumis, Anastasios K.: p. 109, **The Impact of Interstellar Scintillation on Astrometric VLBI**
Tzioumis, Anastasios K.: p. 356, **VLBI Astrometry of 22 Southern Hemisphere Radio Sources**
Ullrich, Dieter: p. 324, **Activities of the IVS Analysis Center at BKG in 2003**
Vandenberg, Nancy: p. 60, **VLBI2010: Networks and Observing Strategies**
Vennebusch, Markus: p. 423, **First Results of SINEX Combinations** (1)
VERA Team: p. 151, **Status and Plan of Geodetic and Astrometric Observations with VERA**

Vereshchagina, Iraida: p. 461, **IVS Tropospheric Parameters - Comparison with DORIS and GPS for CONT02**
Volvach, Alexandr: p. 170, **Single Dish Flux Density Monitoring of Geodetic VLBI Sources** (1)
Volvach, Alexander: p. 225, **A Near Real Time e-Radar/VLBI Network**
Volvach, Larisa: p. 170, **Single Dish Flux Density Monitoring of Geodetic VLBI Sources**
Wada, Hirohito: p. 138, **VLBI-GPS Co-location Results in Japan**
Walker, R. Craig: p. 100, **Future Directions on the VLBA** (1)
Wallace, Patrick: p. 366, **The VLBI Contribution to Precession (Present and Future)**
Weber, Robert: p. 105, **VIEPROJ1 - A Students' VLBI Project**
Weber, Robert: p. 408, **High Resolution Earth Rotation Parameters Determined During the CONT02 Campaign**
Weimin, Zheng: p. 210, **e-VLBI Progress of the Chinese VLBI Network** (1)
Whitney, Alan: p. 80, **Backend Systems – Perspectives in 2010**
Whitney, Alan R.: p. 85, **Data Acquisition and Transport - Looking 2010 and Beyond** (1)
Whitney, Alan R.: p. 90, **Correlators in 2010 and Beyond**
Whitney, Alan R.: p. 177, **The Mark 5B VLBI Data System** (1)
Whitney, Alan: p. 220, **Geodetic VLBI Experiments with the K5 System**
Wi, Sek-O: p. 229, **The Multi-Channel Millimeter Wave Receiver for VLBI**
Willis, Pascal: p. 461, **IVS Tropospheric Parameters - Comparison with DORIS and GPS for CONT02**
Winkler, Wolfgang: p. 105, **VIEPROJ1 - A Students' VLBI Project** (1)
Xiuzhong, Zhang: p. 210, **e-VLBI Progress of the Chinese VLBI Network**
Yang, Zhigen: p. 481, **Relative Deformations between Co-located VLBI Stations and Comparisons with VTRF2003** (1)
Ye, Shuhua: p. 133, **Present Status and Future Plan on the Chinese VLBI Network**
Yoshikawa, Makoto: p. 253, **An Evaluation of VLBI Observations for the Deep Space Tracking of the Interplanetary Spacecrafts**
Yoshikawa, Makoto: p. 258, **VLBI Observation for Spacecraft Navigation (NOZOMI) - Data Processing and Analysis Status Report**
Zhang, Hongbo: p. 133, **Present Status and Future Plan on the Chinese VLBI Network**
Zhang, Jin: p. 133, **Present Status and Future Plan on the Chinese VLBI Network**
Zhang, Liwei D.: p. 75, **Extending the ICRF to Higher Radio Frequencies: 24 and 43 GHz Astrometry**
Zhang, Liwei D.: p. 361, **Extending the ICRF to Higher Radio Frequencies – Imaging and Source Structure**
Zhang, Xiuzhong: p. 133, **Present Status and Future Plan on the Chinese VLBI Network**
Zhang, Xizheng: p. 133, **Present Status and Future Plan on the Chinese VLBI Network**
Zinoviev, Alexis: p. 166, **VLBI Status of the Bear Lakes Radio Astronomy Station**
Zinoviev, Alexis: p. 225, **A Near Real Time e-Radar/VLBI Network**

REPORT DOCUMENTATION PAGE	*Form Approved* *OMB No. 0704-0188*

1. REPORT DATE *(DD-MM-YYYY)*
07-02-2004

2. REPORT TYPE
Conference Publication

3. DATES COVERED *(From - To)*

4. TITLE AND SUBTITLE
International VLBI Service for Geodesy and Astrometry 2004 General Meeting Proceedings

5a. CONTRACT NUMBER

5b. GRANT NUMBER

5c. PROGRAM ELEMENT NUMBER

6. AUTHOR(S)
Nancy R. Vandenberg and Karen D. Baver, Editors

5d. PROJECT NUMBER

5e. TASK NUMBER

5f. WORK UNIT NUMBER

7. PERFORMING ORGANIZATION NAME(S) AND ADDRESS(ES)
NASA Goddard Space Flight Center
Greenbelt, MD 20771

8. PERFORMING ORGANIZATION REPORT NUMBER
2004-02219-0

9. SPONSORING/MONITORING AGENCY NAME(S) AND ADDRESS(ES)
National Aeronautics and Space Administration
Washington, DC 20546-0001

10. SPONSORING/MONITOR'S ACRONYM(S)

11. SPONSORING/MONITORING REPORT NUMBER
CP-2004-212255

12. DISTRIBUTION/AVAILABILITY STATEMENT
Unclassified-Unlimited, Subject Category: 46
Report available from NASA Center for Aerospace Information, 7121 Standard Drive, Hanover, MD 21076-1320, (301)621-0390

13. SUPPLEMENTARY NOTES
N. Vandenberg, NVI Inc., K. Baver, Raytheon

14. ABSTRACT
This volume is the proceedings of the third General Meeting of the International VLBI Service for Geodesy and Astrometry (IVS), held in Ottawa, Canada, February 9-11, 2004. The contents of this volume also appear on the IVS Web site at http://ivscc.gsfc.nasa.gov/ publications /gm2004. The keynote of the third GM was visions for the next decade following the main theme of "Today's Results and Tomorrow's Vision", with a recognition that the outstanding VLBI results available today are the foundation and motivation for the next generation VLBI system requirements. The goal of the meeting was to provide an interesting and informative program for a wide cross section of IVS members, including station operators, program managers, and analysts.

This volume contains 99 papers and two abstracts of papers presented at the GM. The volume also includes a report about a splinter meeting held in conjunction with the GM, the fifth IVS Analysis Workshop.

15. SUBJECT TERMS
Geodesy, astrometry, VLBI, geophysics, Earth orientation, very long baseline interferometry, interferometry, radio astronomy, geodynamics, reference frames, terrestrial reference frame, celestial reference frame, length of day, Earth system science, Earth rotation.

16. SECURITY CLASSIFICATION OF:			17. LIMITATION OF ABSTRACT	18. NUMBER OF PAGES	19b. NAME OF RESPONSIBLE PERSON
a. REPORT	b. ABSTRACT	c. THIS PAGE			Karen Baver
				544	19b. TELEPHONE NUMBER *(Include area code)*

Standard Form 298 (Rev. 8-98)
Prescribed by ANSI Std. Z39-18

INSTRUCTIONS FOR COMPLETING SF 298

1. REPORT DATE. Full publication date, including day, month, if available. Must cite at least the year and be Year 2000 compliant, e.g. 30-06-1998; xx-06-1998; xx-xx-1998.

2. REPORT TYPE. State the type of report, such as final, technical, interim, memorandum, master's thesis, progress, quarterly, research, special, group study, etc.

3. DATES COVERED. Indicate the time during which the work was performed and the report was written, e.g., Jun 1997 - Jun 1998; 1-10 Jun 1996; May - Nov 1998; Nov 1998.

4. TITLE. Enter title and subtitle with volume number and part number, if applicable. On classified documents, enter the title classification in parentheses.

5a. CONTRACT NUMBER. Enter all contract numbers as they appear in the report, e.g. F33615-86-C-5169.

5b. GRANT NUMBER. Enter all grant numbers as they appear in the report, e.g. AFOSR-82-1 234.

5c. PROGRAM ELEMENT NUMBER. Enter all program element numbers as they appear in the report, e.g. 61101 A.

5d. PROJECT NUMBER. Enter all project numbers as they appear in the report, e.g. 1F665702D1 257; ILIR.

5e. TASK NUMBER. Enter all task numbers as they appear in the report, e.g. 05; RF0330201; T4112.

5f. WORK UNIT NUMBER. Enter all work unit numbers as they appear in the report, e.g. 001; AFAPL30480105.

6. AUTHOR(S). Enter name(s) of person(s) responsible for writing the report, performing the research, or credited with the content of the report. The form of entry is the last name, first name, middle initial, and additional qualifiers separated by commas, e.g. Smith, Richard, J, Jr.

7. PERFORMING ORGANIZATION NAME(S) AND ADDRESS(ES). Self-explanatory.

8. PERFORMING ORGANIZATION REPORT NUMBER. Enter all unique alphanumeric report numbers assigned by the performing organization, e.g. BRL- 1234; AFWL-TR-85-4017-Vol-21 -PT-2.

9. SPONSORING/MONITORING AGENCY NAME(S) AND ADDRESS(ES). Enter the name and address of the organization(s) financially responsible for and monitoring the work.

10. SPONSOR/MONITOR'S ACRONYMS). Enter, if available, e.g. BRL, ARDEC, NADC.

11. SPONSOR/MONITOR'S REPORT NUMBER(S). Enter report number as assigned by the sponsoring/monitoring agency, if available, e.g. BRL-TR-829; -215.

12. DISTRIBUTION/AVAILABILITY STATEMENT. Use agency-mandated availability statements to indicate the public availability or distribution limitations of the report. If additional limitations/ restrictions or special markings are indicated, follow agency authorization procedures, e.g. RD/FRD, PROPIN, ITAR, etc. Include copyright information.

13. SUPPLEMENTARY NOTES. Enter information not included elsewhere such as: prepared in cooperation with; translation of; report supersedes; old edition number, etc.

14. ABSTRACT. A brief (approximately 200 words) factual summary of the most significant information.

15. SUBJECT TERMS. Key words or phrases identifying major concepts in the report.

16. SECURITY CLASSIFICATION. Enter security classification in accordance with security classification regulations, e.g. U, C, S, etc. If this form contains classified information, stamp classification level on the top and bottom of this page.

17. LIMITATION OF ABSTRACT. This block must be completed to assign a distribution limitation to the abstract. Enter UU (Unclassified Unlimited) or SAR (Same as Report). An entry in this block is necessary if the abstract is to be limited.